KOSM

60

Kosmos 60 is
furnace black for ru
rubber. It originat
ture is scientifically c
standards. Its super
strength make for

UNITED CARBO

Charle

New York • Akron
Canada: Canadia

Don't get trapped...

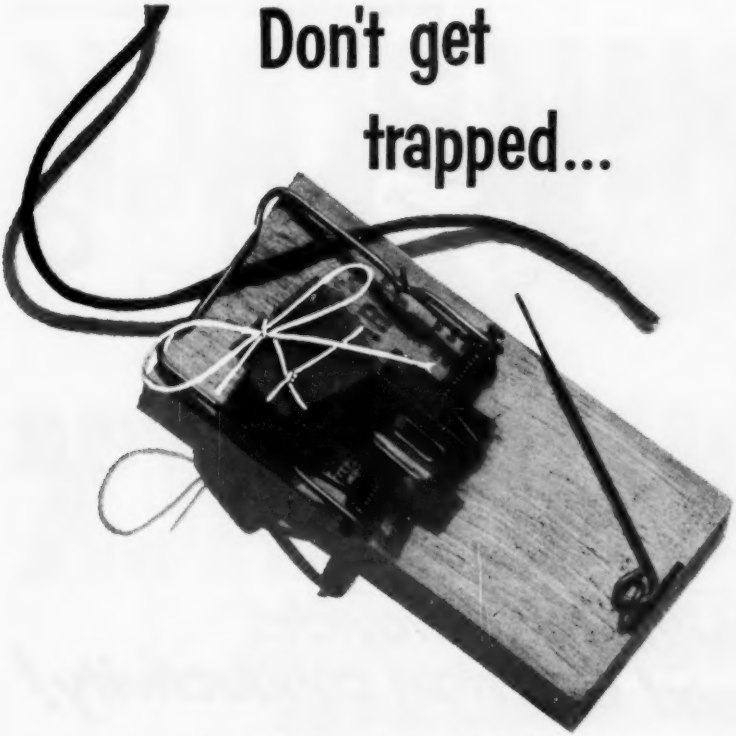

by inferior carbon blacks—
depend on Witco for top performance blacks in your natural and synthetic rubber formulations. Highest manufacturing standards guarantee uniformity and economy... and Witco technical service is unsurpassed.
You can't buy better than Witco.

Witco Chemical Company
Continental Carbon Company
122 East 42nd Street, New York 17, N. Y.

WITCO®

Chicago • Boston • Akron • Atlanta • Houston • Los Angeles • San Francisco
London and Manchester, England

Second-class postage paid at Lancaster, Pa.

PHILBLACK

PHILBLACK

*Philblack*O provides good electrical conductivity!*

Manufacturers can overcome the problem of static electricity in tires, industrial belting and other rubber products by using Philblack O.

By adjusting the recipe and mixing time; selecting the proper Philblack at the appropriate loading, you can get rubber compounds ranging from good conductors to good insulators. Your Phillips technical representative can help you select the proper Philblack.

*A trademark

LET ALL THE PHILBLACKS WORK FOR YOU!

A — **Philblack A, Fast Extrusion Furnace Black.** Excellent tubing, molding, calendering, finish! Mixes easily. Disperses heat. Non-staining.

O — **Philblack O, High Abrasion Furnace Black.** For long, durable life. Good conductivity. Excellent flex life and hot tensile. Easy processing.

I — **Philblack I, Intermediate Super Abrasion Furnace Black.** Superior abrasion. More tread miles at moderate cost.

E — **Philblack E, Super Abrasion Furnace Black.** Toughest black yet! Extreme resistance to abrasion.

Phillips 66

PHILLIPS CHEMICAL COMPANY, Rubber Chemicals Division, 318 Water Street, Akron 8, Ohio
District Offices: Chicago, Dallas, Providence and Trenton • **West Coast:** Harwick Standard Chemical Company, Los Angeles, California • **Warehouse Stocks** at Akron, Chicago, Trenton, Brighton, Mass. and Toronto, Canada • **Export Sales:** 80 Broadway, New York 5, New York • **European Office:** Phillips Chemical Company, Limmatquai 70, Zurich 1, Switzerland.

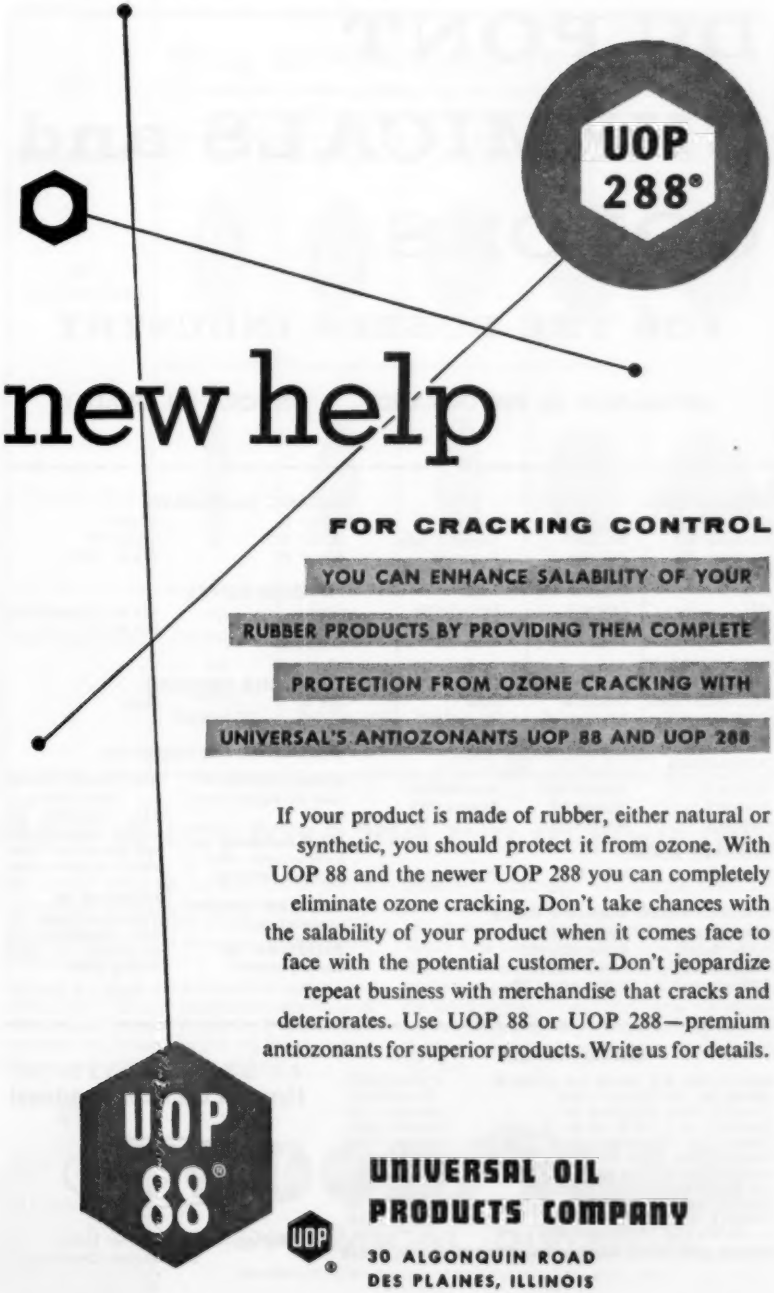
UOP
288®
new help
FOR CRACKING CONTROL
YOU CAN ENHANCE SALABILITY OF YOUR
RUBBER PRODUCTS BY PROVIDING THEM COMPLETE
PROTECTION FROM OZONE CRACKING WITH
UNIVERSAL'S ANTIOZONANTS UOP 88 AND UOP 288
If your product is made of rubber, either natural or synthetic, you should protect it from ozone. With UOP 88 and the newer UOP 288 you can completely eliminate ozone cracking. Don't take chances with the salability of your product when it comes face to face with the potential customer. Don't jeopardize repeat business with merchandise that cracks and deteriorates. Use UOP 88 or UOP 288—premium antiozonants for superior products. Write us for details.
UOP
88®
UOP
UNIVERSAL OIL
PRODUCTS COMPANY
30 ALGONQUIN ROAD
DES PLAINES, ILLINOIS

DU PONT CHEMICALS and COLORS

FOR THE RUBBER INDUSTRY

DEPENDABLE IN PERFORMANCE . . . UNIFORM IN QUALITY

ACCELERATORS

Accelerator 89	MBTS Grains	Thiuram E
Accelerator 552	NA-22	Thiuram E Grains
Accelerator 808	Permalux	Thiuram M
Accelerator 833	Polyac Pellets	Thiuram M Grains
Conac S	Tepidone	Zenite
MBT	Tetrone A	Zenite Special
MBTS	Thionex	Zenite A
	Thionex Grains	Zenite AM

ANTI-OXIDANTS

Akroflex C Pellets	Neozone A Pellets	Thermoflex A Pellets
Akroflex CD Pellets	Neozone D	Zalba
Antox	Permalux	

AQUAREXES (MOLD LUBRICANTS AND DISPERSING AGENTS)

Aquarex D	Aquarex MDL	Aquarex SMO
Aquarex G	Aquarex ME	Aquarex WAQ
Aquarex L	Aquarex NS	

BLOWING AGENTS

Unicel ND	Unicel NDX	Unicel S

COLORS—Rubber Dispersed Colors

Rubber Red PBD	Rubber Green FD
Rubber Red 2BD	Rubber Blue PCD
Rubber Yellow GD	Rubber Blue GD
Rubber Green GSD	Rubber Orange OD

ORGANIC ISOCYANATES

Hylene* M	Hylene* T
Hylene* M-50	Hylene* TM
Hylene* MP	Hylene* TM-65

PEPTIZING AGENTS

Endor	RPA No. 3 Concentrated
RPA No. 2	RPA No. 6
RPA No. 3	

RECLAIMING CHEMICALS

RPA No. 3	RR-10

SPECIAL-PURPOSE CHEMICALS

BARAK—Retarder activator for thiazole accelerators

Copper Inhibitor 65—Inhibits catalytic action of copper on elastomers

ELA, ELA-N—Elastomer lubricating agents

HELIOZONE—Sun-checking inhibitor

NBC—Inhibits weather and ozone cracking of SBR compounds. Improves heat and sunlight discoloration resistance of neoprene stocks.

RETARDER W
Retarder-activator for acidic accelerators. Also an activator for certain blowing agents.

*REG. U. S. PAT. OFF.

DISTRICT OFFICES

Akron 8, Ohio, 40 E. Buchtel Ave. at High St. . . . POrtage 2-8461
Atlanta, Ga., 1261 Spring St., N.W. . . . . TRinity 5-5391
Boston 10, Mass., 140 Federal St. . . . . HAncock 6-1711
Charlotte 1, N. C., 427 W. 4th St. . . . . FRanklin 5-5561
Chicago 3, Ill., 7 South Dearborn St. . . . . ANdover 3-7000
Detroit 35, Mich., 13000 W. 7-Mile Rd. . . . . UNiversity 4-1963
Houston 6, Texas, 2601A West Grove Lane . . . . MOhawk 7-7429
Los Angeles 58, Calif., 2930 E. 44th St. . . . . LUdlow 2-6464
Palo Alto, Calif., 701 Welch Rd. . . . . DAvenport 6-7550
Trenton 8, N. J., 1750 N. Olden Ave. . . . . EXport 3-7141
In New York call WAlker 5-3290

In Canada contact: Du Pont Company of Canada (1956) Ltd., Box 660, Montreal

E. I. du Pont de Nemours & Co. (Inc.)
Elastomer Chemicals Department

DU PONT
REG. U.S. PAT. OFF.

Better Things for Better Living . . . through Chemistry

MILL SHRINKAGE TEST

(Stock placed on cold mill, preset at .050" between rolls. After stock warmed, samples cut and permitted to cool)

HARDNESS: 80 DUROMETER					
40 DUROMETER					
STOCK COMPOSITION:	0% CHEMIGUM N-8 100% Polymer "A"	25% CHEMIGUM N-8 75% Polymer "A"	50% CHEMIGUM N-8 50% Polymer "A"	75% CHEMIGUM N-8 25% Polymer "A"	100% CHEMIGUM N-8 0% Polymer "A"

How to improve the run of your mill

The samples above tell the story. Taken from a series of test mill runs, they graphically illustrate the superior processability of new CHEMIGUM N-8 and how it can be used to improve the processing of other nitrile rubbers.

CHEMIGUM N-8 is an intermediate acrylonitrile content copolymer and exhibits corresponding oil resistance and physical properties. It also exhibits very rapid mill breakdown and will form a smooth sheet immediately, even on a cold mill.

By blending CHEMIGUM N-8 with other nitrile, styrene or natural rubbers, processing characteristics and physical properties can be obtained which previously were not possible. And, since it is stabilized with a nonstaining, non-discoloring antioxidant, it can be used in the most exacting color applications. For full details on unusual CHEMIGUM N-8, including the latest *Tech Book Bulletins*, just write to Goodyear, Chemical Division, Dept. V-9430, Akron 16, Ohio.

GOODYEAR

CHEMICAL DIVISION

Chemigum—T.M. The Goodyear Tire & Rubber Company, Akron, Ohio

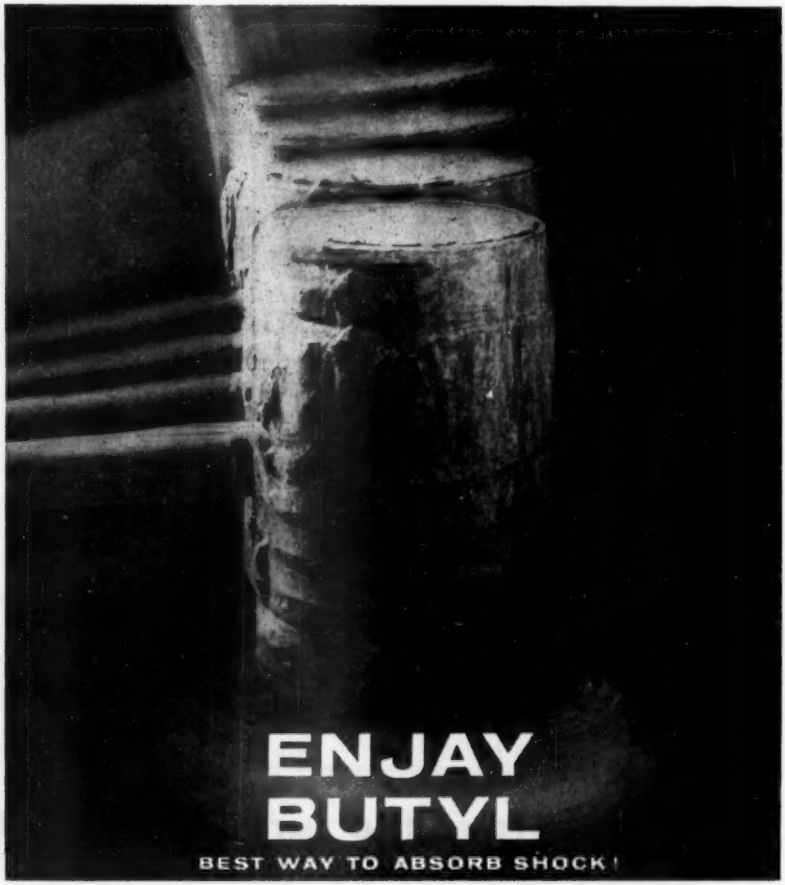

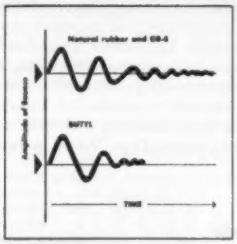

Butyl's superior shock-absorption characteristics reduce amplitude of bounce in much less time as compared with other rubbers.

Enjay Butyl, because of its higher damping factor, absorbs shock energy *more* completely than any other rubber. Through simple variations in compounding or processing, you can build the right degree of resiliency for your requirements. Butyl is the ideal rubber for motor mounts, load cushions, sound deadener insulation, axle and body bumpers—and other shock, noise and mechanical-vibration applications.

Butyl *also* offers outstanding resistance to weathering and sunlight . . . chemicals . . . heat . . . abrasion, tear and flexing . . . unmatched electrical properties and impermeability to gases and moisture.

Find out how this versatile rubber can improve your product. Call or write the Enjay Company, today!

ENJAY® BUTYL

ENJAY *Pioneer in Petrochemicals*

ENJAY COMPANY, INC., 15 West 51st Street, New York 19, N. Y.

Akron • Boston • Charlotte • Chicago • Detroit • Los Angeles • New Orleans • Tulsa

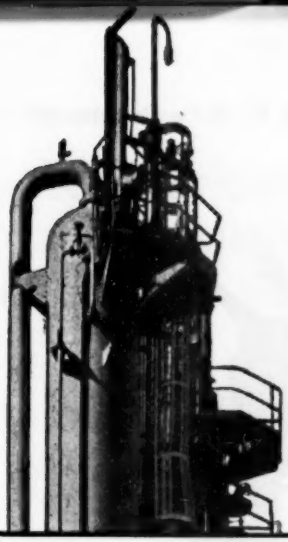

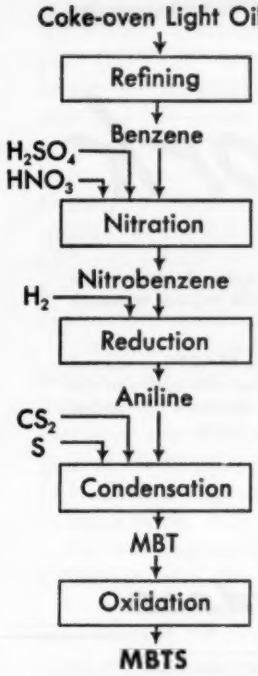

Starting from coke-oven Light Oils, Cyanamid performs and controls each step to the final product...*MBTS*.

If you want the best—*buy Cyanamid MBTS*

CYANAMID

AMERICAN CYANAMID COMPANY
RUBBER CHEMICALS DEPARTMENT
Bound Brook, New Jersey

Cyanamid is basic in the production of MBTS

...teamwork

Successful calf roping requires teamwork between man and horse. A successful business requires teamwork between supplier and customer.

The users of ***TEXAS CHANNEL BLACKS*** are assured of teamwork — not only through the quality of the blacks but also the extra quality they impart to finished product when used alone or in blends.

TEXAS
CHANNEL BLACKS
®

Sid Richardson
CARBON CO.
FORT WORTH, TEXAS

GENERAL SALES OFFICES
EVANS BUILDING
AKRON 8, OHIO

REINFORCED WITH **HI-SIL® 233,** RESILIENT ***RIPPLE® SOLE** REGISTERS RESOUNDING RECEPTION

RIPPLE* Soles, as displayed on these shoes by (left to right) Cardone & Baker, E. T. Wright, and Buster Brown, are available in red, chocolate, natural, grey, black and white. *TM—RIPPLE SOLE CORP.

Beebe Rubber Company of Nashua, New Hampshire, is the licensed producer of the unique and increasingly popular RIPPLE® Sole. Compound requirements are extreme; a combination of singularly good abrasion, tear, and flex life—with outstanding bounce and resilience.

The "Vees" molded into the RIPPLE® Sole must rebound from rough and rugged treatment, since only the limited area of their crowns constitutes the entire walking surface. It's a job of reinforcement tailor-made for our Columbia-Southern Hi-Sil 233, which in Beebe's judgment "just works out better in our compounds than any of the other reinforcers we'd tried."

Excellent physicals in brightly colored stocks are no longer a problem, with Columbia-Southern white reinforcing pigments on the scene. If spectrum-spanning color can give *your* compounds a lift, we suggest you take a look at Hi-Sil 233, Silene® EF, or Calcene® TM, NC, or CO. Each is tops in its field . . . and *should* be in your formula book.

For working samples, contact our nearest District Sales Office or write direct to Room 1929T at Pittsburgh.

Columbia-Southern Chemical Corporation, One Gateway Center, Pittsburgh 22, Pa. Offices in fourteen principal cities. In Canada: Standard Chemical Limited.

COLUMBIA-SOUTHERN CHEMICAL CORPORATION

A Subsidiary of Pittsburgh Plate Glass Company

MONSANTO RUBBER CHEMICALS ANSWER A FREQUENTLY ASKED COMPOUNDING QUESTION

QUESTION: *What new, solid antiozonant guards rubber against ozone cracking with minimum staining ???*

ANSWER: *New Santoflex GP*

Monsanto announces Santoflex GP—the newest and best antiozonant you can use to "vaccinate" rubber against ozone attack. "GP" shows minimum staining. Now you can benefit from an antiozonant in mechanical goods and other industrial products just as tire-makers do in their compounds...Santoflex GP gives prolonged crack resistance to belting, electrical insulation, motor mounts, hose and appliance parts. An easily handled solid, "GP" imparts excellent ozone resistance.

Static Ozone Test (48 Hours) Dynamic Ozone Test (36,000 Flexes—48 Hours) Migration Stain Test

No antiozonant Santoflex GP No antiozonant Santoflex GP (ASTM Test D-925-55, Method B)

See the difference 2-PPH Santoflex GP makes on SBR-1500 in a typical compound. Stocks exposed to approximately 50 parts of ozone per 100 million parts of air at 100°F. for 48 hours show how Santoflex GP substantially retards ozone cracking—yet they show only slight staining of a white auto lacquer.

SEND COUPON FOR SAMPLES...TECHNICAL HELP. Every application, plant and process has different compound requirements. That's why Monsanto recommends no "canned" formulations or "cure-alls"—we do offer samples of Santoflex GP along with technical help in testing it out for your specific application. The coupon is for your convenience.

SANTOFLEX: MONSANTO T. M., REG. U. S. PAT. OFF.

Monsanto

MONSANTO CHEMICAL COMPANY
Rubber Chemicals Department, Akron 11, Ohio

Please send me a sample of new Santoflex GP.

NAME.....

COMPANY.....

ADDRESS.....

CITY.....ZONE STATE.....

Philprene rubber for low water absorption!*

CURRENT PHILPRENE POLYMERS		
	NON-PIGMENTED	PIGMENTED WITH PHILBLACK*
HOT	PHILPRENE 1000 PHILPRENE 1001 PHILPRENE 1006 PHILPRENE 1009 PHILPRENE 1010 PHILPRENE 1018 PHILPRENE 1019	PHILPRENE 1100 ** PHILPRENE 1104 ** Pigmented with EPC Black
COLD	PHILPRENE 1500 PHILPRENE 1502 PHILPRENE 1503	PHILPRENE 1601 PHILPRENE 1605
COLD OIL	PHILPRENE 1703 PHILPRENE 1706 PHILPRENE 1708 PHILPRENE 1712	PHILPRENE 1803 PHILPRENE 1805

Let it rain! Water is no problem with Philprene 1018. Used with other polymers, Philprene 1018 provides protection against water . . . for wire and cable jackets, rubber footwear, storm coats and other rubber articles.

Phillips Chemical Company makes the largest variety of commercially available polymers on the market. You can select one that is practically made to your specifications! Consult your Phillips technical representative for complete information.

*A trademark

PHILLIPS CHEMICAL COMPANY, Rubber Chemicals Division, 318 Water Street, Akron 8, Ohio
District Offices: Chicago, Dallas, Providence and Trenton • **West Coast:** Harwick Standard Chemical Company, Los Angeles, California • **Warehouse Stocks** at Akron, Boston, Chicago and Trenton • **Export Sales:** 80 Broadway, New York 5, New York • **European Office:** Phillips Chemical Company, Limmatquai 70, Zurich 1, Switzerland.

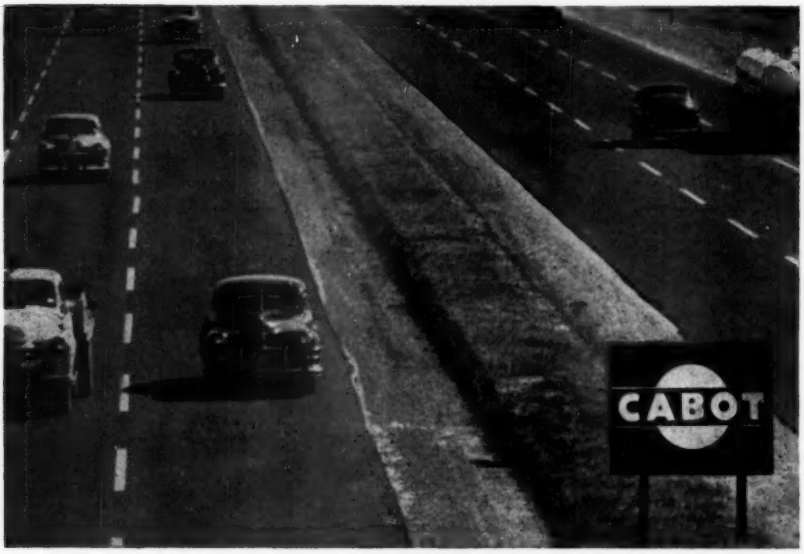

On the Road with
CABOT BLACKS

ON THE ROAD TESTS are an important part of the Cabot testing program... designed to provide the best reinforcing carbon blacks available. In addition to laboratory and factory tests, Cabot blacks are compounded in various types of rubber, and tires are subjected to miles and miles of grueling road tests. That's why Cabot blacks give consistently longer wear and trouble-free performance in all types of rubber. Complete production quality control further assures the same excellence of performance from every shipment of Cabot blacks.

CHANNEL BLACKS:	Spheron 9 EPC	Spheron 6 MPC	Spheron C CC	
FURNACE BLACKS:	Vulcan 9 SAF	Vulcan 6 ISAF	Vulcan 3 HAF	Vulcan XC-72 ECF
Vulcan SC SCF	Vulcan C CF	Sterling 99 FF	Sterling SO FEF	Sterling V GPF
Sterling L HMF	Sterling LL HMF	Sterling S SRF	Sterling NS SRF	Pelletex SRF
Pelletex NS SRF	Sterling R SRF	Gastex SRF		
THERMAL BLACKS:	Sterling FT	Sterling MT	Sterling MT-NS	

Free Samples, Technical Literature Available

CABOT® **GODFREY L. CABOT, INC.**

77 FRANKLIN STREET, BOSTON 10, MASS.

EXPANDED...
TO BETTER SERVE YOU

New, Additional Research and Customer Service Facilities

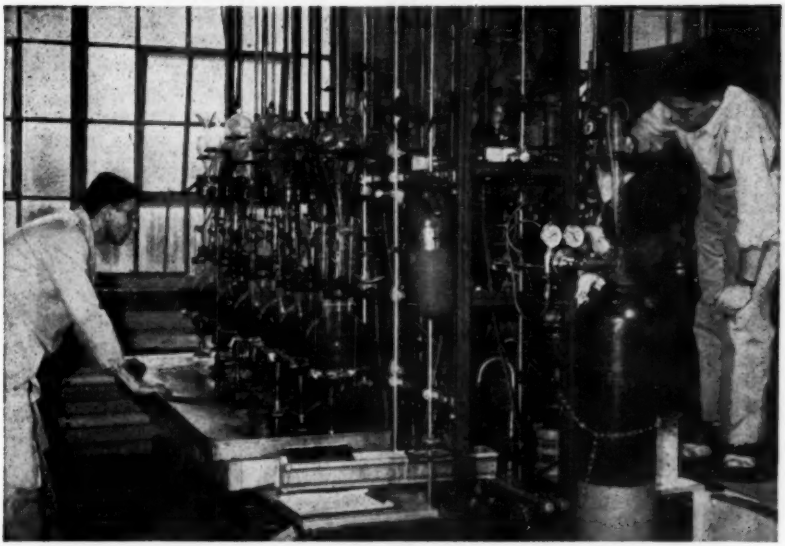

Our research and customer service facilities have been enlarged to help in our mutual search for new and improved products for the industry. These new facilities will enable us to expedite assistance in formulating and processing problems. Some of this equipment is to explore new areas of synthetic rubber and liquid polymer chemistry.

Facilities have been added to develop urethane products with practical properties. Our customer service laboratories, too, have been greatly expanded to meet the increasing number of requests for product evaluation.

Skilled Thiokol technicians have at their fingers vast funds of specialized knowledge available to you.

These facilities...this knowledge...is yours for the asking. FOR INFORMATION, write to: Thiokol Chemical Corporation, 780 N. Clinton Avenue, Trenton 7, N. J.

Thiokol®

PIONEER MANUFACTURER OF SYNTHETIC RUBBER

THIOKOL CHEMICAL CORPORATION

780 NORTH CLINTON AVE. • TRENTON 7, NEW JERSEY

®Registered Trademark of the Thiokol Chemical Corporation for its liquid polymers, rocket propellants, plasticizers and other chemical products.

For Accelerators, Activators, Anti-Oxidants and Special Rubber Chemicals

TRY NAUGATUCK

NAUGATUCK supplies a complete line of proven accelerators, activators, anti-oxidants, and special chemicals to give you thorough control of rubber product manufacture and performance.

ACCELERATORS

THIAZOLES—
M-B-T
M-B-T-S O-X-A-F

THIURAMS—
MONEX*† TUEX†
MORFEX ETHYL TUEX†
PENTEX*

DITHIOCARBAMATES—
ARAZATE* ETHAZATE*†
BUTAZATE* METHAZATE*†
ETHAZATE-50D

ALDEHYDE AMINES—
BEUTENE* HEPTEEN BASE*
TRIMENE* TRIMENE BASE*

XANTHATES—
C-P-B* Z-B-X*

ACTIVATORS

VULKLOR DIBENZO G-M-F
D-B-A G-M-F

ANTI-OXIDANTS

AMINOX* B-L-E*
ARANOX* B-X-A
V-G-B* FLEXAMINE
OCTAMINE* BETANOX* Special

SPECIAL PRODUCTS

BWH-1 SUNPROOF* Improved
CELOGEN SUNPROOF* Junior
CELOGEN-AZ SUNPROOF*—713
E-S-E-N SUNPROOF* Regular
LAUREX* SUNPROOF* Super
TONOX* KRALAC* A-EP

SPECIAL PRODUCTS FOR SYNTHETIC POLYMERS

DDM—modifier
THIOSTOP K&N—short stops
POLYGARD—stabilizer

*Reg. U. S. Pat. Off.

THE WORLD'S LEADING MANUFACTURER OF RUBBER CHEMICALS

LOOKING FOR...
Plastics
Reclaimed Rubber
Synthetic Rubber
Latices

Write, on your letterhead, for technical data or assistance with any Naugatuck product.

†these products furnished either in powder form or fast-dispersing, free-flowing NAUGETS.

Naugatuck Chemical

Division of United States Rubber Company
Naugatuck, Connecticut

IN CANADA NAUGATUCK CHEMICALS DIVISION
Dominion Rubber Company, Limited, Elmira, Ontario
RUBBER CHEMICALS • SYNTHETIC RUBBER • PLASTICS • AGRICULTURAL CHEMICALS
RECLAIMED RUBBER • LATICES • Cable Address: Rubexport, N. Y.

Naugatuck NAUGAPOLS

answer your problems in.....

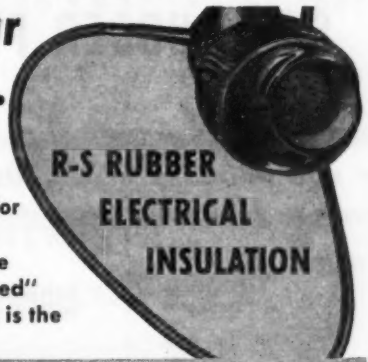

For products requiring excellent electrical properties and for those items designed for low moisture absorption, NAUGAPOL, butadiene-styrene copolymers, "Specially Processed" during the finishing operation, is the best obtainable.

Current NAUGAPOL Polymers for electrical applications

HOT TYPES

GRADE	CLASS	END USES
NAUGAPOL 1016	Staining	Standard grade for wire and cable and mechanical goods.
NAUGAPOL 1018	Non-staining	Crosslinked processing aid. Wire and cable and mechanical goods.
NAUGAPOL 1019	Non-staining	Standard grade for wire and cable and mechanical goods.
NAUGAPOL 1023	Staining	Low styrene content. Wire and cable and mechanical goods for arctic service.

COLD TYPES

GRADE	CLASS	END USES
NAUGAPOL 1503	Non-staining	Standard grade for wire and cable and mechanical goods.
NAUGAPOL 1504	Non-staining	Low styrene content. Wire and cable and mechanical goods for arctic service.

For technical data, information or assistance that will help you in processing of your rubber compounds, write to us on your company letterhead.

Naugatuck Chemical

Division of United States Rubber Company
Naugatuck, Connecticut

IN CANADA: NAUGATUCK CHEMICALS, Elmira, Ontario • Cable Address: Rubexport, N.Y.
Rubber Chemicals • Synthetic Rubber • Plastics • Agricultural Chemicals • Reclaimed Rubber • Latices

HOW YOU BENEFIT WHEN YOU USE SUN RUBBER PROCESS AIDS

IF YOU PROCESS	USE	BECAUSE
OIL EXTENDED POLYMERS GR-S TYPES 1703 1707 1708 1801	CIRCOSOL-2XH	New low cost! Low staining properties on white goods. Improves GR-S rebound. Constant uniformity assures minimum downgrading.
OIL EXTENDED POLYMERS GR-S TYPES 1705 1709 1710	SUNDEX-53	Versatile. Highly compatible with natural rubber, reclaims, GR-S types.
NEOPRENE WHV	SUNDEX-53	Cost of compounds comparable to low-cost elastomers.
REGULAR NEOPRENES and NATURAL RUBBER	CIRCO LIGHT RUBBER PROCESS-AID	True softening by physical changes in rubber structure. Large quantities absorbed without blooming.

To learn more about using Sun Rubber Process Aids to get better physicals, lower costs, and easier processing, see your Sun representative. Or write for your copy of Sun's latest Technical Bulletin describing any of the above products. Address SUN OIL COMPANY, Philadelphia 3, Pa., Dept. RC-4.

INDUSTRIAL PRODUCTS DEPARTMENT

SUN OIL COMPANY SUNOCO

PHILADELPHIA 3, PA.

IN CANADA: SUN OIL COMPANY, LTD., TORONTO AND MONTREAL

DECEMBER • 1958
Volume XXXI • Number Five

RUBBER CHEMISTRY
AND TECHNOLOGY

RUBBER REVIEWS
for 1958

PUBLISHED BY THE DIVISION
OF RUBBER CHEMISTRY OF THE
AMERICAN CHEMICAL SOCIETY

COLUMBIAN offers an outstanding carbon black for every rubber need...

STATEX® 160 SAF Super Abrasion Furnace

STATEX 125 ISAF Intermediate Super Abrasion Furnace

STATEX R HAF High Abrasion Furnace

STANDARD MICRONEX® MPC Medium Processing Channel

MICRONEX W 6 EPC Easy Processing Channel

STATEX B FF Fine Furnace

STATEX M FEF Fast Extruding Furnace

STATEX 93 HMF High Modulus Furnace

STATEX G GPF General Purpose Furnace

FURNEX® SRF Semi-Reinforcing Furnace

plus outstanding pure iron oxide pigments from our MAPICO IRON OXIDES UNIT

REDS . . . 617, 297, 347, 387, 477 and 567

TANS . . . 10, 15 and 20

BROWNS . . . 418, 419, 420, 421 and 422

PLUS YELLOWS . . .

COLUMBIAN CARBON COMPANY

380 Madison Avenue, New York 17, N. Y.

RUBBER CHEMISTRY AND TECHNOLOGY

Published in Five Issues (January–March, April–June, July–September, October–November & December) under the Auspices of the Division of Rubber Chemistry of the American Chemical Society, Prince and Lemon Streets, Lancaster, Pa.

Editor.....DAVID CRAIG
Associate Editor.....S. D. GEHMAN
Associate Editor.....B. L. JOHNSON
Rubber Division Librarian.....MRS. LILLIAN COOK
Business Manager.....D. F. BEHNEY
Advertising Manager.....GEORGE HACKIM
Treasurer.....G. E. POPP

Vol. XXXI **December 1958** **No. 5**

CONTENTS

General Section PAGE

Officers..... iii
Division of Rubber Chemistry of the American Chemical Society..... vi
Future Meetings..... vii
Sponsored Rubber Groups. Officers and Meeting Dates..... viii
New Books and Other Publications..... x

Papers

The Elasticity of Rubber. LAWRENCE WOOD..... 959
Friction and Abrasion of Rubber. A. SCHALLAMACH..... 982
Protection of Rubber Against Atmospheric Ozone-Cracking. B. S. BIGGS..... 1015
The Use of Radioactive Sulfur in Vulcanization. G. A. BLOKH..... 1035
The Reaction of Sulfur and Sulfur Compounds with Olefinic Substances:
VIII. The Reaction of Sulfur with Mono-olefins. L. BATEMAN, R. W. GLAZEBROOK, C. G. MOORE, M. PORTER, G. W. ROSS AND R. W. SAVILLE..... 1055
IX. The Reaction of Sulfur with 2,6-Dimethylocta-2,6-diene. L. BATEMAN, R. W. GLAZEBROOK AND C. G. MOORE..... 1065
X. The Kinetics of the Reaction of Sulfur with Cyclohexene and Other Olefins. G. W. ROSS..... 1077
XI. The Mechanism of Interaction of Sulfur with Mono-olefins and 1,5-Dienes. L. BATEMAN, C. G. MOORE AND M. PORTER..... 1090
Stability of High Polymer Latexes and Their Electrokinetic Potentials. S. S. VOYUTSKII AND R. M. PANICH..... 1105
Foam Stability. A. J. DE VRIES..... 1142

RUBBER CHEMISTRY AND TECHNOLOGY

RUBBER CHEMISTRY AND TECHNOLOGY is published under the supervision of the Editor, representing the Division of Rubber Chemistry of the American Chemical Society. One object of the publication is to render available in convenient form under one cover important and permanently valuable papers on fundamental research, technical developments, and chemical engineering problems relating to rubber or its allied substances. Another object is to publish timely reviews.

RUBBER CHEMISTRY AND TECHNOLOGY may be obtained in one of three ways:

(1) Any member of the American Chemical Society may become a member of the Division of Rubber Chemistry by payment of the dues ($4.00 per year) to the Division and thus receive RUBBER CHEMISTRY AND TECHNOLOGY.

(2) Anyone who is not a member of the American Chemical Society may become an Associate of the Division of Rubber Chemistry upon payment of $6.50 per year to the Treasurer of the Division of Rubber Chemistry, and thus receive RUBBER CHEMISTRY AND TECHNOLOGY.

(3) Companies and libraries may subscribe to RUBBER CHEMISTRY AND TECHNOLOGY at the subscription price of $7.50 per year.

To these charges of $4.00 and $7.50, respectively, per year, postage of $.20 per year must be added for subscribers in Canada, and $.50 per year for those in all other countries not United States possessions.

All applications to become Members or Associates of the Division of Rubber Chemistry, with the privilege of receiving this publication, all correspondence about subscriptions, back numbers, changes of address, missing numbers, and all other information or questions should be directed to the Treasurer of the Division of Rubber Chemistry, George E. Popp, Phillips Chemical Co., 318 Water St., Akron 8, Ohio.

Articles, including translations and their illustrations, may be reprinted if due credit is given RUBBER CHEMISTRY AND TECHNOLOGY.

Second-class postage paid at Lancaster, Pa.

THE DIVISION OF RUBBER CHEMISTRY OF THE AMERICAN CHEMICAL SOCIETY

OFFICERS AND EXECUTIVE COMMITTEE

Chairman.....E. H. KRISMANN, E. I. du Pont de Nemours & Co., Akron, O.

Vice-Chairman. W. J. SPARKS, Esso Research and Engineering Co., Linden, N. J.

Secretary.....R. H. GERKE, U. S. Rubber Co., Wayne, N. J.

Assistant Secretary.....L. H. HOWLAND, Naugatuck Chemical Division, Naugatuck, Conn.

Treasurer.....G. E. POPP, Phillips Chemical Company, Akron, O.

Assistant Treasurer.....D. F. BEHNEY, Harwick Standard Chemical Co., Akron, O.

Editor of *Rubber Chemistry and Technology*.....DAVID CRAIG, B. F. Goodrich Research Center, Brecksville, O.

Advertising Manager of *Rubber Chemistry and Technology*...GEORGE HACKIM, General Tire & Rubber Co., Akron, O.

Directors...R. F. DUNBROOK (Past Chairman), S. C. NICOL (Director-at-Large), K. R. GARVICK (Akron), T. C. EDWARDS (Boston), PAUL SICK (Buffalo), VINCENT LABRECQUE (Chicago), W. C. CARTER (Connecticut), R. W. MALCOLMSON (Detroit), DAVID SHERMAN (Fort Wayne), R. E. BITTER (Los Angeles), S. M. MARTIN, JR. (New York), R. J. REYNOLDS (Northern California), M. A. YOUKER (Philadelphia), R. B. ROBITAILLE (Rhode Island), F. W. GAGE (Southern Ohio), A. W. SLOAN (Washington, D. C.), N. S. GRACE (Canada),

Councilors...H. I. CRAMER, 1956–1959; R. H. Gerke, 1958–1960.
(Alternates, C. S. YORAN, 1958–1960; J. M. BALL, 1956–1959.)

COMMITTEES

Advisory Committee on Local Arrangements....C. A. SMITH, *Chairman* (New Jersey Zinc Co., Cleveland, Ohio), S. L. BRAMS (Dayton Chemical Products, West Alexandria, Ohio), A. J. NORTHAM (E. I. du Pont Company, Wilmington, Delaware).

Auditing Committee....R. B. APPLEBY, *Chairman* (E. I. du Pont Company, Akron, Ohio), C. W. CHRISTENSEN (Monsanto Chemical Company, Akron, Ohio), D. L. SIMOND (Godfrey L. Cabot Company, Akron, Ohio).

Best Papers Committee....W. R. SMITH, *Chairman* (Godfrey L. Cabot Co., Boston, Mass.), E. B. NEWTON (B. F. Goodrich Research Center, Brecksville, Ohio), E. H. KRISMANN (E. I. du Pont Company, Akron, Ohio).

Bibliography Committee....J. MCGAVACK, *Chairman* (U. S. Rubber Co., Passaic, N. J.), O. E. BECKVOLD (U. S. Rubber Research Center, Wayne, N. J.), E. M. BEVILACQUA (U. S. Rubber Research Center, Wayne, N. J), VICTOR BURGER (U. S. Rubber Research Center, Wayne, N. J.), LOIS BROCK (General Tire & Rubber Co., Akron, Ohio), D. E. CABLE (U. S. Rubber Research Center, Wayne, N. J.), LILLIAN COOK (Rubber Div. Library, University of Akron, Akron, Ohio), DOROTHY HAMLEN (Rubber Div. Library, Univ. of Akron, Akron, Ohio), H. E. HAXO (U. S. Rubber Research Center, Wayne, N. J.), JEANNE JOHNSON (U. S. Rubber Research Center, Wayne, N. J.), R. K. KUHNS (U. S. Rubber Research Center, Wayne, N. J.), M. E. LERNER (*Rubber Age*, New York, N. Y.), G. E. POPP, (Phillips Chemical Co., Akron, Ohio), G. S. MILLS (U. S. Rubber Research Center, Wayne, N. J.).

By-Laws Revision Committee....W. L. SEMON, *Chairman* (B. F. Goodrich Research Center, Brecksville, Ohio), R. H. GERKE (U. S. Rubber Company, Wayne, N. J.), G. ALLIGER (Firestone Tire & Rubber Co., Akron, Ohio), W. WARNER (General Tire & Rubber Co., Akron, Ohio).

Charles Goodyear Medalist Committee....B. S. GARVEY, JR., *Chairman*, Pennsalt Chemical Co. (Wayne, Pa.), JOHN BALL, Midwest Rubber Reclaiming Co. (Wilton, Conn.), SEWARD BYAM, E. I. du Pont Co. (Wilmington, Del.), A. E. JUVE, B. F. Goodrich Research Center (Brecksville, O.), W. L. SEMON (B. F. Goodrich Research Center, Brecksville, O.).

Committee on Committees....T. W. ELKIN, *Chairman* (R. T. Vanderbilt Co., New York City), A. E. JUVE (B. F. Goodrich Research Center, Brecksville, Ohio), J. D. D'IANNI (Goodyear Tire & Rubber Co., Akron, Ohio), V. J. LABRECQUE (Victor Gasket & Mfg. Co., Chicago, Ill.), D. C. MADDY (Harwick Standard Chemical Co., Akron, Ohio).

Editorial Board of Rubber Reviews....N. BEKKEDAHL (National Bureau of Standards, Washington, D. C.), G. S. WHITBY (University of Akron, Akron, Ohio), W. R. SMITH (Godfrey L. Cabot Co., Cambridge, Mass.), S. D. GEHMAN (Goodyear Tire & Rubber Co., Akron, Ohio), D. CRAIG (B. F. Goodrich Research Center, Brecksville, Ohio), G. E. P. SMITH, JR. (Firestone Tire & Rubber Co., Akron, Ohio).

Education Committee....C. V. LUNDBERG, *Chairman* (Bell Telephone Laboratories, Murray Hill, N. J.), R. G. SEAMAN (*Rubber World*, New York City), R. D. STIEHLER (National Bureau of Stds., Washington, D. C.), W. F. BUSSE (E. I. du Pont Co., Wilmington, Delaware), M. L. STUDEBAKER (Phillips Chemical Co., Akron, Ohio).

Files and Records Committee....J. D. D'IANNI, *Chairman* (Goodyear Tire & Rubber Co., Akron, Ohio), D. HAMLEN (University of Akron. Akron, Ohio), E. A. WILLSON (B. F. Goodrich Research Center, Brecksville, Ohio).

Finance and Budget Committee....L. V. COOPER, *Chairman* (Firestone Tire & Rubber Co., Akron, Ohio), S. B. KUYKENDALL (Firestone Tire & Rubber Co., Akron, Ohio), E. H. KRISMANN (E. I. du Pont de Nemours & Co., Akron, Ohio), G. E. POPP, *Ex-officio* (Phillips Chemical Co., Akron, Ohio).

Future Meetings....A. E. LAURENCE, *Chairman* (Phillips Chemical Co., Elmhurst, Ill.), G. N. VACCA (Bell Telephone Laboratories, Murray Hill, N. J.), E. B. BUSENBERG (B. F. Goodrich Co., Akron, Ohio).

Library Policy Committee....RALPH F. WOLF, *Chairman* (Columbia-Southern Chemical Co., Barberton, Ohio), O. D. COLE (Firestone Tire & Rubber Co., Akron, Ohio), N. V. SEEGER (Diamond Alkali, Painesville, Ohio), GUIDO STEMPEL (General Tire & Rubber Co., Akron, Ohio), A. M. CLIFFORD (Goodyear Tire & Rubber Co., Akron, Ohio).

Membership Committee....K. GARVICK, *Chairman* (Mansfield Tire & Rubber Co., Mansfield, Ohio), All the Directors from each Local Rubber Group.

New Publications Committee....N. BEKKEDAHL, *Chairman* (National Bureau of Standards, Wash., D. C.), R. G. SEAMAN (*Rubber World*, New York City), D. CRAIG (B. F. Goodrich Research Center, Brecksville, Ohio), M. MORTON (University of Akron, Akron, Ohio).

Nomenclature Committee.....R. G. SEAMAN, *Chairman* (*Rubber World*, New York City), I. D. PATTERSON (Goodyear Tire & Rubber Co., Akron, Ohio), F. W. GAGE (Dayton Chemical Products Laboratories, W. Alexandria, Ohio), E. E. GRUBER (General Tire & Rubber Co., Akron, Ohio), ROY M. VANCE (Columbian Carbon Co., Brooklyn, N. Y.), A. L. BACK (West Chester, Pa.).

Nominating Committee....J. M. BALL, *Chairman* (Midwest Rubber Reclaiming Co., Wilton, Conn.), S. M. MARTIN, JR. (Thiokol Chemical Corp., Trenton, N. J.), L. H. HOWLAND (Naugatuck Chemical Co., Naugatuck, Conn.), J. D. D'IANNI (Goodyear & Tire Rubber Co., Akron, Ohio), PAUL SICK (Hewitt-Robins, Inc., Buffalo, N. Y.).

Officers Manual....A. E. JUVE, *Chairman* (B. F. Goodrich Research Center, Brecksville, Ohio), J. FIELDING (Armstrong Rubber Co., West Haven, Conn.).

Papers Review Committee....E. H. KRISMANN (E. I. du Pont Company, Akron, Ohio), B. S. GARVEY, JR. (Pennsalt Chemical Co., Wayne, Penna.), D. CRAIG (B. F. Goodrich Research Center, Brecksville, Ohio), R. H. GERKE (U. S. Rubber Co., Wayne, N. J.).

Selection Committee for the Rubber Science Hall of Fame, University of Akron, representatives of the Division of Rubber Chemistry....A. E. JUVE (B. F. Goodrich Research Center, Brecksville, O.), RALPH F. WOLF (Columbia-Southern Chemical Co. Barberton, O.).

Tellers....T. W. ELKIN, *Chairman* (R. T. Vanderbilt Co., New York City), W. STUBBLEBINE (Stowe-Woodward Newton Upper Falls, Mass.), B. W. BENDER (U. S. Rubber Co., Wayne, N. J.), H. E. HAXO (U. S. Rubber Co., Bloomfield, N. J.

Program Committee....B. S. GARVEY, JR., *Chairman*. S. C. NICOL (Goodyear Tire and Rubber Co., Akron, Ohio). C. F. GIBBS (B. F. Goodrich Research Center, Brecksville, Ohio), C. A. BARTLE (E. I. du Pont Co., Wilmington, Delaware), W. S. TULEY (U. S. Rubber Co., Wayne, N. J.), A. G. TREADGOLD (United Carbon Co., Charleston, W. Va.).

DIVISION OF RUBBER CHEMISTRY OF THE AMERICAN CHEMICAL SOCIETY

Annual Report—1958

The following report briefly summarizes the activities of the Division of Rubber Chemistry during the year 1958.

Section I

	1957	1958
Membership	2638	2544
Associates	531	580
Subscribers	857	820
Complimentaries	24	26
Total	4050	3970

The membership has decreased in 1958. No research has been made on the cause. It is to be noted that 1958 was a depression year.

The effect of the increase in dues for 1959 is yet to be determined.

A new rubber group, The Southern Rubber Group, was approved by the Executive Committee at the September Meeting. The complete list of sponsored rubber groups is as follows:

Akron	Connecticut	New York	Southern Ohio
Boston	Detroit	Northern California	Southern Rubber Group
Buffalo	Fort Wayne	Philadelphia	Washington, D. C.
Chicago	Los Angeles	Rhode Island	Canada

During the year the following members have passed on:

Henri Chauvin	Elmo E. Hanson
M. S. Kharasch	H. A. Morton
M. H. Laatsch, Jr.	Theo. G. Daub
J. Q. McGiffin	G. G. Balazs
R. L. Sibley	A. J. Kearfott
J. M. Jackson	Ed. Ray Lasser

Section II

The Spring Meeting was held in Cincinnati, Ohio, at which there were four half day sessions. Two half day sessions were devoted to symposia on High Temperature Resistant Elastomers: (1) invited papers, (2) contributed papers. The Fall Meeting was held in Chicago, Illinois, with the Parent Organization. Four half-day sessions of general papers were held.

The Charles Goodyear Medal was presented to J. C. Patrick, retired, Thiokol Corporation, Trenton, N. J. The title of his paper was, "Comments on Polysulfide Elastomers".

Certain by-law changes were made, the most important of which was the increase in dues.

The newly created offices, Assistant Treasurer and Business Manager of RUBBER CHEMISTRY AND TECHNOLOGY, Assistant Business Manager of RUBBER CHEMISTRY AND TECHNOLOGY and the Assistant Secretary, have been filled, respectively, by D. F. Behney, G. Hackim and L. H. Howland.

Section III

The Division publishes four regular issues of RUBBER CHEMISTRY AND TECHNOLOGY each year.

"Rubber Reviews", which will be published annually as a fiifth issue, will constitute the Division of Rubber Chemistry's contribution to the summarization of knowledge on rubber chemistry and technology by experts in the field.

Section IV

In 1959 the Division of Rubber Chemistry will meet in Los Angeles in the Spring at which there will be two symposia: ozone, and polyurethanes, respectively.

In the Fall of 1959 in November there will be an International Rubber Conference sponsored jointly by the Division of Rubber Chemistry, ACSr Committee D-11 on Rubber and Rubber Like Materials, ASTM, and Rubber and Plastics Division, ASME. The meeting is being planned by the International, Rubber Conference Committee. It is planned that the papers shall be preprinted and then published in book form. Sufficient titles of papers have been received by the Program Committee to insure a successful program.

The International Rubber Conference Committee Chairman is A. E. Juve, the Program Chairman is B. S. Garvey, Jr. and the Local Arrangements Chairman is A. W. Sloan.

R. H. GERKE, *Secretary*
Division of Rubber Chemistry
American Chemical Society

FUTURE MEETINGS

Meeting		City	Hotel	Date
1959	Spring	Los Angeles	Biltmore	May 12–15
1959	Fall	Washington*	Shoreham	November 9–13
1960	Spring	Buffalo	Statler	May 3–6
1960	Fall	New York	Commodore	September 13–16
1961	Spring	Louisville	Brown	May 18–21
1961	Fall	Chicago	Sherman	September 5–8
1962	Spring	Boston	Statler	May 15–18
1962	Fall	Atlantic City, N. J.	Chalfonte	September 11–14

* An international meeting jointly sponsored by the Division of Rubber Chemistry ACS, Committee D-11 of ASTM, and the Rubber and Plastics Division of ASME.

SPONSORED RUBBER GROUPS

OFFICERS AND MEETING DATES

1958

Akron Rubber Group

Chairman: George Hackim (General Tire & Rubber Co., Akron). *Vice Chairman:* Milton Leonard (Columbian Carbon Co., Akron). *Secretary:* Irvin J. Sjothun (Firestone Tire & Rubber Co., Akron). *Treasurer:* John Gifford (Witco Chemical Co., Akron). Meetings in 1958: January 24, April 11, June 20, October 24. Meetings in 1959: January 23, April 3, June 19 and October 23.

Boston Rubber Group

Chairman: Roger L. Steller (B. F. Goodrich Chemical Co., Boston). *Vice-Chairman:* William H. King (Acushnet Process Co.). *Secretary-Treasurer:* James J. Breen (Barrett & Breen Co.). *Permanent Historian:* Harry A. Atwater (Malrex Chemical Company). *Executive Committee:* Arthur I. Ross, Thomas C. Edwards, George E. Herbert, John M. Hussey, Charles S. Frary. Meetings in 1958: March 21, June 20, October 17, December 12.

Buffalo Rubber Group

Chairman: John Helwic (Dunlop Tire & Rubber Co., Buffalo). *Vice-Chairman:* Richard Herdlein (Hewitt-Robins, Inc., Buffalo). *Secretary-Treasurer:* Larry Halpin (Dunlop Tire & Rubber Co., Buffalo). *Asst. Sec'y-Treasurer:* Edward Haas (Dunlop Tire & Rubber Co., Buffalo). *Ex-Officio Chairman:* Charles Miserentino. *Directors:* Jack Wilson (Dow Corning), Jack Haller (Linde Air), Eugene Martin (Dunlop Tire & Rubber Co.), Ed Sverdrup (U. S. Rubber Reclaiming), Robert Donner (National Aniline), Robert Pryor (Hewitt-Robins, Inc.). Meeting dates in 1958: May 9—International Rubber Group Meeting, General Brock Hotel, Niagara Falls, Canada, June 10, October 14, December 2.

Chicago Rubber Group

President: V. Labrecque (Victor Mfg. & Gasket Co., Chicago). *Vice-President:* M. J. O'Connor (O'Connor & Co., Inc., Chicago). *Secretary:* J. Groot (Dryden Rubber Div., Sheller Mfg., Chicago). *Treasurer:* S. F. Choate (Tumpeer Chemical Co., Chicago). Term ends July, 1958. *Directors:* James B. Moore, J. B. Porter, H. D. Shetler, E. F. Wagner, R. R. Kann, R. A. Kurtz, Ralph Shell, J. F. Swart. *Legal Counsel & Executive Secretary:* E. H. Leahy, Room 1411, 111 W. Washington Street, Chicago. Meetings in 1958: January 31, March 14, April 25, July 25, October 3, November 14, December 19.

The Connecticut Rubber Group

Chairman: R. T. Zimmerman (R. T. Vanderbilt Co., Inc., East Norwalk, Connecticut). *Vice-Chairman:* W. H. Couch (Whitney Blake Co., Hamden, Conn.). *Secretary:* V. P. Chadwick (Armstrong Rubber Co., West Haven, Conn.). *Treasurer:* J. W. Perkins (Armstrong Rubber Co., West Haven,

Conn.). Terms to end December 31, 1958. *Directors:* One-Year term ending December 31, 1958: H. GORDON (Ideal Rubber Co., Brooklyn, New York), G. R. SPRAGUE (B. F. Goodrich Sponge Products, Shelton, Conn.), D. F. CUMMINGS (General Electric Co., Bridgeport, Conn.). Two-Year terms ending December 31, 1958: R. W. WARD (E. I. du Pont de Nemours & Co., Boston, Mass.), F. W. BURGER (Phillips Chemical Co., Providence, R. I.). Director to National Division—W. C. CARTER (Pequanoc Rubber Co., Butler, New Jersey). Meetings in 1958: February 21, May 23, September 6, November 14.

DETROIT RUBBER GROUP

Chairman: E. J. KVET, JR. (Detroit Arsenal, Detroit). *Vice-Chairman:* W. F. MILLER (Yale Rubber & Mfg. Co., Sandusky, Michigan). *Secretary:* W. D WILSON (R T. Vanderbilt Co., Detroit). *Treasurer:* W. A. WIARD (Dow Corning, Midland). *Directors:* J. F. STIFF, J. M. CLARK, JACK MASDEN, A. F. THOMPSON, FRANK G. FALVEY, R. W. MALCOLMSON, C. H. ALBERS, R. HUIZINGA, E. P. FRANCIS, P. V. MILLARD, J. J. FLEMING, R. C. CHILTON, S. M. SIDWELL, R. H. SNYDER, R. C. WATERS, E. W. TILLITSON, T. W. HALLORAN. *Councilors:* H. F. JACOBER, H. W. HOERAUF, J. T. O'REILLY. Meetings in 1958: February 7, April 18, June 27, October 3, December 5.

FORT WAYNE RUBBER GROUP

Chairman: GEORGE E. KELSHEIMER (U. S. Rubber Co., Ft. Wayne, Ind.). *Vice-Chairman:* PHILIP MAGNER, JR. (General Tire & Rubber Co., Wabash, Ind.). *Secretary-Treasurer:* WALTON D. WILSON (R. T. Vanderbilt Co., 5272 Doherty Dr., Orchard Lake, Michigan). *Directors:* M. J. O'CONNOR, NORMAN KLEMP, E. THEALL, H. CANTWELL, H. GLASSFORD, J. LAWLESS, R. HARTMAN, S. CHOATE, E. BOSWORTH. Meetings in 1958: February 13, April 10, June 6 (outing), September 25, December 4.

LOS ANGELES RUBBER GROUP

Chairman: ALBERT H. FEDERICO (C. P. Hall Co. of Calif.). *Assoc. Chairman:* CHARLES H. KUHN (Master Processing Corp., Lynwood). *Vice-Chairman:* B. R. SNYDER (R. T. Vanderbilt Co., Los Angeles). *Secretary:* L. W. CHAFFEE (Ohio Rubber Co., Long Beach, Calif.). *Asst. Secretary:* EDMUND J. LYNCH (H. M. Royal, Inc. Downey, Calif.). *Treasurer:* W. M. ANDERSON (Gross Mfg. Co., Monrovia, Calif.). *Asst. Treasurer:* R. O. WHITE (Caram Mfg. Co., Monrovia, Calif.). *Directors:* ROY N. PHELAN (Atlas Sponge Rubber Co., Monrovia), WILLIAM J. HANEY (Kirkhill Rubber Co., Brea), CHARLES M. CHURCHILL (Naugatuck Chemical, East Los Angeles), HOWARD R. FISHER (W. J. Voit Rubber Co., Los Angeles), JOHN L. RYAN, (Shell Chemical Corp, Torrance), CARL E. HUXLEY (Enjay Co., Los Angeles), WALTER E. BOSWELL (Thiokol Chemical Corp.). Meetings in 1958: February 4, March 4, April 1, May 5, October 7, November 4.

NEW YORK RUBBER GROUP

Chairman: C. V. LUNDBERG (Bell Telephone Laboratories, Murray Hill, N. J.). *Vice-Chairman:* R. B. CARROLL (R. E. Carroll, Inc., Trenton, N. J.). *Secretary-Treasurer:* M. E. Lerner (Rubber Age, New York). Terms end December 31, 1958. Meetings in 1958: March 28, June 5, August 5, October 17, December 12.

Northern California Rubber Group

President: William "Bill" Deis (Merck & Co., Inc. South San Francisco). *Vice-President:* Drace "Kut" Kutnewsky (Burke Rubber Co., San Jose). *Treasurer:* D. A. "Dell" Driesbough (Plastic & Rubber Products Co., Oakland). *Secretary:* C. P. "Pete" Engelsman (E. S. Browning Co., San Francisco). *Directors:* Claude "Corky" Corkadel, Keith Large, Roy Woodling. Meetings in 1958: February 13, March 13, April 10, September 11, October 9, November 13.

Philadelphia Rubber Group

Chairman: R. A. Garrett (Armstrong Cork Research Center, Lancaster, Pa.). *Vice-Chairman:* R. S. Graff (E. I. du Pont de Nemours & Co., Wilmington). *Secretary-Treasur:* H. C. Remsberg (Carlisle Tire & Rubber, Carlisle, Pa.). *Executive Committee:* T. E. Farrell, R. N. Hendriksen, James Jones, George N. McNamara, J. R. Mills, H. M. Sellers, Merrill Smith. *National Dir.:* Dr. M. A. Youker (E. I. du Pont de Nemours & Co., Wilmington). Meetings in 1958: April 25, August 22, 1958, October 24, November 14, 1958 and January 23, 1959.

Rhode Island Rubber Group

Chairman: W. K. Priestly (Kaiser Aluminum & Chemical Co., Bristol, R. I.). *Vice-Chairman:* H. W. Day (E. I. du Pont de Nemours & Co., Boston). *Secretary-Treasurer:* Harry L. Ebert (Firestone, Fall River, Mass.). *Historian:* R. G. Bolkman (U. S. Rubber Co., Providence). *Executive Committee:* W. J. Blecharczyk, E. S. Uhlig, R. B. Robitaille, J. M. Vitale, C. A. Damicone, G. E. Enser. Meetings in 1958: April 10, June 5, November 6.

NEW BOOKS AND OTHER PUBLICATIONS

Vanderbilt Rubber Handbook (Tenth Edition—1958). Edited by George G. Winspear. The R. T. Vanderbilt Company, 230 Park Avenue, New York 17, New York, $5\frac{1}{2} \times 8\frac{1}{2}$ inches, 620 pages, $15.00. The tenth edition of the most useful compilation of data and information for technical men in the rubber industry is now available in an improved and still more useful form. While the present volume is about 100 pages shorter than the previous edition, this is largely because latex information was omitted from this edition and published (in 1954) in a separate handbook of some 320 pages.

The contents are organized as follows: Sect. 1, Commercial Rubbers, 139 pages; Sect. 2, Compounding Materials and Uses, 46 pages; Sect. 3, Compound Properties and Test Methods, 36 pages; Sect. 4, Compound Design, 54 pages; Sect. 5, Laboratory Examination of Compounding Materials and Rubber Products, 71 pages; Sect. 6, Articles of Theoretical Interest, 19 pages; Sect. 7, Processing Methods and Equipment, 22 pages; Sect. 8, Commercial Rubber Products and Processes, 108 pages; Sect. 9, General Information, 73 pages.

The binding is rugged, the paper of good quality, the printing excellent, the illustrations excellent and an adequate index is included. In an effort of this magnitude there are certain to be typographical errors, erroneous or unclear statements, etc., however in this case these are remarkably few. Some of those which this reviewer noticed are given below.

In reference (3) p. 39 the Davis and Blake monograph is correctly referred to as "Chemistry and Technology of Rubber." In reference (4) it is incorrectly referred to as Rubber Chemistry and Technology.

On p. 40 it is stated that ". . . Subcommittee D-1418 has made . . .". This should be ". . . Subcommittee VIII of Committee D-11 has established a Tentative Recommended Practice for Nomenclature for Synthetic Elastomers and Latices, ASTM Designation: D1418-58T".

Also on p. 40 is the sentence "The letter preceding the diolefin designation signifies a comonomer or *conomer* used in its preparation." The italicized word should have been *comonomers*.

On p. 48 it is stated that the unsaturation of butadiene-styrene rubbers is less than that of natural rubber and on p. 158 it is stated that the butadiene-styrene and butadiene-acrylonitrile copolymers require less sulfur for a full hard rubber than natural rubber. While it is true that the unsaturation of standard butadiene-styrene rubber (77 butadiene-23 styrene) is slightly less than natural rubber, the difference is so small as to be negligible. On p. 466, the calculation is shown for the amount of sulfur required to react with all the double bonds in polybutadiene which turns out to be 59.3 against 47 for natural rubber. Thus the theoretical requirement for standard SBR would be $59.3 \times .77 = 45.7$.

On p. 95 the real usefulness of Hycar 2202 (brominated butyl) is not mentioned. These are the ability to covulcanize in blends with natural rubber and SBR and as adhesives. Also in this section on butyl rubber no mention is made of resin cures.

In the section dealing with Silicone elastomers, neither the vinyl-containing polymers nor the nitrile oil resisting polymers are mentioned.

In numerous places, e.g., p. 147, 158, 389 and 456, the phrase "copolymer synthetics" is used which is apparently intended to mean copolymers of butadiene and either styrene or acrylonitrile. This is not a good designation since there are other copolymer synthetic rubbers, e.g., Kel-F Elastomer which are radically different from the SBR and NBR types.

On p. 204 in the discussion of Mooney cure data, the time required for the viscosity to increase an arbitrary number of units beyond the scorch time is said to be "the rate of cure". It would be better to say that this figure gives a measure of the rate of cure or that its reciprocal or the number of Mooney units rise per minute during this interval is the rate of cure obtained by this method.

On p. 232 it is stated that "Elastomers, such as natural rubber, which crystallize on extension are subject to dilute ozone attack over a narrow range of elongations between 5 and 20 per cent. The so-called random polymers, which do not crystallize on stretching, become more susceptible to attack as stresses above the tolerable minimum are increased." There is no fundamental difference in the behavior of natural rubber (which crystallizes readily) and SBR (which crystallizes only slightly) with respect to the effect of strain on cracking. In both cases the frequency of cracking increases and the crack depth decreases as strain is increased, at least up to 100%.

On p. 218 it is stated that the Ross flexing machine was designed by the Heel and Sole Committee of the American Rubber Association. The latter organization should have been The Rubber Manufacturer's Association.

It should be mentioned again that these comments are minor and almost insignificant compared to the mass of high quality information in the volume.

This volume is, without doubt, the most indispensable volume which an operating rubber technologist can have in his office.

The R. T. Vanderbilt Company should be congratulated again for a very fine service to the industry. [Reviewed for RUBBER CHEMISTRY & TECHNOLOGY by A. E. Jure.]

FORTSCHRITTE DER HOCHPOLYMEREN-FORSCHUNG—ADVANCES IN POLYMER SCIENCE. Published by Springer, Berlin-Göttingen-Heidelberg. Available in the United States through Stechert-Hafner, Inc., 31 East 10th Street, New York 3, N. Y. This new journal first appeared in July, 1958 and will be published, irregularly, four numbers to a volume. The journal will contain reports, in the nature of monographs, in the field of the physics and chemistry of high polymers. Subjects will be covered in the least space required for development of a complete knowledge of the literature pertaining to that subject.

The editorial board is international in its membership consisting of Prof. J. D. Ferry, The University of Wisconsin, Prof. C. G. Overberger, Polytechnic Institute of Brooklyn, Profs. G. V. Schulz and H. A. Stuart, Institut für Physikalische Chemie der Universitat, Mainz, and Prof. A. J. Staverman of Holland. The composition of this editorial board should make it possible for the journal to include reports of outstanding advances without regard to nationality of the author or the sphere of the research. Attempts will be made to avoid the character of a collection of reviews in the make-up of this journal. Articles shall be written in the language of the author but in any case in either German, English or French.

The first issue contains an interesting collection of articles all by American authors. The subjects of these four articles of the first issue of *Advances in Polymer Science* are an illustration of the diversity and timeliness of its articles. This may be an indication of the potential value of this new publication. The first paper is "Specific Ion Binding by Polyelectrolytes" by H. Morawetz of the Polytechnic Institute of Brooklyn. It is followed by a paper on "The Study of High Polymers by Nuclear Magnetic Resonance" by W. P. Slichter of the Bell Telephone Laboratories. The third paper by a group from the Wright Air Development Center is "Fluorine-Containing Polymers. I. Fluorinated Vinyl Polymers with Functional Groups, Condensation Polymers and Styrene Polymers" by William Postelnek, Lester E. Colman and Alan M. Lovelace. The final paper of this first issue is "The Dynamic Mechanical Properties of High Polymers at Low Temperatures" by A. E. Woodward and J. A. Sauer of Pennsylvania State University.

THE ELASTICITY OF RUBBER*

LAWRENCE A. WOOD

NATIONAL BUREAU OF STANDARDS, WASHINGTON, D. C.

INTRODUCTION

The properties of rubber have been regarded in former times as sufficiently novel to call for research activities on the part of a number of scientists better known for their work in other fields. Joseph Priestley, discoverer of oxygen, gave it its name[36]. Electrician Michael Faraday first measured its chemical composition[15]. The first to treat the thermodynamics of elastic deformation and to predict temperature and energy changes on the stretching of rubber was none other than Lord Kelvin[25], while the first careful experimental investigator of the thermoelastic properties of rubber[24] was J. P. Joule, better known for the mechanical equivalent of heat. Boltzmann[12] and Kohlrausch[26] also each devoted considerable attention to the time-dependent elastic effects in rubber, while W. C. Röntgen[41] investigated Poisson's ratio in rubber 20 years before he discovered x-rays.

Rubbers, natural and synthetic, are unique in their high extensibility and forcible quick retraction. These two properties, in suitable quantitative terms serve as the modern definition of a rubber—independent of any mention of chemical structure.

In Figure 1 the upper curve represents a typical stress-strain relation obtained with natural rubber[53]. The lower curve represents values of the stress-temperature intercept at 0° K, which will be discussed later. The upper curve is far from the linearity expressed by Hooke's Law. We note three regions—the first of decreasing slope, the second of almost constant slope, and the third of very rapidly increasing slope. Natural rubber can become semicrystalline on stretching. Measurements of crystallinity by a variety of methods show no evidence of crystals in the first region; in the second region crystallization increases with time; and in the third region the degree of crystallinity may be as high as 30–40 per cent and varies little with time.

Figure 2 shows the same data[53] as Figure 1 with the vertical ordinate or stress scale expanded tenfold. This shows the first two regions and a portion of the third.

Our present conception[30] of crystalline regions in a rubber is that the long chain molecules are parallel and alined in those regions and randomly oriented in the amorphous regions. Rubberlike elasticity is possible only in the amorphous regions. The upturn in the stress-strain curve represents chiefly the stiffening effect of the crystalline regions in an amorphous matrix. To avoid

* In the present century the diversity of facts and theories to be considered has forced such specialization that most of us find it necessary to rely on review papers for a description of work outside our field of immediate interest. The present paper is intended to give a concise summary of the present state of knowledge of the nature and origins of the elasticity of rubber. Almost all of this knowledge has been gained in the past twenty years, as shown by the dates of the publications cited. Reference should be made to several books[1–6] for details which can not be included in the present paper. Most of the illustrative data in the present paper are taken from work performed at the National Bureau of Standards. This paper is essentially the same as the address of the retiring President of the Philosophical Society of Washington printed in the *Journal of the Washington Academy of Sciences* 47, 281–299 (1957). It has been revised slightly to correspond to the interests of the readers of RUBBER CHEMISTRY AND TECHNOLOGY.

the complexities associated with a two-phase system we shall concern ourselves hereafter only with effects obtained in the absence of crystallinity and consequently shall consider only the first region of the stress-strain curve. For the same reason we shall omit reference to the extensive work on the properties of swollen rubbers[3,18,20,22].

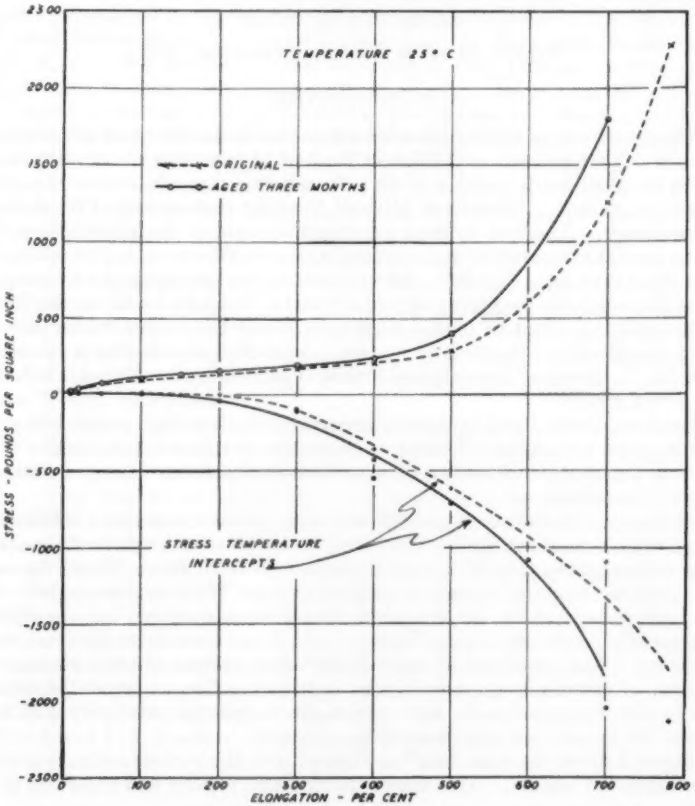

FIG. 1.—Stress-strain relation and stress-temperature intercepts at constant elongation. Natural rubber. Data in Reference 53.

VISCOELASTIC BEHAVIOR

The relation between stress and strain in rubber is quite time-dependent. The curves already shown were obtained after the stress had been applied for several hours. Figure 3 shows the stress-strain relations when the specimen is stretched at a constant speed of about 200 per cent per minute and then allowed to retract at the same rate. A second extension curve, begun 3 minutes after completion of the first, falls considerably below the first curve, but the second retraction curve is almost identical with the first. The specimen in this case was SBR—a noncrystallizing copolymer of butadiene and styrene. If the

length is held fixed (at 100 per cent elongation, for example), the stress is found to decrease with time—rapidly at first and then more and more slowly. If the load is held fixed the length increases rapidly at first and then more and more slowly. The first condition is called stress relaxation; the second is called creep. If the length is held fixed at some point on the retraction curve, one finds an increase of stress with time, or correspondingly a decrease of length with time if the load is held fixed after partial retraction. The curve shown by the dashed line is that obtained after several hours of stress relaxation at each elongation. It is intermediate between the first extension and the retraction curves and is comparable with the curves shown in Figure 1 and 2 for natural

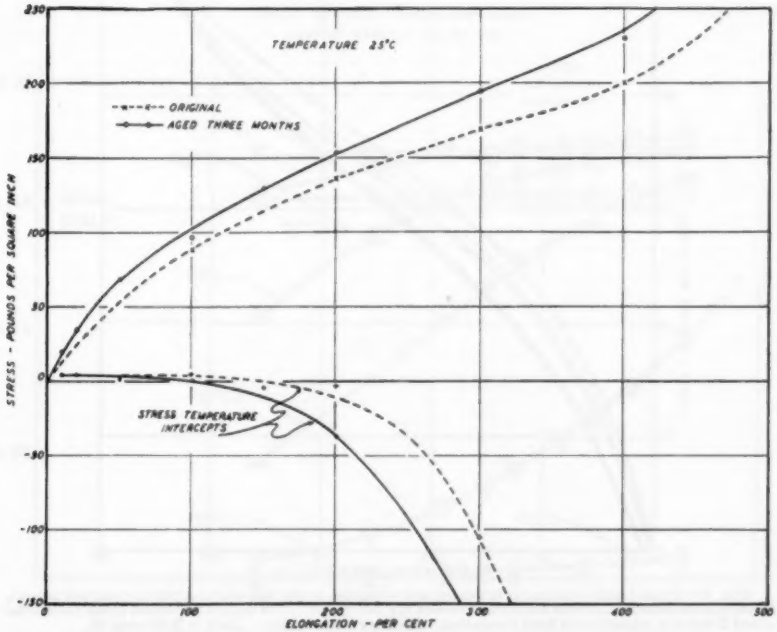

FIG. 2.—Stress-strain relation and stress-temperature intercepts at constant elongation. Ordinate range one-tenth that of Fig. 1. Natural rubber. Data in Reference 53.

rubber. There is relatively little "set"—namely extension remaining after release of load. Almost all this set disappears in time, as will be seen later, and the discussion will be restricted to rubbers which are sufficiently well-vulcanized to show little significant flow or permanent deformation.

The area under the extension curve represents the work done in deforming the rubber and the area under the retraction curve represents the external work done by the rubber in retracting. The difference between these areas—the area between the curves—represents the irrecoverable energy loss on completing a cycle—in exact analogy with the hysteresis losses in magnetic materials. The loss shown by SBR synthetic rubber is much larger than is obtained with natural rubber under the same conditions in the absence of crystallization.

The loss manifests itself in heat of course and causes SBR tires to develop higher temperatures than natural rubber tires in operation.

The loss shown by IIR or butyl rubber is normally much greater than that shown by SBR synthetic rubber, particularly if the cycle is traversed rapidly. Dropped from a height of 6 feet a natural rubber ball is deformed in a period of the order of milliseconds and rebounds giving back about 80 per cent of its original energy; about 20 per cent is lost in hysteresis. A butyl rubber ball dropped under the same conditions gives back about 8 per cent of its original energy; about 92 per cent is lost in hysteresis.

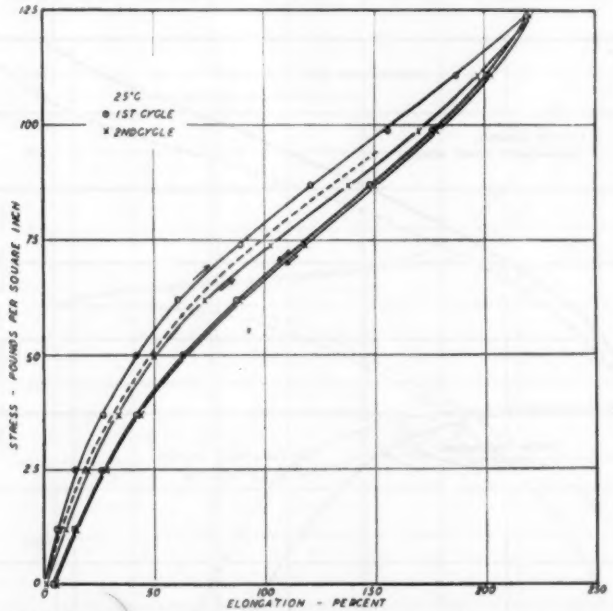

FIG. 3.—Stress-strain relation for extension and retraction at the rate of about 200 per cent per minute. There was an interval of about 3 minutes between the two cycles. The dashed line shows stress value after about 2 hours of relaxation at fixed elongation. SBR synthetic rubber. Data in Reference 42.

Creep, stress relaxation, set, and related effects are examples of viscoelastic phenomena in general. Extensive studies of creep have been made by Leaderman[4,28,29] and extensive research on stress relaxation has been conducted by Tobolsky[44,45]. Ferry[16] has applied dynamic methods in this field.

Figure 4 shows unpublished experimental data obtained by Leaderman on the creep of a pure-gum vulcanizate of natural rubber in shear at different temperatures. The shear strain was observed from 5 seconds to 5 minutes after the application of a constant shear stress of 10.67 psi. At −60° C the strain was too small to be measured for times less than 0.5 minutes. Progressive increases with temperature and time can be noted in Figure 4 up to −40° C. At 0° and 50° C little change with time can be noted on the scale of coordinates shown. However, the strain at 50° is seen to be less than that of 0° C.

All the data shown in Figure 4 can be represented in the form of a single

sigmoid curve by two successive operations on the coordinates, as follows: (1) plotting as ordinate a quantity equal to the shear strain multiplied by a factor of T/298 where T is the temperature of observation in ° K and 298° K (= 25° C) is a reference temperature and (2) displacing the curves along the log-time axis until the new ordinate values coincide. The first operation is based on the conclusions of the statistical theory of an equilibrium modulus of rubber elasticity[5] to be discussed in more detail in a later section. The second operation is based on a principle of equivalence of time-scale and temperature change which has been extensively investigated[4,16,28,44,45]. The shape of the curves in Figure 4 is such that, after these operations, coincidence of the overlapping portions of

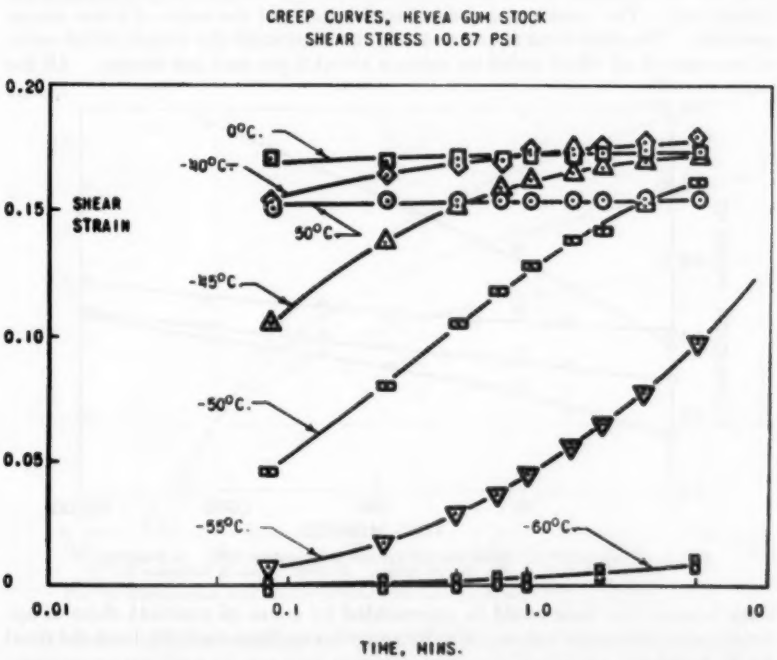

FIG. 4.—Shear creep at various temperatures. Natural rubber. Unpublished data of Leaderman.

the curves is indeed obtained, and the amount of shift necessary for coincidence of the ordinate values agrees very well with general relations found applicable to all polymers[16,45].

A single curve is obtained rising in sigmoid fashion from a strain too small to be observed at short times to a shear strain corresponding to a modulus of the order of 10^7 dynes/cm^2 at long times. Empirical equations have been found which represent this curve over the entire range of experimental values[51]. The curve may be regarded as representing the behavior of the rubber over a very wide range of times at a single reference temperature. The behavior at other temperatures may be obtained by a mere shift of the log-time scale. General confirmation is given to this conception by studies of the dynamic modulus for

sinusoidal stresses of varying frequency[16]. By extending into the megacycle range at 25° C, these studies can give information about the behavior in the range of microseconds, whereas inertial effects prevent direct creep observations on specimens of ordinary size at times shorter than the order of milliseconds.

The sigmoid creep curve for 25° C derived from Figure 4 indicates that a strip of rubber, in the absence of inertial effects, would first deform perceptibly in a time of the order of hundredths of a microsecond. Other work involving the observation of strains smaller by several orders of magnitude has shown that the effective modulus for shorter times is of the order of 10^{11} dynes/cm^2. Between about 0.01 microsecond and 10 microseconds the creep curve indicates that the deformation would rise to correspond to a modulus of the order of 10^7 dynes/cm^2. The most rapid rise occurs for times of the order of a few microseconds. The slope then shows a steady decrease until the time is of the order of one second, at which point its value is about 2 per cent per decade. All the

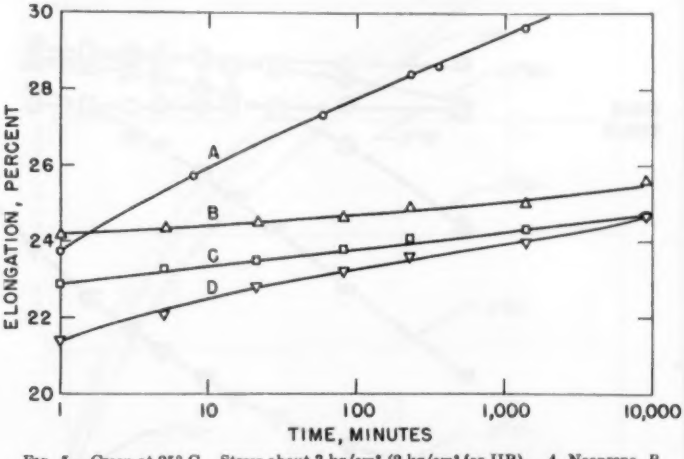

FIG. 5.—Creep at 25° C. Stress about 3 kg/cm^2 (2 kg/cm^2 for IIR). *A*. Neoprene. *B*. Natural rubber. *C*. IIR (butyl) rubber. *D*. SBR. Data in Reference 31.

data beyond this time could be represented by a line of constant slope of approximately the same value. Similar creep curves have recently been obtained by F. Bueche[14].

Entirely analogous results are obtained from stres-relaxation experiments[44,45].

Figure 5 shows experimental observations of Martin, Roth, and Stiehler[31] covering four decades of the creep curve at 25° C beginning at one minute. In this case the specimens were subjected to simple extension at a fixed stress. As far as can be seen the relation of elongation to log time is linear over this range in agreement with the representation of the data of Figure 4 from one second to 5 minutes. Martin, Roth, and Stiehler[31] give the creep of a natural rubber compound vulcanized to approximately the same Young's modulus (13.8 kg/cm^2) as the vulcanizate used by Leaderman in Figure 4 as averaging 2 per cent per decade, in agreement with the figure noted for Leaderman's data. The decrease of slope of the creep curve, evident over the range from microseconds to about one second, apparently does not continue over the next six decades of log time.

The maximum time shown in Figure 5 is about one week, and it is not feasible to extend the observations appreciably farther on the logarithmic time scale at 25° C because of the likelihood of irreversible chemical changes due to aging of the rubber. Likewise degradation and flow[31,42,53] and nonrecoverable stress relaxation[10,11] occur in most elastomers within a few hours if observations are made at temperatures above 50° C. Thus it is not feasible to extend the effective time-scale by observations at temperatures higher than 50° C. Consequently, with the exception of some specially purified silicone rubbers "cross-linked by radiation"[13], we know of no instances where experimenters have been successful in obtaining conditions such that no change of deformation with time could be observed.

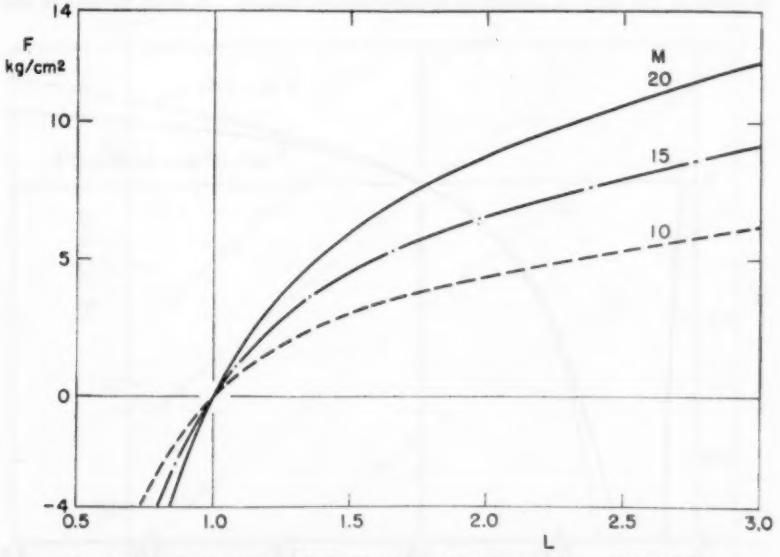

FIG. 6.—Stress-strain relations for rubbers with modulus values of 10, 15, and 20 kg/cm².

A model system possessing a single retardation time would give a sigmoid creep curve reaching 99 per cent of its final value 0.66 decade beyond its point of maximum slope. It has already been noted that the experimental creep curve continues its observable rise for at least 12 decades beyond its point of maximum slope. The conclusion is that each rubber listed in Figure 5 must be represented as a system with a very wide distribution of retardation times, extending up to at least a week.

Recovery curves at 25° C[31] demonstrate that recovery is essentially complete and that the synthetic rubber neoprene, which showed the greatest slope in its creep curve and had the largest temporary set also recovered most rapidly and its recovery in 10,000 minutes was as complete as that of the others.

The recovery curves demonstrate that a once-stretched rubber is still undergoing changes a week after the stress was removed. The importance of previous mechanical history was also brought out by experiments of Martin, Roth, and Stiehler[31] yielding creep curves under a stress of 2 kg/cm² measured (1)

after no prestressing, (2) after prestressing for 1440 min at 4 kg/cm² with no time for recovery, and (3) after prestressing for 1440 min at 4 kg/cm² followed by 5 min of recovery at zero stress. It was found that the effects of the 5-minute interval of recovery disappear after about an hour but that the effects of the one-day prestressing are still evident after a week.

FORM OF STRESS-STRAIN RELATION

Suppose that the stress is maintained constant and the strain measured after a fixed period of creep—1000 min for example. Figure 6 shows the results which would be obtained with three different rubber vulcanizates. The ordinate is the stress F (force divided by undeformed cross section) and the abscissa L the ratio of stretched to unstretched length. A short section of the

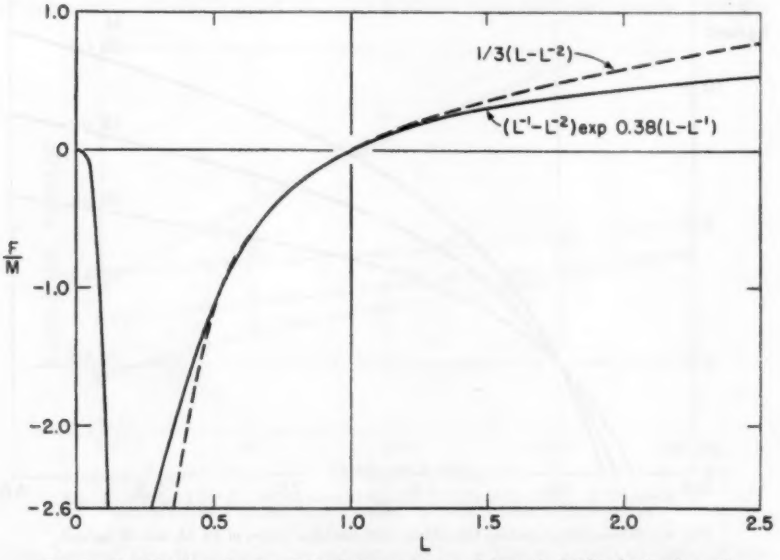

FIG. 7.—Empirical function for relation between stress-modulus ratio F/M and extension ratio L. Dashed line shows function predicted by statistical theory. From Reference 52.

compression curve, where L is less than unity, is shown. The value of Young's modulus M, or slope at $L = 1$, is 10, 15, or 20 kg/cm², respectively, for each of the three curves. This covers about the range of values encountered for rubber vulcanizates containing no fillers—the only ones to be considered here.

The first significant fact to be noted in this connection is that the course of the curve is dependent only on the modulus. The modulus varies with the nature of the rubber, the extent of vulcanization, and the time of creep, but the stress-strain relation does not depend on what particular combination of these factors leads to a given modulus. This means that the curves given are applicable for example to any period of creep; of course all points must be taken after the same fixed time. It should be pointed out that the stress-strain curves observed when the stress and strain are varied simultaneously (as in normal tensile testing) do not fulfill this condition. However, for a rubber

where the creep does not exceed a few per cent per decade of time, the modulus falls by only a few per cent during the time required to elongate the specimen to break at the rate employed in normal tensile testing.

The second significant fact to be noted is the apparent similarity of shape of the curves. This is demonstrated by plotting the ratio of stress to modulus, F/M, against L. The three curves of Figure 6 all coalesce to a single general function having unit slope at $L = 1$.

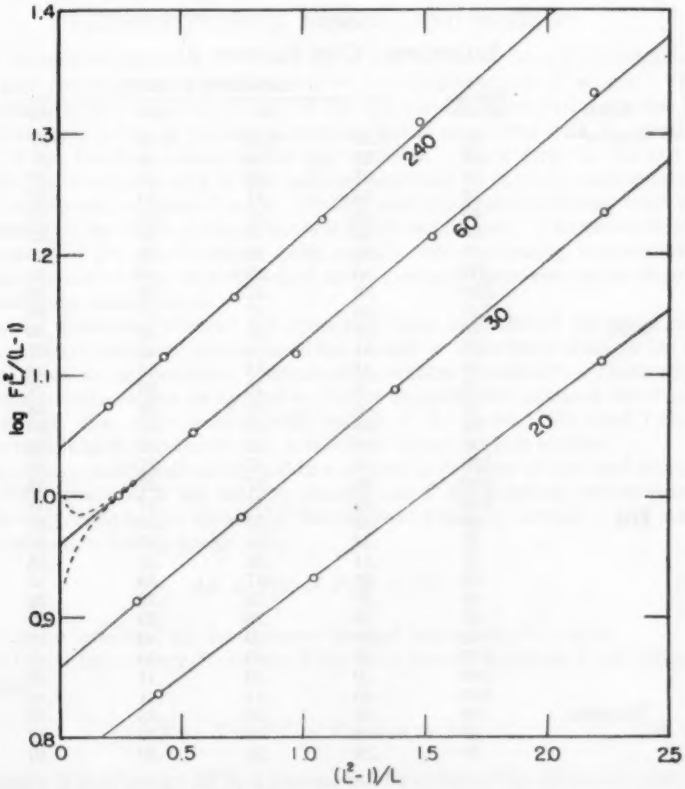

FIG. 8.—Plot for determining validity of empirical function and evaluating the constant A and the modulus M. IIR (butyl) rubber vulcanized 20, 30, 60, and 240 minutes. 100 min creep. Data in Reference 31.

An empirical function representing the observed values of F/M satisfactorily over the range of interest has been found to be:

$$F/M = (L^{-1} - L^{-2}) \exp A(L - L^{-1}) \tag{1}$$

where A is a constant[31]. A plot of this function including the compression region is shown by the full line in Figure 7. The constant A has been taken as 0.38. The relation predicted by the statistical theory to be discussed later is

shown by the dashed line for comparison. Of course no significance is to be attached to the portion of the empirical curve near the origin. The directly observed values of F/M are found to lie on the full line for values of L between 0.5 and about 3. The data of Martin, Roth, and Stiehler[31] offer the best experimental verification of this statement in the region of extension, while the data of Treloar[47] offer the most extensive verification in the compression region between $L = 0.5$ and $L = 1$. The observations are better represented by the

TABLE I

VALUES FOR "A" IN EQUATION (1)

Rubber	Minutes of cure	Time of creep in minutes			
		1	10	100	1000
Natural	20	0.35	0.36	0.36	0.37
	22	.35	.36	.36	.37
	25	.35	.36	.36	.37
	30	.36	.37	.36	.37
	40	.36	.37	.37	.37
	60	.36	.37	.37	.37
	80	.36	.36	.37	.37
	100	.36	.37	.38	.38
	120	.36	.37	.38	.38
	240	.36	.37	.37	.38
SBR	20	.33	.33	.34	.36
	25	.34	.34	.35	.37
	30	.34	.34	.35	.38
	40	.35	.35	.36	.38
	60	.35	.36	.36	.38
	80	.35	.37	.37	.38
	100	.36	.37	.37	.38
	120	.36	.37	.37	.38
	160	.36	.37	.37	.38
	240	.36	.37	.37	.38
IIR	20	.32	.33	.34	.36
	22	.33	.34	.36	.37
	25	.34	.36	.37	.38
	30	.36	.37	.38	.39
	40	.37	.38	.38	.39
	60	.38	.38	.39	.40
	80	.39	.40	.40	.40
	100	.39	.40	.40	.41
	160	.40	.40	.41	.40
	240	.40	.41	.41	.42
Neoprene	20	.38	.38	.38	.39
	40	.38	.38	.39	.40
	90	.38	.39	.39	.40

dashed curve of the statistical theory only for values of L less than 0.5. The success of the single empirical function in representing both compression and extension is a very significant accomplishment[52].

A more logical and more sensitive method of testing the validity of the empirical F/M function is shown in Figure 8. The form of the function is such that a plot of the quantities shown as ordinates should yield a straight line with a slope corresponding to the constant A (taken as 0.38 in Figure 7) and an intercept corresponding to the modulus M. The data[31] shown here are for IIR (butyl) rubber specimens. Table I shows values of the slopes of these and similar lines for pure-gum vulcanizates of natural rubber and the three common synthetic rubbers.

Accepting the validity of the empirical F/M function one can then compile a table of values of F/M for each per cent elongation between 0 and 200; from a single observation of stress and strain the table can be used to evaluate M. M is the most logical quantity to use in characterizing the kind of rubber, the state of vulcanization, and the creep behavior. If desired the table can be used a second time to determine the value of F at any elongation. The utility of such a table in practical work is obvious.

THERMODYNAMICS: ENTROPY AND ENERGY

The retractive force in a stretched metal can be traced back to interatomic forces and potential energy associated with a displacement of atoms. The expansive force of a compressed gas, on the other hand, is not primarily due to any interatomic forces or potential energies, but is associated with the kinetic energy of the thermal motion of the gas particles. Work done on the gas is converted to thermal energy of the particles and may be partially recovered as the gas is allowed to expand again. In this case changes in entropy must be considered and the effect of temperature is highly significant. Correspondingly the pressure of the gas increases quite rapidly with increasing temperature, while the retractive force in a stretched metal generally decreases rather slowly with increasing temperature.

One can determine whether the retractive force in stretched rubber is primarily due to interatomic forces (as in the metal) or to entropy changes (as in the gas) from an examination of stress-temperature relations[32]. Thermodynamic considerations can be applied to derive quantitative relations involving "equilibrium" (i.e., time-independent) values of the stress. We shall follow the thermodynamic treatment and symbols of Flory[3] in this section.

The change in internal energy dE in a process is the sum of the heat energy added TdS, where dS is the entropy change and T the absolute temperature, plus the work done on the system by the external pressure, namely $-PdV$ and by the retractive force, namely fdL.

$$dE = TdS - PdV + fdL \tag{2}$$

where f is the force and dL the distance through which the force acts.

The Gibbs free-energy F and the Helmholtz energy function A are defined as follows:

$$F = E + PV - TS = A + PV \tag{3a, b}$$

The change in free energy dF in a process can be obtained by differentiation of Equation (3a) to give

$$dF = VdP - SdT + fdL \tag{4}$$

It can be seen that

$$\left.\frac{\partial F}{\partial L}\right]_{T,P} = f \tag{5}$$

and

$$\left.\frac{\partial F}{\partial T}\right]_{L,P} = -S \tag{6}$$

Utilizing the well-known property of a double partial derivative that the order of differentiation is immaterial one finds that

$$\frac{\partial f}{\partial T}\Big]_{L,P} = \frac{-\partial S}{\partial L}\Big]_{T,P} \tag{7}$$

The quantity on the right is significant in calculations but not directly observable. The quantity on the left is readily measured.

Solving Equation (2) for the force one finds:

$$f = -T\frac{\partial S}{\partial L}\Big]_{T,P} + \frac{\partial E}{\partial L}\Big]_{T,P} \tag{8}$$

since the quantity $P\frac{\partial V}{\partial L}\Big]_{T,P}$ is negligible. Finally,

$$f = T\frac{\partial f}{\partial T}\Big]_{L,P} + \frac{\partial E}{\partial L}\Big]_{T,P} \tag{9}$$

This means that if the force f measured at constant length and pressure is plotted against the temperature T, then the slope of the tangent to the curve at any point will give $\frac{-\partial S}{\partial L}\Big]_{T,P}$ and the intercept (at 0° K) of the tangent will give $\frac{\partial E}{\partial L}\Big]_{T,P}$.

Plots of this sort are grequently made[7,8], and are usually found to be practically linear. The entropy component of the force $-T\frac{\partial S}{\partial L}\Big]_{T,P}$ is often found to be considerably larger than the energy component $\frac{\partial E}{\partial L}\Big]_{T,P}$ but the latter is by no means negligible in general.

This analysis of the components at constant pressure, while perfectly valid, does not possess as much significance as it would if it had not been found[20,21] that there is a volume increase on stretching rubber, amounting to hundredths of a per cent at an elongation of 100 per cent under constant pressure. This volume increase is responsible for significant parts of the internal energy and entropy changes. Consequently if attention is to be centered on configurational aspects, the analysis should be made at constant volume, not at constant pressure.

In this case, it is found convenient to perform on the Helmholtz energy function A the same operations just performed on the Gibbs free energy F. It will be remembered that A is $E - TS$ and so

$$dA = dE - TdS - SdT \tag{10}$$

$$dA = -PdV - SdT + fdL \tag{11}$$

The partial derivatives of A at constant volume are again f and $-S$ and on cross differentiation we get

$$\left.\frac{\partial f}{\partial T}\right]_{L,V} = \left.\frac{-\partial S}{\partial L}\right]_{T,V} \tag{12}$$

$$f = T\left.\frac{\partial f}{\partial T}\right]_{L,V} + \left.\frac{\partial E}{\partial L}\right]_{T,V} \tag{13}$$

This is identical in form with Equation (9) previously obtained at constant pressure. It calls for maintaining the volume constant by the application of external pressure as the force-temperature relation is investigated. This would be an experimental condition quite difficult to maintain accurately, although consideration has been given to attempting it.

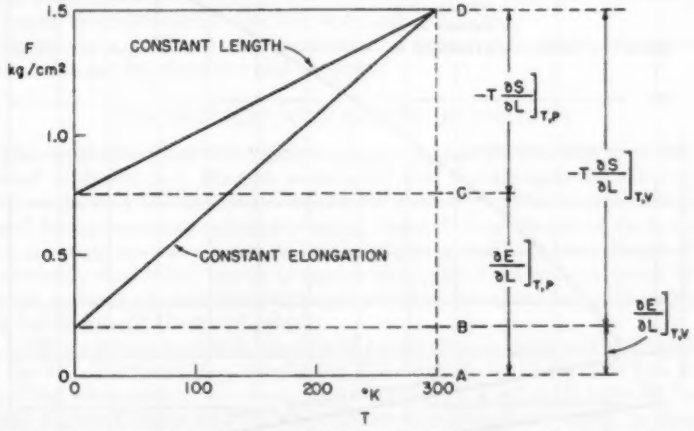

FIG. 9.—Stress-temperature relations. Resolution of stress into entropy and energy components.

The same result can be obtained under much simpler experimental conditions if one makes use of the following approximation:

$$\left.\frac{-\partial S}{\partial L}\right]_{T,V} = \left.\frac{\partial f}{\partial T}\right]_{\alpha,P} \tag{14}$$

where α is the ratio of stretched to unstretched length, the lengths being measured at the same temperature. This approximation may be derived by an extended analysis[3] which will not be repeated here. Finally then

$$f = T\left.\frac{\partial f}{\partial T}\right]_{\alpha,P} + \left.\frac{\partial E}{\partial L}\right]_{T,V} \tag{15}$$

The force required to maintain a constant elongation, $(\alpha - 1)$, is relatively easy to measure as a function of temperature at constant pressure.

Typical schematic force-temperature plots of the types just described are shown in Figure 9, where the resolution of the force into energy and entropy

components at constant pressure and at constant volume can be noted. If the force-temperature plot is not linear the lines shown can be taken to represent the tangents to the cruve at point *D*. If the force is taken as that acting on unit area of original cross section the ordinate in Figure 9 can also represent the stress.

From experimental studies of the type illustrated in Figure 9 one obtains data similar to that shown in the lower curves of Figures 1 and 2, which give values of the stress-temperature intercept for natural rubber which has been maintained at constant elongation for several hours[53]. This period is long

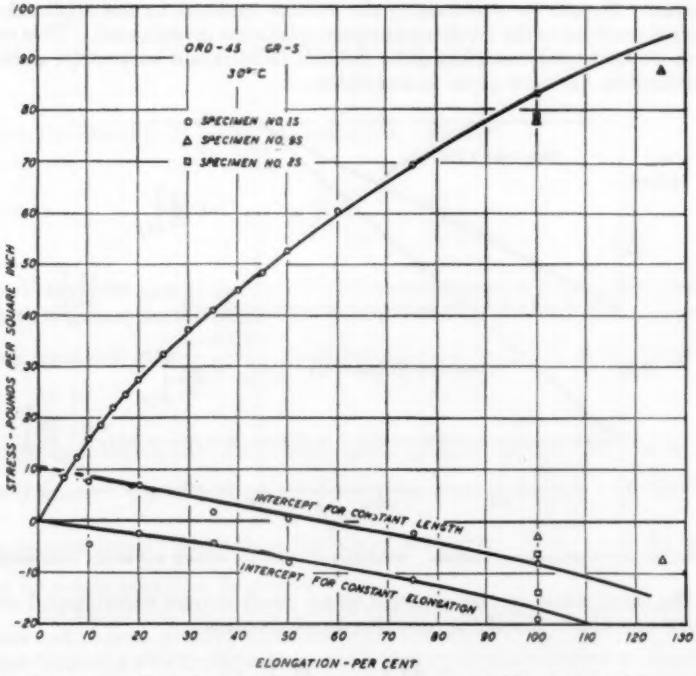

FIG. 10.—Stress-strain relation and stress-temperature intercepts for SBR. Data in Reference 42.

enough to insure that the stress is changing only very slowly with time. However, the true "equilibrium" values required in the thermodynamic analysis are not experimentally accessible, since the stress relaxation of natural rubber at 25° C, like the creep, is normally not less than the order of 2 per cent per decade of time, as discussed in the section on viscoelastic behavior. Some observers have reduced the rate of stress relaxation at 25° C by a previous relaxation at the maximum elongation followed by a recovery period[22] or by a previous swelling of the rubber[18,20]. It is not clear to what extent these procedures may alter the system under investigation.

The intercept of the stress-temperature relation represents, as has just been shown, the internal energy component $\left(\frac{\partial E}{\partial L}\right)_{T,V}$ of the stress. The negative

values at high elongations are due to crystallization, which of course is responsible for large changes in internal energy with stretching. Crystallization by favoring the alinement of molecules in the direction of stretching would be expected to decrease the total force and lead to negative values of the intercept. The positive values which are obtained at low elongations have not received an explanation in molecular terms, but are quite small in comparison with the total stress. The total stress is consequently to be regarded as consisting essentially of the entropy component alone in the case of natural rubber in the absence of crystallization.

A similar type of representation of the results[42] obtained with SBR synthetic rubber is given in Figure 10. The constant-elongation intercept is always negative here, becoming zero at the zero elongation. Thus the observed stress is consistently less than that component arising from the entropy alone. The intercept at constant length also shown here differs from that at constant elongation because of the energy changes associated with the change of volume, as already demonstrated in the thermodynamic analysis.

Similar data for the evaluation of internal energy changes do not appear to be available for butyl rubber and neoprene.

STATISTICAL CALCULATION OF ENTROPY

The conclusion that the retractive force in stretched rubber is chiefly associated with entropy changes stimulated the development of calculations based on the detailed molecular structure of rubber[5,43] These calculations and related background are commonly called the statistical theory of rubber elasticity (because they are based on statistics and probability considerations) or alternatively the kinetic theory of rubber elasticity (because they relate to the thermal motions of molecular segments and are analogous to similar calculations in the kinetic theory of gases).

A typical rubber molecule consists of a long flexible chain of 10,000 to 100,000 atoms. For simplicity, numbering the atoms in the chain from 1 to n and neglecting atoms not in the chain, let us maintain a fixed angle between bonds joining adjacent atoms and no other preferred orientation. Atom A_3 may lie anywhere on a circle formed by rotating the molecule about A_1 A_2 as axis; atom A_4 is correspondingly on a circle formed by rotation about A_2 A_3 as axis, and so on with the other atoms. The calculation of the most probable value of A_1 A_n, the distance between ends, is of course one of the well-known "random flight" problems of statistics.

For visualization Treloar[5] has constructed a model of this sort by bending a wire to make 1000 equal segments with angles of 109° between each segment. A random choice of one of 6 positions for A_2, A_4, A_5, etc. on the circles just mentioned was made by a throw of a die. A photograph of the wire is shown in Figure 11.

This of course represents only one of many possible configurations. Since there are 1000 choices among 6 possibilities the number of configurations is 6^{1000}, which is 10^{778}. The end-to-end distance A_1 A_n shown turned out to be very close to the most probable end-to-end distance calculated from statistics. The actual typical rubber molecule would have a minimum of about 10,000 links rather than the 1000 shown here.

We shall not trace out any exact derivations here but it is easy to see that one can calculate the probability of a given configuration and of a given ensemble of configurations. From this the entropy of the undeformed rubber can

be obtained by the Boltzmann relation that the entropy is the Boltzmann constant k times the logarithm of the probability. A similar calculation can be made for the entropy in the deformed state. The difference in entropies multiplied by the temperature gives the change in the Helmholtz energy function A on stretching, or at least that poriton of it which arises from entropy changes.

Three somewhat different approaches have been used for these calculations of change of A on deformation. If the dimensions of a cube, initially of unit length on each side, become λ_1, λ_2, and λ_3 on deformation, the three approaches

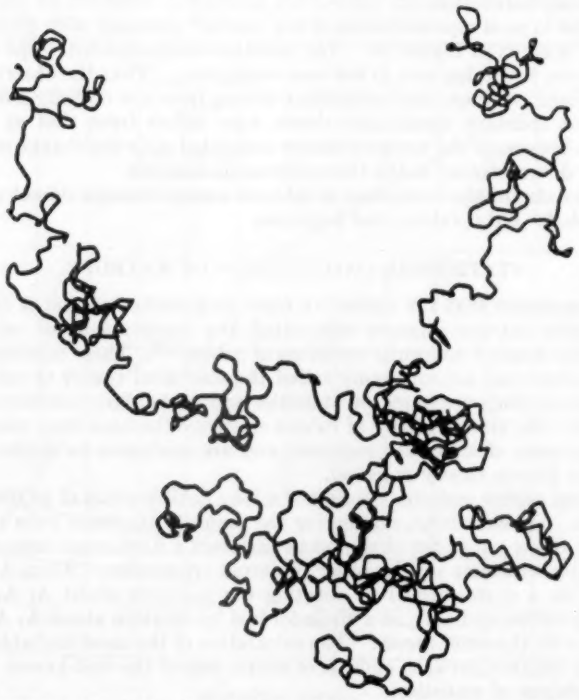

FIG. 11.—1000-link chain with random orientation of links. Described on page 42 of Reference 5.

agree in predicting that the entropy component of the energy function change per unit volume should have the form:

$$\Delta A = -T\Delta S$$
$$= (G/2)(\lambda_1^2 + \lambda_2^2 + \lambda_3^2 - 3) \qquad (16)$$

They also agree in predicting proportionality between the constant G and absolute temperature but differ in the other factors determining G.

The approach proposed by Kuhn[23,27,46] considers only a single molecule of molecular weight M_c and assumes that the deformations of the molecule parallel exactly the deformations of the bulk rubber. This approach yields

$$G = \rho RT/M_c \qquad (17)$$

where ρ is the density and R the gas constant.

The appraoch proposed by F. T. Wall[46,50] considers N chains and yields

$$G = NkT \tag{18}$$

where k is the Boltzmann gas constant.

The approach outlined by Flory and Rehner[3,19,49] considers a network resolved into tetrahedra of average molecular weight M_c between crosslinks. The result is the same as that given in Equation (17), where M_c now has the significance just mentioned.

If the specimen is subject to the type of deformation known as pure shear $\lambda_1 = L$, $\lambda_2 = 1/L$ and $\lambda_3 = 1$, where L is the ratio of stretched to unstretched length for one dimension of the unit cube. When the deformation is simple shear (involving effectively a translation and rotation in addition to pure shear) the shear strain γ is $(L - 1/L)$ and the strain energy is the same as for pure shear.

The strain energy per unit volume for simple shear is thus from Equation (16):

$$W = (G/2)(L^2 + 1/L^2 - 2) = (G/2)(L - 1/L)^2 \tag{19}$$

$$W = (G/2)\gamma^2 \tag{20}$$

The shear stress σ is then:

$$\sigma = dW/d\gamma = G\gamma \tag{21}$$

Equation (21) predicts the validity of Hooke's Law for shear stress and strain and states that the constant G is the shear modulus.

If the specimen is subjected to simple extension or compression $\lambda_1 = L$ and $\lambda_2 = \lambda_3 = L^{-\frac{1}{2}}$. Here, from Equation (16),

$$W = (G/2)(L^2 + 2/L - 3) \tag{22}$$

and the stress F is then

$$F = \frac{dW}{dL} = G(L - L^{-2}) \tag{23}$$

One notes that the slope of Equation (23) at the origin is $3G$; consequently Young's modulus M is three times the shear modulus G,—the relation valid for an incompressible material.

$$F/M = (1/3)(L - L^{-2}) \tag{24}$$

Experimental values of the entropy components of stress can be obtained by subtracting from an observed value of total stress the component due to energy effects. The methods of determining the latter quantity are given in the preceding section. Figures 1 and 2 show observed values of total stress (upper curves) and energy component (lower curves) for a pure-gum vulcanizate of natural rubber. Up to elongations (about 150 per cent) where crystallization becomes apparent in this rubber the energy component is rather small compared

with the total stress; consequently in this instance the total stress arises effect ively from the entropy component alone. In Figure 7 the values of entropy component of the stress-modulus ratio (dashed line) calculated from Equation (24) derived from the statistical theory are compared with the observed values represented by the empirical relation (full line) given by Equation (1). It will be seen that the discrepancy between the observed values and the calculated values is considerable; the calculated values are as much as 50 per cent larger than the observed values at $L = 3$. This discrepancy has been noted repeatedly in natural rubber (References 5, 8, 22, 31, 43, 47, 49), but no revised calculation of the entropy component has been developed which will explain the discrepancy. The discrepancy appears also in butyl rubber[17] and in silicone rubber[13].

In the case of a pure-gum vulcanizate of SBR synthetic rubber[42] the discrepancy is found to be much less. Here the energy component is much larger, is always negative, and its magnitude increases markedly with elongation, as can be seen in Figure 10. When this quantity is added to the observed stress to get an experimental value of the entropy component of the stress-modulus ratio, it is found that the value calculated from statistical theory seldom exceeds this experimental value by more than 10 per cent. It is difficult to understand how SBR should come nearer to the ideal rubber in this respect and yet be farther from it in most other respects.

The statistical theory, in addition to the predictions regarding the functional form of the stress-strain relation as just discussed, calls for proportionality between the shear modulus G and absolute temperature, Equations (17) and (18). For temperatures between $-30°$ and $+70°$ C this proportionality is normally found to be valid[7,32,42,53]. When precise measurements are made at low elongations, curves which are concave toward the temperature axis are observed[8].

Finally the statistical theory in Equations (17) and (18) predicts a definite value of the shear modulus, which can be calculated if one can determine M_c or N. The first attempts[9,17,18] to verify the relationship gave values of the calculated modulus between one-third and one-half of those which are observed. Recent extensive studies[34,35] have given calculated values as high as two-thirds of those observed. In the calculation a correction must be made for the effect of initial molecular weight before crosslinking. Network entanglements, not considered in the measured crosslinkages, are usually considered responsible for the higher observed modulus. On the other hand, in very recent work on silicone rubber crosslinked by radiation, Bueche[13] calculates a modulus about twice that observed.

STRAIN ENERGY CONSIDERATIONS

We have just seen how a single strain energy function can be used to predict stess-strain relations under two different types of deformation. Indeed if completely known, it can predict these relations for any abribrary type of deformation whatever. We can say then that the ultimate problem of rubber elasticity is the derivation of the strain energy function from molecular considerations. We have seen the rather limited success of the statistical calculation of the entropy component.

There are certain general considerations regarding the form of the strain energy function which must apply whatever its molecular origin. Work along these lines was initiated by Mooney[33] and the ideas were put into much more general and rational form by Rivlin[37–40]. For example, the strain energy func-

tion must be expressible as a linear combination of certain functions of the deformation called strain invariants. The three simplest strain invariants are as follows:

$$I_1 = \lambda_1^2 + \lambda_2^2 + \lambda_3^2 \tag{25}$$

$$I_2 = \lambda_1^2\lambda_2^2 + \lambda_2^2\lambda_3^2 + \lambda_3^2\lambda_1^2 \tag{26}$$

and

$$I_3 = \lambda_1^2\lambda_2^2\lambda_3^2 \tag{27}$$

Each must fulfill two conditions: first, it must be symmetrical in λ_1, λ_2, and λ_3, because of the isotropy of the rubber before stretching, and second, it must contain only even powers of the λ's, since the stored energy is unaltered by a change of sign of two of the λ's, corresponding to a rotation of the deformed rubber through 180°. It can be seen that each term in I_1 contains a single λ; in I_2 they appear in pairs and in I_3 they appear as the product of all three. Higher strain invariants contain the fourth and higher even powers of the λ's, but will not be further considered here because of their complexity.

If the volume is constant (as it is in rubber to within some hundredths of a per cent), I_3, the square of the volume of the deformed unit cube, is equal to unity and I_2 becomes the sum of the reciprocals of the squares of the λ's.

For simple extension the relations have already been mentioned

$$\lambda_1 = L, \qquad \lambda_2 = \lambda_3 = L^{-\frac{1}{2}},$$

and consequently

$$I_1 = L^2 + 2L^{-1} \tag{28}$$

and

$$I_2 = 2L + L^{-2} \tag{29}$$

The stress F for simple extension or compression can be obtained by differentiation of the strain energy function W.

$$F = \frac{dW}{dL} = \frac{\partial W}{\partial I_1}\frac{dI_1}{dL} + \frac{\partial W}{\partial I_2}\frac{dI_2}{dL} \tag{30}$$

I_3 does not appear since it is unity, as already mentioned, and higher invariants are being neglected.

$$F = 2(L - L^{-2})\frac{\partial W}{\partial I_1} + 2L^{-1}(L - L^{-2})\frac{\partial W}{\partial I_2} \tag{31}$$

If one wishes to put Equation (31) into a form suitable for a convenient plot, he has two choices suggested by the following two modifications of the equation:

$$(F/M)/2(L - L^{-2}) = \frac{1}{M}\frac{\partial W}{\partial I_1} + \frac{1}{M}\frac{\partial W}{\partial I_2}L^{-1} \tag{32}$$

$$(F/M)/2(1 - L^{-3}) = \frac{1}{M}\frac{\partial W}{\partial I_1}L + \frac{1}{M}\frac{\partial W}{\partial I_2} \tag{33}$$

If in accordance with the conclusion of Mooney[33], the partial derivatives remain constant as L is varied, a plot of

$$(F/M)/2(L - L^{-2}) \text{ against } L^{-1}$$

as suggested by Equation (32) will give a straight line with intercept

$$(1/M)(\partial W/\partial I_1) \text{ and slope } (1/M)(\partial W/\partial I_2).$$

The converse of this statement is not ture: if a straight line is obtained from a plot of the type mentioned it is not necessarily true that the intercept C_1/M and slope C_2/M will be the quantities mentioned, since the partial derivatives may each be functions of L. Rivlin and Saunders[39] present evidence to indicate that

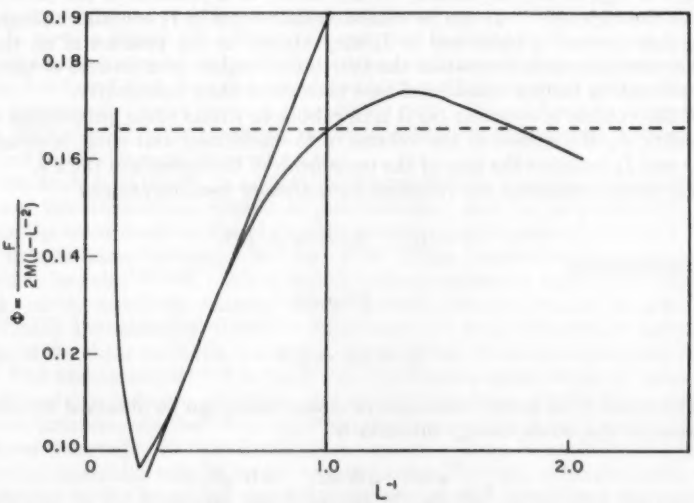

FIG. 12.—Plot of the empirical stress-strain relation of Equation (1) in the form suggested by Equation (32). A taken as 0.38. From Reference 52.

$\partial W/\partial I_1$ is substantially independent of I_1 and I_2, and consequently independent of L. $\partial W/\partial I_2$ is independent of I_1 but decreases with increase of I_2. However the decrease is not more than about ten per cent over the range considered here A plot similar in form to that just mentioned but not containing the factor M has found extensive use[22,39,40,43] in the British literature.

If the plot just mentioned is not a straight line the slope and intercept may be evaluated over limited regions of approximate linearity. Figure 12 shows the empirical F/M function given in Equation (1) with $A = 0.38$, used in a plot suggested by Equation (32). An approach to linearity is seen for the intermediate values of L^{-1}.

Equation (33) suggests a plot of $(F/M)/2(1 - L^{-3})$ against L to evaluate as intercept C_2/M and as slope C_1/M. This general type of plot has been noted in only one instance[11] (again without the factor M), although this form appears to be much more convenient and is more readily visualized than that

suggested by Equation (32). The region of compression also is represented in a more satisfactory fashion.

Figure 13 demonstrates the same facts as Figure 12 somewhat more clearly by using the empirical F/M function in the plot suggested by Equation (33). This figure extends into the region of compression. It shows that in this region the statistical theory represents the data adequately. In fact, for values of L below 0.5 and only in this region, it has already been pointed out that the statistical theory represents the data better than the empirical F/M function. The deviations from the statistical theory are apparent immediately above $L = 1$; there is no region of approximate conformity at low values of extension[52].

For values of L between 1.5 and 3 a straight line with smaller slope and a positive intercept is noted, corresponding to the approach to linearity noted in Figure 12. Both slope and intercept are varying in the region from 1.0 to 1.5.

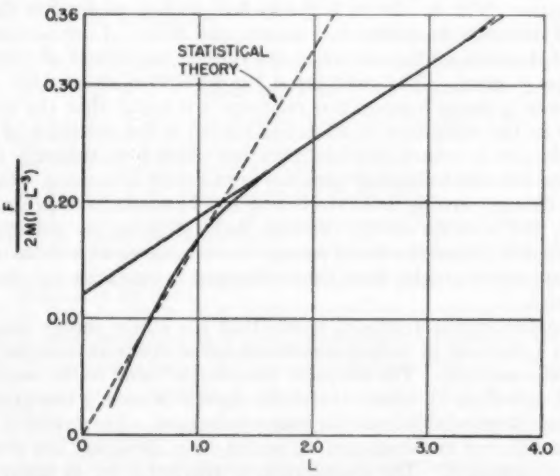

FIG. 13.—Plot of the empirical stress-strain relation of Eq. (1) in the form suggested by Eq. (33). A taken as 0.38. From Ref. 52.

Crystallization effects[3,39], lack of reversibility[40], and the approach to the limiting extension of a network[39,40,49] have been invoked to explain the behavior for values of L greater than 3. There has been a tendency to ascribe the deviations from linearity for L between 1.0 and 1.5 (i.e., for L^{-1} between 0.7 and 1) to errors of observation[22] but the deviations are systematic and the line must form a smooth junction with the values in the compression region (L less than 1), as shown in Figure 13.

The entropy component of the strain energy function predicted by the statistical theory has been given in the preceding section as Equation (16). This is now seen to involve only the first strain invariant I_1 and constants. It is the simplest possible form the strain energy function could assume. The statistical theory offers no explanation of the term involving the second strain invariant I_2 above $L = 1.0$, as shown in Figure 13. The defect, in the case of natural rubber at least, is in the calculated entropy and not in the internal energy term, as has just been shown by the thermodynamic analysis. The decrease of en-

tropy with L is less at larger values of L than would be calculated from pure probability. In other words, the system retains more disorder in the arrangement of the molecular chains than is expected. This is not too surprising. The quantitative calculation of this additional entropy from molecular considerations is one of the most promising fields for further work in the theory of rubber elasticity.

SUMMARY

Rubbers, natural and synthetic, are unique in being highly extensible and in retracting forcibly and quickly to substantially their original dimensions when released.

It has been found that the stress-strain curves for extension and compression of most of the simplest vulcanizates of natural rubber and the three most important synthetic rubbers are similar in shape. The relationship is expressed by the equation $F/M = (L^{-1} - L^{-2}) \exp A(L - L^{-1})$ where F is the stress, L the ratio of stretched to unstretched length, and M and A are constants. The constant M depends on the nature of the rubber, the extent of vulcanization, and the time of creep. The constant A has a value of about 0.38.

By a study of stress-temperature relations it is found that the most important factor in the retraction of stretched rubber is the tendency of long chain flexible molecules to return to a configuration which is statistically more probable than the one which the stretching has forced them to assume. Calculations of entropy changes arising from stretching can be made from probability considerations, and a strain energy function deduced from the entropy changes. Stresses calculated from the strain energy function agree with those observed in compression but are greater than those observed in extension by almost 50 per cent at $L = 3$.

A phenomenological approach shows that the strain energy should be expressible as a function of certain quantities called strain invariants, calculable from the deformations. The simplest behavior is found in the region of compression (L less than 1), where the strain energy is merely the first invariant times a constant calculable from the entropy changes. For values of L between 1.5 and 3 a different constant and an added term involving the second strain invariant are required. The explanation of this behavior in molecular terms is one of the most important current problems of rubber elasticity.

REFERENCES

[1] Alfrey, T., "Mechanical Behavior of High Polymers", Interscience Publishers, Inc., New York, 1948.
[2] Eirich, F. R., editor, "Rheology Theory and Applications", Academic Press, New York, Vols. I–III, 1956–1958.
[3] Flory, P. J., "Principles of Polymer Chemistry", Cornell University Press, Ithaca, N. Y., 1953.
[4] Leaderman, H., "Elastic and Creep Properties of Filamentous Materials and Other High Polymers", Textile Foundation, Washington, D. C., 1943.
[5] Treloar, L. R. G., "The Physics of Rubber Elasticity", Oxford University Press, London, 1949; compare also the 1958 edition.
[6] Stuart, H. A., editor, Vol. 4, "Die Physik der Hochpolymeren. Theorie und Molekulare Deutung Technologischer Eigenschaften von Hochpolymeren Werkstoffen", Springer-Verlag, Berlin, 1956; see especially chapter by Treloar, L. R. G.
[7] Anthony, R. L., Caston, R. H., and Guth, E., *J. Phys. Chem.* **46**, 826 (1942); RUBBER CHEM. & TECHNOL. **16**, 297 (1943).
[8] Baldwin, F. P., Ivory, J. E., and Anthony, R. L., *J. Appl. Phys.* **26**, 750 (1955); RUBBER CHEM. & TECHNOL. **29**, 227 (1956).
[9] Bardwell, J., and Winkler, C. A., *India Rubber World* **118**, 509 (1948); *Can. J. Res.* **B27**, 116, 128, 139 (1949).
[10] Berry, J. P., and Watson, E. F., *J. Polymer Sci.* **18**, 201 (1955); RUBBER CHEM. & TECHNOL. **29**, 398 (1956); *J. Polymer Sci.* **21**, 505 (1956); RUBBER CHEM. & TECHNOL. **30**, 42 (1957).
[11] Blackwell, R. F., *Trans. Inst. Rubber Ind.* **28**, 75 (1952); RUBBER CHEM. & TECHNOL. **25**, 430 (1952).
[12] Boltzmann, L., *Pogg Ann. Physik* **7**, 624 (1876); *Wied Ann. Physik* **5**, 430 (1878).
[13] Bueche, A. M., *J. Polymer Sci.* **19**, 297 (1956).
[14] Bueche, F., *J. Polymer Sci.* **25**, 305 (1957); RUBBER CHEM. & TECHNOL. **31**, 1 (1958).

[16] Faraday, M., *Quart. J. Sci.* **21**, 19 (1826); "Experimental Researches in Chemistry and Physics", p. 174, Taylor and Francis, London, 1859.
[17] Ferry, J. D., "Structure and Mechanical Properties of Plastics", Chapter 6 in Reference 6.
[17] Flory, P. J., *Ind. Eng. Chem.* **38**, 417 (1946); RUBBER CHEM. & TECHNOL. **19**, 552 (1946).
[18] Flory, P. J., Rabjohn, N., and Schaffer, M. C., *J. Polymer Sci.* **4**, 225 (1949).
[19] Flory, P. J., and Rehner, J., Jr., *J. Chem. Phys.* **11**, 512 (1943); *Ann. New York Acad. Sci.* **44**, 419 (1943).
[20] Gee, G., *Trans. Faraday Soc.* **42**, 585 (1946); RUBBER CHEM. & TECHNOL. **20**, 442 (1947).
[21] Gee, G., Stern, J., and Treloar, L. R. G., *Trans. Faraday Soc.* **46**, 1101 (1950); RUBBER CHEM. & TECHNOL. **24**, 767 (1951).
[22] Gumbrell, S. M., Mullins, L., and Rivlin, R. S., *Trans. Faraday Soc.* **49**, 1495 (1953); RUBBER CHEM. & TECHNOL. **28**, 24 (1955).
[23] James, H. M., and Guth, E., *Ind. Eng. Chem.* **33**, 624 (1941); *J. Chem. Phys.* **11**, 455 (1943); *J. Chem. Phys.* **15**, 669 (1947); *J. Polymer Sci.* **4**, 153 (1949).
[24] Joule, J. P., "On Some Thermodynamic Properties of Solids", *Phil. Trans. Royal Soc.*, London **A149**, 91 (1859); "Scientific Papers of J. P. Joule", p. 413, Physical Society, London, 1884.
[25] Kelvin, Lord (W. Thomson), "On the Thermoelastic and Thermo-magnetic Properties of Matter", *Quart. J. Math.* **1**, 5 (1855); "Mathematical and Physical Papers", **1**, p. 309, Cambridge University Press, 1882.
[26] Kohlrausch, F., "Experimental-Untersuchungen uber die Elastischen Nachwirkung bei Torsion, Ausdehnung und Biegung", *Pogg. Ann Physik* (6) **8**, 337 (1876).
[27] Kuhn, W., *Kolloid-Z.* **68**, 2 (1934); *J. Polymer Sci.* **1**, 380 (1946).
[28] Leaderman, H., "Viscoelasticity Phenomena in Amorphous High Polymeric Systems", Chapter in Reference 2.
[29] Leaderman, H., Smith, R. G., and Jones, R. W., *J. Polymer Sci.* **14**, 47 (1954).
[30] Mandelkern, L., *Chem. Rev.* **56**, 903 (1956).
[31] Martin, G. M., Roth, F. L., and Stiehler, R. D., *Trans. Inst. Rubber Ind.* **32**, 189 (1956); RUBBER CHEM. & TECHNOL. **30**, 876 (1957).
[32] Meyer, K. H., and Ferri, C., *Helv. Chim. Acta* **18**, 570 (1935); RUBBER CHEM. & TECHNOL. **8**, 319 (1935).
[33] Mooney, M., *J. Appl. Phys.* **11**, 582 (1940).
[34] Moore, C. G., and Watson, W. F., *J. Polymer Sci.* **19**, 237 (1956); RUBBER CHEM. & TECHNOL. **30**, 11 (1957).
[35] Mullins, L., *J. Polymer Sci.* **19**, 225 (1956); RUBBER CHEM. & TECHNOL. **30**, 1 (1957).
[36] Priestley, J., "Familiar Introduction to the Theory and Practice of Perspective", London, 1770.
[37] Rivlin, R. S., "Large Elastic Deformations", Chapter in Reference 2.
[38] Rivlin, R. S., *Phil. Trans. Royal Soc.*, London **A240**, 459, 491 (1948).
[39] Rivlin, R. S., and Saunders, D. W., *Phil. Trans. Royal Soc.*, London **A243**, 251 (1951).
[40] Rivlin, R. S., and Saunders, D. W., *Trans. Faraday Soc.* **48**, 200 (1952).
[41] Röntgen, W. C., *Ann. Physik* **159**, 601 (1876).
[42] Roth, F. L., and Wood, L. A., *J. Appl. Phys.* **15**, 749 (1944); RUBBER CHEM. & TECHNOL. **18**, 353 (1945).
[43] Thomas, A. G., *Trans. Faraday Soc.* **51**, 569 (1955).
[44] Tobolsky, A. V., "Stress Relaxation Studies of Viscoelastic Properties of Polymers", Chapter in Reference 2.
[45] Tobolsky, A. V., and Catsiff, E., *J. Polymer Sci.* **19**, 111 (1956); *J. Appl. Phys.* **27**, 673 (1956); RUBBER CHEM. & TECHNOL. **30**, 427 (1957).
[46] Treloar, L. R. G., *Trans. Faraday Soc.* **39**, 36 (1943); RUBBER CHEM. & TECHNOL. **16**, 746 (1943); **17**, 296 (1944).
[47] Treloar, L. R. G., *Trans. Faraday Soc.* **40**, 59 (1944); RUBBER CHEM. & TECHNOL. **17**, 813 (1944).
[48] Treloar, L. R. G., *Proc. Royal Soc.* (London) **B139**, 506 (1952).
[49] Treloar, L. R. G., "Structure and Mechanical Properties of Rubberlike Materials", Chapter 5 in Reference 6.
[50] Wall, F. T., *J. Chem. Phys.* **10**, 485 (1942); **11**, 527 (1943); RUBBER CHEM. & TECHNOL. **15**, 806 (1942); **17**, 392 (1944).
[51] Wood, L. A., "Creep of a Pure-gum Rubber Vulcanizate from −60° to +50° C", *J. Research Natl. Bureau of Standards* (in press).
[52] Wood, L. A., *J. Research Natl. Bureau of Standards* **60**, 193 (1958).
[53] Wood, L. A., and Roth, F. L., *J. Appl. Phys.* **15**, 781 (1944); RUBBER CHEM. & TECHNOL. **18**, 367 (1945).

FRICTION AND ABRASION OF RUBBER *

A. SCHALLAMACH

THE BRITISH RUBBER PRODUCERS' RESEARCH ASSOCIATION,
WELWYN GARDEN CITY, ENGLAND

I. INTRODUCTION

Modern work[1] on the mechanism of sliding friction and frictional wear of solids has brought to light the important role played in these processes by the microtopography of the rubbing surfaces whose roughness makes the true area of contact small and produces high pressures where the asperities meet. Under the influence of these local stresses, irreversible junctions are formed between the rubbing members, and the frictional work done in sliding is the energy necessary to break these junctions. Thus, friction of solids is a concomitant of abrasion, and the frictional force is proportional to the true area of contact.

In contrast, rubber friction is not necessarily accompanied by abrasion. Roth, Driscoll and Holt[2] were the first to show that even after prolonged sliding on plate glass rubber samples suffer no abrasive wear. There is no evidence for rubber forming irreversible junctions with track materials unless very high temperatures are sustained during sliding, and the origin of rubber friction must be sought in a source other than that of solid friction. A suggestion as to its origin will be made in the following section.

In spite of this difference between rubber and solid friction, the line of attack which has proved so successful in the theory of solid friction can with advantage be brought to bear on rubber friction. Attention must, however, be paid to the fact that rubber generally experiences friction and wear under conditions different from those common with substances such as metals and fibers. Rubber hardly ever slides on other rubberlike materials but on tracks grossly dissimilar from it in surface texture, chemical constitution and elastic behavior, road surfaces being the most obvious and important examples. It will be shown in the subsequent pages that the concept of local stress concentrations in the area of contact between rubber and track goes a long way in accounting for the observed effects.

FREQUENTLY USED SYMBOLS

A	True area of contact
d	Linear dimension of abrasive grain
E	Elastic modulus defined by Equation (10)
F	Frictional force
L	Normal load
p	Nominal normal pressure
r	Radius of curvature of asperities
s	Spacing of abrasion patterns
t	Temperature ° C
T	Temperature ° K

* Reprinted from *Wear*, Vol. 1, pages 384–417 (1958).

v	Sliding velocity
W	Abrasion per unit area
μ	Coefficient of friction
φ	Force factor defined by Equation (6)

II. VELOCITY AND TEMPERATURE DEPENDENCE OF RUBBER FRICTION

Dynamic rubber friction has a small but definite positive velocity coefficient at low speeds, first demonstrated by Roth et al.[2]. This effect has the interesting consequence that rubber can slide on a horizontal track at constant velocity when a constant tangential force is applied. In this state of motion the tangential force is, of course, equal to the frictional force. The velocity coefficient being small, small differences in the tangential force produce large differences

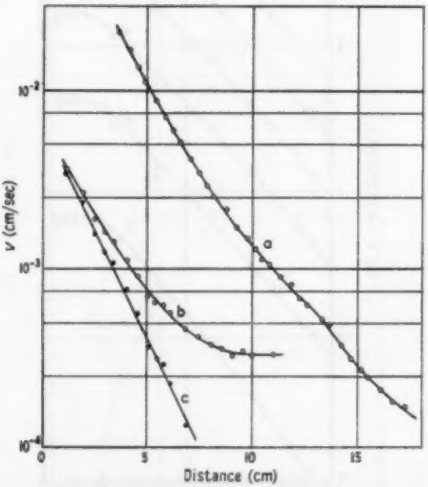

FIG. 1.—Sliding velocity of an acetone-extracted unfilled vulcanizate of natural rubber on finely ground glass plotted against sliding distance. Normal load, 6.44 kg. Tangential force: (*a*), 5.8 kg; (*b*), 7.8 kg. Curve (*c*): curve (*b*) replotted as log [(*v*—0.00036)cm/sec]. From Reference 3.

in the sliding velocity. A measuring method based on this effect[3] is therefore very sensitive. It is found experimentally, however, that the actual sliding behavior of rubber is complicated by time and distance effects which, though transient, can considerably retard attainment of a steady state. This is exemplified by Figure 1. The graphs give the sliding velocities of an acetone-extracted unfilled vulcanizate of natural rubber on a finely ground glass track at two different tangential forces, the larger force having been applied after the experiment with the lower force. It may be mentioned here that in certain measurements it is advisable to extract the samples in order to prevent contamination of the track by impurities oozing out of the samples. This precaution is essential when experiments are carried out at variable temperature, for the rate at which the contamination occurs increases with increasing temperature.

With a pulling force of 5.8 kg, the sliding velocity decreases rapidly throughout the experiment and the sample eventually stops. Despite the initial motion

produced by it, 5.8 kg is obviously lower than the equilibrium force of static friction. On increasing the tangential force to 7.8 kg the sample starts anew, slows down again, but, in contrast to the previous case, reaches a finite steady-state velocity. When the values of this second curve are replotted as log ($v - v_{\text{steady state}}$) the straight line (*c*) is obtained. The effects illustrated by Figure 1 have their counterpart in a slow rise of the frictional force when the sample is moved at constant velocity, as was shown by Roth et al.[2] The phenomenon appears to be due to surface conditioning of the sample; on abrasive tracks where the surface is constantly renewed the effect is absent or very small.

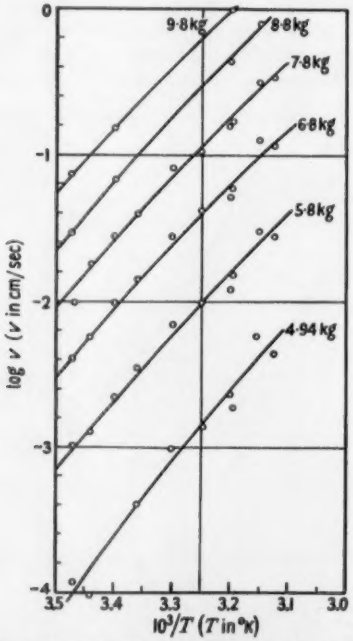

FIG. 2.—Steady-state sliding velocity of an acetone-extracted unfilled vulcanizate of natural rubber on silicon carbide cloth plotted against reciprocal absolute temperature for various tangential forces. Normal load, 6.44 kg. From Reference 3.

For this reason, most experimental results have been obtained on abrasives. Sliding velocities given in the following two graphs (Figures 2 and 3) are all steady-state values.

The most interesting property of sliding velocities is their pronounced temperature dependence. Figure 2 gives the logarithm of the sliding velocity on silicon carbide paper of the natural rubber compound referred to in Figure 1 as function of the reciprocal absolute temperature, the tangential force being the parameter. The curves can be approximated to straight lines and be described by Equation (1)

$$v_{\text{constant force}} = A' \exp(-E'/RT) \qquad (1)$$

where A' and E' are constants.

The force dependence of the sliding velocity can be derived from the curves of Figure 2 by interpolation, the result being shown in Figure 3. Defining static friction as that value of the tangential force at which the velocity approaches zero, a figure of about 5 kg is obtained for sliding on silicon-carbide cloth. At forces above about 7 kg, the curves are nearly straight lines, indicating that an exponential relation between sliding velocity and frictional force obtains at sufficiently high dragging forces.

Equation (1) is strongly reminiscent of the relation between fluidity and temperature observed in viscous flow and also in other phenomena generally referred to as rate processes. In these processes, the elementary particle, or

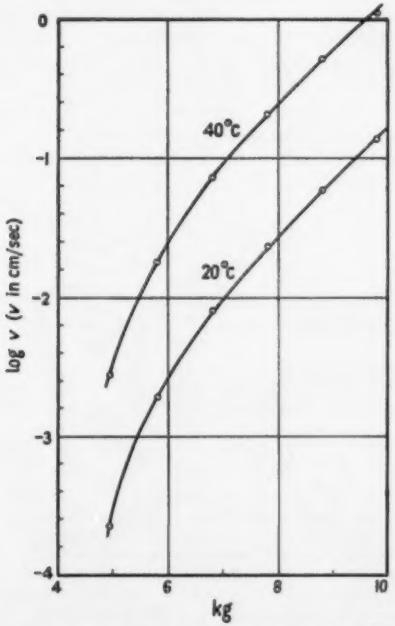

FIG. 3.—Steady-state sliding velocities at two temperatures on silicon carbide cloth plotted against tangential force. Data derived from Figure 2. From Reference 3.

complex of particles involved in the process are thought to be confined to potential wells of depth E' from which they can escape only when they attain through thermal collision kinetic energy equal to, or exceeding E'. The rate of the jumps is proportional to the Boltzmann factor $e^{-E'/RT}$. In the absence of external stress, the direction of escape is random but an applied stress tends to direct the jumps in such a way as to relieve the stress.

It has been suggested[3] that in frictional sliding of rubber the molecular force fields of rubber and track interlock at the true area of contact, similar to the interaction between parallel molecular layers in laminar viscous flow, and that the frictional force of rubber is akin to viscous forces. No breaking of molecular bonds and therefore no frictional wear need be invoked to account for the frictional force in this picture.

The stress dependence of the sliding velocity shown in Figure 3 suggests that rubber friction resembles non-Newtonian rather than Newtonian flow in that the velocity is not proportional to the tangential stress. Following Eyring[4], this effect is thought to be due to a modification of the intermolecular field by the large tangential stresses occurring in rubber friction which effectively lower the energy barrier surrounding the potential well. In the region where the logarithm of the sliding velocity is proportional to the tangential force, the results shown in Figures 2 and 3 can be expressed by Equation (2):

$$v = v_0 \exp - (E_a - \gamma F)/RT \tag{2}$$

where v_0 and γ are constants, E_a is the activation energy and F, the frictional force. The experimentally determined activation energies are 19,880 cal/mole for sliding on ground glass and 16,160 cal/mole on silicon carbide. It is interesting to note that the activation energy for dielectric relaxation has the similar value of about 17,000 cal/mole, suggesting that the moving complexes are of the same order of magnitude in the two processes.

The temperature coefficient of the frictional force as derived from Equation (2) is then given by Equation (3):

$$(\partial F/\partial T)_v = -\frac{R}{\gamma} \log \frac{v_0}{v} \tag{3}$$

This coefficient is always negative because of the high value of v_0 which, as estimated from Figure 2, amounts to 10^{13} cm/sec.

The physical significance of v_0 is as follows:

If λ is the length of the jump executed by the moving complexes after successful activation, then v/λ is the transition rate k, which may be written as

$$k = k_0 \exp - \frac{E_a - \gamma F}{RT}$$

According to the rudimentary theory outlined above, k_0 should be the relevant vibrational frequency of the moving complexes. With 10^{-7} cm as a likely value of λ, k_0 is 10^{20} sec^{-1} which is clearly too high by many orders of magnitude for this interpretation to be valid. The large value of k can be accounted for on the basis of a theory due to Eyring, which considers activation in physical processes as a chemical reaction[4]. In this theory, due consideration is given to the fact that the number of complexes having at any time the activation energy E_a is not solely proportional to the Boltzmann factor $\exp - E_a/RT$ but is also proportional to the ratio of the number of sites available to activated complexes to the number of sites at the disposal of not activated complexes. For this reason, the constant k_0 is actually the product of the vibration frequency and the ratio of sites in the two states. This ratio is introduced in Eyring's theory as $\exp \Delta S/R$; ΔS is called entropy of activation. A large k_0 accordingly indicates that there are many more possible sites for activated than for not activated complexes. This point has been discussed in detail by Kauzmann[27].

Work on the velocity dependence of rubber friction so far referred to has been carried out at velocities not exceeding about 1 cm/sec. With higher velocities, sliding at constant tangential force becomes unstable, presumably because of the temperature rise due to dissipation of frictional energy. It then becomes necessary to reverse the technique and measure frictional forces at prescribed velocities. Experiments have been carried out which allowed the frictional temperature rise to be measured at the same time[6]. The slider was a thermocouple giving a geometric contact area of about 1 mm^2 which was pressed

against a rotating rubber disc. Figures 4(a) and (b) give the results obtained on an unfilled and a carbon black-filled compound of natural rubber. It will be seen that the initial increase of the coefficient of friction with increasing velocity is not maintained at higher speeds but gives way to a gradual decrease.

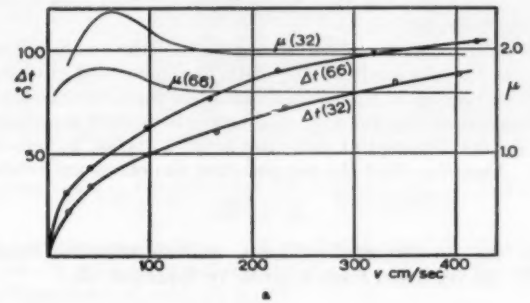

a

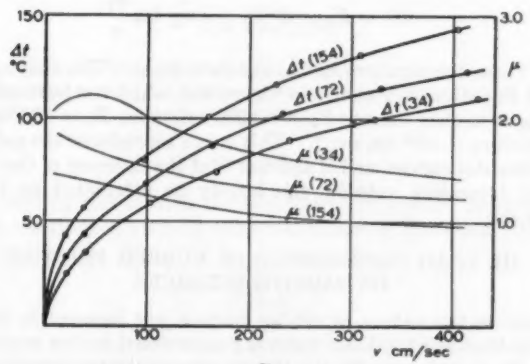

b

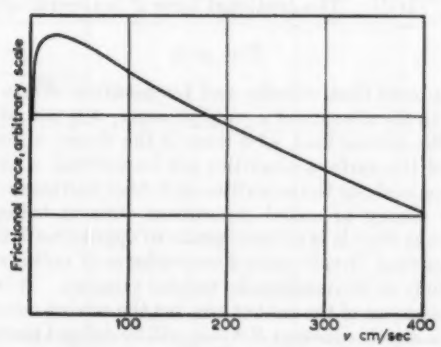

c

FIG. 4.—Frictional temperature rise Δt and coefficients of friction μ plotted against sliding velocity (a), on an unfilled vulcanizate of natural rubber; (b), on a natural rubber tire tread compound filled with 45 phr MPC black. The average normal loads (g) are given in brackets. (c), theoretical velocity dependence of the frictional force, calculated from Equation (5). Graphs (a) and (b) from Reference 5.

The load dependence of the coefficient of friction made evident in these graphs will be treated in detail in later sections.

The considerable temperature rise is approximately proportional to the square root of the velocity. This dependence has been predicted theoretically by Jaeger[6] for very high velocity but appears to be valid for a wider range than given by Jaeger's theory.

It can be shown that the observed decrease of the coefficient of friction at higher velocities agrees qualitatively with the theory of rubber friction expressed by Equation (2) if allowance is made for the simultaneous temperature rise. The comparison can be only qualitative because it is necessary to extrapolate from results obtained at velocities below 1 cm/sec to velocities reaching 400 cm/sec. Assuming that the temperature rise obeys the relation

$$\Delta t = c\sqrt{v} \tag{4}$$

suggested by the experimental evidence, and substituting Equation (4) in Equation (2), the frictional force is given by Equation (5):

$$\gamma F = E_a - R(T_0 + c\sqrt{v}) \log \frac{v_0}{v} \tag{5}$$

where T_0 is room temperature in the absolute scale. The shape of the curve predicted by Equation (5) is shown in Figure 4(c), which has been calculated with the following numerical values: E_a = 20,000 cal/mole, T_0 = 300° K, c = 5 deg $cm^{-1/2}sec^{1/2}$ and $v_0 = 10^{13}$ cm sec^{-1}. This curve reproduces the salient features of the experimental curves, and it appears that the decrease of the coefficient of friction with increasing velocity can largely be attributed to the frictional temperature rise.

III. LOAD DEPENDENCE OF RUBBER FRICTION ON SMOOTH SURFACES

The views on the nature of rubber friction put forward in the preceding section imply that the frictional force is proportional to the true area of contact A, and thus conform with the theory of solid friction briefly reviewed in the INTRODUCTION. The frictional force F is accordingly given by Equation (6)

$$F = \varphi \cdot A \tag{6}$$

and it will be assumed that velocity and temperature effects involve only the force factor φ. In the absence of a yield pressure, it is not admissible to put A proportional to the normal load, as is done in the theory of solid friction where shape and size of the surface asperities are immaterial. An assumption has therefore to be made about the asperities on rubber surfaces which is conducive to treatment by theory or model experiment without being too far-fetched. From both points of view it is advantageous to approximate the rubber surface to an array of identical, closely spaced hemispheres of radius r[7]. This model is meant to apply only to conventionally molded samples. It is further assumed that the elastic behavior of the rubber can, for the strains occurring here, be described by a single elastic constant E which will be defined presently. It follows from dimensional considerations that the true area of contact with an ideally smooth plane under the nominal pressure p must obey a relation of the form

$$A = r^2 \Sigma c_n (p/E)^{\delta n} \tag{7}$$

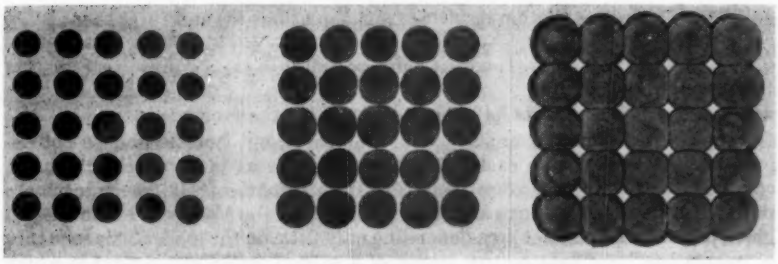

FIG. 5.—Contact area of model rubber surface under 3 different pressures: (a), 2.14 kg/cm²; (b), 7.75 kg/cm²; (c), 66.0 kg/cm². Reduced 0.85 ×.

where the c's and β's are constants. A plotted against (p/E) should yield a universal curve for rubbers of different stiffness. The coefficient of friction derived from Equations (6) and (7) is:

$$\mu = \varphi/E \Sigma c_n (p/E)^{\beta n - 1} \tag{8}$$

and no longer contains the radius r of the asperities.

Model experiments on the compression of large hemispheres[7] have shown that the results fit quite accurately the equation

$$A = \text{const. } p^{2/3} \tag{9}$$

This simple relation agrees with the theoretical expression derived by Hertz[8] from classical elasticity theory for spherical contacts, Equation (10)

$$A = \left(\frac{9}{16}\frac{L}{E}r\right)^{2/3} \tag{10}$$

when the Poisson ratio has the value ½ appropriate for rubber. L is the normal load. Equation (10) will be used to define the effective modulus E.

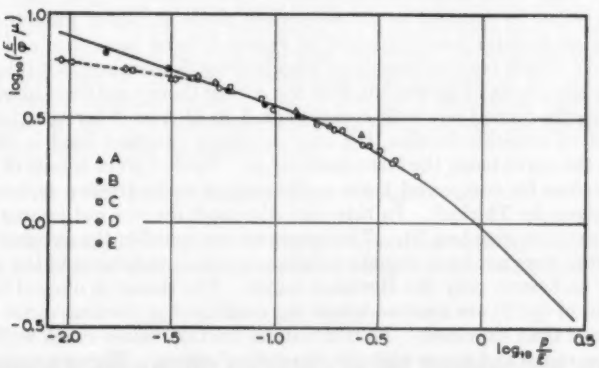

FIG. 6.—Load dependence of the coefficient of rubber friction on plate glass. Full line: theoretical curve determined by means of Equation (11) and the model experiment of Figure 5. A to D, dynamic friction at 0.00216 cm/sec. E, static friction. Values for A to D from Reference 7, for E from Reference 9.

The coefficient of friction resulting from Equations (8) and (9) is then:

$$\mu = (\varphi/E)(p/E)^{-1/3} \tag{11}$$

where numerical constants have been absorbed in the factor φ.

The asperities on rubber surfaces are, however, not isolated and do not deform independently from each other but will jostle as they barrel out during compression. This will cause departure from Equation (11), becoming more pronounced as the load increases and the asperities are squeezed into a solid block presenting a contact area depending only little on the load. This sequence of events has been followed by means of a second model experiment in which a square set of 25 small hemispheres was compressed under variable load. Figure 5 shows the contact areas under 3 different pressures and demonstrates how the asperities at first deform without mutual interference, as is seen from the circular shape of their contact areas, but at higher loads close up finally into a blunted square pattern with little space left in the interstices. The areas of contact under the various loads have been measured, using only theinner 9 hemispheres as the outer hemispheres are subject to end effects. The area so deter-

TABLE I

Compound	E, kg/cm²	φ, kg/cm²
A, unfilled natural rubber	8.88	5.07
B, unfilled natural rubber	18.3	9.12
C, unfilled natural rubber	26.9	12.59
D, natural rubber filled with 50 phr HAF black	41.9	10.47

mined, when divided by the normal load and multiplied with the effective modulus E of the model, should according to Equation (8) represent a universal curve of the product $\left(\frac{E}{\varphi}\mu\right)$ when plotted against (p/E). This curve is shown in the logarithmic plot of Figure 6. At values of (p/E) lower than 0.1, the curve has been continued as straight line of slope $-\frac{1}{3}$ well established by the model experiments with large single hemispheres. This pressure region may be called Hertzian region in contrast to the saturation range at higher pressures.

The experimental points marked in Figure 6 have been obtained on plate glass tracks, which may be considered ideally smooth compared with the rubber, and show the extent of agreement with the simple theory outlined above. The measurements carried out with compounds A to D were determinations of the coefficient of dynamic friction, the only arbitrary constant used in fitting the points to the curve being the force constant φ. Table I gives details of E and φ.

The values for compound E are coefficients of static friction replotted from a curve given by Thirion[9]. In this case, the modulus was not known and had to be adjusted to give best fit. The pressures employed in the dynamic friction experiments were not large enough to bring mutual interference of the asperities into play and cover only the Hertzian range. The theory is obeyed here until low values of (p/E) are reached where the coefficient of friction varies less with normal load than expected. Thirion's static friction values reach well into the saturation range and agree with the theoretical curve. Higher pressures have been employed by Denny[10], who investigated the friction of a number of compounds on polished steel lubricated with olive oil. His results are given in

Figure 7 and show that at large normal loads the coefficient of friction is nearly inversely proportional to the pressure, in agreement with Figure 6.

Denny fitted his results to the empirical Equation (12) the type of which had first been suggested by Thirion[9]:

$$1/\mu A = 1 + 15\,(p/E_0) \tag{12}$$

where A is a material constant (not the area of contact!) and E_0, the compression modulus. According to Equation (12) the coefficient of friction becomes constant at low pressures.

A serious departure from the theory on the load dependence of rubber friction as represented by the full curve in Figure 6 occurs therefore only at low loads. It is suggested that this discrepancy arises from the fact that rubber asperities, even if they can be approximated to hemispheres, are not identical but statistically distributed in size. The influence of this inhomogeneity will

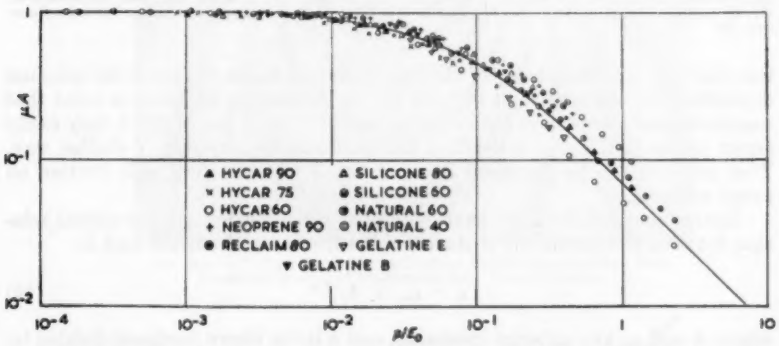

FIG. 7.—Coefficients of dynamic friction on polished steel lubricated with olive oil. Full curve calculated from Equation (12). Figures marked against compounds are BS hardnesses. Velocity 0.01 cm/sec. From Reference 10.

be most pronounced at low normal loads when only the larger asperities are in contact with the track because on increasing the load the true area of contact increases at a greater rate than with identical asperities. A quantitative estimate of this effect can be obtained by assuming that the radii of the asperities have a distribution function $f(r)dr$ becoming zero for a maximum radius r_{max}. At low pressure, where only the largest asperities are involved, the distribution function can be replaced by its tangent, say

$$f(r)dr = \text{const.}\ (r_{max} - r)\,dr \tag{13}$$

Assuming, furthermore, the validity of Hertz's equations both for area of contact and compression of hemispheres, the calculation has the result that

$$\mu_{\text{low}\ (p/E)} = \text{const.}\ (p/E)^{-1/7} \tag{14}$$

Archard[11] has carried out a similar calculation making the assumption that the asperities are identical hemispheres evenly distributed on different levels. The coefficient of friction is in this case proportional to $p^{-1/5}$. It will be seen there-

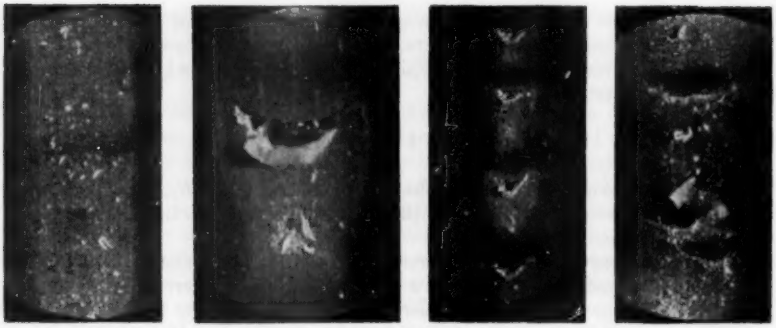

a b c d

FIG. 8.—Traces of a blunt point moving downward on two unfilled vulcanizates of natural rubber with the following moduli: (a), (b) and (c), 11.5 kg/cm²; (d), 18.3 kg/cm². Normal loads and magnifications: (a), 25 g, 30 ×; (b), 80 g, 30 ×; (c) 80 g, 10 ×; (d), 80 g, 30 ×. Photographs (c) and (d) from Reference 13.

fore that any inhomogeneity of the rubber surface tends to reduce the pressure dependence of the coefficient of friction. It should also be borne in mind that macroscopically imperfect contact between rubber and track, which may easily occur under low loads, will affect the frictional behavior in a similar way. This problem will be discussed in more detail when dealing with friction on rough surfaces.

Ratner and Sokolskaya[12] have suggested the following semi-empirical relation between the coefficient of static rubber friction and normal load L:

$$\mu = \mu_\infty + A/L^h \tag{15}$$

where A and μ_∞ are material constants, and h is the Shore hardness divided by 100. At low loads, Equation (15) gives a load dependence difficult to distinguish experimentally from that given by Equation (14), but at higher loads Equation (15) yields, when plotted logarithmically, a curve convex against the log L-axis. In this essential respect, Ratner and Sokolskaya's results differ from those obtained by Thirion, Denny and the author. The divergence is connected with the postulation of a finite coefficient of friction μ_∞ at infinite load, put forward by Ratner and Sokolskaya. We shall return to this point at the end of Section 8.

IV. STRESS CONCENTRATIONS ON RUBBER SURFACES

When rubber slides over a surface with asperities comparable to, or larger than those on the rubber local stress concentrations are produced and abrasion ensues. In treating this matter, a difficulty arises out of the great variety in shape and sharpness of the asperities to be expected on different tracks. In general, only small areas of the asperities will impinge on the rubber. It is known from solid geometry that a small region of any continuous surface can be approximated to an ellipsoid. Employing a sphere as model asperity would therefore not seriously restrict generality. When the load on each asperity is so high that puncture or appreciable penetration of the rubber occur, a cone may be chosen as representative asperity.

Following such considerations, model experiments have been made in which rubber surfaces were scratched by a small hemisphere[13] (1 mm diameter) and by a needle[14] under controlled conditions. Provision was also made for recording the instantaneous tractive forces.

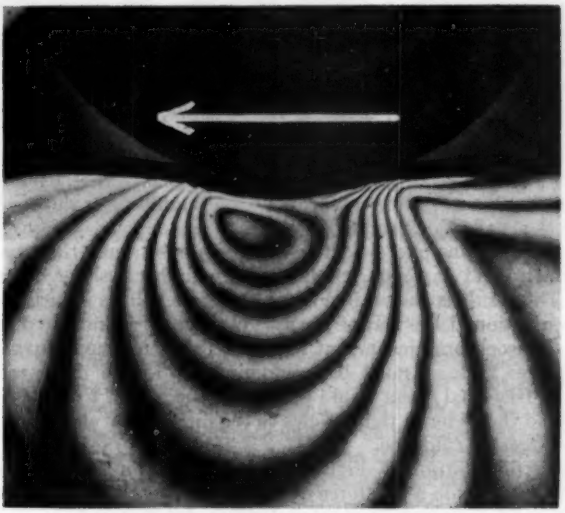

FIG. 9.—(a). Photoelastic picture of stress distribution in rubber under tangential traction of frictional glider. From Reference 13.

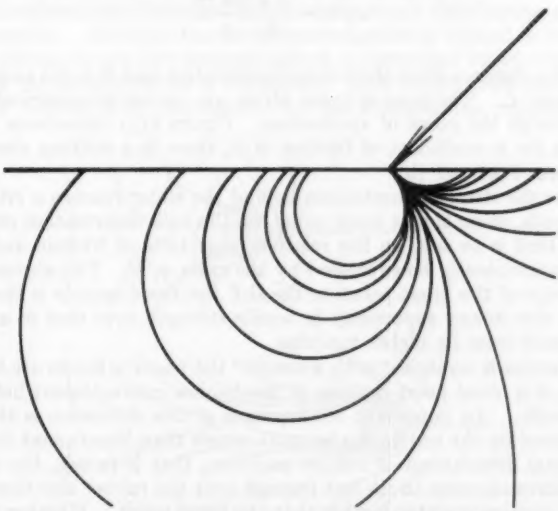

FIG. 9.—(b). Theoretical stress distribution produced by a line force on the edge of a semi-infinite solid.

Examples of traces left by the blunt point on two different compounds are shown in Figure 8. These photographs have been taken with oblique illumination from the right-hand side; the direction of sliding is downward. On the softer of the rubbers hardly any surface damage is created under a load of 25 g (a) but under 80 g a discontinuous trace is produced consisting of lateral tears across the track, one of which is seen in Figure 8(b). Figure 8(c), showing the same trace at lower magnification, demonstrates the periodic nature of the surface damage which has been attributed to a stick-slip mechanism. The rubber adheres frictionally to the hemispherical point and is locally teased out in the direction of sliding until the elastic restoring force exceeds limiting friction and the rubber snaps back. The trace on the harder compound, Figure 8(d), is similar in type but the tears are shallower, less regular and more closely spaced. It has not been possible to produce significant surface damage on carbon-loaded tire tread compounds under the conditions of these experiments.

The stress distribution producing tears like those shown in Figure 8 has been studied by investigating photo-elastically the stresses around the area of contact in the 2-dimensional analogon, employing a cylindrical slider on transparent rubber[13]. The result is shown in Figure 9(a). It will be seen that there is a stress concentration at the rear of the area of contact, as indicated by the close spacing of the isochromatics in that region. This stress concentration, occurring near a free surface, must be predominantly tensile in character. Any failure due to frictional stress would therefore be expected to consist in opening of tears behind the slider at right angles to the direction of sliding, as confirmed by the experimental evidence.

The stress distribution of Figure 9(a) conforms qualitatively to classical theory. In plane strain a line force acting under any angle on the surface of a semi-infinite solid produces a pure radial stress distribution[8]

$$\sigma_\rho = -\frac{2L}{\pi}\frac{\cos\Theta}{\rho}$$

where ρ is the distance from the point of application and Θ is the angle between ρ and the load L. The lines of equal stress are circles symmetrical to L and passing through the point of application. Figure 9(b) reproduces this stress distribution for a coefficient of friction of 2; there is a striking similarity between Figures 9(a) and (b).

Whether the stress concentration behind the slider reaches a critical value or not depends, other things being equal, on the bulk deformation produced by the slider, that is to say, on the relative magnitude of friction and stiffness. This may conveniently be expressed by the ratio φ/E. The absence of tears from the trace of the blunt point on the stiff tire tread sample is therefore not necessarily due to any superiority in tensile strength over that of a pure gum but may result from its higher modulus.

When rubber is scratched with a needle[14] the tractive forces are larger than in the case of a blunt point because of mechanical entanglement between rubber and needle. An important consequence of this difference is that surface damage caused by the needle can be more severe than blunt-point damage and lead to actual detachment of rubber particles; that is to say, the needle can effect primitive abrasion in its first passage over the rubber and therefore take the surface damage one step farther than the blunt point. Whether this occurs or not depends on the mechanical strength of the compound.

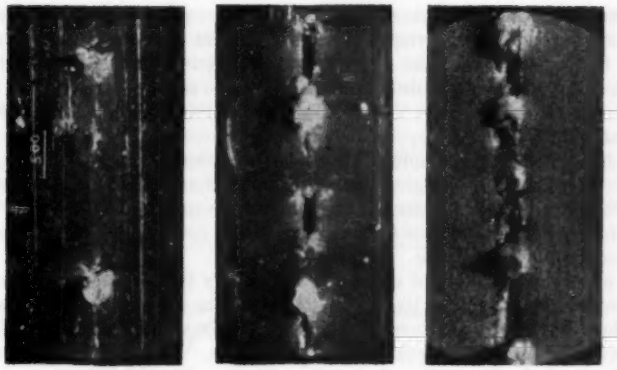

a b c

FIG. 10.—Needle traces on 3 different vulcanizates of natural rubber. (a), unfilled, $E = 11.5$ kg/cm², load 80 g, magn. 13 ×; (b), unfilled, $E = 18.3$ kg/cm², load 50 g, magn. 30 ×; (c), filled with 50 phr MPC black, load 80 g, magn. 30 ×. Photographs (a) and (b) from Reference 14.

A needle trace on the softer of the two unfilled vulcanizates of Figure 8, shown in Figure 10(a), is very similar to that left by the blunt point; the tear resistance of this compound is quite high and amounts to 7.12 kg/cm as defined by Rivlin and Thomas[15]. The harder unfilled vulcanizate of Figure 8(d) has the lower tear resistance of 4.56 kg/cm; as seen from Figure 10(b) the needle here tears out elongated grooves, the trace giving the impression of an incipient scoring mark. The formation of these grooves is explained by the sketch in Figure 11. The family of curves shown are originally equidistant reference lines marked on the surface of the rubber at right angles to the direction of motion. Their subsequent distortion indicates the strain distribution around the entangled needle. Although the stress concentration is highest in front of the needle, no cutting occurs here because failure is prevented by frictional adherence around the circumference of the needle. The rubber tears instead where it first loses contact with the needle, the tears proceeding roughly at right

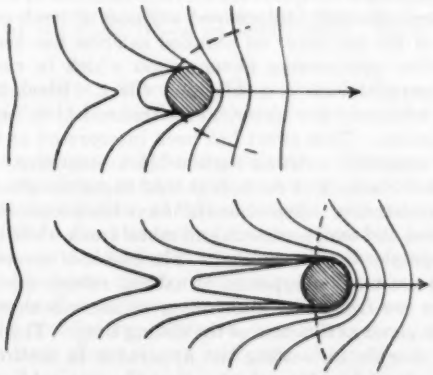

FIG. 11.—Diagrammatic representation of two stages in the deformation of a rubber surface by a needle. The shaded circle is the cross section of the needle.

angles to maximum stress, along the dotted lines. After the needle has passed and the rubber relaxes, the region around the tears turns back through almost 90° and thus gives rise to the grooves seen in Figure 10(b). It may be mentioned in passing that this interpretation of needle traces provides also the reason why it is difficult, if not impossible, to cut soft rubber cleanly with a dry knife blade.

The needle trace on a reinforced compound shown in Figure (10c) differs from all other traces in being continuous but is otherwise similar to that shown in Figure 10(b). It has been pointed out in the original publication[14] that a needle trace will be continuous when the ratio of elastic to frictional forces exceeds a certain critical value.

The exceptional behavior of reinforced rubber both with regard to blunt-point and to needle traces has been attributed to their greater stiffness. It would, however, be premature to draw conclusions from these model experiments as to the abrasion resistance of filled rubbers. The reason why the results cannot be applied without provisos will be discussed in the following section.

V. THE SURFACE CONDITION OF ABRADED, FILLED RUBBER COMPOUNDS

Fillers increase the stiffness of rubber in various degrees depending on quantity and quality of the fillers, the best known of which are carbon blacks. Whatever the filler, most of the stiffening is lost by previous deformation. The phenomenon has been studied by Mullins[16] and more recently by Mullins and Tobin[17]. Once a filled compound has been prestressed, its modulus is lower than that of the virgin material at all stresses lower than the prestress. The absolute value of the modulus and the stress-strain curve of prestressed filled rubber resemble those of unfilled rather than filled compounds. If the abrasion process goes hand-in-hand with the continuous production of large local stresses of the kind suggested by the scratching experiments, the effective stiffness of the surface of filled rubbers should be affected in a similar way. It has therefore been assumed[18] that the surface of abraded filled rubber compounds is covered by a thin, constantly renewed skin the elastic properties of which are not materially different from those of unfilled vulcanizates. For this reason, it would not be appropriate to equate the stiffness effective in the abrasion mechanism with the conventionally determined stiffness of fresh samples.

The existence of the top layer on abraded samples has been demonstrated by means of another prestressing phenomenon which in carbon black-filled compounds runs parallel with the softening effect. Black-filled compounds when new have a relatively low electrical resistance which, however, increases rapidly on deformation. This effect has been interpreted as being due to the breakdown of an originally existing carbon-black structure. The postulated soft skin on abraded black-filled rubbers should therefore also be distinguished by high electrical resistance. Experiments[19] have been made in which both new and abraded samples slid over a smooth and metal track while the resistance between track and sample was determined. The result of measurements carried out with a typical tire tread compound of natural rubber filled with 50 phr of HAF black at two low-frequency alternating voltages is shown in Figure 12, where impedance is given as function of the sliding time. The impedance of the new sample rises sharply on setting the apparatus in motion and reaches a steady-state value about four times higher than the original figure. There is no significant difference between the impedances at the two different frequencies.

After abrasion, the impedance has become frequency-dependent and its equilibrium value has, compared with the fresh sample, risen about 6.5 times at 110 sec^{-1}, and about 26 times at 21 sec^{-1}.

The initial increase of the impedance of the fresh sample is due to deformation of the rubber asperities which are sheared during sliding. The frequency dependence of the impedance after abrasion indicates that the current through the sample has a large capacitive component. The interpretation of this result is that structure breakdown in the surface layer has gone so far that the filler particles are almost completely isolated from each other. The layer has, for

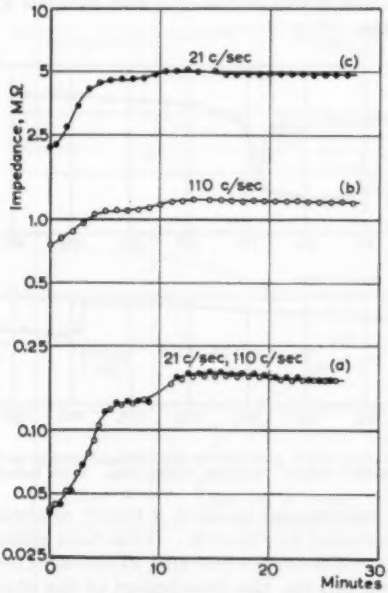

FIG. 12.—Impedance changes during sliding of a carbon black-filled natural rubber vulcanizate plotted against sliding time. (a), new sample; (b) and (c), abraded sample. Velocity, 0.00216 c/sec. From Reference 19.

practical purposes, become a dielectric. That this effect is really due to changes in the surface and not in the bulk of the sample can be shown in the following way.

If, instead of applying an alternating voltage, a direct voltage is connected across the sample, the direct current voltage drop is concentrated in the surface skin and, the layer being thin, should produce a high electric field strength. This, in its turn, should give rise to electrostatic attraction between sample and track, increase the normal load and therefore also the frictional force. This expectation has been borne out by experiment as can be seen in Figure 13. Moderate voltages suffice to increase the frictional force considerably, thus giving independent proof of the existence of an inhomogeneous layer on top of the sample. The time effects shown in Figure 13 are discussed in the original publication.

An estimate for the thickness of the layer can be obtained from the increase

in frictional force under the influence of the applied d.c. potential difference if an assumption is made on the dielectric constant of the layer. The calculation has shown that the order of magnitude of the layer is 10^{-2} cm.

VI. INTRINSIC ABRASION

To judge from the preceding section, no distinction need be made between filled and unfilled rubbers if a picture of the abrasion mechanism is deduced from our scratching experiments. The qualitative difference in surface damage on filled and unfilled compounds observed during that investigation can be attributed to the fact that it was carried out with samples which had undergone no prestressing effects.

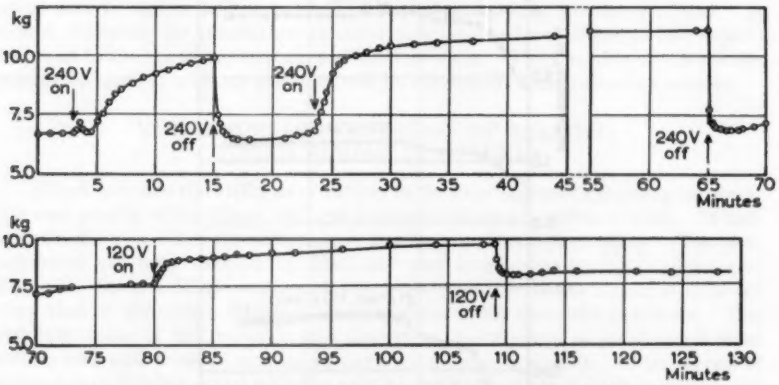

FIG. 13.—The effect of d.c. potentials on the frictional force of an abraded, carbon black-loaded sample. Abscissa, sliding time. From Reference 19.

Bearing these considerations in mind, a theory of abrasion[13] has been built up on the results illustrated by Figure 8. It has been assumed that tears across the path of track asperities are the first and, at the same time, rate-determining stage in the abrasion process, the detachment of the abraded particle during subsequent passes of the abrasive over the tear being governed by a mechanism similar to that discussed in connection with Figure 11. The volume of the abraded particle has been taken to be proportional to the cube of the length of the original tears. Inspection of the photographs in Figure 8 indicates that these tears are of the same order of magnitude as the width of the trace. It has therefore been assumed that length of tear and diameter of the area of contact are proportional to each other so that it only remains to determine the area of contact under various conditions. Model experiments in which a number of compounds have been indented by a large sphere have shown that the diameter of contact a follows to a good approximation the cube root law

$$a = \text{const. } p^{1/3} \tag{16}$$

which has also been found valid for the compression of rubber spheres. It follows from Equation (16) and dimensional considerations that the abrasive wear W per unit area of sample should be given by Equation (17):

$$W = \text{const. } r(p/E) \tag{17}$$

where r is the radius of curvature at the tip of the abrasive grain. According to Equation (17), rubber abrasion should increase linearly with increasing normal load.

When attempting to verify experimentally a theoretical load dependence of rubber abrasion, care must be taken to avoid contamination of the track by impurities issuing from the rubber. As in the case of friction experiments previously referred to, this can be achieved by acetone-extraction of the samples. The erratic nature of the results obtained otherwise is illustrated by Figure 14. Two tire tread samples of natural rubber one of which had been extracted, were

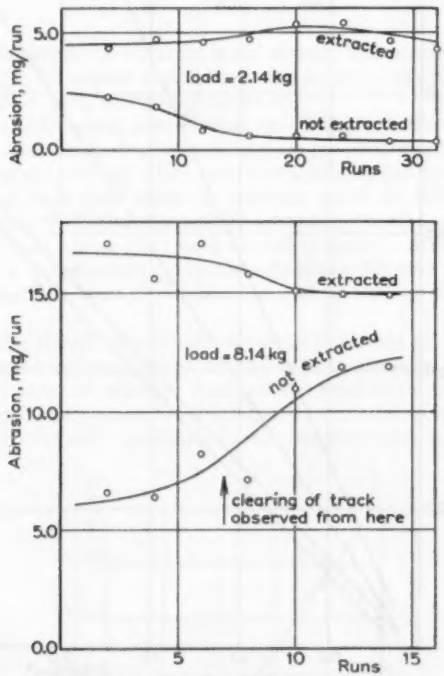

FIG. 14.—Variations in the rate of abrasion of a not-extracted and an extracted natural rubber vulcanisate filled with 50 phr MPC black when using repeatedly the same silicon carbide track (length, 60 cm).

repeatedly abraded each on its own track of 60 cm length. Under a load of 2.14 kg, the rate of abrasion of the extracted sample remained reasonably constant but the rate of the not-extracted sample decreased steadily to very low values. The track became progressively darker in the process. Under the higher load of 8.14 kg. the rate of abrasion of the extracted sample decreased slightly but the abrasion of the not-extracted sample *increased* considerably, while a gradual clearing of this track was observed. In this latter case the sample appeared to function like a rubber eraser. In general, it has been found that contamination of the track becomes progressively more serious with decreasing rate of abrasion. It also tends to be more troublesome with synthetic than with natural rubber.

The results given in Figure 15 have been obtained with flat extracted and vacuum-dried samples on fresh abrasive (Garnet paper with a mean grain size of 0.13 mm). Furthermore, the direction of abrasion was reversed after each run of 64 cm in order to prevent the formation of socalled abrasion patterns which are the subject of the following section. Abrasion taking place under

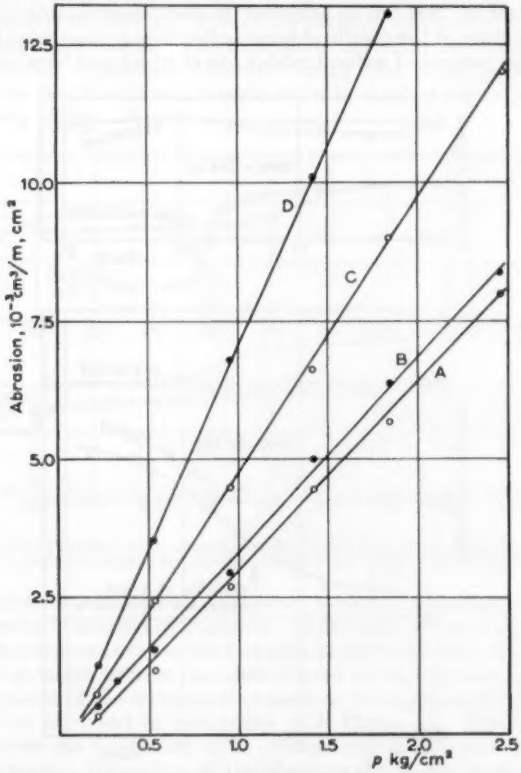

FIG. 15.—Intrinsic abrasion plotted against normal pressure. Compounds: A, Krylene ("Cold rubber") filled with 50 phr HAF black; B to D, natural rubber filled with: B, 50 phr HAF black; C, 75 phr fine thermal black; D, 130 phr Pattinson's activated $CaCO_3$. Velocity, 0.66 cm/sec. From Reference 13.

these conditions will be called "intrinsic" abrasion. Figure 15 shows that the proportionality of intrinsic abrasion and normal load given by Equation (17) is confirmed by experiment.

Equation (17) predicts also that abrasion should be proportional to the radius of curvature of the grain but independent of its size. Two distinct possibilities arise here. In the case of polyhedral grains of different grade there is no *a priori* reason why the sharpness of the corners should be affected by their size so that abrasion should be independent of the coarseness of the abrasive. This conclusion has been tested by carrying out abrasion experiments on garnet papers of different grades; the result is given in Table II.

TABLE II

ABRASION IN 10^{-3} cm^3/m, cm^2 ON GARNET PAPER OF DIFFERENT COARSENESS (FROM REFERENCE 13)

Grain size, mm	0.13		0.29		0.63	
Normal pressure, kg/cm^2	0.53	1.84	0.53	1.84	0.53	1.84
Natural rubber with 50 phr HAF black	1.60	6.09	1.76	6.82	1.81	8.97
Natural rubber with 75 phr fine thermal black	2.00	10.05	2.97	12.05	3.23	13.70
Krylene with 50 phr HAF black	1.43	5.96	1.83	7.50	2.11	10.10

Table II shows that while abrasion is not strictly independent of the coarseness of the abrasive, an almost fivefold increase in grain size leads in the worst case to no more than 70% increase in abrasion.

In contrast to polyhedral grains, wear on abrasive surfaces which can be approximated to close-packed spheres should be proportional to the grain size. Such abrasives are not available but road surfaces may fall into this category. A few experiments have been made on concrete roads of different roughness and it has been found[13] that in this specific instance abrasion on a coarse track was almost four times higher than on a smoother track. Although it was not possible to make a quantitative comparison between the two roughnesses, the result confirms that the laws of abrasion depend in part on the nature of the track.

The tests of the theory of intrinsic abrasion discussed so far concern only the influence of external parameters on the rate of abrasion. An important test of any theory must be whether it allows the relative intrinsic abrasion resistances of any two compounds to be predicted from their physical properties. In this respect only broadly qualitative relations have been ascertained up to

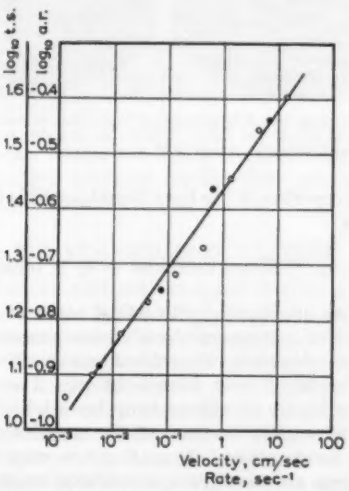

FIG. 16.—Logarithm of the intrinsic abrasion resistance in mg^{-1} plotted against sliding velocity, and logarithm of tensile strength in kg/cm^2 plotted against rate of elongation of an unfilled GR-S vulcanizate. Full points: intrinsic abrasion resistance (a.r.). Tensile strength data from Reference 21.

now. It has been pointed out in section IV that the original tears assumed to be the dominant factor in abrasion resistance are due to tensile failure. Abrasion should therefore increase with decreasing tensile strength. According to Equation (17), abrasion should also increase with decreasing stiffness. It is interesting to note in this context that in empirical attempts[20] to correlate ab-

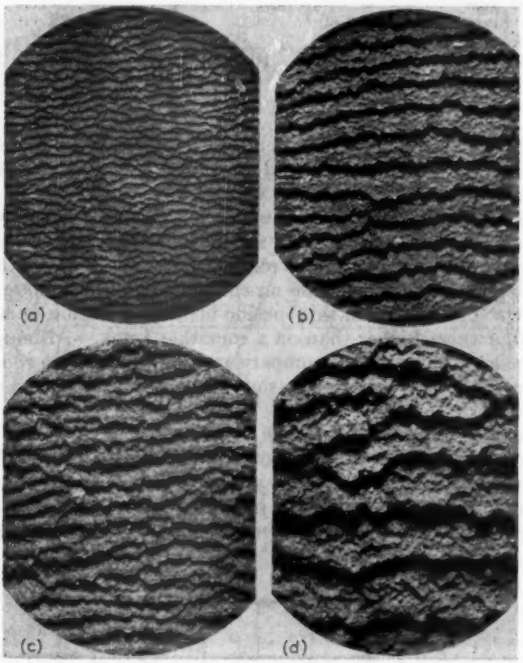

FIG. 17.—Abrasion patterns on two different carbon black-filled vulcanizates of natural rubber. (a) and (c), 45 phr HAF; (b) and (d), 25 phr HAF. Tracks: (a) and (b), fine tarmac; (c) and (d), coarse concrete. Direction of abrasion upward. Magn. 10.8 ×.

rasion with physical properties it has been found possible to establish correlation equations of the type

$$W = a_0 + a_1 \times \text{Shore hardness} + a_2 \times \text{tensile strength}$$

where a_0, a_1 and a_2 are constants. Statistical work of this kind does not, of course, involve a physical picture of the abrasion process.

In assessing relative abrasion values from tensile strength and stiffness, two qualifications must be taken into consideration. The stiffness operating in abrasion is that of the highly prestressed top layer which is lower than that of the bulk material. Secondly, because of the small scale of the elementary abrasion process the local rates of elongation are very high. If for example the contact area between abrasive grain and rubber is about 1/100 mm in diameter, a sliding velocity of 1 cm/sec will give a rate of extension-to-break of about 100,000%/sec. At such rates, tensile strength may appreciably differ

from that determined by conventional methods. Greensmith[21] has recently studied the variation of tensile strength with rate of elongation of rubber compounds and has found that the tensile strength of unfilled GR-S increases pronouncedly with increasing rate of elongation. This compound offers therefore an opportunity to investigate the connection between tensile strength and abrasion on one and the same compound by carrying out abrasion experiments at varying velocity. The result of such measurements and Greensmith's data are given in Figure 16. In the 1000-fold range of velocities covered, tensile strength as function of rate, and intrinsic abrasion resistance (assessed here as the reciprocal of abraded weight for a given track length) as function of velocity

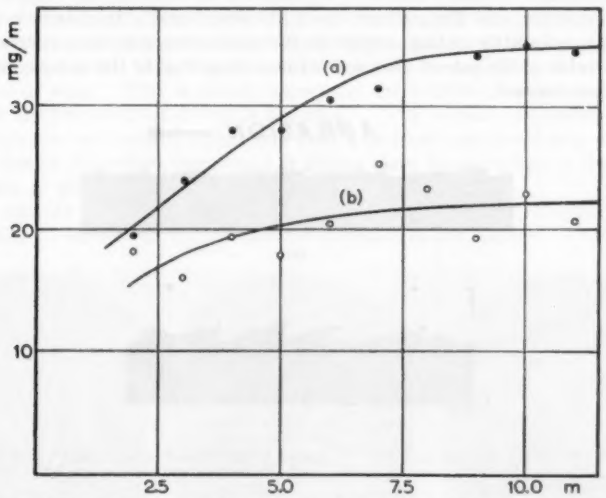

FIG. 18.—Rate of abrasion of an unfilled vulcanizate of natural rubber plotted against distance travelled. (a), sample abraded in constant direction; (b), direction of abrasion changed by 90° every 50 cm. Track: silicon carbide cloth. From Reference 18.

obey the same power law within the limits of experimental error. This result appears to be confirmatory evidence for the close connection between tensile strength and intrinsic abrasion.

VII. THE ABRASION PATTERN

When rubber is abraded without change of direction, sets of parallel ridges are often found on the surface of the samples at right angles to the direction of motion which have been called "abrasion patterns"[18]. Four examples are shown in Figure 17. These particular photographs have been obtained during experiments carried out under laboratory conditions on actual road surfaces, where for reasons to be discussed presently the phenomenon is more readily produced than on commercial abrasives. Another advantage of working on road surfaces is that the need for extraction is largely obviated since road dust prevents the worst effects of smearing. The action of the dust is not understood in detail but appear to be similar to that of pounce.

Figure 17 exhibits clearly two of the relevant characteristics of abrasion

patterns. Their intensity increases with increasing coarseness of the track, and it also increases with decreasing stiffness of the compound. A third, and possibly the most important property of abrasion patterns is that they increase the rate of abrasion. This has been shown by the following experiment. Two samples of the same compound were abraded on the same track but only one was allowed to develop a pattern. On the other sample, formation of pattern was prevented by periodically changing the direction of abrasion by 90°. In other words, the comparison sample underwent only intrinsic abrasion. The rates of abrasion in the two series of measurements are shown in Figure 18 as function of the length of the abrasive path. As seen from Curve (*a*), the rate of abrasion at constant direction increases for a considerable time before becoming constant and the pattern has fully developed. In intrinsic abrasion, Curve (*b*), only little change occurs in the intial stages of the experiment and the final value of the rate of abrasion is lower than that of the sample on which a pattern has formed.

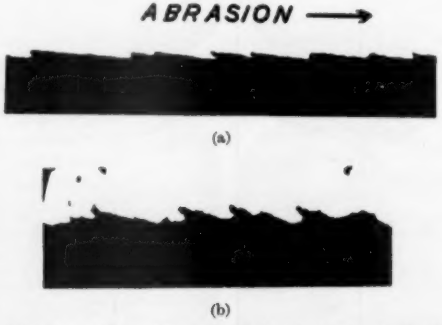

FIG. 19.—Profiles of abrasion patterns: (a), unfilled vulcanizate of natural rubber, abraded under 1.6 kg/cm² on silicon carbide cloth, magn. 5 ×; (b), worn tire surface, horizontal magn. 30 ×, vertical magn. 42.5 ×. From Reference 18.

The explanation of the additional wear caused by abrasion patterns emerges from an examination of their profiles. Cross sections through two different abrasion patterns are reproduced in Figure 19 and show, first of all, that the phenomenon as it occurs on tires resembles in all essentials its laboratory-produced counterpart. The saw teeth seen in both profiles point against the direction of abrasion. When moving over track or road, they are bent backward, thus exposing their underside to abrasion and protecting from abrasion part of the surface in their rear. This gives rise to the peculiar "undercutting effects. The teeth wear progressively thinner until the crests are bodily torn off leaving blunt edges, some of which are seen in Figure 19. In the meantime, the ridges continue to grow out of the underlying bulk material and the pattern is to a certain degree self-perpetuating. When keeping a pattern under observation during an abrasion experiment, it is found that it maintains its general configuration for short times but moves as a whole across the surface in the direction of abrasion[18]. The reason is that the attack of the abrasive on the rubber has, as it were, a forward component.

Because of the great difference in scale between the size of the particles coming off in intrinsic abrasion and the almost macroscopic size of the crests seen in Figure 19, the additional volume loss due to abrasion patterns can constitute a

TABLE III

RATIO, IN %, OF THE ABRASION OF A NATURAL RUBBER COMPOUND FILLED WITH 25 PHR HAF BLACK TO ABRASION OF A COMPOUND FILLED WITH 45 PHR HAF BLACK ON DIFFERENT TRACKS (SEE FIGURE 17)

Intrinsic abrasion	100
Fine tarmac	114
Coarse concrete	135

significant proportion of the total abrasive wear. This contribution to abrasion will be referred to as "pattern abrasion".

As different compounds have different propensities to pattern formation, the relative abrasion rating of given rubber samples depends, in the presence of abrasion patterns, on the intensity of the patterns, and no generally valid figure can be assigned to it. A rating can be quoted only for a given test or for given conditions of wear. This is clearly shown by the relative abrasion figures obtained for the two samples shown in Figure 17. The intrinsic abrasions of these compounds are very nearly equal but once a pattern has developed on them, the abrasion of the softer compound is higher than the abrasion of the harder compound, as shown in Table III.

With equally developed patterns, the relative rates of pattern abrasion may be expected to depend on the mechanical strength of the rubber. Comparison

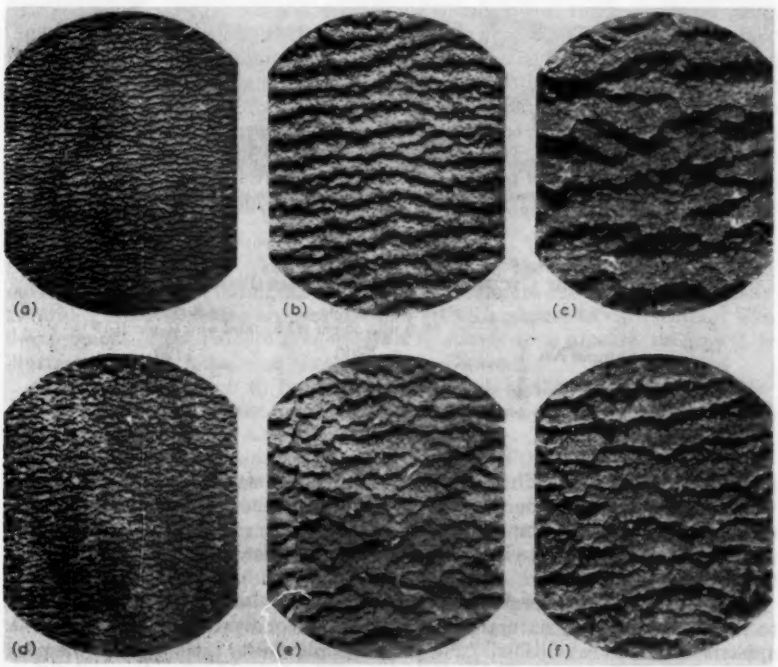

FIG. 20.—Abrasion patterns on vulcanizates filled with 50 phr HAF black. (a), (b), and (c), natural rubber, (d), (e) and (f). GR-S (Krylene). Tracks: (a) and (d), fine tarmac; (b) and (e), concrete; (c) and (f), coarse tarmac. Direction of abrasion, upward. Magn. 10.8 ×.

with experimentally determined strength data should in principal be easier here than in the case of intrinsic abrasion since the larger scale of the phenomenon reduces the rates of strain by several orders of magnitude. An example of similar-sized patterns giving different relative rates of pattern abrasion is provided by carbon black-filled compounds of natural rubber and GR-S. Abrasion patterns produced on these compounds when sliding over different road surfacings are shown in Figure 20. This set of photographs indicates certain differences in the appearance of the abraded surfaces which may be due to different mechanisms of failure operating on the two compounds.

The corresponding relative abrasions are given in Table IV.

TABLE IV

RATIO, IN %, OF THE ABRASION OF A GR-S (KRYLENE) COMPOUND FILLED WITH 50 PHR HAF BLACK TO THE ABRASION OF A NATURAL RUBBER COMPOUND FILLED WITH 50 PHR HAF BLACK ON DIFFERENT TRACKS (SEE FIGURE 20)

Intrinsic abrasion	94
Fine tarmac	107
Concrete	117
Coarse tarmac	138.5

The mode of mechanical failure in pattern abrasion has not yet been definitely established but is thought to be intermediate between tensile break and tear propagation. The tensile strength of the GR-S mix is slightly lower than that of the natural rubber compound, the values being respectively 222 kg/cm² and 241 kg/cm². As for the resistance to tear propagation, the author has carried out a few measurements under the following conditions. A "simple extension" ("trousers")[15] tear testpiece was periodically loaded with an adequate weight until the sample was torn through. The number of cycles necessary to achieve this was taken to be a measure of resistance to tear propagation. The samples were 1 mm thick and 2.54 cm wide, the weight was 414 g

TABLE V

NUMBER OF CYCLES TO FAILURE IN TEAR PROPAGATION

	Natural rubber filled with 50 phr HAF	GR-S (Krylene) filled with 50 phr HAF
Sample No. 1	7800	1420
2	9120	48
3	8760	117
4	8920	2040
Mean	8650	922

and the period of the loading cycle 0.82 sec. When starting the tear, the load was applied for 0.36 sec during each cycle but this time decreased to about 0.14 sec when the tear was completed. Table V gives the results obtained with the two compounds referred to in Table IV. The total length of the tear was 10.5 mm.

In spite of the considerable scatter of the GR-S values, the better resistance to tear-propagation of natural rubber under the conditions of this experiment appears to be well established. No general applicability is claimed for the particular numerical values in Table V, but it will be seen that the observed difference in pattern abrasion on natural rubber and GR-S compounds agrees qualita-

tively with the differences in mechanical strength thought to govern pattern abrasion. Similar results have been obtained with other synthetic rubbers.

A simple theory of abrasion patterns has been developed in close connection with the theory of intrinsic abrasion[13]. The profiles of abrasion patterns shown in Figure 19 make it clear that the phenomenon must begin with part of the abraded rubber surface being pulled out and elongated in the direction of abrasion. It has been suggested that this initial step is facilitated by lips of the type seen in Figure 8(b) which are thrown up behind tears across the track of an abrasive grain. Because of inhomogeneities of the material or because of high pressure exercised by exceptionally tall grains, some of these tears and lips will be larger than the average. As the abrasive passes over the lips and stretches them out they will cover one or more tears in their rear and protect them from further damage before the lips retract. Thus a linear periodic structure is initiated which, however, does not yet constitute an abrasion pattern because of the lack of lateral alignment. When abraded rubber surfaces are examined during early stages of pattern development, such incipient formations are indeed observed as shown in Figure 21(a). These fragmentary abrasion patterns

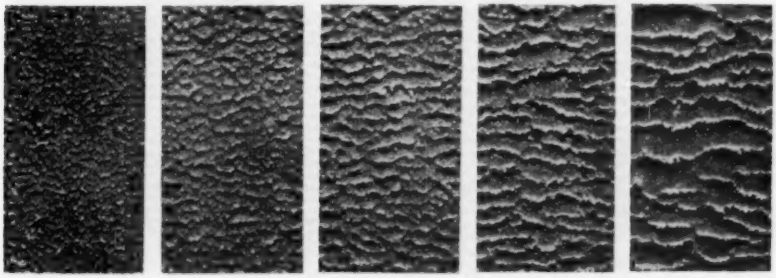

FIG. 21.—Development of an abrasion pattern on an unfilled vulcanizate of natural rubber. Track: garnet paper. Distance travelled: (a), 120 cm; (b), 180 cm; (c), 240 cm; (d), 420 cm; (e), 720 cm; Magn. 10.8 ×.

must be expected to migrate across the surface in the same way as complete patterns but the rate of migration is subject to random effects and occasionally two ridge segments come abreast and line up with respect to each other. The development of the pattern is therefore a relatively slow process; its growth is illustrated by the remaining photographs in Figure 21.

For this mechanism to function, the stiffness of the rubber must be low enough to allow elongation of sufficient magnitude to occur under the tangential stress produced by the asperities of the abrasive. The original modulus of filled compounds of the tire tread type is too high for this purpose and a pattern develops on such samples only after a softened top layer has been created by prestressing. If the rate of abrasion is high, this surface skin is worn away as soon as formed, and it becomes difficult to produce an abrasion pattern under these conditions. This point is illustrated by Figure 22. A typical tire tread compound of natural rubber was abraded under otherwise identical circumstances on garnet and emery paper. Abrasion on the garnet being rapid, only vestiges of an abrasion pattern are formed, whereas a pronounced pattern develops on the blunter emery paper. Similar effects have been observed when comparing rubber surfaces abraded on fresh and repeatedly used specimens of the same abrasive. This is also one of the reasons why abrasion patterns form

with greater ease on road surfacings with their low rate of wear than on commerical abrasives.

Another reason for restricted development of patterns on abrasives is that when the ridges become comparable in size with the dimensions of the abrasive grain, the shape of the grains becomes important. In the case of filled rubbers there is a tendency for the abrasive particles to plough through the ridges and produce scoring marks. This effect is shown by the photographs in Figure 23 which are two pictures of the same abraded rubber surface; the only change made when taking the photographs was to alter the incidence of the illumination. In case (a), the light was parallel to the direction of abrasion and shows up a well defined if not very intense pattern; in case (b), where the light was at right angles to the direction of abrasion, only scoring marks are seen. Because of the lack of continuity in the ridges, such a pattern may be called a "pseudo-abrasion pattern". In general, no scoring marks can be discovered on road-abraded rubber surfaces.

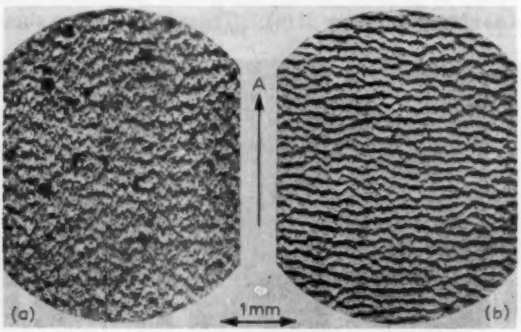

FIG. 22.—Surface of a natural rubber vulcanizate filled with 50 phr HAF black abraded: (a) on garnet paper; (b), on emery paper. Magn. 10.8 ×. From Reference 22.

In the previously published theory of abrasion patterns[13] it has been assumed that their spacing depends only on the size of the lips from which they originate. This lip being solely determined by the length of the tear, it has been deduced that the spacing s_p is given by Equation (18):

$$s_p = \text{const.} \left(\frac{p}{E} r\, d^2 \right)^{1/3} \tag{18}$$

where r is the radius of curvature of the abrasive grain at the point of contact and d, the size of the grain. Equation (18) has been tested both as to load and grain-size dependence by experiments on a commercial abrasive (garnet paper) and has been found to represent the experimental findings remarkably well. Figure 17 shows, however, that Equation (18) will not adequately descrieb patterns produced on road surfaces.

The difference in the spacings of the pattern on the two compounds of different stiffness shown in this figure is larger than predicted by Equation (18) according to which the spacing should be proportional to the inverse cube root of the modulus. The ratio of moduli of these 2 rubbers is 1.85, giving a theoretical ratio of spacings equal to only 1:1.225. The difference in stiffness of the

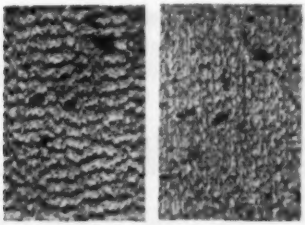

(a) (b)

FIG. 23.—Surface of a natural rubber vulcanizate filled with 50 phr HAF black abraded on garnet paper (a), illumination parallel to the direction of abrasion; (b), at right angles to the direction ofabrasion. Magn. 10 ×.

abraded surfaces will actually be even smaller than 1.85 because of prestressing effects.

It is suggested that on road surfaces or generally on abrasives with grains of large radius of curvature the asperities instead of cutting through the ridges glide over them and elongate them by friction. The spacing is then determined by the equilibrium of frictional and elastic restoring forces. It is shown in the next section that the frictional force F_f of a spherical grain with the diameter d is given by the Equation (20)

$$F_f = \text{const. } \varphi\, d^2\, (p/E)^{2/3}$$

Assuming, furthermore, Hooke's law to hold for the local elongation, the retractive force F_r must be given by a relation of the form

$$F_r = \text{const. } s\, a\, E$$

where s is the spacing and a, the diameter of the area of contact. Substituting for a from Equation (16) and equating F_f and F_r results in the following expression for the spacing:

$$s = \text{const. } \frac{\varphi}{E}\, d \left(\frac{p}{E}\right)^{2/3} \tag{19}$$

where d is the diameter of the close-packed spherical abrasive grains. This equation gives a stronger dependence of the spacing s on both modulus and pressure than Equation (18), but in practice it is difficult to draw a sharp dividing line between the two cases, as is seen from the experimental results given in Table VI.

In this table, r_p is the ratio of the spacings at the two pressures. Its theo-

TABLE VI

SPACINGS OF ABRASION PATTERNS PRODUCED ON TARMAC. NATURAL RUBBER VULCANIZATES FILLED WITH CARBON BLACK

	Spacing (mm)		
	Filler content 25 phr HAF	Filler content 45 phr HAF	r_p
Pressure, 0.66 kg/cm²	0.260	0.155	1.68
Pressure, 2.68 kg/cm²	0.470	0.212	2.22
r_p	1.80	1.37	

TABLE VII

COEFFICIENT OF FRICTION ON GROUND GLASS (FROM REFERENCE 24)

Diameter of silicon carbide grain, mm	Plate glass	0.042	0.067	0.141
Coefficient of friction	1.79	1.48	1.36	1.21

retical value is, according to Equation (18), $(2.68/0.66)^{1/3} = 1.595$, and according to Equation (19), $(2.68/0.66)^{5/9} = 2.18$. The ratio of the spacings on the two compounds is r_c. Assuming, as a guide, that the ratio of the moduli is 1.85, r_c is, after Equation (18), $(1.85)^{1/3} = 1.225$ and after Equation (19), $1.35^{14/9} = 2.604$. It appears therefore from the limited experimental evidence that the influence of the frictional force on the development of patterns gains in importance as the stiffness decreases and the pressure increases.

It should finally be mentioned that abrasion patterns can have considerable diagnostic value when determining the mode of wear taking place under conditions not accessible to direct observation. This applies particularly to tires where the relative motion between tire and track can be deduced from abrasion patterns[23].

VIII. FRICTION ON ROUGH SURFACES

Abrasion of rubber as envisaged in the preceding sections is a consequence of local frictional stresses set up by the asperities of the track and does not, in contrast to solid friction, react on the frictional forces. Friction on rough surfaces can therefore be treated by methods similar to those employed for friction on smooth surfaces, without regard being paid to any mechanical failure ensuing in the wake of the track asperities.

No calculation is necessary to see that the coefficient of friction is lower on a rough than on a smooth surface because of the smaller area of contact. This is shown by the following data obtained with an extracted sample of a natural rubber tire tread compound on glass ground with silicon carbide of different grade.

The essential difference between rubber friction on smooth and rough surfaces lies, however, in their load dependence. The reason for this divergence is that on a rough track both the true and the apparent area of contact depend on the load. A quantitative estimate of the effect can be derived from the model employed in the theory of intrinsic abrasion. The tips of the track asperities are again taken to be spherical and large compared with the rubber

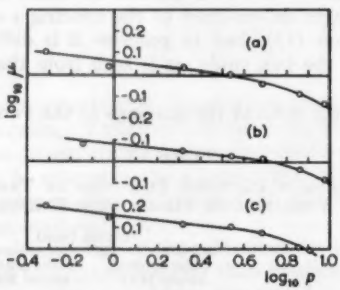

FIG. 24.—Logarithms of coefficients of friction on silicon carbide paper, grade 180, plotted against logarithm of normal pressure. (*a*), unfilled vulcanizate of natural rubber; (*b*), vulcanizate of natural rubber filled with 50 phr HAF black; (*c*), vulcanizate of GR-S (Krylene) filled with 50 phr HAF black. Velocity, 0.00212 cm/sec.

asperities. Gross deformation of the rubber by the track asperities is assumed to obey Hertz's equations for spherical contacts, and the true area of contact contributed by each rubber asperity to be proportional to $(p_l/E)^{2/3}$, where p_l is the local pressure. The calculation has the result that the frictional force produced by a track asperity is

$$F_f = \varphi(p/E)^{8/9}d^{16/9}r^{2/9} \tag{20}$$

and

$$\mu = \text{const.}\ \frac{\varphi}{E}\ (r/d)^{2/9}\ (p/E)^{-1/9} \tag{21}$$

where r is the radius of curvature and d, the size of the track asperities. The relation (21) was first proposed in a slightly different form by Lincoln[25].

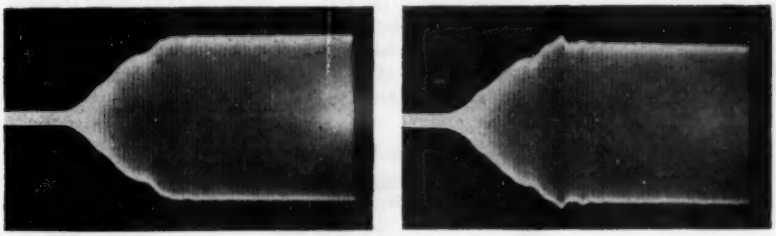

a b

FIG. 25.—Frictional force during start of motion. The amplitude of the envelope is a measure of the tangential force. Normal pressure, 1.28 kg/cm². (a), unfilled vulcanizate of natural rubber; (b), natural rubber filled with 50 phr HAF black.

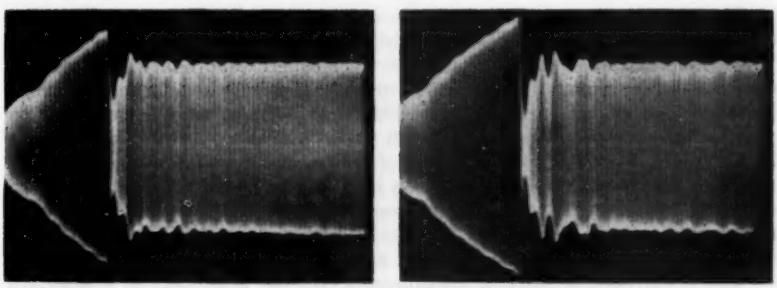

c d

FIG. 25.—(c), vulcanizate of GR-S (Kryiene) filled with 50 phr HAF black; (d), as (c), but sample loaded with 2.23 kg/cm² for 5 minutes before the experiment. Track: garnet paper, grain size 0.29 mm.

Equation (20) has been confirmed experimentally[13,7] with a number of compounds at pressures up to about 2.5 kg/cm². Figure 24 gives the coefficient of friction of three different compounds on silicon carbide paper at pressures up to nearly 10 kg/cm². At higher pressure, Equation (21) fails, the coefficient of friction decreasing more rapidly with increasing pressure than predicted. The reason for this discrepancy is in all probability a saturation effect similar to that demonstrated in Figure 5 for the case of flat contacts. In addition to mutual interference between rubber asperities, saturation can here be produced by the rubber filling the gaps between the track asperities (Denny[10]).

It is at times observed that the force necessary to start a sample on a rough track is greater than the force of dynamic friction sufficient to keep it in motion. This phenomenon of "starting friction" has been investigated in a number of experiments. The time dependence of the tangential force was recorded during the starting period, the deflection of the dynamometer having been converted into the out-of-balance current of a 2000 sec^{-1} alternating current bridge. Representative results are the oscillograms in Figure 25, which show the envelope of the out-of-balance current as function of time (from left to right). With the unfilled natural rubber vulcanizate (a), the force rises monotonously until the sample begins to move and the force becomes constant, but when the compound is filled with 50 phr HAF black (b) the frictional force passes through a slight maximum at the start. This effect is more pronounced with the black-filled GR-S compound (c). The transition from rest to motion is here accompanied by a vibration which takes some time to die out. The excess of starting friction over dynamic friction increases with the time the sample has been in contact with the track. It can also be increased by keeping the sample under a high load before starting the experiment, as shown by the oscillogram Figure 25(d). Table VIII gives typical numerical results.

TABLE VIII

EXCESS OF STARTING FRICTION OVER DYNAMIC FRICTION ON GARNET PAPER, GRAIN SIZE 0.29 MM, NORMAL PRESSURE, 1.28 KG/CM²

Compound	Nat. rubber no filler	Nat. rubber 50 phr HAF	The same, after 90 min under load	Krylene, 50 phr HAF	The same, after 5 min under 2.23 kg/cm²
Excess, %	0	7.1	15.5	33.3	57.8

Noticing the absence of the effect in unfilled natural rubber, the conclusion drawn from these results is that starting friction on rough surfaces is due to plastic deformation of the sample by the track asperities, producing permanent set. At the beginning of movement, work must be done in deforming the rubber which has sagged down into the interstices between track asperities. In practice, starting friction will be difficult to distinguish from static friction, and it is possible that the finite coefficient of static friction at infinite normal load found by Ratner and Sokolskaya[12] is a mechanical hindrance effect similar in character to starting friction. It is interesting to note in this context that in a recent publication[26] Ratner and Lavrent'ev have independently demonstrated the difference between starting friction and static friction.

The occurrence of starting friction indicates the possibility of a negative velocity coefficient of rubber friction and can therefore under certain conditions induce instabilities during sliding. Stick-slip phenomena are, in fact, often encountered in friction experiments with filled GR-S compounds. Starting friction may also have important consequences when rubber is subjected to intermittent sliding, as, for example, on the circumference of tires.

IX. CONCLUSIONS

The work reported in this paper is a first attempt to elucidate some of the most important factors governing friction and abrasion phenomena. Very idealized models had to be chosen in order to reduce the difficulties inherent in the subject to manageable proportions, and at best only semi-quantitative agree-

ment between theory and experiment can be expected. Within these limits, the assumption that local stress concentrations produced by frictional traction are the cause of abrasion has been justified by the available evidence, abrasion thus emerging as a purely mechanical process. In coming to this conclusion, the origin of frictional forces has been completely divorced from abrasion but the existence of starting friction, discussed at the end of the last section, throws doubt on the general validity of this hypothesis. If mechanical entanglement can play a significant role in rubber friction, effects similar to those produced when scratching rubber with a needle may be of greater importance than has been assumed in the present treatment of the subject. It should also be mentioned that no theory is, as yet, available for the mechanism of static friction.

It has been demonstrated that the relative wear resistance of any two compounds is not a constant but can depend pronouncedly on the conditions of testing. This variability is due to the formation of abrasion patterns which develop on different compounds with different intensity and whose contribution to the total abrasive loss depends on the mechanical strength of the compound. Abrasion patterns are thought to influence relative rates of tire wear under different conditions of service[22], but no specific reference has been made in this paper to tires, for the following reason.

Tire wear occurs when there is relative motion in the area of contact between the circumference of the tire and the road and is therefore intimately connected with the mechanics of slipping wheels. This is a topic of some complexity involving the large-scale elastic properties of the wheel, differences in which may overshadow differences in the abrasion resistance of the tire tread. The same considerations apply to abrasion machines which are designed to imitate conditions encountered by tires and employ small rotating samples undergoing various forms of slip. In spite of its intricacy, the problem is amenable to theoretical work and a preliminary result has been given in an earlier publication[22]. It is hoped to present a more advanced approach to it in the near future.

SUMMARY

Experimental evidence is adduced for the view that rubber friction is similar in character to viscous flow and therefore, in contrast to solid friction, not necessarily accompanied by abrasion. This theory implies that the forces of rubber friction are proportional to the true area of contact. The true area of contact is determined by elastic deformation of the asperities on the rubber surface, with the result that Amontons' law is not obeyed by rubber. The laws of rubber friction are deduced from simple models and satisfactorily confirmed by experiment.

Abrasion of rubber is due to mechanical failure under the tractive stresses produced frictionally by the asperities of the track. In this process, certain periodic structures are often created on abraded rubber which have been called "Abrasion Patterns". Abrasion patterns are found to increase the rate of abrasion; a distinction is therefore made between "Intrinsic Abrasion", occurring in the absence of patterns, and "Pattern Abrasion". Both types of abrasion are treated theoretically, and qualitative agreement with the experimental results is obtained.

The phenomenon of pattern abrasion has the important consequence that the relative abrasion rating of any two compounds can depend pronouncedly on the conditions of the test.

REFERENCES

[1] Bowden, F. P., and Tabor, D., "Friction and Lubrication of Solids", Oxford Univ. Press, London, 1954.
[2] Roth, F. L., Driscoll, R. L., and Holt, W. L., *J. Research Natl. Bur. Standards* **28**, 439 (1942).
[3] Schallamach, A., *Proc. Phys. Soc.* (London) **B66**, 386 (1953).
[4] Eyring, H., *J. Chem. Phys.* **4**, 283 (1936).
[5] Schallamach, A., *Trans. Inst. Rubber Ind.* **32**, 142 (1956).
[6] Jaeger, Jr., J. C., *Proc. Roy. Soc.* N.S.W. **76**, 293 (1942).
[7] Schallamach, A., *Proc. Phys. Soc* (London) **B65**, 657 (1952).
[8] Timoshenko, S., and Goodier, J. N., "Theory of Elasticity", McGraw-Hill Book Company, New York, 1951.
[9] Thirion, P., *Rev. gén. caoutchouc* **23**, 101 (1946).
[10] Denny, D. F., *Proc. Phys. Soc.* (London) **B66**, 721 (1953).
[11] Archard, J. F., *J. Appl. Phys.* **24**, 981 (1953).
[12] Ratner, S. B., and Sokolskaya, V. D., *Doklady Akad. Nauk* SSSR **99**, 431 (1954).
[13] Schallamach, A., *Proc. Phys. Soc.* (London) **B67**, 883 (1954).
[14] Schallamach, A., *J. Polymer Sci.* **9**, 385 (1952).
[15] Rivlin, R. S., and Thomas, A. G., *J. Polymer Sci.* **10**, 291 (1953).
[16] Mullins, L., *J. Rubber Research* **16**, 275 (1947); *J. Phys. & Colloid Chem.* **54**, 239 (1950).
[17] Mullins, L., and Tobin, N. R., *Proc. Third Rubber Technol. Conf.*, London, 1954, p. 397.
[18] Schallamach, A., *Trans. Inst. Rubber Ind.* **28**, 256 (1952).
[19] Schallamach, A., *Proc. Phys. Soc.* (London) **B66**, 817 (1953).
[20] Buist, J. M., and Davies, O. L., *Trans. Inst. Rubber Ind.* **32**, 68 (1946).
[21] Greensmith, H. W., Unpublished work.
[22] Schallamach, A., *Kautschuk u. Gummi*, *Sonderheft* "Der Reifen" (1955) p. 27; RUBBER CHEM. & TECHNOL. **29**, 581 (1956).
[23] Gough, V. E., Hardman, J. H., and McLaren, R. J., *Trans. Inst. Rubber Ind.* **32**, 27 (1956).
[24] Schallamach, A., *Kolloid Z.* **141**, 165 (1955).
[25] Lincoln, B., *Nature* **172**, 169 (1953).
[26] Ratner, S. B., and Lavrent'ev, V. V., *Doklady Akad. Nauk* SSSR **108**, 461 (1956).
[27] Kauzmann, W., *Rev. Modern Phys.* **14**, 12 (1942).

THE PROTECTION OF RUBBER AGAINST ATMOSPHERIC OZONE-CRACKING

B. S. Biggs *

Sandia Corporation, Albuquerque, New Mexico

CONTENTS

I. Introduction 1015
II. Molecular Mechanism of Cracking 1016
III. Physical Aspects of Cracking 1018
IV. Accelerated Test Apparatus 1019
A. Static tests 1019
B. High ozone concentrations in urban areas 1020
C. Determination of ozone 1020
D. Dynamic tests 1021
V. Assessment of Damage 1022
VI. Inherent Resistance of Polymers 1024
VII. Protective Agents 1026
A. Waxes 1026
B. Antiozonants 1026
VIII. Mechanism of Action of Antiozonants 1031
IX. Bibliography 1033

I. INTRODUCTION

The cracking of rubber by atmospheric ozone is now a well-known phenomenon and for a number of years rubber scientists and technologists have devoted considerable effort to combating it. While the differences of opinion and the confusion of data in this work are sometimes more conspicuous than the successes, nevertheless, there has been considerable success. In spite of the existence of large areas of uncertainty, much progress has been made. A new word, "antiozonant", has been added to the vocabulary of the rubber man. The substances so designated, together with waxes already well known, enable the compounder to protect natural and synthetic rubbers against both static and dynamic exposure to a fair degree, and this in spite of the fact, now recognized, that certain urban atmospheres may contain much higher concentrations of ozone than were formerly considered normal. In addition, the synthetic polymer chemist has made available a number of commercial rubbers which, because they are saturated, are not at all vulnerable to ozone attack, and serve in many special applications in which extreme resistance to ozone is necessary. The purpose of this paper is to review the present status of the antiozone work.

Ozone has been known as a specific agent for double bonds for many years and, of course, has been the traditional reagent for structure studies in rubber since Harries' classical research on the structure of natural rubber[1]. It should not have been surprising that this same reactivity also makes it an agent for the destruction of useful rubber products, and, indeed, Samuel F. B. Morse is reported to have been aware, even in 1868, that atmospheric ozone has a

* On Leave of Absence from Bell Telephone Laboratories.

deteriorating influence on some kinds of insulation[2]. In 1885, W. Thomson observed[3] that ozone generated in the laboratory could crack stretched vulcanized rubber. The importance of atmospheric ozone in the cracking of rubber articles exposed outdoors has been definitely established by a succession of investigators over the last thirty years[4–11], culminating in the papers of Newton[12], in 1945, and of Crabtree and Kemp[13], in 1946*. These authors surveyed the field thoroughly and made extensive studies of their own. Their reports contain a wealth of information and, to give the reader an idea of the material covered, portions of Newton's own summary of his paper are quoted verbatim:

> "'Exposure-cracking' is the fissuring which occurs when stretched rubber is placed in an atmosphere containing ozone, and is frequently wrongly described as 'sun-cracking'. These cracks form in the rubber at right angles to the applied stress and must be distinguished from crazing, the fissures of which occur in an oxidized surface layer and may run in any direction.
>
> It is shown that there is a 'critical elongation' at which cracking is maximal, but that the relation between the severity of cracking and the surface strain can be greatly modified by changes in the compounding ingredients. Butadiene type of rubbers do not differ greatly in resistance to exposure-cracking, whereas the Neoprene types and Thiokol-FA possess marked resistance.
>
> The only factors essential for the production of exposure-cracking are ozone and strain in the sample, and sufficient ozone must be present in the atmosphere to produce the deterioration observed. Light is not only unnecessary, but actually has a retarding effect on the production of cracks.
>
> . . . The rate of formation of cracks increases with increase of strain until a maximum is reached at about 75 per cent elongation, but the mean rate of growth of cracks is most rapid at 20 per cent elongation because the surface strain is most persistent at this elongation. The actual growth of cracks has been studied microscopically, and it is shown that large cracks are formed by the coalescence of small cracks, and the collapse of neighboring ones."

Crabtree covered much of the same material but devoted a little more attention to the effects of varying temperature and strain, and also described the development of apparatus for accelerated testing. This description was amplified in a subsequent publication[14].

These papers constitute a milestone in our understanding of the ozone problem. Since the time of their publication, much has been done to find ways of improving ozone resistance of rubbers, and in late years this effort has met with rather remarkable success.

II. MOLECULAR MECHANISM OF CRACKING

It would, doubtless, be useful in pursuing the goal of protecting rubber from ozone if the mechanism of cracking were known in a more fundamental way. This is still quite obscure. Unsaturation must, of course, be present in the rubber for it to be susceptible to cracking†. Just how the reaction of ozone on a carbon-to-carbon double bond leads to cracking is not known in detail.

In the first place, it should be noted that ozone apparently reacts with the surface of rubber at rest, but this is not always manifested by outward changes. The reaction is indicated by a slight gain in weight[15]; and careful analysis for

* For further brackground information, see Davis and Blake, "Chemistry and Technology of Rubber", Reinhold, 1937, Chapters 12 and 14.

† Certain polysulfide rubbers appear to constitute an exception to this statement. Presumably, the polysulfide linkage is vulnerable to ozone in some structures.

ozone content of air before and after it passes over rubber reveals the consumption of ozone[16]. Tuley[17] has noted a frosting effect, and Kendall and Mann[18] observed the development of a white film visible under a microscope. The cracking normally observed is a direct result of stress. It was formerly thought that cracking might occur during hydrolysis of the ozonide—in other words, that hydrolysis of the ozonide was an essential step in the cracking of rubber. Crabtree has shown that cracking of rubber by ozone occurs even in a dry atmosphere (completely protected by phosphorus pentoxide)[19], and hence it must be assumed that the cracking does not require the presence of moisture. Newton's view is that in the process of reaction with ozone and the rearrangement of the ozonide, the carbon atoms of the double bond become separated far enough that they can never recombine. When ozone reacts with a double bond, the first product can hardly involve separation of the carbon atoms. Yet, identifiable ozonides have the structure 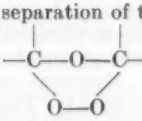 [18,20,21]. It seems plausible to think that the first reaction product, which is presumably a simple adduct, is so unstable that it rearranges with momentary separation of the carbon atoms originally connected by the double bond. In a normal recombination (i.e., in rubber at rest), the atoms regroup themselves in the more stable arrangement shown above, the cage effect preventing the separation from becoming catastrophic. If at the time of this separation and rearrangement, however, a force is acting to pull the carbon atoms apart, they move so far that their recombination becomes impossible. When this happens with several neighboring molecules, all of which are under stress, sufficient movement occurs to concentrate stress on the next nearest neighbors, and thus the stage is set for growth of the crack, both in depth and in length, to microscopic and then to macroscopic size. Why only a few of the millions of potential sites develop into cracks is presumably because cracks form first at the spots of greater molecular extension and the growth of these cracks permits the relaxation of molecules in intervening areas. It is not generally believed that straining the rubber produces any chemical activation.

This is substantially the picture presented by Newton, and by Smith and Gough[22]. It is also alluded to by Cuthbertson and Dunnom[23]. Kendall and Mann[18] have studied the formation of ozonides by infrared analysis and have observed other groupings than that of the simple ozonide, but these could be the result of further reaction, so their work is not really inconsistent with the mechanisms described above.

A few other observations about cracking are worth mentioning. Crabtree and Biggs[24] have reported that certain free radicals, produced by ultraviolet light irradiation of peroxides, cause rubber to crack in a manner indistinguishable from ozone cracking. This does not necessarily indicate that ozone is acting like a free radical, but it causes one to look for similarities of mechanism. It has also been reported that ozone in true solution in water does not crack rubber except under a trapped air bubble[25]*. Similarly, ozone in nitromethane does not cause cracking[26], whereas ozone in silicone oil does. Buist[27] reports that a water film protects rubber against low concentrations of ozone but not against high**. Hydrogen peroxide in aqueous solution irradiated with ultra-

* This was reported privately by Newton, and was subsequently confirmed by Crabtree.

** An as yet unpublished paper by Tucker[28], which bears on this point, has just come to the attention of the author. Tucker finds that while water films protect rubber from the cracking effect of ozone, they do not stop the oxidative effect which eventually may produce severe erosion of the rubber surface.

violet light does not crack rubber, but if rubber is suspended in silicone oil floating above a strong hydrogen peroxide solution, and if the oil is irradiated, the rubber cracks[19]. These facts suggest that ozone, and the OH radicals from hydrogen peroxide, are somehow rendered unreactive by the presence of water and certain other substances[27]. The idea suggests itself that they become hydrated (or solvated) to a less active form. These similarities between the action of ozone and free radicals do not extend, however, to the kinds of agent which protect against them. Typical antioxidants which are active against free-radical oxidation are often not effective against ozone, and the materials most effective against ozone are frequently not good antioxidants. More will be said about this later.

Crabtree[19] has found that stretched rubber is cracked in a gas discharge tube at voltages in excess of 5000 volts, presumably by an ionic bombardment mechanism. The gases used were hydrogen, nitrogen, argon, and helium. Butyl rubber, which is manufactured by ionic polymerization, is particularly susceptible to cracking in a discharge tube. Neoprene and nitrile rubber are the most resistant of the unsaturated rubbers tested. These observations are interesting but do not appear to be related to the phenomenon of exposure cracking.

III. PHYSICAL ASPECTS OF CRACKING

While little is known about the molecular mechanism of cracking, the physical details have been well documented. Norton [1], Powell and Gough[28], Buist[27], and others have studied the formation of cracks, and speculated about their manner of growth. One of the most interesting papers in this connection is that of Smith and Gough[22], who studied the development of ozone cracks by means of time-lapse microphotography. This technique permitted them to produce a moving picture of the cracking phenomenon. Careful examination of this film revealed much valuable information about the physical details of the cracking process. It became apparent that cracks form randomly over the whole surface of a strained area and that there are not necessarily any distinguishing marks on the surface of the rubber at the spots where cracks form. The cracks do not form instantaneously, but require a delay period, and their formation is distributed statistically in time. During the cracking period, some cracks disappear and others join. Cracking continues to develop as long as both stress and ozone are present, although a time is reached when no new cracks appear. Disappearances and crack-joining continue so that in some cases the number of cracks markedly decreases. Incipient cracks have sometimes been referred to as "pin holes"[10], but in the published pictures of Smith and Gough one does not see this stage. Perhaps, if other frames had been selected, this appearance would have been revealed.

Another important paper dealing with physical aspects of cracking is that of Ossefort and Touhey[29]. Many ozone tests are run on strips of rubber which are bent in loops or stretched on boards, and hence are under uniaxial stress. The cracking in such cases is transverse to the direction of strain. Similarly, the folds in stored automobile innertubes or in rubber gloves introduce predominantly uniaxial stress, and the cracking which results is along the line of the fold. Thus, there has arisen the popular idea that ozone cracks must always run in one direction. Where "alligator" patterns have been encountered, the tendency has been to attribute the damage to photooxidation. In 1955, Ossefort and Touhey put an end to this misconception by demonstrating that when biaxial stresses are present in a rubber sample exposed to ozone, cracking occurs in the typical "mud-crack" or "alligator" pattern. They showed pic-

tures of cracked tire sidewalls which appear to be identical in pattern with samples cracked in the dark by ozone while under polyaxial stress. An experienced observer can sometimes see differences between the mud-crack pattern produced by ozone and that resulting from outdoor weathering (the edges and bottoms of ozone cracks may tend to be sharper), but, nevertheless, it appears that ozone may be responsible for even more damage than has been attributed to it previously. While the paper of Ossefort and Touhey was important in directing attention to these facts, it must be pointed out that Norton[10] made the same observation in 1940. He noted that a rubber sheet stretched over a ball and exposed to ozone cracked in a pattern resembling that of dried mud. Norton's observations did not receive the attention they deserved, although reference was made to them by Newton.

IV. ACCELERATED TEST APPARATUS

A. STATIC TESTS

The development of protective agents for rubber is facilitated by reliable methods of test. The fact that ozone has a role in the outdoor deterioration of rubber became recognized only when test conditions became well defined, e.g., light was excluded and ozone was shown to be present. Upon recognition of the problem, each worker has devised equipment to be used in the study. One of the most important contributions of Crabtree and Kemp[14] was the development of a practical method and apparatus for determining in the laboratory, with good reliability, the resistance of a rubber sample to low concentrations of ozone. This made possible the beginning of correlation between indoor and outdoor testing. Previous methods had used too high a concentration of ozone. Prior to 1944, isolated measurements of ozone concentration in air were made in various parts of the world. Crabtree made analyses of the air at Murray Hill, New Jersey, on a daily basis for a year and determined that the ozone concentration ranged from 0 to 6 parts per hundred million of air. Later analyses in Japan[30], Austria[31], and in many places in America[32], are in accord with Crabtree's results. The early ASTM test[33], which was aimed at measuring resistance to corona rather than to atmospheric ozone, used concentrations thousands of times higher than that of the air. Crabtree found that for accelerated testing one needed to stay near atmospheric values to obtain meaningful results and, hence, chose a concentration of 25 parts per hundred million as being reasonably dilute and yet still offering some acceleration over field conditions. (In later years, it has been learned that even this value is exceeded under some circumstances. More will be said about this later.) For generation of this low concentration of ozone, he chose a small quartz mercury lamp which was available commercially and which had a long life. Close regulation of the ozone output was obtained by voltage control. The chamber itself was an aluminum cylinder, two feet in diameter and three feet high, with a vented cover and baffles so arranged as to allow free passage of ozonized air without admitting light. Movement of the air was by convection, aided by a small fan. Regulated heaters were used to maintain the chamber at a prescribed temperature ranging from 90 to 120° F, depending on the kind of rubber being studied. The ozone concentration was brought to 25 parts by repeated analysis and adjustment. The analytical procedure was a modification of that described by Paneth[34] and was based on iodimetry. Samples were disposed on racks around the wall and could be removed easily for observations.

The Crabtree-Kemp apparatus met with wide acceptance and, after a fairly long tryout period, was adopted by ASTM as Test Method D1149-51T (cur-

rently D1149-55T). It has been used with considerable success, both in its original form and also with modifications. Several commercial units embodying its general principles have been made[35]. One of the chief criticisms of it has been inadequate provision for forced movement of ozonized air through the chamber. In a paper presented before the St. Louis Symposium of ASTM, in February 1958, A. G. Veith[36] describes an improved system. He points out that rubber cracking will not be proportional to the measured ozone concentration if large numbers of rubber samples are exposed in a chamber with inadequate air flow. He describes a new chamber which is larger than the Crabtree unit and which is equipped with a highly efficient circulating fan. It can be operated at temperatures ranging from room temperature up to 150° F, at ozone concentrations from 10 to 700 parts per hundred million, and with flow rates up to 7 cubic feet per minute. It is equipped with a revolving test rack for mounting samples, and this is further assurance of uniform exposure to ozone. Positive and substantial air flow is believed to increase the reproducibility of results appreciably.

B. HIGH OZONE CONCENTRATIONS IN URBAN AREAS

An important development of recent years has been the accumulating evidence that in many areas of the country[37], and conspicuously in Los Angeles, ozone concentration can be much higher than the values quoted above. Values of up to 12 parts per hundred million have been reported in several cities[38], and readings of 50 to 90 parts have been measured in Los Angeles during periods of bad smog[39]. Bartel and Temple[40], in 1949, 1950, and 1951, took a portable laboratory into the Los Angeles area and made analyses in various places. They found values ranging as high as 50 parts in the city and a high value of 27 parts 110 miles away, apparently well outside the smog area. Haagen-Smit[41], who has been active in studying the causes of smog, has been able to demonstrate that mixtures of low molecular weight hydrocarbons and nitrogen dioxide, when present at low concentrations in air, can undergo photo reactions which generate ozone. The studies of Stanford Research Institute[42] and of the Los Angeles County Air Pollution Control District[43] have confirmed these results and suggest that automobile exhaust is one important source of ozone-generating material. The fact that high values of ozone have been found in other cities indicates that the combinations of air pollution which accompany modern urban life have in them the raw materials for ozone generation, and leads one to believe that during periods of air stagnation ozone concentrations may build up almost anywhere. An alarming symptom of this is reported by Lundberg, Vacca, and Biggs[44], who repeated at Murray Hill in 1955 the daily analyses carried out by Crabtree and Kemp in 1944. They found values for the month of June almost twice as high as any values found in the earlier series. Only after such tests are repeated in many areas can one say that this represents a significant trend, but the possibility is suggested. The fact that high ozone concentrations are to be expected at times in many areas has raised the question of whether or not 25 parts per hundred million is really high enough for an accelerated test. Some workers have chosen to use 50 or even 100 parts per hundred million[45,46]. Since high outdoor concentrations of ozone usually do not persist for more than a few hours at a time, continuous exposure at 25 parts is still found to constitute an accelerated test.

C. DETERMINATION OF OZONE

Frequent analysis is required for control of ozone concentration in test chambers, or for following the concentration in outdoor air. The classical

method of determining ozone is by iodimetry, based on the strong oxidizing property of ozone. The chief problem in the use of this method is that of quantitative scrubbing of large volumes of air to extract the ozone which may be present in concentrations as low as one or two parts per hundred million. Crabtree and Kemp[14] devised for this purpose an automatic device for producing a fine mist of KI solution which was subsequently trapped in liquid. It is an excellent technique and has given good results in repeated checks. A. G. Veith[36] has been concerned that the vacuum used to draw air through the aspirating system might cause a loss of the released iodine, and has designed a counter-current extraction column to replace the spray jet system. Tests show that the column removes all the ozone from the air stream at flow rates of .3 cubic meter per hour at concentrations up to 250 parts per hundred million. It is said that no loss of iodine vapor occurs since the maximum pressure drop in the system is only 5 to 10 mm and since the dissolved iodine is quickly carried out of the path of the air stream. Refinements in the iodimetry method have also been reported by Bowen and Regener[47], who have devised automatic equipment for the purpose. Automatic ozone measuring devices have been widely used in Los Angeles County. Other refinements have been made by Wadelin[48].

Several methods of analysis for ozone, based on the rate of cracking of rubber, have been developed. These tests are convenient because they do not require complicated laboratory apparatus. Their accuracy is limited by the errors in calibration of the rubber; by the skill of the observer; and by time factors. Even so, Bradley and Haagen-Smit[49] have made good use of the method in smog studies, and Crabreee and Erickson[50] have used it in obtaining readings from remote areas. A very convenient device of this sort is that devised by Beatty and Juve[51] and known as the Goodrich Ozonometer. It represents a considerable improvement in that it does not rely on observations of cracking but on the decrease of stress in the exposed arm of a stretched rubber loop. The progressive cracking of the exposed rubber causes movement of a needle on a scale and hence permits quite precise readings. The instrument is easily calibrated and is then very useful for making quick determinations of ozone concentration in areas remote from laboratory facilities.

The National Bureau of Standards[52] has developed a spectroscopic method of analysis for atmospheric ozone, based on absorption of light in the ultraviolet region. It requires a path of 1450 feet and must be run at night, and hence is not a practical method for routine use. An ultraviolet light method for concentrated ozone is described in ASTM Test Method D470-56T.

D. DYNAMIC TESTS

The Crabtree-Kemp chamber, which, with its modifications, has been so useful in laboratory studies, was designed for static tests only. In many applications, for example, automobile tires, it is important to know the ozone resistance of a compound under occasional or continuous flexing. Many chambers have been devised which provide for flexing of the samples during exposure to ozone. A few of these will be mentioned briefly. The apparatus described by Fielding (1947)[53] provided for periodic flexing of a large number of tapered rubber strips at 60 cycles per minute by attaching one end of each strip to a long oscillating mandrel. The Firestone machine (Ford and Cooper, 1951)[54] was quite versatile, providing for wide variations in temperature, humidity, strain, and ozone concentration. This machine has also been used by the Burke Laboratories in contract work for the Detroit Arsenal. The Rock Is-

land Arsenal[55] has designed a much simpler machine which stretches O-ring specimens from 0 to 25% elongation four times a minute as they rotate over two pulleys. This machine has been used in much of the extensive program at the Rock Island Arsenal. The Monsanto apparatus (Creed, Hill, and Breed, 1953)[56] rotates belt-type samples over two rollers at a frequency of 75 flexes per minute, the flexing being derived from the curvature of the rollers. Meyer and Sommer (1957)[45] mount flat sheet specimens on a canvas belt which is rotated over two pulleys several feet apart and of such dimensions that the surface of the sample is elongated about 15% as it goes around each pulley. One of the most recently described methods is that of Carlson[57], which has the advantage that its testpiece is a very small sample cut from sheet stock.

These machines, and others, have proved themselves useful and it is difficult to say that one is better than another. The choice probably depends on the kinds of samples available and the particular application in mind. Dynamic tests, as a class, have been important in the development of antiozonants. In a very recent paper, Smith and Tuley[58] report on an extensive survey comparing various combinations of protective agents in laboratory and outdoor tests, both static and dynamic. They conclude that dynamic testing is essential for the true evaluation of protective agents for use in tires.

Laboratory tests are primarily of value because they give answers faster than outdoor, or service tests. There are at least two principal weaknesses of laboratory tests for antiozonants: (1) that by subjecting a sample to ozone continuously and in higher concentration than it would experience in service, one might fail an antiozonant whose rate of migration to the surface is slow, but adequate for coping with atmospheric concentrations; and (2) that a particularly volatile antiozonant might be effective in a laboratory test, but in outdoor service might soon be lost. Fortunately, today's best antiozonants have been thoroughly tested in outdoor service as well as in accelerated tests.

V. ASSESSMENT OF DAMAGE

One of the difficult problems in ozone testing has been evaluation of the damage. As pointed out by many people, the cracking pattern varies with strain, samples at low strain showing fewer and larger cracks, and samples at high strain showing many small cracks. Increase in temperature has the same effect as increase in strain [3]. The effect of protective agents will be discussed more completely in another section, but it is pertinent to point out that insufficient amounts of protectant may have the result that a few very deep cracks will form under conditions in which, otherwise, many small cracks might have been produced. This fact complicates evaluation. Various schemes have been adopted for assessing the extent of cracking. Some workers have measured the number of cracks; some the depth; and some the volume. The latter was ingeniously accomplished, in one case, by rubbing a heavy powder in all the cracks and measuring the increase in weight[59]; and, in another, by rubbing radioactive powder into the cracks and counting the total activity[60]. One author has used the cracked sample as a rubber stamp and printed the crack pattern on paper in ink[22]. This is useful in making records, but, of course, leaves the question of assessment unanswered.

A scheme for quantitative evaluation of extent of cracking is the depth measurement technique described by Rugg[61]. As Powell and Gough[28] have pointed out, cracks grow in depth as they grow in length, and Rugg feels that depth is measured more easily. He views a sample in cross-section with a 20-power microscope containing, in its field, a scale divided into millimeters. The

deepest crack, and those within 10% of the deepest, are measured and their depths averaged. Reproducibility is said to be good.

Another system is that of Creed, Hill, and Breed[56]. They chose samples of varying degrees of cracking and rated them from 1 to 6 in order of increasing severity of cracking. These are used as observational standards with which to compare the samples under test. A formula is applied to the results in such a way as to give a numerical rating for the antiozonant. This scheme was subsequently used by Meyer and Sommer[45]. Edwards and Storey[62] also use a rating system, theirs being based on functions of number and depth of cracks. Measurement of the loss of electrical conductivity in a stretched sample as cracking occurs (with consequent reduction in cross-section) has been used to assess damage[63]. This method tends to emphasize the importance of the deepest cracks.

A still different method which has been used successfully is measurement of stress relaxation as cracking proceeds. One version of this method was used by Norton[10] in 1940. Weights were hung on rubber strips and the time for the weight to fall was taken as the end point. Thompson and his associates[64] used a somewhat similar method in their study of neoprene compounds. Buckley[65] used a refined version in some experiments on the ozone resistance of IIR. His sample was attached rigidly at the bottom, and the top was connected to a beam which supported a counter-weight on its other end. Increase in elongation at constant stress was recorded during ozonization. More recently, Veith[36] has described a quite elaborate and quantitative system for evaluating ozone damage by stress relaxation. A test rack holds 12 samples in simple extension. The initial elongation is obtained by adding lead shot to a small bucket clamped to the lower end of each sample. After being mounted, the samples are held for an overnight period in an ozone-free atmosphere to reduce the viscoelastic creep to a negligible rate. The samples are then inserted in a glass-fronted ozone chamber and the ozone-induced creep is followed with a cathetometer.

In discussing evaluation of cracks, one must mention that many investigators have used samples fashioned in such a way as to vary the strain over the length or breadth of the sample. For example, Van Rossem and Talen[6] used thin wedge-shaped pieces and Fielding[53] used long tapered strips of sheet. Edwards and Storey[62] used trapezoidal strips, and they, as well as Winkleman[66], used extruded stock of triangular cross-section, which, when bent in a loop, had maximum strain at the apex of the triangle. Use of such samples has confirmed that for many stocks maximum crack damage occurs at elongations of from 10 to 20%. Whether or not there is a true "critical elongation" as suggested by Newton is still a moot question[67]. Ball, Youmans, and Rausell[68] point out that the elongation at which maximum damage occurs varies with the modulus of the stock, being lower for a high modulus stock, and they suggest that it is more appropriate to compare compounds at equal stress than at equal strain. However, Popp and Harbison[69] and van Pul[70] find little correlation between cracking and modulus.

The criterion of damage easiest to use is that of "time required for the first cracks to appear" as judged with a magnifying glass. This becomes a "go no-go" test and eliminates most subjective factors. It is true that a certain degree of skill is required to recognize the first evidence of damage, but each new reading is a check on previous ones and it is not hard to determine the time of first detectable cracking. This criterion has been used for years on products intended for static use, such as telephone wires.

For dynamic use, it has been felt that to require "no cracking" was unreal-

istic. With the advent of the true antiozonants, it now appears that a degree of protection is obtainable which, in view of the difficulties of evaluating cracks, justifies use of the criterion of no cracks. This has been used, for example, in the extensive tests carried on by the Rock Island Arsenal. As better antiozonants are found, and as their use becomes more widespread, it is anticipated that "time-to-first-evidence-of-damage" at a specified magnification will be adopted as the normal criterion.

VI. INHERENT RESISTANCE OF POLYMERS

It was mentioned early in this paper that there are now several commercial rubbers which are entirely saturated and hence are completely resistant to ozone. The resistance of other polymers varies widely, and this subject was discussed thoroughly in a recent paper by Ossefort[71]. He groups rubbers in two large groups: (I) those inherently resistant to ozone; and (II) those whose resistance is a function of compounding. The Group I list is as follows:

Acrylic ester/acrylonitriles (Acrylons)
Chlorosulfonated polyethylene (Hypalon)
2 (2-cyanoethoxy)ethyl acrylate (Vyram)
Ethyl acrylate/chloroethyl vinyl ether (Hycar 4021)
Fluorinated silicone (LS-53)
Monochlorotrifluoroethylene/vinylidene fluoride (Kel-F Elastomer)
Poly-1,1-dihydroperfluoro butyl acrylate (Poly FBA)
Silicone rubbers
Vinylidene fluoride/hexafluoropropylene (Viton A)

These polymers are all saturated and are unaffected by ozone in atmospheric concentrations.

Group II is divided into two parts, those which do not need a chemical antiozonant, and those which do. These lists are as follows:

Chemical Antiozonant Not Needed for Ozone Resistance

Brominated Butyl
Butyl (IIR)
Neoprene (CR)
Polyurethane

Chemical Antiozonant Required for Ozone Resistance

Butadiene/Acrylonitrile (NBR)
Butadiene/Acrylonitrile/Carboxylic Acid
Butadiene/Styrene (SBR)
Butadiene/Vinyl Pyridine
Cis-1,4-polyisoprene (NR)
Cis-polybutadiene
Conventional polybutadiene (BR)
Mercaptan modified adducts of polybutadiene
Polysulfides
Polyurethanes

The headings of these lists are somewhat misleading, because whether or not the resistant polymers need chemical antiozonant depends on circumstances. Neoprene contains the same number of double bonds as natural rubber, but the

reactivity of the double bond is decreased very appreciably by the presence of the chlorine atom, presumably an example of the phenomenon described by Noller[72] for small molecules. Neoprene gum stocks are quite ozone-resistant. The ozone resistance of neoprene compounds has been studied by Thompson, Baker, and Brownlow[64], and by Hartmann and Glander[73]. When pigments and plasticizers normally used in practical compounding are added, the natural resistance of neoprene is decreased (as is that of natural rubber and SBR[69]). However, even compounded neoprene usually can be protected from ozone by addition of waxes.

The ozone resistance of IIR results from a different cause. Unsaturation is tailored into IIR during synthesis in the amounts needed for satisfactory vulcanization. Many of the double bonds are used during the curing process and hence there is very little unsaturation left at optimum cure[74]. Even this small amount, however, remains an Achilles heel, and IIR is sometimes found to be susceptible to ozone cracking. The literature is quite contradictory on the ozone resistance of such rubbers, and this, no doubt, reflects the extreme importance of curing conditions and formulation[75,76,77,78]. It is generally accepted that low unsaturation is helpful, but results still tend to be erratic. Waxes and antiozonants afford good protection[44].

The butadiene and isoprene rubbers, which make up a large proportion of all rubber used, are quite vulnerable to ozone, and it is this vulnerability which has given impetus to the antiozone work. Most studies of protective agents have been concerned with natural rubber and SBR, which, of course, fall in this group. Nitrile rubbers, also in this group, are considered to be poor in ozone resistance (although Elliott and Newton[79] did not find them so), and the fact that they are usually used in highly plasticized compounds aggravates the situation[75]. They can be improved considerably by use of waxes and antiozonants. Special studies of the protection of nitrile rubbers have been made by the Rock Island Arsenal[80] and by Meyer and Sommer[45].

The polyurethanes appear in two places in Ossefort's table. This is because they vary in degree of unsaturation. Since the polysulfides do not contain unsaturation, the attack on them is believed to consist of oxidation of the disulfide linkage. Members of the family differ widely in their ozone resistance and some of them (Types A and FA) are highly resistant and should be placed in the table at a position near that of neoprene and IIR[81].

Hydropol, a substance prepared by the Phillips Petroleum Company and consisting of hydrogenated butadiene[82], is not listed in the table because it is more of a plastic than a rubber, but it is interesting in its behavior toward ozone. Even the grade which contains 29% residual unsaturation (far more than is present in IIR) is, nevertheless, quite ozone-resistant[83]. Two hypotheses have been offered to explain this. One is that the most accessible double bonds have already reacted during hydrogenation and hence only relatively inactive ones are left. The other is that the low molecular weight fraction of the polymer, probably more readily hydrogenated than the high molecular weight portion, has been converted to a saturated wax which acts like other waxes in protecting the surface from ozone. The latter explanation seems plausible, but at the present time is sheer speculation.

The placement of mercaptan adduct rubbers in the last group is misleading. These products can vary widely in unsaturation. Pierson et al.[84] report data on samples which were 69% saturated and find them to be as resistant as neoprene. Meyer, Naples, and Rice[85], in tests with high concentrations of ozone (10,000 pphm), find them superior to both IIR and neoprene. There may be

similarities between the adduct rubbers and Hydropol with respect to the nature of the residual double bonds.

VII. PROTECTIVE AGENTS

At the time of the Newton and Crabtree papers, a few preventive measures for ozone attack were already known. Williams[4] had noted that oxidized rubber was less susceptible to ozone cracking than fresh rubber, and had suggested the rather drastic measure of treating the surface of the sample with copper chloride. Many workers realized that continuous inert coatings offered protection. Norton[10] mentioned the use of alkyl resin films and Newton[12] and Buist[37] used Vulcaprene. Patents have been issued on hydrogenation of the surface of rubber articles to protect them from ozone[86], on covering them with phenol formaldehyde resin[87], and on addition of certain adducts of hydrogen sulfide[88]. Polyvinyl chloride paints have been used[75]. Some of these measures were useful in special circumstances but they are certainly not general solutions to the problem.

A. WAXES

For many years, wax has been widely used as a protective agent and several authors have studied the relative benefit of various types of wax[44,58,66,70,89,90]. Microcrystalline waxes have been highly regarded and some special blends reputed to be particularly efficacious have been placed on the market. There seems little doubt that the beneficial effect of wax arises from the fact that it blooms to the surface and there interferes mechanically in the contact between ozone and the rubber. It is general knowledge that too little wax is worse than none at all because a break in the film concentrates the ozone attack, and hence the crack growth, at those few places where the wax film has failed. If large quantities of wax are used, on the other hand, there is a tendency for it to crystallize in heavy layers which are easily broken. Paraffin wax, in particular, acts in this manner. Also, heavy layers of wax are unsightly and, in some cases, cause sticking of surfaces.

Any factor which affects the rate of migration of a wax to the surface of a rubber compound may alter the degree of ozone resistance. Some of these are solubility in the rubber polymer; molecular weight and chemical nature of the wax; adsorptive character of any fillers or pigments present. There is at least one instance known in which a change of brand of the whiting used in a wire stock had a marked effect on the ozone resistance. Some compounds of natural rubber and SBR can be given quite good resistance to ozone in static service with no other protective agent than wax, but it is usually dangerous to rely on wax alone. Neoprene and IIR, however, which have high inherent resistance to ozone, can, in many cases, be given entirely adequate resistance to outdoor atmospheres with use of no other protective agent than wax of suitable type and in suitable amount. Neoprene jacketed telephone wires, protected with three or four parts of wax, have stood up for ten years in Los Angeles with no sign of cracking[44].

B. ANTIOZONANTS

It has been abundantly evident that wax alone is not an adequate answer to the ozone problem with the butadiene and isoprene rubbers, particularly when they are subject to flexing in service, and, therefore, the search for better protective agents has continued. In his study of frosting in 1939, Tuley[17] found that, in addition to waxes, certain chemicals were effective in preserving the shiny surface of natural rubber. After mentioning that most antioxidants were

not effective, and that the aldehyde-amines and ketone-amines were slightly so, he had this to say: "A limited number of chemicals have been found which are of any value. The most effective of these are all members of one class, the diprimary arylamines, represented by *p*-phenylenediamine, benzidine, and 4,4′-diaminodiphenylmethane". In the light of the discussion to follow, these words take on great significance. Tuley was aware of the toxicity of these compounds and used them in fractional parts. Derivatives of these compounds, used in amounts of three to five parts per hundred, are our best antiozonants today.

In 1943, a patent was issued to Barton[91] for the use of 1-(*p*-aminophenyl)-2,5-dimethyl pyrrole as a protective agent. This substance seemed to exert a strongly beneficial effect on fresh stocks. Many other pyrroles, notably hexamethylene bisdimethyl pyrrole[19], were tried. In fresh stocks, they appeared to be very helpful in static tests, but after a shelf-aging period of six months, they failed badly on retest. It appeared that a heavy bloom had developed on the surface and this was broken when the samples were stretched. Thus, some members of a class of compound which, at first, was thought to be protecting by chemical means finally appeared to act more like wax. It is probable that the original member bore a closer relationship to modern antiozonants.

Nickel dibutyldithiocarbamate has been said to have value as a protective agent against ozone, particularly at atmospheric concentrations. Its protective action is aided by the presence of wax and is probably related to the bloom which is produced[92].

In the late forties, certain condensation products of ketones and amines were advocated as contributing to the ozone resistance of rubber and SBR. These substances were shown to react with ozone to form dark resinous skins, but they did not become widely used.

It has long been thought that antioxidants, in general, have some protective effect against ozone, but the data have always been erratic. Gaughan[93] states that "conventional antioxidants give protection against ozone cracking mostly by accident". Thompson and coworkers[64], in a systematic study, found some antioxidants which were very good antiozonants, some which were inert, and some which were actually harmful. Similar results were reported by van Pul[70]. However, the idea that antioxidants might be helpful has led investigators to work with various amines, and, in doing so, Creed, Hill, and Breed[56] at Monsanto discovered a substance which might be called a true antiozonant. This was 6-ethoxy-1,2-dihydro-2,2,4-trimethylquinoline. At a level of 3 parts per hundred of rubber or SBR, this compound afforded very substantial protection even in dynamic testing.

While these experiments were going on, workers in other laboratories were testing many other substances, and out of this work came the best antiozonants which are known today. These are the N,N′-dialkyl-*p*-phenylenediamines and related compounds, remarkably closely akin to Tuley's antifrosting agents. One of the earliest ones tried was N,N′-dibutyl-*p*-phenylenediamine. The fact that it is an excellent antiozonant was demonstrated in several laboratories. Gaughan[93], of the Detroit Arsenal, refers to this discovery as a "major advance". It soon developed, however, that this compound was alarmingly toxic for routine use and that its vapor pressure was too high. Continued work at Rock Island Arsenal led to a study of N,N′-di-*secondary*-butyl benzidine which was less toxic and less fugitive, but was not as economically available. From these beginnings, extensive programs were initiated by the Rock Island Arsenal and their contractor, Augustana Research Foundation, and by the Detroit Arsenal and their contractors, Burke Research Company and Dayton Rubber Company.

These programs screened a large number of compounds for antiozonant properties in accelerated and outdoor tests in both static and dynamic exposure. Some of this work was reported by Shaw, Ossefort, and Touhey[55] in 1954. This paper presents data on tests of the following compounds in SBR, both in accelerated and outdoor exposure, with and without other additives:

p,p'-Diaminodiphenylmethane
N,N'-Dinonyl-*p*-phenylenediamine
N,N'-Dioctyl-*p*-phenylenediamine
p-Aminophenol
p-Aminodiethylaniline
o-Aminophenol
p-Phenylenediamine
N,N'-Diphenylbenzidine
0.65 Diarylamine-ketone reaction product
0.35 N,N'-Diphenyl-*p*-phenylenediamine
nickel-dibutyl-dithiocarbamate
N,N'-Diphenyl-*p*-phenylenediamine
6-Ethoxy-1,2-dihydro-2,2,4-trimethylquinoline
N,N'-Di-4(2,6-dimethylheptyl)-*p*-phenylenediamine
N,N'-Di-*n*-octyl-*p*-phenylenediamine
N,N'-Di-(1'-methyloctyl)-*p*-phenylenediamine
N,N'-Di-(1'-methyldodecyl)-*p*-phenylenediamine
N,N'-Di-(1'-methylhexadecyl)-*p*-phenylenediamine
N,N'-Di-2-naphthyl-*p*-phenylenediamine
Mixture of mono- and diheptyl diphenylamines
N,N'-Di-4(2,6-dimethylheptyl)-*o*-phenylenediamine
N,N'-Di-4-(2,6-dimethylheptyl)-*m*-phenylenediamine

The outstanding antiozonants from this list are:

p,p'-Diaminodiphenylmethane
N,N'-Dinonyl-*p*-phenylenediamine
N,N'-Dioctyl-*p*-phenylenediamine
N,N'-Di-4(2,6-dimethylheptyl)-*p*-phenylenediamine
N,N'-Di-(1'-methyloctyl)-*p*-phenylenediamine

Further data on two of these substances are shown in the following table taken from their paper.

TIME TO FIRST CRACK FOR 80/20 GR-S COMPOUNDS CONTAINING VARIOUS ANTIOZIDANTS* IN THE FIRESTONE WEATHERING APPARATUS

Ozone concentration: 50 ± 5 pphm
Temperature: 100 ± 1° F
Dynamic flex: 0 to 20%
Static stress: 20%

Note: This test was run continuously Monday through Friday.
OK: Indicates specimen crackfree, test continuing.

Antiozidant*	Amt. 100 RHC	Amt. wax	Time to first crack in hours	
			Static	Dynamic
N,N'-Dinonyl-*p*-phenylenediamine	3	3	OK1440	7
N,N'-Dinonyl-*p*-phenylenediamine	3	1	OK1440	7
N,N'-Dioctyl-*p*-phenylenediamine	3	3	OK1440	23
N,N'-Dioctyl-*p*-phenylenediamine	3	1	OK1440	23

* The word "antiozonant" is used more commonly now.

Interesting facts from this paper are: The efficiency of the antiozonant is enhanced by the presence of wax; is diminished by a period of oxidation before the ozone test; and, in general, samples last longer outdoors than they do in the accelerated test. In particular, 6-ethoxy-1,2-dihydro-2,2,4-trimethylquinoline gives much better protection outdoors than in the accelerated test. This is believed to result from the fact that a sample outdoors is normally exposed to much lower concentrations of ozone, and even when the concentration is high it is intermittent. Thus, an antiozonant which diffuses to the surface quite slowly might still be able to cope with the ozone in the outdoor test. As pointed out earlier, this is a weakness of accelerated tests.

In other reports [70,94], N-phenyl-N′-cyclohexyl-*p*-phenylenediamine, along with the same N,N′-dioctyl and N,N′-dinonyl derivatives, was found to be outstanding. Smith and Tuley[58] in fact obtained repeated readings which indicated N-phenyl-N′-cyclohexyl-*p*-phenylenediamine to be measurably superior to other antiozonants.

In recent work at the Burke Research Company[95], on contract to the Detroit Arsenal, the following range of antiozonant activities was found for various substituted *p*-phenylenediamines in SBR compounds after being aged 24 hours at 100° C:

Excellent to Good

N-substituent	*N′-substituent*
t-Butyl	*t*-Butyl
s-Alkyl (C_7–C_9)	*s*-Alkyl (C_7–C_9)
s-Alkyl (C_6–C_{12})	Cyclohexyl (C_6–C_9)
Alkyl (C_3–C_{12})	Phenyl
Cyclohexyl (C_6–C_9)	Aryl (C_6–C_{10})
Cycloalkyl (C_5–C_8)	Cycloalkyl (C_5–C_8)

Good to Fair

N-substituent	*N′-substituent*
s-Alkyl (C_3–C_6)	*s*-Alkyl (C_3–C_6)
s-Alkyl (C_{10}–C_{13})	*s*-Alkyl (C_{10}–C_{13})
s-Alkyl (C_{14}–C_{17})	Cyclohexyl
s-Alkyl (C_{14}–C_{17})	Phenyl
Cyclohexyl (C_9 or higher)	Cyclohexyl (C_9 or higher)
Aralkyl (Phenylethyl)	Aralkyl (Phenylethyl)

Fair to Poor

N-substituent	*N′-substituent*
n-Alkyl (C_8 optimum)	*n*-Alkyl (C_8 optimum)
s-Butyl	*s*-Alkyl (C_9–C_{12})
Aryl (C_6–C_{10})	Aryl (C_6–C_{10})
Alkylidene (C_7–C_9)	Alkylidene (C_7–C_9)
Aralkyl (benzyl)	Aralkyl (benzyl)
Cyanoethyl	Cyanoethyl

For a while, in these studies, it was believed that the presence of an active hydrogen atom, which is generally thought of as being important in antioxidants, was also desirable in antiozonants. This idea has still not been abandoned completely, although it has been found that certain tetra-substituted *p*-phenylenediamines can also be good antiozonants. The Burke Research report gives the following ratings on antiozonants of the formula RNA-C_6H_4-N′R′B with R, R′, A, and B, as indicated:

Excellent

N-substituents		*N'-substituents*	
A	*R*	*B*	*R'*
Methyl	*s*-Alkyl (C_3–C_8)	Methyl	*s*-Alkyl (C_3–C_8)
Cyanoethyl	*s*-Alkyl (C_3–C_8)	H	*s*-Alkyl (C_3–C_8)
Cyanoethyl	*s*-Alkyl (C_3–C_8)	Cyanoethyl	*s*-Alkyl (C_3–C_8)
Methyl	Cyclohexyl	Methyl	Cyclohexyl
Methyl	Methyl	H	*s*-Alkyl (C_8)
Methyl or ethyl	Methyl or ethyl	H	Cyclohexyl
Methyl	Methyl	H	Phenyl
Methyl	Methyl	Methyl	*s*-Alkyl (C_3–C_8)

Good to Fair

N-substituents		*N'-substituents*	
A	*R*	*B*	*R'*
Methyl	*n*-Alkyl (C_8)	Methyl	*n*-Alkyl (C_8)
Methyl	Phenyl	Methyl	Phenyl
*Iso*butyl	*Iso*butyl	*Iso*butyl	*Iso*butyl
Methyl	*t*-Butyl	Methyl	*t*-Butyl
Methyl	Methyl	Cyanoethyl	Cyclohexyl
Cyanoalkyl (C_7–C_8)	*s*-Alkyl (C_3–C_8)	H	*s*-Alkyl (C_3–C_8)
Cyanoalkyl (C_3–C_8)	Aryl (C_6–C_7)	H	Alkyl or Cycloalkyl (C_3–C_8)

Fair to Poor

N-substituents		*N'-substituents*	
A	*R*	*B*	*R*
*Iso*butyl	Cyclohexyl	*Iso*butyl	Cyclohexyl
Cyclohexyl	Cyclohexyl	H	H
Methyl	Methyl	Cyanoethyl	Cyanoethyl
Methyl	Methyl	H	Cyanoethyl
Methyl	Methyl	←——Benzylidene——→	
Cyanoethyl	Cyanoethyl	H	Cyanoethyl
Cyanoethyl	Cyanoethyl	Cyanoethyl	Cyanoethyl
Methyl	Methyl	Methyl	Methyl
n-Propyl	*s*-Alkyl (C_7)	*n*-Propyl	*s*-Alkyl (C_7)
Cyanoethyl	Cyanoethyl	H	Phenyl
*Iso*butyl	*s*-Butyl	*Iso*butyl	*s*-Butyl

Although the tetra-substituted compounds in the first list are rated "excellent" in this table, their effectiveness does not compare with that of N,N'-dioctyl or N,N'-dinonyl-*p*-phenylenediamine.

Studies with compounds having other nuclei between the amino groups in place of phenylene showed that ozone resistance decreased in the order phenylene, diphenylene, methylene, diphenylene and amino diphenylene derivatives.

It will be evident to the reader that extensive screening programs of this sort require the mixing, curing, mounting, and observing of hundreds of samples. In all cases, the results are affected by the specific conditions of test. Hence it would be surprising, indeed, if universal agreement were found in all cases, particularly on the relative effectiveness of quite similar substances. One should, therefore, regard the above comparisons as qualitative trends.

From these and other tests, it appears to be sound practice to use at least 3 parts of a good antiozonant, and for many formulations 5 parts are needed. It is also desirable to add 1 to 3 parts of wax along with the antiozonant. This is borne out in a comparison between Los Angeles and accelerated exposure of a large number of SBR compounds by Lundberg, Vacca, and Biggs[35,44], and in a recent paper by Edwards and Storey[96]. The latter authors, using both

the ozone chamber and an ingenious technique of mounting samples on actual tire sidewalls, obtained excellently correlating data showing that combinations of wax and standard antiozonants offer effective protection.

The level of protection which can be obtained by good antiozonants in outdoor exposure has been shown in some of the tables quoted above. Information on many specific articles of manufacture is also available, and indicates that they can be protected[45]. For example, it has been demonstrated that tires containing proper amounts of good antiozonants will remain uncracked outdoors for prolonged periods[58,94].

VIII. MECHANISM OF ACTION OF ANTIOZONANTS

The mechanisms by which antiozonants and antioxidants act appear to be completely different. An interesting paper which bears on this point is that of Delman, Simms, and Allison[97]. These workers carried out experiments in which rubber was dissolved in benzene and the viscosity of the solution was measured while ozonized air was passed through it. The viscosity fell at rates much higher than were found in similar experiments in which the air contained no ozone. When conventional antioxidants, such as phenyl-2-naphthylamine or diphenyl-*p*-phenylenediamine, were added to the solution, practically no change in the rapid rate of fall of viscosity was found, but when antiozonants, such as N,N′-dibutyl-*p*-phenylenediamine or 6-ethoxy-1,2-dihydro-2,2,4-trimethylquinoline, were added, the viscosity stayed almost constant until the antiozonant was used up. When the viscosity began to fall, it could be stabilized again by further additions of antiozonant*. Kendall and Mann[18] found that phenyl-2-naphthylamine inhibited the development, during oxidation, of certain bands observable in the infrared spectrum, but that it did not inhibit ozone cracking of natural rubber vulcanizates. Together with the fact, already mentioned, that many antioxidants are useless as antiozonants, these results seem to support the viewpoint expressed above that protection against oxidation and protection against ozonization follow different mechanisms. It is also suggested that antiozonants work by stoichiometry rather than by chain-stopping. If this is true, then the action of the antiozonant must be to migrate to the surface of a rubber sample and there preferentially react with ozone.

The Augustana Research Foundation[16], in contract work for the Rock Island Arsenal, has carried out some most interesting experiments which throw light on how antiozonants function. They devised a sensitive technique for measuring the change in concentration of ozone in air before and after passing over the substances under study. By means of this technique, they were able to show not only the absorption of ozone by SBR raw polymer dispersed on silica gel, but also by unstretched vulcanized SBR rods. In the latter case, absorption fell off very rapidly as the surface became saturated. This technique was used to measure the ozone absorption of the antiozonants themselves dispersed on silica gel, and it was found that most of the typical N,N′-dialkyl-*p*-phenylenediamines consume four moles of ozone per mole. Corresponding derivatives of benzidine absorb eight moles. A substituted *p*-amino phenol absorbs only two moles. These reactions need much more investigation. (Infrared analysis of the products of ozonization of antiozonants shows that the aromatic characteristics of the original compound have been destroyed to a large extent, and that carboxyl and carbonyl groups are predominant functional groups in the reaction

* Smith and Tuley[45] have used this procedure successfully as a screening test for antiozonants. The results correlate with outdoor dynamic tests.

products. Nitro groups are present, and oxalic acid has been identified.) Mixtures of antiozonants with unsaturated hydrocarbons (models for unsaturated rubber) were treated with ozonized air and it was found that the antiozonant is attacked first and is consumed before appreciable attack occurs on the olefin. These experiments make entirely plausible the hypothesis that antiozonants function by reacting preferentially with the ozone which reaches the surface. The amount of antiozonant on the surface at any time is a function of its concentration and solubility in the polymer; its rate of diffusion through the polymer; previous contact of the surface with ozone; volatility of the antiozonant; and perhaps other factors. In this connection, the following paragraph quoted from the Augustana report (page 17) is pertinent:

> "A number of GR-S vulcanizates which included both an antiozonant and wax in their formulation were placed under static stress and exposed to ozone at low concentrations (30 pphm) intermittently for extended periods of time without obtaining any ozone cracks on the surface of the rods. . . . In particular, samples S12B68 and S47A3B7 were completely protected by the antiozonant each contained, in that no ozone cracking could be detected in over 100 hours for S12B68 and over 60 hours for S47A3B7. In all cases, it was found that the initial rates of absorption of ozone were high (nearly 100% removal of the ozone from the ozone-air stream) but the rates gradually declined as a residue of oxidized products accumulated on the surface of the rod. During an idle time between successive exposures, it was found that fresh ozone-sensitive materials had effused to the surface of the rods so that the initial rate of absorption in each successive run was higher than the end rate of the preceding run. After a certain number of runs, a steady state of absorption of ozone was reached in which the rate of absorption (after a few initial higher rates) became constant for a given vulcanizate. It is believed that in the steady state the rate of the reaction of ozone with a particular sample is fixed by the rate at which the antiozonant migrates to the surface of the rubber. In practice, it was found that if the quantity of ozone absorbed for various times were plotted against the corresponding time, a curve was obtained for each run which could be assembled into a composite curve."

Some disadvantages of present day antiozonants, in addition to the toxicity already mentioned, are that they are oil extractable and they tend to discolor as they react with ozone, and hence spoil the appearance of light-colored goods. Investigators in this field have been mindful of these weaknesses and are continuing their search for better materials. There is some evidence that the tetra-substituted *p*-phenylenediamines are not as bad stainers as the disubstituted derivatives, although they are still much worse than conventional phenolic antixoidants. There are few clues on which to proceed to develop antiozonants free of these difficulties, but if ease of reaction with ozone is a controlling property, there should be other systems which would work as well as the substituted aromatic amines. In view of the great strides already made in finding compounds with desired properties, it seems quite likely that further refinements are attainable.

ACKNOWLEDGMENT

The author is grateful for aid received during the preparation of this paper. Constructive comments on the manuscript were offered by A. G. Veith and

A. E. Juve, of the Goodrich Research Center; F. H. Winslow, G. N. Vacca, H. Peters, and C. V. Lundberg, of the Bell Telephone Laboratories; members of the staffs of the Detroit and Rock Island Arsenals; G. E. P. Smith, of the Firestone Research Laboratories; and James Crabtree. Reports not yet published, or not readily available to the author, were supplied by H. Tucker, A. G. Veith, G. N. Vacca, G. E. Meyer, F. B. Smith (and W. F. Tuley), G. E. P. Smith, the Detroit and Rock Island Arsenals.

IX. BIBLIOGRAPHY

[1] Harries, C., *Ber.* **38**, 1195 (1905).
[2] Reported in Royle Forum (John Royle and Sons), No. 40, Sept. 15, 1940.
[3] Thomson, W., *J. Soc. Chem. Ind.* **4**, 710 (1885).
[4] Williams, I., *Ind. Eng. Chem.* **18**, 367 (1926).
[5] Haushalter, F. L., Jones, W. N., and Schade, J. W., *Ind. Eng. Chem.* **20**, 300 (1928).
[6] Van Rossem, A., and Talen, H. W., *Kautschuk* **7**, 79 (1931); Rubber Chem. & Technol. **4**, 490 (1931).
[7] Rainier, E. T., and Gerke, R. H., *Ind. Eng. Chem. Anal. Ed.*, **7**, 368 (1935).
[8] Somerville, A. A., Ball, J. M., and Cope, W. H., *Ind. Eng. Chem.* **21**, 1183 (1929).
[9] Kearsley, E. P. W., *Rubber Age* **27**, 649 (1930).
[10] Norton, F. J., *Rubber Age* **47**, 87 (1940).
[11] Eccher, S., *Gomma* **4**, 1 (1940); Rubber Chem. & Technol. **13**, 566 (1940).
[12] Newton, R. G., *India Rubber J.* **121**, 257 (1951).
[13] Crabtree, J., and Kemp, A. R., *Ind. Eng. Chem.* **38**, 278 (1946).
[14] Crabtree, J., and Kemp, A. R., *Ind. Eng. Chem. Anal. Ed.*, **18**, 769 (1946).
[15] Fisher, H. L., Quoted by Tuley, Ref. 17 below.
[16] Augustana Research Foundation, Rock Island, Ill., Final Report on Contract No. DA-11-022-ORD-329 and Contract No. DA1-11-022-ORD-508-(P)-40, Project No. TB4-521, Aug. 1, 1957.
[17] Tuley, W. F., *Ind. Eng. Chem.* **31**, 714 (1939).
[18] Kendall, F. H., and Mann, J., *J. Polymer Sci.* **19**, 503 (1956).
[19] Crabtree, J., Private Communication.
[20] Pummerer, R., and Richtzenhain, H., *Ann.* **529**, 33 (1937); Rubber Chem. & Technol. **11**, 7 (1938).
[21] Lahous, G., *Chem. Ber.* **87**, 1708 (1954).
[22] Smith, D. M., and Gough, V. E., *Trans. Inst. Rubber Ind.* **29**, 219 (1953).
[23] Cuthbertson, G. R., and Dunnom, D. D., *Ind. Eng. Chem.* **44**, 834 (1952).
[24] Crabtree, J., and Biggs, B. S., *J. Polymer Sci.* **11**, 280 (1953).
[25] Newton, R. G., Private Communication.
[26] Barnard, D., Private Communication.
[27] Buist, J. M., *Rev. gén. caoutchouc* **31**, 479 (1954); Rubber Chem. & Technol., **28**, 230 (1955).
[28] Powell, E. G., and Gough, V. E., *Trans. Inst. Rubber Ind.* **21**, 102 (1945).
[29] Ossefort, Z. T., and Touhey, W. J., *Rubber World* **132**, 62, 70 (1955).
[30] Matsuda, T., and Tanaka, M., *J. Soc. Rubber Ind. Japan* **26**, 407 (1953).
[31] Kainradl, P., *Kautschuk und Gummi* **8**, 117 (1955); Rubber Chem. & Technol. **29**, 1102 (1956).
[32] Bergstrom, E. W., Rock Island Arsenal Laboratory Report No. 56-3729, Dec. 12, 1956.
[33] A.S.T.M. Test Method D574.
[34] Paneth, F. A., and Edgar, J. L., *Nature* **142**, 112 (1938).
[35] Vacca, G. N., Presented at St. Louis Symposium A.S.T.M., Feb. 1958, to be published by A.S.T.M.
[36] Veith, A. G., Presented at St. Louis Symposium A.S.T.M., Feb. 1958, to be published by A.S.T.M.
[37] Nellen, A. H., Dunlap, W. B., Jr., Glaser, C. J., Jr., and Landes, R. A., *Rubber Age* **66**, 659 (1950).
[38] Kettering Lab., University of Cincinnati, "Concentration of Oxidizing Substances in the Atmosphere of a Number of American Cities", Sept. 1954.
[39] Air Pollution Foundation, 704 South Spring St., Los Angeles, Calif., "An Aerometric Survey of the Los Angeles Basin", July 1, 1955.
[40] Bartel, A. W., and Temple, J. W., *Ind. Eng. Chem.* **44**, 857 (1952).
[41] Haagen-Smit, A. J., Bradley, C. E., and Fox, M. M., *Ind. Eng. Chem.* **45**, 2086 (1953).
[42] Stanford Research Institute, "The Smog Problem in Los Angeles County", 1954.
[43] Larson, G. P., Chipman, J. C., and Kauper, E. K., *J. Air Pollution Control Association* **5**, 84 (1955).
[44] Lundberg, C. V., Vacca, G. N., and Biggs, B. S., *Rubber World* **135**, 699 (1957).
[45] Meyer, D. A., and Sommer, J. G., Dayton Rubber Co. Final Report to Detroit Arsenal, June 30, 1957, A.S.T.I.A. Catalogue No. AD 143312.
[46] Van Pul, B. I. C. F., *Kautschuk und Gummi* **8**, WT184 (1955); *C. A.* **49**, 13679 (1955).
[47] Bowen, G., and Regener, V. H., *J. Geophys. Research* **56**, 307 (1951).
[48] Wadelin, C. W., *Anal. Chem.* **29**, 441 (1957).
[49] Bradley, C. E., and Haagen-Smit, A. J., *Rubber Chem. & Technol.* **24**, 750 (1951).
[50] Crabtree, J., and Erickson, R. H., *India Rubber World* **125**, 719 (1952).
[51] Beatty, J. R., and Juve, A. E., *Rubber World* **131**, 232 (1954).
[52] Stair, R., Bagg, T. C., and Johnston, R. G., *J. Research Natl. Bur. Standards* **52**, 133 (1954).
[53] Fielding, J. R., *India Rubber World* **115**, 802 (1947).
[54] Ford, E. W., and Cooper, L. V., *India Rubber World* **124**, 696 and **125**, 55 (1951).
[55] Shaw, R. F., Ossefort, Z. T., and Touhey, W., Jr., *Rubber World* **130**, 636 (1954).
[56] Creed, K. E., Hill, R. B., and Breed, J. W., *Anal. Chem.* **25**, 241 (1953).
[57] Carlson, L. E., Presented at Meeting of Rubber Division, A.C.S., May 1958.
[58] Smith, F. B., and Tuley, W. F., Presented at Chicago Meeting of Rubber Division, A.C.S., Sept. 1958.
[59] Werkenthin, T. A., *Rubber Age* **59**, 697 (1946).
[60] Kalinsky, J. L., and Werkenthin, T. A., *Rubber Age* **75**, 375 (1954).
[61] Rugg, J. S., *Anal. Chem.* **24**, 818 (1952).
[62] Edwards, D. C., and Storey, E. B., *Trans. Inst. Rubber Ind.* **31**, 45 (1955).
[63] Shaw, R. F., and Adams, S. R., *Anal. Chem.* **23**, 1649 (1951).
[64] Thompson, D. C., Baker, R. H., and Brownlow, R. W., *Ind. Eng. Chem.* **44**, 85 (1952).
[65] Buckley, D. J., and Robison, S. B., *J. Polymer Sci.* **19**, 145 (1956).
[66] Winkleman, H. A., *Ind. Eng. Chem.* **44**, 841 (1952).

[67] Zuev, Yu. S., Pravednikova, S. I., Proceedings of the Academy of Sciences, USSR, Section: Physical Chemistry, Vol. 116, Sept.–Oct. 1957, English Translation (Consultants Bureau, Inc., 227 West 17th St., New York 11, N. Y.), 641.
[68] Ball, J. M., Youmans, R. A., and Rausell, A. F., *Rubber Age* **55**, 481 (1944).
[69] Popp, G. E., and Harbison, L., *Ind. Eng. Chem.* **44**, 837 (1952).
[70] Van Pul, B. I. C. F., *Trans. Inst. Rubber Ind.* **34**, 28, 37, 86 (1958).
[71] Ossefort, Z. T., Presented at St. Louis Symposium A.S.T.M., Feb. 1958, to be published by A.S.T.M.
[72] Noller, C. R., Carson, J. F., Martin, H., and Hawkins, K. S., *J. Am. Chem. Soc.* **58**, 24 (1936).
[73] Hartmann, A., and Glander, F., *Kautschuk und Gummi* **8**, WT35 (1955); RUBBER CHEM. & TECHNOL. **29**, 166 (1956).
[74] Zapp, R. L., Decker, R. H., Dyroff, M. S., and Rayner, H. A., *J. Polymer Sci.* **6**, 331 (1951).
[75] Rinne, W. W., and Kvet, E. J., Presented at Army Conference on Elastomers, Ft. Belvoir, Va. April 24–25, 1957.
[76] Neu, R. F., *Rubber World* **137**, 398 (1957) (Butyl Symposium at Ft. Wayne Meeting).
[77] Enjay Co., Report ELD-6815, "Ozone Resistance and Weatherability of Butyl Compounds".
[78] Dunkel, W. L., and Phelan, R. R., *Rubber Age* **83**, 281 (1958).
[79] Elliott, R., and Newton, R. G., *J. Rubber Research* **17**, 17 (1948).
[80] Bergstrom, E. W., Rock Island Arsenal Laboratory Report No. 56-1946, July 5, 1956.
[81] Thiokol Company, Butyl Bulletin No. 105.
[82] Jones, R. V., Moberly, C. W., and Reynolds, W. B., *Ind. Eng. Chem.* **45**, 1117 (1953).
[83] Peters, Henry, Private Communication.
[84] Pierson, R. M., Gibbs, W. E., Meyer, G. E., Naples, F. J., Saltman, W. M., Shrock, R. W., Tewksbury, L. B., and Trick, G. S., *Rubber and Plastics Age* **38**, Nos. 7 and 8 (1957).
[85] Meyer, G. E., Naples, F. J., and Rice, H. M., Presented at Chicago Meeting of Rubber Division, A.C.S., Sept. 1958.
[86] Harvey, M. T., U. S. Patent 2,678,892.
[87] Shinkle, S. D., U. S. Patent 2,648,613.
[88] McMillan, F. M., U. S. Patent 2,514,661.
[89] Sharpe, P. D., *Rubber Age* **77**, 884 (1955).
[90] Best, L. L., and Moakes, R. C. W., *Trans. Inst. Rubber Ind.* **27**, 103 (1951).
[91] Barton, B. C., U. S. Patent 2,324,056.
[92] Pinazzi, C. P., and Billuart, M., *Rev. gén. caoutchouc* **31**, 123 (1954); RUBBER CHEM. & TECHNOL. **28**, 438 (1955). See also du Pont Report No. 56-9, 11/56.
[93] Gaughan, J. E., *Rubber World* **132**, 136 (1956).
[94] Bergstrom, E. W., Rock Island Arsenal Laboratory Report No. 58–105, Jan. 1958.
[95] Bruce, F. C., Isley, R. E., and Hunt, B., Report No. 57 (Final and Summary Report) ,Burke Research Co. to Detroit Arsenal on Project No. TT1-718, Oct. 1, 1957, Contract No. DA-20-089-ORD-36531.
[96] Edwards, D. C., and Storey, E. B., *Rubber Age*, **79**, 787 (1956).
[97] Delman, A. D., Simms, B. B., and Allison, A. R., *Anal. Chem.* **26**, 1589 (1954).
[98] Tucker, H., Presented at St. Louis Symposium A.S.T.M., Feb. 1958, to be published by A.S.T.M.

THE USE OF RADIOACTIVE SULFUR IN VULCANIZATION *

G. A. Blokh

Kiev Technological Institute of Light Industry, Kiev, USSR

One of the newest and most promising physical-chemical methods consists of the use of radioactive tracer atoms, particularly in such varying fields of knowledge[1,2,3,4,5] as research, industry, agriculture, etc.

It should not be surprising therefore that these methods are favored in the study of rubber, especially in connection with the very complex vulcanization process. The use of the isotope method introduces new, realistic prospects to the experimental study of vulcanization. These include the interaction of sulfur-containing chemicals, such as accelerators, in mixtures subjected to vulcanization.

A study of the interaction of accelerators with vulcanizing agents, based on isotopic exchange, makes possible a determination of the mobility of sulfur atoms at carbon-sulfur bonds and other bonds of organic substances. By the isotope method it is possible to observe the movements of sulfur tracer atoms and of tagged sulfur compounds in the complex and manifold curing process. The mobility of sulfur in various combinations with carbon is directly related to accelerator structure and activity and, consequently, to the synthesis of new accelerator types. It is very important to clarify the question as to whether the mobility of sulfur atoms and the intensity of the isotope exchange can serve as a criterion for accelerated activity in curing. Tracer atoms can be used extensively to solve many technological problems[33,34,35] in the rubber industry.

This review deals with scientific studies made in the field of tagged sulfur vulcanization.

THE INTERACTION OF ACCELERATORS AND VULCANIZING AGENTS

This interaction and its influence on the structure of rubber form the core of the study of vulcanization and have not been solved experimentally[6] as yet. In order to rationalize vulcanization, it must be determined whether an interaction of accelerators and vulcanizing agents takes place in the rubber mix during cure, whether intermediate products emerge which decompose as active sulfur forms, and whether the sulfur belonging to the accelerator or to the vulcanizate is mobile. An investigation of these matters experimentally became feasible when the method of tracer atoms was introduced. The reactions occurring during cure involving the isotopic exchange of sulfur atoms found in some of the best known accelerators such as thiazoles, carbamates, thiurams, xanthates, sulfenamides, and others, as well as of sulfur as a curing agent, both melted and in solution, or, in the rubber itself, have been made the subject of numerous studies (see, in this connection References 7–15, 24, 30, 32, 37–42, 44 and 45). These studies cover the wide temperature range of 25° to 190°.

* A translation (with minor revisions) of an article[47] by G. A. Blokh in *Gummi und Asbest*, Vol. 10, page 610–616 and 672–684 (1957).

The basis of the experimental procedure was that the sulfur containing accelerator and radioactive sulfur, S*, were either melted together, refluxed in solvents, e.g., xylene, alcohol, benzene, and the like, or they were mixed with rubber and heated at 140° to 150°. Next, the accelerators and curing agents were chemically isolated from the melts, solutions or rubber vulcanizates. The separation of the accelerator from free radioactive sulfur must be absolutely

TABLE I

ISOTOPIC EXCHANGE OF ELEMENTARY SULFUR WITH SULFUR FROM THE ACCELERATOR

Reactants	Temp., °C	Time, hr/min	Exchange, %	Velocity constant, K (hr^{-1})	Act. energy kcal/mole
Potassium xanthate + sulfur (alcohol-toluene solution)[12]	0	0/60	85.8	0.0324	—
Same as above	18	0/15	80.9	0.0996	—
Isopropyl xanthate + sulfur (naphthalene)	115	5/0	100	—	—
Potassium diethyldithiophosphate + sulfur (alcohol-toluene solution)	100	—	None	—	—
Sodium diethyldithiocarbamate + sulfur (alcohol-toluene solution)[11]	60	15/30	100	0.089	22.3
Same as above	70	5/0	100	0.242	
Nickel diethyldithiocarbamate + sulfur (decalin)[41]	150	8/0	None	—	—
Tetramethylthiuram disulfide + sulfur[5,14,26,34]					
(melt)	100	1/0	36.2		
(rubber)	145	1/0	65.0	0.110	—
(naphthalene)	150	—	—	—	21.5
Tetraisobutylthiuram disulfide + sulfur[41] (xylene)	148.5	—	—	—	24.0
Tetraethylthiuram disulfide + sulfur[41] (acetone)	58	2/0	None	—	—
MBT + sulfur[7,26,30]					
(melt)	100	3/0	0.8		
(melt)	145	0/30	47.0	0.365	—
(melt)	190	0/7	100		
(xylene)	125	5/0	20.3	—	—
(xylene)	140	8/0	93	—	24
(rubber)	150	0/20	17.1	—	—
MBT + H_2S	135	18/0	49	0.039	—
(toluene)[12]	150	10/0	73	0.117	25.1
MBTS + sulfur (naphthalene)[41]	178.5	—	—	—	23.0
MBT + sulfur + DPG (toluene)[30]	100	8/0	12.8	—	—
	125	5/0	46.6	—	—
Sulfenamide BT + sulfur (melt)[26]	140	0/24	29.6	—	—
MBT methylether + sulfur (melt)[26]	140	2/0	None	—	—
Methylbenzothiazole + sulfur (melt)[7]	145	2/0	None	—	—
MBT benzylether + sulfur (melt)[10]	145	2/0	None	—	—
Aminobenzothiazole + sulfur (melt)[26]	145	1/0	None	—	—

complete because the presence of a mere trace of radioactive sulfur will distort the results. In the case of an MBT-sulfur mixture (MBT = mercaptobenzothiazole) the separation was done with the help of 0.5 to 1 per cent aqueous sodium hydroxide. MBT was separated as its sodium salt which was then decomposed with hydrochloric acid. The precipitated MBT was washed in water and dried to constant weight. To separate the components of the melts of thiuram (TMTD) and radioactive sulfur, TMTD was converted to nickel

dimethyldithiocarbamate according to the method worked out by Ginzburg and Derechinskaya[16]. We separated MBT from TMTD in the same manner.

The melt of sulfenamide BT and radioactive sulfur was separated by the conversion of sulfenamide into MBT and further treatment as above. Sodium carbamate and potassium xanthate were separated from radioactive sulfur by utilizing their various solubilities in water.

After separation of the accelerator, washing and drying to constant weight, its radioactivity was checked[17] with a Geiger-Mueller counter for soft β radiation. The determination[17] of the radioactivity in the accelerators recovered after interaction with radioactive sulfur serves as proof for the interaction of accelerator with sulfur during the cure and discloses the curing mechanism.

The results of the isotopic exchange reactions of elementary sulfur and combined sulfur in accelerators and derivatives are summarized in Table I. They show the presence of an interaction between accelerators and sulfur acting as a curing agent. The accelerators isolated after interaction with radioactive sulfur proved to be radioactive. The appearance of radioactivity here was a result of the formation of unstable polysulfide combinations the decomposition of which brought about an isotopic exchange of sulfur atoms. The sulfur in the thiazole ring of MBT and the disulfide, MBTS, does not participate in the isotopic exchange. The sulfur of the mercapto group like that in the thione form proved to be mobile. Table I indicates also that ultra accelerators, such as xanthates, dithiocarbamates, and thiurams, are characterized by a more intense isotopic exchange at lower temperatures compared with that of accelerators in the thiazole and sulfenamide class.

On the other hand, our results given in Table I show that 2-methylbenzothiazole, the methyl and benzyl ethers of MBT, 2-aminobenzothiazole, O,O-diethylphosphorodithioic acid and its potassium salt, do not enter into isotopic exchange with elementary sulfur. Appropriate curing tests show that these compounds do not accelerate vulcanization. Thus, the inability of the sulfur atoms in them to exchange at curing process temperatures is closely related to their action as accelerators. Apparently the presence of mobile sulfur in an accelerator's structure is a most important characteristic of effectiveness in the acceleration of cure and depends on the type of carbon-to-sulfur linkage. The isotopic exchange of sulfur atoms in many organic sulfur compounds has been the object of numerous studies. Thus, the influence of structure of organic sulfur compounds on their ability to undergo isotopic exchange was explored in work by Guryanova, Vasilyeva and Kuzina[41]. Such studies are very important for the disclosure of the mechanism of accelerator action. These authors investigated the exchange of polysulfide sulfur with elementary radioactive sulfur and observed a big difference in behavior of the middle sulfur atoms (R—S—S*—S—R) of polysulfides with aliphatic and aromatic radicals. For instance the energy of activation for the exchange reaction amounts to 14.5 kcal/g mole with ditolyltrisulfide and to 27.3 kcal/g mole with diethyltrisulfide. It was also demonstrated that the exchange of organic disulfides, for instance MBTS, with the corresponding thiol, MBT, does occur in the R—S group:

$$RS^*—S^*R + RSH \longrightarrow RS^*H + RS—S^*R$$

The conditions of exchange for the RS* groups, between disulfides and thiols, vary considerably from one system to another. Thus the exchange in the RS* groups of diphenyl disulfides with thiophenol takes place with notice-

able speed even at 35°, while between *p*-nitrophenyl disulfide and *p*-nitrothiophenol at the same speed the exchange takes place not below 100° to 105°. It occurs with even greater difficulty in systems of compounds with aliphatic and benzyl radicals. A study of the dependence of reaction rate on the concentration of the reacting compounds showed that the controlling stage is the decomposition of the disulfide into RS* radicals which, on colliding with the thiol molecules, abstracts from them a hydrogen atom and results in a tagged thiol molecule and an untagged radical RS.

The substituents in aromatic disulfides (CH_3, OCH_3, C_6H_5, and NO_2) exert a similar influence on the homolytic strength of the S—S bond which is independent of their polarity. In every case this S—S combination becomes stronger when compared with the unsubstituted disulfide. The authors studied the effect of molecular structure on the mobility of sulfur in C—S and C=S compounds. The sulfur in a C—S compound in most cases is exchanged with elementary sulfur with greater difficulty than is that in an S—S compound. The interchangeability of sulfur combined with carbon depends to a large extent on molecular structure. Thus, the sulfur of thiurams or that of the derivatives of 2-mercaptobenzothiazole which are accelerators enters into exchange with elementary sulfur at 100° to 130° while the sulfur of thiophenol, butyldisulfide, and phenyldisulfide, which are not accelerators, does so only at 200° to 230°. The activation energy for the exchange is an indication of the strength of the C—S bond and possibly is also one of the criteria for characterizing the ability of vulcanization accelerators to form radicals by rupture of the C—S bond[41]. For instance, in the exchange of the following system the activa-

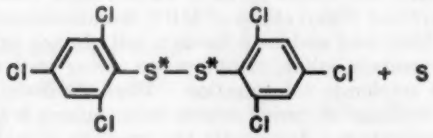

tion energy amounts to 47.3 kcal/g mole, but in the exchange of accelerators, such as MBTS, MBT, or TMTD, with sulfur it amounts, respectively, to 23, 24, and 21.5 kcal/g. In the esters of diethyldithiocarbamic acids contrary to

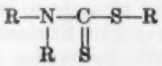

what occurs with the salts of these acids, or in corresponding thiurams, only one sulfur atom is exchanged, presumably the C=S sulfur. The second sulfur atom, namely, the one that is connected with the ethyl radical is not exchanged. The equations for an eventual mechanism of exchange reaction between sulfur atoms of the accelerators and vulcanizing agents are as follows.

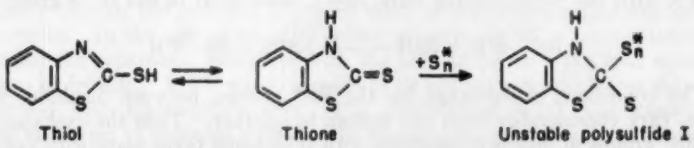

The unstable polysulfide can lose radiosulfur to reform MBT[10], or, it can lose $S^*_{n-1}S$ to form radioactive MBT:

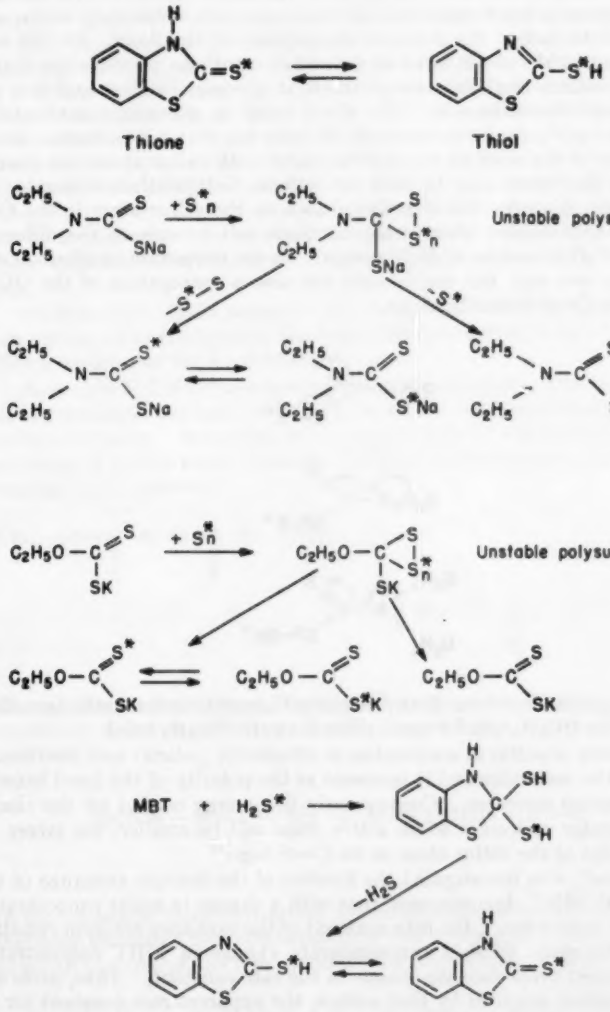

It is fully justifiable to assume[10–13,18,29,44] that the bonds between sulfur atoms in the molecules of elementary sulfur are easily polarized. Therefore when a molecule of a compound having a polar bond $\overset{+}{C}—\overset{-}{S}$ collides with a sulfur molecule having an S_8 ring structure, an ionic or radical cleavage of —S—S— bonds occurs and the formation of an unstable polysulfide intermediate com-

pound takes place. The decomposition of this then leads to an exchange of sulfur atoms at which point sulfur appears in a reactive form and reacts with the rubber. Seen from this point of view, the sulfur in the C-to-S bonds of organic compounds must enter into an exchange with elementary sulfur at a rate that will be faster, the stronger the polarity of the bond. Of the compounds examined the C=S bond in potassium xanthate presents the highest polarity; in sodium diethyldithiocarbamate it is somewhat less and it is still less in mercaptobenzothiazole. The C=S bond in potassium xanthate[13] is obviously strongly polar because the S—K bond has an ionic character, and as a consequence of the shift of the electron cloud both sulfur atoms are charged negatively. The same may be said for sodium diethyldithiocarbamate. In this latter case, however, the negative charge on the sulfur atom in the C=S bond is probably smaller than in the xanthate salt because of the difference between the C_2H_5O and the C_2H_5N groups. In the potassium xanthate system there appears not only the conjugation but also a conjugation of the OC_2H_5 bond with the C=S double bond, i.e.,

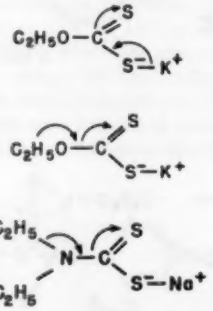

Such a conjugation in sodium diethyldithiocarbamate is undoubtedly less effective because the OC_2H_5 bond is more polar than the NC_2H_5 bond.

The mobility of sulfur in accelerators is affected by polarity and distribution of charge in the molecules and it increases as the polarity of the bond between sulfur and carbon increases. Consequently the energy needed for the change of the accelerator molecules to an active state will be smaller, the larger the negative charge of the sulfur atom in its C=S bond[44].

Guryanova[14], who investigated the kinetics of the isotopic exchange of sulfur atoms with MBT, demonstrated that with a change in sulfur concentration of from three to five times, the rate constant of the exchange reaction remained practically the same while a commensurate change in MBT concentration caused an almost proportionate change in the rate constant. Thus, according to the information supplied by that author, the apparent rate constant for the exchange depends first of all on the concentration of MBT and not of sulfur. It would seem that this exchange is not a simple bimolecular reaction but rather that it proceeds in stages, the slowest being the process of changing MBT into a condition capable of reaction. The fact that the rate constant is independent of sulfur concentration indicates that the exchange reaction proceeds faster and with less activation energy. Guryanova observed only an insignifi-

cant change in rate constant when the exchange between sulfur and the sulfur from MBT was compared in polar and nonpolar solvents. From this the author concludes that the speed of exchange between MBT and sulfur is determined by a radical transformation of MBT rather than by a tautomeric one.

The isotopic exchange of sulfur atoms of TMTD with elementary sulfur has been studied by Blokh[24], Bresler[15], Guryanova[14], Craig[20], Mochel[42], and others. It was found[8] that during the curing of rubber an intensive isotopic exchange of sulfur atoms takes place which can be observed even at 100°, but that heating sulfur and MBT alone at this temperature for as long as 3 to 5 hours does not produce an isotopic exchange of sulfur atoms. According to Craig and others[20], who studied the pyrolysis of radioactive TMTD at 100–200° all products of decomposition of the thiuram show the same radioactivity. On the basis of these results a conclusion was reached in regard to the equivalence of all the four sulfur atoms and TMTD was held to have the flat structure of a six membered ring.

Studies of the dipole moment[14] of TMTD indicate a nonsymmetrical structure for the molecule because the dithiocarbamate groups may be connected at different angles at the S—S bonds.

As we know, TMTD can cure rubber without sulfur. The energy of TMTD decomposition is not high, 36 kcal/mole, and so isotopic exchange can assume a radical character. According to Guryanova's data[14] the mechanism of isotopic exchange of sulfur atoms between TMTD and elementary sulfur unfolds according to the pattern:

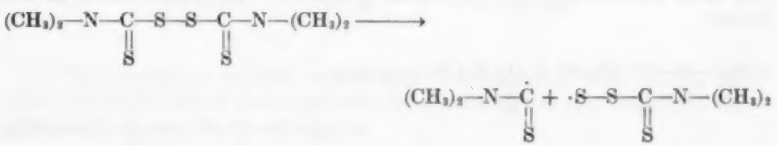

The resulting radicals attack the tracer S^*_8, and as a consequence there occurs a separation of tracer sulfur from the S^*_8 ring and its attachment to the radical:

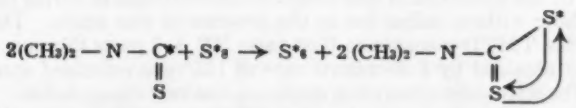

In such a radical the sulfur atoms are indistinguishable and equivalent. Furthermore through a new combination of two radicals, a TMTD molecule arises in which any one of the four sulfur atoms can be tagged thus:

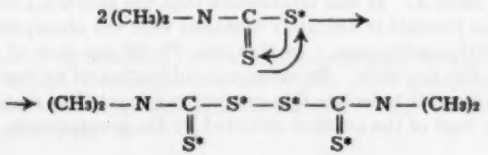

Hence, the same interchangeability of all four sulfur atoms in the thiuram is a result of the chemical equivalence of both sulfur atoms in the radical.

As regards the participation in the exchange of the second radical, i.e., the sulfenyl radical $\cdot S_2C(S)N(CH_3)_2$, it is in this case possible for a sulfur atom to separate with the formation of the dithiocarbamate, radical $\cdot SC(S)N(CH_3)_2$, or for two sulfur atoms to separate to form another thiocarbamoyl radical, $\cdot C(S)N(CH_3)_2$.

Bresler[15], on the assumption of a bimolecular process of exchange, is of the opinion that in TMTD both sulfur atoms of the disulfide bridge are exchanged. This would take place in three stages. The first is a monomolecular decomposition:

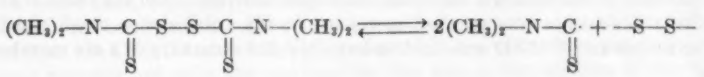

In the second, the thiocarbamoyl radical attacks the sulfur rings and splits away from them sulfur atoms, a process requiring only a little activation energy:

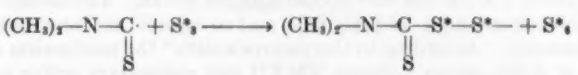

The third step leads to the formation of TMTD with tagged sulfur in the bridge:

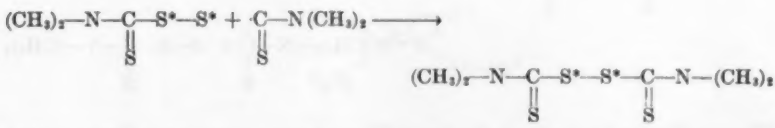

Most likely, the decomposition of TMTD occurs at the S—S bond. This is confirmed by the formation of zinc dimethyldithiocarbamate during the TMTD cure of rubber without sulfur but in the presence of zinc oxide. The acetone extract of the TMTD vulcanizate (100 parts NR + 3 parts thiuram + 2 parts zinc oxide) obtained by a 30 minute cure at 125° was examined spectroscopically[21]. The ultraviolet absorption spectrum was very characteristic. Absorption maxima appeared at wave lengths of 2800 and 2600 A while the original TMTD shows only one absorption band at 2650 A. As we know, only a single very wide absorption band corresponds to the thiuram monosulfide at around 2750 A. Moreover, the results obtained cannot be ascribed to the formation of tetramethylthiourea because this compound shows a very narrow absorption band at about 2500 A. It was established that the spectrum observed for the TMTD reaction product is definitely identical with the absorption spectrum of zinc dimethyldithiocarbamate. In this case 70–76 per cent of the TMTD is converted into the zinc salt. By using a combination of solvents, alcohol and acetone, it was possible to isolate this product in a crystalline state in an amount of about 90 per cent of the amount detected by the spectograph. The identity

of the precipitated product as pure zinc dimethyldithiocarbamate was established by an analysis for sulfur, nitrogen and zinc as well as by the close conformity of the melting temperature, 247°.

Bresler[15] ascertained that the rate constant for the attachment of sulfur to rubber is the same as the rate constant of the isotopic exchange of sulfur with TMTD. The same activating energy in both processes and the conformity of the preexponential factors indicate that the rate of the curing process is determined by the interaction of elementary sulfur, S_8, with the accelerator. The presence of substituent methyl groups in TMTD, as against butyl groups in TBTD, exerts no particular influence on the kind of sulfur combinations in the thiuram[14]. The velocity constant for the exchange of sulfur atoms at 130° was, in the case of TBTD, $0.14 \cdot 10^{-3}$, which came very close to the level for TMTD which was $0.11 \cdot 10^{-3}$:

On the premise of the above representations in regard to the isotopic exchange of sulfur with TMTD and for the results of the spectroanalysis, colorimetric and other analyses, it is possible to advance theoretical patterns for thiuram vulcanization[21]:

1. The decomposition of thiuram into radicals and their entrance into the structure of rubber:

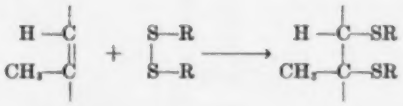

2. The interaction between rubber molecules sulfurized with TMTD, ZnO and nonmodified rubber molecules with the elimination of zinc dimethyldithiocarbamate:

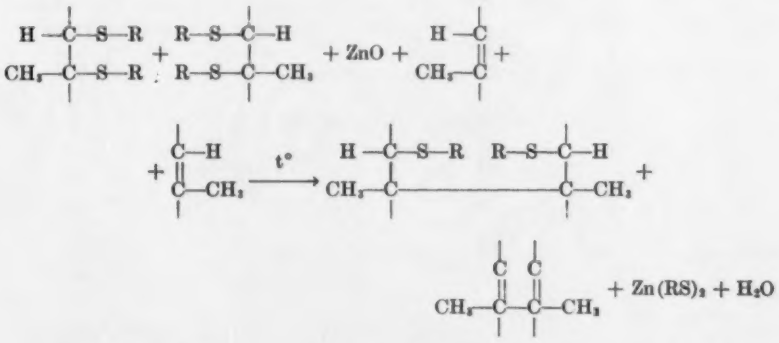

3. Interaction of structurized rubber molecules among themselves with zinc oxide and with nonmodified sections of the rubber chain concurrently with the elimination of zinc dimethyldithiocarbamate and a further combination of the structural elements of rubber:

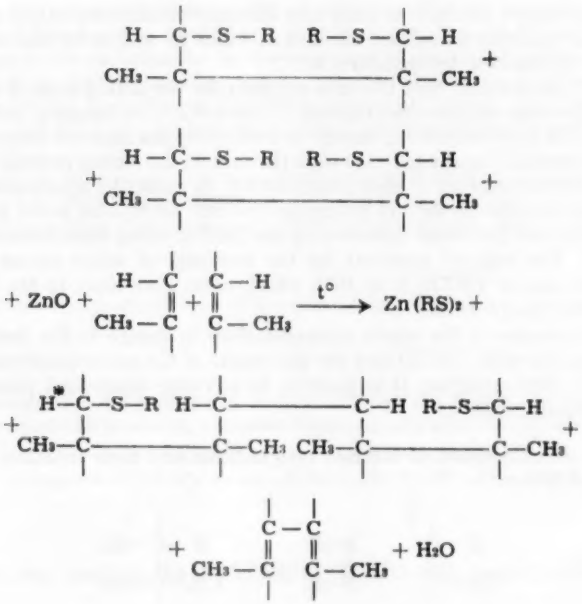

Thus, this assumed pattern explains the formation of the zinc dithiocarbamate as well as the partial consumption of TMTD during cure, all of which coincides with the results of the isotopic exchange and the spectroanalysis of the vulcanizates.

A detailed pattern of thiuram curing has been given by Scheele, Lorenz and Dummer[22]. According to them vulcanization consists of the following steps:

a. Decomposition of the thiuram into radicals:

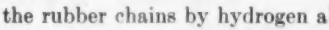

b. Activation of the rubber chains by hydrogen abstraction:

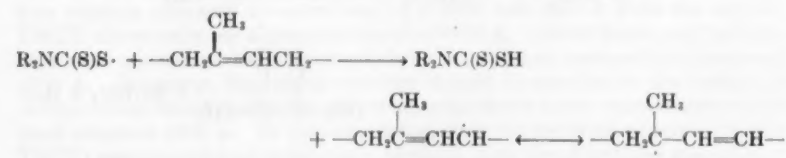

c. Dimerization of the activated rubber molecules (i.e., the rubber radicals) thus leading to structurization of the system. There are three structures obviously possible for crosslinks formed in this way.

d. Addition of the thiuram radical to the rubber molecule double bond to give a structure in which thiuram radicals participate:

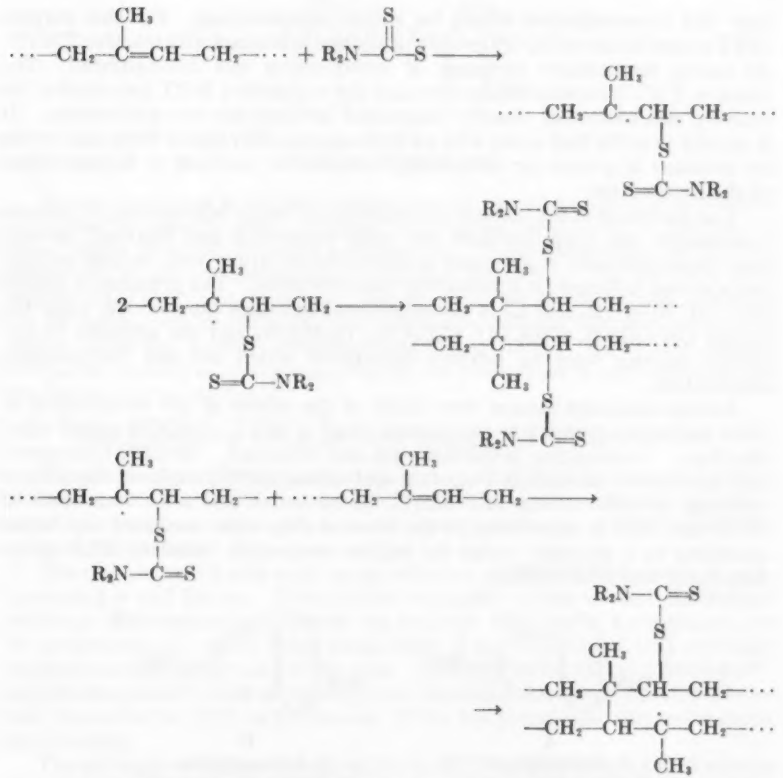

In work by Dogadkin and associates[25,42] the character of sulfur-free vulcanization by radioactive MBTS (A) as well as by Sulfenamid BT (B) was established experimentally. The entrance of the decomposition products of MBTS and Sulfenamid BT, respectively, into the rubber structure was demonstrated analytically, that is by the determination of the bound sulfur and nitrogen in the vulcanized rubber, and, as well, by a measurement of the radioactivities:

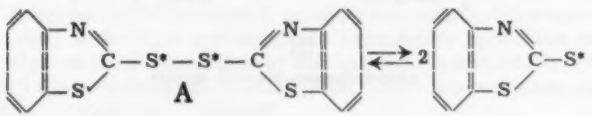

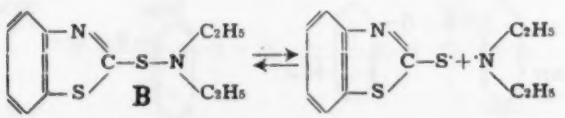

Blokh and Golubkova[9], using the tracer technique, made a study of the interaction[46] of MBT and TMTD as an example of a combination of accelera-

tors (the two-accelerator effect) for rubber compounding. For this purpose MBT tagged in the sulfhydril group was allowed to interact with inactive TMTD. At curing temperature exchange of sulfur atoms was demonstrated. The inactive TMTD became radioactive and the radioactive MBT lost much of its activity, demonstrating thereby interaction between the two accelerators. It is equally possible that along with an exchange of sulfur atoms there also occurs an exchange of groups (or of radicals) between the products of decomposition of the accelerators.

The disclosure of the influence of substituents in the benzene ring of thiazole accelerators and their disulfides was most interesting and Harman[23] showed that the substitution of hydrogen in the sulfhydril group with various radicals has a strong influence on accelerating characteristics. The presence of groups CO, NH, NO_2, OH, S or Cl in the substituent increases the activity, while the groups CH_2CONH, CH_2COO, $C_6H_5CH_2$, $C_{10}H_7CH_2$ and the aliphatic hydrocarbon radicals tend to produce derivatives which are not vulcanization accelerators.

Isotope exchange studies were made of the effects of the introduction of nitro and amino groups into the benzene ring[26] of MBT, of MBTS and of other disulfides. Accelerating properties were also examined. Blokh[24], Guryanova and associates[41], as well as Dogadkin and colleagues[25,43], explored the isotope exchange of sulfur atoms with MBT. Some amino and nitro derivatives of MBT and MBTS, substituted in the benzene ring, were produced and tested according to a standard recipe for rubber compounds based on SKB (polybutadiene) and SKS (SBR):

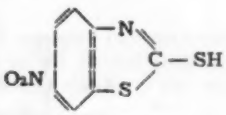

I

Nitrocaptax
(6-Nitro-2-mercapto-benzothiazol)

(32)

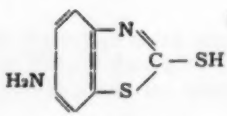

II

Aminocaptax
(6-Amino-2-mercapto-benzothiazol)

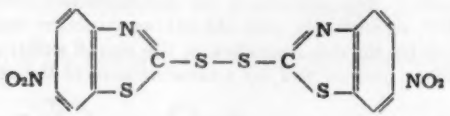

III

Bis(6-dinitrobenzothiazolyl) disulfide

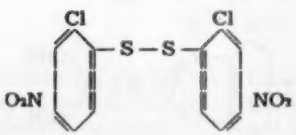

IV

2-Chloro-4-nitrophenyl disulfide

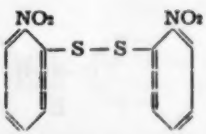

V

2-Nitrophenyl disulfide

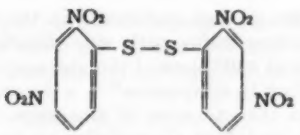

VI

2,4-Dinitrophenyl disulfide

It was found that MBT derivatives I and II as well as the nitro derivative III of MBTS produce rubber of good physical and mechanical properties, in other words they are effective accelerators. These compounds participate intensively in the isotope exchange of sulfur atoms[26,41]. The disulfide compounds III, IV, V, and VI extend their effectiveness as vulcanizing agents to the sulfurless cure in SKB (sodium butadiene rubber) mixtures containing carbon black and kaolin. Disulfide compounds III, IV, V, VI, and others, offer great promise as curing materials for the production of heat resisting and insulating types of rubber.

INFLUENCE OF SULFUR-FREE AUXILIARY COMPONENTS

The effects of such important materials as zinc oxide, sulfur free accelerators containing nitrogen like diphenylguanidine (DPG), age resisters like phenyl-2-naphthylamine, and carbon black, on the isotope exchange of sulfur atoms are of particular interest.

The role played by zinc oxide as an activator of organic accelerators in rubber curing is well known. It would be reasonable to assume that the isotope exchange of elementary sulfur with the sulfur in MBT or in a sulfenamid, in the presence of zinc oxide, takes place faster, if the intensity of that exchange characterizes the acceleration of the cure. Findings by Blokh[27] and Auerbach[28], had the unexpected result of showing that the isotope exchange of sulfur atoms with the sulfur in MBT or Sulfenamid BT in the presence of zinc oxide drops precipitously.

The exchange of sulfur with the sulfur in MBT in SKB[26] during a 15 minute cure at 145° in the presence of zinc oxide dropped from 14 to 6 per cent. This apparent contradiction is easily explained. As is well known during the course of a cure in the presence of zinc oxide, MBT forms the zinc salt of the mercaptobenzothiazole, involving a change in structure with respect to the sulfur atom. It would seem that during the conversion of MBT into the zinc salt we lose the possibility of a tautomeric transition. Thus the formation of the thione form of the C=S compounds which is essential to an exchange of the thiazole accelerator[27] is prevented. Therefore it must be assumed that the activation of the sulfur, even without an exchange, will consistently follow the path to a formation of an unstable polysulfide of zinc mercaptide and which, by decomposition, will separate sulfur in reactive form. This process takes place very intensively in the presence of amines[29].

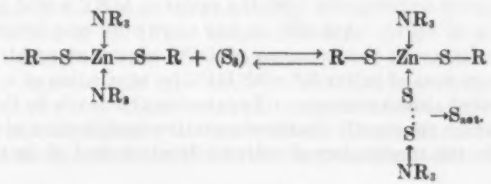

Zinc dithiocarbamates do not participate in the isotope exchange either. The heating of radioactive sulfur with zinc dimethyldithiocarbamate (ZnDMDC) for 60 minutes at 140° showed the absence of an isotope exchange of sulfur atoms[20]. According to Guryanova[14,41], a decomposition with separation of zinc sulfide occurs in the exchange of zinc salts. Consequently the conclusions of that author no longer characterize an exchange with zinc dithiocarbamate but rather with the products of its decomposition. On the other hand the heating of a mixture[20] consisting of 0.01 mole radioactive sulfur, 0.01 mole ZnDMDC and 0.0005 mole TMTD in a xylene solution at 140° for 30 minutes showed that the precipitated ZnDMDC retained 22 per cent radioactivity of the original sulfur. A study was also made of an isotope exchange involving the heating of 1 mole equivalent of ZnDMDC with 2 moleequivalents of radioactive TMTD in xylene for 60 minutes at 120–125°. The separated TMTD and ZnDMDC showed identical radioactivity. Therefore the absence of an isotope exchange of elementary radioactive sulfur with the sulfur of the ZnDMDC on the one hand and the existence of such an exchange in the presence of thiuram on the other may well indicate that apparently an exchange of the group radicals can take place, that is, that the combinations of sulfur and zinc atoms can transfer from one base of dithiocarbamate to another. Thus the accelerating effect of the zinc dithiocarbamates can be explained by the formation of an unstable intermediate product, a polysulfide, which decomposes when separating active sulfur fragments:

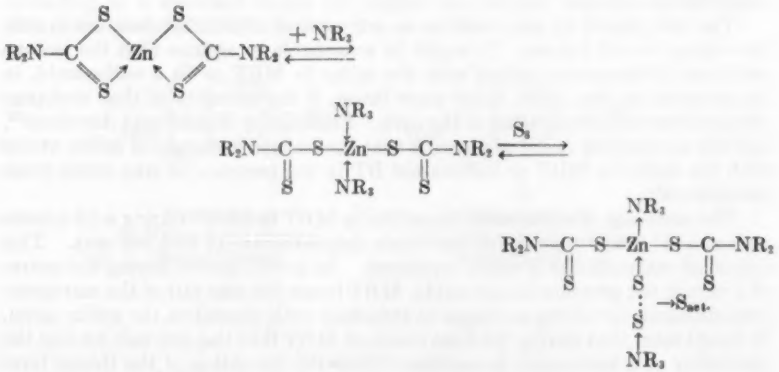

The role of the sulfurless, hydrogen containing accelerator DPG is generally known. In terms of accelerating properties it falls behind MBT. However the frequent use by industry of DPG and MBT, together, produces a considerably greater activity than is the case for either used separately. From the standpoint previously submitted one might expect that the intensity of the isotope exchange of sulfur atoms with the sulfur in MBT would increase greatly in the presence of DPG. Actually it was shown by one investigation[30] that the isotope exchange in the presence of DPG occurs at greater speed. The immediate interaction of sulfur S_8* with DPG by separation of hydrogen sulfide was demonstrated simultaneously. Apparently this leads to the formation of a polysulfide which constantly liberates an active modification of sulfur. These facts illuminate the mechanism of sulfur activation and of its transition from

the ring structure into the radical or ion structure which reacts with rubber under the influence the sulfurless DPG accelerator. Sulfur activation with diphenylguanidine can, presumably, be explained along the lines:

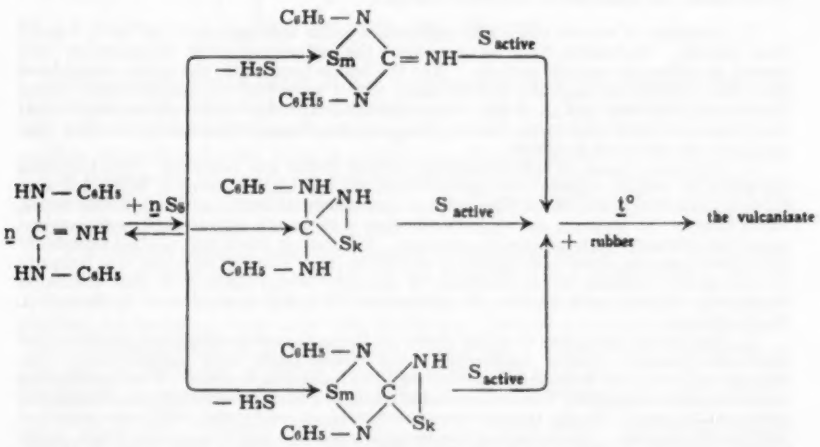

In an interesting study Krebs[29] mentions the mechanism of sulfur activation with amines by forming amine polysulfides which decompose with separation of active sulfur.

Phenyl-2-naphthylamine (PBNA) which is an antioxidant and not an accelerator is different from DPG. The isotope exchange of the sulfur atoms occurs with the same intensity in its presence as in its absence[30]. In this connection when PBNA is sulfurized, it reacts with radioactive sulfur to liberate hydrogen sulfide. Without doubt the sulfurization of PBNA is important in evaluation of its protective properties and in the study of the kinetics of vulcanization. As already mentioned, zinc sulfide and hydrogen sulfide are produced during cure. Blokh[27] has shown that free sulfur and the sulfur from MBT enter into an isotope exchange with the sulfur from zinc sulfide and also with that from the hydrogen sulfide. From all these facts we can conclude that in the vulcanization of rubber not only elementary sulfur but also sulfur from all the sulfur containing components of a compound will participate in the isotope exchange, even of such components as are produced during the process[27] itself.

THE INTERACTION OF CURING SYSTEM, RUBBER AND FILLER

A method involving tracer atoms offers promising possibilities in the study of the adsorption processes in rubber mixes. By this method an attempt was made to establish the conditions under which stable bonds (possibly chemical) between the carbon black structure and sulfur are formed. It is not improbable that the interaction of sulfur and accelerator, namely the isotope exchange of sulfur atoms, takes place on the very large surface of the carbon black particles added to the compound. It is precisely on this surface that the active form of sulfur separates as a consequence of the decomposition of the intermediate polysulfide combinations of accelerator and sulfur. This sulfur is not only adsorptively and chemically attached to the microcrystalline carbon structure of the

carbon black, displacing oxygen and hydrogen combinations, but also is attached to the oriented film of rubber at the carbon black surface.

The strength of the bond between carbon black and sulfur is best judged by these facts, as established experimentally:

1. A mixture of carbon black and radioactive sulfur was heated at 145° for 3, 6 and 9 hour periods. Thereafter, in order to separate the radioactive sulfur, the mixtures were heated in xylene for various periods. Had the bonds been weak, the sulfur would have gone into the solvent and the carbon black would have lost its radioactivity. After three hours, however, not all of the radioactive sulfur attached to the carbon black could be extracted from it, and as the heating time was lengthened the quantity of sulfur that could not be detached increased.
2. A mixture based on polyisobutylene rubber P-200 was prepared. The following are parts by weight: rubber 100, carbon black 60, radioactive sulfur 3, MBT 1.8, zinc oxide 5, and stearic acid 2.5. The mixture was heated at 145° for two and four hours, respectively. To separate the rubber and other components and to remove the carbon black the mixture was treated with solvents. The carbon black was washed repeatedly with fresh benzene, dried and tested for radioactivity. The carbon black was found to be radioactive because of the presence of strongly bound sulfur. It was calculated tentatively that as much as 70 to 80 per cent of the sulfur used adhered to the carbon black surface.
3. The isotopic exchange of sulfur atoms on the surface of carbon black particles is of particular interest. Sulfur (radioactive) and carbon black were coprecipitated from benzene solution, the benzene being evaporated at room temperature. The same carbon black was then coagulated from an alcohol solution of mercaptobenzothiazole, the alcohol being evaporated. Finally the mixture of carbon black, sulfur and MBT was heated at 130° for 60 minutes. A control test was made in a solution free from carbon black, under similar conditions. The activity of the MBT isolated from the carbon black mixture was 1260 counts per minute, while that of the MBT from the solution was only 580, thus showing that the isotopic exchange on the surface of carbon black is much more intensive. The carbon black from the mixture was treated for 100 hours with large quantities of benzene in order to separate any free radioactive sulfur. It was then dried and tested for radioactivity. It still showed a residual radioactivity of 19.3 per cent based on the mixture before extraction. An approximate calculation indicated that in this test up to 18.4 per cent of the original radioactive sulfur combined with the carbon black. These facts signify that the sulfur not only forms a strong chemical bond with the film-like rubber on the surface of the carbon black but that it also combines very firmly with the carbon black. The vulcanizate structure must therefore include not only rubber and sulfur but carbon black as well. It is on the filler surface that the isotopic exchange between sulfur and accelerators and the elimination of active sulfur takes place. This is confirmed by the fact that a preliminary thermal activation of the black, sulfur and MBT mixture at 130 to 150° for 1 to 4 hours, followed by mixing with rubber and cure will result in an enhanced vulcanization and produce rubber goods possessing better physical and mechanical characteristics.

MOBILITY OF SULFUR BONDS AND MIGRATION PROCESSES IN THE VULCANIZATE

In an analysis of the available experimental material relating to the isotopic exchange of sulfur atoms in organic compounds and their accelerating action during cure we must point out an apparent contradiction[45]. This is that an isotopic exchange with sulfur is over after a few hours while the cure of most rubber products requires less than one hour. This contradiction is dispelled if we consider that sulfur in a rubber compound even under curing conditions is in the form of 8-atom rings[15]. During vulcanization and interaction between sulfur and accelerator there develops an unstable polysulfide intermediate compound. The formation of the thiuram tetrasulfide was detected by Klebanskii[19] and that of benzothiazolyl tetrasulfide by Dogadkin[25]. So, for instance, we may imagine the polysulfide from mercaptobenzothiazole resulting from the isotope exchange with sulfur to have the following structure:

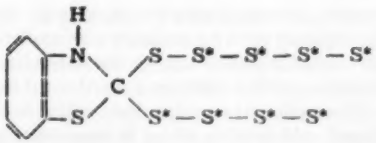

For an exchange of sulfur atoms, a separation of S*··S groups is essential which means the cleavage of the strong C—S bonds. For the structurizing of the molecular rubber chains a cleavage of 1 to 2 sulfur atoms from the polysulfide chain is sufficient, that is, a splitting of the weaker —S—S—S— bonds. Thus there takes place during vulcanization along with an isotope exchange a faster process of progressive dissociation of the intermediate compounds with separation of the sulfur atoms in a reactive form.

The isotope method makes it possible to regard in a new light the question of the mobility of sulfur contained in the structure of a vulcanizate. One of the earliest mentions of the different nature of mono and polysulfide bonds in rubber, as resulting from cure with sulfur and various accelerators, is found in the interesting work of Dogadkin and Tarasova[31]. Their study was made of the isotope exchange of sulfur from the structures of MBT, MBTS, TMTD, ZnDMDC, or Sulfenamid BT, with the sulfur that is variously bound with the polymer in soft and hard rubber[24,27,32] cures. Their study disclosed that the sulfur of mono and disulfide bonds in a TMTD vulcanizate during hot immersion of the stock in a solution of accelerators tagged with radio sulfur did not enter into any exchange reaction[27,32]. This finding shows the immobility and stability of these sulfur bonds. A different picture resulted from the investigation of soft and hard rubber[24,32,39] containing polysulfide sulfur bound to the polymer. In this particular case during the immersion of soft or hard rubber in solutions of accelerators at 78 to 138° we observed an intense isotopic exchange of sulfur atoms from the accelerators with the sulfur atoms from the disassembled polysulfide units. The participation of exchanged atoms varied, according to circumstances, from 12 for soft rubber to 22 per cent for hard rubber. This vouches beyond any doubt for the mobility of the polysulfide bound sulfur both in soft and hard rubber and is of considerable significance for the usefulness of this material[36]. During this same work we recognized experimentally a combination of radioactive MBT with the rubber structure during cure[32].

Bresler, Kushner and Saminskii[39] carried out an extended inquiry into the mobility of polysulfide sulfur in soft and hard rubber. These authors worked out a diffusion method for the investigation of the mobility of sulfur bonds and established a mathematical procedure for quantitative measurements. Detailed descriptions of this diffusion method are given[15,39]. On the premise that the energy in the cleavage of the polysulfide bond is not high and that under conditions of cure it amounts to only 27,000 plus or minus 500 cal/mole, as they indicate, the polysulfide bridge which is only 10–20 sulfur atoms long is easily dissociated. The mobility of the bound sulfur which occurs through a chemical dissociation of the polysulfide chains and their attachment to other unsaturated bonds of sulfur or rubber, is referred to by the authors as chemical diffusion.

The complete diffusion method[15,39] for investigating the curing of rubber and the mobility of polysulfide sulfur with the aid of radioactive sulfur consists of the following: pulverized radioactive sulfur is brought into contact with the

vulcanizate, or conversely, a vulcanizate prepared with the aid of radioactive sulfur may be brought together with an ordinary vulcanizate or uncured rubber, in a special metal thermostat which is sealed hermetically. During the heating process free radioactive sulfur diffuses into the rubber, or, conversely is freed and rebound. The radioactive polysulfide sulfur bound with the rubber diffuses into the ordinary rubber with which it has come in contact. Eventually a steady state is reached. Then, with the aid of a Geiger-Mueller counter, the radioactivity of the opposing surface of the rubber sample, i.e., the receiver, is measured. The results, with the aid of a standard curve, are used to calculate the diffusion coefficients and the sulfur concentration. It may be mentioned here that, guided by the diffusion method and with the help of radioactive sulfur, Auerbach and Gehman[40] explored such technologically important questions as the blooming of sulfur, solubility, and diffusion.

Bresler[30] demonstrated that the degree of dissociation of the migrating polysulfide sulfur at 100° is 3 per cent and at 160° is 22 per cent. As was to be expected the coefficient of chemical diffusion was considerably smaller than the coefficient of diffusion of the free molecularly soluble sulfur and amounted to $1.82 \cdot 10^{-7}$ cm²/sec for natural rubber at 151° and to $1.10 \cdot 10^{-7}$ cm²/sec for SKB.

It was found that the amount of radioactive sulfur diffusing into the top layer of rubber making contact, the receiver, was large only if that layer was vulcanized. If the top layer was raw rubber only a small amount of radioactive sulfur penetrated.

The experimental results[24,27,32] of the isotopic exchange of labile polysulfide sulfur bound with rubber with the immobile sulfur in the —C—S—C— and —C—S—S—C— combinations were confirmed in later work[37,38]. Tikhomirova and Kuzminskii[37], who studied the mobility of sulfur bonds dependent on the types of accelerators and on the agents used to counteract oxidation in accordance with the method of tracer atoms, obtained some very interesting results. They established that:

1. In all sulfur vulcanizates labile sulfur bonds are present which are easily cleaved regardless of the type of accelerator used; the number of mobile sulfur bonds is determined by the type of accelerator; and, the number of labile bonds is negligible in the presence of TMTD.
2. The content of mobile sulfur bonds in the vulcanizates remains the same regardless of the type of material used to counteract oxidation, namely, PBNA or diphenylamine.
3. The relative number of mobile sulfur bonds diminishes as the curing temperature is increased.

Tarasova, Kaplunov and Dogadkin[33] investigated exchange reactions in vulcanized rubber according to the diffusion method and obtained data on the isotopic exchange between the sulfur structures of vulcanizates. The authors showed that the exchange of sulfur atoms between vulcanizates that come in contact with one another takes place either through intermolecular interaction of colliding polysulfide groups of different vulcanizates or through the splitting off of sulfur radicals with subsequent penetration into and attachment to the vulcanization structure. Further tests made by the authors disclosed that the diffusion of sulfur groups is negligible.

The decomposition of polysulfide bonds occurs, without any doubt, through the separation or even the removal of sulfur compounds during lengthy cures in heaters, reclaiming operations and thermal aging of rubber of various compounds. It is unavoidable that the quality of rubber stocks, testpieces of which lie close to one another, will be affected. The truth of this was demonstrated in the following experiment. Some radioactive vulcanizates were

made with polysulfide bonds, S*. Strips from them were hung from glass tripods under a glass bell. At a distance of 1 cm from them were placed sheets of nonradioactive vulcanizates of identical composition. The glass bells were heated in a thermostat at 70, 100 and 140°. Every strip was then tested for radioactivity. At 140° radioactivity dropped 15 per cent in one hour, 26.5 per cent in six hours and in 13 hours 36 per cent. At 70° the reduction was 4.3 per cent after 25 hours and 13.9 per cent after 62 hours. In the originally nonradioactive sheets a radioactivity within a range of 75 to 320 counts per minute was observed. The formation of hydrogen sulfide was also analytically detected.

OTHER STUDIES

Finally we wish to call attention to the utilization of sulfur tracer atoms in the solution of concrete technical problems. One study[33] demonstrates the possibility of the distribution of sulfur between rubber stocks, the likely migration of sulfur from one compound to another during the storage of raw mixtures on shelves or in transit, and the migration of sulfur from the carcass to the tread during the vulcanization of rubberized tire cords. Inquiries into the diffusion of sulfur and accelerators during the vulcanization of multiple-ply articles like tires, cables and similar products also offer considerable interest. The study[34] of sulfur diffusion from tubing to insulating stock containing TMTD, as in a cable, serves as an example of the emergence of an increased concentration of diffused radioactive sulfur into the microscopic contact layers between two different types of stock. Here an intense isotopic exchange occurs, and new sulfur structures are formed in the bordering layer. This will cause various types of injuries to the contact surface, such as cracking, stratification, etc. It was shown that neither talc, nor a rubberized fabric, nor even polyvinylchloride nor polyethylene can protect the rubber mixture against the migrating sulfur. These findings are of real practical value to the entire industry. The utilization of tracer atoms and of radioactive isotopes by the rubber industry should promote future technical progress.

An isotopic exchange among accelerating and vulcanizing substances obtained at room temperature under the influence of gamma rays from Co 60 is of particular significance.

REFERENCES[47]

[1] Brodskiĭ, A. I., "Chemistry of Isotopes," Acad. Sci. USSR Press, Moscow, Izdatel stvo Akad. Nauk SSSR, 1952, 352 pp; *C.A.* **48**, 3808i.
[2] Bresler, S. E., "Radioactive Elements", Moscow, Tekh.-Teoret. Lit. 1952; *Chem. Zentr.* **124**, 2248 (1953).
[3] Hevesy, George, "Radioactive Indicators", Interscience, New York, 1948, 572 pp; *C.A.* **43**, 8866c.
[4] "Proceedings of the Conference of the Academy of Sciences of the USSR on Peacetime Uses of Atomic Energy"; Rubber Chem. & Technol. **29**, 516–529 and 534–554 (1956).
[5] Symposium on the "Mechanism of Organic Reactions", Academy of Sciences, USSR, 1953.
[6] Dogadkin, B. A., "The Science of Rubber", 1938; "The Physics and Chemistry of Rubber", Moscow, Goskhimizdat, 1947, 421 pp; *C. A.* **43**, 5624b.
[7] Blokh, G. A., Golubkova, E. A., and Miklukhin, K. P., *Doklady Akad. Nauk SSSR* **86**, 569 (1952); Rubber Chem. & Technol. **29**, 1369 (1956).
[8] Blokh, G. A., and Sasonova, L. P., *Zhur. Legkaya Prom.* **12**, 40 (1952); Rubber Chem. & Technol. **28**, 804 (1955).
[9] Blokh, G. A., and Golubkova, E. A., *Doklady Akad. Nauk SSSR* **91**, No. 7 (1953); *C. A.* **48**, 1047c.
[10] Blokh, G. A., Golubkova, E. A., and Miklukhin, G. P., *Doklady Akad. Nauk SSSR* **90**, 201 (1953); Rubber Chem. & Technol. **29**, 63 (1956).
[11] Kukhtenko, I. I., Blokh, G. A., and Miklukhin, G. P., *Ukrain. Khim. Zhur.* **21**, 227 (1955); *C. A.* **50**, 3858a.
[12] Rekasheva, A. F., Blokh, G. A., and Miklukhin, G. P., *Zhur. Obschel Khim.* **25**, 1351 (1955); *C. A.* **50**, 35 (1956).
[13] Foka, M. N., and Burksev, L. E., *Doklady Akad. Nauk SSSR* **99**, 1011 (1954); *C. A.* **50**, 187i.
[14] Guryanova, E. N., and Vasilyeva, V. I., *Zhur. Fiz. Khim.* **28**, 60 and 67 (1954); *C. A.* **48**, 11888a. Cf. *Zhur. Fiz. Khim.* **29**, 576 (1955).
[15] Bresler, S. E., Pryadilova, V. I., and Khalman, V. Ya., *Zhur. Tekh. Fiz.* **24**, 577 (1954); Rubber Chem. & Technol. **29**, 946 (1956).
[16] Ginsburg, Z., and Derechinskaya, A., *J. Rubber Ind. USSR*, **1936**, 310; *C. A.* **30**, 4790.

[17] Bochkarev, W., "Measurement of β and γ Ray Activity", *Akad. Nauk SSSR*, Moscow, SSSR, 1953, 241 pp.
[18] Miklukhin, G. P., "Progress of Chemistry", (USSR) **17**, 663 (1948); *Doklady Akad. Nauk SSSR* **73**, 117 (1950).
[19] Hantzsch, A., and Bucerius, W., *Ber.* **59**, 793 (1936).
[20] Craig, D., *J. Polymer Sci.* **6**, 1 (1951); RUBBER CHEM. & TECHNOL. **24**, 262 (1951).
[21] Jarrijon, A., RUBBER CHEM. & TECHNOL. **19**, 1061 (1946).
[22] Scheele, W., Lorenz, O., and Dummer, W., *Kautschuk und Gummi* **8**, 27 (1955); RUBBER CHEM. & TECHNOL. **29**, 1 (1956). See, however, Bielstein, G., and Scheele, W., *Kolloid-Z.* **147**, 152 (1956); RUBBER CHEM. & TECHNOL. **30**, 393 (1957); see also Ref. d (Ed. of *R. C. & T.*).
[23] Harman, M. W., *Ind. Eng. Chem.* **29**, 205 (1937); RUBBER CHEM. & TECHNOL. **10**, 329 (1937).
[24] Blokh, G. A., *Doklady Akad. Nauk SSSR* **91**, 1107 (1953); RUBBER CHEM. & TECHNOL. **27**, 974 (1954).
[25] Dogadkin, B. A., and Selyukova, V., and others, *Kolloid. Zhur.* **17**, 215 (1955); RUBBER CHEM. & TECHNOL. **29**, 917 (1956). See also RUBBER CHEM. & TECHNOL. **29**, 933 (1956).
[26] Blokh, G. A., Work at the Kiev Technical Institute for Light Industry, 1954, No. 6.
[27] Blokh, G. A., see Reference 26, No. 1.
[28] Auerbach, I., *Ind. Eng. Chem.* **45**, 1526 (1953); RUBBER CHEM. & TECHNOL. **27**, 134 (1954).
[29] Krebs, H., *Gummi und Asbest* **8**, 68 (1955); RUBBER CHEM. & TECHNOL. **30**, 962 (1957).
[30] Blokh, G. A., Golubkova, E. A., and Kurskay, K. W., *Doklady Akad. Nauk SSSR* **105**, 275 (1955); RUBBER CHEM. & TECHNOL. **29**, 1363 (1956).
[31] Dogadkin, B., and Tarasova, S., *Doklady Akad. Nauk SSSR* **85**, 1069 (1952); RUBBER CHEM. & TECHNOL. **26**, 759 (1953).
[32] Blokh, G. A., and Chuprina, L. F., *Doklady Akad. Nauk SSSR* **99**, 575 (1954); RUBBER CHEM. & TECHNOL. **29**, 67 (1956).
[33] Blokh, G. A., Demidionova, W. J., Prshebylski, M. I., and Rekasheva, A. F., Reference 26, **1955**, No. 1.
[34] Blokh, G. A., Miklukhin, G. P., and Nikulina, R., *Communications of the Electrical Industry, USSR* (1952), No. 1.
[35] Tarasova, S. I., Kaplunova, M. J., and Dogadkin, B. A., *Works Laboratory, USSR* (1955), No. 4/21.
[36] Kuzminskil, A. S., and Lyubchanskaya, L. I., *Doklady Akad. Nauk SSSR* **90**, 409 (1953); RUBBER CHEM. & TECHNOL. **29**, 530 (1956).
[37] Tikhomirova, I. N., and Kuzminskil, I. N., *Zhur. Fiz. Khim.* **29**, 1278 (1955); RUBBER CHEM. & TECHNOL. **30**, 61 (1957).
[38] Tarasova, S., Kaplunov, M., and Dogadkin, B. A., *Doklady Akad. Nauk SSSR* **99**, 819 (1954); RUBBER CHEM. & TECHNOL. **29**, 511 (1956).
[39] Bresler, S. E., Kushnev, V. P., and Samenskil, *Zhur. Tekh. Fiz.* **24**, 2150 (1954); RUBBER CHEM. & TECHNOL. **29**, 980 (1956).
[40] Auerbach, I., and Gehman, S. D., *Anal. Chem.* **26**, 685 (1954); RUBBER CHEM. & TECHNOL. **27**, 773 (1954).
[41] Guryanova, E. N., Vasilyeva, V. N., and Kuzina, L. S., Ref. 4, Session of the Division of Chemical Sciences, pages 163–175; RUBBER CHEM. & TECHNOL. **29**, 534 (1956).
[42] Mochel, W. E., and Peterson, J. H., *J. Am. Chem. Soc.* **71**, 4 (1949); RUBBER CHEM. & TECHNOL. **22**, 1092 (1949).
[43] Dogadkin, B. A., and Reznikovskil, M. M., *Uspekhi Khim.* **24**, 801 (1955); *C. A.* **50**, 3790d.
[44] Miklukhin, G. P., and others, Ref. 4, Session of the Division of Chemical Sciences, pages 153–162.
[45] Dogadkin, B. A., Kaplunov, M., and Tarasova, Z., *Doklady Akad. Nauk SSSR* **99**, 819 (1954).
[46] Blokh, G. A., Golubkova, E. A., and Kulberg, L. M., *Ref.* **26**, **1949**, No. 9.
[47] The references have been checked with *Chemical Abstracts* and *R. C. & T.* Some supplementary references have been added. Editor of *R. C. & T.*

SUPPLEMENTARY REFERENCES

[a] Dogadkin, B. A., *J. Polymer Sci.* **30**, 351 (1958); Compare also the paper presented on vulcanization by this author at the Cologne meeting of the Deutsche Kautschuk Gesellschaft, May, 1958.
[b] Dolgoplosk, B. A., *J. Polymer Sci.* **30**, 315 (1958).
[c] Klebanskil, A. L., Zukerman, N. Ya., and Fomina, L. P., *J. Polymer Sci.* **30**, 363 (1958).
[d] Scheele, W., and Cherubim, *Verhandlungsber. Kolloid-Gesellschaft* **18**, 115 (1958).
[e] Kuzminskil, A. S., and Chertkova, V. F., *Doklady Akad. Nauk SSSR* **107**, 428 (1956); *C. A.* **50**, 16167b.
[f] Blokh, G. A., and Yaroshevich, A. G., *Doklady Akad. Nauk SSSR* **116**, 105 (1957); *C. A.* **51**, 13301*f*.
[g] "Vulkanizatsiya Resin" ("Vulcanized Rubber"), Goskhimizdat, Moscow, 1954.

THE REACTION OF SULFUR AND SULFUR COMPOUNDS WITH OLEFINIC SUBSTANCES

PART VIII. THE REACTION OF SULFUR WITH MONO-OLEFINS

L. Bateman, R. W. Glazebrook, C. G. Moore, M. Porter, G. W. Ross, and R. W. Saville

The British Rubber Producers' Research Association, Welwyn Garden City, Herts., England

INTRODUCTION TO PARTS VIII–XI

Earlier Parts of this series[1–6] reported the partial separation and identification of the complex products of certain sulfur-olefin and related reactions chosen as models for examining the mechanism of vulcanization of natural and synthetic rubbers by sulfur. The main conclusion was that sulfur-olefin interaction proceeds by free-radical chain processes, and this has been quoted elsewhere[7] and widely accepted.

Results are now presented which extend and correct the earlier findings and lead to the different mechanistic conclusion that the reactions are *polar* in type, involving heterolysis of S—S and C—H bonds. This paper and Part XI deal with the products of the reactions of sulfur with mono-olefins and a 1,5-diolefin[8], respectively, and Part X[9] presents a complementary kinetic investigation, the first for such reactions. All the experimental evidence is collated in Part XI[10] in a general theory of sulfur-olefin interaction.

Reaction of sulfur with mono-olefins at about 140°.—Previous workers[2,11,12] have reported that the products are mainly polysulfides $R \cdot S_x \cdot RH_2$ in which the hydrocarbon attachments are alkenyl (R) and alkyl (RH_2), as deduced from elementary analyses and from the results of degradation with ozone[11]. Ozonization was, however, of limited diagnostic value, since the method was applied before the response of different sulfide units to ozone had been ascertained[13]. The comparable use of methyl iodide[14] is also inadmissible since its reaction with sulfide to yield trimethylsulfonium iodide is nonspecific[15] with respect to the structures of R and R′ in $R \cdot S \cdot R'$ and occurs to negligible extent with di- and polysulfides[16].

The products of the sulfuration of differently substituted alkenes (1-octene cyclohexene, 2-heptene, 2-methyl-2-pentene, 1-methylcyclohexene, and 2,6-dimethyl-2-octene) have now been examined in greater detail, and their structures determined by a combination of conventional analyses, hydrogenolysis by reaction with lithium aluminium hydride[17], and spectroscopic comparison of original and hydrogenolysis products with synthetic reference compounds.

Reaction of sulfur with 1-octene.—At 140° complete combination of the sulfur (0.350 g-atom/mole) occurs in 14 hr (see also Part X)[9]. The product consisted of (i) unchanged olefin, spectroscopically identical with the original

* Reprinted from the *Journal of the Chemical Society*, 1958, pages 2838–2846. The following three papers, this issue, constitute Parts IX, X and XI.

material, (ii) a small quantity of a volatile sulfur compound, probably 1,2-epithio-octane, and (iii) the main product, "octene polysulfide."

The polysulfide had an average composition $(C_8H_{16.1}S_{2.33})_{2.12}$, apparently indicative of two octene units joined by a polysulfidic link, with the retention of the H:C ratio of the original olefin. The inference that on the average one octyl and one octenyl group are present per molecule (cf. Refs. 2 and 12) is, however, incorrect since the infrared spectrum showed the polysulfide to be predominantly saturated, there being no vinylic (CH_2:CHR) unsaturation and a maximum of 0.22 double bond as *trans*-CHR:CHR′ group per molecule. On hydrogenolysis, only 45% of the total sulfur was liberated as hydrogen sulfide (an octenyl octyl polysulfide of the above composition should yield ca. 60%), and the remainder was located in (*a*) a monothiol fraction, mainly octane-2-thiol with a minor amount of an unsaturated thiol having *trans*-CHR:CHR′ groups, (*b*) octane-1,2-dithiol, (*c*) a monosulfide comprising dioctyl and/or octenyl octyl sulfide, and (*d*) a high-boiling fraction whose analyses indicated formula $(C_8H_{15.6}S_{1.0})_{2.4}$. No evidence for the presence of octane-1,3-dithiol could be obtained; oxidation of the dithiol fraction and attempts to detect the formation of the disulfide (I) by the characteristic ultraviolet absorption of the 1:2-dithiolan ring system[18] were unsuccessful.

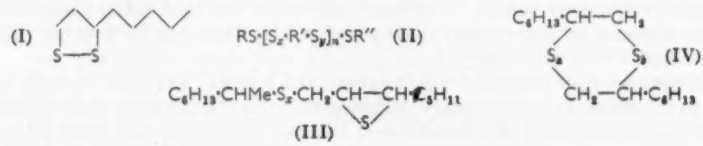

On less complete evidence, it had previously been inferred[19] that the dithiol results from the hydrogenolysis of polymeric polysulfides typified by (II). The observed composition of the bulk polysulfide precludes the presence of appreciable amounts of such structures unless (i) the ebullioscopic method for determining the molecular weight gives an erroneously low value, or (ii) products of low molecular weight, containing only one olefinic unit per molecule, are also present. Both these possibilities have been investigated and must be dismissed: the ebullioscopic method shows no anomalous features when applied to authentic di- and poly-sulfides, and fractionation of the total polysulfide yields no material containing single olefin units. Further, the relative molar yield of mono- and di-thiols of 1.1:1 is incompatible with their derivation from a structure (II). The dithiol could result from hydrogenolysis of an alkenyl alkyl structure $C_8H_{17}\cdot S_x\cdot C_8H_{15}$ (one double bond), followed by combination of the hydrogen sulfide and octenethiol produced, but this would be at variance with the spectroscopic data, and with negative results from experiments to test the formation of dithiols by secondary reactions during the hydrogenolysis of authentic alkenyl alkyl and dialkenyl polysulfides. Thus, the hydrogenolysis of di(cyclohex-2-enyl) polysulfides gives solely hydrogen sulfide and cyclohex-2-ene-1-thiol.

The only remaining explanation is that the dithiol is primarily derived from products composed of two hydrocarbon units joined by sulfur bridges in such a way that one or both units have more than one sulfur attachment, i.e. (III) or (IV). On hydrogenolysis, a compound (IV) would yield only the observed octane-1,2-dithiol, but a compound (III) would be expected to give the 1,2- and the 1,3-isomers unless scission of the epithio-ring is specifically oriented.

Such orientation is unlikely, and positive evidence favoring structure (IV) has been obtained by treating the polysulfide with potassium hydrogen sulfide. A product (V), $(C_8H_{16.1}S_{1.4})_3$, resulted, which was practically free from thiol groups and polysulfide units greater than S_2. Hydrogenolysis of product (V) yielded a C_8 thiol, octane-1,2-dithiol, dioctyl and/or octenyl octyl sulfide, and a polymer $(C_8H_{15.3}S_{1.1})_{3.6}$, i.e., products similar to those obtained likewise from the parent polysulfide. The observed transformations are consistent with the attack of HS^- ions on the S—S bonds in compound (IV), but not with attack on a structure (III), which would give, *inter alia*, a product containing free thiol groups, disulfide or shortened polysulfide linkages, and hydrocarbon units with three sulfur atoms directly attached to them, and on hydrogenolysis would give either an octanetrithiol or a dimercaptodioctyl monosulfide. Evidence based on other related aspects of episulfide reactivity[20] is also against the presence of compound (III).

TABLE I

YIELDS OF HYDROGENOLYSIS PRODUCTS FROM OCTENE POLYSULFIDE AND THE SULFURATED PRODUCT (V) (MOLE PER MOLE OF REACTANT)

Reactant	H_2S	Mono-thiol	Di-thiol	Mono-sulfide	Residue	Recovery, wt %
$(C_8H_{16.1}S_{2.33})_{2.12}$ (V); $(C_8H_{16.1}S_{1.4})_3$	2.3	0.62	0.60	0.15	0.17*	90
	0.16	0.71	1.25	0.30	0.05†	94

* Average composition $(C_8H_{15.6}S_{1.0})_{2.4}$.
† Average composition $(C_8H_{15.3}S_{1.1})_{3.6}$.

The monosulfide and the high-boiling fraction (*d*) obtained after hydrogenolysis of the parent octene polysulfide (p. 1059) appear to be original constituents of the latter and not derived products. The monosulfide is dioctyl sulfide and/or octenyl octyl sulfide, formation of the former paralleling that of dicyclohexyl sulfide in the corresponding sulfuration of cyclohexene[2]. The fraction (*d*), $(C_8H_{15.6}S_{1.0})_{2.4}$, on the basis of its predominantly saturated nature, its low thiol content, and its resistance to hydrogenolysis (confirmed by

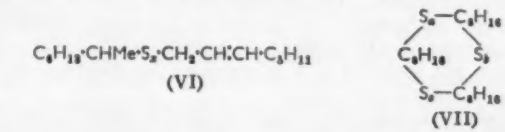

independent experiment) appears to be mainly Compound IV ($a = b = 1$), mixed with minor amounts of Compound II ($x = y = 0$; $n = 1$) and a mercaptomonosulfide, $C_8H_{17}\cdot S\cdot C_8H_{16}\cdot SH$, the latter being derived from (II; $x = 0$, $y \geqslant 1$; $n = 1$). The resistance of the C—S bonds in Compounds IV ($a = b = 1$) and II ($x = y = 0$; $n = 1$) to hydrogenolysis is comparable with the resistance of C—S bonds in monolsulfides and in the polymer $(C_8H_{16}S)_n$ obtained from 1,2-epithio-octane[20].

After allowance for loss on isolation, the yields of hydrogenolysis products recorded in Table I allow a semiquantitative analysis of the octene polysulfide to be made as follows: octenyl octyl polysulfide (VI; $x = 6.7$), 25 mole %; (IV; $a + b = 6.7$), 30 mole %; dioctyl- and/or octenyl octyl sulfide, 15 mole %; (II; R = R′ = R″ = C_8; $x + y = 4.7$, $n = 1$), 15 mole %; and a mixture of (IV; $a = b = 1$) and (II; R = R′ = R″ = C_8; $x = y = 0$, $n = 1$), 15

mole %. The elementary analysis and bulk unsaturation of this mixture agree with the above values. Similarly, the product (V) obtained on reaction with hydrosulfide (see above) appears to consist of compounds: (II; R = R′ = R″ = C_8; $x + y = 3.9$; $n = 1$), 15 mole %; (II; R = R′ = R″ = C_8; $x + y = 1.95$; $n = 2$), 25 mole %; dioctyl and/or octenyl octyl sulfide, 30 mole %; (VII; $a + b + c = 5.9$), 25 mole %; and nonreducible material $(C_8H_{15.3}S_{1.1})_{3.6}$, 5 mole %. This composition fulfils the analytical requirements and is also in accord with the derivation of (V) from the parent polysulfide.

The above structures, while in agreement with the hydrogenolysis and analytical data, are to some extent arbitrary in respect of molecular complexity and length of the polysulfide linkage. The compositions detailed above should be regarded as typifying the relative contributions of the various generic structures whose presence is experimentally well founded.

Reaction of sulfur with sym-dialkyl- and trialkylethylenes.—The average compositions of polysulfides formed from these olefins conform to the pattern observed with 1-octene, viz., the major constituents consist of two hydrocarbon units joined by either one or two chains of sulfur atoms, with the C:H ratio of the parent olefin retained (Table II). Likewise, spectroscopic examination

TABLE II

COMPOSITIONS OF OLEFIN POLYSULFIDES, AND YIELDS OF HYDROGENOLYSIS PRODUCTS (MOLE PER MOLE OF POLYSULFIDE)

Polysulfide from	Formula	Mono-thiol	Di-thiol	Molar ratio mono- to di-thiol	H_2S	Residue	Recovery, wt. %
Oct-1-ene	$(C_8H_{16.1}S_{2.33})_{2.12}$	0.62	0.60	1.1 :1	2.3	0.32	90
Cyclohexene	$(C_8H_{14.6}S_{2.57})_{2.1}$	0.90	0.53	1.67:1	—	0	63
Hept-2-ene	$(C_7H_{14.8}S_{2.77})_{2.2}$	—	—	—	—	—	—
2,6-Dimethyloct-2-ene	$(C_{10}H_{20.7}S_{2.5})_{2.16}$	1.29	0.90	1.47:1	2.88	0	~100
1-Methylcyclohexene	$(C_7H_{12.8}S_{2.69})_{2.17}$	1.14	0.42	2.3 :1	2.90	0.12	84
2-Methylpent-2-ene	$(C_6H_{12.4}S_{2.18})_{2.06}$	1.12	0.31	3.7 :1	2.30	0.05	84

reveals that the total unsaturation present is in all cases less than is required for alkenyl alkyl structures. The residual unsaturation of the several polysulfides is not uniform, however, and varies in the order: 2-methylpent-2-ene > 1-methylcyclohexene > cyclohexene > hept-2-ene > oct-1-ene. (2,6-Dimethyloct-2-ene is not included in this series as the spectroscopic analysis is less accurate.)

Hydrogenolysis of the polysulfides gave hydrogen sulfide, mono- and dithiols containing one olefin unit per molecule, and higher-boiling material containing sulfurgroups resistant to lithium aluminium hydride. The following conclusions can be drawn about the nature of these products: (i) the monothiols are partly unsaturated; (ii) the saturated monothiols derived from the polysulfides of the trialkylethylenes are tertiary; in no case has the secondary isomer been identified; (iii) the dithiols are saturated, and by analogy with the formation of octane-1,2-dithiol from "octene polysulfide" are believed to have the thiol groups on vicinal carbon atoms. The dithiol obtained from "cyclohexene polysulfide" gave on treatment with benzaldehyde a phenyldithiolan, m.p. 133–134°, different from the hexahydro-2-phenylbenzo-1,3-dithiol (VIII), m.p. 115.5° (see Culvenor et al[21]), and yielded a trithiocarbonate, m.p. 99–99.5°, different from the compound (IX), m.p. 169° (see Culvenor et al.[22]). As the dithiol used by these authors was almost certainly the *trans*-form it is inferred that the dithiol now obtained is cyclohexane-*cis*-1,2-dithiol.

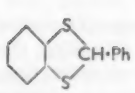

(VIII)

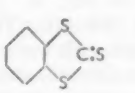

(IX)

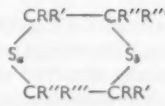

(X)

The above findings indicate that the polysulfides listed in Table II are composed of constituents similar in type to those present in octene polysulfide, viz., alkenyl alkyl polysulfides, cyclic structures (X; R = R′ = alkyl; R″ = H or alkyl; R‴ = H) analogous to (IV), and polymeric compounds (II). The yields of hydrogen sulfide, mono- and dithiols, and nonreducible sulfur-compounds obtained on hydrogenolysis (Table II) show that the polysulfides from the di- and tri-alkylethylenes contain a higher proportion of the alkenyl alkyl polysulfide and a lower proportion of the cyclic and polymeric structures, (X) and (II), respectively, than the products from oct-1-ene. The order in which the alkenyl alkyl polysulfides are formed preferentially is: 2-methylpent-2-ene > 1-methylcyclohexene > cyclohexene > 2,6-dimethyloct-2-ene > oct-1-ene, which parallels the order of retention of the olefinic unsaturation in the bulk sulfurated product. As for "octene polysulfide," it is possible to calculate the approximate compositions of those polysulfides for which the product recovery on hydrogenolysis approached 100% (Table III).

TABLE III

APPROXIMATE COMPOSITIONS OF BULK POLYSULFIDES (MOLE FRACTION)

Polysulfide from	Alkyl-S_x-alkenyl	(X)	(II)	RSR′	Residual material	Value of z $(a+b)$
2-Methylpent-2-ene	0.80	0.15	0	—	0.05	4.5[5]
1-Methylcyclohexene	0.60	0.20	0.10	—	0.10	6.1
2,6-Dimethyloct-2-ene	0.45	0.35	0.20	—	—	.60
Oct-1-ene	0.25	0.30	0.15	0.15	0.15	6.7

Olefinic structure of the polysulfides.—Spectroscopic examination of the "octene polysulfide" shows that the unsaturation present is wholly of the type CHR:CHR′, there being none of the vinylic type of the parent olefin; only *trans*-CHR:CHR′ groups have been identified, but the *cis*-isomer cannot be definitely excluded on the available evidence. This complete double-bond shift is a special feature of the oct-1-ene system which is not observed with the other unsymmetrical olefins studied. The polysulfides from the trialkylethylenes show only minor changes in unsaturation type, there being only small amounts of the CHR:CHR′ and CH_2:CRR′ forms present. Ultraviolet spectra show the absence of vinyl sulfide groups, $C{=}C{\cdot}S_x{\cdot}$.

EXPERIMENTAL

Preparation of materials.—Sulfur was purified by Bacon and Fanelli's method[23]. Oct-1-ene and hept-2-ene were Phillips Petroleum Company "Pure Grade" materials. The other olefins were prepared by standard methods and were analytically and spectroscopically pure.

General procedures.—(1) *Hydrogenolysis of polysulfides.*—The polysulfide (10 g) in dry tetrahydrofuran (50 ml) was added slowly with stirring to lithium aluminium hydride (3–5 g) in tetrahydrofuran (100 ml) and the mixture refluxed for 4–6 hr. Excess of reagent was destroyed with ice, and the products were

hydrolyzed with 2*N*-sulfuric acid (200 ml). The thiols were extracted with light petroleum, the extract was washed with water and dried (Na_2SO_4), the solvent was carefully removed through a column, and the thiols were fractionated.

(2) *Determination of "removable sulfur" in polysulfides.*—"Removable sulfur", defined as the percentage of total sulfur in the polysulfide liberated as hydrogen sulfide by hydrogenolysis with lithium aluminium hydried, was determined as previously described[1].

(3) *Determination of thiols.*—The thiols (10–20 mg) in aqueous ethanol (100 ml, 95%) was titrated against aqueous 0.01*N*-silver nitrate and the endpoint determined by the amperometric method[24].

(4) 2,4-*Dinitrophenyl sulfide derivatives of thiols.*—These were prepared by the method of Bost, Turner, and Norton[25].

(5) Molecular weights were determined ebullioscopically in benzene.

(6) *Spectrometric analysis.*—Infrared spectra were recorded on a Grubb-Parsons single-beam spectrometer with a rock salt or lithium fluoride prism, or on a Hilger H.800 spectrometer. Ultraviolet absorption spectra were determined in ethanol or cyclohexane with a Hilger Uvispek spectrophotometer. Unsaturated groups were identified by the characteristic bands of the olefinic ν(C:C) and δ(CH) vibrations[26], and (unless stated otherwise) were estimated in CCl_4 or CS_2 solution by reference to the absorption characteristics of the δ(CH) band of relevant olefins. Identification of the types of C—S linkages in the polysulfides and their hydrogenolysis products was based on the infrared spectroscopic characteristics of synthetic thiols, sulfides, and polysulfides. The absence of conjugated olefinic unsaturation was based on the absence of absorption at ~2400 A; the absence of the C=C·S_x-chromophore in the polysulfides was established by comparison of their ultraviolet absorption characteristics with those of authentic saturated and unsaturated mono- and polysulfides.

Reaction of oct-1-ene with sulfur.—This is described in detail as illustrative of the procedure used with all the olefins listed on p. 1055. The olefin (101.6 g) and sulfur (10.16 g) were heated together *in vacuo* at 140° ± 0.1° for 14.0 hr. No sulfur was deposited from the product during 24 days at −20°. Evaporative distillation of the product at $<50°/<10^{-3}$ mm gave: (i) unchanged olefin (83.09 g), n_D^{20} 1.4092 (Found: C, 85.5; H, 14.3%), which contained only CH_2: CHR groups and was devoid of conjugated unsaturation; (ii) a volatile fraction (3.10 g) which was fractionated further into (ii*a*) oct-1-ene (2.10 g), n_D^{20} 1.4095 (Found: C, 85.8; H, 14.2; S, 0.2%), and (ii*b*) a yelllw liquid (0.42 g) (Found: C, 66.6; H, 10.8; S, 21.9; thiol-S, 0.4. Calc. for $C_8H_{16}S$: C, 66.6; H, 11.2; S, 22.2%), which was predominantly saturated, devoid of thiol and thioketone groups, and shown by infrared spectral analysis to be mainly 1,2-epithio-octane; and (iii) "octene polysulfide" (24.84 g), a dark brown liquid residue, n_D^{20} 1.5611 [Found: C, 51.4, 51.7; H, 8.6, 8.8; S, 40.0, 40.3; "Removable sulfur", 44.8, 45.3%; *M*, 412, 410. Corresponds to $(C_8H_{16.1}S_{2.33})_{2.12}$], which was largely saturated.

The polysulfide (iii) (10.02 g) with lithium aluminium hydride (4.76 g) gave the following thiol fraction : (iii*a*) b. p. 71–75°/17 mm, n_{20}^{D} 1.4564 (2.09 g) (Found: C, 66.0; H, 12.0; S, 21.9; thiol-S, 22.6; C: H, 8: 17.3. Calc. for $C_8H_{16}S$: C, 66.6; H, 11.2; S, 22.2. Calc. for $C_8H_{18}S$: C, 65.7; H, 12.4; S, 21.9%); (iii*b*) b. p. 75–110°/17 mm., n_D^{20} 1.4817 (0.26 g) (Found: thiol-S, 30.8%); (iii*c*) b. p. 55–56°/0.08 mm, n_D^{20} 1.5004 (2.12 g) (Found: C, 54.5; H, 10.3; S, 35.9; thiol-S, 36.4, 36.6; C: H, 8: 18.0. Calc. for $C_8H_{18}S_2$: C, 53.95; H, 10.15; S, 35.95%); (iii*d*) b. p. 56–110°/0.08 mm, n_D^{20} 1.4779 (1.29 g) (Found: C, 67.6; H,

12.0; S, 20.6; thiol-S, 12.9, 13.2%; *M*, 220, 240. Calc. for 43:57 mole % mixture of octanedithiol and dioctyl sulfide; C, 67.4; H, 12.2; S, 20.4; thiol-S, 12.3%; *M*, 224); and (iiie) a residue, n_D^{20} 1.5075 (1.42 g) [Found: C, 65.3; H, 10.7; S, 22.2; thiol-S, ~6%; *M*, 330,260. Corresponds to $(C_8H_{15.6}S_{1.02})_{2.39}$].

Examination of the hydrogenolysis fractions.—Fraction (iii*a*) was mainly saturated, although absorption at 967 cm^{-1} could be due to up to 0.20 double bond as *trans*-CHR:CHR′ group per mole. Fraction (iii*a*) gave a 2,4-dinitrophenyl sulfide which was separated chromatographically into: (*a*) 2,4-dinitrophenyl 1-methylheptyl sulfide, m. p. and mixed m. p. 44–45° (Found: C, 53.7; H, 6.3; N, 8.9. Calc. for $C_{14}H_{20}O_4H_2S$: C, 53.8; H, 6.5; N, 9.0%), having an infrared spectrum identical with that of the synthetic material; and (*b*) an orange-red oil (Found: C, 52.1; H, 6.15; N, 9.1%) which crystallized after 3 months to give 2,4-dinitrophenyl 1-methylheptyl sulfide, m. p. and mixed m. p. 46–48°.

The dithiol fraction (iii*c*) was saturated, weak absorption at 967 cm^{-1} being attributed to a skeletal vibration also observed in the spectrum of octane-1,2-dithiol. The dithiol was identified as octane-1,2-dithiol by formation of the bis-2,4-dinitrophenyl sulfide which was separated chromatographically into two forms (from ethanol-acetone) having m. p.s and mixed m. p.s 58–60° (Found: C, 46.9; H, 4.35; N, 10.9, 10.8. Calc. for $C_{20}H_{22}O_8N_4S_2$: C, 47.1, H, 4.3; N, 11.0%) and 95–97.5° (Found: C, 47.1; H, 4.5; N, 10.7, 10.9%). Recrystallization of the two forms from acetone at −78° gave the form of m. p. 39–40°, and recrystallization from ethanol-acetone gave other forms, m. p. 61–62.5° and 70.5–72°.

Fractions (iii*d*) and (iii*e*) were largely saturated; fraction (iii*d*) contained a saturated dithiol, but other constituents were not identified (conjugated structures were absent).

Hydrogenolysis of fraction (iii*e*) (1.05 g) gave hydrogen sulfide (equiv. to 0.4% of "removable sulfur") and the following fractions: (iiie*i*) b. p. <99°/10^{-2} mm (0.08 g) (Found: C, 62.0; H, 10.8; S, 25.5%); (iiie*ii*) b. p. 99–100°/10^{-2} mm. (0.306 g) (Found: C, 65.9; H, 11.3; S, 22.15%; *M*, 249, 277. Calc. for $C_{16}H_{34}S_2$: C, 66.1; H, 11.8; S, 22.1%; *M*, 291. Calc. for $C_{16}H_{32}S_2$: C, 66.6; H, 11.2; S, 22.2%; *M*, 289), which showed no infrared absorption in the 6μ region but slight absorption at 970 cm^{-1} which could be due to 0.13 *trans*-CHR:CHR′ group per mole, while the presence of 1.1–1.4 thiol groups per mole was also indicated, and (iiie*iii*) a residue (0.51 g) (Found: C, 68.4; H, 10.4; S, 19.3%; *M*, 569, 576) which was mainly saturated and devoid of thiol groups.

Absence of octane-1,3-dithiol in the hydrogenolysis fraction (iii*c*).—Fraction (iii*c*) (0.879 g) in light petroleum (40 ml) was oxidized with excess of iodine in aqueous potassium iodide. The final excess of iodine was destroyed, the organic layer separated, washed with water, and dried (Na_2SO_4), and the solvent removed *in vacuo*, to give a *disulfide polymer* (0.700 g) [Found: C, 57.2; H, 9.8; S, 32.7%; *M*, 710, 737, 745. $(C_8H_{16}S_2)_4$ requires C, 54.2; H, 9.7; S, 36.1%; *M*, 705] which showed no ultraviolet absorption maximum at 3300 A. Comparable oxidation of octane-1,2-dithiol (0.886 g) gave a disulfide polymer (0.740 g) (Found: C, 56.0; H, 9.4; S, 34.7%; *M*, 947, 1015) showing no maximum absorption at 3300 A. Oxidation of propane-1,3-dithiol in light petroleum gave 1,2-dithiolan having maximum absorption at 3270–3280 A. Comparable results to the above were obtained by partial aerobic oxidation of *dilute* ethanolic solutions of fraction (iii*c*) and propane-1, 3-dithiol.

Reaction of "oct-1-ene polysulfide" with potassium hydrogen sulfide.—The

polysulfide (iii) [Found: C, 52.15; H, 8.65; S, 39.6%; *M*, 427, 405. Corresponds to $(C_8H_{15.8}S_{2.28})_{2.25}$] (8.23 g) was shaken for 48 hr at room temperature with an ethanolic solution of potassium hydrogen sulfide [prepared by saturating a solution of potassium hydroxide (7.1 g) in ethanol (78 ml) with hydrogen sulfide at 0°]. Ethanol was removed under reduced pressure, and the product treated with water (200 ml) and extracted with light petroleum (3 × 75 ml). Acidification of the aqueous portion with dilute hydrochloric acid gave sulfur (1.37 g, corresponding to 42% of "removable sulfur") but no organic material. Removal of the solvent from the light petroleum extract gave a dark brown liquid (V) (6.76 g), n_D^{20} 1.523 [Found: C, 60.9; H, 10.3; S, 29.2; thiol-S, 0.3; "removable sulfur", 3.9%; *M*, 463, 470. Corresponds to $(C_8H_{16.1}S_{1.41})_{2.97}$], which was devoid of thiol groups and predominantly saturated; absorption at 970 cm^{-1} could correspond to a maximum of 0.17 *trans*-CHR:CHR′ unit per molecule. The polysulfide (5.04 g) with lithium aluminium hydride (1.0 g) gave the following thiol fractions: (1) b. p. 65–70°/15 mm., n_D^{20} 1.4508 (0.9995 g) (Found: C, 66.6, 67.2; H, 12.3, 12.5; S, 20.0, 20.15; thiol-S, 22.3. Calc. for $C_8H_{16}S$: C, 66.6; H, 11.2; S, 22.2; thiol-S, 22.2. Calc. for $C_8H_{18}S$: C, 65.7; H, 12.4; S, 21.9; thiol-S, 21.9%); (2) b. p. <50°/0.08 mm (0.10 g); (3) b. p. 56–57°/0.08 mm, n_D^{20} 1.4953 (2.025 g) (Found: C, 54.7; H, 10.2; S, 35.7; thiol-S, 35.4. Calc. for $C_8H_{18}S_2$: C, 53.95; H, 10.15; S, 35.95; thiol-S, 35.95%); (4) b. p. 60–80°/0.01 mm (0.07 g); (5) b. p. 80–100°/0.01 mm, n_D^{20} 1.4811 (1.12 g) [Found: C, 67.8; H, 11.8; S, 20.4; thiol-S, 9.2%; *M*, 245, 256. Corresponds to $(C_8H_{16.6}S_{0.90})_{1.77}$. Calc. for 38:62 mole % mixture of octanedithiol and dioctyl sulfide: C, 68.1; H, 12.4; S, 19.5; thiol-S, 10.8%; *M*, 228); (6) a residue, n_D^{20} 1.525 (0.30 g) [Found: C, 64.2; H, 10.3; S, 23.6%; *M*, 510, 543. Corresponds to $(C_8H_{15.3}S_{1.10})_{3.58}$]. The infrared spectra of fractions (1), (3), (5), and (6) closely resembled those of the corresponding fractions from the hydrogenolyzed unchanged polysulfide with the exception that *all* fractions were predominantly saturated.

Evaporative distillation of "oct-1-ene polysulfide."—Distillation of the polysulfide $(C_8H_{15.8}S_{2.28})_{2.25}$ (1.986 g) at 100°/10^{-2} mm in a pot-type "molecular still"[12] gave (1) an orange liquid (0.231 g) (Found: C, 66.1; H, 11.2; S, 22.45%; *M*, 269, 257. Calc. for $C_{16}H_{32}S_2$: C, 66.6; H, 11.2; S, 22.2%; *M*, 289. Calc. for $C_{16}H_{34}S_2$: C, 66.1; H, 11.8; S, 22.1%; *M*, 291), and (2) an orange liquid (0.121 g) (Found: *M*, 376, 343). Distillation was continued at 10^{-5} mm (bath-temp. up to 115°) to give fractions (3) an orange liquid (0.598 g) [Found: C, 47.9; H, 8.3; S, 43.7%; *M*, 493, 450. Corresponds to $(C_8H_{16.5}S_{2.74})_{2.4}$], (4) an orange-brown liquid (0.429 g) [Found: C, 47.45; H, 8.1; S, 44.7%; *M*, 520, 483, 462. Corresponds to $(C_8H_{16.3}S_{2.82})_{2.4}$], and (5) a dark brown residue (0.352 g) [Found: C, 54.05; H, 9.8; S, 36.6%; *M*, 843, 800. Corresponds to $(C_8H_{17.3}S_{2.03})_{4.6}$]. Recovery of the polysulfide was 87%. All fractions were spectroscopically similar to the parent polysulfide.

Synthesis of reference compounds for the oct-1-ene reaction.—(1) *Octane-1-thiol* (*cf. Brown, Jones, and Pinder*[27]).—1-Acetylthio-octane, b. p. 116–117°/10 mm, n_D^{20} 1.4641 (64%) (Found: C, 63.7; H, 10.6; S, 16.8. Calc. for $C_{10}H_{20}OS$: C, 63.9; H, 10.65; S, 17.0%), was prepared by addition of mercaptoacetic acid to oct-1-ene. Hydrolysis of the thiolester with aqueous-ethanolic potassium hydroxide under nitrogen gave octane-1-thiol, b. p. 77–78°/10 mm, n_D^{20} 1.4542 (85%) (Found: C, 65.65; H, 12.2; S, 21.2. Calc. for $C_8H_{18}S$: C, 65.7; H, 12.4; S, 21.9%). The 2,4-dinitrophenyl octyl sulfide had m. p. 75–76° [from light petroleum (b. p. 60–80°)] (Found: C, 54.2, 54.1; H, 6.5, 6.4; N, 9.15.

Calc. for $C_{14}H_{20}O_4N_2S$: C, 53.9; H, 6.4; N, 9.0%) (Brown et al. report m. p. 78°). The mercuric salt crystallized as plates (from ethanol), m. p. 71–72° (Found: C, 39.15; H, 6.95. Calc. for $C_{16}H_{34}S_2Hg$: C, 39.1; H, 6.95%).

(2) *Octane-2-thiol.*—This thiol, b. p. 64–65°/10 mm, n_D^{20} 1.4506 (79%) (Found: C, 66.1; H, 12.4; S, 20.7%), was prepared from 2-bromo-octane and thiourea by the normal method[28]. It gave 2,4-dinitrophenyl 1-methylheptyl sulfide, m. p. 44.5–45° (from ethanol) (Found: C, 53.75; H, 6.3; N, 8.8%) (Norman, LeSuer, and Mastin[29] report m. p. 47.5°).

(3) *Octane-1,2-dithiol.*—A solution of potassium ethyl xanthate (33.6 g) in acetone (700 ml) was filtered from insoluble material and then added with stirring during 1 hr to 1,2-dibromo-octane (19.0 g; b. p. 53–56°/0.15 mm; n_D^{20} 1.4969) in acetone (35 ml). The product was filtered, the solvent removed, the yellow residue dissolved in chloroform (50 ml), washed with water, and dried (Na_2SO_4), and the solvent removed under reduced pressure. The resulting xanthic ester in dry tetrahydrofuran (50 ml) was hydrogenolyzed for 4 hr by lithium aluminium hydride (7.6 g) in refluxing tetrahydrofuran (75 ml) (cf. Djerassi et al.[30]), to give *octane-1,2-dithiol* (4.3 g, 35%), b. p. 56–59°/0.05–0.1 mm, n_D^{20} 1.4981 (Found: C, 54.0; H, 10.1; S, 36.1; thiol-S, 35.1. $C_8H_{18}S_2$ requires C, 53.95; H, 10.15; S, 35.95; thiol-S, 35.95%). The dithiol showed a weak infrared band at 967 cm^{-1}. The *bis-2,4-dinitrophenyl sulfide* exhibited polymorphism, being obtained in a number of forms whose color and m. p. depended on the conditions of crystallization. Thus, slow crystallization from dilute ethanol-acetone solution gave a pale yellow solid, m. p. 56–57°, whereas more concentrated solutions gave deep yellow crystals, m. p. within the ranges 97–98°, 92–94°, and 70–72°. Satisfactory analyses were obtained for all forms (e.g., form of m. p. 97–98°: Found: C, 47.0; H, 4.3; N, 10.95. $C_{20}H_{22}O_8N_4S_2$ requires C, 47.1; H, 4.3; N, 11.0%). Crystallization from concentrated acetone solutions at −78° gave a form, m. p. 38–38.5°, which changed in 1 month into the form, m. p. 71.5–73°. Attempted preparation of other derivatives of the dithiol for diagnostic purposes was unsuccessful; the bis-(2,4-dinitrophenyl sulfone) was unstable, and the trithiocarbonate and benzylidene derivative were oils.

Reaction of sulfur with di- and trialkylethylenes.—The olefin and sulfur (10% w/w) were heated together *in vacuo* at 140° for 5 hr. The products were isolated and examined as described above for the oct-1-ene-sulfur reaction. The major experimental findings are summarized in Tables II and III and in the text (p. 1059).

Synthesis of reference compounds.—(1) *Di(cyclohex-2-enyl) polysulfide.*—Reaction of cyclohex-2-enethiol (7.0 g, b. p. 44–46°/10 mm) with sulfur (3.0 g) in the presence of a trace of diethylamine at room temperature gave the polysulfide (8.0 g) [Found: C, 48.3; H, 5.95; S, 45.8; removable sulfur," 47.0%; *M*, 300, 316. Corresponds to $(C_6H_{8.9}S_{2.15})_{2.05}$]. Hydrogenolysis of the polysulfide (5.0 g) yielded only hydrogen sulfide and cyclohex-2-enethiol (2.93 g), b. p. 48–50°/10 mm, n_D^{20} 1.5242 (Found: C, 63.3; H, 8.8; S, 27.8. Calc. for $C_6H_{10}S$: C, 63.1; H, 8.8; S, 28.1%).

(2) *2,6-Dimethyloctane-2-thiol.*—2-Benzylthio-2,6-dimethyloctane (74%; b. p. 100–112°/0.01 mm n_D^{20} 1.5147) was prepared by the sulfuric acid-catalyzed addition of toluene-ω-thiol to 2,6-dimethyloct-2-ene (cf. ref. 31). Reduction of the sulfide with sodium in liquid ammonia (cf. Ref. 31) gave *2,6-dimethyloctane-2-thiol* (91%), b. p. 84–85°/10 mm, n_D^{20} 1.4543 (Found: C, 68.9; H, 12.65; S, 18.35. $C_{10}H_{22}S$ requires C, 69.0; H, 12.6; S, 18.4%).

(3) *2,6-Dimethyloctane-3-thiol.*—2,6-Dimethyloct-2-ene (14 g) reacted exothermically with mercaptoacetic acid (10 ml) under ultraviolet light to give 3-acetylthio-2; 6-dimethyloctane, b. p. 117–118°/10 mm, n_D^{20} 1.4670 (18.5 g, 86%) (Found: C, 66.1; H, 11.05; S, 15.35. Calc. for $C_{12}H_{24}OS$: C, 66.7; H, 11.1; S, 14.8%). Hydrolysis of the thiolester (18.4 g) with boiling aqueous-ethanolic potassium hydroxide during 30 min gave 2,6-*dimethyloctane-3-thiol*, b. p. 88–89°/10 mm, n_D^{02} 1.4584 (13.2 g, 89%) (Found: C, 69.0; H, 12.7; S, 18.4; thiol-S, 18.4%).

The synthesis of other reference compounds has been described previously[31].

Thermal stability of olefin sulfuration products.—Samples of olefin polysulfides" were heated *in vacuo* at 140° for 5 hr. Elementary and spectroscopic analysis of the products revealed the changes in molecular constitution and complexity as tabulated.

No.	Polysulfide from	Original composition	No.	Composition after heating
1	1-Octene	$(C_8H_{15.3}S_{2.28})_{2.25}$	1*a*	$(C_8H_{16.1}S_{2.28})_{2.83}$
2	2-Methyl-2-pentene	$(C_6H_{12.6}S_{2.15})_{2.06}$	2*a*	$(C_6H_{12.1}S_{1.22})_{2.41}$
3	1-Methylcyclohexene	$(C_7H_{12.6}S_{2.68})_{2.17}$	3*a*	$(C_7H_{12.1}S_{2.66})_{2.27}$
4	2,6-Dimethyl-2-octene	$(C_{10}H_{20.7}S_{2.8})_{2.18}$	4*a*	$(_{10}H_{20.6}S_{2.76})_{1.61}$

Polysulfides 1 and 1*a* had similar spectra except for slightly less pronounced absorption at 970 cm^{-1} in the latter. Samples 2 and 2*a* had similar spectra except for some reduction in trialkylethylenic unsaturation; comparable differences were shown between 3 and 3*a*, and 4 and 4*a*.

We thank Mr. G. M. C. Higgins for the spectroscopic data.

SYNOPSIS

Reaction of sulfur with mono-olefins at 140° gives, not only alkenyl alkyl polysulfides as previously supposed, but also substantial amounts of more saturated compounds having two attachments of sulfur per olefin moiety. The latter appear to have mainly cyclic structures (derived from the linking of two ethylenic centers) and include polymeric polysulfides (derived from similar linking of three or more olefin units); epithio-groups could not be detected in these polysulfides. The proportion of alkenyl alkyl polysulfide to these other products varies in a regular manner among different types of olefin.

REFERENCES

[1] Part VII, Farmer, Ford, and Lyons, *J. Appl. Chem.* **4**, 554 (1954); RUBBER CHEM. & TECHNOL. **28**, 470 (1955).
[2] Farmer and Shipley, *J. Chem. Soc.* **1947**, 1519; RUBBER CHEM. & TECHNOL. **20**, 341 (1947).
[3] Naylor, *J. Chem. Soc.* **1947**, 1532.
[4] Bloomfield, *J. Chem. Soc.*, **1947**, 1546.
[5] *Idem, ibid.*, p. 1547.
[6] Idem, *J. Soc. Chem. Ind.* **68**, 66 (1949).
[7] Flory, "Principles of Polymer Chemistry", Cornell Univ. Press, 1953, p. 454; Burnett, "Mechanism of Polymer Reactions", Interscience Publ. Inc., New York, 1954, p. 89; Grassie, "The Chemistry of High Polymer Degradation Processes", Butterworths, London, 1956, p. 246.
[8] Bateman, Glazebrook, and Moore, following paper.
[9] Ross, Part X, this issue.
[10] Bateman, Moore, and Porter, Part XI, this issue.
[11] Armstrong, Little, and Doak, *Ind. Eng. Chem.* **36**, 628 (1944); RUBBER CHEM. & TECHNOL. **17**, 788 (1944).
[12] Selker and Kemp, *ibid.* **39**, 895 (1947).
[13] Barnard, *J. Chem. Soc.* **1957**, 4547.
[14] Selker and Kemp, *Ind. Eng. Chem.* **36**, 16 (1944).
[15] Bloomfield, Proc. Second Rubber Tech. Conf., London, 1948, p. 79.
[16] Selker, *Ind. Eng. Chem.* **40**, 1467 (1948).
[17] Arnold, Lien, and Alm, *J. Amer. Chem. Soc.* **72**, 731 (1950); Moore and Saville, *J. Chem. Soc.* **1954**, 2082.
[18] Baritrop, Hayes, and Calvin, *J. Amer. Chem. Soc.* **76**, 4348 (1954).
[19] Bateman, Glazebrook, Moore, and Saville, Proc. Third Rubber Tech. Conf., London, 1954, p. 298.
[20] Moore and Porter, *J. Chem. Soc.*, **1958**, 2062.

[21] Culvenor and Davies, *Austral. J. Sci. Res.* **1,A**, 236 (1948).
[22] Culvenor, Davies, and Pausacker, *J. Chem. Soc.* **1946**, 1050.
[23] Bacon and Fanelli, *Ind. Eng. Chem.* **34**, 1043 (1942).
[24] Kolthoff and Harris, *Ind. Eng. Chem. Anal. Ed.* **18**, 161 (1946).
[25] Bost, Turner, and Norton, *J. Amer. Chem. Soc.* **54**, 1985 (1932).
[26] Bellamy, "The Infrared Spectra of Complex Molecules", Methuen, London, 1954, pp. 31 et seq.
[27] Brown, Jones, and Pinder, *J. Chem. Soc.* **1951**, 2123.
[28] *Org. Synth.* **21**, 36 (1941).
[29] Norman, LeSuer, and Mastin, *J. Amer. Chem. Soc.* **74**, 161 (1952).
[30] Djerassi, Gorman, Markley, and Oldenburg, *J. Amer. Chem. Soc.* **77**, 568 (1955).
[31] Moore and Saville, *J. Chem. Soc.* **1954**, 2089.

PART IX. THE REACTION OF SULFUR WITH 2,6-DIMETHYLOCTA-2,6-DIENE*

L. Bateman, R. W. Glazebrook, and C. G. Moore

The British Rubber Producers' Research Association, Welwyn Garden City, Herts., England

Farmer and Shipley[1] showed that reaction of sulfur with 2,6-dimethylocta-2,6-diene (I) at 140° yields a cyclic monosulfide and a crosslinked polysulfide. No detailed investigation of the structures of these cyclic monosulfide or polysulfide products was undertaken, but it was deduced[1] that the former contained 6-ethyl-2,2,6-trimethylthiacyclohex-3-ene (VIII) and a compound having vinylidene unsaturation, $CH_2{:}CRR'$, as apparently revealed by the infrared spectrum, and this has formed part of the evidence on which broad mechanistic conclusions have been based[2].

This reaction has now been re-examined in greater detail; the compositions of the cyclic sulfide and crosslinked polysulfide fractions and their variation with time of reaction have been determined. Results and conclusions differing in important respects from those advanced by the earlier workers have been reached, as reported preliminarily elsewhere[3].

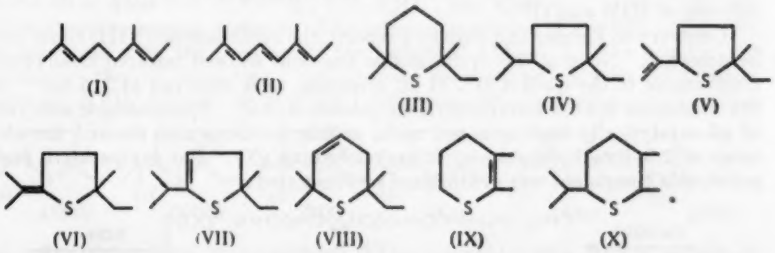

Constitution of the cyclic sulfide fraction.—This fraction contains 2,6-dimethylocta-2,4,6-triene (II) (*allo*ocimene), two saturated cyclic sulfides ($C_{10}H_{20}S$) [2-ethyl-2,6,-trimethylthiacyclohexane (III) and 2-ethyl-2-methyl-5-isopropylthiacyclopentane (IV)], and two monounsaturated cyclic sulfides [2-ethyl-2-methyl-5-*iso*propenyl- (V) and 2-ethyl-2-methyl-5-*iso*propylidenethiacyclopentane (VI)].

The triene (II) and the cyclic sulfides (III)–(VI) were identified mainly by infrared and ultraviolet spectroscopic examination of the bulk cyclic sulfide and

* Reprinted from the *Journal of the Chemical Society*, 1958, pages 2846–2856. See the preceding paper, this issue, for Part VIII.

of constituent fractions given by a combination of distillation, chromatography, and catalytic hydrogenation.

By a combination of fractional distillation and chromatography on alumina or silica gel, the triene (II) was removed from the cyclic sulfide mixture (which then gave analyses for a mixture of $C_{10}H_{18}S$ and $C_{10}H_{20}S$), and the latter partially resolved into (III)–(VI). The triene (II) was shown by spectroscopy to be predominantly the *trans*-C_4, *cis*-C_6 isomer (cf. O'Connor and Goldblatt[4]) and was estimated by absorption at 2730 A. The presence of the isomers (III) and (IV) in the cyclic sulfide mixture was established by comparison of the infrared absorption spectrum with those of synthetic (III) and (IV)[5]; chromatography gave a fraction which was devoid of (IV), (V), and (VI) and had an infrared spectrum identical with that of pure (III) Although isomers (V) and (VI) have not yet been synthesized (cf. Glazebrook and Saville[5]), evidence for their presence in the mixture can be adduced as follows. Infrared absorption at 1640 and 890 cm^{-1} in the bulk cyclic sulfide indicated vinylidene unsaturation, $CH_2:CRR'$; this is attributed to compound (V) since chromatography on silica gel gave a fraction which was free from (II) and (VI) and contained only minor amounts of (III) and (IV), but had ca. 50–60 mole % of $CH_2:CRR'$ groups, and on catalytic hydrogenation[6] gave the pure thiophan (IV), as shown by direct comparison with a synthetic specimen. Evidence for the presence of compound (VI) is: (i) selective ultraviolet absorption at 2290–2300 A, associated with the vinylic sulfide, C:C—S—, chromophore, also shown by the synthetic cyclic sulfide (IX)[7]; (ii) removal of ingredients (II), (III), (IV), and (V) by chromatography to give a fraction which had maximum absorption at 2290 A (ϵ 7750) but had no infrared absorption attributable to olefinic unsaturation other than the tetrasubstituted type, and on catalytic hydrogenation absrobed hydrogen equivalent to 0.95 double bond per $C_{10}H_{18}S$ molecule to give the cyclic sulfide (IV). The presence of the skeletal structures of (III) and (IV) in the cyclic sulfide fraction was confirmed by conversion of the latter into a cyclic sulfone mixture, $C_{10}H_{18-20}O_2S$, which on catalytic hydrogenation absorbed hydrogen equivalent to 0.35 double bond per $C_{10}H_{18}O_2S$ molecule to give the sulfones of (III) and (IV)[6].

Contrary to Farmer and Shipley's report[1], the cyclic sulfide (VIII) could not be detected. None of the cyclic sulfide fractions showed infrared absorption attributable to the *cis*-R·CH:CH·R′ grouping, as is observed at 715 $cm.^{-1}$ in the analogous 2,2,6,6-tetramethylthiacyclohex-3-ene[8]. Spectroscopic analysis of all catalytically hydrogenated cyclic sulfide fractions also showed the absence of 2,3-dimethyl-6-*iso*propylthiacyclohexane (X). For comparative purposes, this compound was syntheiszed as illustrated:

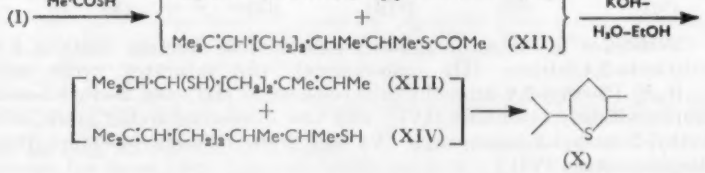

Certain of the cyclic sulfide fractions which had been subjected to considerable heating during distillation probably contained some 5-ethyl-5-methyl-2-*iso*propylthiacyclopent-2-ene (VII). However, this compound does not ap-

pear to be a primary reaction product but results from the sulfur- or polysulfide-catalyzed isomerization of (VI) (cf. p. 1070).

Constitution of the crosslinked polysulfide fraction.—The polysulfide mixture obtained from the diene (I)–sulfur reaction at 140° has been less completely analyzed, but it has been established that the composition varies considerably with the reaction time and that the crosslinked structures do not, as previously envisaged[1,2], consist solely of acyclic di-isoprene (C_{10}) units linked as alkenyl alkyl polysulfides but contain cyclic units based on the skeletal structure of (IV) at point vicinal to the polysulfide crosslink. More information about the polysulfide structures follows from fission of the —S—S— bonds with lithium aluminium hydride[5,9] in conjunction with spectroscopic and elementary analyses of the original polysulfide and its hydrogenolysis products.

Analyses of the polysulfide obtained in a 5 hours' reaction indicated a composition $(C_{10}H_{18}S_{2\cdot9})_{1\cdot82}$; the product therefore consists mainly of two di-isoprene units linked by a polysulfide bridge and does not involve repetitive interlinking of diene units by sulfur atoms (cf. Refs. 3 and 10). It has much less unsaturation than is required for an alkenyl alkyl polysulfide structure (3 double bonds per C_{20} unit), there being only 0.5—1.0 RR′C:CHR″ group per molecule and smaller amounts (<0.05) of CH_2:CRR″ and possibly *trans*-R·CH:CH·R′ groups (<0.1–0.2 per molecule); these findings suggest the presence of cyclic structures. Hydrogenolysis of the polysulfide yielded hydrogen sulfide (indicative of polysulfide crosslinks), acyclic monothiol and dithiol, and mercaptocyclic sulfides [$C_{10}H_{18-20}S_2$ (1 SH)], together with a noncleavable residue (Table II, expt. 1). The monothiol proved to be a mixture of a doubly

$Me_2C(SH)\cdot CH_2\cdot[CH_2]_2\cdot CMe(SH)\cdot CH_2Me$
(XV)

$Me_2C(SH)\cdot CH(SH)\cdot[CH_2]_2\cdot CMe{:}CHMe$
(XVI)

unsaturated compound ($C_{10}H_{17}\cdot SH$) and a monounsaturated compound ($C_{10}H_{19}\cdot SH$), in which the unsaturation is mainly trialkylethylenic with smaller amounts of *trans*-R·CH:CH·R′, CH_2:CRR′, and C:C·C:C groups, and the thiol grouping mainly tertiary. The infrared spectrum of the dithiol fraction is consistent with the presence of the saturated dithiol (XV) or unsaturated analogues thereof containing 1 double bond per C_{10} unit, or with a 1,2-dithiol such as (XVI), comparable with the 1,2-dithiols obtained from hydrogenolyses

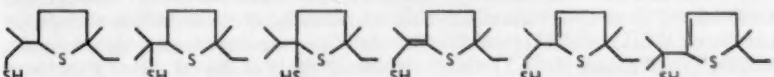

(XVII) (XVIII) (XIX) (XX) (XXI) (XXII)

of polysulfides from mono-olefins[10]. The mercaptocyclic sulfide is largely saturated and appears to consist of the thiphans (XVII) and (XVIII), with possibly (XIX), and minor amounts of their unsaturated analogues (XX), (XXI), and (XXII) containing the C:C-S– chromophore. For reference the mercaptocyclic sulfide (XVII) was prepared by the reaction sequence:

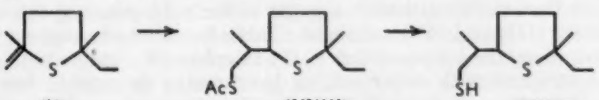

(V) (XXIII) (XVII)

The preparation of the isomer (XVIII) has been previously described[5], but unambiguous syntheses of the mercaptocyclic sulfides (XIX)–(XXII) have not been realized. The uncleavable material is predominantly saturated, and contains cyclic structures based on (XVII)–(XXII), and smaller amounts of acyclic structures, crosslinked by monosulfide units.

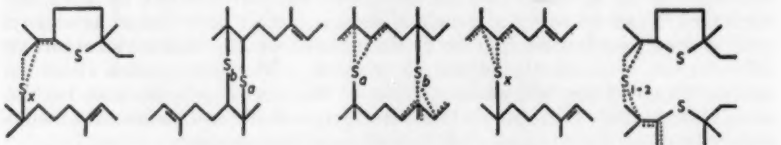

(XXIV) (XXV) (XXVI) (XXVII) (XXVIII)

The above results show that the polysulfide obtained after 5 hours' reaction is composed of both cyclic and acyclic units crosslinked by a mono- or poly-sulfide group as typified by (XXIV)–(XXVII) in which the dotted lines represent the aternative positions of the C—S and C:C bonds.

Analyses of the polysulfide obtained after 50 hours' reaction indicated a composition $(C_{10}H_{17.6}S_{1.46})_{1.74}$, incomplete removal of small amounts of the

TABLE I

REACTION OF 2,6–DIMETHYLOCTA–2,6–DIENE (I) (100 G) WITH SULFUR (10 G) AT 140°

Expt. no.	Reaction time, (hr)	Cyclic sulfide (*A*), g	Poly-sulfide (*B*), g	Triene (II), g	*A*/*B*	Diene in *A* / Diene in *B*	*S* (%) in *B*	"Removable sulfur" in *B**
1	5.0	5.0†	12.0	0.48	0.42	0.56	40.0	52
2	50.0	20.6‡	24.4	1.6	0.85	0.92	25.3	8

* Removed as hydrogen sulfide on hydrogenolysis.
† Contains (III) plus (IV), 48%; (V), 41%; (VI), ≯11%.
‡ Contains (III) plus (IV), 43%; (V), 26%; (VI), 30%; (VII) 1–2%.

triene (II) and cyclic sulfides causing the slight departure from a C_{20} unit structure. It consisted essentially of the crosslinked sulfides (XXIV; $x = 1$—2) and (XXVIII). Hydrogenolysis yielded only 8% of the total sulfur as hydrogen sulfide, showing that crosslinks greater than —S_2— occurred only to a very small extent. The other hydrogenolysis product were mainly uncleavable material (67% of the original polysulfide), containing cyclic sulfide structures based on (XVII)–(XXII) joined by monosulfide crosslinks, and mercaptocyclic sulfides $[C_{10}H_{18-20}S_2$ (1-SH)] which consisted mainly of the saturated structures (XVII)–(XVIII), with smaller amounts of (XX)–(XXII).

Influence of reaction time on diene (I)-sulfur reaction.—Increasing the reaction time from 5 to 50 hours leads to an increased yield of sulfurated product (Table I) (cf. Bloomfield[11] and Ross[12] and a redistribution of the polysulfide sulfur, reflected in the decreased sulfur content of the polysulfide and the increased amount of cyclic sulfide in the total product. The compositions of the products also change markedly; the yield of the cyclic sulfide (VI) increases relatively to that of (V), although changes in the proportions of the saturated cyclic sulfides (III) and (IV) are slight (Table I). The two reasons for these changes are: first, the incorporation of the thiophan (V) into polysulfide structures by interaction with sulfur and/or decomposing polysulfide (see below); secondly, the sulfur- or polysulfide-catalyzed isomerization of the compound

(V) to (VI), analogous to the base-catalyzed isomerization of allylic (C:D·D·S—) to vinylic (C·C:D·S—) sulfides[12]. The occurrence of these secondary reactions was confirmed by independent experiment; reaction of a cyclic sulfide fraction containing predominantly vinylidene unsaturation [due to (V)] with 10% of sulfur at 140° yielded a crosslinked polysulfide (~40% of the reactant mixture) consisting of crosslinked cyclic sulfides typified by (XXVIII), together with a cyclic sulfide fraction in which (VI) was the sole unsaturated species. Further, reaction of a cyclic sulfide containing 60% of (V) and only 4.5% of (VI) with a catalytic amount of sulfur (1.5%) for 48 hours at 140° yielded a cyclic sulfide containing 37% of (V) and 23% of (VI). No isomerization of (V) to (VI) occurred when the cyclic sulfide was heated alone *in vacuo* for 48 hours at 140°. These reactions are further discussed in Part XI.

With the crosslinked polysulfide, increasing the reaction time leads to redistribution of the polysulfidic sulfur with a decrease in the crosslink to mainly $—S_1—$ and $—S_2—$ units and with more cyclic sulfide structures incorporated in the polysulfide (Tables I and II). Similar changes were observed on heating

TABLE II

COMPOSITION OF POLYSULFIDE HYDROGENOLYSIS PRODUCTS
(YIELD: WT % OF POLYSULFIDE)

Reaction time, hr.	Polysulfidic sulfur*	Cyclic sulfide $C_{10}H_{18-20}S$	Monothiol $C_{10}H_{17-19}·SH$	Mercaptocyclic sulfide $C_{10}H_{18-20}S_2$(1 SH)	Dithiol $C_{10}H_{18-20}S_2$(2 SH)	Higher-boiling products	Loss
5†	21	0	30	16	18	12	3
50	2	5‡	8	17	1	67	0

* Removable as hydrogen sulfide by hydrogenolysis.
‡ Main fraction.
‡ Impurity in polysulfide.

the polysulfide, isolated after 5 hours' reaction, at 140° for 7 hours: this gave a small amount of cyclic sulfide, consisting mainly of (III) (~75%) with some (VI) (≤27%) and a polysulfide which was largely saturated and contained an increased proportion of cyclic structures as present in (XXVIII).

EXPERIMENTAL

2,6-Dimethylocta-2,6-diene (*I*).—This was prepared by the reduction of purified geraniol[14], and had b. p. 56.0°/14 mm., n^{20} 1.4520.

Synthesis of cyclic sulfides.—Compounds (III) and (IV) were prepared as described by Glazebrook and Saville[5]. The thiacyclopentane (IV) formed a *mercuric chloride complex*, m. p. 115–116° (Found: C, 26.9; H, 4.7; Cl, 15.6, 15.65; Hg, 45.2. $C_{10}H_{20}S$, $HgCl_2$ requires C, 27.0; H, 4.5; Cl, 16.0; Hg, 45.3%).

2,3-Dimethyl-6-isopropylthiacyclohexane (X). The 1,5-diene (I) (55 g) reacted exothermically with mercaptoacetic acid (15.2 g) at room temperature; the reaction was completed on the steam bath (30 min) and the product then fractionated to give a mixture of mercaptoacetates (XI) and (XII), b. p. 126–128°/10 mm, n_D^{20} 1.4828 (28 g, 66%) (Found: C, 67.0; H, 10.25; S, 15.1. Calc. for $C_{12}H_{22}OS$: C, 67.3; H, 10.3; S, 14.95%). This (28 g) was refluxed under nitrogen with potassium hydroxide (20 g) in water (100 ml) and ethanol (100 ml) for 15 min, and the cooled solution was diluted with water (500 ml), acidified with acetic acid, extracted with ether, dried, and fractionated, then having b. p. 92–94°/10 mm, n_D^{20} 1.4800 (17 g, 71%) (Found: C, 69.3; H, 11.4; S, 18.3; thiol-S, 10.2. Calc. for $C_{10}H_{19}·SH$: C, 69.8; H, 11.6; S, 18.6; thiol-S, 18.6%).

This product in cyclohexane was cooled in running water and irradiated with ultraviolet light for 2 hr (until the thiol content fell to zero); fractionation then gave compound (X), b. p. 86–89°/8 mm, n_B^{20} 1.4805 (Found: C, 70.3; H, 11.8; S, 18.3. Calc. for $C_{10}H_{20}S$: C, 69.8; H, 11.6; S, 18.6%), which had an infrared spectrum similar to that of a specimen prepared by Naylor[15].

Determination of thiols.—The thiol in ethanol was titrated against standard aqueous silver nitrate and the endpoint determined by the amperometric method[16]. In earlier work the thiol was determined by titration against a standard butanol solution of copper butyl phthalate[17]; such determinations are designated C.B.P. below.

Spectrometric analyses.—(i) *Cyclic sulfide fractions.*—The amounts of triene (II) and the cyclic sulfides (III)–(VII) in these were determined as follows: (*a*) The triene (II) by absorption at 2730 A in EtOH; ϵ = 42,870 at 2730 A for pure (II)[4]; (*b*) (III) by means of a sharp band of medium intensity at 872 cm^{-1} characteristic of synthetic (III) (this determination is satisfactory except where large amounts of CH_2:CRR′ groups, which absorb strongly at 890 cm^{-1}, are present); (*c*) (V) by absorption at 890 cm^{-1}; ϵ determined for 2-methylnon-1-ene and 2,4,4-trimethylpent-1-ene under comparable conditions; (*d*) (VI) by absorption at 2290 A; ϵ 7750 at 2290 A in EtOH found for fraction (*A*vii) (Table IV) which is assumed to be pure (VI) [this method is applicable only when (VII) is absent]; (*e*) when (VI) and (VII) are both present approximate estimates were obtained from equations correlating the absorption of pure (VI) and of 2-methyl-5-*iso*propylthiacyclopent-2-ene[7] ($\lambda_{max.}$ 2400 A; ϵ 2800 in EtOH) at 2290 and 2400 A with the experimentally observed absorption of the cyclic sulphide mixture at these wavelengths; (*f*) (IV) was estimated by difference since pure (IV) lacks a distinctive band of sufficient intensity to permit estimation in mixtures.

(ii) *Polysulfide fractions.*—The types and amounts of olefinic unsaturation in these were determined as described in Part VIII[10]. Identification of the types of C–S linkages was based on spectroscopic characteristics of relevant synthetic sulfides and polysulfides (Higgins, unpublished data).

Reaction of 2,6-dimethylocta-2,6-diene (I) with sulfur.—(1) *Preliminary investigation.*—A mixture of the olefin (466 g) and sulfur (120 g) was heated with stirring under nitrogen for 52 hr at 140°. Fractional distillation then gave (i) unchanged olefin (120 g), b. p. 55–57°/10 mm, n_B^{20} 1.4490; (ii) a small intermediate fraction (16 g), b. p. 57–85°/10 mm, n_B^{20} 1.4840; (iii) a cyclic sulfide fraction (150 g), b. p. 85–95°/10 mm, n_B^{20}1.4870; and (iv) an undistillable polysulfide residue (300 g).

Examination of the cyclic sulfide fraction (iii).—Refractionation through a glass-helix-packed Fenske column gave three approximately equal fractions: (iii*a*) b. p. 84–90°/10 mm, n_B^{20} 1.4840 (Found: C, 69.25, 68.9; H, 11.2, 11.2; S, 18.2; C: H, 10: 19.3, 19.4. Calc. for $C_{10}H_{18}S$: C, 70.5; H, 10.65; S, 18.85. Calc. for $C_{10}H_{20}S$: C, 69.8; H, 11.6; S, 18.6%); (iii*b*) b. p. 90–92°/10 mm, n_B^{20} 1.4839 (Found: C, 69.85, 69.85; H, 11.3, 11.55; S, 18.65%; C:H, 10: 19.3, 19.7); (iii*c*) b. p. 92–94°/10 mm, n_D^{20} 1.4934 (Found: C, 69.4, 69.95; H, 10.3, 10.65; S, 18.65%; C: H, 10: 17.7, 18.2). Fractions (iii*b* and *c*) were combined, and a portion was dissolved in light petroleum and eluted through alumina under nitrogen; the solvent was removed from the eluate and the products were distilled, to give cyclic sulfide (*A*), b. p. 82–90°/10 mm, n_D^{19} 1.4875 (Found: C, 70.75; H, 11.6; S, 18.3%), containing a little of the solvent. Repetition of the above procedure with a further portion of the combined fractions (iii*b*) and

(iiic) gave cyclic sulfide (*B*), b. p. 88–90°/10 mm, n_D^{19} 1.4880 (Found: C, 70.3; H, 11.25; S, 18.7%; C: H, 10: 19.1). Spectroscopic analysis of (*A*) indicated approximately 0.7% of the triene (II), 30% of (III), 4% of (V), 27% of (VI), 14% of (VII) and 24% (by difference) of (IV). The product (*A*) in light petroleum was rechromatographed on alumina and then distilled, to give cyclic sulfide (*Ai*), b. p. 83–86°/10 mm, n_D^{20} 1.4867 (Found: C, 69.8; H, 11.1; S, 18.5%; C:H, 10: 19.0), which on catalytic hydrogenation[6] absorbed 0.35 H_2 per $C_{10}H_{18}S$ unit. Distillation of the reaction product gave: (*AiH*), b. p. 82–85°/10 mm, n_D^{20} 1.4791 (Found: C, 69.2; H, 11.45; S, 18.8%; C: H, 10: 19.7), which contained (III) and (IV) in approximately equal proportions, but not the thiacyclohexane (X); ultraviolet absorption indicated a maximum of 2% (VI) plus (VII). Cyclic sulfide (*B*) absorbed 0.38 H_2 per $C_{10}H_{18}S$ unit and gave the product (*BH*), b. p. 82–85°/10 mm, n_D^{20} 1.4796 (Found: C, 69.85; H, 11.25; S, 18.7%), which was mainly (IV) (90–95%) with a little (III), there being no (X) and only a trace of unsaturated groups revealed by a very weak band at ~1640 cm^{-1}. Treatment of product (*BH*) with mercuric chloride gave the mercurichloride derivative of (IV), m. p. and mixed m. p. 117° (Found: C, 27.0; H, 4.6; Hg, 45.4. Calc. for $C_{10}H_{20}S,HgCl_2$: C, 27.0; H, 4.5; Hg, 45.3%). The

TABLE III

COMPOSITIONS OF FRACTIONS DERIVED FROM CYCLIC SULFIDE (A)

Fraction no.	B.p./mm	Vol. ml	n_D (temp.)	Composition (wt %)				
				Formula	(III)	(IV)	(V)	(VI)	(VII)
(*Aii*)	131—133°/83—84	4	1.4851 (19.5°)	$C_{10}H_{18.6}S$	35	0	0	43	35
(*Aiii*)	133—138°/83—84	6	1.4837 (19°)	$C_{10}H_{18.7}S$	72	16*	0	12	—
(*Aiv*)	138—139°/83—84	5	1.4834 (19°)	$C_{10}H_{18.7}S$	55	32*	6	8	—
(*Av*)	105—110°/10	0.5	1.4951 (22°)	$C_{10}H_{18.4}S$	≤25	0	2	63	Trace
(*Avi*)	100—115°/10	0.5	1.5010 (21.5°)	$C_{10}H_{18.1}S$	Trace	Trace	7	80	Trace

* By difference.

apparent disparity in the relative amounts of (III) and (IV) present in samples (*AiH*) and (*BH*) suggests the nonidentity of their respective precursors and this was in part confirmed when infared analysis of cyclic sulfide (*B*) revealed 16% of (V) and probably <25% of (III). These results indicate partial separation of the components in combined fractions (iii*b* and *c*) to different extents during chromatography and distillation, confirmed by the distillative and chromatographic separations of the components of cyclic sulfide (*A*) described below.

Distillative fractionation of cyclic sulfide (*A*).—Fractionation of sample (*A*) (20 ml) through a concentric-tube column gave the fractions listed in Table III.

Chromatographic fractionation of cyclic sulfide (*A*).—A sample in light petroleum was chromatographed on silica gel (100–200 mesh) and eluted with the same solvent. Four approximately equal fractions were obtained which, after removal of solvent, gave the cyclic sulfide fractions whose compositions are given in Table IV. Confirmation that fraction (*Avii*) was substantially pure (VI) was the absorption of 0.95 H_2 per $C_{10}H_{18}S$ unit, to give a cyclic sulfide (*AviiH*) consisting of substantially pure (IV) with a maximum of 2% of (VI) and no (III), (V), or (X).

Oxidation of cyclic sulfide (*Ai*) *to sulfone.*—Cyclic sulfide (*Ai*) (8.8 g) on oxidation with hydrogen peroxide-acetic acid at 0° gave sulfone (*AiS*), b. p. 92–94°/0.01 mm, n_D^{20} 1.4880 (8.4 g, 80%) (Found: C, 58.95; H, 9.5; S, 15.55; C: H, 10: 19.2. Calc. for $C_{10}H_{18}O_2S$: C, 59.5; H, 8.9; S, 15.85. Calc. for

$C_{10}H_{20}O_2S$: C, 58.9; H, 9.8; S, 15.7%), which absorbed 0.35 H_2 per $C_{10}H_{18}O_2S$ molecule, to give a saturated sulfone (*AiSH*), b. p. 78–79°/0.01 mm, n_D^{20} 1.4836 (Found: C, 58.9; H, 9.8; S, 15.65%; C: H, 10: 19.8). This consisted of the sulfone derivatives of (III) (47%) and (IV) (53%).

Reaction of 2,6-Dimethylocta-2,6-diene (I) with sulfur.—*(2) 50 hours' reaction.*—A mixture of the olefin (90.0 g) and sulfur (9.0 g) was heated *in vacuo* for 50 hr at 140°. Fractional distillation then gave unchanged olefin, a cyclic sulfide fraction (*C*), b. p. 88–94°/10 mm, n_D^{20} 1.4950 (20.5 g) (Found: C, 71.5; H, 11.2; S, 16.9%; C: H, 10: 18.7), and a polysulfide residue (*D*) (21.9 g) involatile at 60°/0.001 mm [Found: C, 64.7; H, 9.55; S, 25.3%; *M*, 313, 327. Corresponds to $(C_{10}H_{17\cdot6}S_{1\cdot46})_{1\cdot74}$]. Fraction (*C*) contained approximately 7% of the triene (II), 24% of (V), 28% of (VI), 1–2% of (VII), and (III) and (IV) in roughly equal proportions.

Hydrogenolysis of polysulfide (D).—The polysulfide (*D*) (10.0 g) in tetrahydrofuran (50 ml) was added to lithium aluminium hydride (3 g) in tetrahydrofuran (100 ml) and the mixture refluxed for 6 hr. The product was decomposed with 2*N*-sulfuric acid (100 ml) at 0° and the evolved hydrogen sulfide removed in a current of nitrogen and collected in aqueous lead acetate to give lead sulfide (1.5 g; i.e., 8% of "removable sulfur"). The hydrogenolysis prod-

TABLE IV

CYCLIC SULFIEDS (%) IN FRACTIONS DERIVED FROM CYCLIC SULFIDE (A) BY CHROMATOGRAPHIC SEPARATION

Fraction no.	n_D^{20}	(III)	(IV)	(V)	(VI)
(*A*vii)	1.5049	0	0	0	100
(*A*viii)	1.4885	0	50–60	8	40
(*A*ix)	1.4828	35	55	7	6
(*A*x)	1.4822	100	0	0	—

ucts were extracted with light petroleum and fractionated, to give: (*D*i), b. p. <55°/0.01 mm, n_D^{20} 1.5073 (1.05 g) (Found: C, 66.8; H, 10.15; S, 22.1; thiol-S, 11.5%; C: H, 10: 18.1; *M*, 176, 190); (*D*ii), b. p. 55–57°/0.01 mm n_D^{20} 1.5189 (0.96 g) (Found: C, 64.7; H, 9.9; S, 25.9; thiol-S, 13.7%; C: H, 10: 18.2; *N*, 183, 196); (*D*iii), b. p. 57–60°/0.01 mm, n_D^{20} 1.5236 (1.12 g) [Found: C, 60.5; H, 9.7; S, 29.55; thiol-S, 18.1%; C: H, 10: 19.1; *M*, 199, 213. Calc. for $C_{10}H_{18}S_2$ (1SH): C, 59.5; H, 8.9; S, 31.7; thiol-S, 15.8%; *M*, 202. Calc. for $C_{10}H_{20}S_2$ (1SH): C, 58.8; H, 9.8; S, 31.4; thiol-S, 15.6%; *M*, 204]; (*D*iv), b. p. <100°/0.001 mm, n_D^{20} 1.5336 (4.16 g) [Found: C, 67.3; H, 10.05; S, 22.25; thiol-S, 6.75%; C: H, 10: 17.8; *M*, 287, 300. Corresponds to $(C_{10}H_{17\cdot8}S_{1\cdot24})_{1\cdot66}$]; and (*D*v) an undistillable residue (ca. 2.5 g), not further examined. The sulfur and thiol contents of the above fractions together with their molecular weights permitted the determination of the amounts of monothiol, dithiol, and mercaptocyclic sulfide formed (Talbe II).

A second polysulfide (*Da*) (Found: C, 61.5; H, 9.3; S, 29.2%), comparable to polysulfide (*D*), was obtained by evaporative distillation at <110°/10^{-3} mm of the polysulfide residue obtained from reaction of (I) with sulfur for 52 hr at 140°, (p. 1070). Hydrogenolysis of polysulfide (*Da*) (16.0 g) gave negligible hydrogen sulfide and the following fractions: (*Da*i), b. p. <60°/0.01 mm, n_D^{20} 1.5041 (1.4 g) [Found: C, 62.3; H, 10.2; S, 27.3; thiol-S (C.B.P. method), 16.2%; C: H, 10: 19.5; *M* (cryoscopic in C_6H_6), 188]; (*Da*ii), b. p. 60°/0.01 mm, n_D^{20} 1.5160 (2.7 g) [Found: C, 60.15; H, 9.85; S, 29.95; thiol-S

(C.B.P. method), 15.8%; C: H, 10: 19.5; *M*, 203, 208]; (*Da*iii), b. p. 60°/0.01 mm, n_D^{20} 1 5210 (2.7 g) [Found: C, 59.9; H, 9.6; S, 30.9; thiol-S (C.B.P. method), 16.4%; C: H, 10: 19.1; *M*, 202, 203. Calc. for $C_{10}H_{18}S_2$(1 SH): C, 59.35; H, 8.95; S, 31.7; thiol-S, 15.85%; *M*, 202.4. Calc. for $C_{10}H_{20}S_2$ (1SH): C, 58.75; H, 9.9; S, 31.35; thiol-S, 15.7%; *M*, 204.4]; (*Da*iv), b. p. 60°/0.01 mm, n_D^{20} 1.5278 (1.4 g); and (*Da*v), residue (6.0 g) which on molecular distillation at 60–105°/10^{-3} mm gave: (*Da*vi), n_D^{18} 1.5340 [Found: C, 65.4; H, 9.95; S, 24.25; thiol-S (C.B.P. method), 5.6%; *M*, 310. Corresponds to $(C_{10}H_{18\cdot1}S_{1\cdot39})_{1\cdot70}$]; (*Da*vii), n_D^{18} 1.5350 [Found: C, 66.45; H, 10.05; S, 23.2; thiol-S (C.B.P. method), 3.0%; *M*, 322, 328. Corresponds to $(C_{10}H_{18\cdot0}S_{1\cdot31})_{1\cdot81}$]; and (*Da*viii), n_D^{18} 1.5400 [Found: C, 66.6; H, 9.9; S, 23.8: thiol-S (C.B.P method), 1.9%; *M*, 365. Corresponds to $(C_{10}H_{17\cdot7}S_{1\cdot34})_{2\cdot02}$].

Spectroscopic examination of polysulfides (*D*) *and* (*Da*) *and their hydrogenolysis products.*—Sample (*D*) showed weak infrared absorption bands attributable to minor contamination with cyclic sulfide and triene (II), which is also indicated by the analyses of the polysulfide and its hydrogenolysis products (*D*i) and (*D*ii), and by ultraviolet absorption thereof at 2300–2350 and 2800 A, attributed to ~6–10% of (VI) and ⩽2% of (II), respectively. The infrared spectrum of (*Da*) resembled that of the mercaptocyclic sulfide (XVIII), suggesting that (*Da*) consists essentially of cyclic sulfide units crosslinked by sulfur atoms, and this accords with the analysis of the hydrogenolysis products (*Da*i)–(*Da*iv). The spectra of the latter resemble that of the tertiary mercaptocyclic sulfide (XVIII) more than that of the primary-mercapto-analogue (XVII). The higher-boiling hydrogenolysis fractions (*Da*vi–viii), substantially devoid of thiol groups, are spectroscopically similar to (XVIII); apart from weak infrared absorption attributed to 0.3–0.6 RR′C:CHR″ group per molecule, these samples appear to be saturated. However, they show maximum ultraviolet absorption at 2350–2360 A attributed to C:C—S groups [(*Da*vi and vii), ~0.45; (*Da*viii), ~0.6]. Similarly, the major hydrogenolysis fraction (*D*iv) of polysulfide (*D*) showed maximum ultraviolet absorption at 2400 A, indicating ~0.6 C:C—S— group per molecule. It is thus inferred that the fractions (*Da*vi–viii) contain structures (XXIX)–(XXXIV). Since structures (XXXIII) and (XXXIV) contain trisubstituted double bonds and as there is an apparent correlation between the amounts of C:C—S and RR′C:CHR″ groups the observed absorption in (*Da*vi–viii) at ~830 cm.$^{-1}$ may be associated solely with structures (XXXIII) and (XXXIV).

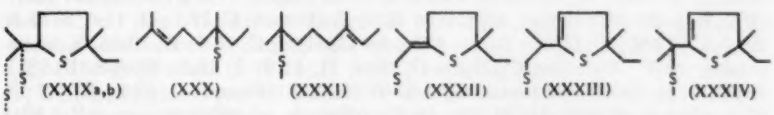

Reaction of 2,6 dimethylocta-2,6-diene (*I*) *with sulfur.*—*(3) 5 hours' reaction.*—A mixture of the olefin (200 g) and sulfur (20.0 g) was heated *in vacuo* for 5 hr at 140°. The product was cooled at −20° overnight, sulfur (7.0 g) which had separated was filtered off, and the filtrate fractionated, to give (i) unchanged olefin (168 g) which contained 2.7% of CH_2:CRR′- and 2.1% of CH_2:CHR-type unsaturation in addition to the original trialkylethylene unsaturation, (ii) a cyclic sulfide fraction (12.0 g), collected at 0.1 mm (bath-temp. at 80–90°) in a trap cooled in acetone-carbon dioxide; and (iii) a polysulfide residue (24.0 g).

Examination of the cyclic sulfide fraction (*ii*). Distillation gave a main

cyclic sulfide fraction (*E*), b. p. 82–88°/10 mm, n_D^{20} 1.4968 (Found: C, 72.2; H, 10.9; S, 15.65%; C: H, 10: 18.0) which contained triene (II) 8%, (V) 38%, (VI) ≯ 10%, and roughly equal amounts of (III) and (IV); no reliable estimate of (III) was possible owing to the large amount of (V) which masks absorption at 874 cm^{-1}. Cyclic sulfide fractions comparable to (*E*) gave similar analyses: for example, a cyclic sulfide fraction (*F*), b. p. 85–95°/10 mm, n_D^{20} 1.4970 (Found: C, 71.7; H, 10.9; S, 16.45%), contained triene (II) 9.3%, (V) 35–40%, (VI) 15%, and (III) and (IV). Attempts to hydrogenate the cyclic sulfide fraction catalytically failed owing to thiol formation and poisoning of the catalyst (cf. Bateman and Shipley[6]). Fractional elution of cyclic sulfide (*E*) in light petroleum through a silica gel column gave main fractions: (*E*i), n_D^{20} 1.5300; (*E*ii), n_D^{20} 1.5001; (*E*iii), n_D^{20} 1.4902; (*E*iv), n_D^{20} 1.4908; (*E*v), n_D^{20} 1.4897; (*E*vi), n_D^{20} 1 4897. Fraction (*E*i) contained 73.6% of the *trans*-C_4, *cis*-C_5-triene (II), as indicated by ultraviolet absorption at 2730 A; identification of other components was not possible because of the large amount of (II) present, but (V) and a small amount of (VI) were probably present. Fraction (*E*ii) contained (II) 12%, (V) ~50%, and (VI) ~20%. Fractions (*E*iii–vi) had similar spectra; (*E*iii) contained 54% of (V) and the other fractions ~50–60% of this compound; the ultraviolet spectra showed a maximum of ~1% of conjugated material [i.e., (II) and (VI)] to be present in these fractions; identification of other compounds was hampered by the large amount of (V) present. Fractions (*E*iii–vi) were combined (1.7 g) (Found: C, 70.2; H, 11.0; S, 18.2%; C: H, 10: 18 65); it did not absorb hydrogen catalytically. The cyclic sulfide (1.13 g) was recovered and a portion (0.85 g) catalytically hydrogenated; 0.93 H_2 per $C_{10}H_{18}S$ molecule was absorbed, to give a cyclic sulfide (*E*iii–vi*H*), b. p. 80–90°/10 mm, n_D^{20} 1.4728, shown spectroscopically to be almost pure (IV) and confirmed by the formation of the mercurichloride derivative of (IV), m. p. and mixed m p. 115–116°.

Examination of the polysulfide fraction (*iii*).—A portion (20 g) in light petroleum was eluted through alumina. After evaporation and removal of a little sulfur, the residue was heated at 60–80°/0.1 mm for several hours to give a small distillate (Found: C, 59.2; H, 8.75; S, 31.95%; C: H, 10: 17.6) and a main polysulfide residue (*G*) [Found: C, 51.75; H, 7.8; S, 40.0%; *M*, 414, 428. Corresponds to $(C_{10}H_{18}S_{2\cdot9})_{1\cdot82}$].

Hydrogenolysis of (*G*) (10.0 g) as above gave hydrogen sulfide (equiv. to 52% of "removable sulfur") and fractions: (*G*i), b. p. <95°/10 mm, n_D^{20} 1.4840 (0.39 g) (Found: C, 71.75; H, 11.45; S, 16.5; thiol-S, 16.2%; C: H, 10: 19.0); (*G*ii), b. p. 90–96°/10 mm, n_D^{20} 1.4890 (2.25 g) (Found: C, 70.1; H, 11.0; S, 18.6; thiol-S, 19.4%; C: H, 10: 18.7. Calc. for $C_{10}H_{18}S$: C, 70.5; H, 10.65; S, 18.85; thiol-S, 18.8. Calc. for $C_{10}H_{20}S$: C, 69.8; H, 11.6; S, 18.6; thiol-S, 18.6%); (*G*iii), b. p. 56–60°/0.01 mm, n_D^{20} 1.5140 (1.16 g) (Found: C, 62.2; H, 9.7; S, 27.6; thiol-S, 21.9%; C: H, 10: 18.6); (*G*iv), b. p. 60°/0.01 mm, n_{20}^{D} 1.5218 (2.66 g) (Found: C, 59.35; H, 9.7; S, 30.85; thiol-S, 23.7, 24.0%; C: H, 10: 19.5; *M*, 224. Calc. for $C_{10}H_{20}S_2$: C, 58.8; H, 9.8; S, 31.4; 1 thiol-S, 15.6 *M*, 204); (*G*v), a residue (1.27 g) which was evaporatively distilled at 140°/0.01 mm to give (*G*vi), n_D^{20} 1.5377 (0.61 g) [Found: C, 64.0; H, 9.75; S, 25.5; thiol-S, 7.8, 8.1%; *M*, 383. Corresponds to $(C_{10}H_{18\cdot2}S_{1\cdot49})_{2\cdot06}$], and (*G*vii), a residue (ca. 0.6 g) [Found: C, 60.3; H, 10.6; S, 27.4; thiol-S, 3.0%. Corresponds to $(C_{10}H_{20\cdot9}S_{1\cdot7})_n$].

Spectroscopic examination of polysulfide (*G*) *and its hydrogenolysis products*.—The infrared spectrum of polysulfide (*G*) indicated that it was more unsaturated

than the polysulfides (*D*) and (*Da*), and this was confirmed by comparison of their ultraviolet spectra, viz., higher absorption in (*G*) at 2150–2500 A, attributable to isolated C:C groups or singly conjugated structures. The unsaturation was predominantly of the RR'C:CHR'' type, absorption at 824 cm^{-1} indicating 0.5–1.0 double bond per molecule. There was evidence of *trans*-R·CH:CH·R' groups (<10–20%), but the presence of saturated cyclic sulfide structures which also absorb at ~960 cm^{-1} precluded an accurate estimate. Despite the lack of well-defined bands in the infrared spectrum of (*G*) to allow the types of C—S links present to be definitely identified, it was concluded that the polysulfide had a complex acyclic-cyclic sulfide structure.

The hydrogenolysis fractions (*Gi*) and (*G*ii) contained approximately the same amounts and types of unsaturation (RCH:CR'R'', 1.5 per mole; RCH:CHR', 0.1; CH_2:CR'R'', 0.1; C:C·C:C, 0.1). The infrared spectra of both fractions indicated the presence of a saturated tertiary thio group, $Me_2C(S—)R$; weak bands at 1240 cm^{-1} suggested that small amounts of primary or secondary thiols may also be present. Fractions (*G*iii and iv) were more saturated than (*G*i and ii); they could both contain the mercaptocyclic sulfides (XVII), (XVIII), and (XIX), the intensities of relevant infrared bands indicating a total of ~50% of these structures in agreement with the elementary analytical data. Ultraviolet absorption at 2390–2420 A in (*G*iv) probably indicates both C:C·C:C and C:C—S— chromophores, the latter being associated with mercaptocyclic sulfide structures such as (XX), (XXI), and (XXII). The maximum amounts of the above chromophores are 5–5.5% of the former or 19% of the latter. (*G*vi) was similar to (*G*iv) and contained only a small amount of unsaturation which was mainly trialkylethylenic; it contained an appreciable amount of cyclic sulfide structures possessing the skeletal structure of the thiacyclopentane (IV). Sharp-maximum ultraviolet absorption at 2400 A in (*G*vi) could be due to 0.75 C:C—S— group or to 0.44 C:C·C:C group per molecule.

Thermal treatment of polysulfide.—A sample (5.0 g) of a polysulfide (*Ga*), similar to (*G*) [Found: C, 51.9; H, 7.95; S, 40.2%; *M*, 407, 413. Corresponds to $(C_{10}H_{18\cdot3}S_{2\cdot9})_{1\cdot77}$], which had been freed from cyclic sulfide by 5 hours' heating at 60°/0.001 mm., was heated *in vacuo* for 7 hr at 140°, the material becoming darker and more viscous. The product was eluted through alumina with light petroleum, and the eluate fractionated at 90°/0.1 mm, to give cyclic sulfide (*H*) (0.41 g), n_D^{20} 1.4846 (Found: C, 71.6; H, 11.0; S, 16.8%; C: H, 10:18.3), containing (III) ~75%, and (VI) (max. amount 27%); the material also showed very weak maximum absorption at 2820 A ($E_{1\,cm}^{1\%}$ 45), which may be due to a small amount of highly conjugated material. The residual polysulfide (*Ia*) (2.64 g) [Found: C, 52.35; H, 8.55; S, 40.1%; *M*, 430, 431. Corresponds to $(C_{10}H_{19\cdot5}S_{2\cdot87})_{1\cdot86}$] yielded no further distillate from a pot still at 100°/0.01 mm in 1 hr. Stripping the alumina column with chloroform gave polysulfide (*Ib*) (1.62 g) [Found: C, 51.3; H, 7.3; S, 39.9%; *M*, 503, 509. Corresponds to $(C_{10}H_{17}S_{2\cdot9})_{2\cdot2}$]. The infrared spectra of polysulfides (*Ia*) and (*Ib*) were similar and suggested that both samples are nearly saturated, those bands in (*Ga*) assigned to trialkylethylenic groups having practically disappeared; between 1150 and 900 cm^{-1} the spectra of (*Ia*) and (*Ib*) are similar to those of both mercaptocyclic sulfides (XVII) and (XVIII). Ultraviolet absorption of (*Ib*) at 2150–3000 A was less than that of (*Ga*), the greatest difference occurring at 2450–2500 A; this decrease is ascribed to a decrease in content of conjugated structures.

Synthesis of mercaptocyclic sulfide (XVII).—The cyclic sulfide mixture used had n_D^{20} 1.4924 (Found: C, 70.15; H, 11.2; S, 18.6%; C: H, 10: 19.0). It was free from triene (II) and contained (V) 55%, (VI) ⩾ 7%, and (III) and (IV) (total ~38% by difference). A mixture of the sulfide (1.8 g) and redistilled mercaptoacetic acid (5 g) was irradiated with ultraviolet light in a quartz tube *in vacuo*. Removal of unchanged acid and fractionation gave fractions: (iE, b. p. 29–30°/0.01 mm, n_D^{20} 1.4890 (0.31 g) (Found: C, 68.75; H, 11.35; S, 19.3%; C: H, 10: 19.7) which contained only (III) (67% based on a band at 874 cm^{-1}) and (IV); (ii), b. p. <103°/0.01 mm (0.1 g); and (iii), b. p. 103–105°/0.01 mm, n_D^{20} 1.5207 (1.58 g), predominantly *5-(2-acetylthio-1-methylethyl)-2-ethyl-2-methylthiacyclopentane* (XXIII) (Found: C, 58.65; H, 9.0; S, 25.7. $C_{12}H_{22}OS_2$ requires C, 58.5; H, 8.95; S, 26.0%). Hydrolysis of the thiolester (iii) (1.0 g) with boiling aqueous-ethanolic potassium hydroxide under nitrogen gave *2-ethyl-5-(2-mercapto-1-methylethyl)-2-methylthiacyclopentane* (XVII), b. p. 65°/0.01 mm, n_D^{20} 1.5214 (0.76 g, 92%) (Found: C, 59.1; H, 9.8; S, 31.3; thiol-S, 17.0, 17.1%; C: H, 10: 19.8. $C_{10}H_{20}S_2$ requires C, 58.85; H, 9.8; S, 31.35; thiol-S, 15.6%), which gave a red color with the Rheinboldt test indicating a primary or secondary thiol.

Sulfur-catalyzed thermal isomerization of cyclic sulfide (V).—The cyclic sulfide had b. p. 98–100°/18 mm, n_D^{20} 1.4895 (Found: C, 70.35; H, 11.0; S, 18.9%; C: H, 10: 18.7) and contained 60% of (V), 4.5% of (VI), and (IV), but no triene (II). It was unchanged at 140° ± 0.1° *in vacuo* for 48 hr. The sulfide (0.5276 g) and sulfur (7.8 mg) were heated *in vacuo* in 140° ± 0.1° for 48 hr. Evaporative distillation *in vacuo* of a portion (0.33 g) of the product, n_D^{20} 1.4979, gave (i), a cyclic sulfide fraction, n_D^{20} 1.4910 (0.30 g) (Found: C, 70.5; H, 11.2; S, 18.35, 18.8%; C: H, 10: 19.0), $\lambda_{max.}$ 2290 A ($E_{1\,cm}^{1\%}$ 113) in EtOH, and (ii) a polysulfide residue (0.03 g) (Found: C, 61.65; H, 9.1; S, 29.15%. Corresponds to $(C_{10}H_{17.6}S_{1.77})_n$]. If the polysulfide (ii) results from the reaction of (V) with sulfur, (VI) and the saturated cyclic sulfides being unaffected, then spectroscopic analysis of (i) indicates 37% of (V) and 23% of (VI); thus of the 0.60 mole of (V) present in the original cyclic sulfide 0.33 mole is unaffected, 0.16 mole is isomerized to (VI), and 0.12 mole is converted into polysulfide.

Reaction of diene (I)-cyclic sulfide with sulfur.—The cyclic sulfide had n_D^{20} 1.4920 (Found: C, 70.3; H, 10.85; S, 18.3%), $E_{1\,cm}^{1\%}$ 38 at 2290 A, and contained 45% of (V), ⩾7% of (VI), and the saturated cyclic sulfides (III) and (IV) [(III) > (IV)], but no triene (II). The cyclic sulfide (3.0 g) and sulfur (0.3 g) were heated *in vacuo* at 140° for 48 hr. Fractionation of the product gave: (i) cyclic sulfide (1.67 g) b. p. 90–95°/10 mm, n_D^{20} 1.4937 (Found: C, 70.2; H, 11.2; S, 18.65%), $E_{1\,cm}^{1\%}$ 268 at 2290 A in EtOH, containing 59% of (VI) and ~30–40% of (III), but no (V); and (ii) a polysulfide, b. p. <140°/0.01 mm, n_D^{20} 1.5691 (1.3 g) [Found: C, 57.5; H, 8.85; S, 34.0%; *M*, 385. Corresponds to $(C_{10}H_{18.3}S_{2.2})_{1.84}$)]. The polysulfide was predominantly saturated. The presence of crosslinked structures based on the mercaptocyclic sulfides (XVII)–(XIX) is indicated by the infrared spectrum, although this does not resemble (XVII) or (XVIII) sufficiently closely to indicate whether the polysulfide has primary and/or tertiary C—S crosslinks. However, the presence of a *gem*-dimethyl group, indicated by the splitting of the methyl deformation band, shows that some tertiary C—S groups must be present.

We thank Mr. G. M. C. Higgins for the spectroscopic data.

SYNOPSIS

Reaction of 2,6-dimethylocta-2,6-diene (I) with sulfur at 140° yields 2,6-dimethylocta-2,4,6-triene (II), the cyclic monosulfides (III)–(VI), and a crosslinked polysulfide fraction containing two diene (C_{10}) units joined by one or two sulfur crosslinks. Increasing the reaction time leads to redistribution of the polysulfidic sulfur in terms of increasing the proportion of cyclic monosulfides and of converting acyclic crosslinked polysulfide into structures having cyclic units based on the skeletal structure of (IV) vicinal to shorter sulfur crosslinks.

REFERENCES

[1] Farmer and Shipley, *J. Chem. Soc.*, **1947**, 1519.
[2] Farmer, *J. Soc. Chem. Ind.* **66**, 86 (1947); Bloomfield and Naylor, Proc. XIth Internat. Congr. Pure Appl. Chem., London, 1947, Vol. II, p. 7; Bloomfield, Proc. Second Rubber Tech. Conf., London, 1948, p. 79.
[3] Bateman, Glazebrook, Moore, and Saville, Proc. Third Rubber Tech. Conf., London, 1954, p. 298.
[4] O'Connor and Goldblatt, *Anal. Chem.* **26**, 1726 (1954).
[5] Glazebrook and Saville, *J. Chem. Soc.* **1954**, 2094.
[6] Bateman and Shipley, *J. Chem. Soc.* **1958**, 2888.
[7] Bateman and Glazebrook, *J. Chem. Soc.* **1958**, 2834
[8] Naylor, *J. Chem. Soc.* **1949**, 2749.
[9] Arnold, Lien, and Alm, *J. Amer. Chem. Soc.* **72**, 731 (1950).
[10] Bateman, Glazebrook, Moore, Porter, Ross, and Saville, preceding paper, this issue.
[11] Bloomfield, *J. Soc. Chem. Ind.* **68**, 66 (1949).
[12] Ross, following paper, this issue.
[13] Tarbell and McCall, *J. Amer. Chem. Soc.* **74**, 48 (1952); Tarbell and Lovett, *ibid.* **79**, 2259 (1956).
[14] Chablay, *Ann. Chim.* (*France*) **8**, 145 (1917); Dupont, Dulou, and Desreux, *Bull. Soc. Chim. France* **6**, 84 (1939).
[15] Naylor, *J. Chem. Soc.*, **1947**, 1532.
[16] Kolthoff and Harris, *Ind. Eng. Chem. Anal. Ed.* **18**, 161 (1946).
[17] Turk and Reid, *ibid.* **17**, 713 (1945).

PART X.[1] THE KINETICS OF THE REACTION OF SULFUR WITH CYCLOHEXENE AND OTHER OLEFINS*

G. W. Ross

THE BRITISH RUBBER PRODUCERS' RESEARCH ASSOCIATION, WELWYN GARDEN CITY, HERTS., ENGLAND

As stated in Part VIII[2], the kinetic studies now reported are complementary to product studies described in Parts VIII and IX in a program of work aimed at elucidating the mechanism of sulfur-olefin interaction at about 140°.

Attention has been given mainly to the reaction of sulfur with cyclohexene, because the latter is a relatively good solvent for sulfur, but reactions with 1-methylcyclohexene, oct-1-ene, hept-2-ene, 2-methylpent-2-ene, 2,6-dimethyloct-2-ene, and the 1,5-diene, 2,6-dimethylocta-2,6-diene, have also been examined. The rate of reaction increases until about 20% of the sulfur has reacted and then continues at an almost steady value until nearly all the sulfur is consumed. Further reaction between the product and excess of olefin proceeds at a diminishing rate. Kinetic analysis has been confined mainly to the period of accelerating rate (r_a), and the information obtained appears to justify this procedure rather than considering the steady maximum rate (r_m).

* Reprinted from the *Journal of the Chemical Society* **1958**, pages 2856–2866. For Part IX see the preceding paper, this issue.

EXPERIMENTAL

Materials.—Cyclohexene was freed from peroxides and purified as described by Bateman and Hughes[3] and stored under nitrogen at −25° until required. The other olefins were as described in Parts VIII[2] and IX[1]. Immediately before use, the olefin was passed under nitrogen through activated alumina and then distilled under a high vacuum. Sulfur was purified by Bacon and Fanelli's method[4], and converted into a form suitable for introduction into the dilatometer (capillary tube of 1.5 mm internal diameter) by grinding and sieving or by recrystallization from cyclohexane. Cyclohexane was purified by nitration and fractionation (b. p. 80.5°/756 mm), followed by passage through a column of silica gel. Pure 2,2-diphenyl-1-picrylhydrazyl and dibenzyl tetrasulfide were supplied by Lyons and Watson[5], and Moore, respectively. 1-Azobis-1-phenylpropane was prepared as described by Cohen, Crosvos, and Sparrow[6]. Benzoquinone, trichloroacetic acid, triethylamine, and ethyl sulfide were purified by standard methods; other substances were of "AnalaR" grade and were used directly.

Procedure.—Reaction was followed by observing the volume contraction in a dilatometer with a cathetometer. The dilatometer had a bulb of capacity 4–8 ml and a capillary tube of 1.5 mm internal diameter. The olefin was degassed and then distilled at $<10^{-3}$ mm into the dilatometer containing a weighed quantity of sulfur. Rapid dissolution of the sulfur was effected with vigorous magnetic stirring. Temperature variation during reaction was generally <0.01°; if greater (as over long periods) the volume changes were corrected. Allowance was made for the initial time lag (ca. 3 min) in reaching temperature equilibrium in the thermostat. At the end of a run, the dilatometer was cooled rapidly, the products were transferred to a wide-mouthed tube and degassed, and the unchanged olefin was distilled into a receiver cooled in liquid air and weighed. Unchanged sulfur in the residue was separated by successive filtration and cooling to −25°; the quoted sulfur contents of the polysulfides are probably a little high owing to the solubility of sulfur in these products. Weighings were made at each stage in these operations when it was necessary to correlate volume changes with extent of reaction.

Reaction of cyclohexene with sulfur.—(*a*) In a typical experiment, sulfur (0.3048 g) and olefin (4.0582 g) were heated at 139.3° for 5 hr; the contraction in the dilatometer tube was 42 mm. The volatile portion (3.79 g) of the mixture was unchanged olefin which was analytically (Found: C, 87.6; H, 12.2. Calc. for C_6H_{10}: C, 87.8; H, 12.2%) and spectroscopically pure but contained a trace of thiol (smell and darkening of lead acetate paper). The sulfurated residue (0.56 g) [Found: C, 39.8; H, 5.5; S, 54.5%; *M* (ebulliscopic in C_6H_6), 367. Calc. for $(C_6H_{10}S_{3\cdot1})_2$: C, 39.7; H, 5.5; S, 54.7%; *M*, 362] did not give a precipitate of sulfur even after one year at −25°. (*b*) Sulfur (2.0 g), cyclohexene (8.1 g), and benzene (8.8 g) were heated *un vacuo* at 150° for 6 hr with gentle rocking. Evaporation *in vacuo* then gave a fraction of b. p. 79–80° (13.6 g) and a yellow mobile oil (0.3 g) (Found: C, 70.1; H, 9.8; S, 19.6%; C: H, 6: 10). The residue (4.2 g) (Found: C, 45.1; H, 6.7; S, 48.0; C: H, 6: 10.6. Calc. for $C_{12}H_{20}S_5$: C, 44.5; H, 6.2; S, 50.8%) contained no phenyl groups as shown spectroscopically.

RESULTS

Until all the sulfur is consumed the sulfurated product can be formulated as two olefin units (RH) linked by several sulfur atoms, i.e., $(RH)_2S_x$ (Table I).

TABLE I

COMPOSITION OF CYCLOHEXENE POLYSULFIDE (139.3°)

Sulfur concn., g-atom/l	Time, hr	S atoms per cyclohexene unit ($x/2$)	No. of cyclohexene units in polysulfide molecule
1.6	1.5	3.5	2
1.6	2	3.5	2
3.2	2.3	3.7	2
3.2	4	3.4	2
0.8	5	3.2	2
1.6	5	3.1	2
3.2	5	3.1	2
3.2	6*	2.9	2
1.6	7*	2.3	2.2
1.6	49*	0.9	2.5

* Sulfur totally combined.

The data are consistent with the product being a mixture of alkenyl alkyl polysulfide, RS_xRH_2, and a polysulfide with two intermolecular sulfur linkages, RH$\overset{S_y}{\underset{S_y}{<}}$RH ($x = y + z$), as revealed by structural studies[2]. During this period, to which the present kinetic study is restricted, the value of x remains sensibly constant, but it decreases thereafter, while the molecular complexity of the product increases, an effect which reflects the formation of a polymer species, $RS\cdot[S_aRHS_b]_n\cdot SRH_2$, which has also been identified earlier[2].

Comparable data to those of Table I were obtained at 120° and 130°, indicating that the composition of the polysulfide is independent of temperature up to the stage of total combination of sulfur.

Calibration of volume contraction.—The linear contraction in the capillary tubing was directly proportional to the amount of cyclohexene which reacted, up to 5 hr at 139.3° (Figure 1), as determined by the difference between the original and the recovered amounts of olefin. In certain calibration experi-

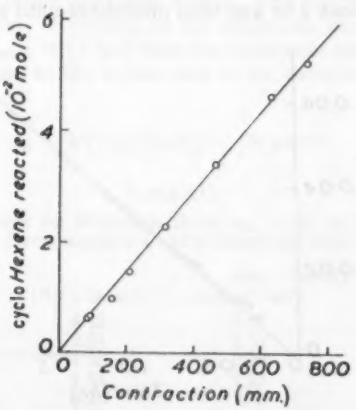

FIG. 1.—Relation between contraction in a 1.5 mm diam. capillary and the amount of cyclohexene reacted.

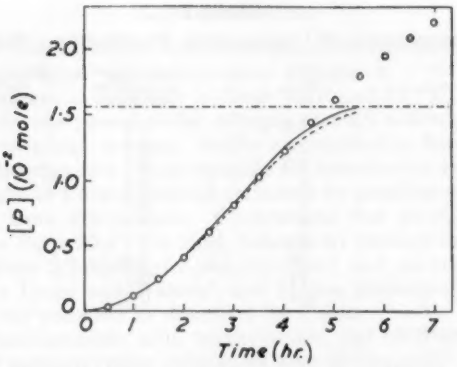

FIG. 2.—Course of reaction of sulfur (2.0 g-atom/l) with cyclohexene (8.2 mole/l) at 139.3°. ○ Experimental. (————) Eqn. 10 ([RH] assumed constant). (- - - - -) Change in [RH] allowed for. (————) Limit of applicability of kinetic scheme.

ments a dilatometer of 45 ml capacity with a 4 mm diameter capillary was used; in Figure 1 the contraction given is for a 1.5 mm diameter capillary. The amount of sulfur which reacted was deduced from the composition of the polysulfide produced and the amount of olefin which reacted. Since each polysulfide molecule contains two cyclohexene units:

$$[P] = \tfrac{1}{2}[RH]_{changed} = \frac{1}{x}[S]_{changed} \qquad (1)$$

where [P] is the concentration of polysulfide formed in mole/l, and RH and S denote the olefin and sulfur, respectively.

A similar relation applied for the other olefins studied.

Kinetic study of the cyclohexene-sulfur reaction at 139.3°.—A typical run is shown in Figure 2. During the first 2.5 hr the rate increases to a maximum which persists for about 2 hr and then diminishes until after 50 hr the volume

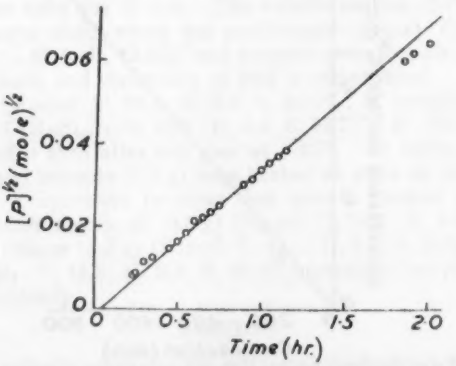

FIG. 3.—Plot of square root of polysulfide formed against time during period of accelerative rate of the sulfur-cyclohexene reaction (reaction conditions as for Figure 2).

TABLE II

DEPENDENCE OF ACCELERATING RATE, r_a, ON REACTANT AND PRODUCT CONCENTRATIONS (139.3°)

$[S]_0$ (g-atom/l)	$[RH]_0$ (mole/l)	$10^5 r_a[P]^{-\frac{1}{2}}$ (mole$^{\frac{1}{2}}$ l$^{-\frac{1}{2}}$ sec^{-1})	$10^5 r_a[P]^{-\frac{1}{2}}[S]_0^{-\frac{1}{2}}[RH]_0^{-\frac{1}{2}}$ (mole$^{-\frac{1}{2}}$ l$^{\frac{1}{2}}$ sec^{-1})
0.47	8.43	4.29	2.20
0.71	8.40	5.21	2.14
0.88	2.24	3.19	2.27
0.88	4.65	4.41	2.19
0.88	8.33	5.46	2.02
1.59	8.28	2.44	2.13
1.99	8.22	2.86	2.20
2.26	8.18	3.19	2.34
3.20	8.06	3.44	2.14

change becomes negligible. For the first 5 hr the volume change reflects the formation of a polysulfide of approximagely constant average composition (Table I).

For the first tenth of reaction, the following relation was found to hold (Figure 3 and Table II):

$$[P]^{\frac{1}{2}} = k(t - t_i)[S]_0^{\frac{1}{2}}[RH]_0^{\frac{1}{2}} \tag{2}$$

where t represents total time, t_i an induction period, the suffixes indicate initial concentrations, and k is a proportionality constant. (Variation of $[RH]_0$ was achieved by using cyclohexane as diluent.) The induction periods, t_i, increased with reductions in the sulfur and olefin concentrations and in temperature (e.g., from ca. 0.05 hr at 139.3° to 1.5 hr at 115° for the concentration conditions of Figures 2 and 3), but definite correlations with these variables were not established.

The rate in this accelerating period, r_a, is then given by:

$$r_a = d[P]/dt = 2k([P][S]_0[RH]_0)^{\frac{1}{2}} \tag{3}$$

Precise correlation of the maximum rate, r_m, with the reactant variables has not been found possible. However, at the arbitrarily chosen time of half reaction, $t_{\frac{1}{2}}$, when $[S]_{reacted} = [S]_0/2$ then the maximum rate, r_m, is found to be proportional to $[S]_0$ and to the square root of the concentration of olefin then present (Table III), i.e.,

$$r_m = k'[S]_0([RH]_0 - [S]_0x^{-1})^{\frac{1}{2}} \tag{4}$$

TABLE III

DEPENDENCE OF MAXIMUM RATE, r_m, AT $t_{\frac{1}{2}}$ ON SULFUR AND CYCLOHEXENE CONCENTRATIONS (139.3°)

$[S]_0$ (g-atom/l)	$[RH]_0$ (mole/l)	$10^5 r_m$ (mole l^{-1} sec^{-1})	$10^5 r_m[S]_0^{-1}([RH]_0 - [S]_0x^{-1})^{-\frac{1}{2}}$ (mole$^{\frac{1}{2}}$ l$^{\frac{1}{2}}$ sec^{-1})
0.47	8.43	0.67	4.93
0.88	2.24	0.51	4.04
0.88	4.65	0.78	4.18
0.88	8.33	1.25	4.95
1.59	8.28	2.05	4.57
1.99	8.22	2.45	4.39
3.20	8.06	3.34	3.83

TABLE IV

TEMPERATURE DEPENDENCE OF r_a AND r_m

Temp.	115	120	125	130	139.3
$10^6 r_a[P]^{-\frac{1}{2}}[S]_0^{-\frac{1}{2}}[RH]_0^{-\frac{1}{2}}$ (mole$^{-\frac{1}{2}}$ l$^{\frac{1}{2}}$ sec^{-1})	0.136	0.216	—	0.725	2.22
$10^6 r_m[S]_0^{-1}([RH]_0 - [S]_0 x^{-1})^{-\frac{1}{2}}$ (mole$^{\frac{1}{2}}$ l$^{\frac{1}{2}}$ sec^{-1})	0.27	0.43	0.75	1.4	4.5

Effect of temperature.—The relations (2), (3), and (4) also hold at 120° and 130°. From results at these temperatures and more limited results at 115° and 125° (Table IV), the Arrhenius energies of activation for the reactions in the accelerating and the maximum rate regions were the same within experimental error (37 kcal/mole).

TABLE V

EFFECT OF ADDED CYCLOHEXENE POLYSULFIDE (P) ON THE CYCLOHEXENE–SULFUR REACTION AT 120°. $[S]_0$ = 0.49 G-ATOM/L

[P] (mole/l)	0.077	0.163	0.236
10^6 rate (mole l^{-1} sec^{-1})	1.46	2.07	2.46
10^6 rate $[P]^{-\frac{1}{2}}$	5.25	5.14	5.06

Effect of additives.—"Cyclohexene polysulfide" (Found: C, 54.2; H, 6.3; S, 48.5%) promoted the reaction and gave a constant rate in the early stages which was proportional to the square root of the concentration of the added polysulfide (Table V).

Neither 1,1′-azo*iso*butyronitrile at 70° nor 1-azobis-1-phenylpropane at 110° appreciably affected the reaction.

TABLE VI

EFFECT OF FREE RADICAL INHIBITORS ON THE SULFUR–CYCLOHEXENE REACTION

Free radical inhibitor	Concn. (10^{-2} mole/l)	Temp.	$10^6 r_a[P]^{-\frac{1}{2}}[S]_0^{-\frac{1}{2}}$ (sec^{-1})	Free radical inhibitor	Concn. (10^{-2} mole/l)	Temp.	$10^6 r_m[S]_0^{-1}$ (sec^{-1})
—	—	130°	2.1	—	—	120°	1.22
Hydroquinone	12	130	2.1	Iodine	6.9	120	1.27
Benzoquinone	8.6	130	3.1	Diphenylpicryl-hydrazyl	0.25	120	0.6

Irradiation of the reaction mixture in a silica dilatometer with light from high- or low-pressure mercury lamps failed to induce reaction at 80–100°

Typical inhibitors and retarders of free radical chain reactions (Table VI) and of cationic polymerizations (*tert*-butyl alcohol, pyridine, and dioxan) failed to retard sulfur-olefin reactions. On the contrary, iodine and diphenylpicrylhydrazyl eliminated the period of build-up to maximum rate, while benzoquinone increased r_a.

TABLE VII

EFFECT OF TRIETHYLAMINE ON THE SULFUR–CYCLOHEXENE REACTION

[Et$_3$N] (mole l^{-1})	$[S]_0$ (mole l^{-1})	Temp.	$10^{-2} r_m[S]_0^{-1}$ (mm hr^{-1} mole l^{-1})	[Et$_3$N] (mole l^{-1})	$[S]_0$ (mole l^{-1})	Temp.	$10^{-2} r_m[S]_0^{-1}$ (mm hr^{-1} mole^{-1}) l
0	1.65	120°	1.2	0	1.69	135°	8.4
0.33	1.65	120	3.8	0.33	1.69	135	17.0

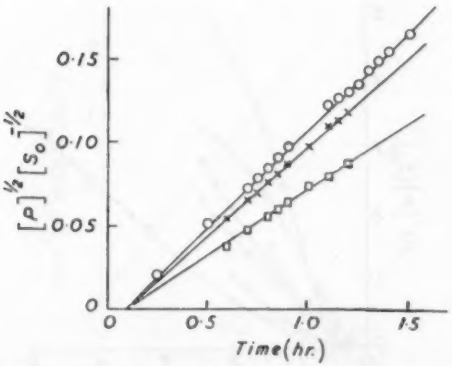

FIG. 4.—Effect of solvent medium on the sulfur-cyclohexene reaction at 139.3°. (—□—□—□—) Cyclohexane, $\epsilon = 2$ at 20°. (—×—×—×—) Diethyl sulfide, $\epsilon = 7.2$ at 20°. (—○—○—○—) Nitromethane, $\epsilon = 39.4$ at 20°.

Trichloroacetic, benzoic, propionic, and stearic acid at 0.05–0.15 *M*-concentrations increased the rate of reaction by 20–50% throughout its course, without affecting the composition of the product.

Triethylamine (0.33 mole l^{-1}) at 120° and 135° decreased the time to reach, and gave a higher, maximum rate (Table VII), in agreement with earlier qualitative observations on amine catalysis of sulfur-olefin reactions[7]. The overall activation energy was reduced from 37 to 31 kcal/mole. During the period when the sulfur is not wholly combined, little change in product composition was detected.

Changing from cyclohexane as diluent to solvents of higher dielectric constant, viz., diethyl sulfide and nitromethane, increased the rate of reaction in this order (Figure 4), without affecting the sigmoid nature of the extent of reaction-time curve. The product composition was unaffected, and there was no interaction of the sulfur with the solvent.

Although thiols have often been postulated as intermediates[8,9], only traces have been detected in the products described in Parts VIII[2] and IX[1]. Addition

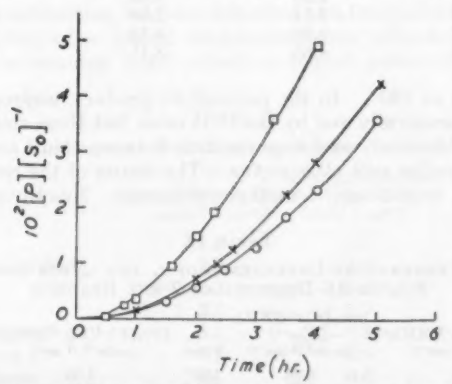

FIG. 5.—Effect of propane-2-thiol on sulfur-cyclohexene reaction at 130°. Thiol concn. (mole/l): (—○—○—○—), 0.0. (—×—×—×—), 0.26. (—□—□—□—), 1.34.

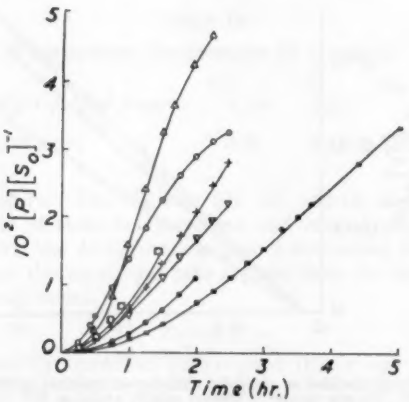

FIG. 6.—Course of reaction of sulfur with olefins at 140°. (—■—■—■—) Oct-1-ene. (—×—×—×—) Hept-2-ene. (—▽—▽—▽—) cyclohexene. (—○—○—○—) 1-Methylcyclohexene. (—△—△—△—) 2-Methylpent-2-ene. (—□—□—□—) 2,6-Dimethyloct-2-ene. (—●—●—●—) 2,6-Di-methylocta-2,6-diene.

of propane-2-thiol in concentrations from 1 to 50 molar % of the cyclohexene promoted the reaction at 130° without altering the shape of the reaction-time curve (Figure 5). The increase in rate is not large, however, and does not indicate that the thiol is an active intermediate. Moreover, the volatile material recovered at the end of the reaction always contained unchanged thiol

TABLE VIII

REACTION OF SULFUR WITH 2,6-DIMETHYLOCT-2-ENE AT 140°

$[S]_0$ (g-atom/l)	$[RH]_0$ (mole/l)	$10^4 r_a[P]^{-\frac{1}{2}}[S]_0^{-\frac{1}{2}}[RH]_0^{-\frac{1}{2}}$ (mole$^{-\frac{1}{2}}$ l$^{\frac{1}{2}}$ sec^{-1})	$10^4 r_m[S]_0^{-1}([RH]_0 - [S]_{ax^{-1}})^{-\frac{1}{2}}$ (mole$^{\frac{1}{2}}$ l$^{\frac{1}{2}}$ sec^{-1})
0.49	4.70	3.05	6.9
0.57	0.45	3.05	6.8
0.57	0.92	3.22	6.0
0.57	2.23	3.02	6.6
0.57	3.14	2.94	6.6
0.77	4.68	3.18	7.3
1.10	4.65	3.11	7.3

even after 25 hr at 130°. In the polysulfidic product, isopropyl groups were detected spectroscopically and by the C:H ratio, but these could result wholly or in part from the ready exchange reaction between thiols and polysulfides[10].

Reactions of sulfur with other olefins.—The course of the reactions of sulfur with oct-1-ene, hept-2-ene, 1-methylcyclohexene, 2-methylpent-2-ene, 2,6-

TABLE IX

TEMPERATURE-DEPENDENCE OF r_a AND r_m FOR THE SULFUR-2,6-DIMETHYLOCT-2-ENE REACTION

Temp.	$10^4 r_a[P]^{-\frac{1}{2}}[S]_0^{-\frac{1}{2}}[RH]_0^{-\frac{1}{2}}$ (mole$^{-\frac{1}{2}}$ l$^{\frac{1}{2}}$ sec^{-1})	$10^4 r_m[S]_0^{-1}([RH]_0 - [S]_{ax^{-1}})^{-\frac{1}{2}}$ (mole$^{\frac{1}{2}}$ l$^{\frac{1}{2}}$ sec^{-1})	Temp.	$10^4 r_a[P]^{-\frac{1}{2}}[S]_0^{-\frac{1}{2}}[RH]_0^{-\frac{1}{2}}$ (mole$^{-\frac{1}{2}}$ l$^{\frac{1}{2}}$ sec^{-1})	$10^4 r_m[S]_0^{-1}([RH_0] - [S]_{ax^{-1}})^{-\frac{1}{2}}$ (mole$^{-\frac{1}{2}}$ l$^{\frac{1}{2}}$ sec^{-1})
113.5°	0.11	0.28	130°	1.05	2.16
124.5	0.41	0.89	134.5	2.14	3.54
126.8	0.68	1.31	140	3.08	6.8

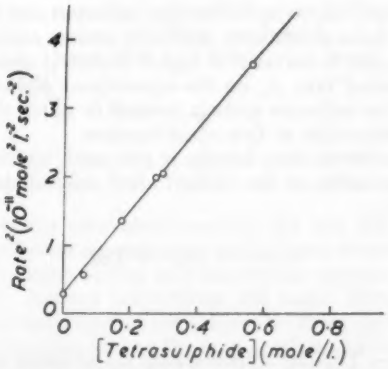

FIG. 7.—Effect of dibenzyl tetrasulfide on rate of reaction of sulfur with 2,6-dimethyloct-2-ene at 125°.

dimethyloct-2-ene, and 2,6-dimethylocta-2,6-diene simulates that with cyclohexene (Figure 6). The reaction was 2,6-dimethyloct-2-ene has been studied in some detail, and kinetic characteristics similar in all respects to those reported above were observed. Equations (3) and (4) are obeyed (Table VIII), and the energies of activation associated with the accelerative and maximum rates (38 and 37 kcal/mole, respectively; cf. Table IX) are practically identical with those found for cyclohexene. 1-Azobis-1-phenylpropane had no effect on the reaction, and the free radical inhibitor tetraphenylhydrazine caused no retardation. The polysulfide product catalyzed the reaction, as did dibenzyl tetrasulfide at 125°, the square of the rate being a linear function of the polysulfide concentration (Figure 7).

Analysis of the rate measurements on the several olefins on the basis of Equations (3) and (4) gives the data recorded in Table X.

DISCUSSION

Olefin-sulfur interaction has been described as a free radical chain process[8,9]. A polar rather than a free radical mechanism is now indicated by (*a*) the non-retardation by substances which retard or inhibit known free radical chain

TABLE X

REACTION OF SULFUR WITH OLEFINS AT 140°

Olefin	$10^{4}r_0[P]^{-\frac{1}{2}}[S]_0^{-\frac{1}{2}}[RH]_0^{-\frac{1}{2}}$ (mole$^{-\frac{1}{2}}$ l$^{\frac{1}{2}}$ sec^{-1})	$10^{4}r_m[S]_0^{-1}([RH]_0^{-\frac{1}{2}} - [S]_{0x}^{-\frac{1}{2}})^{-\frac{1}{2}}$ (mole$^{\frac{1}{2}}$ l$^{\frac{1}{2}}$ sec^{-1})	Composition of polysulfide
Oct-1-ene	1.6	4.1	$[C_8H_{16}S_{2\cdot4}]_{2\cdot2}$*
2,6-Dimethylocta-2,6-diene	2.0	4.6	$[C_{10}H_{18}S_{3\cdot1}]_{2\cdot1}$
Cyclohexene	2.3	4.9	$[C_6H_{10}S_{2\cdot1}]_{2\cdot0}$
Hept-2-ene	2.6	6.7	$[C_7H_{14}S_{2\cdot8}]_{2\cdot2}$
2,6-Dimethyloct-2-ene	3.1	6.8	$[C_{10}H_{20}S_{2\cdot5}]_{2\cdot1}$
2-Methylpent-2-ene	3.9	12.9	$[C_6H_{12}S_{2\cdot2}]_{2\cdot2}$
1-Methylcyclohexene	4.1	6.6	$[C_7H_{12}S_{2\cdot2}]_{2\cdot5}$

* For oct-1-ene the reaction time was 11 hr; for other olefins this was 5 hr.

processes; (*b*) the noncatalysis by free radical initiators and by ultraviolet light; (*c*) the catalysis by polar substances, especially amines and iodine; and (*d*) the increase in reaction rate in solvents of higher dielectric onstant. The dependence of the accelerating rate, r_a, on the square root of the sulfur, olefin, and product concentration indicates a chain process in which the termination step involves mutual destruction of two chain carriers.

The annexed *formal* reaction scheme is proposed, which for convenience is restricted to the formation of the alkenyl alkyl polysulfide component of the reaction product.

Chain initiation

$$P \longrightarrow TS_a^+ + TS_b^- \qquad R1$$

Propagation

$$TS_a^+ + RH \longrightarrow TS_aRH^+ \text{ Persulfenium ion addition to double bond} \qquad R2$$

$$TS_aRH^+ + RH \begin{cases} \nearrow \; TS_aR(\equiv P) + RH_2^+(\equiv T^+) \quad \text{Proton transfer} & R3' \\ \searrow \; TS_aRH_2(\equiv P) + R^+(\equiv T^+) \quad \text{Hydride ion transfer} & R3'' \end{cases}$$

$$T^+ + S_8 \longrightarrow TS_a^+ \qquad R4$$

Termination

$$\left.\begin{array}{lll} T^+ + TS_b^- \longrightarrow & & R5 \\ TS_a^+ + TS_b^- \longrightarrow & \text{Nonchain carriers} & R6 \\ TS_aRH^+ + TS_b^- \longrightarrow & & R7 \end{array}\right\}$$

It will be shown in the following paper that the other main products of mono-olefin sulfuration which have been revealed by the structural studies reported in Part VIII[2] can be explained by rational and kinetically equivalent variants of the propagation steps R2–R4.

Three basic features of the mechanism require comment. First is the heterolysis of an S—S bond as the initiation step, rather than a homolysis as previously supposed[8,9]. This is a novel postulate, but is not at variance with present knowledge of the reactivity of S—S bonds in sulfur and polysulfides[11]. Secondly, the chain carriers are identified with cations, although a kinetically similar mechanism can be based on participation of the persulfenyl anion in the propagation. This choice is based (i) on the known susceptibility of "non-activated" double bonds to electrophilic attack, and their resistance to nucleophilic reagents[12], and (ii) on the structures of the products. Thirdly, although the intermediates are formulated as ions, it is not imagined that these exist as such in the reaction environment, but rather that highly polarized molecules and ion pairs or aggregates are formed which react with the ionic character specified. All three features are of considerable general interest and justify a fuller discussion which is given in the following paper.

Application of the formal scheme to cyclohexene indicates how a product having an average alkenyl alkyl polysulfide structure is formed:

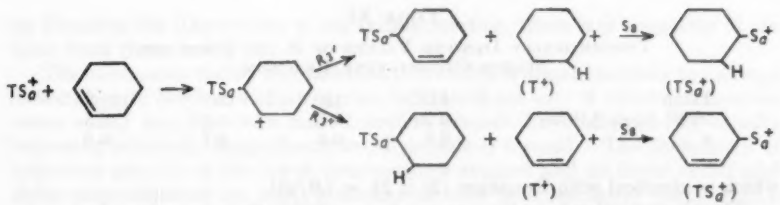

In this case the kinetically equivalent reactions R3′ and R3″ yield structurally identical products and thus no means is available to determine their relative participation. With olefins having unsymmetrically substituted double bonds, however, structurally distinct polysulfides will result from the occurence of R3′ and R3″ and thus their relative importance for these olefins can be deduced. The relative rates of reaction among the mono-olefins (Table X) are consistent with increase in nucleophilic power and facilitation of reaction R2 by increased alkyl substitution at the double bond. The variation in rate is small, however, probably in part owing to some compensating change of reactivity in the other chain carriers (TS_aRH^+ and T^+) and in part because of the much larger contribution of the initiation reaction, R1, to the overall energetics of the reaction.

Kinetic requirements of the reaction mechanism.—By assuming stationary-state conditions and long kinetic chains, the following rate equation is derived:

$$r^{-2}[P][S][RH] = A^{-1}[S]^{-1}x^2[RH] + B^{-1}x + C^{-1}[S][RH]^{-1} \qquad (5)$$

where

$$r = d[P]/dt = -\tfrac{1}{2}d[RH]/dt = -\frac{1}{x}d[S]/dt \qquad (6)$$

$$A^{-1} = k_1^{-1}k_4^{-2}k_5 \qquad (7)$$

$$B^{-1} = (k_5 + k_6)k_1^{-1}k_2^{-1}k_4^{-1} + (k_5 + k_7)k_1^{-1}k_3^{-1}k_4^{-1} \qquad (8)$$

$$C^{-1} = k_1^{-1}(k_2^{-1}k_6 + k_3^{-1}k_7)(k_2^{-1} + k_3^{-1}) \qquad (9)$$

and reactions R3′ and R3″ are treated as a composite reaction R3.

Equation (5) is seen to be equivalent to the experimentally determined rate in the accelerating region (Equation 3) provided A^{-1} and C^{-1} are neglected. This condition holds if the reactions involving the hydrocarbon ion T^+ are either very much faster or slower than the reactions involving the other intermediates. The former case is supported indirectly by the fact that benzene does not participate in the reaction (p. 1078). An interesting consequence of the greater reactivity of the T^+ species is apparent experimentally in the 2,6-dimethylocta-2,6-diene reaction (see below).

During the early stages of the reaction when [RH] is practically constant, integration of Equation (5) (terms in A and C being neglected) gives

$$2x[P] = [S]_0[1 - \cos(B[RH]_0)^{\frac{1}{2}}t] \qquad (10)$$

Expressing $\cos(B[RH]_0)^{\frac{1}{2}}t$ as a power series and ignoring powers of t greater than the second then leads to:

$$[P] = B[S]_0[RH]_0t^2/4x \qquad (11)$$

TABLE XI

THEORETICALLY DERIVED VALUES OF B AND x FOR THE SULFUR–CYCLOHEXENE REACTION

Temp.	115°	120°	130°	139.3°
$10^4B^{\frac{1}{2}}$ (mole$^{-\frac{1}{2}}$ l$^{\frac{1}{2}}$ sec^{-1})	0.29	0.55	1.9	5.5
x	6.4	6.4	6.7	6.0

which is identical with Equation (2) if $2k = (B/x)^{\frac{1}{2}}$.

The theoretical rate in the accelerating period is therefore given by:

$$r_a = (B/x)^{\frac{1}{2}}([P][S]_0[RH]_0)^{\frac{1}{2}} \tag{12}$$

By choosing the time in the region of maximum rate where half the sulfur reacts and substituting the appropriate polysulfide and olefin concentrations then obtaining {viz., $[S]_0/2x$ and $([RH]_0 - [S]_0x^{-1}$, respectively} into Equation (5), and again neglecting terms in A and C, gives the theoretical maximum rate at $t_{\frac{1}{2}}$ as:

$$r_m = B^{\frac{1}{2}}[S]_0([RH]_0 - [S_0]x^{-1})^{\frac{1}{2}}/2x \tag{13}$$

This is identical with the experimental expression (Equation 4), with $k' = B^{\frac{1}{2}}/2x$.

From the found values of k and k', B and x can be separately evaluated, as for cyclohexene in Table XI. On substituting these into Equation (10), then the full lines in Figures 2 and 8 give the course of the reaction. Agreement with the experimental points is good until 90% of the sulfur has reacted and its further improved by correcting for the change in olefin concentration (broken lines). The values of x determined in this way agree well with experiment (cf. Table I).

Although Equations (5), (12), and (13) have been derived on the assumption of long kinetic chains, this assumption is superfluous if termination occurs solely

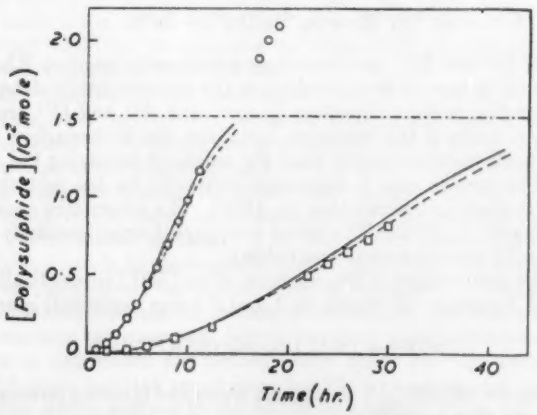

FIG. 8.—Course of reaction of sulfur (2.0 g-atom/l) with cyclohexene at 120° and 130°. □ Experimental at 120°. ○ Experimental at 130°. (————) Eqn. 10 (RH] assumed constant). (- - - - -) Change in [RH] allowed for. (————) Limit of applicability of kinetic scheme.

by Reaction R6 (the reverse of the inition reaction) since rate equations of the same form then result.

The mechanism tacitly assumes that polysulfide is present initially to undergo dissociation to produce a chain carrier, but this is not so. A direct reaction between sulfur and the olefin must therefore precede the chain process, rapidly becoming relatively insignificant as polysulfide is formed. The occurrence of induction periods at the lower temperatures studied and at lower sulfur and olefin concentrations (p. 1081) is consistent with both reactants' engaging in a prior reaction of this kind which proceeds far less readily than the later multistage interaction. The influence of promoters of the overall reaction appears informative in this sense. One class, e.g., acids, do not affect the sigmoid nature of the reaction-time curve and appears to facilitate the propagation reactions, probably by aiding the proton exchange process R3′. Another class, e.g., iodine, amines, and 2,2-diphenyl-1-picryhydrazyl, gives an enhanced and initially linear rate of reaction, almost certainly by reacting or forming complexes with the sulfur to give polarized persulfenyl species more readily than does the olefin by direct reaction[11].

Cyclic sulfide formation in the 1,5-diene system.—An apparently anomalous feature of the comparative rates of reaction of different olefins (Table X) is that 2,6-dimethylocta-2,6-diene reacts more slowly than a strictly comparable mono-olefin (2,6-dimethyloct-2-ene) despite having twice the concentration of double bonds as reactive sites. This diene also differs from mono-olefins in yielding a cyclic monosulfide mixture as a major product[1]. These two features now appear to be related and to reflect a special variant of the reaction mechanism in 1,5-diene systems, viz., interaction of an S—S bond of a polysulfide, formed as outlined above, with a carbonium ion formed at an adjacent double bond by prior proton-transfer with TS_aRH^+, as illustrated. The esseitial

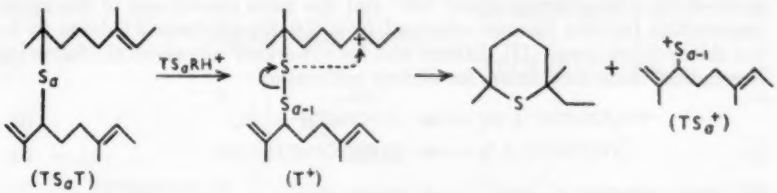

kinetic feature of this process is that the carbonium ion (T^+) is transformed into a cyclic sulfide and the less reactive chain carrier TS_a^+ without consuming elemental sulfur. By thus explaining the reduced rate of reaction, as well as exactly defining the cyclic sulfides formed, strong evidence for the validity of the proposed formal mechanism is provided.

ACKNOWLEDGMENT

The author is indebted to Dr. L. Bateman and Dr. C. G. Moore for guidance during the course of this work and for much assistance in preparing this paper for publication.

SYNOPSIS

The interaction of sulfur and cyclohexene at 110–140° has been studied dilatometrically. The reaction is autocatalytic, and in the early stages the rate is proportional to the square root of the sulfur, olefin, and product con-

centrations. Other mono-olefins react similarly. 2,6-Dimethylocta-2,6-diene reacts more slowly than comparable mono-olefins, despite having two double bonds per molecule, and this feature is associated with the formation of cyclic monosulfides in addition to the crosslinked polysulfides similar to those formed from mono-olefins.

The kinetic and product data are consistent with a polar, not a free radical, chain reaction.

REFERENCES

[1] Part IX, Bateman, Glazebrook, and Moore, preceding paper, this issue.
[2] Bateman, Glazebrook, Moore, Porter, Ross, and Saville, this issue, p. 1055.
[3] Bateman and Hughes, *J. Chem. Soc.* 1952, 4594.
[4] Bacon and Fanelli, *Ind. Eng. Chem.* **34**, 1043 (1942).
[5] Lyons and Watson, *J. Polymer Sci.* **18**, 141 (1955).
[6] Cohen, Crosvos, and Sparrow, *J. Amer. Chem. Soc.* **72**, 3947 (1950).
[7] Moore and Saville, *J. Chem. Soc.* 1954, 2082, 2089.
[8] Farmer and Shipley, *J. Polymer Sci.* **1**, 293 (1946).
[9] Bloomfield and Naylor, Proc. XIth Internat. Congress Pure Appl. Chem., 1947, Vol. II, p. 7.
[10] Birch, Cullum, and Dean, *J. Inst. Petroleum* **39**, 206 (1953).
[11] Bateman, Moore, and Porter, following paper, this issue.
[12] Dewar, "The Electronic Theory of Organic Chemistry," Oxford Univ. Press, 1949, p. 142.

PART XI. THE MECHANISM OF INTERACTION OF SULFUR WITH MONO-OLEFINS AND 1,5-DIENES *

L. Bateman, C. G. Moore, and M. Porter

British Rubber Producers' Research Association, 48 Tewin Road, Welwyn Garden City, Herts., England

Believing an alkenyl alkyl polysulfide to be the major product of sulfur-mono-olefin interaction at about 140° and the main constituent of the cyclic monosulfide fraction likewise obtained from 2,6-dimethylocta-2,6-diene to be the thiacyclohex-3-ene (II), Farmer and his coworkers[1] advanced the following free-radical chain mechanism for olefinic sulfuration:

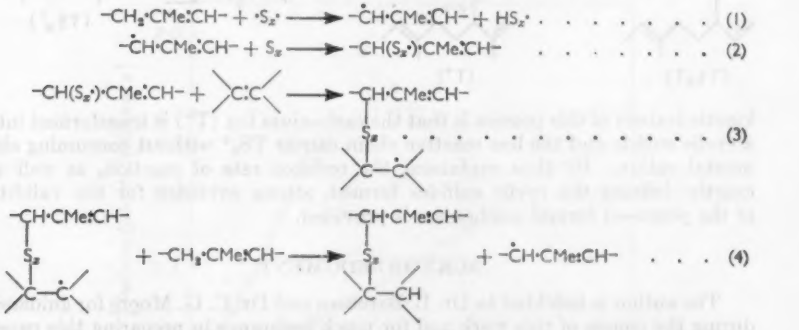

In the special case where the sulfurated radical formed in (2) contains one sulfur atom, alternative reactions to (3) and (4) were proposed, viz., capture of a hydrogen atom, followed by polar or radical addition of the alkenethiol to a second double bond, and this was regarded as the main route to the cyclic monosulfides from 1,5-dienes:

* Reprinted from the *Journal of the Chemical Society*, 1958, pages 2866–2879.

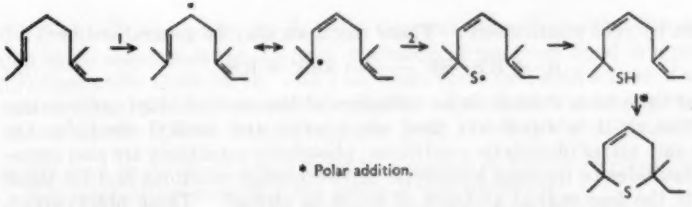

This mechanism has been widely quoted[2] despite little supporting evidence; it was based mainly on an assumed analogy with olefinic autoxidation whose radical-chain nature is well founded[3].

The detailed structural and kinetic studies reported in the preceding three papers now show: (i) that alkenyl alkyl polysulfides are not the sole primary products of the reaction of mono-olefins with sulfur; (ii) that the alkenyl alkyl polysulfides formed have not the structures to be expected from reactions (1)–(4); (iii) that 2,6-dimethylocta-2,6-diene does not yield cyclic monosulfides having structures consistent with a wholly free radical reaction (e.g., III), or with a free radical reaction yielding a dienethiol (e.g., I) which then undergoes polar intramolecular addition to give (II) as detailed in (5); and (iv) that the kinetic characteristics indicate a polar and not a free radical mechanism.

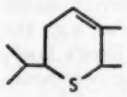

(III)

The above mechanism is therefore rejected and a polar mechanism is proposed, which is represented in its simplest form by Reactions (6)–(14):

$$\text{Initiation: Polysulfide} \longrightarrow TS_a^+ + TS_b^- \quad (6)$$

$$\text{Propagation: } TS_a^+ + RH(C{:}C) \longrightarrow TS_aRH^+ \text{ (sat.)} \quad (7)$$

$$TS_aRH^+ \text{ (sat.)} + RH(C{:}C) \longrightarrow TS_aRH_2 \text{ (sat.)} + R^+ \quad (8)$$

$$TS_aRH^+ \text{ (sat.)} + RH(C{:}C) \longrightarrow TS_aR(C{:}C) + RH_2^+ \quad (9)$$

$$\left.\begin{matrix} R^+ \\ RH_2^+ \end{matrix}\right\} + S_b \longrightarrow \begin{cases} RS_a^+ & (10) \\ RH_2S_a^+ & (11) \end{cases}$$

$$\text{Termination: } \left.\begin{matrix} R^+ \\ RH_2^+ \\ TS_aRH^+ \end{matrix}\right\} + TS_b^- \longrightarrow \text{Nonchain carriers} \quad \begin{matrix} (12) \\ (13) \\ (14) \end{matrix}$$

where RH(C:C) is a mono-olefin; (sat.) denotes absence of C:C; H is an α-methylenic hydrogen atom; T is R or RH_2; and a and $b \geqslant 1$. The validity of this mechanism kinetically has been demonstrated by Ross[4]; it will be shown here that Reactions (6)–(14) and rational extensions thereof logically account for the major products from mono-olefins or 1,5-dienes and sulfur.

The fundamental feature of the proposed mechanism is heterolysis of S—S bonds. Since the reactivity of organic di- and polysulfides has often been considered to reflect a susceptibility to homolysis, it is necessary to examine the justification for these suppositions.

Homolysis of S—S bonds.—Convincing evidence exists for the homolysis of S—S bonds in certain thermal and photochemical reactions. Thus, disulfides are efficient radical-acceptors for hydrocarbon radicals formed in vinyl polymerizations initiated by free radicals[5] and during mechanical degradation of

elastomers by cold mastication[6]. These reactions may be generalized as:

$$R\cdot + R'S{-}SR' \longrightarrow RSR' + R'S\cdot \qquad (15)$$

Disulfides have been shown[7] to be initiators of free radical vinyl polymerizations, although it is significant that alkyl, aryl, and aralkyl disulfides are effective only under photolytic conditions; photolytic conditions are also essential for disulfides to undergo homolytic thiyl-exchange reactions and for them to initiate the free radical addition of thiols to olefins[8]. These observations suggest that homolysis of S—S bonds cannot be effected by purely thermal means at temperatures commonly used in reactions of olefins with sulfur (about 140°), but requires either an external free radical source [e.g., Reaction (15) or photochemical activation[9] as in Reaction (16)]:

$$R'S{-}SR' \xrightarrow{h\nu} 2R'S\cdot \qquad (16)$$

Kharasch and others[7] and Lecher[10] regard as inconclusive or incorrect earlier evidence cited in favor of thermal homolysis of S—S bonds, such as, e.g., the thermochromic behavior of disulfides and their nonobeyance of Beer's law[11], and the reaction of disulfides with hexaphenylethane in solution to give a monosulfide[12]. Stronger physicochemical evidence is that hot solutions of benzothiazolyl disulfide in toluene are paramagnetic[13], but Cutforth and Selwood[13] have pointed out that even this is not critical since excitation of the disulfide to a triplet state would produce a comparable effect. No evidence is available[14] that simple alkyl or aryl disulfides display paramagnetism at temperatures up to 140°.

Discussion of the homolysis of S—S bonds in the sulfur molecule, S_8, and in organic polysulfides is especially relevant. Gee and his coworkers[14,15] have described the increase in molecular complexity of liquid sulfur which occurs quite abruptly at 159° in terms of the formation of a linear polymeric diradical form of sulfur which is in equilibrium with S_8 rings:

$$S_8 + \cdot S_x\cdot \rightleftharpoons \cdot S_{x+8}\cdot \qquad (17)$$

for which confirmation is provided by recent paramagnetic studies of liquid sulfur at 189° and above[16]. However, the existence of diradical forms of sulfur at $\geqslant 159°$ cannot be offered as evidence that a significant concentration of such species is present in olefinic solutions at ~140°, as required by the free radical chain mechanism of Farmer and others[1]. Sulfur and organic polysulfides are as reactive as disulfides towards hydrocarbon radicals, e.g., alkyl and alkenyl radicals derived from alkyl- or alkenyl-phenyltriazens[17]. By contrast with disulfides, sulfur inhibits the free radical polymerization of vinylic monomers[18], this being ascribed to homolysis of the S—S bond in the S_8 molecule by the polymeric radical [Reaction (18)], giving a persulfenyl radical incapable of reinitiating polymerization:

$$R_n\cdot + S_8 \longrightarrow R_nS_x\cdot \qquad (18)$$

Organic polysulfides, $R'S_xR'$ ($x > 2$), also act as polymerization inhibitors[7] and do not initiate vinyl polymerization even under photolytic conditions. Birch and others[7] state that di-*tert*-butyl trisulfide is an exception in this respect, since it photolytically initiates polymerization of acrylonitrile. No explanation appears to have been offered, for the reduced reactivity of $R'S_x\cdot$ ($x \geqslant 2$) compared with $R'S\cdot$ in initiating vinyl polymerization, but one is probably revealed by recent work[15] which suggests that $R'S_x\cdot$ radicals are partly stabilized by a resonance structure containing a "three-electron bond":

$R-\ddot{S}-\ddot{S}-\ddot{S}\cdot \longleftrightarrow R-\ddot{S}-\ddot{S}\cdots\ddot{S}$. Gee and others[15] consider this stabilization to be responsible for the heat of scission of the S—S bond in a polymeric diradical sulfur chain being <35 kcal/mole, compared with a heat of atomization of about 428 kcal/mole for the S_8 ring (equivalent to a heat of scission of 53 kcal per S—S bond in the ring), and point out that in organic polysulfides

$$R'-\overset{a}{S}-S-\overset{b}{S}-S-R'$$

it will lead to an S—S bond stability sequence in R′—S—S—S—S—R′ of $a > b$, if interactions involving the group R′ are neglected.

To summarize: purely thermal homolysis of S—S bonds in sulfur and organic di- and polysulfide molecules at temperatures below 140° has not yet been conclusively demonstrated; such fission occurs only when induced photolytically or by a radical displacement reaction such as (15) and (18).

Heterolysis of S—S bonds.—The S—S bonds in sulfur and organic polysulfides are readily broken by nucleophilic reagents, as represented by (19):

$$X^- + -S-\overset{\curvearrowright}{\underset{\cdot\cdot}{S}}-S- \longrightarrow -S-\underset{\cdot\cdot}{S}-X + \overset{-}{\underset{\cdot\cdot}{S}}- \quad . . . . . (19)$$

Common examples include the attack of SO_3^{2-}, CN^-, RS^-, or HS^- ions on sulfur and di- and polysulfides[19] and reactions with Grignard reagents (RMgX) and lithium aluminium hydride[20] are probably other examples, the respective nucleophilic species being R^- and AlH_4^-. More recently, evidence has been offered that the nonionic nucleophiles R_3N: and R_3P: participate in S_N2 reactions at S—S bonds. Jennen and Hens[21] and Krebs[22] formulate the reaction of molecular sulfur with tertiary amines as:

$$R_3N: + S_8 \longrightarrow R_3N^+-S-S_6-S^- \quad (20)$$

and Bartlett and Meguerian[23] obtained kinetic evidence that the reaction of sulfur with triphenylphosphine, to give triphenylphosphine sulfide, involves an initial rate-determining S_N2 heterolysis of S_8 [Reaction (21)], followed by a rapid sequence of comparable reactions typified by (22):

$$R_3P: + S_8 \longrightarrow R_3P^+-S-S_6-S^- \quad . . . . . (21)$$

$$R_3P^+-S-S-S_5S^- \longrightarrow R_3PS + R_3P^+-S-S_5-S^- \quad . . . . . (22)$$

The reaction of triphenylphosphine with allyl disulfide has also been interpreted[24] as a polar process [Reaction (23)], contrary to the free radical postulate of Schönberg and others[11,25]:

$$RS-SR \longrightarrow RS^+ + RS^- \xrightarrow{Ph_3P:} [Ph_3P-SR]^+\overset{-}{S}R \longrightarrow Ph_3PS + RSR \quad . . . . (23)$$

and a similar view is taken of the reaction of triethyl phosphite with diethyl disulfide[26]:

$$(EtO)_3P: + EtS-SEt \longrightarrow [EtS\cdot P^+(OEt)_3]S^-Et \longrightarrow EtS\cdot P:O(OEt)_2 + EtSEt \quad (24)$$

The relevance of Reactions (20) and (21) to the function of vulcanization accelerators and zinc salts in increasing the rate of sulfur-olefin reactions will be discussed elsewhere.

Electrophilic fission of S—S bonds, as is now envisaged in olefin sulfuration, is less well authenticated. One example is thought to be the acid-catalyzed interaction of alkyl disulfides with olefins to give bis monosulfides, as in the

chain sequence (25)–(28)[27]:

$$RS{-}SR + H^+ \longrightarrow [\overset{H}{RS{-}SR}]^+ \quad (25)$$

$$[\overset{H}{RS{-}SR}]^+ + CH_2{=}CH_2 \longrightarrow RS{-}CH_2{-}CH_2^+ + RSH \quad (26)$$

$$RS{-}CH_2{-}CH_2^+ + RS{-}SR \longrightarrow RS{-}CH_2{-}CH_2{-}SR + RS^+ \quad (27)$$

$$RS^+ + CH_2{=}CH_2 \longrightarrow RS{-}CH_2{-}CH_2^+ \quad (28)$$

To explain the formation of monosulfides as minor products when *strong* acids such as hydrofluoric acid are used, Reactions (29)–(31) are then postulated as an additional chain-initiation process:

$$CH_2{=}CH_2 + H^+ \longrightarrow CH_3{-}CH_2^+ \quad (29)$$

$$CH_3{-}CH_2^+ + RS{-}SR \longrightarrow [\overset{R}{RS{-}S{-}}CH_2{\cdot}CH_3]^+ \quad (30)$$

$$[\overset{R}{RS{-}S{-}}CH_2{\cdot}CH_3]^+ \longrightarrow RS{\cdot}CH_2{\cdot}CH_3 + RS^+ \quad (31)$$

Reactions comparable to (27) and (30)–(31) have been advanced to explain the formation of monosulfides from the thermal reaction of dialkyl disulfides with betaine ($Me_3N^+{\cdot}CH_2{\cdot}CO{\cdot}O^-$) which acts as a source of Me^+ cations [Reaction (32)][28]:

$$RS{-}SR + Me^+ \longrightarrow [\overset{Me}{RS{-}SR}]^+ \longrightarrow RSMe + RS^+ \quad (32)$$

Similarly, the fission of S—S bonds in carboxyl-substituted alkyl disulfides by dimethylformamide (B:) has been formulated as an acid-base catalyzed reaction[29]:

$$B{:}H^+ + RS{-}S{-}CH_2R' \longrightarrow \overset{H}{RS^+}{-}S{-}CH_2R' + B{:} \longrightarrow$$

$$RSH + {}^+S{-}CH_2R' \xrightarrow{B:} RSH + S{:}CHR' + B{:}H^+ \quad (33)$$

Interaction of S—S bonds with olefinic double bonds.—Reaction (6) has been formally represented as the dissociation of a polysulfide into free persulfenyl ions, which in the prevailing nonpolar medium must be associated either as an ion pair or as constituting a highly polarized molecule. Species of this kind have been postulated in other polar reactions in nonpolar solvents where solvation forces cannot provide the large amount of energy necessary for separation (as distinct from formation) of two unlike ions[30]. Polarization of S—S bonds in sulfur and polysulfide molecules will be promoted by the electron-donor activity of olefinic double bonds, just as this promotes complex formation with iodine[31], silver ions[31,32], and various metallic salts[32,33], cf.:

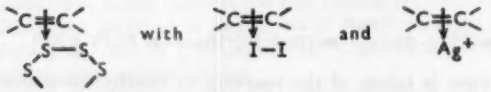

Such association is essentially similar to, although of a lower order than, the nucleophilic attack of tertiary amines[21,22] and triarylphosphines[23] on sulfur. A truer representation of Reactions (6) and (7) is therefore:

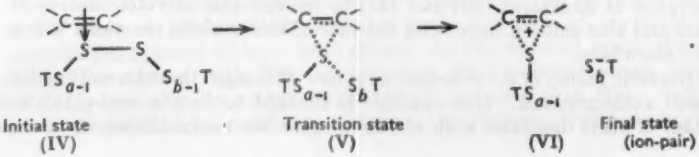

....(34)

The sulfuration process as represented by Reaction (34) is thus mechanistically analogous to other reactions involving the addition of electrophilic reagents to olefins in nonpolar media, e.g., halogen addition[34] and "allylic" chlorination[35], ozonolysis[36], and addition of sulfenyl halides[37]. The cationic moiety of (VI), formulated as a bridged persulfonium ion by analogy with comparable structures[38] and because of certain reactivity characteristics discussed below, appears to be the dominant intermediate in determining the course and products of the overall sulfuration process. The highly complex nature of the products[39] can be related logically to the various possibilities of reaction of this cation, viz., combination with the associated anion or with a sulfur molecule, and proton or hydride ion-exchange with an olefin molecule, the differences in product compositions in different olefinic systems reflecting changes in the relative importance of these competing reactions as detailed below.

The persulfenyl anion, TS_b^-, does not appear to participate in the olefinic sulfuration, although it may well facilitate the breaking of the S_8 ring, in keeping with the known ability of sulfenyl anions to induce S—S bond scission[19], and it will certainly engage in exchange reactions with the polysulfide products[19]. There is no evidence for the addition of this anion to an olefin, this being in accord with the fact that base-catalyzed addition of thiols to double bonds occurs only when the latter are activated by electron-attracting substituents (CO_2R, CHO, CN[40].

Sulfuration of 1-Octene.—2-Methylheptyl 2-octenyl sulfides (VII; $a \geqslant 1$), the cyclic compounds (VIII; a'' and $b \geqslant 1$), and the polymeric material (IX; a and $b \geqslant 0$; $n \geqslant 1$) are major products, and 1,2-epithio-octane (X) a minor product, of this reaction[39]. The formation of these compounds (which are not obviously related) and their derivation from common intermediates can be rationalized on the basis of the arguments developed in the last section, as indicated in the annexed reaction scheme, where R′ = C_6H_{13} and the numbers refer to reactions already designated.

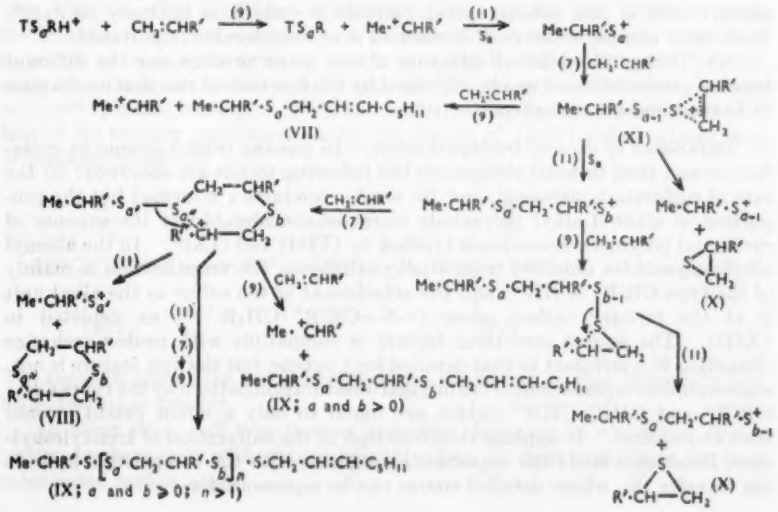

Important features of this scheme are:

(i) The reactions leading to the different products are the propagation steps in the basic chain mechanism (p. 1091), or kinetically equivalent variants which generate carbonium or persulfenium ionic-type intermediates in the product-forming reactions (to give VIII–X). This justifies kinetic analysis in terms of the basic mechanism, notwithstanding the complexity of the product[4].

(ii) The bridged persulfonium ion (XI) appears to react mainly (*a*) by combining with sulfur, to give subsequently (VIII), (IX), and (X), and (*b*) by transferring a proton to an olefin, thereby giving (VII). The effect of (*b*) is to cause the sulfur chain in (VII) to be attached to the secondary position of the alkyl unit and to the primary position in the alkenyl unit, as is found experimentally[39].

(iii) The unsaturation pattern in (VII) is that of an allyl sulfide. This strongly suggests that proton elimination occurs in a process specifically involving the bridged persulfonium unit and a β-CH_2 group (Reaction 35):

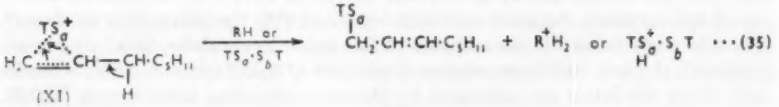

(XI)

rather than from the carbonium ion $TS_a—CH_2\cdot\overset{+}{C}H\cdot CH_2\cdot C_5H_{11}$, which would be expected to give at least a proportion of the more stable vinyl isomer, $TS_a—CH{:}CH\cdot CH_2\cdot C_5H_{11}$[39,41]. This mode of deprotonation and its structural consequences are also evident in the diisoprenoid system (p. 1100).

(iv) Hydride ion transfer (Reaction 8) appears not to occur to an appreciable extent. Its occurrence would generate the mesomeric cation

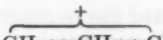

which should lead to a small but readily detectable amount of the 1-vinylhexyl sulfide structure, $CH_2{:}CH\cdot CH(C_5H_{11})\cdot S_a—$ in the alkenyl unit of the octenyl octyl polysulfide—which is contrary to fact[39]. With other olefins, however, this reaction is of considerable importance.

(v) Neither the detailed structure of any given product nor the different types of product formed can be explained by the free radical reaction mechanism of Farmer and his coworkers[1].

Sulfuration of di- and trialkylethylenes.—In passing from 1-octene to cyclohexene and then to trialkylethylenes the following trends are observed: (i) the rate of sulfuration increases[4], and (ii) similar products are formed but the proportion of alkenyl alkyl polysulfide increases considerably at the expense of cyclic and polymeric compounds typified by (VIII) and (IX)[39]. In the alkenyl alkyl polysulfides obtained from trialkylethylenes, the unsaturation is mainly of the type $CR'R''{:}CHR'''$, and the attachment of the sulfur to the alkyl unit is at the tertiary carbon atom $(—S—CR'R''\cdot CH_2R''')$[39], as depicted in (XIII). The second structural feature is compatible with proton-exchange (Reaction 9) equivalent to that detailed for 1-octene, but the first feature is not, since complete replacement of the original unsaturation pattern by the types $CH_2{:}CR'R''$ and $CHR'{:}CHR''$ (which are found to only a minor extent) would then be required. It appears therefore that in the sulfuration of trialkylethylenes, Reaction 9 is of little importance compared with the competitive hydride ion transfer (8), whose detailed course can be represented as:

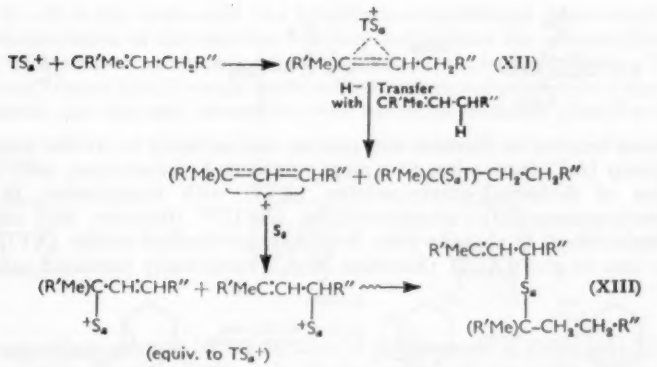

Olefins are known to participate in hydride ion transfers of this type[42], which will be promoted by alkyl substitution at the far side of the adjacent double bond owing to the greater resonance stabilization of the resultant allylic carbonium ion (cf. the comparable influence in free-radical olefin autoxidation[3]). Such substitution can thus be expected to facilitate the above sequence of reactions, and in doing so to repress relatively the alternative reactions of the bridged persulfonium ion involving proton transfer and addition of sulfur. The rate and product changes through the olefin series detailed above are, therefore, mutually consistent and understandable. In the case of the particular trialkylethylene, 2,6-dimethylocta-2,6-diene, there is a specific consequence of hydride-ion transfer (p. 1100).

One special feature of the hydride ion transfer represented above may be noted, viz., the attachment of the hydride ion to the least substituted carbon atom of the bridged persulfonium ion (XII), leading to the *tert*-alkylperthiolinkage in (XIII). The opening of the bridged persulfonium ion (XII) in this way, which in effect is contrary to Markownikoff's rule for polar addition of the electrophile TS_a^+ to a double bond, is unusual but not unique. The usual direction of opening of bridged 'onium ions (XIV; AX = NR_2, SR, or OH, etc.) by attack of a nucleophilic reagent Y^-, recognized in numerous reactions[38,43], is that leading to (XV), and is attributed[44] to the preferential formation of the tertiary carbonium ion by ring fission of (XIV) before attachment of the addendum Y^-:

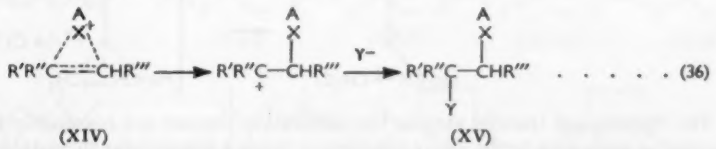

The reaction conditions are generally those conducive to this essentially S_N1 type, two-stage process.

An alternative, S_N2 type process is possible, however, in which ring fission occurs synchronously with nucleophilic attack by Y^- preferentially at the least substituted carbon atom:

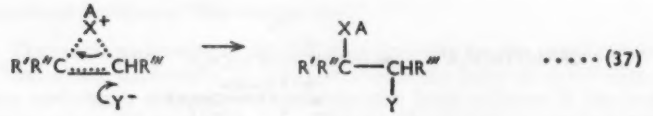

..... (37)

Reactions believed to illustrate this process, and certainly to involve migration of a group (AX) from a less to a more substituted carbon atom, are: (i) the reaction of 3-chloro-1-ethylpiperidine (XVI) with benzylamine to give 2-(benzylaminomethyl)-1-ethylpyrrolidine (XVII)[45] (Reaction 38); and (ii) the displacement of chlorine from 2-chloropropyl methyl sulfide (XVIII) by sulfite ions to give (XIX) (Reaction 39)[46]. Particularly pertinent examples

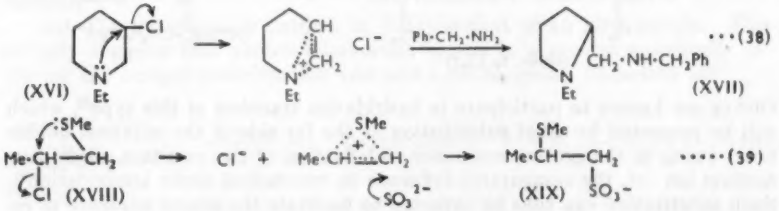

...(38)

.....(39)

are the reactions of chlorine and of bromine with propylene sulfide in anhydrous chloroform and carbon tetrachloride, which are formulated[47] as shown (for chlorine). It is to be noted that this series of reactions, in which opening of the episulfide ring occurs exclusively to give sulfur attachment at the more substituted carbon atom, proceeds in nonsolvating media where S_N2 type interaction of the postulated ionic intermediate will be favored, whereas ring opening in which a bridged sufonium ion is first converted into a much more labile carbonium ion will not.

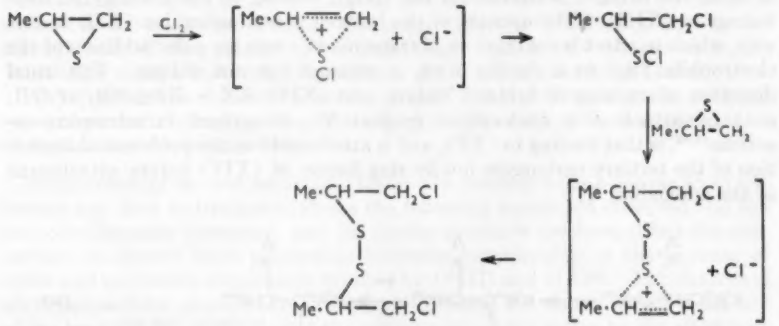

The hydride ion transfer step in the sulfuration process can reasonably be regarded as analogous to the above reactions in being a bimolecular substitution at the least substituted carbon atom of (XII) (Reaction 40):

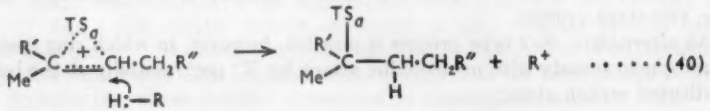

..... (40)

where H—R is the olefin and the hydride ion transferred is α-methylenic. This interpretation of the reaction not only rationalizes the present findings but allows apparently anomalous data in the literature to be understood. Thus, Bloomfield[48] found that the main product from the thermal reaction of 1-methylcyclohexene and diphenyl tetrasulfide was 1-methylcyclohexyl phenyl sulfide,

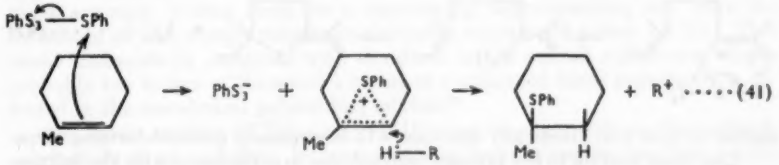

and was unable to account for the addition of the elements of PhSH, or addition in accord with Markownikoff's rule, having regard to the belief in the free radical nature of sulfuration processes then current[1]. The reaction appears now to be analogous to the reaction of a trialkylethylene with sulfur, with hydride ion transfer proceeding as specified above (Reaction 41).

Sulfuration of 2,6-dimethylocta-2,6-diene.—The products of this reaction are the triene (XX), a cyclic sulfide mixture, consisting mainly of (XXI) and (XXIII), with some (XXII); (XXIV) appears in greater amount at the expense of (XXIII) as reaction proceeds, and complex polysulfides whose composition also changes with reaction time[39]. In the early stages of reaction, there is a predominance of acyclic polysulfidic structures typified by (XXV) and (XXVI), but compounds containing cyclic sulfide units and having short sulfide crosslinks (S_1 or S_2) as in (XXVII) and (XXVIII) (a = 1 or 2, and the dotted lines represent alternative positions of the sulfur linkage and possible sites of unsaturation) are later formed to an increasing extent.

It was previously believed that the cyclic sulfides (XXI)–(XXIII) were primary products[49]. Thus, (XXIII) was thought to result from direct attack of sulfur at one double bond of the diene followed by cyclization of an intermediate perthiol (reaction 42). Oxidation of the perthiol to liberate hydrogen sulfide ($2R{\cdot}S_xH \xrightarrow{S} R{\cdot}S_{2x}{\cdot}R + H_2S$) which can then add in a polar manner to the diene to give a mono-olefinic tertiary thiol susceptible to intermolecular

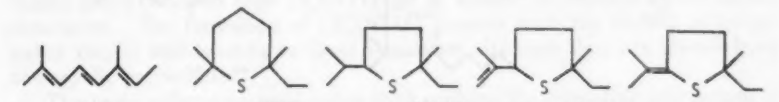

(XX) (XXI) (XXII) (XXIII) (XXIV)

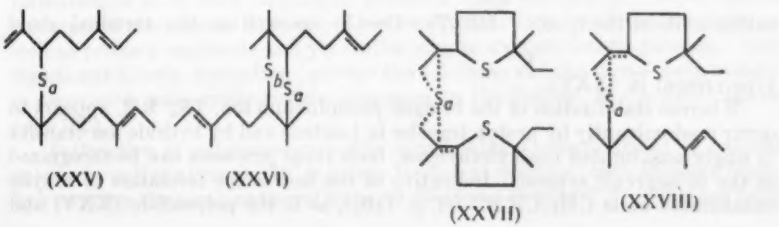

(XXV) (XXVI) (XXVII) (XXVIII)

addition was held to be the origin of the saturated sulfides (XXI) and (XXII). However, recent evidence does not accord with the participation of thiols as intermediates in these reactions[4], and it is now believed that the acyclic polysulfides are the sole primary products and that the cyclic sulfides, both free and combined in later formed polysulfides, arise wholly from secondary reactions

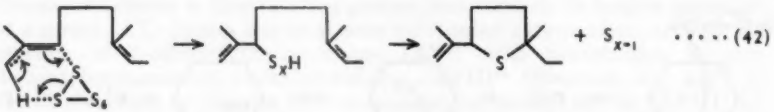

(42)

similar in type and kinetically equivalent to the primary product-forming steps.

Reactions leading to the primary polysulfides in accordance with the sulfuration mechanism now advanced are set out below. Only the more important possibilities for isomerism are given; it is to be understood that deprotonation

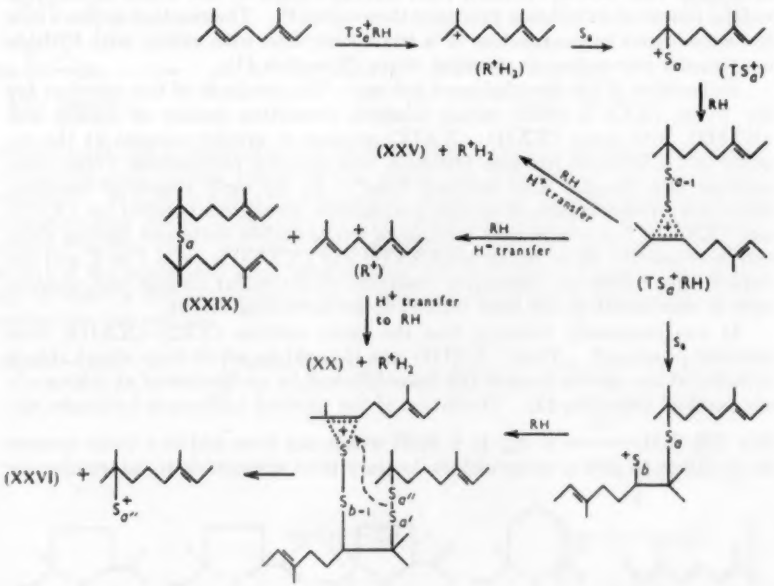

of the persulfonium ion, TS_a^+RH, for example, may lead to some unsaturated sulfide units of the type 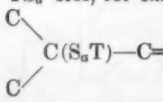 as well as the terminal vinyl type present in (XXV).

Whereas stabilization of the bridged persulfonium ion, TS_a^+RH, appears to occur predominantly by proton transfer in 1-octene and by hydride ion transfer in singly unsaturated trialkylethylenes, both these processes can be recognized in the di-isoprenic system. Indicative of the first is the formation of vinylic unsaturated units $CH_2{:}CR'R''$ (cf. p. 1101), as in the polysulfide (XXV) and

the derived cyclic sulfide (XXIII) (see below), while strong evidence for the second is the formation of the triene (XX). The latter feature further indicates an understandable difference in reactivity of the allylic carbonium ions formed by loss of a hydride ion from the structures $CMe_2{:}CH{\cdot}CH_2R$ and $CMe_2{:}CH{\cdot}CH_2{\cdot}CH_2{\cdot}CMe{:}CHMe$; in the first case, combination with sulfur ensues to give a persulfenium ion (p. 1096); in the second, the unsaturation pattern provides a strong driving force for a preferential deprotonation, and thus the formation of the highly resonance-stabilized conjugated triene (XX). This triene undoubtedly competes with the diene in the overall sulfuration and is probably the source of the small amount of conjugated diene unsaturation detected in the crosslinked polysulfidic mixture[39].

The cyclic sulfides (XXI) and (XXIII) can be derived from the primary polysulfides (and also from isomers resulting from initial protonation at the other double bond in the diene) by intramolecular reactions induced by, and involving, active intermediates analogous to those postulated for the primary sequence of reactions as exemplified in the annexed scheme. The allylic sulfide (XXIII) is known[39] to undergo a sulfur-catalyzed isomerization to the vinylic isomer (XXIV), and would be expected to undergo other reactions leading to

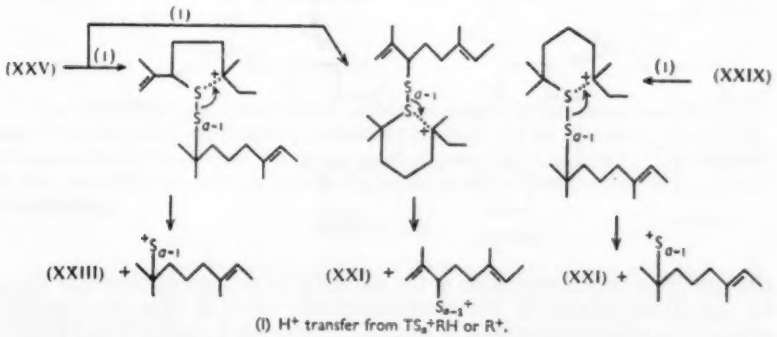

the saturated thiacyclopentane (XXII) and to polysulfidic-cyclic sulfide structures such as (XXVII) and (XXVIII): analogous reactions applied to crosslinked polysulfides of type (XXVI) lead to similar polysulfidic cyclic sulfide structures. The formation of (XXVIIb) accords with the finding of conjugated vinylic sulfide units in these structures although they are absent from the acyclic polysulfides[39].

The basic sulfuration mechanism thus explains the formation and nature of the numerous products detailed above. Conversely, it definitely implies the formation of a complex mixture of products which changes in composition as sulfuration proceeds as a result of successive reactions involving products as well as primary reactants and yet conforming to a single kinetic pattern. One significant kinetic distinction between the 1,5-diene and the mono-olefin system is associated with cyclic sulfide formation in the former, as discussed below (p. 1102).

Sulfuration of polyisoprenes.—The crosslinking (vulcanization) of natural rubber by sulfur alone at 140° is a very inefficient reaction; each effective crosslink requires the combination of some 40–60 atoms of sulfur[49,50]. This has been

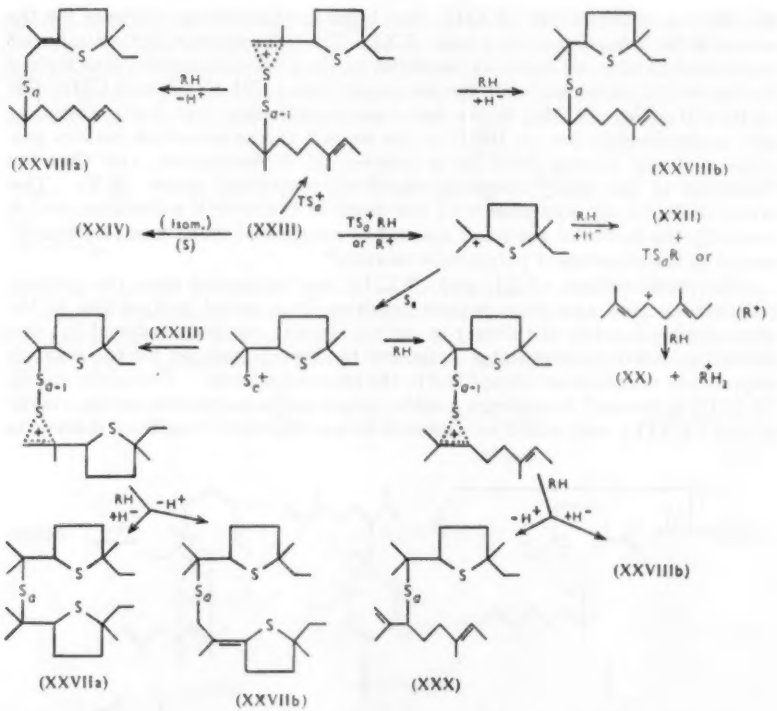

attributed[51] to the incorporation of the sulfur (*a*) in multiatom crosslinks (S_4–S_8), and (*b*) in cyclic sulfide (noncrosslinking) structures; to these must now be added (*c*) in adjacent crosslinks, as in (XXVI), which act physically as a single crosslink. The present work throws light on three aspects of this technologically important and hitherto little understood subject.

First, contrary to earlier ideas[49,51] no acceptable mechanism can be advanced to explain the formation of cyclic sulfide independently of, and yet competitive with, the formation of polysulfide. Secondly, although acyclic polysulfides are now held to be the precursors of the cyclic sulfides, this conversion does not result in the ultimate destruction of a crosslink (cf. Ref. 51); a persulfenium ion, TS_a^+, is concurrently produced and this forms a new crosslink by reaction with the polyisoprene. The inefficient use of sulfur in this sense is in fact more subtle than previously supposed[51]; it involves not the destruction of crosslinks, but the diversion of carbonium and bridged persulfonium ion intermediates (R^+ and TS_a^+RH, respectively) from reactions which directly create crosslinks to those giving cyclic sulfides. Thus, protonation of double bonds vicinal to sulfur attachments by the species R^+ or TS_a^+RH (p. 1101) leads to cyclic sulfide rather than to the crosslinking which directly follows the protonation of other double bonds. In the formation of cyclic sulfide, a carbonium ion is in effect transformed into a persulfenium ion without combination of sulfur. It is this transformation which is held responsible for the lower rate of sulfura-

tion of 1,5-dienes compared with comparable mono-olefins[4], and otherwise peculiar feature of these reactions.

The third point to be made is that the mechanism now proposed for cyclic sulfide formation in a di-isoprene does not readily explain an important feature of the polyisoprene system, viz., the formation of many *isolated* cyclic sulfide structures (i.e., not associated with crosslinking units), as inferred from the low crosslinking efficiency of vulcanization. Protonation at a double bond vicinal to a polysulfide linkage has been postulated as a prerequisite for formation of a cyclic sulfide. In a polymeric olefin such as natural rubber, random protonation would be expected greatly to outweigh this directed protonation, unless special factors come into play. Two possible factors are: (i) polarization of specific double bonds, creating an enhanced affinity for protons, by interaction with neighboring sulfur atoms (e.g., XXXI) (cf. p. 1094); (ii) preferred protonation of the polysulfidic chain, followed by attack of the resultant persulfonium ion (XXXII) at an adjacent double bond (Reaction 43) (cf. Ref. 27).

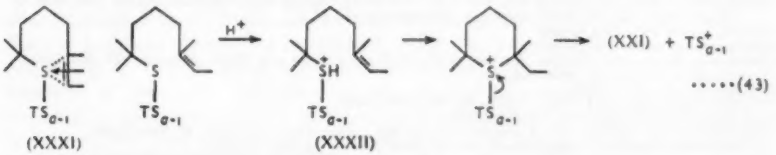

The effect on these reactions of the technologically important accelerators and other auxiliary vulcanizing agents for rubbers will be discussed elsewhere; a major effect is to increase the importance of persulfenyl anions (TS_b^-) relative to the persulfenium ions in promoting combination of sulfur and in favoring crosslinking.

SYNOPSIS

A polar chain mechanism is advanced for reaction of olefins with sulfur at about 140°; the initiation step is heterolysis of a polysulfide into polar persulfenyl intermediates, at variance with the current view that thermal dissociation of S—S bonds under these conditions occurs homolytically. A review of the literature indicates that, while such homolysis can be induced photochemically or by reaction with other free radicals, it does not occur simply on heating sulfur or organic di- and polysulfides at about 140°.

The reaction mechanism, which is consistent with kinetic data (Part X), accounts for the formation of complex polysulfides, including cyclic structures, from 1-octene, di- and trialkylethylenes and 2,6-dimethylocta-2,6-diene. The products are complex because a bridged persulfonium intermediate can lose a proton to, or gain a hydride ion from, the olefin (thereby becoming a polysulfide), or combine with sulfur to produce a persulfenium ion which ultimately forms a multibridged polysulfide derived from two or more olefin units. These competitive reactions occur in different proportions with different olefins—proton loss is more important than hydride ion gain in a 1-alkene, while the converse is true for trialkylethylenes.

Cyclic monsulfides formed from the 1,5-diene are essentially secondary products resulting from the first formed polysulfides which engage in proton-transfer processes to give sulfurated carbonium ion species: these effect intramolecular heterolysis of adjacent polysufide linkages, the processes being similar to those postulated for the initial reaction.

ACKNOWLEDGMENT

The work described in this paper and Papers VIII–X forms part of the program of research undertaken by the Board of the British Rubber Producers' Research Association.

REFERENCES

[1] Farmer and Shipley, *J. Polymer Sci.* 1, 293 (1946); Farmer and Shipley, *J. Chem. Soc.* **1947**, 1519; Farmer, *J. Soc. Chem. Ind.* **66**, 86 (1947); Bloomfield and Naylor, XIth Internat. Congr. Pure Appl. Chem., London, **1947**, Vol. II, p. 7.
[2] Flory, "Principles of Polymer Chemistry", Cornell Univ. Press, 1953, p. 454; Burnett, "Mechanism of Polymer Reactions", Interscience Publ. Inc., New York, 1954, p. 89; Grassie, "Chemistry of High Polymer Degradation Processes", Butterworths, London, 1956, p. 246.
[3] Bateman, *Quart. Rev.* **8**, 147 (1954).
[4] Ross, *J. Chem. Soc.* **1958**, 2856, preceding paper this issue.
[5] Pierson, Costanza, and Weinstein, *J. Polymer Sci.* **17**, 221 (1955); Costanza, Coleman, Pierson, Marvel, and King, *ibid.*, p. 319, and references therein; Dinaburg and Vansheidt, *J. Gen. Chem.* (*USSR*) **24**, 839 (1954) (English translation).
[6] Ayrey, Moore, and Watson, *J. Polymer Sci.* **19**, 1 (1956).
[7] Kharasch, Nudenberg, and Meltzer, *J. Org. Chem.* **18**, 1233 (1953); Birch, Cullum, and Dean, *J. Inst. Petroleum*, **39**, 206 (1953); Ferington and Tobolsky, *J. Amer. Chem. Soc.* **77**, 4510 (1955); Kern, *ibid.*, p. 1382; Otsu, *J. Polymer Sci.* **21**, 559 (1956).
[8] Rueggeberg, Cook, and Reid, *J. Org. Chem.* **13**, 110 (1948); Rueggeberg, Chernack, Rose, and Reid, *J. Amer. Chem. Soc.* **70**, 2292 (1948); cf. Kharasch et al., ref. 7.
[9] Lyons, *Nature* **162**, 1004 (1948).
[10] Lecher, *Science* **120**, 220 (1954).
[11] Schönberg, Rupp, and Gumlick, *Ber.* **66**, 1932 (1933); Schönberg and Rupp, *Naturwiss* **21**, 561 (1933); Koch, *J. Chem. Soc.* **1949**, 394, 401.
[12] Lecher, *Ber.* **53**, 577 (1920).
[13] Cutforth and Selwood, *J. Amer. Chem. Soc.* **70**, 278 (1948).
[14] See Gee, *Trans. Faraday Soc.* **48**, 515 (1952).
[15] Fairbrother, Gee, and Merrall, *J. Polymer Sci.* **16**, 459 (1955); Gee, *Sci. Progr.* **43**, 193 (1955).
[16] Gardner and Fraenkel, *J. Amer. Chem. Soc.* **76**, 5891 (1954); **78**, 3279 (1956).
[17] Tinyakova, Dolgoplosk, and Tikhomolova, *J. Gen. Chem.* (USSR) **25**, 1333 (1955) (English translation).
[18] Bartlett and Trifan, *J. Polymer Sci.* **20**, 457 (1956) and references therein; Kice, *J. Amer. Chem. Soc.* **76**, 6274 (1954); *J. Polymer Sci.* **19**, 123 (1956).
[19] Foss, *Acta Chem. Scand.* **4**, 404, (1950); Bertozzi, Davis, and Fettes, *J. Polymer Sci.* **19**, 17 (1956).
[20] Arnold, Lien, and Alm, *J. Amer. Chem. Soc.* **72**, 731 (1950); Bordwell and McKellin, *ibid.* **73**, 2251 (1951).
[21] Jennen and Hens, *Compt. Rend.* **242**, 786 (1956).
[22] Krebs, *Gummi u. Asbest*, **8**, 68 (1955); RUBBER CHEM. & TECHNOL. **30**, 962 (1957).
[23] Bartlett and Meguerian, *J. Amer. Chem. Soc.* **78**, 3710 (1956).
[24] Challenger and Greenwood, *J. Chem. Soc.*, **1950**, 26.
[25] Schönberg, *Ber.* **68**, 163 (1935).
[26] Jacobsen, Harvey, and Jensen, *J. Amer. Chem. Soc.* **77**, 6064 (1955).
[27] Lien, McCaulay, and Proell, General Papers, Division of Petroleum Chem., Amer. Chem. Soc. **1952**, No. 28, p. 169.
[28] Challenger, Taylor, and Taylor, *J. Chem. Soc.* **1942**, 48; Challenger, *Quart. Rev.* **9**, 255 (1955).
[29] Schöberl and Gräfje, *Naturwiss*, **43**, 445 (1956).
[30] Hughes, Ingold, Mok, Patai, and Pocker, *J. Chem. Soc.* **1957**, 1265 and references therein; Ingold, *Proc. Chem. Soc.* **1957**, 279.
[31] Evans, *J. Chem. Phys.* **24**, 1244 (1956) and references therein.
[32] Chatt, in "Cationic Polymerization", Ed. Plesch, Heffer, Cambridge, 1953, pp. 40 et seq.
[33] Douglas, "The Chemistry of the Co-ordination Compounds", Ed. Bailar, Reinhold Publ. Corp., New York, 1956, pp. 487 et seq.
[34] de la Mare, *Quart. Rev.* **3**, 126 (1949).
[35] Taft, *J. Amer. Chem. Soc.* **70**, 3364 (1948); Salomon, *Proc. Inst. Rubber Ind.* **3**, 176 (1956).
[36] See Waters, *Ann. Reports* **49**, 111 (1952).
[37] Hogg and Kharasch, *J. Amer. Chem. Soc.* **78**, 2728 (1956).
[38] Winstein and Grunwald, *J. Amer. Chem. Soc.* **70**, 828 (1948); Winstein and Ingraham, *ibid.* **74**, 1160 (1952).
[39] Bateman, Glazebrook, Moore, Porter, Ross, and Saville, *J. Chem. Soc.* **1958**, 2838; Bateman, Glazebrook, and Moore, *J. Chem. Soc.* **1958**, 2846.
[40] Schöberl and Wagner, "Methoden der Organischen Chemie", Houben-Weyl, Georg Tiheme, 1955, Vol. IX, pp. 123 et seq.
[41] Tarbell and McCall, *J. Amer. Chem. Soc.* **74**, 48 (1952); Tarbell and Lovett, *ibid.* **78**, 2259 (1956).
[42] Bartlett, Condon, and Schneider, *ibid.* **66**, 1531 (1944); Schneider and Kennedy, *ibid.* **73**, 5013, 5017, 5024 (1951); Moore and Waight, *J. Chem. Soc.* **1952**, 4237; Baddeley and Pickles, *J. Chem. Soc.* **1953**, 3726.
[43] Fuson, Price, and Burness, *J. Org. Chem.* **11**, 475 (1946); Kharasch and Buess, *J. Amer. Chem. Soc.* **71**, 2724 (1949); Davies and Savige, *J. Chem. Soc.* **1950**, 317; **1951**, 774; Kerwin, Ullyot, Fuson, and Zirkle, *J. Amer. Chem. Soc.* **69**, 2961 (1947).
[44] Alexander, "Ionic Organic Reactions", Wiley, New York, 1950, pp. 97 et seq.
[45] Reitsema, *J. Amer. Chem. Soc.* **71**, 2041 (1949).
[46] Marvel and Weil, *ibid.* **75**, 61 (1954).
[47] Stewart and Cordts, *ibid.* **74**, 5880 (1952).
[48] Bloomfield, *J. Chem. Soc.* **1947**, 1547.
[49] Bateman, Glazebrook, Moore, and Saville, Proc. Third Rubber Technol. Conf., London, **1954**, p. 298.
[50] Moore and Ross, unpublished work.
[51] Bloomfield, *J. Soc. Chem. Ind.* **68**, 66 (1949).

STABILITY OF HIGH POLYMER LATEXES AND THEIR ELECTROKINETIC POTENTIALS *

S. S. Voyutskiĭ and R. M. Panich

M. V. Lomonosov Institute of Fine Chemical Technology, Moscow, USSR

The stability of colloid systems is a central problem of colloid chemistry. Therefore, many papers have been devoted to studies of coagulation and to the development of criteria of stability for colloid systems. For a long time a prevalent opinion was that the stability of colloidal particles could be explained by the fact that like charge on the particles prevents agglomeration of particles which collide due to Brownian motion. This opinion was first expressed by Hardy[1] and later developed by Powis[2], Ellis[3] and a number of other scientists. According to this point of view, electrokinetic potential (ζ potential) is the measure of stability. However, after detailed investigation of coagulation phenomena and accumulation of experimental data the correctness of this point of view became less obvious, and the statement that the electrokinetic potential is a criterion of stability of colloidal systems underwent vigorous criticism.

The reasons for the measured values of electrokinetic potentials not always corresponding to the stability of certain systems are as follows: firstly, the exact determination of electrokinetic potential is work of great experimental difficulty which seems to some investigators insuperable. Some of these difficulties are (1) the necessity of performing the mocroelectrophoresis in a medium which has the same characteristics as the colloidal system under investigation, (2) the influence on electrophoresis of the simultaneously occurring electrolysis (3) the wash out of the boundary line between the solution and the colloidal system, and a number of others. In the case of microelectrophoresis, these difficulties are replaced by others, which are not less difficult to overcome.

Secondly, very great difficulties arise on calculation of electrokinetic potential using the experimentally determined electrophoretic mobility. Quite recently the question of which equation to use for calculation of the electrokinetic potential, the formula of Helmholz-Smoluchowsky[4] or the formula of Hückel[5], was raised. Thanks to the work of Henry[6] this question has been clarified. Furthermore, the question of values of viscosity and dielectric constant to use for calculation of electrokinetic potential was not solved[7,8] until recently. Therefore, the values of electrolkinetic potential which are given even in the latest papers, performed by taking into account all possible correction terms, have only relative meaning. Here also, a recent advance has been the accounting for the effect on determination of electrokinetic potential[9] of the conductivity of the particles of the disperse phase and the deformation of the double layer on electrophoresis (electrical relaxation).

Thirdly, other investigators are of the opinion that the electrokinetic potential cannot characterize the stability of colloids in general. Kargin believes molecular nonionic solvation of the products which form on the phase boundaries as a result of surface reactions to be the most important factor for the

* Translated for Rubber Chemistry and Technology from *Uspekhi Khimii*, Vol. 25, pages 57 to 90 (1956) by George Shkapenko and John C. Park.

stability of lyosols. Rebinder's theory is that mechanico-structural properties of gel-like films on the surface of particles mechanically prevent their drawing together. Naturally, neither of these factors can be characterized by electrokinetic potentials.

Deryagin believes that in the case of the absence of polymolecular layers strongly bound by molecular forces to the particle surface (lyophobic colloids) the splitting force, which determines the stability, is determined by the mutual deformation of the diffuse ionic atmosphere which surrounds the particles. However, according to Deryagin, the electrokinetic potential can be indicative of the stability of such a system only on condition that

$$\zeta \leqslant \zeta_c = \sqrt{\alpha \frac{A}{Dh}}$$

where ζ_c is the critical value of electrokinetic potential, α the coefficient of proportionality, A a constant which characterizes molecular interaction, D the dielectric constant and h the thickness of the diffuse double layer. The above expression, which is similar to the well known Euler-Korf criterion, is in good agreement with experiments concerning coagulation of sols and emulsions by electrolytes only in the zone near the isoelectric point, i.e., at relatively small values of the electrokinetic potential.

When the electrokinetic potential is greater than 100 mV, the repulsive forces between the particles no longer depend appreciably on electrokinetic potential and are determined only by composition and concentration of the coagulating electrolyte. With increased concentration and increase of the charge of counterion the diffuse double ionic layer contracts and the energy barrier disappears. In this case Deryagin's calculations lead to the following condition of coagulation:

$$C_e > 40 f(\beta) \frac{D^3 (kT)^5}{A^2 e^6 z^6}$$

where C_e is the counterion concentration in g ions/cm^3 corresponding to the threshold of coagulation, $f(\beta)$ is a multiplier depending on the value (β), i.e., the ratio of the charge of the ion with the same sign as the surface to the charge of the counterion (at $\beta = 1, f(\beta) = 1$), e is the electron charge, z is the counterion valency, k the Boltzmann constant, and T the absolute temperature.

In spite of the fact that many objections against the use of the electrokinetic potential as a criterion for stability of colloidal systems were fair, none of these objections completely abrogate this criterion. Actually, all of the experimental difficulties noted, keeping in mind modern techniques of electrophoresis, can be more or less overcome. Using some criteria, which were deduced from the theory of strong electrolytes by Debye and Hückel, the effect of such phenomena as electrical relaxation and electrophoretic retardation on electrokinetic potential can be correctly evaluated.

Finally, the last group of objections which maintain that the electrokinetic potential, in principle, cannot characterize the stability of colloidal systems, has significance only in the case of certain colloidal systems, namely:

1) Systems whose particle solvation is basically due to molecular (nonionic) solvation.

2) Systems whose particles have an absorption film with clearly expressed mechanico-structural properties (for example—foams).
3) Systems with very large charges on the particles.

A great number of lyosols do not fall in the classes which are listed above and for characterization of their stability the electrokinetic potential certainly can be used. Besides, it can be assumed that even in the case when the stability of the system under investigation is not solely determined by the energy barrier due to particles of the double electric layer, the determination of the electrokinetic potential can give much information toward an understanding of the reasons for stability of the system. To supplement this it is necessary to investigate also the molecular solvation of the particles and the presence on their surface of an elasto-viscous absorbed layer.

In connection with all that has been said about electrokinetic potential as a characteristic of stability of disperse systems, it is interesting to note the opinion of many investigators that, up to this time, electrophoresis has been the most important source of information about the stability of lyophobic colloids[9,10,11]. This explains the fact that the number of papers devoted to investigation of electrokinetic potentials of colloid particles has considerably increased of late. Pertinent investigations have been conducted to perfect the methods of electro-osmosis and electrophoresis, as well as to clarify the action of various factors on the electrokinetic potential of particles and establish the relation between this potential and the stability of colloids.

A number of papers of principal importance in the field of electrochemistry of high polymer dispersions should be especially noted. Beginning in 1936 papers by Kemp and Twiss[12], Hauser and Bender[11] Jordan[13] and Bowler[14] appeared which were devoted to the electrochemistry of natural latex. More recently papers concerning synthetic latex began to appear. In this connection the works of Maron and his collaborators in the United States[15,16] Voyutskiĭ and his collaborators in the USSR[17–19] and Munro and Sexsmith in Canada[20] should be mentioned.

Such an interest in the electrochemistry of aqueous dispersions of high polymers can be explained first of all by their great practical importance, and by the technologists' need for methods to control their mechanical stability. Besides that, the natural and synthetic latexes are especially suitable materials for the solution of very important theoretical questions about the relation between electrokinetic potential and colloid stability. This results from the following characteristics of these high polymer systems.

1. The chemical composition of the aqueous phase of relatively simple latexes and the hydrocarbon phase usually consist of chemically inert material. Therefore, it can hardly be expected that destruction of these systems would involve any chemical reactions on the surface of the particles except those well studied reactions in which a stabilizer takes part.

2. In these systems molecular solvation of particles which can influence the stability of a collodial system is of course absent since the hydrocarbon phase itself is poorly wet by the disperse water phase.

3. In dispersions of high polymers, according to our visualization, the mechanico-structural factor does not play an essential role. As will be further shown, it is established, at the present time, that latex globules, stabilized by soap, are covered by an emulsifier layer which is far from saturation. In this

condition the formation of a mechanically durable gel on the surface is hardly possible.

4. Latex particles have, as a rule, a spherical shape. This eliminates any effect of their surface topography on their interaction and therefore it can be assumed that in the collision of two globules an interaction of two ideal spheres takes place. All investigators come to this point of view in considering interaction between colloidal particles.

5. The dispersed phase of a latex is usually a dielectric which makes it possible to ignore the correction for particle conductivity in this case.

6. Mechanical properties of high polymers allow one to consider that latex globules are rigid particles. This considerably simplifies the treatment of experimental results, since liquid particles would deform under action of the motion of a surrounding liquid. On the other hand, the double layer on the boundary between two liquids arises in both phases and its part in the disperse phase leads to circulation in the droplet which can affect the electrophoretic mobility.

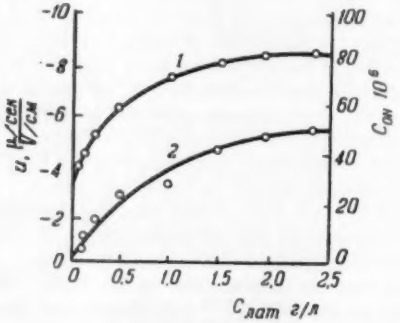

FIG. 1.—Effect of solids content (C_L) on the electrophoretic mobility (u) (Curve *1*) of the globules of natural latex and on the hydroxyl concentration (C_{OH}) in the serum (Curve *2*).

7. Finally, in coagulation of high polymer dispersions coalescence of individual particles does not occur. In the latex, immediately after coagulation, globules still are surrounded by very fine films of the medium. This fact allows use to neglect the total drop in potential (ζ-potential) which, as is well known, determines the stability against coalescence of the droplets in the emulsion. It also allows the assumption that, for latexes, the stability against coupling of particles which are at comparatively large distances can be well enough characterized by the value of the electrokinetic potential. This review summarizes the work done in the field of electrochemistry of high polymers and demonstrates that electrokinetic potential is a measure of the stability of such a system.

EFFECT OF DILUTION AND VARIATION OF STABILIZER CONTENT ON THE ELECTROKINETIC POTENTIAL OF LATEX GLOBULES

Hauser and Bender[11] investigated the effect of dilution on the electrophoretic mobility of globules in ammoniacal, natural latex containing 38% solids and having a pH of 9.9 using the method of micro electrophoresis. As can be seen

in Figure 1, dilution of the latex with water decreases the rate of electrophoresis slowly at first and then more rapidly. The curve given in the same graph showing the dependence of concentration of the hydroxide ion on dilution has the same shape. The authors believe that the decrease of electrophoretic mobility with dilution of the latex is caused not by desorption of stabilizer but by decrease of the pH value. This assumption, it appears, is confirmed by the fact that the electrophoretic mobility is directly proportional to the concentration of the hydroxyl ions in the latex. The last is clearly visible from Figure 2.

The insignificant effect of desorption of the stabilizer was confirmed also by direct experiments of the authors which showed that the rate of electrophoresis in latex diluted with a borate buffer with pH = 10.2 and having solids of 1.52, 0.38, 0.057 g/l proved to be practically the same, namely 3.2(μ/sec/V/cm).

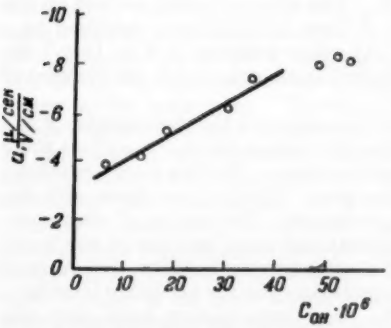

FIG. 2.—Relationship between the concentration of hydroxyl ions (C_{OH}) in the serum and electrophoretic mobility (u) of the globules of natural latex.

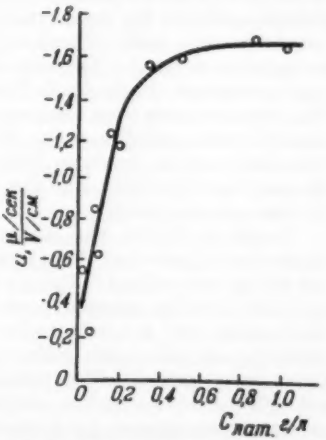

FIG. 3.—Relationship between the solids content (C_L) and electrophoretic mobility (u) of the globules of natural latex. Buffer ionic strength I =0.02 and pH =5.4–5.5.

Later, the effect of dilution on the electrophoretic mobility of globules of natural latex was investigated by Bowler[14]. He used the microelectrophoresis techniques of Abramson, Moyer and Gorin[21]. Freshly obtained latexes diluted with buffer solutions were investigated. The ionic strength of all solutions was 0.02; the value of pH was 5–5.5. The results of Bowler's experiments performed with two samples of natural latex are shown in Figure 3. The experimental points are located on one curve in which the mobility decreases rapidly when the concentration of solids becomes less than 0.5 g/l. The reason for this decrease, as the author believes, is the desorption of stabilizer.

When the concentration of solids in latex was higher than 1 g/l, it was difficult to measure the rate of electrophoresis of the individual latex particles. Bowler did not perform experiments involving solutions with higher concentrations. Obviously, there are some discrepancies between the data of Hauser and Bender and that of Bowler. However, it is possible to conclude that if desorption of the protein from the globules of the natural latex takes place, it occurs in any case at solids concentrations of the order of magnitude of 0.5 g/l and lower.

TABLE I

EFFECT OF TOTAL SOLIDS CONTENT ON MOBILITY OF TYPE II LATEX

Total solids, g/l	Average mobility, $\frac{\mu/sec}{V/cm}$
9.5	−5.58
14.7	−5.61
29.4	−5.44

Maron et al.[15] investigated the effect of solids content in synthetic latexes on the electrokinetic potential. These investigators used the macro electrophoresis method using conditions which insured accurate results. The current in the electrophoretic tube never exceeded 1.5mA. In calculating the electrophoretic mobility the mean values of the rates of ascending and descending boundaries were used. These were close in value when the latexes taken were not too concentrated. The value of pH in the latexes was maintained approximately constant (in the limits from 8.4 to 9.0) by addition of a borate buffer. The measurements were made at 30° C. The effect of solids content on the electrophoretic mobility of the globules of Type II GR-S latex stabilized by a fatty acid soap is shown in Table I. At solids contents of 9 to 15 g/l the electrophoretic mobility, and also the electrokinetic potential of the globules of this latex are constant.

Voyutskiĭ, Panich and Kal'yanova[18] investigated the dependence of the electrokinetic potential of synthetic latex globules on the solids content using the well known method of Rabinovich and Fodiman. For this work a synthetic latex stabilized by ammonium oleate was used. Dilution was made with distilled water, and a borate buffer was employed. The values of electroconductivity and pH of the buffer were maintained equal to those of the liquid under investigation. Observations of electrophoretic mobility were carried out with the aid of a reading microscope and always on the ascending boundary, as was recommended by Gerasinov[22]. Most investigators have used this method. The calculation of the electrokinetic potential was performed using the well known Helmholz-Smoluchovsky formula. The results obtained by the authors are given in Figure 4.

As one can see, the value of the electrokinetic potential of globules on dilu-

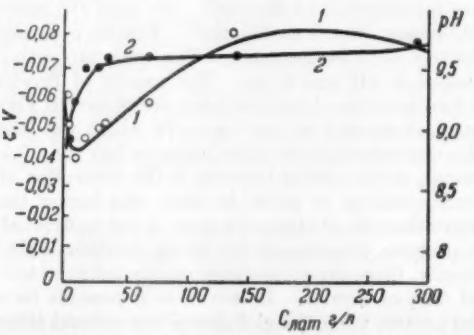

FIG. 4.—Effect of solids content (C_L) on the electrokinetic potential (ζ) of particles of synthetic latex and on pH of the serum: *1*.—curve of ζ; *2*.—curve of pH.

tion rises slightly at first then drops and finally increases somewhat again. The increase of the electrokinetic potential as dilution is begun can be explained by the decrease in absolute concentration of foreign electrolytes which are always present in the system. This of course must lead to broadening of the double electric layer. It is much more difficult to explain the decrease of electrokinetic potential on further dilution. The soap desorption at such relatively small dilutions, which was mentioned in connection with the desprotion of proteins, is scarcely probable. It is impossible to assume that the decrease of the electrokinetic potential is connected with conversion of the soap to an acid, since according to Figure 4 this decrease occurs in general at a constant value of pH. Probably, the decrease of electrokinetic potential is fictitious and is a result of the fact that the authors did not take the ionic strength variation on dilution into account in their calculations. Finally, the increase of the electrokinetic potential in the range of solids concentrations of 3.0–8.5 g/l can be explained by the continuing decrease of the ionic strength of the solution.

Munro and Sexsmith[20] studied the effect on the rate of electrophoresis of dilution of two synthetic latexes with double distilled water. One of these was stabilized by polyvinyl alcohol and gum tragacanth, and the other was made using a cationic soap as an emulsifier. Determination of electrophoretic mobility was carried out at 20° C using a modified Briggs' microphoretic method. The electro-conductivity of all solutions under investigation was brought always to the same value. The experiments showed that the electrophoretic mobility of the first latex in the range of solids concentrations from 0.1 to 1.4 g/l had a practically constant value of 2.6(μ/sec/V/cm). Such a constant electrophoretic mobility is explained by the nonionic character of one of the stabilizers—polyvinyl alcohol. The second latex demonstrated a slight decrease in electrophoretic mobility of from +7.4 to +6.1 (μ/sec/V/cm) when the solids content was decreased from 0.7 to 0.1 g/l. This was probably due to the desorption of the cationic active soap. The variation of electrokinetic potential upon dilution of the latex is closely related to the variation of electrokinetic potential of the latex globules as a function of the stabilizer content in the latex.

In order to determine the effect of removal of the natural protein stabilizer on electrokinetic mobility of globules of freshly prepared natural latex, Bowler[14] centrifuged a latex 8 times and after each centrifugation diluted the upper layer with a 3 per cent ammonia solution. In another case, dilutions were made with 2 per cent ammonium oleate solution. The resultant latexes were diluted with buffers of different pH but with the same ionic strength of 0.02. In these solutions the electrokinetic mobility of the globules was determined using the micro electrophoresis method. The results of Bowler's experiments are given in Figure 5.

Before washing, the latex had an isoelectric point at pH = 4.35. After treatment with ammonia the latex showed a considerably lower isoelectric point, of 3.86. Latex washed with a soap solution contained negatively charged particles at pH's extending down to pH = 3.5.

Maron et al.[15] studied the effect of creaming on the electrophoretic mobility of GR-S Type II synthetic latex stabilized by a fatty acid soap. The creaming in this case was promoted with the aid of sodium chloride followed by dilution of the creamed latex phase which was then brought to values of pH and ionic strength which were equal to those of the initial latex. Creaming increased the electrophoretic mobility of the latex particles by 8.5 per cent.

Very interesting results were obtained by Maron and Bowler[16] in an in-

vestigation of the effect of supplemental addition of a rosin soap (which was previously present in Type III GR-S latex as a stabilizer) on the electrophoretic mobility of its particles. A solution of a sodium or patassium soap of abietic acid was added to the latex and then disodium phosphate buffer to bring the ionic strength to 0.05. The electrophoretic mobility was measured with the aid of macroelectrophoresis at 30°, and the results are illustrated in Figure 6. The content of rosin soap in the original latex was 0.0021 mole/1. Therefore, in order to get the total amount of soap in the latex, 0.0021 should be added to the readings on the abscissa.

On addition of both soaps, the electrophoretic mobility did not increase but decreased linearly with the increase of the soap concentration. The soap concentration which corresponds to the beginning of micelle formation and at which the globules are covered by a monomolecular layer of soap was experimentally determined by Maron and Bowler to be 0.0136 mole/l of total soap, or 0.0115 mole/l if expressed in the amount of added soap (see Figure 6, line B). The

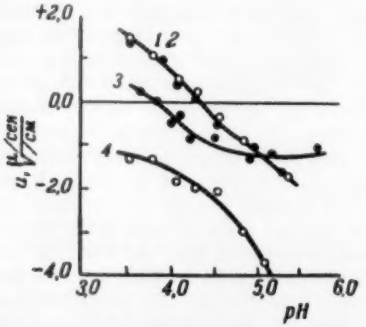

FIG. 5.—Effect of the removal of stabilizer on the electrophoretic mobility (u) of the globules of natural latex as a function of pH; temperature =30° C, I =0.02.

Curve *1*.—Unwashed latex No. 1.
Curve *2*.—Unwashed latex No. 2.
Curve *3*.—Washed latex No. 1 treated with ammonia.
Curve *4*.—Washed latex No. 2 washed with soap.

data corresponds to the case where no electrolyte is added to the soap solution. In the presence of Na_2HPO_4, the point corresponding to the formation of micelles and the covering of their surface with a monomolecular soap layer is, of course, somewhat displaced toward smaller concentrations of soap.

The straightness of the lines indicates that on formation of micelles, no great changes occur in the state of the soap absorbed on the surface of the globules and that the electrophoretic mobility does not depend on the aggregation of soap in solution. These data conflict with the observations of Munro and Sexsmith[20] which will be described later. It could be expected that the electrophoretic mobility should increase with increasing soap concentration in cases where the surface of the globules is not yet saturated. However, an inverse relationship, which is probably a result of the gradually increasing ionic strength and viscosity of the medium on addition of soap was found by Maron and Bowler. The effect of these two factors overbalances the increase of electrophoretic speed resulting from additional absorption of the soap.

As is visible from Figure 6, sodium ions decrease the electrophoretic mobility

more than potassium ions. This is probably due to the lower viscosity of the potassium rosin soap solution and the larger absorptive power of the sodium ion. The larger value for the electrokinetic potential of globules of a latex stabilized by potassium soaps in comparison with one stabilized with sodium soaps is in complete agreement with the experimental fact that potassium soaps are better emulsifiers than sodium soaps[23].

The data of Maron and Bowler which shows that the maximum electrophoretic mobility and hence the maximum electrokinetic potential correspond to incomplete saturation of the adsorption layer on the surface of the latex particles and that both of these values decrease on complete saturation of the layer does not conflict with the fact that the electrokinetic potential is a measure of the stability of colloidal and microheterogenic systems. As is well known, the stabilizing effect of soaps and albumin increases at first on increasing their concentration, and then after reaching a maximum begins to decrease. This phenomenon can also be explained by the fact that at high concentrations of stabilizer, a saturated fragile adsorption layer forms which, when damaged,

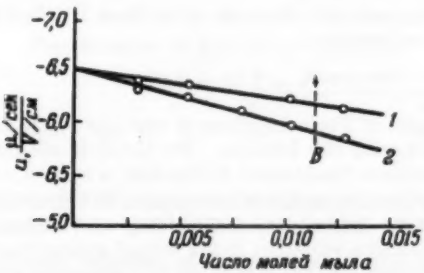

FIG. 6.—Effect of soap addition on the electrophoretic mobility (u) of globules of latex. Curve *1*.—potassium soap. Curve *2*.—sodium soap.

cannot be reestablished as rapidly as in the case of nonsaturated easily movable adsorption layers[24]. However, the same phenomenon can also be explained by the decrease of the electrolkinetic potential of the globules as a result of the increasing ionic strength caused by the increasing content of ionic stabilizer. Further investigation should show how universal this last explanation is. At very high concentrations of emulsifier the electrokinetic potential of latex globules, as well as the drops of an emulsion, can have significant effects on mechanical stability of the system owing to the fact that in this condition compact, possibly polymolecular gel-like layers, which are very durable, can be formed on the interphase surface.

EFFECT OF TEMPERATURE ON THE ELECTROKINETIC POTENTIAL OF LATEX GLOBULES

The temperature effect on the electrophoresis of colloidal systems in general and latexes in particular has not been adequately studied. Only in the papers of Maron and his collaborators[15,16], mentioned above, was the effect of temperature on the rate of electrophoresis investigated for Type II GR-S latex, stabilized by a fatty acid soap, and for Type III GR-S latex, stabilized by a rosin soap. The effect of temperature on the electrophoretic mobility of globules of the

TABLE II

ELECTROPHORETIC MOBILITY OF GLOBULES OF TYPE II LATEX AS A FUNCTION OF TEMPERATURE

Temperature in ° C	Electrophoretic mobility in $\frac{\mu/sec}{V/cm.}$	
	Experijentally found	Calculated
1	−2.54	−2.51
20	−4.48	−4.54
30	−5.62	−5.61
35	−6.13	−6.15

Type II latex with buffers was investigated at pH = 7.7–9.9 and at an ionic strength of 0.144. The results of these experiment are given in Table II.

The temperature effect on the rate of electrophoresis in the case of Type III latexes with phosphate buffers at various ionic strengths but with pH values in the range of 8.8–9.2 is shown in Figure 7. As is visible, the electrophoretic mobility is a linear function of the temperature. The effect of temperature on the rate of electrophoresis in the case of the Type II GR-S latex can be well represented by the expression

$$u = 2.40 + 0.107t$$

In the last column of Table II values of mobility of the globules are given which are calculated using this formula. For the Type III GR-S latex, Maron and others give the more complicated expression: $u = 2.32 - 365\ I^4 + [0.102 + (0.0092/\sqrt{I})]t$ where the mobility is expressed as a function of temperature t, and ionic strength I. The variation of mobility with temperature in Maron's experiments amounts to a variation in the rate of approximately two per cent per degree in comparison with the rate at 25° C. Since this value is of the same order of magnitude as the variation of the mobility with temperature for ions[27,26], it is possible to conclude that the variation of the mobility of the globules of the latex with temperature is a result of variation of the viscosity of the medium.

However, a precise calculation which was carried out taking into account

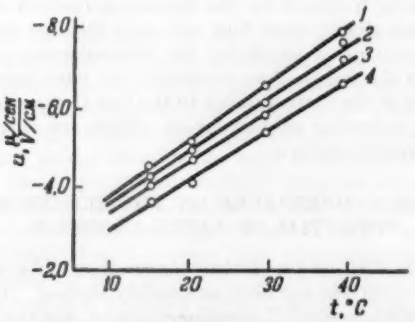

FIG. 7.—Effect of temperature (t) on the electrophoretic mobility (u) of the globules of Type III latex.

Curve *1*, I=0.05. Curve *3*, I=0.15.
Curve *2*, I=0.1. Curve *4*, I=0.2.

the variation of the viscosity of the interglobular liquid, showed that the electrokinetic potential itself is slightly increased when the temperature is raised. In the case of Type III latex the increase is approximately 0.3 per cent per degree in comparison with the potential at 25° C. Such an increase can be explained, from our point of view, only by an increase in the thickness of the diffuse part of the double electric layer due to the more intense thermal motion of the antiions. Desorption of the stabilizer molecules from the surface of the globules, which can occur with increasing temperature and which could lead to a lowering in the mobility of the latex particles, is obviously negligible. The temperature effect on electrokinetic potential shows that on heating, the stability of synthetic latexes should increase if this potential is really a measure of the stability of the colloidal system. This is completely confirmed by experiment. Firstly, synthetic latexes, stabilized by soaps, withstand heating to the boiling point. Secondly, as indicated by Maron and Bowler[16], more electrolyte is required for coagulation of a hot latex than for coagulation of a cool latex.

TABLE III

EFFECT OF STORAGE ON MECHANICAL STABILITY

Natural rubber, 61.5% solids; 0.7% NH_3

	Storage period	
	30 day	90 day
Mech. stability, sec.	450	810
KOH number	0.59	0.66

EFFECT OF THE LENGTH OF STORAGE ON THE ELECTROKINETIC POTENTIAL OF LATEX GLOBULES

Bowler[14] investigated variation of electrophoretic mobility of particles of freshly prepared natural latex which had been concentrated and stored. As was indicated, this investigator used microelectrophoresis and the experiments were performed so that, in the case of latex concentrates which were stored for different amounts of time, determination of the electrophoretic mobility was made at different pH. For this purpose, aqueous latex solutions or their concentrates were diluted with acetate or phosphate buffers adding such amounts of HCl or NaOH as were necessary. Bowler's experiments showed that the electrophoretic mobility of the globules increased with concentration and with storage of the concentrates. This increase is especially remarkable at high values of pH. The variation in mechanical stability and KOH number upon storage of concentrated, natural latex is illustrated in Table III.

It can be seen that storage of natural latex concentrate increases its mechanical stability. Bowler explains this increase of stability and electrophoretic mobility by hydrolysis of the esters of high molecular weight fatty acids followed by formation of ammonia soaps. The soap anions carrying a negative charge, when adsorbed on uncovered parts of the latex globules, displace the proteins which are present on their surface or react with them to form a soap-protein complex. All of this increases the stability of the latex and the electrophoretic mobility of its particles. The increase in mobility becomes less marked at lower pH in the range where, according to Bowler, the soaps are not too easily adsorbed.

The explanation given for the increase in the stability of natural latex with time coincides with the opinion of Baker[28] that splitting of protein-lipoid com-

plexes takes place on storage to liberate fatty acids which accumulate as ammonium soaps at the rubber-water interface.

There are no investigations on the variation of the electrokinetic potential of globules of synthetic latexes as a function of the length of storage. Let us note only that, according to the data of S. L. Tolmud et al. on storage of synthetic latexes, the soap from the surface of the globules goes into the water phase. This, of course, can promote a lowering in the electrophoretic rate of the latex globules and lead to a decrease in the stability.

VARIATION OF ELECTROKINETIC POTENTIAL AS A FUNCTION OF pH OF THE LATEX

The question of the effect of pH on the electrokinetic potential of emulsions and dispersions of high polymers has attracted attention of physical chemists for a long time. Ellis[29] showed that the electric charge on globules of diluted emulsions, which do not contain a special stabilizer, arises from adsorption of

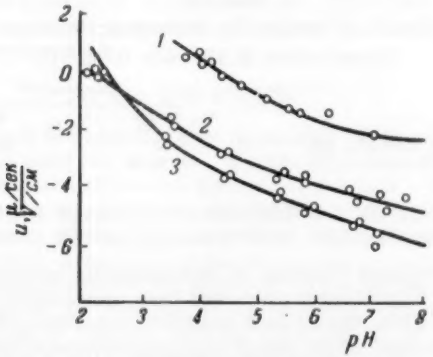

FIG. 8.—Effect of pH on the electrophoretic mobility (u) of various components of natural latex: $I = 0.01$.

Curve *1*.—protein. Curve *2*.—resins. Curve *3*.—rubber hydrocarbon.

hydroxyl ions on the surface. According to Ellis, the electrokinetic potential of droplets of a diluted oil emulsion has a negative value in basic as well as in acidic media. However, the data of older investigations should be noted with some care since at that time the techniques of electrophoretic measurements were not perfected and the effects of ionic strength of solutions, electrophoretic retardment, electrical relaxation and a series of other factors on electrophoresis were not taken into account; these essentially influence the results in determination of electrokinetic potential.

In 1936, Kemp and Twiss[12] investigated all of the factors mentioned above. They studied the effect of pH on the electrokinetic mobility of model systems; one being an emulsion of pure rubber hydrocarbon, another was a suspension of silica particles on the surface of which rubber proteins were adsorbed. The third system was a dispersion of rubber resin. These proteins and resins were obtained from natural latex. The data illustrating the variation of the electrophoretic mobility of the particles in the various systems as a function of pH are given in Figure 8.

With decreasing pH, the electrophoretic mobility of rubber hydrocarbon and of resin decreases to zero at pH = 2.4 and 2.1, respectively. The reason for this, according to the author's belief, is the adsorption of hydrogen ions and a decrease in the ionization of the resin acids. For the proteins the isoelectric point was obtained at pH = 4.4. On further decrease of pH the charge becomes positive and its absolute value begins to increase.

The results of experiments involving model systems were compared by Kemp and Twiss with the mobility of globules of latices of various concentrations as a function of pH at an ionic strength of 0.01. The results of these last experiments are illustrated in Figure 9. As is visible, the electrophoretic mobility increases with increase of pH and decrease of latex concentration. In comparing Figures 8 and 9 it becomes apparent that in basic media at low concentrations, the mobility of latex globules is comparable to the mobility of particles of pure rubber hydrocarbon. This can be explained by the fact that

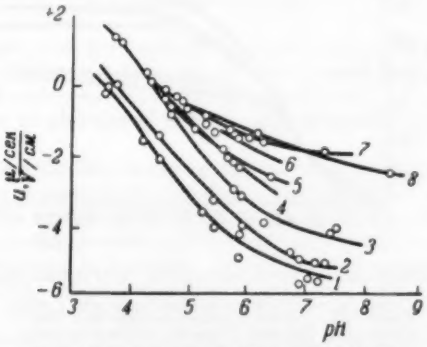

FIG. 9.—Effect of pH on the electrophoretic mobility (u) of the globules of natural latex: $I = 0.01$ (at various solids contents).

Curve 1. 0.016 g/l. Curve 5. 39.1 g/l.
Curve 2. 0.98 g/l. Curve 6. 67.6 g/l.
Curve 3. 3.9 g/l. Curve 7. 89.8 g/l.
Curve 4. 11.8 g/l. Curve 8. 195 g/l.

under such conditions it is virtually impossible for the proteins and resins to be adsorbed due to the low concentration of the solution and to their good solubility in a basic medium. Kemp and Twiss showed that the fractions of the rubber-globule surface covered with protein and with rubber resin vary with latex-dilution and the pH of the serum. Such a conclusion is in good agreement with the data of Limburg[30] who investigated the relationship between emulsifying power of gelatin as a function of pH and established that the gelatin concentration at which complete saturation of the layer around the oil droplets occurs increases with increasing pH.

The effect of pH on the electrophoretic mobility of globules of natural latex was investigated by Jordan[13]. This investigator employed the method of microelectrophoresis and applied it to studies of diluted latexes containing 0.22 g/l of rubber. Figure 10 shows the effect of pH on the electrophoretic mobility of a latex solution diluted with buffers of various ionic strength containing mono- or bivalent cations in combination with a monovalent anion.

These data enable us to draw the following conclusions:

1. In solutions of constant ionic strength, the electrophoretic mobility of the globules increases as pH increases to a value of 8. On further increase of pH, the mobility remains practically constant.

2. The globules of a latex in diluted solutions of potassium or calcium salts of mono basic acids are negatively charged at pH above 4.2. However, at the same pH and ionic strength, the electrophoretic mobility and the electrokinetic potential are considerably lower in calcium buffer solutions than in those of potassium. This indicates a strong adsorption of bivalent calcium ions by latex globules and suggests an explanation for the well known destabilizing effect of calcium salts on latex.

3. At constant values of pH, as calculation based on the curves of the Figure shows, the electrokinetic mobility of latex globules in potassium buffers is inversely proportional to the square root of the ionic strength.

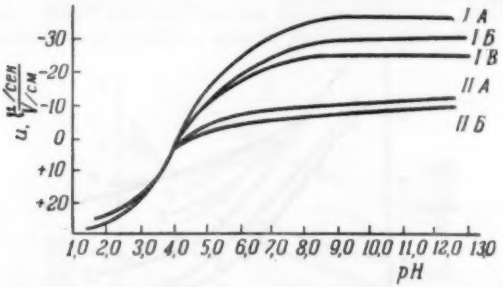

FIG. 10.—Effect of pH on electrophoretic mobility (u) of globules of natural latex.

Curve *1A.*—globules in potassium buffer with $I = 0.05$.
Curve *1B.*—globules in potassium buffer with $I = 0.1$.
Curve *1C.* globules in potassium buffer with $I = 0.2$.
Curve *IIA.*—globules in calcium buffer with $I = 0.05$.
Curve *IIB.*—globules in calcium buffer with $I = 0.1$.

Bowler[14], using the method of microelectrophoresis, investigated the effect of pH on the electrophoretic mobility of globules of freshly prepared Hevea latex. For the experiment, solutions made by dilution of the latex by buffers of constant ionic strength of 0.02 were used. A limitation of this work appears to be the narrow range of pH in which the variation of electrophoretic mobility was investigated*. The results obtained by him are given in Figure 11. Experiments performed with latexes which were collected in different seasons (February and April) were similar and indicated no effect of seasonal variation on mobility. The curves for electrophoretic mobility are similar to those obtained for proteins.

As was shown by Belgrave[21], on acidifying natural latex under certain conditions, its globules change their electric charge to the opposite one and so a latex can be obtained with positively charged particles. The reason usually advanced for this was the amphoteric character of the protein stabilizer whose molecules have two functional groups: amino—which causes the positive charge of the globules in an acidic medium, and carboxylic—which provides the negative charge for globules in a basic medium. However, the investigation

* Editor's Note. The object of these mobility investigations was to determine the isoelectric point as a measure of clonal variation. The pH range was fully adequate for this purpose.

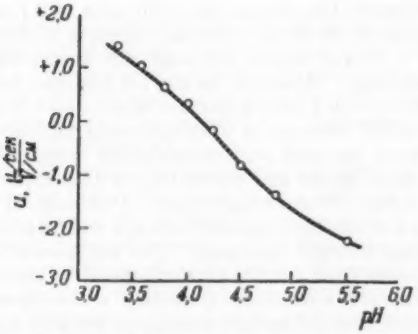

FIG. 11.—Effect of pH on the electrokinetic mobility (u) of the globules of natural latex. Temperature = 30° C, I = 0.02.

by Voyutskiĭ, Panich, and Kal'yanova[17–19] showed that particles of synthetic latex stabilized by soaps, the molecules of which have only one carboxylic group, also have the ability to reverse charge on addition of acid. The question of change in charge of globules of natural latex is complicated and requires further investigation.

Methods for reversing the charge of natural latex are described in detail by Sarrut[32]. In the process of charge reversal, the latex goes through the isoelectric state and the system can coagulate. In order to avoid this the acid should be added as fast as possible and it is also expedient to add a protective colloid, for example casein, to the latex. Fullerton[33], who studied the relationship between stability, concentration and charge, was unable to get a stable latex of more than 15 per cent solids with positively charged particles. However, Rhodes and Sekar[34] succeeded in obtaining a stable natural latex containing 30 per cent solids and with positively charged globules.

Maron and others[15] also investigated the effect of pH on the electrophoretic mobility of globules of Type II GR-S latex stabilized by a fatty acid soap. The investigation was performed with the aid of macroelectrophoresis at 30° at constant ionic strength of 0.150. The pH was controlled by addition of NaOH or HCl to the solutions of disodium phosphate used. The results obtained are illustrated in Figure 12.

As is evident, the relationship between electrokinetic mobility and pH is expressed by a broken line. If the second part of the curve is extrapolated to

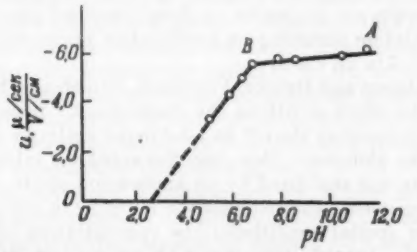

FIG. 12.—Effect of pH on the electrophoretic mobility (u) of the globules of Type II GR-S latex. Temperature = 30° C, I = 0.150.

zero mobility, it intersects the abscissa at a pH value of 2.7 which corresponds to the isoelectric point of the latex at an ionic strength of 0.150. The authors believe that at pH = 10 and higher, the emulsifier is present in the latex entirely as the sodium soap. However, as the pH becomes lower than 10, the soap is gradually transformed into a mixture of soap and fatty acid. This is accompanied by gradual decrease of electrophoretic mobility of the globules (AB in Figure 12) since the fatty acid molecules are comparatively poorly dissociated. Besides that, Maron and others believe that fatty acids are not adsorbed as strongly as the corresponding soaps. This point of view is doubtful. The fatty acid, as a less soluble compound, always will be adsorbed on the surface of the rubber more strongly than soap. The well known fact that acidification of latexes decreases their surface tension should be explained not by dissolution of particles of fatty acid formed from soap, as is supposed by Maron and others, but by the fact, that the surface activity of the acid is greater than that of the soap. At pH = 6.9, according to Maron and others, most of the soap contained in latex is changed into acid. Upon further lowering of pH, all the

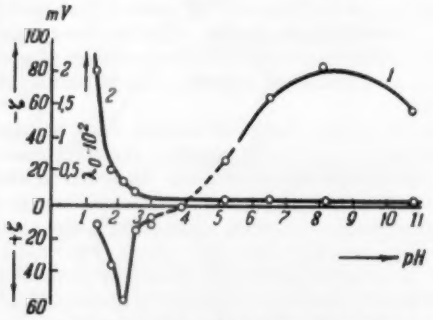

FIG. 13.—Variation of electrokinetic potential (ζ) (Curve *1*) and specific conductivity (λ_s) (Curve *2*) as a function of pH of the latex.

soap is transformed into an acid, the electric charge and the mobility of the particles decrease rapidly and the system becomes unstable and coagulates. For coagulation of the latex is it not necessary to bring the charge or mobility to zero, but only to lower them to a low critical value which lies at a pH of of about 5 at $I = 0.150$.

In another paper Maron and Bowler[16] investigated the effect of pH on the electrophoretic mobility of latex stabilized by rosin soap at four different ionic strengths. The results are analogous to those described above. It is remarkable that the coagulation occurring on acidification prevented lowering the pH of the latex below 5.5 in all cases.

In contrast to Maron and Bowler, Voyutskiĭ, Panich and Kal'yanova[19], who also investigated the effect of pH on the electrokinetic potential of synthetic latexes, succeeded in lowering the pH to 1.5-3.0 and getting a reversal of charge on the surface of the globules. However, the synthetic latex which was used in these experiments was stabilized by an ammonium oleate, which is not amphoteric. The experiments showed that the lowering of pH and reversion are possible only under special conditions; low concentration of latex and rapid introduction of acid. Introduction of a 0.1*N* solution of HCl into latex containing 28 per cent solids always led to immediate and complete coagulation.

However, if HCl was introduced into latex diluted so that it contained only 2–4 per cent solids, coagulation was not observed at all or occurred only partially. For establishing the values of electrokinetic potential of the latex on variation of its pH, Voyutskiĭ, Panich and Kal'yanova used the macroelectrophoretic method, which they also used previously[17,35]. The results obtained by these authors are illustrated in Figure 13.

On lowering of pH, a small increase of the absolute value of the negative electrokinetic potential takes place first then a decrease occurs. A zone in which the determination of the electrokinetic potential is impossible follows which is due to instability of the latex. After this zone, on addition of large quantities of acid, the particles show a positive potential, the value of which again increases on addition of acid and then decreases. Since the negative charge of the latex particles on acidification becomes positive, an isoelectric point should exist for the latex. This point was impossible to find by the method of electrophoresis because of coagulation of the latex. Therefore, it was found by determination of the pH corresponding to the maximum coagulation. It turned out that the isoelectric point of the latex under investigation occurred at pH = 3.9. Thus, Voyutskiĭ, Panich and Kal'yanova showed that on acidification of synthetic latexes which are stabilized by soaps, destabilization occurs at high latex concentrations when the conditions for coagulation are the most favorable.

On acidifying emulsions with low solids contents, the collisions are infrequent and the system does not coagulate so that the charge on the globules can be reversed. The reason for the last phenomenon consists, probably, in adsorption of positive hydrogen ions by the globules. As is well known, the hydrogen ion is highly adsorbable and in many cases can be a stabilizer. There are indications in the literature of the possibility of reversing the charge of particles of some colloids and emulsions of rubber particles, which were initially stabilized by hydroxyl ions[12], by adsorption of hydrogen ions. The presence of two extremes on the curve expressing the dependence of the electrokinetic potential on pH (Figure 13) can be explained by the contraction of the double electric layer and by decrease in the absolute value of the electrokinetic potential at high concentrations of base or acid.

Similar phenomena for diluted emulsions of mineral oil have been observed previously[11,29,30,36]. The positive electrokinetic potential in acid media is considerably smaller in absolute value than the negative potential in basic media. This is in good agreement with the fact that a latex of reversed charge is less stable than it was initially. The reason for the decreased stability of the latex with positively charged globules is probably connected with the fact that, in this case, a less active stabilizer is present. The fact that on the right side of the isoelectric point the electrokinetic potential curve slopes more than on the left side of this point can probably be explained by the nature of the stabilizer. However, the lowering of the electrokinetic potential in strongly acidic media as well as the smaller experimental value of this potential in an acidic zone than in a basic one, can also be explained by increased ionic strength of the solution due to addition of considerable quantities of HCl.

In the recently published investigations by Munro and Sexsmith[20], the effect of pH on the electrophoretic mobility of globules of three synthetic latexes stabilized by nonionic polyvinyl alcohol, by anionic gum arabic, and by cationic active soap, is described. The determination of the electrophoretic mobility was performed using the microelectrophoretic method. In order to bring the

pH to the desired value, various quantities of HCl, NaCl or NaOH were added to the latexes after dilution. The results of the measurements performed by Munro and Sexsmith are illustrated in Figure 14.

In the case of the nonionic stabilizer, the electrophoretic mobility of the latex globules is practically independent of pH. The light negative charge which the particles have can be explained in this case by adsorption by the globules of negative ions as, for example, Cl^- ions or by chemical reactions which take place in the system on polymerization. Particularly, the authors believe that oxidation of alcoholic or other groups of stabilizers by peroxides used as initiators in the polymerization reaction can lead to the formation, on the molecule, of a carboxylic group and thus cause the negative charge on the globules. A similar explanation of charge on a lecithin dispersion was sug-

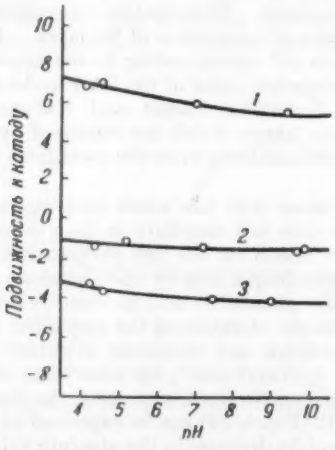

FIG. 14.—Effect of pH on the electrophoretic mobility of the globules of synthetic latexes.

Curve *1*.—Latex containing cationic soap as a stabilizer.
Curve *2*.—Latex containing nonionic stabilizer-polyvinyl alcohol.
Curve *3*.—Latex containing anionic stabilizer-gum arabic.

gested by Price and Lewis[37]. These authors believe that the total charge of the particle is the result of two independent phenomena—adsorption of hydroxyl ions on the surface of the fatty portions of the particles and ionization of the amphoteric groups.

In the case where an anionic stabilizer such as gum arabic, which generally contains arabinic acid, was used, an increase of pH increased the electrophoretic mobility to a certain value and then it became constant. This agrees with the observations of Maron and others.

Finally, in the case of the cationic stabilizer, as could be expected, an inverse dependence was observed—the electrophoretic mobility decreased with increasing pH.

According to Munro and Sexsmith it is essential, that the cationic soap impart to the particles considerably greater electrophoretic mobility than an anionic soap. This obviously is stipulated by the fact that quaternary ammonium compounds, such as the cationic soaps which were used by the authors,

are capable of strong ionization; whereas, the long chain organic acids are weakly dissociated.

DEPENDENCE OF ELECTROKINETIC POTENTIAL ON THE ELECTROLYTE CONTENT IN LATEX

Effect of electrolytes on electrokinetic potential of particles and their stability has been studied by a number of investigators[2,30,38] of very dilute emulsions of oils in water. There is little information about the action of electrolytes on the electrokinetic potential of droplets in the case of concentrated emulsions containing stabilizers. However, there are reasons for thinking that alkalis and their salts have the same action on the electrokinetic potential of emulsion droplets stabilized by sodium oleate as on the electrokinetic potential which exists at the "oil-water" boundary in the absence of stabilizer[39].

TABLE IV

CATAPHORETIC VELOCITY AND ζ-POTENTIAL AS A FUNCTION OF NaCl CONCENTRATION

NaCl, %	Cataphoretic velocity, $\frac{\mu/\text{sec}}{\text{V/cm}}$ 25°C	ζ-Potential, millivolts
0	6.4	−81
0.0001	7.0	−88
0.001	7.2	−91
0.01	6.9	−87
0.1	5.6	−71
0.5	3.5	−44
1.0	2.9	−37
2.0	1.8	−23
4.0	1.4	−18
7.0	1.1	−14

In spite of the great number of papers devoted to the clarification of the action of electrolytes on the electrokinetic potential of dilute emulsions, these results can be applied to dispersions of high polymers only with great care. Firstly, the experimental techniques of these investigations which were performed a long time ago suffered from a series of drawbacks. These measurements were performed without accounting for the effect of electrophoretic retardation, electrical relaxation, and other factors influencing the electrophoretic mobility. Secondly, these investigations were performed mostly with emulsions which did not contain stabilizers, i.e., on systems essentially different from the concentrated emulsions in which class dispersions of high polymers belong.

Hauser and Bender[11], to the best of our knowledge, first investigated the effect of introduction of various quantities of NaCl on the electrophoretic speed of natural latex particles. Table IV indicates that the electrokinetic potential increases at first with increasing content of NaCl in the latex and then drops. At four per cent NaCl in the latex, the agglomeration of particles is noticeable. At 7 per cent NaCl the electrokinetic potential reaches some constant, very low value. Under these conditions the attractive forces predominate, and this favors the aggregation of the particles and their adhesion to the cover glass and to the slide when observed under a microscope.

Hauser and Bender came to the interesting conclusion that the small increase of electrolyte content with a monovalent cation causes the increase of

electrokinetic potential of particles of natural latex. The same phenomenon was observed by Maron and others using synthetic latexes. We believe that the increase of electrokinetic potential observed at small concentrations of non-coagulating electrolytes explains the increase of stability of latexes observed by Voyutskiĭ, Musatova and Bernstein[40] when the latexes were diluted and salts of the type Na_2CO_3, $NaHCO_3$, NaCl, and others were introduced.

Somewhat later Kemp and Straitiff[41] investigated the action of various salts on the quantity of alcohol which is necessary for coagulation of natural latex. Although the authors in this investigation did not determine the electrokinetic potential, their work has a certain interest for us since the electrolyte content in latex is connected with the electrokinetic potential of its particles. The experiments were performed in such a way that, to the dialyzed latex of pH = 7.4 or 5.4 (in the last case the value of pH was established with the aid of

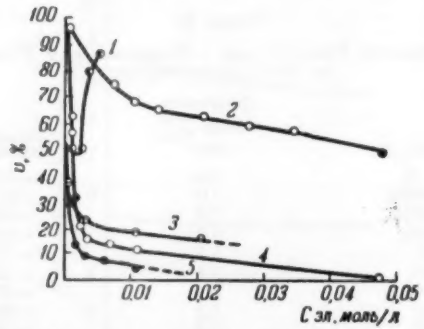

FIG. 15.—Effect of the electrolyte concentration (C_{el}) on the alcohol quantity (v) necessary for coagulation of dialyzed latex.

Curve *1*.—$AlCl_3$; pH =7.4.
Curve *2*.—KCl; pH =7.4.
Curve *3*.—KCl; pH =5.4.
Curve *4*.—$BaCl_2$; pH =7.4.
Curve *5*.—$BaCl_2$; pH =5.4.

acetic acid) containing 15 per cent solids, an equal amount by volume of electrolyte solution of known molarity was added and then the amount of alcohol necessary for coagulation was determined. The results of these experiments are given in Figure 15.

The rapid downward slope of the curves (Figure 15) corresponding to the area of small concentrations of electrolyte shows that the coagulation by the alcohol is not simply a result of dehydration of the adsorbed proteins, as was believed before. Curve 4 for $BaCl_2$ intersects the abscissa at an electrolyte content of 0.0475 mole/l while at the same molarity of KCl, 47 per cent of methanol by volume is required for coagulation (curve 2). Curve 1 for $AlCl_3$ is quite peculiar because it shows that in small quantities, this salt acts similar to the other salts, but at high concentrations it has a very small effect. The anomalous behavior of the latex when $AlCl_3$ is introduced is believed by the authors to be an effect of hydrolysis of this salt and variation of the pH of the solution. From our point of view the peculiarities observed can be explained by reversion of the latex globules as a result of their adsorption of Al ions or the products of hydrolysis of $AlCl_3$.

The effect of electrolytes on the electrokinetic mobility of globules of natural latex was also investigated by Bowler[14] using microelectrophoresis. The experiments were performed with latexes of various pH's (9–9.4) diluted by disodium hydrogen phosphate buffers of varying ionic strength. Diluted latexes were made from a 62 per cent concentrate which was obtained by centrifugation and stored for 90 days in the presence of 0.7 per cent ammonia. The results of this investigation are given in Figure 16. The increase of ionic strength at first lowers the electrophoretic mobility very strongly and then less rapidly, the curve being logarithmic.

The effect of electrolytes on the electrokinetic mobility in the case of synthetic latexes was studied by Maron and others with the aid of macroelectrophoresis. Maron, Turnbull and Elder[15] investigated the mobility of globules of the synthetic latex, Type II GR-S, stabilized by the soap of a fatty acid and diluted by a phosphate buffer into which different electrolytes were introduced.

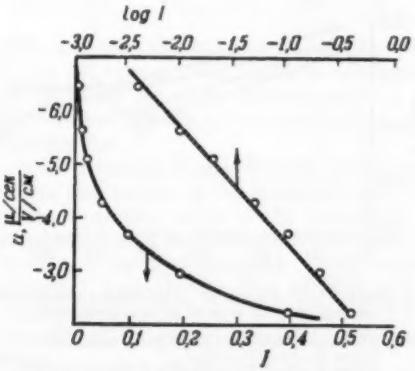

FIG. 16.—Effect of ionic strength (I) on the electrophoretic mobility (u) of globules of natural latex. Temperature = 30° C, pH = 9.0–9.4.

The amount of dry residue in the solution under investigation was in the range of 9–15 g/l; the pH = 8.2–9.0. The electrical conductivity of the solutions was adjusted to the electro-conductivity of the latex with the aid of the same electrolyte which the latex contained. The temperature in all cases was 30° C. The results are illustrated in Figure 17.

As is visible from comparison of the curves for the mixtures of various electrolytes, the ionic strength is not the only factor causing variation of the electrophoretic mobility. The nature of the electrolyte is also of importance. At the same ionic strength NaCl is the most effective in lowering mobility, followed in turn by Na_2HPO_4, Na_2SO_4 and KCl. The same order is observed, according to Maron and others, for the effectiveness of these salts on the coagulation of Type II GR-S latex. It is important to note that in the case of Na_2HPO_4 at high ionic strengths aggregation and coagulation were observed which encumbered the determination of mobility. However, the authors succeeded in establishing that the electrophoretic mobility decreases sharply.

The shape of the curves in Figure 17 reveals that, with increasing ionic strength, the mobility of the latex globules at first increased, reached a maximum and then decreased. The shape of the curve is explained as follows. The

initial rise in mobility at low ionic strengths is probably a result of ion adsorption which leads to increase of the electrokinetic potential. It is possible that the ionic strength at which this increase takes place is too small to cause appreciable desolvation of the soap. At this point the effect of the electrolyte on the ionic atmosphere begins to exert some influence, and probably adsorption of cation takes place causing a decrease of the electrophoretic mobility and the curve goes over its maximum. The levelling off of mobility decrease, which is observed at ionic strengths 0.3–0.4 is probably a result of the counterbalancing action of desolvation. The last has a tendency to increase the charge density and thus the electrophoretic mobility. A sharp lowering of the mobility near the end of the curve, according to Maron and others, is caused by desorption of the soap and neutralization of the latex particles. A proof that the desorption process takes place is indicated by the fact that a sharp lowering of the surface tension on the boundary "latex-air" is observed near the coagulation point.

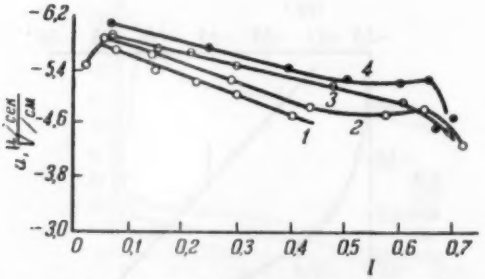

FIG. 17.—Effect of ionic strength (I) on the electrophoretic mobility (u) of Type II GR-S latex at 30° C, pH =8.2–9.0.

Curve *1*.—Na_2HPO_4+NaCl (1:4.5 mole ratio).
Curve *2*.—Na_2HPO_4 only.
Curve *3*.—Na_2HPO_4+Na_2SO_4 (1:3 mole ratio).
Curve *4*.—Na_2HPO_4+KCl (1:4.5 mole ratio).

The authors of the present survey cannot completely agree with the explanations of the form of the curves of Figure 17 given by Maron and others. Firstly, in giving an explanation for the shape of the curves they did not take into account the electrophoretic retardation and electrophoretic relaxation which are very much dependent on the value of X. The last value is ini ts turn a function of the ionic strength. Secondly, it is unbelievable that desolvation can lead to an increase in electrophoretic mobility. As a rule, the desolvation is connected with the contraction of the double electric layer and leads to the opposite effect. Thirdly, it is also unbelievable that at the high ionic strength (end of the curve) soap desorption takes place. In the solutions under investigation the solids content was always 9–15 g/l independent of the ionic strength. In such conditions the increase of ionic strength (concentration of the electrolyte) can only favor soap adsorption on the surface of the globules. It is much more probable that the decrease of electrophoretic mobility at high ionic strength can be explained by strong contraction of the double electric layer as a result of the anti-ion action.

In another paper Maron and Bowler[16] described the effect of concentration of the electrolyte on the electrophoretic mobility of the globules of Type III GR-S latex stabilized by potassium rosin soap. The relationship between the

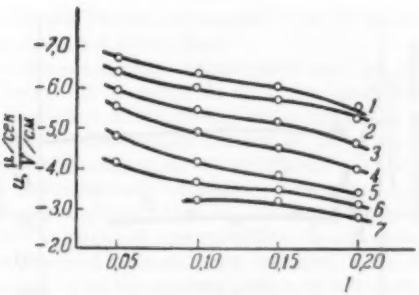

FIG. 18.—Effect of the ionic strength (I) on the electrophoretic mobility (u) of globules of Type III GR-S latex.

Curve	1	2	3	4	5	6	7
pH	10	8.0	7.0	6.5	6.0	5.7	5.5

electrophoretic mobility and the ionic strength at constant pH was determined at 30° for seven different pH values. The results so obtained are illustrated in Figure 18. At all values of pH the electrophoretic mobility decreases with increasing ionic strength. This decrease is more noticable at high and low ionic strengths than at medium ones.

Munro and Sexsmith[20] investigated the effect of concentration of electrolyte with monovalent cations and anions on the electrophoresis of very dilute synthetic latexes in the concentration range of the electrolyte, 0–0.01 M. The authors believe that at such small concentrations the effect of electrolytes on the electrophoretic mobility is the most apparent. NaCl was used as an electrolyte for these experiments. Immediately after addition of the electrolyte the latex samples were shaken well and allowed to stand for 12 hours. After that the electrophoretic mobility of the particles was determined using the modified micro method of Briggs.

In Figures 19, 20, and 21 curves are shown representing the dependence of the electrophoretic mobility on the concentration of electrolyte for latexes stabilized by nonionic hydroxy ethyl cellulose, by anionic gum arabic, and by a cationic soap respectively. The pecularities of the curves of Figures 19 and 20 which are characteristic for all the latexes containing nonionic and anionic

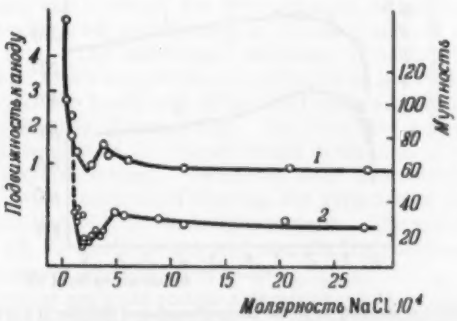

FIG. 19.—Effect of the electrolyte concentration on the electrophoresis and stability of a synthetic latex containing hydroxyethyl cellulose as a stabilizer: Curve *1*.—electrophoretic mobility. Curve *2*.—stability.

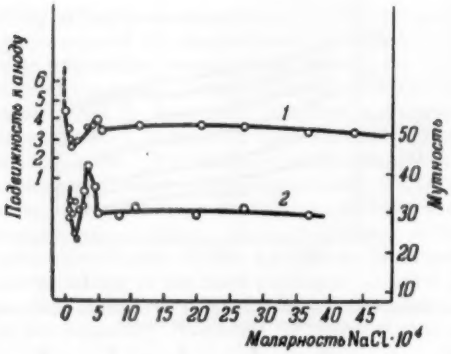

FIG. 20.—Effect of the electrolyte on the electrophoresis and stability of a synthetic latex containing gum arabic as a stabilizer.

Curve *1*.—electrophoretic mobility. Curve *2*.—stability.

stabilizers is the presence of two extreme points. The authors believe that the presence on the curve of a minimum followed immediately by a maximum is related to the formation of micelles in the latex. It is very probable that on reaching a certain concentration of electrolyte favoring adsorption, the quantity of emulsifier on the surface of the particles is sharply increased. As a result of that, the density of the electric charge on the surface of the globules increases. This in turn leads to an increase in electrophoretic mobility. Simultaneously, the formation of the micelles begins in the water phase. Further addition of the electrolyte results in contraction of the ionic atmosphere around the particles and this then causes the decrease in the electrophoretic mobility. The latex particles which contain nonionic stabilizer and which behave, on electrolysis, similarly to those stabilized by anionic stabilizers can acquire a charge as a result of adsorption on their surface of the anionic sub-

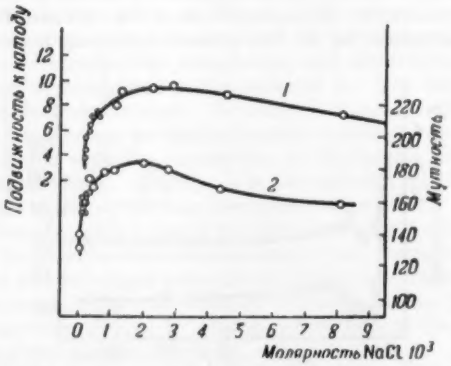

FIG. 21.—Effect of electrolytes on the electrophoresis and stability of a synthetic latex containing a cationic soap as a stabilizer.

Curve *1*.—electrophoretic mobility. Curve *2*.—stability.

stances which were formed during polymerization or in consequence of adsorption of negative ions from the water phase.

In the case of latexes containing cationic stabilizer, the curve (Figure 21) is of quite different form. It is probable that the concentration of cationic emulsifier which is present in dilute latexes still exceeds the critical concentration of micelle formation. Under such conditions, the addition of a salt causes a notable increase of micelle migration toward the surface of the globules resulting in an increase in electrophoretic mobility. This is true up to comparatively high concentrations of sodium chloride. Doscher[42] showed that actionic emulsifiers at higher than critical concentrations have a greater tendency toward adsorption as charged aggregates or micelles, than as ions. Another explanation for the absence of the extreme points on the curve of Figure 21 can be given using the point of view of Schulman and Cockbain[43]. These authors, in contrast to Doscher, believe that long chain compounds, due to their ability to ionize, are very soluble in water. Therefore, on the boundary "hydrocarbon-water", only very broadened adsorption films can form. The correctness of such an explanation is confirmed by the fact that Powis and Wood on observation of the electrophoretic mobility of oil drops in a solution of dodecylpyridinechloride did not find the extremes on the curves which are supposed to correspond to the formation of micelles.

It is necessary to note that the difference between the maximum and minimum electrophoretic mobilities near the critical concentration for the formation of micelles increases with increasing anionic character of the stabilizer. The limiting mobility value follows the same regularity. Ham and Dean[44] investigated the effect of salt addition on the electrophoresis of dispersions of octadecane and also found limiting values of electrophoretic mobilities. The electrophoretic mobility did not fall to zero in these experiments but decreased logarithmically to approach certain limiting values which were dependent on the nature of the salt added. Their results indicate the existence of a certain salt concentration after which further addition of salt does not affect the electrophoretic mobility of particles. This contradicts the usual concept that the electrolyte, if it is present in sufficient quantity, can cause complete discharge of the particles or even impart a charge of the opposite sign.

In summarizing the work of Munro and Sexsmith, the experiments concerning the relationship between the electrophoretic mobility of globules and the stability of latexes should be mentioned. For determination of stability the same solutions which served for determination of electrophoresis were used. Dilute latexes, after introduction of electrolyte, were centrifuged for 30 min at 2070 rpm. The centrifuged solutions were then transfered into clean test tubes and underwent further centrifugation for 10 minutes. After that, the turbidity of the liquid was determined using a photoelectric colorimeter with blue light filter Number 342. The turbidity was always proportional to the solids content of the latexes except in the case of very dilute suspensions of polydisperse latexes. Using the data thus obtained, so called "stability curves" were constructed showing the variation of the turbidity of the latexes as a function of their electrolyte content. The stability curves are given on Figures 19, 20 and 21 which also contain the corresponding electrophoretic mobility curves discussed previously.

The stability curves are quite comparable with the curves of electrophoretic mobility for each given latex. Besides that, each of the latexes which contain a nonionic or anionic surface active stabilizer, has a minimum in the stability

curve at approximately the same electrolyte concentration at which the mobility minimum occurs. The stability curve for a latex which contains a cationic stabilizer is also similar to the corresponding curve of the electrophoretic mobility. Neither curve possesses a minimum but both are steeply inclined at low salt concentrations, and then pass into a slanting maximum. It is worthwhile to note that the latexes which contain cationic stabilizers and have the most mobile globules exhibit the greatest stability on electrophoresis. It was impossible to establish any traces of precipitate in these even after storage for one week. The results of the investigation performed by Munro and Sexsmith perfectly confirm our opinion that the stability of latexes is a function of the electrokinetic potential of their particles.

Voyutskiĭ, Panich and Kal'yanova[18,19] studied the effect of cations on the electrokinetic potential of globules of a synthetic latex stabilized by ammonium oleate. The most interesting results of this investigation were that under certain conditions electrolytes with trivalent cations, for example aluminum

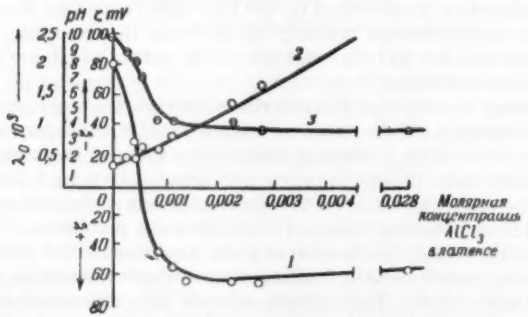

FIG. 22.—Variation of electrokinetic potential (ζ), specific electroconductivity (λ_s), and pH as a function of $AlCl_3$ concentration in the latex.

Curve *1*.—ζ.
Curve *2*.—λ_s.
Curve *3*.—pH.

chloride, are able to reverse the charge on the surface of the latex globules. Preliminary experiments showed that the reversal in charge by aluminum chloride or acid was possible only in the case where the solution of electrolyte was introduced into a dilute latex that contained only 2–4 per cent solids. Besides that, the charge reversal occurred only in the case when about an equal volume of a 0.001 *M* or higher aluminum chloride solution was added to the latex. Aluminum chloride solutions of lower concentration could not cause the reversal. The introduction into latex of calcium chloride solutions of any concentration under any conditions always led to complete coagulation. However, introduction of saturated solutions of potassium chloride into latex did not cause coagulation but only caused reversible flocculation.

In order to establish the relationship between the electrokinetic potential of latex globules and the quantity of aluminum chloride introduced, the authors used the same method which was used in experiments concerning the reversal of charge of latex globules by acid described in the previous section of this review. Latex, containing 4 per cent solids was diluted with an equal volume of aluminum chloride solution of a certain concentration. The solu-

tion underwent electrophoresis at a pH value which the solution had after the introduction of electrolyte. The solution of aluminum chloride was used at a concentration which was equal to the electrolyte concentration under investigation. The specific electroconductivity of the medium was established with the aid of a sodium chloride solution, the pH of which was controlled by introduction of borax or sodium hydroxide. The results of these measurements are shown in Figure 22.

As more and more aluminum chloride is introduced into the latex, the absolute value of negative electrokinetic potential at first sharply decreases, passes through zero at an electrolyte concentration of 0.00055 M, and then goes over into the positive region. The positive values decrease somewhat upon further addition of electrolyte. The stability of the latex globules, on which the charge was reversed by the aluminum salt, decreased. The same was true for the case of charge reversal with acid. This corresponded to the smaller value of electrokinetic potential of particles in acidic media. In the zone near the 150 electric point the latex was quite unstable.

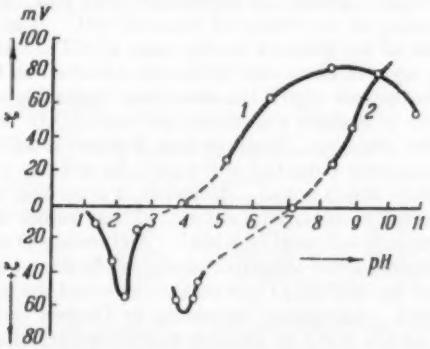

FIG. 23.—Variation of the electrokinetic potential (ζ) as a function of pH of the latex.

Curve *1*.—HCl.
Curve *2*.—$AlCl_3$.

In interpreting the phenomena which take place on reversal of charge on latex globules by aluminum chloride, it is necessary to take into account the following: Firstly, on introduction into latex of aluminum chloride, it undergoes partial or complete hydrolysis depending on the pH of the latex. As a result of this, the system becomes acidic. Thus, on addition of aluminum chloride to latex, the electrokinetic potential of globules is affected by aluminum ions and also by a change of pH of the solution. Secondly, starting from pH = 4 and higher, formation of an insoluble amphoteric aluminum hydroxide which is absorbed on the surface of the globules occurs in the system. The fact that the coagulum obtained under these conditions is quite different from the coagulum which is formed on acidification of the latex can be advanced as proof for the absorption of aluminum hydroxide. It is a fine precipitate or friable lumpy substance easily pulverizable between the fingers. This characteristic of the precipitate is obviously caused by the fact that each globule is surrounded by a layer of aluminum hydroxide, which prevents direct contact between the globules and hinders formation of the usual compact coagulum.

In order to exclude the influence of pH on the electrokinetic potential of

latex globules, when the effect of aluminum chloride is considered, it is convenient to use Figure 23. The variation of the electrokinetic potential as a function of pH in the series of experiments where aluminum chloride was added is shown (curve 2) as well as the series of analogous experiments where different quantities of hydrochloric acid were used (curve 1). Comparing curves 1 and 2, one sees that the introduction of aluminum chloride into the system considerably displaces the curve of "electrokinetic potential—pH of dispersion" toward the right. However, their shapes are similar. The question concerning which ions can determine the charge of the globules on introduction of the aluminum chloride into latex arises. The positive electrokinetic potential in this case can be determined by the aluminum ions only at pH = 4.1 and lower. At higher pH values amphoteric aluminum hydroxide which is absorbed by the globules will be formed so that the positive charge of the particles can be explained by the presence, on their surface, of ions such as $Al(OH)_2^+$ or $Al(OH)^{++}$ or hydrogen ions which are still present in the system and which also can be adsorbed.

The isoelectric point of aluminum hydroxide according to the literature[45] lies in the range of pH 7.5–8.0. In accordance with this, curve 2 crosses the abscissa approximately at the indicated values of pH. It is obvious that the electrical properties of the globules in this zone of pH are almost completely determined by the layer of aluminum hydroxide adsorbed on the surface of the globules. At higher values of pH, the aluminum hydroxide which is adsorbed by the globules now is charged negatively, and $Al(OH)_2O^-$ ions will be found on the surface of the globules. It seems that this fact should favor increasing the negative electrokinetic potential of the globules in basic media at the same pH value. In reality, this is not so. However, it is necessary to keep in mind that for charge reversal by aluminum chloride at high values of pH only a small amount of the aluminum salt need be added. An increase of the absolute value of the negative electrokinetic potential caused by hydroxyl ions due to additional adsorption of the $Al(OH)_2O$ ions on the surface of the particles can occur but not be observed. Aluminate, according to Daniels (compare[45]) usually cannot be formed at pH = 6.8 in the case under consideration.

The latex which was used for the experiments contains ammonia and, as is known, in the presence of ammonia, aluminate is completely transformed into aluminum hydroxide. The experiments concerning charge reversal on the latex globules with the aid of aluminum chloride addition as well as by acidification are illustrative examples which prove how important the electrokinetic potential is in stability of latexes. Really, latex turns out to be quite stable, if its globules possess sufficiently high potential, independent of pH of the medium and the nature of the stabilizer. At low potentials, the latex is unstable and undergoes coagulation. As experiment shows, the lower the electrokinetic potential is, the more complete is coagulation. At the isoelectric point the coagulation is complete and takes place almost instantly. It is important to note, that latex with globules of reversed charge is noticably less stable than the initial one. This can probably be explained by the different nature of a cationic stabilizer. The lower stability of this latex is in agreement with the fact that the absolute value of the electrokinetic potential of the globules of this latex is smaller than the potential of the globules of a latex of normal charge.

DISTRIBUTION OF STABILIZER IN LATEXES

Baker[28] performed detailed studies of the distribution of the stabilizer—native albumin—in natural latexes and their concentrates. This investigator

judged the protein distribution between the disperse phase and the dispersing medium by the nitrogen content. According to Baker, the amount of nitrogen in the disperse phase in natural latex and its concentrates varies considerably depending on the origin and method of treatment of the product. In fresh latexes the quantity of nitrogen which is contained in the disperse phase is approximately 25 per cent of the total present in the latex. In products which have been centrifuged, the absolute nitrogen content is always lower, but the per cent of nitrogen combined with the disperse phase is considerably higher. Baker investigated the effect of dilution of latex on the protein desorption from the surface of the latex globules. The experiments were performed so that the latex underwent numerous creamings followed each time by removal of the serum liberated from the globules. The residue was then diluted with the precipitating agent. As a precipitating agent, sodium alginate was used, which as the author and Bondy[46] showed is not readily adsorbed by the globules. Distribution of the protein in the latex was established from the quantity of nitrogen combined with the disperse phase (N_D) and that present in the serum (N_S). In both cases the quantity of nitrogen was expressed in per cent of the total quantity of rubber.

TABLE V

THE EFFECT OF DILUTION ON THE DISTRIBUTION OF PROTEIN IN LATEXES

40% Latex–Ammonia preserved

Storage time in months	Number of creamings	N_S in % of rubber		N_D in % of rubber	
		Initial	Final	Initial	Final
6	10	0.208	0.0016	0.173	0.131
15	7	0.198	0.0036	0.135	0.134
15	7	0.194	0.0027	0.108	0.100

The results are given in Table V. The quantity of adsorbed protein is smaller on the globules of latexes which have been stored for a long time than on the particles of fresher latex.

On investigation of various fractions of latexes, Baker established that, in accordance with the size and total surface of the latex particles, the fractions with increasing nitrogen content could be classified in the following order; 1) Centrifuged concentrate, 2) Settled concentrate, 3) Initial latex, 4) Serum, remaining after centrifugation. Treatment with base sharply lowers the nitrogen combined with the disperse phase. Most of the protein is desorbed from the globules during the first hours of treatment. Baker showed that even upon numerous protracted treatments of the latex by a base, it was impossible to remove completely all of the protein from the dispersed phase. About 4 per cent of the total nitrogen or 0.02–0.03 per cent if calculated with respect to the rubber always remained. It is impossible to remove this nitrogen by extraction with acetone. On the basis of these experiments, Baker assumed that a certain part of the nitrogen is combined with the rubber chemically. Removal of the nitrogen containing substance from the surface of globules is considerably faster at 70° C than at 50° C.

Another method for the removal of protein from the surface of the globule consists in its displacement by any surface active substance, for example, by soap. Table VI lists the results of nitrogen determinations (N_D and N_S) in concentrate, obtained by creaming of a latex, into which various quantities of

potassium oleate were introduced. It is shown that the potassium oleate displaces the protein from the surface of the rubber globules. Most of the protein (except 0.03 per cent) can be displaced by potassium oleate. In addition, the author showed that the soap not only displaces the protein from the surface of rubber particles but also some substances of unknown structure. Since these substances of unknown structure are displaced last by the soap, it is plausible to assume that they are more surface active than the protein, and are therefore lipoids, which are strongly bound to the rubber. Investigation of variation of the distribution of the nonrubberlike components in ammoniated latex during twelve months storage showed that the quantity of nitrogen which is connected with the disperse phase decreases with time. According to Baker, this is explained by existance in the fresh latex of complexes from which proteins and fatty acids can be split.

In the investigations by Roberts[47,48] there are indications that chemical complexes whose components can be split on hydrolysis are present in fresh latex. The hydrolyzing agents are enzyme and bacteria. The changes in the chemical composition of a latex to which ammonia was added are explicable by the joint action of enzymes and ammonia. They split off and destroy the pro-

TABLE VI

EFFECT OF SOAP ON PROTEIN DISTRIBUTION IN NATURAL LATEX

Amount of potassium oleate (in g) added to 100 g of latex containing 19.1% solids	N_S in % of rubber	N_D in % of rubber
0	0.088	0.180
0.16	0.099	0.130
0.35	0.102	0.115
0.62	0.107	0.095
1.35	0.118	0.046
2.57	0.122	0.036

teins, forcing them to transfer from the surface of the globules into the water phase. They also liberate fatty acids which concentrate themselves as the ammonium soaps on the "rubber-water" boundary. The first process decreases, and the second one increases the stability against acid coagulation of the latexes. Existence of the opposite tendency which affects the latex stability on coagulation is confirmed by the experiments of Rhodes[49].

Very interesting information concerning the ratio of stabilizer adsorbed on the globule's surface and that present in the water phase of GR-S latex is given in the review of Zwicker[50]. In GR-S latex of 0.1 μ particle diameter stabilized by the soaps of fatty acids, each 100 parts of polymer contains about 7 parts of soap. If the latex contains 40 per cent solids, less than 0.04 per cent of the soap is present in the water phase, representing only 60 per cent of practical saturation. In other words, 99 per cent of the total amount of soap in the latex is present on the surface of the globules. Furthermore, the experiments show that four more parts of soap, in respect to polymer, can be added before there is any appreciable increase of soap concentration in the water phase. It is necessary to note that, according to Zwicker, such a relationship observed in the case of synthetic GR-S latex differs from that for Hevea. In the case of natural latex the surface of the globules can be saturated by addition of a relatively small quantity of soap. If one neglects this difference between many synthetic latexes and natural ones, it can lead to difficulty. For example, the addition

of a well stabilized dispersion of filler to a soap-starved latex leads to microflocculation of the latter. This is explained by the fact that the stabilizer goes from the particles of the filler on to the globules of latex.

Soap adsorption up to saturation of the surface of the latex particle and formation of a homogeneous monomolecular layer is used by Maron and others for determination of the size of latex particles. The latex is titrated by the soap solution. After the formation of the homogeneous monomolecular layer on the surface of the globules the formation of soap micelles begins in the water phase. This can be established by a series of indications:[51] a minimum in the surface tension[52]; a break in the electroconductivity vs. soap concentration curve[53]; ability of the solution to dissolve, colloidally, hydrocarbons and pigments[54]; change of the structure of the foam; gelatinization at change of viscosity; and change in light scattering[55].

STRUCTURE OF THE ADSORBED LAYER ON THE SURFACE OF LATEX GLOBULES

Electrophoretic investigations, studies of stabilizer distribution between the dispersed phase and the dispersing medium, and also observations by a number of investigators who studied latexes with the aid of other methods enable us to make some generalizations concerning the structure of the adsorbed stabilizer layer which covers the surface of the latex globules. Such generalizations are very useful for a deeper understanding of the importance of the electrokinetic potential as a factor responsible for the stability of latexes.

Natural latex.—According to Kemp[56], a layer of protein is present on the surface of globules of natural latex. The external part of it consists of substances whose structure is not well known. Proof of the presence of this layer lies in the constancy of the acetone extractable material which is obtained after repeated creaming of the latex. This layer is usually removed in centrifugation. It can also be removed by heating the latex with alkali and subsequent coagulation of the latex with alcohol[57]. Upon such treatment the acetone extract is decreased from 2.4 to 1.2 per cent. The acid number of the acetone extract is simultaneously decreased from 109 to 11. Ordinary coagulation of the latex by acid liberates fatty acids which are found in the acetone extract. This indicates that fatty acids are present in the latex serum as soaps or as more complicated compounds which are split upon acidification. In Figure 24, the structure of the latex globule, taken from the paper by Kemp, is shown.

Baker[28] believes that proteins, soaps and other surface-active substances probably of lipoid nature are present on the surface of globules of natural latex as complex films. These films, at sufficiently high concentrations, can become a double layer with the hydrophobic lipoid part directed toward the rubber phase and the hydrophilic part, which consists of proteins and soaps, facing outwards. Baker assumes that the thickness of such a double layer is hardly more than 40 A.

The works of van Gils[58] and of Cook and Sekhar[59] established that fresh Hevea latex is not solely a dispersion of rubber globules in the serum, but that there are also present large gel-like particles of their agglomerates which form in the rubber dispersion as a separate phase. These substances were named lutoids because they contain the yellow coloring matter of the rubber. The lutoids probably play a certain role in the process of rubber formation in the tree. It is supposed that the lutoids partly consist of three-component coacervates and positively charged magnesium ions. These coacervates not only

form a separate lutoidic fraction, but also envelop the rubber globules. On introduction of ammonia into latex, the lutoids are partially dissolved.

In spite of a disagreement among some investigators concerning the details of structure of the adsorbed layer, all the investigators come to the conclusion that the stability of natural latex is due to the presence of the adsorbed layer of protein on its globules. Since in natural latex, at least two proteins are present—A and B, investigations aiming to clarify which of these proteins determine the colloidal properties of the latex have been carried out. Omitting the details of these investigations and referring to the papers in question[41,60] let us note only that all the investigators assign the stability of the latexes in basic and neutral media to protein A. The authors come to this conclusion on the basis of the following facts: protein A is adsorbed more strongly on the interphase surface; it can be precipitated by all substances which provoke the coagulation of the latex; and the latex globules at pH = 5.5 and higher have the

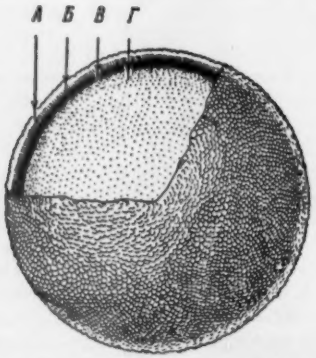

FIG. 24.—Schematic drawing of natural latex globule.

A.—Transitory layer of soap or lipide.
B.—Adsorbed protein layer.
C.—Gel+rubber hydrocarbon layer.
D.—Sol+rubber hydrocarbon emulsion containing sterol bodies.

same electrokinetic mobility as protein A. In acidic media, in the pH range of 4.5–5.4 where association of the globules begins, the results of electrophoresis show that there is a layer consisting of a mixture of proteins A and B on the surface of the aggregates. From pH 3.7–4.5 only B is present.

An electrophoretic investigation of proteins carried out later with the serum of rubber latex[61] showed that, while in the serum of latex preserved with ammonia there are two proteins, unpreserved Hevea latex contains seven electrophoretically separable proteins. On investigation of the relationship between the electrophoretic mobility of these proteins and pH, it was established that not all of these proteins have an isoelectric point in the acidic zone and that the isoelectric points of two prtoeins lie at pH = 7.9 and 9.7. Preservation with the aid of ammonia not only decreases the number of the resolvable proteins from seven to two, but also more than doubles their electrophoretic mobility at pH = 6.85. The authors assume that this at least partially accounts for the superior mechanical stability of preserved latexes within a short time after ammonia preservation. However, the authors do not reject the possi-

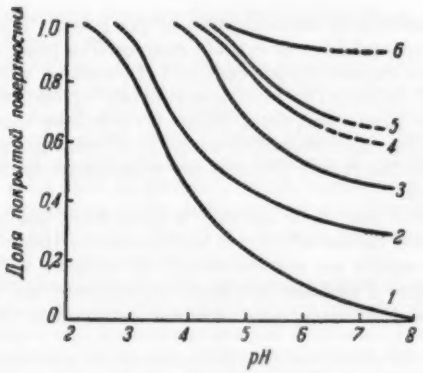

FIG. 25.—Relationship between fraction of the globule-surface covered with protein and the pH of the serum.

Curve	1	2	3	4	5	6
Latex Conc., g/l	0.016	0.98	3.9	11.8	39.1	67.6.

bility that the increased stability of the latexes might also be a result of soap formation by hydrolysis of resins.

The structure of the adsorbed layer on the surface of natural latex globules can be essentially affected by a number of factors. Kemp and Twiss[12] attempted to measure the variation in protein and rubber resin adsorbed at the surface of the natural latex globule as function of pH of the serum and degree of dilution of the latex. The method employed is based on the assumption that the resultant surface charge-density of a composite colloidal particle depends on the surface-charge densities of the capillary-active substances adsorbed at the particle surface, and on the fraction of the surface area occupied by those substances.

Figures 25 and 26 illustrate the change in surface fraction covered with protein as a function of pH in latexes of various concentration.

Figure 27 shows the variation in composition of the surface of latex globules

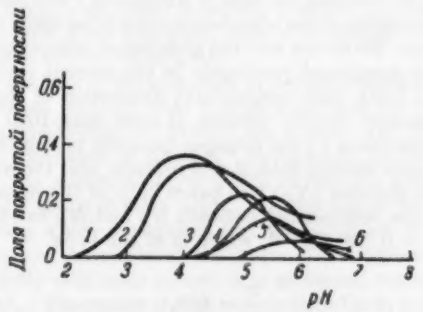

FIG. 26.—Relationship between fraction of the globule-surface covered with rubber resin and the pH of the serum.

Curve	1	2	3	4	5	6
Latex Conc., g/l	0.016	0.98	3.9	11.8	39.1	67.6.

at pH = 8 as a function of concentration of the latex. The external surface of the globules of natural latex is entirely composed of protein when the solids content of the latex exceeds 12 per cent and the surface, at the concentration indicated above, is indicated to remain completely covered with protein up to pH = 10. On the other hand, from Figure 25 it follows that in natural latex at large dilutions (for example, solids contents of 0.016 g/l and at sufficiently high values of pH) the rubber globules are completely deprived of their protective protein shell.

Obviously, in this case, their stability is determined not by the protein adsorption, but by other factors which will be discussed further. Kemp and Twiss believe that these results are not necessarily at variance with the presence of protein on the surface of globules as a lipoid-protein complex, though they agree more naturally with the simpler view as to the independence of the protein and the rubber-resin.

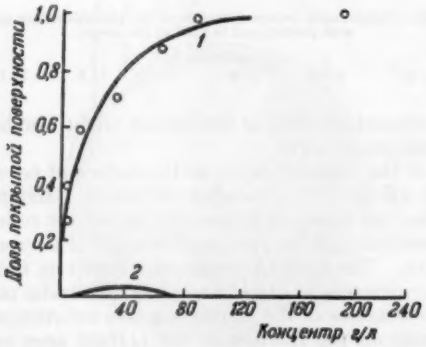

FIG. 27.—Variation in surface composition of natural latex at ph 8.0 as a function of concentration.

1. Protein.
2. Resin.

It is interesting to compare the data of Kemp and Twiss with that of Baker[28], who judged the saturation of the adsorbed protein layer using the distribution of the nitrogen between the serum and the globules of natural latex. The results obtained by Baker mentioned previously in the present review show that on dilution of natural latex, only insignificant desorption of the proteins can be observed. For example, despite dilution of more than 1000 times in one of a series of experiments (latex P) the nitrogen quantity present in the serum (N_S) became 100–130 times smaller than it was initially, and the nitrogen remaining combined with the globules (N_D) was hence 76% of the initial quantity. According to Baker, the relationship between N_D and N_S can be represented by the equation: $N_D = 0.128\ N_S^{0.056}$, which is of the type

$$\frac{x}{m} = k^{1/n},$$

suggested by Freundlich for adsorption equilibria of the liquid-solid type. Due to the very small value of $1/n$ for the given case, the adsorption of protein

by rubber is considerably stronger than that of liquids on porous absorbates, such as charcoal or silica gel.

It is worthwhile to note, that in the case of natural latex stabilized by protein, irreversible adsorption of the stabilizer on the surface of the latex globules is also possible. In any case, a good example of irreversible adsorption of protein on the surface of drops of the disperse phase was observed by Schorter[62] in preparation of an oil emulsion in the presence of common albumin. On shaking, a quasi solid shell of albumin, which immediately underwent denaturalization due to the action of the surface forces, was formed around each drop of oil. As a result of this, the change which took place in the adsorbed layer had the character of an irreversible coagulation.

The question of the spontaneously occurring process of concentration of the dissolved substance in the interphase layer is very important in connection with stability of emulsions and dispersions toward dilution. It is thought that, in the case of irreversibility of the adsorption of stabilizer, latexes should be considerably more stable upon dilution by water. However, the stability of very dilute latexes depends also on other factors, which will be considered further.

TABLE VII

SOAP REQUIRED FOR THE FORMATION OF A SATURATED MONOMOLECULAR LAYER ON GLOBULES IN LATEXES OF VARIOUS DISPERSITY

Diameter of globules in μ	Number of globules per kg of polymer	Total surface sq meters/ kg polymer	Milliequivalents of soap per 100 parts of polymer
0.02	2.39×10^{20}	300,000	236
0.06	8.84×10^{18}	100,000	78.6
0.20	2.39×10^{17}	30,000	23.6
0.60	8.84×10^{15}	10,000	7.9
2.0	2.39×10^{14}	3,000	2.4
6.0	8.84×10^{12}	1,000	0.8

Synthetic latexes.—The structure of the layer which covers the surface of the globules of a synthetic latex is considerably less complicated, and therefore the phenomena observable upon its formation and destruction are much more simple than in the case of natural latex. First of all, in the serum of synthetic latexes one quite definite stabilizer is usually present. Secondly, the stabilizer in this case is, as a rule, a low molecular weight compound such as the soap of a fatty acid, a sulfonic acid or its salt etc.

In the general concept of the structure of layers of surface active substances on interphase surfaces, we think that in such adsorbing layers the hydrocarbon part of the adsorptive is directed toward the rubber, and the ionic group, toward the water. The paper of Zwicker[50] contains an indication of the degree of saturation by the adsorbing layer which covers the globules, of synthetic latexes stabilized by soaps of fatty acids. In this paper the calculation of the quantity of the soap which is required for the formation of a monomolecular layer on the globules of various latexes is given. The surface area to which the molecules of the fatty acid soap adhere in a saturated monomolecular layer is assumed to be $21 A^2$. The results of such calculations for hypotethical, mono disperse latexes are given in Table VII.

Experience has shown that in order to get a GR-S latex stable enough for purposes of transportation and storage it is sufficient to add only 40–60% of the

soap necessary for the formation of a saturated surface layer[63]. This, the adsorbed layers on the globules of synthetic latexes are not polymolecular (as some authors think[64,65,66,67]) and are not even saturated as a rule. This conclusion that the surface of the globule is not saturated is a serious argument against the assumption that the formation of gel-like shells around the globules can affect the stability of synthetic latexes. The importance of this shell for the stability of emulsions and some other colloids was underlined by Ramsden[68], Lewis[69], Rebinder[70] and by a number of other investigators. It is hardly possible to speak about the presence of two dimensional gels surrounding the particles and about the mechanico-structural properties of these gels if one keeps in mind the lack of saturation by the adsorbed layer of the surface of the globules of common synthetic latexes. However, it is necessary to keep in mind that in a homologous series of fatty acid salts, the stabilizing effect toward foams and emulsions probably passes through a critical point showing a sharp increase at C_{11}, i.e., when soap like properties become evident. The adsorption, however, in a homologous series increases in accordance with the Traube rule, and therefore, constancy of the adsorption of the potential determining ion could be preserved by a simple increase in the concentration of the surface active substance by 3–3.5 times on going to a lower homolog. However, it is known that the lower homologs of the salts of fatty acids are not able to stabilize emulsions and foams in any concentration. Rebinder indicated that these considerations were the facts confirming the specificity of the stabilizing effect of soaps as protecting colloids. In concluding what has been said about the structures of the adsorbed layers on the globules of synthetic latexes it is worthwhile to mention that there is no direct relation between the degree of saturation and the electrokinetic potential. As we saw, Maron and Bowler showed that with increasing soap content in synthetic latex, the electrokinetic potential does not increase and it can even be decreased.

Very dilute latexes.—It was noted already that at comparatively moderate dilutions of latexes with water only a small part of the stabilizer undergoes desorption and transfers to the serum. However, at very large dilutions the surface of the globules loses a considerable amount of stabilizer which goes over into the water phase. Both the considerations based on the reversibility of the adsorption phenomenon, and the electrophoretic data obtained by Bowler confirm this. However, simple experiment shows that even at very large dilution latex systems do not lose their stability if the pH of the water which is used for dilution is adjusted to the pH of the initial latex and does not contain polyvalent cations. The question of what causes the stability of such dilute latexes then arises. This stability of very dilute latexes as well as the stability of very dilute emulsions can be explained in a number of ways. Firstly, in the case of large dilutions the coagulation of dispersed systems is slowed because of the decrease in probability of collision which would lead to adherence and coagulation of the particles. Secondly, in very dilute emulsions and latexes the particles can adsorb hydroxyl and hydrogen ions which are always present in water and thus obtain a charge and a hydrate shell. This can favor the stability of the system. Schorter[62] believes that, at large dilutions, the emulsion droplets preferentially adsorb hydroxyl ions from the water and therefore are charged negatively. In more concentrated solutions the specific activity of the hydrogen and hydroxyl ions disappears and the ion of the opposite sign is adsorbed which leads to a lowering of the free charge. This question can be solved definitely only after detailed experimental investigation.

REFERENCES

[1] Hardy, *Z. physik. Chem.* **33**, 385 (1900).
[2] Powis, *Z. physik. Chem.* **89**, 91 (1914).
[3] Ellis, *Z. physik. Chem.* **89**, 145 (1914).
[4] Smoluchowsky, *Bull. Acad. Sci. Cracovie 184* (1903).
[5] Hückel, *Physik. Z.* **25**, 204 (1924).
[6] Henry, *Proc. Roy. Soc. (London)* **133**, 106 (1941).
[7] Kruyt and van der Willigen, *Z. physik. Chem.* **130**, 170 (1927).
[8] Robinerson, "Problems of Colloid Chemistry, Khimtheoretizdat, p. 123, Moscow, 1937.
[9] Oberbeek, "Advances in Colloid Science", Interscience Publishing Co., New York, N. Y., 1950, p. 97.
[10] Kruyt, *Colloid Science I*, 81 (1950).
[11] Hauser and Bender, *Proc. Rubber Technol. Conf.*, London, **1938**, p. 101.
[12] Kemp and Twiss, RUBBER CHEM. & TECHNOL. **9**, 551 (1936).
[13] Jordan, *Proc. Rubber Technol. Conf.*, London, **1938**, p. 111.
[14] Bowler, *Ind. Eng. Chem.* **45**, 1790 (1953); RUBBER CHEM. & TECHNOL. **27**, 472 (1954).
[15] Maron, Turnbull and Elder, *J. Am. Chem. Soc.* **70**, 582 (1948).
[16] Maron and Bowler, *J. Am. Chem. Soc.* **70**, 3893 (1948).
[17] Voyutskil, Smetkin, Panich and Kal'yanova, *Doklady Akad. Nauk SSSR.* **70**, 1013 (1950).
[18] Voyutskil, Panich and Kal'yanova, *Proceedings of CNIKZ*. "Theory and Practice of Adhesives", Gizlegprom, 1952, p. 90.
[19] Voyutskil, Panich and Kal'yanova, *Trudy M.I.T.Ch.T. Goskhimizdat* 1953, V, p. 30.
[20] Munro and Sexsmith, *Canadian J. Chem.* **31**, 287, 985, 1189 (1953).
[21] Abramson, Moyer and Gorin, "Electrophoresis of Proteins" Reinhold Pub. Corp., N. Y., **1942**.
[22] Gerasimov, *Zhur. Russ. Fiz. Khim. Obshchestva*, **58**, 601 (1926).
[23] King and Mukherjee, *J. Soc. Chem. Ind. (London)* **59**, 185 (1940).
[24] Rebinder, "Conspectus of General Course in Colloid Chemistry", Moscow State University Press, 1949 p. 74.
[25] King, *Trans. Faraday Soc.* **37**, 168 (1941).
[26] Thompson, *Trans Electrochem. Soc.* **81**, 941 (1936).
[27] Glesston, "Introduction to Electrochemistry", I. L. (1951) p. 89.
[28] Baker, RUBBER CHEM. & TECHNOL. **14**, 641 (1941).
[29] Ellis, *Z. physik. Chem.* **78**, 321 (1912).
[30] Limburg, *Rec. trav. chim.* **45**, 772, 854, 875 (1926).
[31] Belgrave, *Malayan Agr. J.* **11**, 348 (1923).
[32] Sarrut, RUBBER CHEM. & TECHNOL. **20**, 63 (1947); RUBBER CHEM. & TECHNOL. **4**, 310 (1931).
[33] Fullerton, *J. Rubber Research Inst. Malaya* **2**, 156 (1930).
[34] Rhodes and Sekar, *J. Rubber Research Inst. Malaya* **7**, 169 (1937).
[35] Voyutskil and Dzyadel, *Kolloid, Zhur.* **7**, 237 (1941).
[36] Bull and Gortner, *Proc. Nat. Acad. Sci. US.* **17**, 288 (1931).
[37] Price and Lewis, *Trans. Faraday Soc.* **29**, 775 (1933).
[38] Ellis, *Trans. Faraday Soc.* **9**, 15 (1913).
[39] Donnan, *Chem. Age (London)* **31**, 282 (1923).
[40] Voyutskil, Musatova and Bernstein, *Legkaya Prom.* **1944** No. 1–2, 23.
[41] Kemp and Straitiff, *J. Phys. Chem.* **44**, 788 (1940); RUBBER CHEM. & TECHNOL. **13**, 705 (1940).
[42] Doscher, *J. Colloid Sci.* **5**, 100 (1950).
[43] Schulman and Cockbain, *Trans Faraday Soc.* **36**, 662 (1940).
[44] Ham and Dean, *Trans Faraday Soc.* **36**, 52 (1940).
[45] Nicolskil and Paramonova, *Z. physik. Chem.* **2**, 687 (1931).
[46] Bondy, *Trans. Faraday Soc.* **35**, 1093 (1939).
[47] Roberts, *J. Rubber Research Inst. Malaya* **7**, 46 (1936); **8**, 179 (1938); RUBBER CHEM. & TECHNOL. **11**, 445 (1938); **10**, 1 (1930).
[48] Roberts, *J. Chem. Soc.* **1938**, 2032.
[49] Rhodes, *J. Rubber Research Inst. Malaya* **9**, 126 (1939).
[50] Zwicker, *Ind. Eng. Chem.* **44**, 774 (1952).
[51] McBain, *Colloid Chem.* Reinhold Publ. Co., N. Y., (1944).
[52] Antonoff, *Colloid Chem.*, Reinhold Publ. Co., N. Y., (1950).
[53] Maron, Elder and Ulevitch, Div. of Rubber Chem., ACS, 112th Meeting, N. Y., 1947.
[54] Gorin and Harkins, *J. Am. Chem. Soc.* **69**, 679 (1947); Gorin, Klevens and Harkins, *J. Chem. Phys.* **14**, 216, 640 (1949).
[55] Debye, *J. Applied Phys.* **15**, 232 (1944); *J. Phys. & Colloid Chem.* **53**, 1 (1949).
[56] Kemp, *Ind. Eng. Chem.* **30**, 154 (1938).
[57] Kemp, *Ind. Eng. Chem.* **29**, 643 (1937).
[58] Homans and van Gils, Proc. Second Rubber Technol. Conf., London, **1948**, p. 292; van Gils, *Ind. Eng. Chem.* **45**, 452 (1953).
[59] Cook and Sekhar, RUBBER CHEM. & TECHNOL. **27**, 297 (1954).
[60] Bondy and Freundlich, *India-Rubber J.* **95**, 513 (1938).
[61] Roe and Ewart, RUBBER CHEM. & TECHNOL. **16**, 542 (1943).
[62] Schorter, *J. Soc. Dyers Colorists* **31**, 64 (1915); **34**, 136 (1918).
[63] Willson, Miller and Rowe, *J. Phys. & Colloid Chem.* **53**, 357 (1949).
[64] Nonaka, *J. Soc. Chem. Ind. Japan* **31**, 297 (1928).
[65] Serrallach and Jones, *Ind. Eng. Chem.* **23**, 1016 (1931).
[66] Heymann, *Allgem. Oel-u. Fett-Ztg.* **29**, 389 (1932).
[67] Seymour, Tartar and Wright, *J. Phys. Chem.* **38**, 839 (1934).
[68] Ramsden, *Proc. Roy. Soc. (London)* **A72**, 156 (1903); *Z. Physik. Chem.* **47**, 336 (1904).
[69] Lewis, *Phil. Mag.* **15**, 499 (1908); **17**, 466 (1909).
[70] Rebinder, *Zhur. Fiz. Khim.* **2**, 754 (1931); *Kolloid Zhur.* **8**, 157 (1946); "Conspectus of General Course in Colloid Chemistry", Moscow State Univ. Press, 1949, p. 74.

FOAM STABILITY *

A FUNDAMENTAL INVESTIGATION OF THE FACTORS CONTROLLING THE STABILITY OF FOAMS

A. J. DeVries

Centre de Recherches de la Compagnie de Saint-Gobain, Antoine (Seine), France

CONTENTS

		PAGE
I.	Structure and stability of foams	1143
1.1	Introduction	1143
1.2	Surface tension and foam stability	1144
1.3	Drainage and foam stability	1147
1.4	Foam drainage and bubble shape	1148
II.	Gas diffusion in foams	1151
2.1	Introduction	1151
2.2	Experimental methods	1152
2.3	Pressure differences and diffusion between foam bubbles	1153
2.4	Discussion of the mechanism of gas diffusion in foams	1155
2.5	Experimental verification of the diffusion mechanism	1157
2.6	The degree of dispersion of the gaseous phase	1160
III.	Spontaneous foam destabilization resulting from gas diffusion	1162
3.1	Bubble size frequency distribution in various foams	1163
3.2	Kinetics of foam destabilization caused by transfer of gas between the bubbles	1167
3.3	Experimental investigations of the kinetics of foam destabilization	1169
3.4	Conclusion	1173
IV.	Kinetics and activation energy of film rupture	1173
4.1	Introduction	1174
4.2	Results of cinematographic observations at high speeds	1175
4.3	Activation energy of film rupture	1179
4.4	Stability of "black spots"	1184
V.	Mechanism of film rupture	1186
5.1	Collapse of "unstable" films	1187
5.2	Collapse of "stable" films provoked by a local surface tension depression	1189
5.3	Effect of an adsorption layer on the local thinning of foam lamellae	1191
5.4	Conditions of film rupture induced by a temperature difference	1193

* Reprinted from Communication No. 326 (1957) of the Rubber-Stichting, Oostsingel 178, Delft, The Netherlands and from *Recueil des travaux chimiques des Pays-Bas*, Vol. 77 pages 81–91, 209–223, 283–296, 383–399, and 441–461 (1958). This work formed part of a program of fundamental research on latex problems of the Research Department of the Rubber-Stichting, under the management of the former Director, H. C. J. de Decker.

5.5 Film collapse resulting from induced local temperature differences 1194
5.6 Effect of spontaneous temperature fluctuations in the liquid .. 1196
5.7 Action of antifoaming agents 1200
5.8 Other causes of film rupture 1200
VI. Summary 1201
VII. References 1204

Although the production of foam rubber on an industrial scale has been for a considerable time a rather well-controlled process, all factors involved are still insufficiently known. The most critical phase of the manufacturing process is undoubtedly the gelation of the foam produced. This consists of a clotting of the dispersed rubber particles while a simultaneous destabilization of the dispersed gas bubbles has, however, to be prevented. In order to gain a better insight into the present and similar processes, a fundamental knowledge of foams in general and of their stability conditions in particular is indispensable.

The author studied the technology of foam rubber manufacture in the laboratories of the Rubber-Stichting at Delft and carried out the research described in this review in order to get at the "fundamentals". Since he comes from the University of Utrecht, the school of thought inherent to the laboratories of physical chemistry there has been the basis of his reasoning. He is indebted to Professor J. Th. G. Overbeek for many helpful suggestions.

I. STRUCTURE AND STABILITY OF FOAMS

A critical survey is given of the various factors governing the stability of foams. Special attention is paid to the role of surface tension and to the importance of Gibbs' effect of surface elasticity of thin liquid films. The contribution of the last factor to the free energy of deformation of foam lamellae is estimated.

The two different forms of foam structure which may occur, foams with spherical bubbles and foams containing polyhedral cells, are described. Their differences are explained in particular with respect to the processes responsible for the spontaneous destabilization of foams: transfer of gas between the bubbles and collapse of the lamellae.

1.1. INTRODUCTION

Foams are colloidal systems containing a gas as the dispersed phase. The continuous phase may be liquid or solid. Both solid and liquid foams possess the fundamental characteristic common to all "irreversible" colloids, viz. a very large interfacial area. The interfacial tension and consequently the total free energy of the interface is always positive. Reduction of the interfacial area is, therefore, accompanied by a gain in total free energy and hence foams, like other irreversible colloids, are unstable in the thermodynamic sense. Spontaneous decrease of interfacial area may be observed in liquid foams and in foams in which the continuous phase is slowly changing from the liquid to the gel state (e.g., a rubber latex foam during gelation). Approach to thermodynamic equilibrium (i.e., total phase separation) proceeds at a finite rate; measurements of the rate constants of the irreversible processes leading to equilibrium should provide quantitative information about the factors governing the most conspicuous property of foams, viz. their (relative) stability.

Theories accounting for the stability of foams appeared already in the nineteenth century and were based mostly on the peculiar features of foam structure. Though a liquid foam may be properly defined morphologically as a dispersion of a gas in a liquid, such dispersions are not generally named foams unless the volume concentration of dispersed gas is very high (from 50% to > 90%). This remarkably high volume concentration of the dispersed phase, which is not often encountered in other irreversible colloidal systems, necessitates the average distance between the dispersed gas bubbles to be very small compared with the diameter of the bubbles. A liquid foam may, therefore, be alternatively defined as a two-phase system consisting of the three-dimensional continuous structure of liquid lamellae keeping the enclosed gas subdivided. This is not merely a formal question of definition: more often foam stability has been (or is) discussed not in terms of interaction between dispersed colloidal particles but as a problem of strength and rheological properties of thin liquid films. The best known of these properties is the "elasticity" due to the existence of an interfacial tension between the liquid and the adjacent gas phase. Foam lamellae are highly deformable and may, therefore, be subject to important variations in interfacial area. Any extension of a surface is accompanied by an increase of free energy because work has to be done to bring molecules from the interior to the surface. An equal amount of free energy is released when the surface contracts isothermally. The resistance of a lamella to any deformation leading to extension of its total surface area will be dependent on the surface tension of the liquid. It may be easily demonstrated (see Part IV) that one of the processes responsible for foam collapse, viz. rupture of lamellae, requires indeed a temporary increase of the surface area. The conclusion that a high surface tension will increase the resistance of foam lamellae against rupture seems, nevertheless, to be contradicted by the general notion that a low value of the surface tension of the liquid is desirable in order to obtain a stable foam. A more detailed discussion of the relationship between foam stability and surface tension may bring out its complexity.

1.2. SURFACE TENSION AND FOAM STABILITY

When a given volume of gas is to be dispersed in a unit volume of liquid, the free energy increase coupled with this process will be equal to the product of surface tension and total interfacial area. Therefore, with a given method of producing the foam, lowering the surface tension will permit a higher degree of dispersion of the foam bubbles[1]. Once the foam has been formed, its interfacial area starts to decrease immediately. The gas pressure in the bubbles will be larger than the pressure in the surrounding liquid as indicated by the classical equation of Laplace[2] and Young[3]. For a spherical foam bubble of radius R the pressure excess is equal to $2\gamma/R$, if γ is the surface tension of the liquid. It follows that a pressure difference will exist across a liquid film separating two bubbles of unequal size and hence diffusion of gas will proceed from the smaller to the larger bubble. This phenomenon has already been investigated by Dewar[4]; in accordance with theory it was found by Clark and Blackman[5] that the smallest bubbles in a foam shrink and disappear while the largest ones grow in size. This means that the average bubble size in a polydisperse foam increases with time. The decrease of interfacial area will be slower the smaller the surface tension.

Formation of foam and stability towards the influence of internal pressure differences are thus both promoted by a low surface tension. The influence of

this parameter on the stability against film rupture is less simple. Firstly, it must be borne in mind that pure liquids are unable to form "stable" foams. Liquid lamellae containing no more than one component collapse very rapidly irrespective of the value of the surface tension. Persistent foams have a liquid phase which contains at least two components one of which is preferentially adsorbed at the interface. The surface tension is determined by the amount of adsorbed solute as defined by Gibbs' theorem:

$$d\gamma = -\sum_i \Gamma_i d\mu_i \tag{1.1}$$

where μ_i is the chemical potential and Γ_i the surface excess of the i-th component. Any deformation of the lamella which is accompanied by an increase of its surface area will disturb the adsorption equilibrium and instantaneously decrease the amount of adsorbed solute per unit of area. According to Equation (1.1) the surface tension rises and this increase of tension should counteract further extension of the surface and tend to restore the initial equilibrium. The "elasticity" of foam lamellae is usually attributed to this effect only, although it is evident that extension of the surface always requires a certain amount of free energy, even when the surface tension remains constant. Let us suppose that a liquid film of surface area S will be extended by an amount ΔS as a result of local deformation; the surface tension increases simultaneously by an amount $\Delta\gamma$. Here and throughout the following discussion $\Delta\gamma$ is the average increase of tension of the total deformed surface $S + \Delta S$. The surface free energy change will be positive and equal to:

$$\Delta F_s = \gamma \cdot \Delta S + (S + \Delta S) \cdot \Delta\gamma \tag{1.2}$$

The first term on the right hand side represents the increase of free energy in the absence of a surface tension change, the second term gives the contribution of the variation in tension. The value of the last term has been derived by Gibbs[6] for a film containing two components one of which occurs in greater proportion at the surface than in the interior. The "modulus of surface elasticity" was defined by Gibbs as:

$$E = 2S \frac{d\gamma}{dS} \tag{1.3}$$

Starting from (1.1) the following result was obtained:

$$E = 4\Gamma_2^2 \left(\frac{\partial \mu_2}{\partial G_2} \right)_{G_1} \tag{1.4}$$

G_1 and G_2 are the total quantities of the components per unit area of the film and the subscript 2 refers to the surface active component. Equation (1.4) implies that the extension is performed at an infinitely small rate, because the equilibrium between surface and bulk composition has to be maintained in order to satisfy Gibbs' theorem (1.1). In reality, however, the deformations in a foam lamella are so rapid that equilibrium may be disturbed for an appreciable period of time depending upon the rate of diffusion of the molecules or ions to and from the surface. The surface tension increase following a rapid extension of the surface will, therefore, be larger than given by Equation (1.4). The

relative magnitude of the terms in Equation (1.2) may, nevertheless, be estimated if we consider the two extreme cases: ΔS small and ΔS large.

When $\Delta S \ll S$, Equation (1.2) may be rewritten as follows:

$$dF_s = \gamma dS + S d\gamma \tag{1.5}$$

$$= \left[\gamma + \left(S \frac{d\gamma}{dS}\right)\right] dS \tag{1.6}$$

$$= (\gamma + \tfrac{1}{2}E)\, dS \tag{1.7}$$

where E is given by Equation (1.3).

The relative importance of Gibbs' "surface elasticity" is now given by the ratio $\frac{1}{2}E/\gamma$. An approximate value of E may be either calculated from the surface tension dependence on the activity of the surface active solute, or derived directly from surface pressure measurements in a Langmuir trough if the adsorbed monolayer is insoluble in the substrate. In the latter case the relative increase of surface area dS/S will be equal to the relative increase of area per adsorbed molecule dA/A, and hence:

$$\tfrac{1}{2}E = S \frac{d\gamma}{dS} = - A \frac{d\pi}{dA} \tag{1.8}$$

where the surface pressure π is equal to $\gamma_0 - \gamma$, if γ_0 is the surface tension of the bare surface. The value of the right hand side of Equation (1.8) follows immediately from surface pressure measurements; it can also be derived from surface tension data[7] by putting A equal to $1/\Gamma$:

$$\tfrac{1}{2}E = - A \frac{d\pi}{dA} = - \Gamma \frac{d\gamma}{d\Gamma} \tag{1.9}$$

At very low surface concentrations ($\pi < 1$ dyne/cm) the adsorbed layer behaves as a two-dimensional ideal gas:

$\pi = RT\Gamma$, and hence $\frac{1}{2}E = \pi$. The contribution of the change of surface tension to the free energy increase is, in this case, negligible in comparison with the effect of increasing surface area. The value of the right hand side of Equation (1.8) or Equation (1.9) increases rapidly when the surface concentration becomes higher. From the experimental results reported by various authors[7,8] it may be deduced that $\frac{1}{2}E$ varies between 50 and 125 dynes/cm for condensed adsorption layers of a great many surface active agents. It is, therefore, possible that the contribution of Gibbs' surface elasticity will be 2 to 3 times as large as the free energy change due to the increase of surface area, the value of γ being in the order of 30–40 dynes/cm.

The relative importance of Gibbs' effect will be smaller when ΔS becomes very large. If the deformation of the foam lamella is confined to a small volume element of the film, e.g., at the place where rupture is about to occur, ΔS is of the same order of magnitude as S, the initial surface area of the volume element under consideration.

The instantaneous increase of surface tension is now only of importance in the deformed film element and we may apply Equation (1.2) to this element while neglecting the minor changes occurring in the rest of the film.

Putting $\Delta S = S$, Equation (1.2) can be reduced to:

$$\Delta F_s = (\gamma + 2\Delta\gamma)\, S$$

The instantaneous decrease of surface concentration will now be equal to half the initial value of Γ; the corresponding rise in surface tension is dependent on the composition of the system[7] but will, in general, never be far less than the value of $\gamma_0 - \gamma$.

It follows that the relative importance of Gibbs' effect is now given by the magnitude of the ratio: $2(\gamma_0 - \gamma)/\gamma$.

For very low values of the surface concentration this ratio will be smaller than 1; it increases with increasing surface concentration and will reach a maximum value of the order of 2 for most aqueous foams where the surface tension is about half as great as the surface tension of pure water.

Our discussion of both extreme cases of surface deformation thus leads to the conclusion that, in all instances of practical interest, the contribution of the rise in surface tension to the free energy of deformation is of the same order of magnitude as the effect of increasing surface area if, at least, the rate of deformation is much larger than the rate of attainment of equilibrium.

Rapid deformations of foam lamellae are not necessarily caused by mechanical disturbances but may also be due to a change of thermal equilibrium leading to a local temperature rise in the foam lamella. The surface tension of liquids generally decreases with increasing temperature and hence a local increase of temperature will be followed by a decrease of surface tension in the warmer portion of the film. Free energy might be gained when the surface area of this part of the film increases in relation to the surface of the colder surrounding part. The warmer part will, consequently, become thinner. This phenomenon, already known to Dupré[9], was probably demonstrated for the first time by Plateau[10], who was able to show that the warmth of a finger brought near to a very large soap bubble was sufficient to cause a diminution of thickness indicated by a change of color from yellow to green.

It is generally recognized that liquid lamellae are more liable to rupture the smaller their thickness; a local temperature rise followed by thinning should, therefore, increase the probability of rupture. It is, however, evident that the ultimate degree of thinning will be dependent on the relative magnitudes of the local surface tension depression caused by the temperature difference and the rise of tension due to the increase of surface area of the warmer film element. The influence of a local temperature rise on the stability of foam lamellae will be discussed in more detail in Part V.

1.3. DRAINAGE AND FOAM STABILITY

All liquid foams are subject to drainage of the liquid from between the bubbles due to the action of gravity. Drainage is accompanied by a progressive thinning of the lamellae and may, therefore, enhance the probability of film collapse. Brady and Ross[11] have developed a quantitative theory of foam stability based on a simplified picture of the foam structure. They assume that the rate of thinning due to drainage is the same for all lamellae and that rupture takes place instantaneously after a certain "critical" thickness has been reached. The total lifetime of a foam should then be proportional to the kinematic viscosity of the liquid and to the initial height of the foam column if the foam is regarded as a series of vertical films. Although this relationship was

confirmed for the foams of some hydrocarbon oils the proposed theory is not generally valid. Its main fallacy is the assumption that every lamella ruptures immediately after attaining the critical thickness. It is wellknown from the experiments of Plateau and Dewar, for example, that thin liquid films are able to persist for very long times (depending upon the external circumstances) without any appreciable change of thickness, if the film is composed of a solution able to form stable foams. In these cases no unique relationship can exist between the rate of thinning and the lifetime of a foam lamella. A critical thickness at which rapid collapse takes place may, however, exist in the case of films of pure liquids[12] and of solutions[13] that are not able to form stable foams. It will be shown in Part V that the spontaneous collapse of these films can be explained perfectly by the interaction of the mutual attractive forces of the liquid molecules. The magnitude of these forces increases rapidly with decreasing film thickness, which explains the fact that sudden collapse takes place only after attainment of a certain critical thickness.

In order to account for the arrest of drainage in stable films at a certain limiting thickness (which may be as low as 120 A) Gibbs supposed that the interior of these films, as well as the upper layer of a large volume of liquid, will behave as having a "gelatinous consistency". The extremely large resistance towards deformation of the surface layer of foam-forming solutions was already known to Plateau who introduced the concept of "surface viscosity". Although many theoretical and experimental investigations in the field of surface rheology have been reported since then[14], the influence of surface viscosity and surface yield value on the stability of foams has only recently been demonstrated[15]. The effect of these properties is, probably, not only due to their influence on drainage in the very thin lamellae but also to the increased resistance towards rapid deformations of all lamellae in a foam.

Drainage in thin films can also be retarded and even totally arrested as a result of double layer repulsion in the case of charged interfaces[13]. The importance of double layer interaction might, in principle, be deduced from the influence of the ionic strength on foam stability. The problem is, however, complicated by the fact that various parameters affecting foam stability (density of the adsorbed monolayer, rate of lowering of surface tension, surface viscosity) may all be dependent on the activity of electrolytes. A straightforward and unique relationship between foam stability and ionic strength is, therefore, in general not to be expected. The same is true for the relation between foam stability and surface potential. A detailed discussion of the mechanism and kinetics of film collapse will allow us, however, to estimate the importance of double layer interaction (Parts IV and V).

1.4. FOAM DRAINAGE AND BUBBLE SHAPE

The most stable shape of a single gas bubble surrounded by liquid is the sphere, having the smallest possible surface area for a given volume of gas. When a gas is dispersed in a liquid all bubbles will tend to attain the spherical shape. It is, therefore, necessary that the bubbles in a foam be polydispersed if the volume concentration of gas becomes higher than 74% and the spherical shape is to be conserved. Polydispersity promotes, however, instability of a foam because of the pressure differences existing between spherical bubbles of unequal size. Many persistent foams do not consist of spherical bubbles but contain very regularly built cells of polyhedral shape all of which may be of equal or nearly equal size.

Foam structure and bubble shape are independent of the method by which the foam is produced but are determined only by the concentration of gas in the foam. The influence of the gas concentration is illustrated by Figures 1.1 and 1.2. The first picture (1a) is a photomicrograph of a foamed oil-in-water emulsion. This emulsion was prepared by dispersing a mixture of 57 volumes of monochlorobenzene and 43 volumes of paraffin oil in 100 parts of a 0.18 molar solution of sodium laurate. The emulsion did not cream and its viscosity was 11.0 centipoises at a rate of shear of 900 sec^{-1}. The foam contained 7.5 volumes of liquid and 92.5 volumes of air.

The foam was produced by whipping the emulsion by means of an ordinary, electrically driven, household beating apparatus. The foam bubbles are nearly perfectly spherical as is equally the case with the foam on picture 2a, which was produced by the same method from an emulsion of similar composition, but

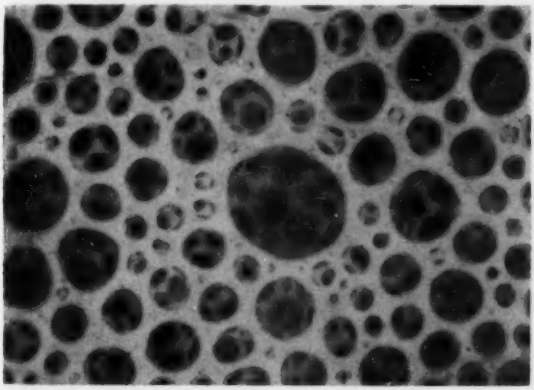

a) Time = 0; magnification (linear) = 16.

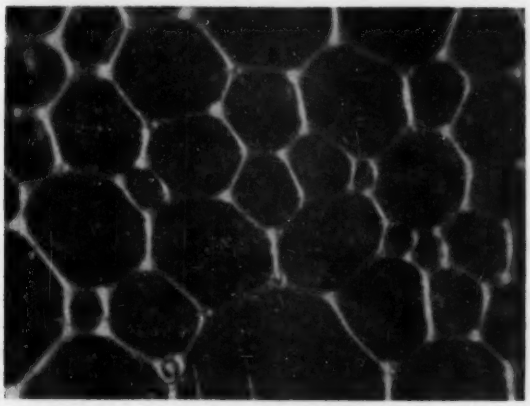

b) Time = 15 min; magnification (linear) = 16.

FIG. 1.1.—Foamed oil-in-water emulsion. Concentration of air = 92.5 vol %. Viscosity of liquid = 11 cp.

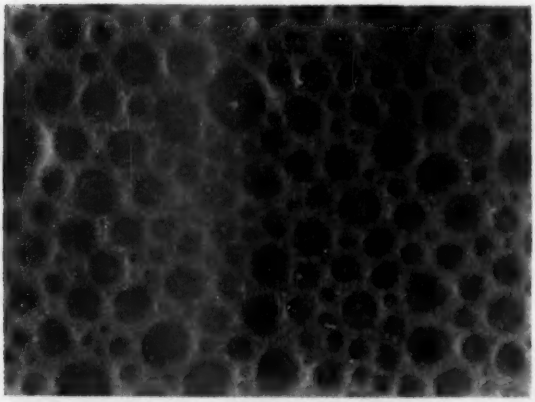

a) Time = 0; magnification (linear) = 16.

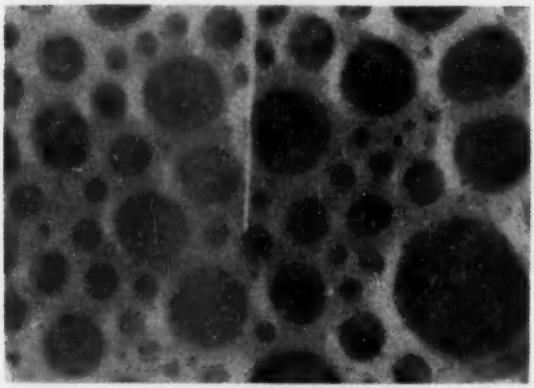

b) Time = 15 min; magnification (linear) = 16.

FIG. 1.2.—Foamed oil-in-water emulsion. Concentration of air = 92.5 vol %. Viscosity of liquid = 65 cp.

having a volume concentration of 70% and consequently an appreciably higher viscosity viz. 65 centipoises (rate of shear 900 sec^{-1}). The air content of the foam was the same as in 1a (92.5 vol%).

Pictures 1b and 2b show both foams 15 minutes after they had been produced.

Whereas the bubbles in foam 2 have changed only in size but have preserved their spherical shape, the morphological structure of foam 1 has totally changed. The rate of drainage in foam 1 was much larger than in foam 2: as a result, the liquid content of foam 1 has considerably decreased during 15 minutes and the lamellae have become planes meeting at angles of 120°. Since the original foam was polydisperse, the polyhedral air cells formed after drainage are also of unequal size. If, however, the original spherical bubbles are monodispersed (which may be accomplished, e.g., by pressing the air into the liquid through

narrow orifices of equal diameter), a very regular structure of equal-sized polyhedral foam-cells is obtained.

A peculiar feature of polyhedral foam structure is the strong curvature of the surfaces of a lamella at the edges where three bubbles meet. According to the fundamental equation of Laplace and Young the pressure in the liquid of these edges should be lower than in the liquid of the bubble walls. This pressure difference will be the cause, as was first pointed out by Plateau, of a suction exerted upon the liquid in the walls, by which the lamella thickness will be reduced. Hence in foams with polyhedral gas bubbles two different forces are active in effecting a progessive thinning of the lamellae, viz. gravitation and capillary suction. The effects of both forces may be additive in some parts of a lamella and opposite in other parts; the flow pattern in such a lamella is, therefore, very complex as may be easily observed in a single, vertically placed liquid film. The edges contain a much larger volume of liquid than the thin walls between two bubbles (on photograph 1b the walls are totally invisible because of their thinness). It may be expected that foams with polyhedral gas bubbles will be more liable to film rupture: on the other hand, pressure differences across the lamellae will be much smaller because of the very slight curvature of the larger part of the bubble walls. The decrease of total interfacial area resulting from gas transfer between the bubbles has been investigated in foams containing spherical cells; the results are reported in Parts II and III. The process of film collapse, which is of overwhelming importance in polyhedral foams, will be examined in Parts IV and V.

II. GAS DIFFUSION IN FOAMS

Pressure differences between foam bubbles of unequal size are the cause of gas transfer from small to larger bubbles. The rate at which the small bubbles decrease in size is calculated as a function of the radius of the bubbles, the surface tension of the liquid and the thickness and permeability of the liquid lamellae between the bubbles. The calculation is based on the assumption that the pressure difference between a small and an adjacent large bubble is dependent only, to a first approximation, on the radius of the smaller bubble.

Values of the average lamella thickness calculated by means of the derived rate equation from the observed rate of shrinking of small bubbles in various foams, are of the right order of magnitude, if it is supposed that the permeability of the lamellae is determined by the solubility and the diffusion constant of the gas in the liquid.

The rate equation enables the number of bubbles per unit volume of foam to be expressed as a function of time if the initial bubble size frequency distribution is known. It is shown that the bubble size distribution function can be calculated from the bubble sizes observed in the plane of contact between the foam and the glass wall of a container. An experimental method of determining the number and sizes of the bubbles in this plane is described.

2.1. INTRODUCTION

Spontaneous decrease of the interfacial area between liquid and gas takes place in all liquid foams. The resistance towards this reduction of interfacial area may be regarded as a measure of the stability of the foam; measurements of the rate at which the decrease of interfacial area proceeds may thus provide a quantative evaluation of the foam stability.

It has already been mentioned in Part I of this series that two different processes are responsible for the changes in degree of dispersion of the gas bubbles in a foam, viz.:

a) diffusion of gas from high pressure regions to regions of lower pressure, which entails total disappearance of part of the gas bubbles.
b) collapse of liquid lamellae and subsequent coalescence of adjacent gas bubbles.

In the present and the following section the mechanism and kinetics of the first process will be discussed in connection with the results of experimental investigations of various liquid foams.

2.2 EXPERIMENTAL METHODS

The foams were prepared by whipping 50 mls of the liquid in a container by means of an ordinary, household whipping apparatus equipped with an electric motor (Precision Scientific Co., Chicago). Whipping was executed with constant speed until the desired volume of gas (in most of the experiments air was used) was entrained. Immediately after whipping, a sample of the foam was poured into a small rectangular glass container, on one of the outer flat walls of which 16 squares were engraved each occupying an area of 0.0025 cm^2. By four successive countings of the number of bubbles in four different squares the average total number of gas bubbles per unit area of cross section was determined. The plane of contact between the flat wall and foam was observed with a microscope (magnification: 27 $\times$). Determination of the total number of bubbles was repeated every second minute and, in this way, the degree of dispersion of the gas bubbles could be assessed rapidly as a function of time.

In many cases photomicrographs were also taken in order to determine the bubble size distribution in the cross section. Representative micrographs are reproduced in Figure 1.2 of Part I. Bubble size distribution functions were calculated by assuming the observed bubbles to be perfect spheres.

In general the measured diameters will differ slightly from the true ones. The angle of contact between liquid and glass does not appear to have any influence on the observed diameters since coating the inner glass wall with paraffin or replacing the glass by other materials like polymethyl methacrylate did not appreciably affect the results obtained. The presence of the surface-active agent in the aqueous phase is evidently sufficient to assure complete wetting of the walls of the container. Disagreement between the real and observed values of the bubble diameters will be caused mainly by

(a) distortion of the gas bubbles in the front layer next to the glass wall. As a result of hydrostatic pressure the bubbles in the front layer will be somewhat flattened and their shape will, therefore, deviate from that of a perfect sphere. Because of this effect the observed diameters will be larger than the real diameters of equal-sized bubbles in the interior of the foam.

(b) limited transparency of the liquid in the foam. In order to observe the real diameter of a sphere in the front layer light should be transmitted through the liquid between the bubble and the glass wall over a distance equal to the radius of the sphere. In the case of opaque liquids like oil or rubber emulsions this distance might be somewhat smaller; then the observed diameter is not that of the sphere but that of a cross section cut through the sphere by an imaginary plane parallel to the wall. As a result of this effect the observed diameters will be smaller than the real ones.

Distortion of the bubbles and limited transmission of light affect the discrepancy between real and observed values of the bubble diameters in opposite directions. The total effect has been assumed, therefore, to be negligible. The relationship between the bubble size distribution in the interior of the foam and the bubble size distribution in the front layer next to the wall of the container will be discussed in Section 2.6.

Foam densities were determined by weighing a given volume of foam; the volume concentrations of dispersed gas were calculated from the densities of the foam and the liquid.

2.3. PRESSURE DIFFERENCES AND DIFFUSION BETWEEN FOAM BUBBLES

A most important consequence of the existence of free surface energy is the presence of a pressure difference across a curved liquid-gas interface. The pressure deficiency under a concavely curved meniscus gives rise to the well known capillary elevation of a liquid in a small tube. If the curved liquid surface fully encloses the volume of gas, as occurs with the bubbles in a foam, the pressure excess of the gas in the bubbles can be easily calculated from the curvature of the surface and the surface tension of the liquid[16].

If γ is the surface tension of the liquid and r the radius of the bubble, the pressure excess will be equal to:

$$\Delta p = \frac{2\gamma}{r} \tag{2.1}$$

It appears from Equation (2.1) that the pressure excess in a foam bubble is proportional to the surface tension of the liquid and inversely proportional to the radius if the bubble is a perfect sphere. In general, for any shape of bubble:

$$\Delta p = \gamma \left(\frac{1}{r_1} + \frac{1}{r_2} \right) \tag{2.2}$$

where r_1 and r_2 are the principal radii of curvature of the bubble.

The pressure in the bubbles of a foam may be calculated by means of Equation (2.1) if the size of the globules is known. Since foams with spherical gas bubbles are nearly always polydisperse, the pressures in the different bubbles will not be the same and hence diffusion of gas takes place from regions of high pressure (small bubbles) to regions of lower pressure (large bubbles). The rate at which the diffusion proceeds will be proportional to the pressure difference and the permeability of the liquid film separating the bubbles of unequal size.

All bubbles in the interior of a foam will either grow or become smaller and disappear depending on their diameter and the diameter of the bubbles in their environment. All bubbles in the top layer of a foam column which are adjacent to the atmosphere above the foam will shrink and disappear because of their pressure excess.

In general, each large bubble is surrounded by a great many smaller ones that disappear as a result of the transfer of gas from the smaller bubbles to the large one. The pressure difference between the gas in a small bubble and that in the large one is equal to:

$$2\gamma \left(\frac{1}{r} - \frac{1}{R} \right) \tag{2.3}$$

where r = radius of small bubble and R = radius of large bubble.

R will be many times larger than r (e.g., 20 times as large) and $1/R$ may therefore be neglected in comparison with $1/r$ to a first approximation. The pressure difference causing diffusion is then equal to the pressure excess in the small bubble. The rate at which a small bubble in the foam shrinks and disappears is thus assumed to be dependent only on its own radius.

The diffusion equation may be written as:

$$-\frac{dn}{dt} = D \cdot A \frac{\partial c}{\partial x} \tag{2.4}$$

where $-dn/dt$ is the number of moles of gas passing per second through the film separating the bubbles and D the diffusion constant.

A, the area of the film through which the gas diffuses will be approximately equal to the surface area of the small bubble, i.e. $= 4\pi r^2$. (Figure 2.1.)

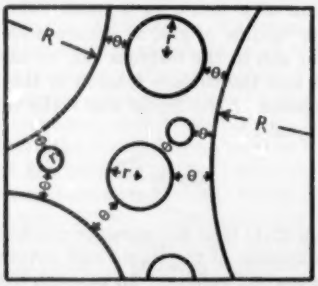

FIG. 2.1.—Schematic representation of cross section through a foam.

$\partial c/\partial x$ is the concentration gradient of the gas in the liquid film which, assuming the diffusion to be in the stationary state, may be put equal to $\Delta c/\Theta$, where Θ is the average thickness of the liquid film and ΔC the difference in concentration across the film from $x = 0$ to $x = \Theta$.

According to Henry's law the concentration difference is proportional to the pressure difference across the film, or:

$$\Delta C = S \cdot \Delta p = S \cdot \frac{2\gamma}{r}$$

if S is the solubility of the gas expressed in moles of gas per ml of liquid at a pressure of 1 dyne/cm^2.

From Equation (2.4) if follows that:

$$-\frac{dn}{dt} = D \cdot 4\pi r^2 \cdot \frac{2\gamma S}{r\Theta} \tag{2.5}$$

The number of moles of gas in the small bubble may also be expressed as a function of the bubble radius. If the ideal gas law is obeyed.

$$n = \frac{4/3\pi r^3}{RT}\left(p_0 + \frac{2\gamma}{r}\right) \tag{2.6}$$

where p_0 is atmospheric pressure. The excess pressure in the bubble, $2\gamma/r$, is always very small compared with the atmospheric pressure and may be neglected in Equation (2.6).

After inserting n from Equation (2.6) into the diffusion Equation (2.5) integration gives:

$$r_0^3 - r^3 = \frac{4RT}{p_0} \cdot \frac{D \cdot S\gamma}{\Theta} t \tag{2.7}$$

where r_0 = initial value of the bubble radius at $t = 0$. It follows that a plot of r^3 against time should be a straight line, the slope of which is proportional to the diffusion constant and the solubility of the gas in the liquid, proportional to the surface tension and inversely proportional to the average thickness of the liquid films separating the small vanishing bubbles from the large ones.

With the aid of Equation (2.7) it should be possible to calculate the number of bubbles in a foam disappearing per unit of time if the initial bubble size distribution in the foam is known. Before proceeding to this calculation, however, it will be useful to consider critically the assumptions and approximations underlying the derivation of Equation (2.7).

2.4 DISCUSSION OF THE MECHANISM OF GAS DIFFUSION IN FOAMS

a) In the foregoing section it has been assumed that the transfer of gas from relatively small to larger foam bubbles is governed by the rate of steady state diffusion of the gas molecules in the liquid films between the bubbles and the solubility of the gas in the liquid. This assumption implies that the rate of dissolution of the gas at the interface of the small bubble and the rate of evaporation at the interface of the large bubble are very large compared with the rate of diffusion.

If, however, the diffusion of gas molecules through the liquid membrane is not the rate-determining part of the permeation process, Equation (2.5) is no longer valid, because the concentrations of dissolved gas at the boundaries of the liquid film then are not equal to the equilibrium concentrations given by Henry's law.

Equation (2.4) may be rewritten as:

$$-\frac{dn}{dt} = P \cdot A \cdot \frac{\Delta p}{\Theta} \tag{2.8}$$

where P is defined as the permeability of the film.

It has been shown[17,18] that, in general, in a stationary state of permeation:

$$P = \frac{D \cdot S}{1 + 2D/K\Theta} \tag{2.9}$$

In the derivation of this equation the rate of passage through the boundary surfaces has been assumed to be:

$$-\frac{dn}{dt} = K(C_0^{eq} - C_0) \tag{2.10}$$

where C_0 is the concentration of dissolved gas at $x = 0$, and C_0^{eq} is the equilibrium concentration at $x = 0$ as given by Henry's law: $C_0^{eq} = S \cdot p$.

It follows from Equation (2.9) that:

$$P \simeq D \cdot S \tag{2.11}$$

if $2\,D/K\Theta \ll 1$.

In this case the rate of diffusion is much smaller than the rate of dissolution and hence Equation (2.5) will be valid to a high approximation. In the other extreme case: $2D/K\Theta \gg 1$, Equation (2.9) may be written as:

$$P \simeq \tfrac{1}{2} K \cdot S \cdot \Theta \tag{2.12}$$

Equation (2.8) may then be reduced to:

$$-\frac{dn}{dt} = \tfrac{1}{2} A \cdot K \cdot S \cdot \Delta p$$

which means that the transfer of gas has become independent of the diffusion constant and the thickness of the liquid film.

In our derivation, Equation (2.11) is used instead of the more complete expression for P, Equation (2.9). The inaccuracy resulting from this approximation depends on the value of the factor $2D/K\Theta$.

Since no reliable data on the value of K are known in this case, it is not possible to estimate the error introduced by using the approximate Equation (2.11). Its use should result in too high a value for P and consequently for Θ. In Section 2.5 it will be shown, however, that the values for Θ calculated by means of Equation (2.7) are in general *lower* than the real ones from which it may be inferred that the correction for a finite rate of dissolution and evaporation is not very important.

b) The pressure difference existing between a small bubble and a large one is equal to $2\gamma\ (1/r - 1/R)$, Equation (2.3).

The assumption that $1/R \ll 1/r$ and that consequently the last term of Equation (2.3) may be neglected, introduces an error the magnitude of which can be estimated from the observed bubble size distributions of a great many foams. The determination of the bubble size distribution in various foams shows that in the foams investigated, usually more than 30% of the bubbles have a radius smaller than $2.5 \cdot 10^{-3}$ cm whereas the largest bubbles have radii larger than $25 \cdot 10^{-3}$ cm. Should transfer of gas occur from a bubble with radius r to one with radius $10\ r$ the calculated rate of diffusion according to Equation (2.5) would be 10% higher than the real value. Taking into account the measured bubble size distributions and the fact that the small vanishing bubbles will be preferentially situated in the neighborhood of much larger bubbles, a maximum deviation of 20% between real and calculated rate of bubble size change may be expected.

c) The area through which the gas escapes from a small bubble and diffuses to a larger one has been taken equal to the surface area of the small bubble. This will be approximately true if a small bubble "loses" its enclosed volume of gas to more than one large bubble at the same time. If, however, transfer of gas takes place between two bubbles only, the "escape area" will be smaller and approach the value of half the surface area of the small bubble. The latter case will, probably occur less often than the former one as may be inferred from the Figures 1.2a (in Part I) and 2.1. A quantitative estimation of this

correction has not been attempted but it might be accounted for by multiplying the theoretical rate of bubble size change (right-hand side of Equation (2.7) by a factor a where $\frac{1}{2} < a < 1$.

All corrections discussed tend to decrease the rate of change of bubble size. A calculation of the film thickness Θ from the observed rate of decrease in bubble size if D, S and γ are known, will, therefore, be rather inaccurate but may nevertheless be expected to give values of the right order of magnitude.

2.5. EXPERIMENTAL VERIFICATION OF THE DIFFUSION MECHANISM

If the transfer of gas between the bubbles in a foam is really caused by the existing pressure differences, this diffusion should result in small bubbles becoming smaller and large bubbles becoming larger. The rate at which the

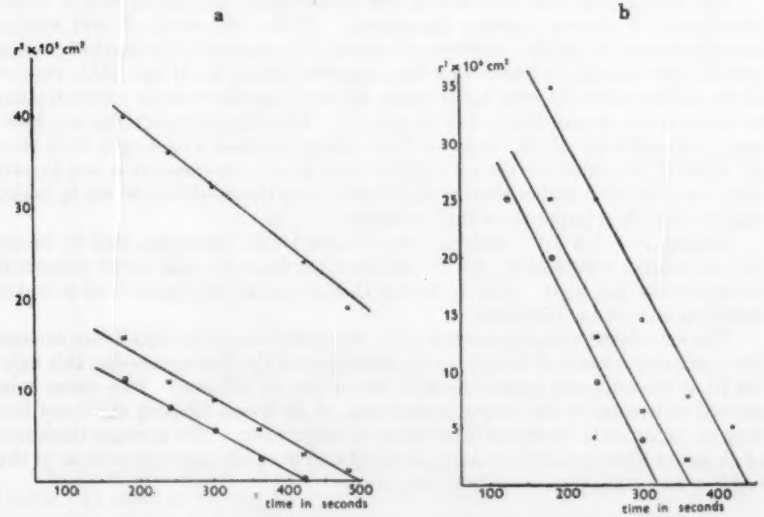

FIG. 2.2—Square of bubble radius as a function of time. a) Foams of oil-in-water emulsion. Composition of liquid phase: 57 vol of monochlorobenzene, 43 vol of paraffin oil, 43 vol of water (air content of foam: 92.5 vol %). A photomicrograph of this foam has been reproduced in Figure 1.2 of Part I. b) Foam of 60% Hevea rubber latex (air content of foam: 92.5 vol %).

small bubbles become smaller and finally disappear is then given by Equation (2.7). The progressive disappearance of small bubbles will result in a decrease in the number of bubbles per unit volume of foam with time. A determination of the rate of change of bubble concentration should, in principle, allow us to calculate the rate at which the small foam bubbles disappear.

Before showing how such a calculation may be accomplished, in the next section, some results will be given of an attempted direct experimental verification of the diffusion mechanism.

The change in radius of various foam bubbles was followed by taking photomicrographs of a given area of the plane of contact between the foam and the glass wall of the container. The foams investigated were prepared by whipping the desired volume of air into an oil-in-water emulsion or into a sample of Hevea rubber latex. The foams of these relatively viscous emulsions have a

very low rate of drainage and contain approximately spherical air bubbles at the densities investigated. From comparison of photomicrographs taken at different moments it could be shown that the largest bubbles grow and the smaller bubbles decrease in size. Identification of some individual bubbles made it possible to follow the process of change in bubble size. In Figure 2.2 data are plotted for the square of radius as a function of time. It appears that for both oil-in-water emulsion foam and Hevea latex foam this function is fairly well represented by a straight line. From the slope of the curve the average thickness of the liquid film surrounding the shrinking air bubble may be calculated by means of Equation (2.7). Taking the permeability $P(= D \cdot S)$ of water for air to be equal to $1.5 \cdot 10^{-11}$ mole $cm^{-1} \cdot sec^{-1} \cdot atm^{-1}$ the value of Θ would be equal to $4 \cdot 10^{-4}$ cm for the oil emulsion foam and $1.6 \cdot 10^{-4}$ cm for the latex foam.

The assumption that the value of the permeability is equal to that of water introduces, of course, another inaccuracy. If the dispersed oil and rubber globules should be totally impermeable to air, the amount of permeated gas per unit of time should be equal, to a first approximation, to 30 and 40%, respectively, of the value for pure water (these figures being the volume concentration of water in the oil and the rubber emulsion). The dispersed particles are, however, permeable to air: the value of P for rubber is about 4 times less than that for water[19], the value for the oil mixture used in our experiments is not known but it may be even higher than that of water since the solubility of air in many organic liquids is larger than that in water.

Taking $P = 1.5 \cdot 10^{-11}$ mol $cm^{-1} \cdot sec^{-1} \cdot atm^{-1}$ will, therefore, lead to incorrect calculated values of Θ; for the rubber latex foam the calculated value will be somewhat too high. The deviation in the case of the foamed oil-in-water emulsion cannot be predicted.

The calculated value represents only the thickness of the liquid film around the particular identified bubble or the thickness of the film separating this bubble from the adjacent larger one into which the air diffuses. This value is in general not equal to the average thickness of all liquid films in the foam but may be expected to be of the same order of magnitude. The average thickness of all liquid films in the foam may be calculated from the average volume of the bubbles and the average surface area, since

$$1 - \sum N_i v_i = \tfrac{1}{2}\Theta \sum N_i s_i \qquad (2.13)$$

where N_i is the number of bubbles per unit volume of foam with volume v_i and surface area s_i.

Equation (2.13) may be written as: $1 - N\bar{V} = \tfrac{1}{2}\Theta \cdot N\bar{S}$, where $N = \sum N_i$ and $\bar{V}$ and $\bar{S}$ are the average volume and the average surface area of the foam bubbles. After introducing φ, the volume concentration of gas in the foam, the following expression is finally obtained:

$$\Theta = 2\left(\frac{1}{\varphi} - 1\right)\bar{V}/\bar{S} \qquad (2.14)$$

The calculation of average bubble volume $(4/3\ \pi\overline{r^3})$ and average bubbel surface area $(4\pi\overline{r^2})$ from the observed diameters of the bubbles in the plane of contact between the foam and the wall of the container will be described in Section 2.6. For the oil emulsion and the rubber latex foam the value of the

average film thickness calculated according to Equation (2.14) is $6.6 \cdot 10^{-4}$ cm and $6.2 \cdot 10^{-4}$ cm, respectively. These values are appreciably larger than the values calculated from the measured rate of change in bubble size though they are of the same order of magnitude. Both values are relatively inaccurate; too much importance should not be attached, therefore, to the exact magnitude of the difference between the two calculated values. Yet it appears reasonable to conclude that the value of Θ calculated from the rate of bubble size change is certainly not too high. This means that it is not necessary to postulate the presence of a potential barrier against diffusion at the gas-liquid interface because in that case the calculated thickness of the liquid film should be larger than the value given by Equation (2.14).

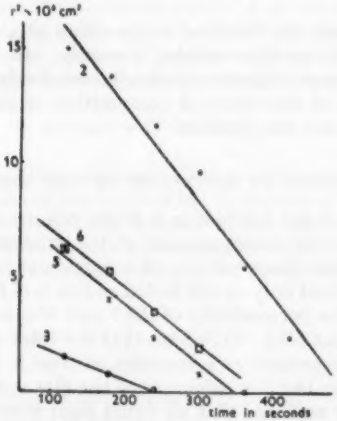

FIG. 2.3—Square of bubble radius as a function of time. Data derived from Clark and Blackman[20], Figure 3.

Clark and Blackman[20] have performed similar experiments with a number of foams. In order to explain the experimental results they derived an expression for the rate of change in bubbles size by assuming the pressure difference to be equal to:

$$2\gamma(1/r - 1/r_m)$$

where r_m is constant over a certain time interval. The predicted dependence of the bubble diameter as a function of time was obeyed by a foamed solution of sodium isopropylnaphthalenesulfonate and hydrolyzed glue. In Figure 2.3 some of their results are plotted according to our Equation (2.7). This equation appears to give also a fair description of the experimental results. From the slope of the four straight lines a value of $14 \cdot 10^{-4}$ to $30 \cdot 10^{-4}$ cm can be calculated for the thickness of the liquid films in the foam, which may be compared with the value of about $10 \cdot 10^{-4}$ cm for the average film thickness calculated from the observed approximate bubble size distribution.

The effect of diffusion of gas from a single, isolated bubble on the decrease of bubble diameter has recently been reported by Brown, Thuman and McBain[21]. These authors determined the rate of decrease in bubble size by observation of single bubbles floating at the surface of detergent solutions.

Their data appeared to fit an r^2 *versus* time plot as demanded by theory. The slope of the plots was dependent on the composition of the detergent solution. The authors suggest that the dependence on composition is caused by the effect of the structure and coherence of the adsorbed detergent film at the gas-liquid interface on the permeability of the liquid bubble wall. The results might also be explained, however, by assuming the thickness of the liquid layer to be dependent on the composition. Unfortunately, the thickness of the bubble walls in these experiments is not known; application of Equation (2.7) to the case of a single bubble and insertion of the experimental results shows that the thickness Θ should have varied between $0.2 \cdot 10^{-4}$ cm and $2.2 \cdot 10^{-4}$ cm if no specific effects of the surface structure exist. These extreme values have been taken from the data of Brown, Thuman, and McBain on solutions of various commercial detergents.

The relation between the chemical composition of a detergent solution, its physical properties like surface tension, viscosity, etc. and the thickness of lamellae arising from such a solution is very incompletely known, which makes a definite explanation of the effect of composition of solution on the rate of change of bubble size not yet possible.

2.6. THE DEGREE OF DISPERSION OF THE GASEOUS PHASE

The total number of gas bubbles in a given volume of foam will gradually decrease as a result of the disappearance of the smallest bubbles. The time interval needed for total disappearance of a particular bubble is, according to Equation (2.7), dependent only on the initial radius r_0 of the bubble, the surface tension of the liquid, the permeability of the liquid film surrounding the bubble and the thickness of that film. It follows that the total number of bubbles per unit volume may be expressed as a function of time if the initial bubble size distribution in the foam and the thickness of the film surrounding each bubble are known. It will be assumed that all liquid films surrounding the small disappearing bubbles have the same average thickness Θ. In that case the total number of bubbles N per unit volume of foam at a time $t = t_\rho$ will be equal to the initial number N_0 at the time $t = 0$ diminished by the number of bubbles vanished during tye time-interval t_ρ, i.e., the number of bubbles with initial radius equal to or smaller than ρ, where the relationship between ρ and t_ρ is given by:

$$\rho = \left(\frac{4RT \cdot D \cdot S \cdot \gamma}{p_0 \Theta} t_\rho \right)^{\frac{1}{4}} \tag{2.15}$$

This equation is derived from Equation (2.7) by putting $r_0 = \rho$ and $r = 0$.

If $F(r)$ is the size frequency distribution function of the bubbles in the foam at $t = 0$,

$$N_{t_\rho} = N_0 \left\{ 1 - \int_0^\rho F(r) dr \right\} \tag{2.16}$$

Integration of the initial bubble size frequency distribution function between the limits $r = \rho = \left(\frac{4RT \cdot D \cdot S \cdot \gamma}{p_0 \Theta} t_\rho \right)^{\frac{1}{4}}$ and $r = 0$ will thus enable us to calculate N as a function of t with the aid of Equation (2.16).

The distribution function $F(r)$ must be determined from the observed radii

of the bubbles counted in a given area of the plane of contact between the foam and the wall of the container. All bubbles counted on the enlarged photomicrographs were assigned to a number of groups according to their radii. From the number of bubbles in every size group and their mean radius, a frequency distribution may be computed. This function, however, does not represent the frequency distribution of the bubble sizes in an arbitrary volume of foam but only the size frequency distribution of the bubbles in the front layer of the foam next to the glass wall.

In order to calculate the relationship between the two distribution functions let us consider the distribution of bubble sizes in any arbitrary plane cut through a volume of foam. If n is the total number of bubbles counted in one square cm of this plane and $f(r)$ is their size frequency distribution function, the number of bubbles with radius between r and $r + dr$ coming within reach of the plane per unit of area is equal to: $nf(r)dr$. It will be obvious that this number is proportional to the total number of bubbles with radius between r and $r + dr$ per unit of volume multiplied by the diameter of these bubbles, or:

$$nf(r)dr = C \cdot 2r \cdot N \cdot F(r)dr \tag{2.17}$$

where C is a proportionality constant. For an exact calculation of C the distribution of the positions of the bubbles in the volume of foam should be specified. If the bubbles are randomly distributed throughout the whole foam volume, C will be equal to 1 for any plane cut through the foam. The relation between n and N is then found immediately by integrating Equation (2.17):

$$n = 2N \int_0^\infty rF(r)dr = 2N\bar{r} \tag{2.18}$$

where $\bar{r}$ is the mean radius of all bubbles in the foam.

In general for any value of C:

$$n = 2CN\bar{r} \tag{2.19}$$

The relationship between the two distribution functions can be derived by combination of Equations (2.17) and (2.19):

$$f(r) = r/\bar{r} \cdot F(r) \tag{2.20}$$

The plane of contact between foam and glass is, however, not an arbitrary plane. The bubbles in the front layer next to the glass wall all have their centers lying at one side of the plane of contact only, whereas the bubbles in the interior of the foam which are within the reach of an arbitrary plane have their centers at either one or the other side of that plane. It has, nevertheless, been established by various authors[22] that the bubble size frequency distribution function in the front layer is nearly the same as that in any other section of the foam. The distribution of bubble sizes in the front layer is, consequently, also given by Equation (2.20). The number of bubbles per unit area of the observed layer will be given by Equation (2.19) where C is smaller than 1, which means that the number of bubbles counted in 1 square cm of the plane of contact will be less than the number present in a volume of foam numerically equal to twice the average radius of the bubbles.

Equation (2.20) may also be written as follows:

$$f(r) = r \cdot \frac{\overline{1}}{r_f} \cdot F(r) \tag{2.21}$$

where $\overline{1}/r_f$ is the average inverse radius of the bubbles in the front layer. Equation (2.21) is derived from Equations (2.17) and (2.19) and allows the distribution function $F(r)$ to be calculated from the observed function $f(r)$.

The moments of $F(r)$ can be directly derived from the observed radii in the front layer. Multiplication of both sides of Equation (2.21) by r (or r^2) and subsequent integration from $r = 0$ to $r = \infty$ gives:

$$\overline{r^2} = \overline{r_f} \Big/ \frac{\overline{1}}{r_f}, \quad \text{and} \quad \overline{r^3} = \overline{r_f^2} \Big/ \frac{\overline{1}}{r_f} \tag{2.22}$$

where $\overline{r_f}$ and $\overline{r_f^2}$ are average radius and average square radius of the bubbles in the front layer.

Average surface area and average volume of the foam bubbles may now be calculated from the experimental data by means of Equation (2.22). The expression for the average thickness of the liquid lamellae (Equation 2.14) becomes finally:

$$\Theta = \frac{2}{3}\left(\frac{1}{\varphi} - 1\right) \overline{r_f^2} \Big/ \overline{r_f} \tag{2.23}$$

Use of the above results will be made in the next part in order to interpret the experimental investigations of spontaneous foam destabilization.

III. SPONTANEOUS FOAM DESTABILIZATION RESULTING FROM GAS DIFFUSION

Bubble size frequency distribution in foamed Tee-pol solutions, oil-in-water emulsions and Hevea rubber latex have been calculated from the observed bubble sizes in the plane of contact between the foam and the glass wall of the container. The bubble size distribution in these foams can be satisfactorily described by the same mathematical expression containing one adjustable parameter.

Using this expression for the distribution function, a relation is derived between the total number of bubbles per unit area of the cross section and the age of the foam, assuming that the disappearance of the small bubbles is caused only by transfer of gas to larger bubbles. With the aid of the derived relationship the average thickness of the liquid lamellae in a number of foams is calculated from the observed rate of decrease in the number of bubbles in the front layer.

The calculated values of the average film thickness are of the same order of magnitude as those calculated directly from the observed bubble size distribution and the liquid content of the foam. Additional evidence of the proposed destabilization mechanism is obtained from experiments, in which the nature of the gaseous phase was varied and from comparison of the rate of decrease in the number of bubbles with the rate of shrinking of individual bubbles.

TABLE I

OBSERVED BUBBLE SIZE FREQUENCY DISTRIBUTION IN VARIOUS FOAMS

Bubble radius in 10^{-4} cm	Number of bubbles in each size group: Hevea latex No. 4 ($\varphi = 0.8$)	Oil-in-water emulsion No. 5 ($\varphi = 0.86$)	Solution of "Teepol"+Na alginate No. 1 ($\varphi = 0.9$)
0 – 12.5	130	55	141
12.5– 25	227		
25 – 37.5	152	185	175
37.5– 50	60		
50 – 75	35	89	110
75 –100	4	60	69
100 –125	—	25.5	58
125 –150	—	6	50
150 –175	—	2	25
175 –200	—	—	21
200 –225	—	—	5.5

3.1. BUBBLE SIZE FREQUENCY DUSTRIBUTION IN VARIOUS FOAMS

The size frequency distribution function of the bubbles in the foams examined may be calculated from the microscopic measurement of a large number of bubbles in a randomly chosen area of the cross section as has been described in Part II. Photomicrographs were made two minutes after whipping of the liquid had been stopped. The observed bubbles were assumed to be perfect spheres and assigned to a number of size groups according to the value of their radii. Representative frequency distributions for various foams are given in Table I.

In order to solve Equation (2.16), given in Part II, explicitly it is necessary to find an adequate mathematical expression for the distribution function. Several methods are available, in principle, to develop such an expression, e.g., Pearson's method of fitting by moments[22].

One of the main objections against application of such a method in our case, however, is the relative inaccuracy of the values of the observed radii. Deviations from the spherical shape and limited sharpness of the outer contours of

TABLE II

COMPARISON OF OBSERVED BUBBLE SIZE FREQUENCY DISTRIBUTIONS IN DIFFERENT FOAMS OF THE SAME COMPOSITION (HEVEA LATEX: $\varphi = 0.94$)

Bubble radius in 10^{-4} cm	Number of bubbles in $17.5 \cdot 10^{-2}$ cm²: Latex foam No. 17	Latex foam No. 18
0– 25	220	211
25– 50	64	50
50– 75	35	43
75–100	40	28
100–125	34	35
125–150	21	17
150–175	11	16
175–200	5	8
200–225	3	4.5
225–250	2	—
250–275	1	1
275–300	1	1
	437	414.5

the bubbles on the photomicrograph may be the cause of substantial errors in the observed sizes, particularly in the case of the smallest bubbles. An example of the errors involved is shown in Table II where the values are compared of bubble sizes observed in equal areas of the front layer in different foams of the same composition. Determination of the total *number* of bubbles per unit area has, evidently, a higher experimental accuracy than determination of the bubble sizes. Experimental results of the determination of the number of bubbles as a function of time can be satisfactorily described by a very simple mathematical expression as will be shown in Section 3.3. This expression may be used in combination with Equation (2.16) to derive a bubble size frequency distribution function $F(r)$ which should correspond to the observed distribution function $f(r)$ in the front layer of the investigated foams. The empirical mathematical expression necessary to solve Equation (2.16) has thus been derived from the most accurate experiments, viz. the kinetic measurements.

For the sake of logical continuity the mathematical expression for the bubble size frequency distribution function will be introduced in this section as an empirical relationship. With its aid a theoretical expression for the kinetics of the foam destabilization process under consideration will be derived in the next section, whereas finally in Section 3.3, the derived rate equation will be applied to the experimental results of the kinetic investigations.

The mathematical expression for the bubble size frequency distribution function which appears to give an adequate description of the frequency distribution observed in a large number of foams, is as follows:

$$F(r) = \frac{6\alpha r}{(1 + \alpha r^2)^4} \tag{3.1}$$

where α is a parameter of the distribution function.

According to Equation (2.21) (see Part II) the size frequency distribution function of the bubbles in the front layer should be:

$$f(r) = \frac{6\alpha r^2}{\bar{r}(1 + \alpha r^2)^4} \tag{3.2}$$

The average radius $\bar{r}$ may be expressed in α:

$$\bar{r} = \int_0^\infty rF(r)dr = 6\alpha \int_0^\infty \frac{r^2}{(1 + \alpha r^2)^4}\, dr = \frac{3\pi}{16}\alpha^{-\frac{1}{2}} \tag{3.3}$$

Inserting the value of $\bar{r}$ into Equation (3.2) results in:

$$f(r) = \frac{32\alpha^{\frac{1}{2}}r^2}{\pi(1 + \alpha r^2)^4} \tag{3.4}$$

For comparison with the observed frequencies Equation (3.4) may be simplified by introduction of the reduced variable $\alpha^{\frac{1}{2}}r$.

If $u = \alpha^{\frac{1}{2}}r$,

$$f(r)dr = \frac{32u^2}{\pi(1 + u^2)^4}\, du = f(u)du \tag{3.5}$$

After equating the observed number of bubbles with radii between the class limits r and $r + dr$ to the number of bubbles with radius $r + \frac{1}{2}\,dr$ the various averages $\overline{r_f}$, $\overline{r_f^2}$, etc. may be calculated. The value of α is found from the value of $\overline{r_f^2}$ with the aid of the following expression:

$$\overline{r_f^2} = \frac{32\alpha^4}{\pi} \int_0^\infty \frac{r^4}{(1 + \alpha r^2)^4}\, dr = 1/\alpha \tag{3.6}$$

With this value of α the observed fraction of bubbles with radii between r and $r + dr$ may be plotted against $u + \frac{1}{2}\,du$ and compared with the calculated value of $f(u)du$. This has been done for a number of various foams in Figure 3.1, where the drawn curve presents the function $f(u)$.

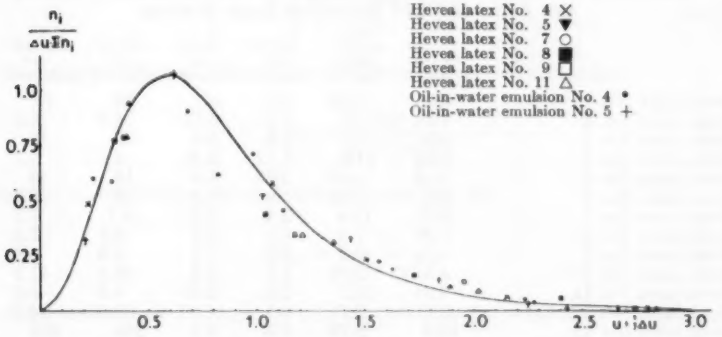

FIG. 3.1—Comparison of proposed frequency distribution function $\frac{32\,u^2}{\pi(1 + u^2)^4}$ with observed bubble size frequencies in various foams.

It is evident that the function $f(u)$ and consequently $f(r)$ gives a fair description of the observed frequency distribution in the foams investigated. Some of the data agree better with the proposed equation than others, which is not surprising in view of the experimental inaccuracy and because of the fact that it is improbable that all foams investigated should possess exactly the same bubble size frequency distribution.

If a large volume of gas has to be dispersed as spherical particles, space filling requirements will, of course, limit the number of possible size frequency distributions. Though the total number of possibilities may be infinitely large, it is not unjustified to assume that, apart from differences in detail, the general shape of many of the possible distribution functions will be the same. If the volume concentration of dispersed gas becomes very high the shape of the bubbles will deviate appreciably from that of a sphere and the proposed distribution function will then be no longer valid.

More information about the difference between calculated and observed values of the bubble size distribution can be obtained by application of the χ^2 test[24].

The value of the quantity $\sum_m (n_i - n_0)^2/n_0$, where n_i is the observed and n_0 the calculated number of bubbles in each size group and m the total number of

size groups is a measure of the degree of conformity between the observed and proposed frequency distribution function.

For the oil-emulsion foam No. 4 and the rubber latex foam No. 4, for example, values were found which could occur between 10 and 50 times in 100 on pure chance, which indicates, accepting the 5% level of probability, that there is no reason to doubt the appropriateness of the theoretical distribution function for these foams.

For some of the other foams presented in Figure 3.1, the values of χ^2 appeared to have a probability of occurrence less than 5%, which means that the proposed expression is certainly not the most probable distribution function for these foams.

TABLE III

COMPARISON OF OBSERVED AND CALCULATED VALUES OF AVERAGE RADIUS AND AVERAGE CUBE RADIUS OF FOAM BUBBLES

	$\overline{r_f^2}\cdot 10^3$ cm^2	$\alpha\cdot 10^{-4}$ cm^{-2} (Eq. 3.6)	$\overline{r_f}\cdot 10^2$ cm (Eq. 3.7)	$\overline{r_f}\cdot 10^2$ cm (observed)	$\overline{r_f^3}\cdot 10^5$ cm^3 (Eq. 3.8)	$\overline{r_f^3}\cdot 10^5$ cm^3 (observed)
Hevea-latex No. 1	6.15	1.62	6.5	6.1	80	90
Hevea latex No. 2	1.34	7.5	3.1	2.85	8.3	8.0
Hevea latex No. 3	4.3	2.3	5.6	5.3	48	46
Hevea latex No. 4	0.85	11.8	2.47	2.46	4.1	3.7
Hevea latex No. 5	2.15	4.65	3.95	3.8	18	16
Hevea latex No. 6	3.5	2.85	5.0	4.8	35	32.7
Hevea latex No. 7	0.78	12.8	2.4	2.3	3.7	3.2
Hevea latex No. 8	1.32	7.6	3.1	2.9	8.1	7.8
Hevea latex No. 9	1.02	9.8	2.7	2.5	5.8	5.4
Hevea latex No. 10	4.3	2.32	5.6	5.2	48.1	41.9
Hevea latex No. 11	0.94	10.7	2.6	2.45	5.0	5.2
Hevea latex No. 12	3.7	2.71	5.1	4.3	38.2	44.8
Hevea latex No. 13	12.8	0.78	9.4	9.1	246	253
Oil-in-water emulsion No. 1	9.5	1.04	8.3	7.8	162	140
Oil-in-water emulsion No. 2	5.5	1.83	6.3	6.0	68	64
Oil-in-water emulsion No. 3	3.64	2.75	5.12	5.18	37.2	31.1
Oil-in-water emulsion No. 4	1.5	6.62	3.3	3.3	9.9	8.9
T-pol + alginate No. 1	6.95	1.44	7.1	6.7	98.5	90.7
T-pol + alginate No. 2	9.66	1.03	8.3	7.7	161.5	147.4

Another test of the appropriateness of the proposed distribution function is shown in Table III where calculated and observed values of the average radius and the average cube of the radius are compared.

The "theoretical" values have been calculated from the following expressions:

$$\bar{r}_f = \frac{32\alpha^4}{\pi}\int_0^\infty \frac{r^3}{(1+\alpha r^2)^4}\,dr = \frac{8}{3\pi}\alpha^{-\frac{1}{2}} \tag{3.7}$$

$$\overline{r^3}_f = \frac{32\alpha^4}{\pi}\int_0^\infty \frac{r^5}{(1+\alpha r^2)^4}\,dr = \frac{16}{3\pi}\alpha^{-\frac{3}{2}} \tag{3.8}$$

The value of α has been determined by means of Equation (3.6).

Summarizing it may be concluded that, although the bubble size frequency distributions in different foams cannot be exactly described by one, generally valid, mathematical expression, the proposed Equation (3.1) may be considered

as a satisfactory approximation to the real frequency distribution observed in the foams investigated.

3.2. KINETICS OF FOAM DESTABILIZATION CAUSED BY TRANSFER OF GAS BETWEEN THE BUBBLES

In Part II it has been shown that the total number of bubbles per unit volume of foam will decrease with time as a result of the transfer of gas from the smaller to the larger bubbles, as expressed by the following relationship:

$$N_{t_\rho} = N_0 \left\{ 1 - \int_0^\rho F(r)dr \right\} \tag{2.16}$$

where

$$\rho = \left(\frac{4RT \cdot D \cdot S \cdot \gamma}{p_0 \Theta} t_\rho \right)^{\frac{1}{3}} \tag{2.15}$$

If now the bubble size frequency distribution obeys the function

$$F(r) = \frac{6\alpha r}{(1 + \alpha r^2)^4} \tag{3.1}$$

Equation (2.16) can be reduced, after integration, to:

$$N_{t_\rho} = \frac{N_0}{(1 + \alpha\rho^2)^3} \tag{3.9}$$

After insertion of Equation (2.15), the relationship being sought is found to be:

$$N_t = N_0 \Big/ \left(1 + \frac{4RT \cdot D \cdot S \cdot \gamma \cdot \alpha}{p_0 \Theta} t \right)^3$$

which may be written as:

$$N_t = \frac{N_0}{(1 + kt)^3} \tag{3.10}$$

where k is given by:

$$k = \frac{4RT \cdot D \cdot S \cdot \gamma \cdot \alpha}{p_0 \Theta} \tag{3.11}$$

In order to check Equation (3.10) experimentally, it is necessary to replace the number of bubbles N per unit volume of foam by the observable number of bubbles n counted in unit area of the front layer.

The relationship between n and t can be found immediately if the following assumptions are made:

(i) the bubble size distribution function is given by Equation (3.1) at any value of t, but the parameter α is a function of time;
(ii) the factor C in Equation (2.19), which is characteristic of the deficiency of the number of bubbles in the front layer compared with the number of bubbles in an arbitrary plane cut through the foam, is independent of time.

The dependence of the distribution function on time is now derived from the condition that the total volume of gas must remain constant, or:

$$\varphi = N \cdot \frac{4\pi}{3} \cdot \overline{r^3} = N \cdot \frac{\pi^2}{4} \cdot \alpha^{-\frac{1}{2}} \tag{3.12}$$

since $\overline{r^3} = 3\pi/16\alpha^{-\frac{1}{2}}$, as follows from Equation (3.1)

From Equation (3.12): $N_0 = 4/\pi^2 \cdot \varphi \cdot \alpha_0^{\frac{1}{2}}$, or in general:

$$N_t = \frac{4}{\pi^2} \cdot \varphi \cdot \alpha_t^{\frac{1}{2}} \tag{3.13}$$

Insertion of these values of N into Equation (3.10) gives:

$$\alpha_t = \frac{\alpha_0}{(1 + kt)^2} \tag{3.14}$$

The dependence of α on time may now be used to determine the relationship between n and t. According to Equation (2.19):

$$n_t = 2C \cdot N_t \bar{r}_t.$$

After insertion of the values, given by Equations (3.3) and (3.10):

$$n_t = 2C \frac{N_0}{(1 + kt)^3} \cdot \frac{3\pi}{16} \alpha_t^{-\frac{1}{2}} \tag{3.15}$$

Insertion of the value of α_t, given by Equation (3.14), leads to:

$$n_t = \frac{2CN_0\overline{r_0}}{(1 + kt)^2} \tag{3.16}$$

or:

$$n_t = \frac{n_0}{(1 + kt)^2} \tag{3.17}$$

Equation (3.17) may also be written as follows:

$$n_t^{-\frac{1}{2}} = n_0^{-\frac{1}{2}}(1 + kt) \tag{3.18}$$

The inverse square root of the number of bubbles per unit area of the cross section, divided by the inverse square root of the number at $t = 0$ will give a straight line if plotted against t.

The slope of this line is given by Equation (3.11) and is a function of the physical parameters of the foam, viz.: permeability of the liquid for the gas, surface tension of the liquid, mean square radius of the bubbles at $t = 0$, and average thickness of the liquid lamellae.

The value of the rate constant k, which may be properly considered as a measure of the foam stability with respect to gas diffusion, is proportional to α/Θ, i.e., inversely proportional to the average volume of the bubbles in a foam at $t = 0$, if φ is kept constant as follows from Equations (2.14) and (3.1).

This result is of some practical importance. If a certain amount of gas has to be dispersed in a given volume of liquid, this might be done in two ways, viz.:

I) by means of a very efficient whipping apparatus, which will produce a foam with large specific interfacial area, i.e., with many small bubbles, or:

II) by dispersing the gas in a relatively poor manner which will result in a foam with many large bubbles.

It is evident from the expression for k that foam I will be less stable than foam II as far as transfer of gas between the bubbles is concerned. Average bubble growth will be faster in foam I and both foams will, therefore, approach each other in the course of time with respect to average bubble size.

In practice, foams of type II may be less stable with respect to film collapse because of the higher rate of drainage which may provoke rupture of the lamellae (see Part V). If, on the other hand, the rate of drainage is not very important because of a high viscosity of the liquid, foams of type II will also be more stable with respect to film rupture since the average thickness of the lamellae will be larger than in foams of type I.

3.3. EXPERIMENTAL INVESTIGATIONS OF THE KINETICS OF FOAM DESTABILIZATION

Determination of the number of bubbles per unit area of the front layer as a function of time was performed as described in Section 2 of Part II. Three different liquids were used for preparing the foams, viz.

a) preserved concentrated Hevea rubber latex to which various amounts of different detergents were added.

b) an oil-in-water emulsion of the following composition:
57 volumes of monochlorobenzene
43 volumes of paraffin oil
34–43 volumes of an aqueous sodium laurate solution (0.18 molar).
(This emulsion does not cream since the density of the dispersed phase is slightly greater than 1).

c) a 1% solution of Tee-pol (a commercial detergent supplied by Shell Chemical Co. and containing a mixture of sodium alkyl sulfates). To this solution was added 1% sodium alginate in order to increase the viscosity up to about 50 centipoises.

Because of the relatively high viscosity of these liquids the foams prepared therefrom do not show appreciable drainage during the first 30 minutes of their existence. Collapse of liquid lamellae did not occur in these foams during the measurements. Decrease of interfacial area was only caused by diffusion of gzs from small to larger bubbles. In foams with very high volume concentrations of dispersed air (~95%) some film clloapse may possibly have taken place but this could not be detected by ordinary visual means.

In Figures 3.2, 3.3 and 3.4 some representative results of the kinetic measurements have been plotted as $n^{-\frac{1}{2}}$ against t. It follows from Equation (3.18) that:

$$n^{-\frac{1}{2}} = n_0^{-\frac{1}{2}} + kn_0^{-\frac{1}{2}}t \tag{3.19}$$

From the slope of the lines drawn and the value of n_0 the average thickness of the liquid lamellae in the foams investigated may be calculated by means of

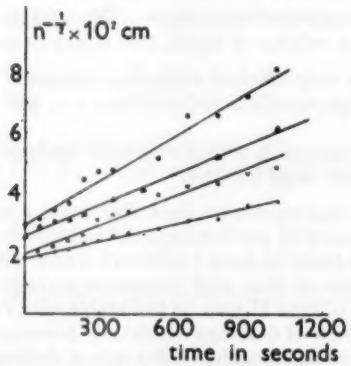

FIG. 3.2—Inverse square root of the number of bubbles per unit of cross section as a function of time for various Hevea latex foams.

○ Latex foam No. 13; $\varphi = 0.957$
△ Latex foam No. 1; $\varphi = 0.91$
× Latex foam No. 8; $\varphi = 0.89$
● Latex foam No. 11; $\varphi = 0.81$

Equation (3.11). Table IV shows the results of this calculation for a number of foams. In the last column of this table the values are given of the average lamella thickness calculated from the observed bubble size distribution with the aid of Equation (2.23).

It appears from this table that both theoretical and observed values of the average lamella thickness of most foams are between 1 and 10 microns. The agreement between theoretical and observed values is not perfect but may be considered very satisfactory, taking account of the various approximations introduced into the theory and the limited accuracy of the experimental values. The opinion of various authors[21] that diffusion of gas is appreciably retarded by the presence of the adsorbed layer of surface active molecules or ions at the

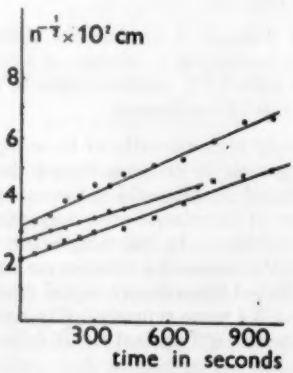

FIG. 3.3—Same as Figure 3.2 for a number of foamed oil-in-water emulsions.

% Emulsion foam No. 7; $\varphi = 0.935$
● Emulsion foam No. 1; $\varphi = 0.925$
× Emulsion foam No. 4; $\varphi = 0.86$

interface, does not seem to be confirmed by our results. Some of the theoretical values of the average lamella thickness may, however, be too low due to the incorrectness of the assumed bubble size distribution function which underestimates somewhat the frequency of the smallest bubbles. Introduction of a more accurate distribution function will in some cases result in higher calculated values of the average film thickness. It is, therefore, not impossible that the transfer of gas through the foam lamellae proceeds, in reality, slightly slower than is assumed in our theory. It appears justifiable to conclude from the results shown in Table IV however, that the effect of the adsorption layer is only small, if it exists at all.

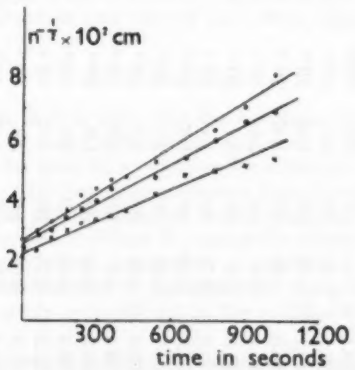

FIG. 3.4—Same as Figure 3.2 and 3.3 for three foamed Tee-pol solutions.

● Tee-pol foam No. 2; $\varphi = 0.93$
○ Tee-pol foam No. 4; $\varphi = 0.918$
× Tee-pol foam No. 1; $\varphi = 0.90$

From the experiments with the foamed oil-in-water emulsions Nos. 5 and 6 the influence of the solubility and diffusion coefficient of the dispersed gas may be deduced. The value of the product $D \cdot S$ for oxygen in water at 20° C is equal to $2.9 \cdot 10^{-11}$ and mole $\cdot$ cm$^{-1} \cdot$ sec$^{-1} \cdot$ atm^{-1}, for nitrogen: $1.32 \cdot 10^{-11}$ mole $\cdot$ cm$^{-1} \cdot$ sec$^{-1} \cdot$ atm^{-1}.

It follows from Equation (3.11) that:

$$(D \cdot S)_{\text{oxygen}} / (D \cdot S)_{\text{nitrogen}} = \left(\frac{k \cdot \Theta}{\gamma \cdot \alpha} \right)_{\text{oxygen}} \Big/ \left(\frac{k \cdot \Theta}{\gamma \cdot \alpha} \right)_{\text{nitrogen}} \tag{3.20}$$

Insertion of the experimentally determined values of k, Θ, α and γ into Equation (3.20) leads to a value of 1.83 for the calculated ratio of the permeabilities of water for oxygen and nitrogen, which is somewhat lower than the real value 2.17.

That transfer of gas between the bubbles causes the sponteneous decrease of interfacial area in the foams investigated can also be demonstrated by comparing the rate of shrinking of an individual bubble with the observed rate of decrease in the total number of bubbles. For the foamed oil-in-water emulsion No. 1 the rate of bubble size change has been measured for a number of bubbles as described in Section 5 of Part II. Comparison of Equations (2.7) and (3.11)

Table IV

Comparison of Calculated and Observed Values of Average Lamella Thickness

Composition of liquid	Composition of gas	Vol fraction of gas φ	Permeability[1] $= D \cdot S$ moles cm^{-1} sec^{-1} atm^{-1}		Surface tension[2] γ dynes cm^{-1}	α^2 in cm^{-2}		k sec^{-1}		Θ theor.[4] cm		Θ observed[5] cm	
T-pol-solution 1	air	0.90	1.5	10^{-11}	29.1	1.44	10^4	2.0	10^{-3}	2.8	10^{-4}	7.7	10^{-4}
T-pol-solution 2	air	0.93	1.5	10^{-11}	29.1	1.03	10^4	2.1	10^{-3}	1.94	10^{-4}	5.9	10^{-4}
T-pol-solution 3	air	0.88	1.5	10^{-11}	29.1	1.52	10^4	1.88	10^{-3}	3.2	10^{-4}	8.8	10^{-4}
Hevea Latex 1	air	0.91	1.5	10^{-11}	36.5	1.62	10^4	1.47	10^{-3}	5.4	10^{-4}	6.2	10^{-4}
Hevea Latex 8	air	0.89	1.5	10^{-11}	35.8	7.6	10^4	2.5	10^{-3}	14.6	10^{-4}	3.6	10^{-4}
Hevea Latex 9	air	0.875	1.5	10^{-11}	35.8	9.8	10^4	2.4	10^{-3}	19.6	10^{-4}	3.9	10^{-4}
Hevea Latex 12	air	0.93	1.5	10^{-11}	35.8	2.71	10^4	1.7	10^{-3}	7.6	10^{-4}	4.3	10^{-4}
Hevea Latex 13	air	0.957	1.5	10^{-11}	35.8	0.78	10^4	1.6	10^{-3}	2.4	10^{-4}	4.1	10^{-4}
Hevea Latex 15	air	0.90	1.5	10^{-11}	33.7	5.81	10^4	2.7	10^{-3}	9.6	10^{-4}	4.05	10^{-4}
Hevea Latex 16	nitrogen	0.94	1.32	10^{-11}	36.5	1.93	10^4	3.3	10^{-3}	2.6	10^{-4}	4.0	10^{-4}
Hevea Latex 17	air	0.94	1.5	10^{-11}	36.5	1.8	10^4	1.8	10^{-3}	4.9	10^{-4}	4.0	10^{-4}
Oil-in-water emulsion 1	air	0.925	1.5	10^{-11}	37.3	1.04	10^4	1.0	10^{-3}	5.2	10^{-4}	6.6	10^{-4}
Oil-in-water emulsion 2	air	0.93	1.5	10^{-11}	37.3	1.83	10^4	2.0	10^{-3}	4.6	10^{-4}	4.6	10^{-4}
Oil-in-water emulsion 3	air	0.91	1.5	10^{-11}	37.3	2.75	10^4	1.77	10^{-3}	7.8	10^{-4}	4.4	10^{-4}
Oil-in-water emulsion 4	air	0.86	1.5	10^{-11}	37.3	6.62	10^4	2.4	10^{-3}	13.8	10^{-4}	4.9	10^{-4}
Oil-in-water emulsion 5	oxygen	0.857	2.9	10^{-11}	34.6	2.7	10^4	1.67	10^{-3}	14.4	10^{-4}	7.7	10^{-4}
Oil-in-water emulsion 6	nitrogen	0.86	1.32	10^{-11}	34.6	4.2	10^4	1.61	10^{-3}	10.4	10^{-4}	6.8	10^{-4}

[1] "International Critical Tables", McGraw-Hill, New York.
[2] Measured by means of the du Noüy method.
[3] Calculated from Equation (3.6).
[4] Calculated from Equation (3.11).
[5] Calculated from Equation (2.23).

shows that:

$$k = \alpha \left(- \frac{dr^2}{dt} \right)$$

if the lamella thickness Θ around the observed bubbles is equal to the average film thickness in the foam.

For this particular foam the value of k, calculated from three individual measurements (see Figure 2.2a of Part II) is equal to $1.3 \cdot 10^{-3}$ sec^{-1}, whereas the experimental value (see Table IV) is equal to $1.0 \cdot 10^{-3}$ sec^{-1}.

The agreement appears fair enough to conclude that k is indeed a measure of the resistance towards spontaneous foam destabilization caused by the permeability of the foam lamellae and not by any other mechanism such as film rupture for example.

3.4. CONCLUSION

It has been shown in this part that the simple experimental technique of counting the number of foam bubbles per unit area of the cross section as a function of time may be used for evaluating foam stability if no rupture of the foam lamellae occurs. In these circumstances foam destabilization is a result of the diffusion of gas from smaller to larger bubbles. The (approximate) theory developed in Section 6 of Part II enables the rate of foam destabilization to be expressed by the physical parameters of the foam. The rate constant is proportional to the permeability of the liquid for the gas, the surface tension of the liquid and inversely proportional to the average thickness of the liquid films.

Moreover, the expression for the rate constant contains a parameter characteristic of the initial bubble size distribution.

After expressing the initial bubble size distribution in a mathematical form, the theory has been applied with good results to measurements of the stability of various foams.

Application of the theory not only permits a quantitative evaluation of foam stability with respect to transfer of gas between the bubbles, but may also be useful in explaining the effect of different variables on the stability of foams. It should be possible for example, with the aid of the theory, to decide if the effect of a particular variable (kind of detergent, concentration of detergent) on the foam stability is caused by its influence on the average lamella thickness, on the bubble size distribution, on the permeability, or merely by its influence on the surface tension of the liquid. Investigations along these lines might provide valuable information about the relationship between the composition of a foam and its stability towards gas transfer.

IV. KINETICS AND ACTIVATION ENERGY OF FILM RUPTURE

High-speed cinematography of collapsing lamellae of an aqueous Tee-pol solution reveals that spontaneous rupture always takes place in the thinnest part of the lamella. The rate of hole expansion is dependent on the thickness of the lamella; its value is found to be in the order of some hundreds of cms per second. Dupré's assumption that the released surface energy will be completely converted into kinetic energy of the liquid appears to be essentially correct. Film rupture in a foamed aqueous solution of ammonium oleate is

shown to proceed at a rate which is at least of the same order of magnitude as that in the isolated lamellae.

Deformation of a foam lamella occurs locally when a hole is about to be formed. The deformation and the very first beginning of hole expansion require an energy of activation which is calculated with the aid of a geometrical model. The energy is more than 1000 kT units in a "black" film of an aqueous soap solution. This amount of energy has to be supplied in order to increase the interfacial area. The activation energy is proportional to the square of the film thickness and its value is hardly influenced by the mangitude of the electric double-layer interaction.

The formation and relative stability of "black spots" in films of much larger thickness than the spot itself is shown to be the result of an equilibrium, existing at a thickness between 100 and 150 A, of the three forces coming into play: London-Van der Waals attraction, double-layer repulsion and surface tension.

4.1. INTRODUCTION

In the foregoing sections one spontaneous process of foam destabilization has been discussed, viz.: the decrease of interfacial area caused by the transfer of gas between bubbles of different sizes. In this and the following paper the second physical process responsible for the spontaneous decrease of interfacial area in many foams, i.e., the collapse of bubble walls, will be investigated.

If a liquid film separating two bubbles in a foam collapses, the bubbles will unite and form one larger bubble, consequently film collapse will be accompanied by a decrease in the total number of bubbles per unit volume of foam. However, in most foams the probability of collapse is not the same for all liquid lamellae. As will be shown in Section 4.3, the probability of collapse is larger the smaller the thickness of the lamella and hence the bubble walls in the top layer of a foam will be more liable to rupture than other lamellae because of their smaller thickness as a result of drainage under the influence of gravitation. Observation of the process of film collapse in a randomly chosen volume of a foam will not yield, therefore, representative information on the rate of decrease in the number of bubbles in other parts of the foam. Nevertheless, it may be assumed, that if a foam lamella collapses the process of rupture will be independent of the position of the lamella, i.e., the mechanism and rate of rupture will be essentially the same for all collapsing films in a foam though the moment at which rupture starts may be different for different lamellae.

Because of the extremely high rate of rupture phenomena a quantitative evaluation of the mechanism of such processes is only possible by means of high speed experimental techniques. High speed cinematography of collapsing foams with the aid of the available apparatus (a camera with a maximum speed of 3000 frames per second) did not, however, provide the information desired. Yet this experimental technique proved to be successful for the study of the rupture process in single, isolated liquid lamellae. There is no reason to suppose that the mechanism of rupture in single liquid films will be different from the similar phenomenon in foam lamellae of the same composition. In the following section the experimental results of the study of single liquid films will be discussed whereas finally their relationship with the problem of foam stability will be considered.

It may be noted that rupture of liquid lamellae and subsequent coalescence of colloidal particles originally separated by those lamellae is a process not con-

fined to foams but occurring as well in other colloidal systems, notably emulsions[25].

It might therefore be expected that a study of this rupture process will also throw some light upon the questions, not yet solved, regarding the mechanism of coalescence in aggregates of emulsion particles.

4.2. RESULTS OF CINEMATOGRAPHIC OBSERVATIONS AT HIGH SPEEDS

The liquid lamellae were prepared by immersion of a circular or rectangular frame into a soap solution. The frames were made of glass or of stainless steel wire. After lifting such a frame slowly from the solution, a liquid lamina is formed within the frame. These lamellae have, evidently, two liquid-air interfaces the area of each being 10–20 cm^2 depending upon the fame used. The lifetime of the lamellae is limited and dependent on various conditions. Rupture and subsequent breakdown were observed by means of an Eastman High

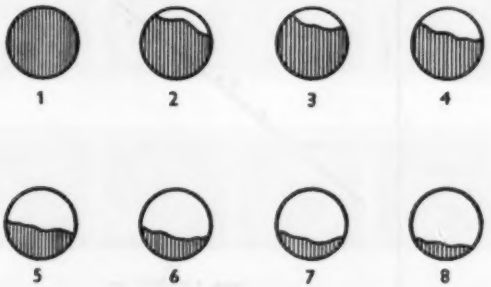

FIG. 4.1—Sequence of images taken from a high speed film of spontaneous rupture in a lamella of a Tee-pol solution. (Diagrammatic representation). Time interval between two images equal to 1700^{-1} sec. Hole formation takes place in the top of the lamella.

Speed camera and 16 mm Kodak Super-XX High Speed Panchromatic Films. These experiments have been executed with the equipment of the "Werkgroep voor Spannings- en Trillingsonderzoek, T.N.O." at Delft.

Illimination of the object was provided by a carbon-arc lamp. The length of the films used was 100 feet; the speed of the film in the camera attains a value of 2500–3000 frames per second after about two thirds of the length of the film has been exposed. This means that observation at such high speeds is only possible during the short period (less than one second) of exposure of the last 30 feet of the film. The existence of these very narrow limits of the time of observation is, of course, a serious drawback to this experimental method when the application concerns a spontaneously occurring process. The liquid lamellae prepared from an aqueous solution of 1% "Tee-Pol" and 1% sodium alginate (the last component had been added in order to increase the viscosity of the solution) had a life of 40–50 seconds under the conditions of the experiment. This means that the variations of the observed values of the lifetime are larger than the total time of exposure of the high speed film. It is, therefore, impossible to predict the moment of rupture with an inaccuracy of less than 1 second as should be necessary for one to be sure that rupture occurs at maximum speed of the film. Nevertheless some films of the spontaneous rupture of liquid lamel-

lae have been made: Figure 4.1 gives a schematic representation of a sequence of 8 images taken from a high speed film of the rupture of a circular lamella. The speed of the film during rupture of the liquid was 1700 frames per second. Rupture occurred about 45 seconds after formation of the lamella. During the lifetime of the lamella a gradual thinning took place as a result of drainage. The wire frame containing the lamella was held in a vertical position and consequently the thickness of the lamella was the smallest at the top. The thickness may be estimated from the color shown by the liquid film; the upper half of the circular lamellae investigated very shortly after formation showed different interference colors arranged in such an order that the colors corresponding to the thinner portions of the film were in general the nearest to the top. The

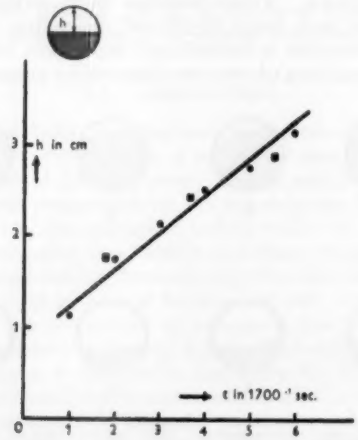

FIG. 4.2—Rate of hole expansion after spontaneous rupture in lamellae of a Tee-pol solution.

● Speed of film: 1700 frames/sec.
■ Speed of film: 920 frames/sec.

boundaries between the colored striations were not formed by perfectly straight horizontal lines but by sinuous curves bent downwards at the borders of the film, indicating the presence of internal flow of the liquid in other directions than merely the vertical. At a certain moment "black spots" begin to form in the thinnest part of the film near the top. The surface area occupied by these black spots grows very rapidly until the lamella suddenly ruptures. In all experiments rupture took place near the top of the lamella, i.e., in the "black" part of the film, as shown in Figure 4.1. The exact value of the thickness of this part of the film has not been determined but, in any case, it will be smaller than 1000 A as has been established by many investigations of "black films"[26]. From the values reported in the literature, determined either by optical or by electrical measurements it may be inferred that the thickness of "black films" prepared from soap solutions ranges from about 120 A to 500 A.

Even if the mean thickness of the black part of the lamellae investigated had been determined, the exact value of the thickness at the spot where rupture starts would still be unkown because the first image of the high speed film after the onset of rupture showed in all cases a hole in the lamella which occupied an

area at least as large as the total area of the "black spot" ($\sim$ 1 cm^2). It was, therefore, impossible to localize the beginning of rupture exactly: the cinematographic observation permits one to conclude only that rupture starts somewhere in the thinnest, viz., the "black", part of the lamella.

An approximate value of the rate of rupture, i.e., the speed with which the hole in the film expands may be deduced from Figure 4.2 where the perpendicular distance of the border line of the hole from the top of the wire frame has been plotted as a function of time. The results of two determinations (one at a speed of 1700 frames per second, the other at 920 frames per second) are fairly well represented by a rectilinear plot. The rate of expansion of the hole calculated from the slope is 680 cm/sec. After having established that spontaneous rupture always starts in the thinnest part of the liquid, a second kind of experiment has been carried out in which rupture was provoked by means of an electric discharge. In this experiment the lamella was placed between the poles of a Ruhmkorff coil. The spark passed through the center of the lamella

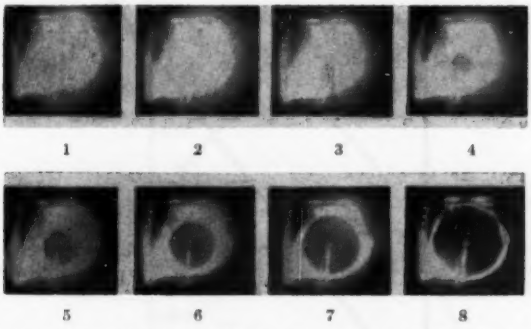

FIG. 4.3.—Sequence of images taken from a high speed film of a collapsing lamella of a Tee-pol solution. Induced hole formation in the center of the lamella by means of an electric discharge. Time interval between two images equal to 1408^{-1} sec except between pictures 2 and 3 where the interval is half as long.

and caused an immediate rupture of the liquid. The electric cricuit comprising the coil was closed automatically by an interrupter attached to the camera; this device permitted one to "trigger" the rupture of the lamella at the moment at which the film in the camera had attained its maximum speed. Some pictures are reproduced in Figure 4.3 taken at a speed of 2815f/sec. The rectangular frame containing the lamella was made of glass and had a surface area of 16 cm^2. The dark patches at the corners of the frame and along its lower side are a result of the uneven illumination of the surface of the lamella which was not absolutely plane but showed an appreciable curvature. Since only one source of illumination was used the presence of shadows on the surface was inevitable.

Figure 4.3 shows clearly that the hole formed by the spark discharge is circularly shaped. During the expansion the hole remains circular, its diameter being a linear function of time. From the plot in Figure 4.4 it may be deduced that the rate of increase of the radius of the hole is equal to 355 cm/sec.

Dupré[27] calculated the speed with which a hole in a liquid film expands, assuming that the surface energy released is completely converted into kinetic energy of the liquid. In this case the following equation holds:

$$2\gamma S = \tfrac{1}{2} S t d v^2$$

where γ = surface tension of the liquid, $2S$ = total surface of the liquid replaced by the hole, t = thickness of the film, d = density, and v = rate of expansion of the hole.

It follows that:

$$v = (4\gamma/td)^{\frac{1}{2}} \tag{4.1}$$

Inserting the values of the surface tension (30 dynes/cm) and of the density (1 g/cm^3) the relationship between rate of expansion and thickness of the lamella becomes for the experiments described: $v^2 = 120/t$, if v is expressed in cm/sec and t in cm.

According to this relation the average thickness of the rupturing lamellae in the first experiments (spontaneous rupture) should have been 2.5 microns, in the last experiment (rupture by means of electric discharge): 9.5 microns. These values seem to be of the right order of magnitude though they are not

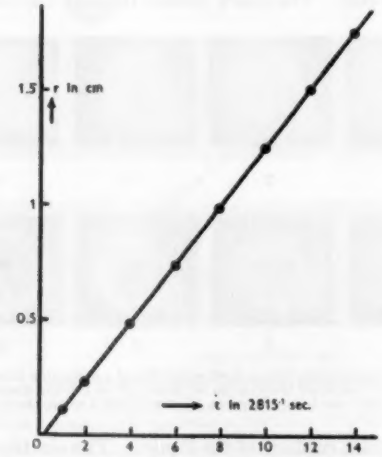

FIG. 4.4 Rate of hole expansion in a lamella ruptured by an electric discharge.

known exactly. In both cases the greatest part of the lamella was uncolored which proves that the thickness was at least 1 micron. The thickness of the lamella ruptured by means of a spark was larger than those of the spontaneously ruptured films because drainage had proceeded to a lesser degree at the moment of rupture. Probably the initial thickness of that lamella was also somewhat larger because the relatively thick glass frame will entrain more liquid than the steel wire frames used in the investigations of spontaneous rupture.

The experimental values of the rate of expansion of the hole show that probably a very great part of the released surface energy will be converted into kinetic energy of the liquid and that Dupré's equation is, therefore, essentially correct. The energy dissipated in overcoming the frictional resistance of the liquid appears to be negligible in comparison with the kinetic energy of the liquid as might be expected at these speeds. The rate of expansion of the hole should therefore be independent of the viscosity of the liquid in this case. Density and surface tension will, in general, not be very different for various

lamella-forming liquids; hence the thickness of the liquid film will be the most important factor in determining the rate of rupture once a hole has been formed. This does not explain, however, the fact that hole formation itself preferentially takes place in the thinnest part of a lamella. The energetics of the hole formation process will be discussed in the next section.

Film rupture in a real foam has also been studied with the high speed camera. In this case it was not possible, however, to determine the rate of hole expansion as has been done for single lamellae. The presence of many curved liquid surfaces all of which are differently orientated gives rise to disturbing optical effects when the foam is illuminated, in particular during the rupture of one of the lamellae because such a rupture provokes rapid movements and changes in orientation of the adjacent lamellae. These rapid local agitations following the rupture of a lamella had a duration from 10^{-3} to 10^{-2} seconds in a foamed aqueous solution of 10% ammonium oleate. It may be deduced that the rate of

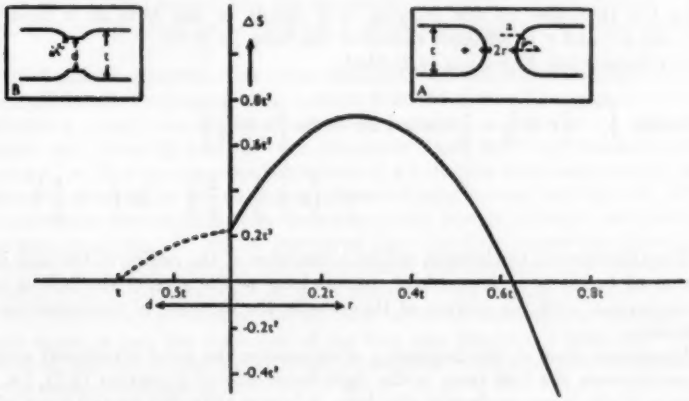

FIG. 4.5—Increase of interfacial area of a rupturing lamella. - - - - - - - thinning before hole has been formed. ——— expansion of hole.

hole expansion in these foam lamellae was at least of the same order of magnitude as the speed with which rupture proceeds in single liquid films. The formation of a hole is, evidently, dependent on local conditions (which will be time-dependent) in the lamellae because rupture took place in different parts of the rectangular foam layer (area: 27 × 20 cm). It is possible that the rupture of a lamella entails sometimes the immediate rupture of an adjacent one, but it appears probable from the observations at high speed that most ruptures are completely independent of each other. It is, therefore, justified to base a discussion of film rupture in foams on model considerations applied to isolated liquid lamellae.

4.3. ACTIVATION ENERGY OF FILM RUPTURE

After a hole has been formed in a liquid lamella, either spontaneously or by any external cause, rapid expansion of that hole will take place because of the considerable amount of surface free energy released as a result of the disappearance of the film. Nevertheless liquid films may persist for very long times, in

particular if they are kept in closed vessels and protected from external disturbances. It is obvious, therefore, that the formation of a hole requires a certain energy of activation.

A closer examination of the rupture process even reveals that the *formation* of a hole not only requires energy, but also that the *expansion* of the hole is accompanied, initially at least, by an increase of free energy.

In Figure 4.5 the total area of the liquid-air interface of a lamella has been plotted as a function of the radius of the hole. It has been assumed that the inner surface of the hole remains curved during expansion (radius of curvature equal to half the thickness of the lamella). The increase of interfacial area upon expansion of the hole is then equal to (see Figure 4.5 inset A):

$$\Delta S = 2\int_0^{\pi/2} 2\pi a \cdot \frac{t}{2}\, d\varphi - 2\pi\left(r + \frac{t}{2}\right)^2 \tag{4.2}$$

where t = thickness of the lamella, a = radius of the hole at a depth $t/2$ $(1 - \sin \varphi)$, and r = smallest radius of the hole ($\varphi = 0$).

It follows from Equation (4.2) that:

$$\Delta S = 2\pi t \int_0^{\pi/2} \left(r + \frac{t}{2} - \frac{t}{2}\cos\varphi\right) d\varphi - 2\pi\left(r + \frac{t}{2}\right)^2$$

$$= \pi^2 t\left(r + \frac{t}{2} - \frac{t}{\pi}\right) - 2\pi\left(r + \frac{t}{2}\right)^2 \tag{4.3}$$

The thickness of the lamella will be a function of the radius of the hole if the volume of liquid is kept constant, but as long as the area of the hole is small in comparison with the surface of the lamella the increase of thickness may be neglected.

It appears that at the beginning of expansion the total interfacial area increases because the first term in the right hand side of Equation (4.2), i.e., the increase of the inner surface of the hole, is larger than the second term which represents the decrease in area of the plane surface of the film. The maximum increase of interfacial area is attained for $r = (\pi/4 - \frac{1}{2})\, t$ and is equal to 0.73 t^2. The activation energy, which has to be supplied in order to expand the hole, is proportional to the square of the film thickness:

$$E_{act.} = \Delta F^s{}_{max} = 0.73 \cdot t^2 \cdot \gamma \tag{4.4}$$

where $\Delta F^s{}_{max}$ is the maximum increase of free surface energy.

Equation (4.4) shows that for a very thin "black" film of an aqueous soap solution ($\gamma = 30 - 40$ dynes/cm, $t = 150$ A) the activation energy has already a value of the order of $5 \cdot 10^{-11}$ ergs., i.e., about 1300 kT-units at room temperature. The increase of interfacial area upon expansion of a hole is, evidently, sufficient to explain the relative stability of these films. Lamellae of pure liquids will, under the influence of gravitation or other forces, attain much smaller thicknesses and the activation energy may then become too small to provide a potential barrier against rupture. Many authors[28] have assumed that the persistence of liquid films, containing one or more surface active components, is caused by the fact that deformation and, consequently, increase of the interfacial area of these films is accompanied by a local increase of surface

tension which counteracts the deformation leading to rupture. The importance of this property, the so-called "surface elasticity", for the stability against rupture has already been discussed in Part I and will be considered in more detail in Part V. It may be noted here, however, that a local increase of surface tension has not much influence on the value of the activation energy as given by Equation (4.4). In an aqueous soap solution, for example, the surface tension may rise locally, as a result of extension of the surface and subsequent disturbance of the adsorption equilibrium, to a value that is at most twice the original one (the surface tension of pure water being about 73 dynes/cm). Even if surface elasticity is totally absent, the difference in limiting thickness between films of a pure liquid and films containing at least one surface active component explains sufficiently the relative stability of the latter. In general, it may be stated that the exact value of the surface tension is of no great importance for the stability of the film against rupture because of its slight influence on the activation energy. More important is the value of the film thickness, which enters as a second power into the expression for the activation energy. It follows that the probability of rupture is greater the smaller the thickness of the film.

Hitherto the discussion has been limited to the increase of free surface energy required by the expansion of a hole in a liquid film. The calculation of the activation energy was straightforward because the mechanism of expansion is simple and perfectly known. On the other hand the very first beginning of rupture, i.e., the spontaneous formation of a hole, is a very complex and totally unknown process, on which no experimental information is available. Nevertheless some assumptions may be made which permit a rough estimate of the energies involved. It will be supposed that the film, before its ultimate rupture, will thin locally over a circular surface, the diameter of which initially is equal to or larger than the thickness of the film. During the progressive thinning of this very small portion of the film the radius of curvature is assumed to remain equal to half the thickness of the film (see Figure 4.5, inset B). The increase of interfacial area is then a function of the initial thickness of the film and of the degree of thinning:

$$\Delta S = 2\int_{\text{arc sin } d/t}^{\pi/2} 2\pi\left(r + \frac{t}{2} - \frac{t}{2}\cos\varphi\right)\frac{t}{2}\,d\varphi + 2\pi \times \left(r + \frac{t}{2} - \frac{t}{2}\sqrt{1 - \left(\frac{d}{t}\right)^2}\right)^2 - 2\pi\left(r + \frac{t}{2}\right)^2 \quad (4.5)$$

where d = thickness of the thin portion of the film, and $2r + t$ = initial diameter of this portion (see Figure 4.6, inset) or:

$$\Delta S = \pi^2 t\left(r + \frac{t}{2}\right)\left\{1 - \left(\text{arc sin}\,\frac{d}{t}\right)\Big/\frac{\pi}{2}\right\} - \pi t^2\left(1 - \frac{d}{t}\right) + 2\pi\left(r + \frac{t}{2} - \frac{1}{2}\sqrt{t^2 - d^2}\right)^2 - 2\pi\left(r + \frac{t}{2}\right)^2 \quad (4.6)$$

$r = 0$ if the initial diameter of the thin section is equal to the film thickness as has been supposed in calculating the dotted curve in Figure 4.5. The complete curve in this figure (dotted + drawn) thus presents the change in interfacial

area which accompanies the formation of a hole and the beginning of its expansion. It is equally possible that the initial surface area of the thinning portion of the film will be larger than supposed in drawing Figure 4.5. It has been observed by various authors[29] that very thin portions may occur in liquid lamellae, the so-called "black spots", which are extended over a considerable area. In the second section of this part the formation of these spots near the top of a vertically held film has been described. They may also occur in the center of a lamella, e.g., under the influence of a centrifugal force as has been demonstrated by Hagenbach[29] or by application of a temperature gradient (see Section 5 of Part V). The most remarkable fact about these "black spots" is their persistance in a film of much greater thickness than the spot itself and the existence of a sharp boundary between the spot and the surrounding liquid. Yet the formation of such a thin patch in a liquid film will require an important amount

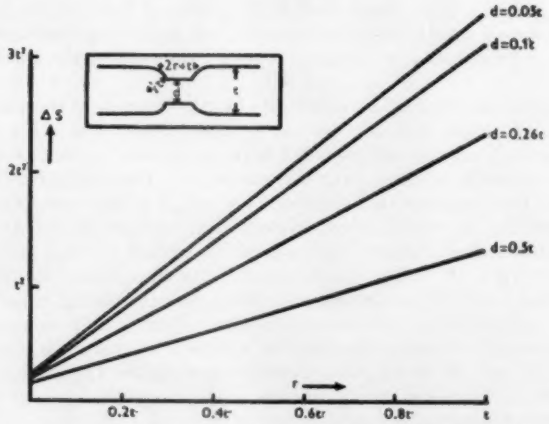

FIG. 4.6.—Increase of interfacial area as a function of the degree of extension of a local thin section in a lamella.

of free surface energy as is shown in Figure 4.6, where the increase of interfacial area has been plotted as a function of the extension of the thinner portion of the film. The increase will be larger the smaller the thickness of this portion. It is evident from a comparison of Figures 4.5 and 4.6 that the formation of a "black spot" in a film of given thickness t may require a much larger amount of free surface energy than the rupture of the same film. If only surface energy had to be supplied, rupture of the film would be more probable than the formation of a "black spot".

It has been proposed to account for the resistance of a liquid film to thinning by assuming a strong electric double layer repulsion between the two surfaces of the film[13,30]. Such a repulsion should, evidently prevent the film from attaining very low values of thickness and might be the reason why any energy available will be dissipated in extending a thin portion of the film rather than in reducing its thickness still further. Deryagin and Titievskaya[13] have reported some experimentally determined values of the pressure which is needed for decreasing the thickness of a liquid film between two gas bubbles in aqueous solutions of undecylic acid and sodium oleate. The pressure increases with

decreasing thickness and may be decreased by the addition of electrolytes to the solution. When the concentration of electrolyte (NaCl) was raised to 0.01 *N*, the film in a sodium oleate solution attained a limiting thickness of ~120 A which was independent of the pressure applied in the range from 300 to 2500 dynes/cm². A similar influence of the electrolyte concentration has already been observed by Reinold and Rücker[31] who found that the limiting thickness of "black" films of sodium oleate solutions is decreased by the addition of potassium nitrate; the smallest thickness observed was also equal to about 120 A.

The theory of electric double-layer repulsion applied by Deryagin in order to explain his experimental observations enables him to describe the measurements in solutions of undecylic acid at various concentrations; the calculated interfacial potentials range from 50–80 millivolts. The theory does not explain, however, the occurrence of a limiting thickness after the addition of at least 0.01 *N*-sodium chloride to the solution of sodium oleate. Even for an infinitely high interfacial potential, the applied pressures should be sufficient to decrease the film thickness to lower values than those observed. The experiments might be explained, according to Deryagin, by assuming that the limiting thickness is due to the presence of polymolecular hydrate layers which are built up on the sodium oleate adsorption monolayers at the interface. The existence of solvate layers having such a considerable thickness (~60 A) has, however, never been proven.

The work of Deryagin and his collaborators appears thus to confirm the notion that electric double-layer repulsion may be important in determining the limiting thickness of liquid films. Since the probability of rupture will be larger the smaller the thickness of the film, the interfacial potential and the ionic strength of the liquid may be parameters of some interest for the strength of liquid films and consequently for the stability of foams. For the rupture process itself the magnitude of double-layer interaction appears, however, too small to supply an important contribution to the activation energy of rupture, as may be shown by the following considerations. If we suppose the interfacial potential to be as high as 250 mV (in general this value will be lower in actual conditions) the potential energy due to double-layer repulsion will have a value of 5–10 ergs/cm², depending upon the electrolyte concentration, when the two charged surfaces have approached to a distance of 10 A[32]. If we consider now a very thin "black" film (t = 120 A) the surfaces of which locally approach to a distance of 10 A and we assume that the radius of the circular area of this thin section is also equal to 10 A, the increase of interfacial energy due to the deformation of the surfaces will be given by Equation (4.6) and may be deduced from Figure 4.6. For this particular case the energy appears to be equal to $\frac{1}{4}t^2 \cdot \gamma$ ergs (t expressed in cms, γ in dynes/cm), i.e., $2.5 \cdot 10^{-11}$ ergs (~625 kT-units) if the value of the surface tension is equal to 35 dynes/cm.

The potential energy increase resulting from the double-layer interaction between the two approaching surfaces each having an area of $\pi \cdot 10^{-14}$ cm², will be no more than 3.10^{-13} ergs (~7 kT-units) which may be neglected in comparison with the increase of interfacial energy. The contribution of the double-layer interaction will gain in importance the larger the surface area of the thin section and its value may even surpass that of the interfacial energy increase when the area of the approaching surfaces becomes very large as in the case of a "black spot" for instance. For a disc-shaped thin spot of diameter 10^{-2} cm in a film, the thickness of which is equal to $1.5 \cdot 10^{-5}$ cm, the increase of interfacial energy will have a value of about $0.8 \cdot 10^{-5}$ ergs if the thickness of the "black

spot" is equal to 150 A. The potential energy due to the double-layer interaction will now be of the same order of magnitude in actual cases where the interfacial potential may be assumed to range from 100 to 150 mV. The surface area of a "black spot" may attain still larger values (of the order of 1 cm^2) and in those cases the increase of interfacial energy will be negligible in comparison with the potential energy of the double-layer interaction. We might, therefore, expect that the interaction between the interfaces of a large "black spot" in an aqueous film is comparable to the interaction between two large hydrophobic colloidal particles. In the next section Verwey and Overbeek's theory of the stability of colloids will be applied to "black spots".

4.4. STABILITY OF "BLACK SPOTS"

According to the theory of the stability of colloids two different types of forces play a role in determining the interaction between charged interfaces, viz. the electric double-layer repulsion and the long-range London-van der Waals attraction forces. The existence of the long-range attractive forces has recently been established by means of painstaking experimental methods[32]; the results obtained by the various authors differ appreciably as to the dependence of the attractive force on the distance between the surfaces and to the exact magnitude of the constant A, which enters as a first power into the expression for the attractive potential. These differences might, in part, be explained by the fact that the experimental procedures employed by the Dutch and the Russian investigators were not exactly the same. The average distance between the surfaces of the plane and the sphere in the experiments of Deryagin and Abrikosova was, apparently, large enough to make the electromagnetic retardation of preponderant importance. Making allowance for this effect, the value of A for quartz calculated from their experiments, is equal to $3 \cdot 10^{-12}$ ergs, i.e., about 3 times as high as the value given by the existent theories. Overbeek and Sparnaay did not find any influence of electromagnetic retardation in the attractive force measured between two plane surfaces. Application of the London-Hamaker theory to the experimental results leads to a value for A, which is about 40 times larger than the theoretical one. It may be deduced from both experimental investigations that application of the London-Hamaker theory to the attraction between the interfaces of a "black spot" will result in values for the attractive potential that are certainly not too high. The value of A has been assumed, in our calculations, to be equal to 2.10^{-12} ergs. It is to be noted that the attraction between two particles of air, dispersed in water, is equal to the attraction between two water particles of the same size and shape, dispersed in air as follows from Hamaker's theory[34].

The total potential energy per cm^2 of surface, due to double-layer repulsion and London-van der Waals attraction, is given in Figure 4.7 as a function of the distance between two charged plane surfaces. The curves for two values of the surface potential have been calculated from the data given by Verwey and Overbeek for an electrolyte concentration of 0.025 N of a monovalent electrolyte. A conspicuous feature of these curves is, next to the presence of a very high potential energy barrier, the minimum for a value between 100 and 150 A for the distance between the surfaces. For this thickness of the "black spot" the mutual attractive forces of the molecules of the liquid, which will tend to reduce the thickness still further, have the same absolute value as the double-layer repulsion which will counteract the thinning of the film. The resulting nega-

tive potential energy has already a value of $-2.7 \cdot 10^{-3}$ ergs for a surface area of 0.1 cm², i.e., about 7.10^{10} kT units. The increase of interfacial energy in this case (Equation 4.6) is only $2.5 \cdot 10^{-4}$ ergs, assuming again that the initial thickness of the film is equal to $1.51 \cdot 0^{-5}$ cm and the surface tension 35 dynes/cm. The London-van der Waals attraction is, therefore, largely sufficient to counteract both double-layer repulsion and surface forces; the equilibrium of the three forces ensures the relative stability of a "black spot" in a film of much larger thickness. For "black spots" of larger surface area the depth of the "potential minimum" will become correspondingly larger and the relative importance of the surface forces smaller.

The theory outlined above explains very well the experimental observations reported in Section 4.2. If a liquid film prepared from a soap solution gradually thins under the action of gravitation or other forces, the two faces of the film may approach locally over a considerable area to a distance where the

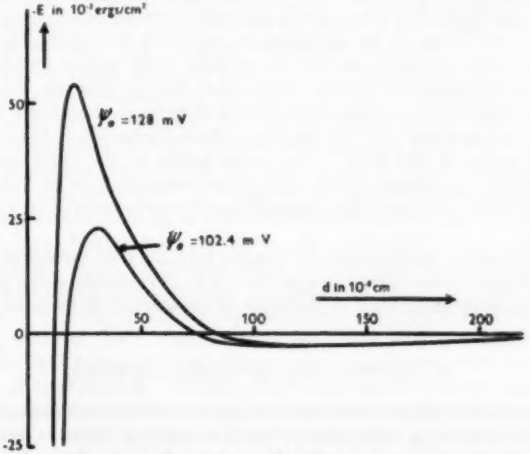

FIG. 4.7.—Total potential energy due to double layer repulsion and London-Van der Waals attraction as a function of the distance between two surfaces of a "black spot". ψ_0 =surface potential.

London-van der Waals attraction between the liquid molecules will enhance appreciably the action of the external forces. The process of thinning will be accelerated resulting in the formation of a "black spot", whose ultimate thickness will be determined by the position of the "potential minimum", hence dependent on the values of the ionic strength of the solution, the constant A and—to a lesser degree—the interfacial potential. In a film held vertically and perfectly undisturbed by any external force except gravity, the "black spot" will start in the top of the film and grow downward, the frontier between the black part and the rest of the film being formed by a straight horizontal line. In general, however, a liquid film, either isolated or forming part of a foam, will be subject to forces acting in different directions, due to pressure differences in the liquid, which may originate from local fluctuations of the gas pressure or from differences in curvature of the gas-liquid interface. The thickness, at which the influence of the London-van der Waals attraction becomes appreciable, will be attained, therefore, in different parts of the film at the same time or in the

same short interval of time. Various "black spots" will be formed and grow rapidly in different directions, thus increasing the total "black" area. The rate of this process of growth will be dependent on the value of the London-van der Waals attraction and the viscosity of the liquid which has to be pushed from between the approaching surfaces. When two or more growing "black spots" meet colaescence of these spots, i.e. formation of one large spot, does not necessarily take place as has often been observed during the experiments described in Section 4.2. When the upper part of a vertically placed film has become "black" this part of the film does not consist, in general, of one alrge continuous "black spot" but it is subdivided into numerous small "black spots". Their coalescence will proceed slowly because of the difficulty for the liquid in the thicker intermediate layers to "escape" from between the "black spots". In all cases observed, rupture of the film occurred before total coalescence of the agglomerated "black spots" had taken place. Rupture was always preceded by a very rapid growth of the total "black" area which seems to indicate that the accelerated liquid flow may be the immediate cause of the breakdown of the film. This hypothesis is in accordance with the well-established fact that liquid films which are kept as free as possible from any external disturbance may have a considerable lifetime even after having become totally "black". The internal liquid flow in these films will be very limited and of a more uniform character in comparison with the lamellae where formation of black spots occurs in different parts of the film. The large value of the activation energy of rupture prevents a collapse of the film unless spontaneous or induced fluctuations of the equilibrium conditions supply a suffiicent excess of energy to provoke rupture.

Various possible mechanisms of film rupture may be proposed in theory; it will be the object of the discussion in Part V to investigate some of these possibilities and to determine their probability of occurrence in isolated lamellae and in foams.

V. MECHANISM OF FILM RUPTURE

Lamellae of pure liquid and small molecule solutions are unstable because of the absence of a limiting thickness. Rapid collapse of these lamellae may start at relatively large thickness ($\sim$500 A) under influence of the London-van der Waals attractive forces. Small quantities of surface active ions will prevent this collapse mechanism from occurring in aqueous lamellae. A sufficient amount of activation energy for rupturing a "stable" lamella may be supplied by a local depression of surface tension in a small volume element of the film. The minimum surface area of such an element is calculated as a function of the film thickness, and its dependence on the rheological properties of the superficial layers of liquid (plasticity, viscosity and elasticity) is explained.

Some results are given of an experimental investigation of the influence of a local rise in temperature on the lifetime of isolated lamellae of a Tee-pol solution. The destabilizing effect of local heating is interpreted as a result of the decrease of surface tension in the warmer portion of the film. The importance of local temperature variations for the instability of foams is discussed. A calculation is given of the magnitude, frequency and average lifetime of spontaneous temperature fluctuations in liquid lamellae under adiabatic conditions. It is shown that these fluctuations are able to affect the stability of very thin lamellae only (thickness of the order of some tens of A).

A general explanation of the action of anti-foaming agents is given, based

on the occurrence of local depressions in surface tension. Finally the effect of mechanical disturbances on the probability of film rupture is considered.

5.1. COLLAPSE OF "UNSTABLE" FILMS

Rupture and collapse of a liquid lamella will always be preceded by the formation of a hole somewhere in the liquid and will demand, therefore, a certain amount of activation energy as has been calculated in Part IV. The energy required will be relatively small for lamellae of pure liquids whose thickness may attain very low values as a result of drainage. The ultimate thickness of these films will be limited only by the dimensions of the liquid molecules. If this ultimate thickness will have been reached anywhere in the liquid, hole formation and rupture will immediately follow since the activation energy in this case will be only a few kT units (see Equation (4.4)), hence insufficient to prevent the spontaneous collapse of the film. Lamellae of pure liquids are, therefore, essentially unstable and incapable of forming a persistent foam structure. The same reasoning is valid for all solutions of substances of low-molecular weight. In general many of these unstable" films will suddenly collapse at a thickness whose mean value is considerably larger than the sum of a few molecular diameters. According to Deryagin and Titievskaya, films formed by aqueous solutions of alcohols and undissociated fatty acids may already collapse at a thickness of 500 A. Before collapse took place the films gradually decreased in thickness down to this "critical" value at which the rapid transition to an unstable state occurred. It might be supposed that the London-van der Waals attractive forces will be of sufficient significance at this distance to cause a very rapid local thinning of the film. In contradistinction with the same process in stable" films of a soap solution, for example, the thinning of unstable films will be practically unhampered (or hampered to a much lesser degree) by the existence of electric double-layer repulsion. In the films investigated by the Russian authors cited, double-layer repulsion was probably not totally absent since it was observed that the process of collapse was accelerated by the addition of electrolytes. In such cases, the exact value of the surface potential will become rather important because the transition from instability to stability is very sensitive to the value of the potential in collodial systems with a low surface charge[35].

The sum of double-layer repulsion and London-van der Waals attraction may be negative for all values of the thickness as is shown in Figure 5.1 for a surface potential of 25.6 mV but nevertheless contain a maximum which is found at about 250 A when the electrolyte concentration is 1 mmol/liter. A corresponding maximum is shown by the curve which represents the total potential energy, i.e., the above mentioned repulsion and attraction energy increased by the repulsion potential due to the surface energy. The values of the various parameters are: $A = 2 \cdot 10^{-12}$ ergs, $\gamma = 70$ dynes/cm and $r = 0.1$ cm. The value of the maximum ($2 \cdot 10^{-5}$ ergs for the chosen example) will, of course, rapidly decrease as the area of the approaching surfaces becomes smaller but a decrease of the surface area will, at the same time, enhance the relative importance of the surface energy (which is proportional to the first power of r). If the value of the surface area should be 10 times as small as in Figure 5.1, the London-van der Waals attraction should be insufficient to counteract the surface forces and film collapse in the absence of external forces at a thickness of 500 A should be inexplicable. The only means of decreasing the value of the potential maximum is lowering the surface potential or increasing the electraolyte con-

centration. It follows that a lamella containing water or an aqueous electrolyte solution will rapidly collapse unless a potential difference exists across the interfaces, whose values does not need to exceed a few tens of millivolts for an electrolyte concentration smaller than 0.001 molar (univalent electrolytes). The rate of collapse will be proportional to the attractive force and inversely proportional to the viscosity of the liquid, if the flow is assumed to be laminar. Thus relatively small quantities of surface active ions will be sufficient to prevent the described collapse mechanism occurring in aqueous lamellae. In

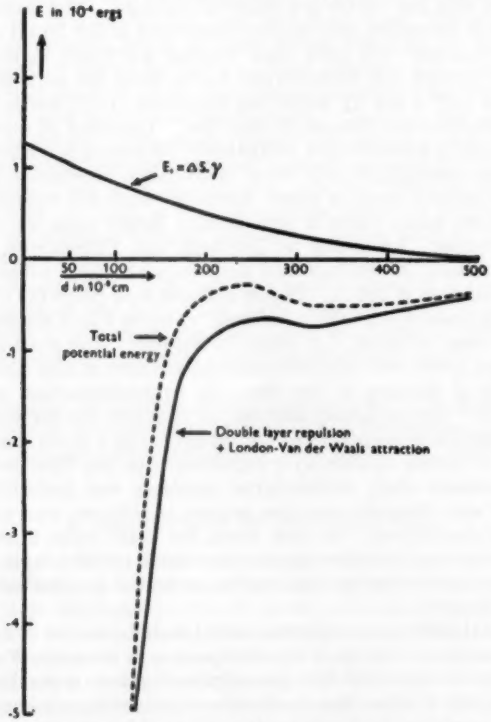

FIG. 5.1.—Total potential energy of two approaching surfaces of a lamella at the limit of stability. $\varphi_0 = 25.6$ mV.

organic liquids, which possess a much lower dielectric constant, the double-layer repulsion is of lesser importance; lamellae of these liquids will, consequently, become unstable at large thickness and will rapidly collapse. The lifetime of these lamellae, like the foam stability of these liquids, will be mainly determined by the rate of drainage. An example of this behavior has been provided by the experiments of Brady and Ross[36] on the foam stability of a number of hydrocarbon oils. The breakdown of these foams proceeds very regularly because all lamellae will collapse at about the same thickness releasing the enclosed gas at a constant rate. The foam stability may be conveniently defined in those cases as the total lifetime of the foam and will be proportional to the

kinematic viscosity of the liquid and the initial height of the foam column. For "stable" foams, in particular those containing surface active components, this simple model of spontaneous collapse will not hold, however, since film rupture in these foams is only possible after a sufficient supply of energy. The probability of rupture does not now need to be the same for all foam lamellae of equal thickness.

Possible mechanisms of "activated" rupture in these lamellae will be discussed in the following sections.

5.2. COLLAPSE OF "STABLE" FILMS PROVOKED BY A LOCAL SURFACE TENSION DEPRESSION

The availability at a certain moment of an extra amount of energy will be determined by the magnitude of

a) spontaneous energy fluctuations in the liquid and in the gas phase;
b) energy "shocks" (mechanical, thermal, acoustic) emanating from any external source.

A positive fluctuation of the energy content of a very small part of a liquid lamella will be equivalent to a temporary rise in temperature of that part of the film. Its effect on the stability of the film will be the same as that of an external heat source. Local heating of a foam may lead to its collapse and it is probable that this phenomenon is related to the thinning of liquid lamellae under the influence of a temperature gradient as has already been demonstrated by Plateau (see Part I). The diminution of thickness is explained by the flow of liquid from the warmest part of the film where the value of the surface tension will be lower than in the surrounding cooler areas. The increase of surface energy caused by a local thinning of the film will, therefore, be partly or totally compensated by a gain in surface energy resulting from the extension of the warmer surface area if, at least, the temperature differences remain large enough during the deformation. Local surface tension depressions are not necessarily due to a spontaneous temperature fluctuation or the presence of an external heat source. They may also originate from chemical reactions in the liquid phase or a sudden change of composition (addition of an anti foaming agent). Before proceeding to a detailed discussion of these various possibilities, the general effect of a constant local surface tension decrease on the free energy of deformation will be calculated.

The total change in free surface energy may be derived with the aid of the model developed in Part IV. We prefer, however, to introduce here a slightly modified picture of the local thinning of a lamella, which will allow us to obtain a very simple mathematical expression for the total energy change. The increase of surface area is only slightly dependent on the exact geometrical shape of the local deformation, which makes the expression for the energy rather insensitive to the pecularities of any model.

We shall suppose that the film element where the tension is lower has a circular cross section (radius = a_0) and that its surface tension will be lower than that of the surrounding liquid by an amount $\Delta\gamma$. The difference in surface tension will cause the film element under consideration to extend in a radial direction accompanied by a corresponding shrinkage of the surrounding area. Both surfaces of the thinning portion of the film will remain symmetrically curved during the deformation, each forming part of a spherical surface (see Figure 5.2). The degree of thinning is given by h whose maximum value (i.e.,

at the moment of rupture) will be equal to half the value of the initial thickness t.

The degree of extension is expressed by the value of a. These various parameters are interdependent because the volume of the deformed film element must remain constant during the extension as expressed by the following condition:

$$\pi a_0^2 t = \pi a^2 t - 2 \cdot \tfrac{1}{6}\pi h(3a^2 + h^2) \tag{5.1}$$

The total increase of surface free energy upon extension is given by:

$$\Delta F_s = 2\pi(h^2 + a^2)\gamma - 2\pi a_0^2\gamma - 2\pi(a^2 - a_0^2)(\gamma + \Delta\gamma) \tag{5.2}$$

where γ is the surface tension of the liquid in the element.

If the surface area of the film element is small, the influence of double-layer repulsion and London-van der Waals attraction may be neglected in compari-

FIG. 5.2.—Local thinning of a lamella due to a surface tension gradient.

son with the contribution of the surface forces. It may be assumed, therefore, that extension and thinning of the film element will occur when

$$\Delta F_s \leqslant 0, \quad \text{and} \quad \frac{d\Delta F_s}{dh} \leqslant 0$$

for all values of h.

Combination of (5.1) and (5.2) enables us to express these conditions in the parameters a_0, t and h. In all cases of practical importance (see below) h^2 is much smaller than $3a^2$ and may therefore, be neglected in the right hand side of Equation (5.1).

The following result is obtained:

$$\Delta F_s \leqslant 0 \quad \text{if:} \quad a_0^2 \geqslant h(t - h)\cdot\gamma/\Delta\gamma \tag{5.3}$$

$$\frac{d\Delta F_s}{dh} \leqslant 0 \quad \text{if:} \quad a_0^2 \geqslant \frac{2h(t - h)^2}{t}\cdot\gamma/\Delta\gamma \tag{5.4}$$

It can be easily verified that the right hand side of (5.4) is always equal to or larger than that of (5.3) for all possible values of h. We have thus only to examine if a minimum value of a_0 exists for which condition (5.4) is always satisfied.

The function $[h(t - h)^2/t]$ has a maximum for $h = \frac{1}{3}t$. Insertion of this value into (5.4) shows that thinning of the film element leading to ultimate rupture is only possible when the initial area of the element has a minimum value which is given by:

$$a_0^2 \geqslant \frac{8}{27} t^2\cdot\gamma/\Delta\gamma \tag{5.5}$$

For smaller values of a_0 thinning will not exceed a certain degree h the value of which may be calculated from (5.4).

Condition (5.5) shows that the radius a_0 has to be at least of the same order of magnitude as the film thickness t if immediate collapse is to take place. The influence of the presence of an adsorption layer at the interfaces of the lamella on the mechanism of film rupture described will be discussed in the following section.

5.3. EFFECT OF AN ADSORPTION LAYER ON THE LOCAL THINNING OF FOAM LAMELLAE

It has already been mentioned in Part I that the presence of adsorbed layers of surface active solutes may appreciably affect the rheological properties of the liquid surface. In certain cases (solutions of proteins, and also aqueous solutions of synthetic detergents[37] the existence of a "surface yield value" could be detected which means that flow of the superficial layers of liquid will occur only when the shear stress exceeds a minimum value. Experimental data are only occasionally reported in the literature; the highest values found by Brown, Thuman and McBain for aqueous solutions of sodium lauryl sulfate, containing small amounts of lauryl alcohol are between 0.1 and 0.15 dynes/cm. These values are of the same order of magnitude as those of the surface pressure ($\Delta\gamma$) to be expected between the surface of a temporary warmer film element and the surrounding surface in the case of spontaneous temperature fluctuations (see Section 5.6). The "surface yield value" of protein solutions may still be higher and it is therefore not unreasonable to attribute the remarkable persistence of the foams prepared from these solutions to the plasticity of the surface layer. Even if plasticity is absent the "surface viscosity" of many foam-forming solutions may attain values which are some orders of magnitude higher than the viscosity in the bulk of the liquid. A high viscosity of the superficial layers of liquid will, of course, never be able to *prevent* the deformation of a volume element of a foam lamella; it may, however, *retard* its thinning. When the deformation is caused by an equilibrium disturbance that is only active during a short period of time, the rate of thinning has to be sufficiently high in order to lead to film collapse before the system has regained its initial equilibrium. The rate of thinning is inversely proportional to the viscosity of the flowing liquid if the flow is laminar. The flow behavior of the liquid in the small volume element is very complex and its elucidation constitutes a difficult hydrodynamical problem. The surface tension difference will cause an outward radial flow of the superficial layers of liquid at both interfaces of the lamella. As a result of this surface flow the liquid in the interior of the film will become successively part of the surface and participate in its movement. The resistance against flow is, therefore, only partly determined by the value of the bulk viscosity but mainly by the viscosity of the superficial layer at the liquid-gas interface. All components which are adsorbed at the interface and thereby increase the surface viscosity of the liquid may be expected to increase the stability of the film against any disturbance acting during a limited period of time.

It has been tacitly assumed throughout this discussion that the initial surface tension difference will remain constant during the total deformation process. If, however, the liquid contains one or more surface active components the sudden increase of the interfacial area of the thinning film element will result in a temporary diminution of the adsorbed amount of these components

per unit of area. The surface tension of the deformed liquid will rise and $\Delta\gamma$ will correspondingly decrease until the initial value of the surface tension is restored by a renewed adsorption of surface active material. For dilute aqueous solutions the new equilibrium value of the surface tension after deformation may often be higher than before and the "restoring elastic force" can be calculated for this case as shown by Gibbs (see Part I). In all cases however, the nonequilibrium value of the surface tension immediately after deformation will be still larger than that given by Gibbs. Attainment of the new equilibrium will be reached at a finite rate whose value has been determined for various solutions and compared with calculated data of diffusion rates[38]. The values are strongly dependent on the composition and concentration of the solution; it appears that the time necessary for restoring the equilibrium value of the surface tension may range from 10^{-3} second to some hours. The initial surface tension difference will rapidly decrease during the deformation when the rate of thinning is larger than the rate of attainment of surface tension equilibrium. In extreme cases the deformation process will cease after having reached a certain degree of thinning and may even become reversed because $\Delta\gamma$ will change in sign when the effect of decreased surface concentration is more important than the influence of the initial surface tension depression. This may readily occur in many practical instances as the following considerations will show. The relative increase of interfacial area of the deformed film element is equal to (see Figure 5.2):

$$\frac{\Delta S_w}{S_w} = \frac{h^2 + a^2 - a_0^2}{a_0^2}$$

Its maximum value is attained at the moment of rupture ($h = \frac{1}{2}t$) and, according to Equation (5.1), is equal to:

$$1 + t^2/3a_0^2$$

In most cases $t^2 < 3a_0^2$ and the final surface area is, therefore, about twice as large as the initial one. The influence of a diminution of the surface concentration by a factor 2 on the value of the surface tension can be deduced from the surface tension dependence on the activity of the solute(s) with the aid of Gibbs' theorem or from surface pressure measurements in a Langmuir trough (see Part I). Both methods show that the rise in surface tension caused by a decrease of surface concentration to half its initial value may, in many cases, amount to some tens of dynes/cm, which is much higher than the surface tension depression expected from a moderate temperature increase (see below).

Arrest and reversal of the thinning process may even occur when the rate of surface tension equilibrium attainment is very high. In that case the rise of tension is given by Gibbs' expression:

$$d\gamma = \frac{2\Gamma_2^2}{S}\left(\frac{\partial\mu_2}{\partial G_2}\right)_{G_1} dS \qquad (5.6)$$

where G_1 and G_2 are the total quantities of the two components per unit area of the film and the subscript 2 refers to the surface active solute. For a given volume element of the film G_2 is proportional to the thickness and hence the rise in tension per unit of relative area increase will, according to Equation (5.6), be

larger the smaller the film thickness. This is a direct consequence of the fact that the ratio between the number of adsorbed and dissolved solute molecules is a decreasing function of the thickness. If A is the area occupied by an adsorbed molecule or ion, the total number adsorbed at both interfaces of the film is equal to $2/At$ per unit volume of the lamella. In a "black" film of thickness $t = 150$ A this number will represent a concentration of 0.44 mole/1 when $A = 50$ A^2. The concentration of dissolved molecules will, in general, be much lower; when an element of such a film increases its surface area by a factor 2 the number of molecules in the interior of the element will be largely insufficient to restore the surface concentration to its original value. Surface deformation of very thin films will, therefore, always lead to an increase of surface tension even at high rates of equilibrium attainment, and give rise to a restoring elastic force as postulated by Gibbs. Film collapse will, nevertheless, result from a local thinning when its driving force is greater than the restoring one. The probability of such an occurrence in the case of a local temperature increase will be examined in the following section.

5.4. CONDITIONS OF FILM RUPTURE INDUCED BY A TEMPERATURE DIFFERENCE

A local temperature rise in a liquid lamella may provoke thinning and ultimate rupture as described in Section 5.2 when the radius of the disc-shaped warmer film element has a minimum value which is given by:

$$a_0^2 \geqslant \frac{8}{27} t^2 \cdot \gamma / \Delta\gamma \tag{5.5}$$

The minimum values of a_0 can be calculated for any value of the local temperature difference ΔT if the temperature dependence of the surface tension is known.

The temperature function of the surface tension of water is equal to[39]:

$$\frac{\partial\gamma}{\partial T} = -0.145$$

dynes/cm/° C for all temperatures between 10° and 60° C. The addition of surface active solutes not only decreases the absolute value of the surface tension but also its dependence on temperature, as shown by the following data: aqueous sodium oleate sol.: $\gamma_{20°C} = 34$ dynes/cm; $\partial\gamma/\partial T = -0.07$ dyne/cm/° C[40]: aqueous potassium laurate sol. (0.01 mol(: $\gamma_{20°C} = 34$ dynes/cm; $\partial\gamma/\partial T = -0.06$ dyne/cm/° C[41]: aqueous Tee-pol sol. (1%); $\gamma_{20°C} = 33$ dynes/cm; $\partial\gamma/\partial T = -0.05$ dyne/cm/°C.

A combination of low surface tension together with an appreciable temperature dependence is encountered only in the case of unassociated organic liquids[42] where $\partial\gamma/\partial T$ is equal to -0.12 dyne/cm/° C, and $\gamma_{20°C}$ may vary between 20 and 40 dynes/cm.

Use has been made of these data in order to calculate the minimum values of a_0 by means of Equation (5.5). The results are given in Table V for a number of temperature differences.

The calculated data show that the ratio a_0 (min)/t is of the same order of magnitude for all liquids and solutions concerned.

TABLE V

MINIMUM VALUES OF THE RADIUS OF A WARMER VOLUME ELEMENT IN A LAMELLA LEADING TO COLLAPSE

Temp. difference ΔT in ° C	Minimum value of a_0 in		
	Water	Aqueous soap- and detergent sol.	Unassociated organic liquids
1	12.3 t	13 t	6.7 t
2	8.81 t	9.3 t	4.8 t
3	7.1 t	7.5 t	3.9 t
4	6.1 t	6.5 t	3.4 t
5	5.5 t	5.8 t	3 t
10	3.9 t	4.1 t	2.1 t

5.5. FILM COLLAPSE RESULTING FROM INDUCED LOCAL TEMPERATURE DIFFERENCES

In this section some results obtained by two different experimental methods which have been applied in order to permit a more or less rough estimate of the temperature differences necessary to induce film collapse will be reported. The results may be compared with the theoretical data given in the foregoing section; finally, the probability of spontaneous film collapse in foams caused by local temperature differences will be discussed.

The lamellae investigated were prepared again by immersion of a wire frame in a solution of 1% Tee-pol (~0.03 normal) to which 1% sodium alginate was added in order to increase its viscosity. After lifting the liquid film from the solution, its center was heated by means of a thin copper wire (diameter = 0.01 cm) pierced through the film and forming part of an electrical circuit comprising a battery and a resistance. The temperature of the wire was measured by means of a thermocouple at a point near the surface of the lamella. A range of temperatures could be attained by varying the potential difference

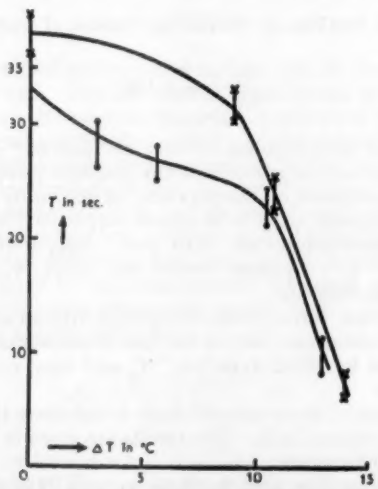

FIG. 5.3.—Effect of local heating on the lifetime of a lamella of a Tee-pol solution. ● heating by a copper wire pierced through the lamella. × heating by a copper needle at 40 microns distance from the lamella.

with the aid of the sliding resistance. A disadvantage of this method is the introduction of a new unknown factor, viz., the interface between the metal wire and the liquid which might influence the stability of the film.

A second method has therefore been employed in which the localized temperature increase of the film was effectuated by means of an electrically heated copper needle, which was brought at a distance of about 40 microns from the center of the film by means of a micrometer screw. The temperature of the needle top was measured again with the aid of a thermocouple. The results obtained with both methods are represented by the two curves in Figure 5.3. At each chosen temperature, on the average, the lifetimes of six films have been determined by each method; in all about 60 measurements have been made.

The lifetime of a film at a given temperature of the copper wire appears more or less to correspond with an equal lifetime in the second series of measurements when the copper needle was heated to the same temperature. This may be purely coincidental and does not necessarily mean that the temperature distribution around the center of the film was the same in both cases.

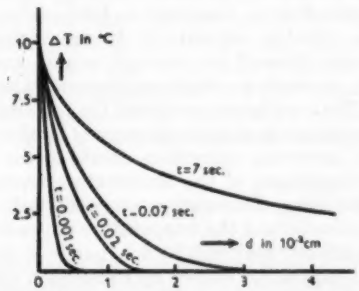

FIG. 5.4.—Claculated temperature distribution in a lamella as a function of the radial distance from the heated wire. Effects of increasing time. Diameter of wire = 0.01 cm. d = radial distance from circumference of wire.

An important destabilizing influence manifests itself at a temperature difference of about 10° C between the wire (or the needle) and the liquid from which the film has been prepared. The conditions of these experiments differ, however, to a large extent from those of the simplified model described in Section 5.2, which makes a direct comparison of theoretical and experimental results hardly possible. The volume of the warmer film element in the experiments is not constant but increases rapidly with time because of the conductivity of the liquid. Moreover its temperature is not the same throughout the whole volume but depends on the radial distance from the center and on time. The temperature distribution around the heated wire as a function of time may be calculated when heat transfer is caused only by conduction[43] (i.e., for a liquid at rest). Some results of such a calculation are given in Figure 5.4. It may be deduced that the heat from the wire expands very rapidly over a considerable volume of liquid during the lifetime of the lamella. Because of the flow of liquid from warmer to colder regions the influence of local heating will manifest itself at still larger distances from the wire than those given by the theory of conduction. According to the theoretical data given in Table V the linear dimensions of the surface of the warmer film element have to be at least of the same order of magnitude as the film thickness. This was certainly the case in

both experiments described; local heating gave rise to the development of a number of "black spots", which were clearly visible and the more or less circular surface area of which had a diameter of a least 0.01 cm, whereas the film thickness was of the order of a few microns.

At temperatures for which the influence on the lifetime of the film was only slight, the "black spots" formed in the center of the film rose to the top and united with the "black spots" already present in that part of the lamella. In those cases film rupture probably took place near the top in contradistinction with collapse in very short-lived films ($\Delta T \sim 10°$ C), which ruptured before the "black spots" had risen to the top. It might be concluded from these observations that a temperature difference may decrease the lifetime of a lamella even when the value of the local temperature increase is insufficient to provoke rupture of the warmer film element; in the latter case its effect may be indirect, viz. an increase of the "black" area of the lamella and a corresponding increase of the probability of rupture.

Local temperature differences of sufficient magnitude and affecting a sufficiently large area to decrease the film stability, can also be produced when the persistence of liquid films is measured at temperatures higher than about 35° C in an apparatus, which is not perfectly thermostatted as has been demonstrated by Gillespie and Rideal[44] for films of paraffin and benzene (thickness from 10^{-5} to 10^{-4} cm), separating a flattened drop of water from a large volume of the same liquid. These authors found that the probability of film rupture is independent of temperature when the occurrence of local temperature variations is greatly reduced; if, however, convection effects in the thermostatted water jacket could cause disturbance of the temperature equilibrium, a decreasing film stability with increasing temperature was observed. Similar phenomena might readily occur in foams and the temperature dependence of foam stability reported by various authors[45] may well be due, partly or totally, to the presence of local variations of temperature caused by convection currents in the thermostat liquid and in the foam lamellae. This effect will be still more pronounced when heating takes place after the foam has been formed because of the relatively slow heat transfer in the foam itself. Important local temperature variations may then be produced in the lamellae.

Uneven temperature distributions might equally be expected in the case of exothermic (or endothermic) chemical reactions taking place between components of the liquid phase. The influence of local temperature differences on the rupture of foam lamellae is, therefore, of more than merely academic interest. In the manufacture of latex foam rubber for instance, the gelation of the rubber latex is brought about by ionic reactions in the liquid phase of the foam. These reactions tend to reduce the charge density of the rubber-water interface, either at room or at elevated temperatures depending upon the particular gelation agents used[46]. Gelation of these foams is always accompanied by an appreciable degree of film rupture, in particular when the foam is heated; it will be evident from the foregoing that the existence of local temperature variations may play an important role in these and other technological processes.

5.6. EFFECT OF SPONTANEOUS TEMPERATURE FLUCTUATIONS IN THE LIQUID

Local temperature variations in foams will arise even when heat exchange with the exterior is rigorously excluded. It will be the object of the following

discussion to investigate the influence of spontaneous temperature fluctuations in the lamellae on the probability of rupture.

Temperature fluctuations in a volume element of liquid are relatively small; their average value may be derived from the theory of statistical mechanics[47].

In any volume element of a liquid film in contact with a large amount of gas of average temperature T_0 the mean value of the temperature fluctuations will be given by:

$$\overline{\Delta T^2} = \frac{kT_0^2}{C} \tag{5.7}$$

where k is the Boltzmann constant and C the heat capacity at constant volume of the considered element of liquid. Hence the average temperature fluctuation in a volume element of water equal to 10^{-18} cm³ will, at room temperature, be of the order of 0.5° C ($k = 1.38 \cdot 10^{-16}$ ergs/° K, molecular heat capacity of water $c_v = 1.26 \cdot 10^{-15}$ ergs/molecule/° K). Let us suppose now that this volume element is part of a very thin black film (thickness $\sim 10^{-6}$ cm); the radius of the circular cross section a_0 will then be equal to 0.5 t. It is evident from a comparison with the values calculated in Section 5.4 that a temperature increase of 0.5° C will be insufficient to provoke a thinning of this volume element leading to ultimate rupture. The probability of larger temperature fluctuations may be determined by application of a very general method given by Slater[48]. If $W(T)\,dT$ represents the probability of finding a temperature between T and $T + dT$ in a volume element of average temperature T_0, we have

$$W(T)dT = \text{const. exp} - \frac{E - T_0S}{kT_0}\,dT \tag{5.8}$$

where E and S are the energy and the entropy of the liquid at the temperature T. Expanding the free energy function in Taylor's series about T_0 and remembering that this function will have a minimum at the average temperature, the following result is obtained:

$$E - T_0S = E(T_0) - T_0S(T_0) + \tfrac{1}{2}\left(\frac{d^2E}{dT^2} - T\frac{d^2S}{dT^2}\right)_{T=T_0}(T - T_0)^2 + \cdots \tag{5.9}$$

Using the thermodynamic equations:

$$\left(\frac{\partial E}{\partial T}\right)_v = C \quad \text{and} \quad \left(\frac{\partial S}{\partial T}\right)_v = \frac{C}{T} \tag{5.10}$$

Equation (5.9) may be solved:

$$E - T_0S = E(T_0) - T_0S(T_0) + \frac{C}{2T_0}(T - T_0)^2 \tag{5.11}$$

Insertion of this result into Equation (5.8) and evaluation of the normalization constant by integration over all values of $T - T_0$ leads to the following expression:

$$W(T)dT = \left(\frac{C}{2\pi kT_0^2}\right)^{\frac{1}{2}} \text{exp} - \frac{C(T - T_0)^2}{2kT_0^2}\,dT \tag{5.12}$$

This equation is analogous to Gauss' well-known error function. The probability of a fluctuation larger than ΔT will now be given by:

$$W_{\Delta T} = \left(\frac{C}{2\pi k T^2}\right)^{\frac{1}{2}} \int_{\Delta T}^{\infty} \exp - \frac{C(\Delta T)^2}{2kT^2}\, d(\Delta T) \tag{5.13}$$

$$= (2\pi)^{-\frac{1}{2}} \int_{X}^{\infty} \exp - \tfrac{1}{2}X^2\, dX \tag{5.14}$$

where

$$X = \Delta T/T \cdot (C/k)^{\frac{1}{2}} \tag{5.15}$$

The value of the integral in Equation (5.14) may be read from the tables of Gauss' error integral for any ΔT, T and C.

The results of the calculation for a volume element of water equal to 10^{-18} cm^3 are given in Table VI.

TABLE VI

PROBABILITY OF A TEMPERATURE FLUCTUATION $> \Delta T$ IN 10^{-18} CM^3 WATER AT $T = 300°$ K

ΔT in ° K	$W_{\Delta T}$
0.5	0.184
1	0.034
2	0.000126
3	$2 \cdot 10^{-9}$
4	$3 \cdot 10^{-13}$
5	10^{-19}
6	$2 \cdot 10^{-28}$

The data given show that the probability decreases very rapidly for increasing values of the fluctuation. In larger volume elements the probability of a given temperature fluctuation will be correspondingly smaller since X is proportional to $C^{\frac{1}{2}}$, and the heat capacity C is proportional to the volume of the element. The probability of a fluctuation larger than 3° C, which for 10^{-18} cm^3 water is equal to $2 \cdot 10^{-9}$, will for $4 \cdot 10^{-18}$ cm^3 water be no more than $2 \cdot 10^{-28}$, i.e., a decrease by a factor 10^{20} for a 4-fold increase of volume. It follows that spontaneous temperature fluctuations, which are sufficiently large to affect appreciably the stability of a lamella, will only occur in very thin films. The number of fluctuations per unit of time and its distribution will be the same for all volume elements of equal size in the lamella. In a "black" film or spot with a total surface area $= 2S$ cm^2 and a thickness $\sim 10^{-6}$ cm, the total number of fluctuations per second in all volume elements of 10^{-18} cm^3, which are larger than ΔT, is therefore equal to:

$$S/10^{-12} \cdot W_{\Delta T} \cdot \frac{dN_f}{dt} \tag{5.16}$$

$S/10^{-12}$ is the number of volume elements of 10^{-18} cm^3, and dN_f/dt is the total number of fluctuations per second in each element.

If a fluctuation ΔT leads to immediate rupture of the film, expression (5.16) may be put equal to $1/\tau$, where τ is the average lifetime of the lamella.

In order to calculate the number of fluctuations per second in each volume element, the duration of one fluctuation should be known. It will be obvious

that the duration of any fluctuation will be longer the larger the magnitude of ΔT; it is impossible to define exactly the value of the fluctuation at a given moment since the time function of the temperature will never be constant but composed of a series of sinusoidal waves. We may nevertheless define the duration of the fluctuation as the period of time, in which the temperature fluctuation continually increases from its mean value, passes through a maximum and finally falls off again until the average value is regained. The time, in which a fluctuation ΔT decreases to its mean value $\overline{\Delta T}$, may be calculated if it is assumed that the warmer element transfers its excess of heat to the surrounding elements by conduction only. Carslaw and Jaeger[49] have given a treatment of this case for a very small spherical element of radius a. Their approximated expression for $a^2 < \kappa t$ (where κ is equal to thermal conductivity/density $\times$ specific heat) reads as follows:

$$\overline{\Delta T} \Big/ \Delta T = \frac{a^3}{6\pi^{\frac{1}{2}}(\kappa t)^{\frac{1}{2}}} e^{-a^2/4\kappa t} \tag{5.17}$$

In a volume element of water equal to 10^{-18} cm^3 the time t necessary for decreasing ΔT from 5 or 6° C to its mean value 0.5° C is, according to Equation (5.17) about 10^{-9} second, κ being equal to $1.14 \cdot 10^{-3}$ cm^2/sec. For these extremely low values of t, Equation (5.17) is at the limits of its validity; in view of the approximate character of the reasoning given it does not seem worthwhile to attempt a more precise calculation. We will assume that the total number of fluctuations will be at least of the order of 10^9 per second. Insertion of this value into Equation (5.16) leads to the conclusion that only fluctuations of about 5° C or smaller may be of any practical importance as far as their frequency of occurrence is concerned. The number of fluctuations, which are larger than ΔT in a "black spot" of 1 cm^2, will be equal to 100 per second for $\Delta T = 5°$ C and only 1 per $5 \cdot 10^6$ seconds for $\Delta T = 6°$ C. According to Equation (5.5), a temperature increase of 5° C in a cylindrical volume element of an aqueous solution at room temperature will lead to collapse of the lamella when the radius of the circular cross section is at least equal to 5.8 times the film thickness (see Table V). This means that in a lamella of thickness $\sim 10^{-6}$ cm the volume of the warmer element has to be much larger than 10^{-18} cm^3 as assumed in our calculation.

Condition (5.5) will be satisfied when the volume element of 10^{-18} cm^3 forms parts of a lamella or a "black spot" having a thickness smaller than 25 A. Only in that case the stability of the lamella may be affected by spontaneous temperature fluctuations; the lifetime of the fluctuations in such a volume element will be appredably larger than given by Equation (5.17) since the greater part of the surface (more than 80%) is now formed by the liquid-gas interface which will have a retarding influence on the heat transfer from the warmer element. The lifetime may now be sufficiently large to provoke an immediate breakdown of the lamella. The time interval in which a volume element of liquid will thin from, e.g., 25 A to 5 A, can be estimated from Stephan's expression[50] for the rate of thinning of a cylindrical volume of liquid under the influence of a normal force F:

$$\text{time} = \frac{3\pi\eta a_0^4}{4F}\left(\frac{1}{d_2^2} - \frac{1}{d_1^2}\right) \tag{5.18}$$

where $d_1 = 25 \cdot 10^{-8}$ cm and $d_2 = 5 \cdot 10^{-8}$ cm.

The force F is to be calculated by differentiation of Equation (5.2) for the free energy: its value is dependent on the exact magnitude of the surface area of the warmer volume element and may amount to $10^{-5} - 10^{-4}$ dynes when the lamella consists of an aqueous soap solution. It follows from Equation (5.18) that the element will have attained a thickness of 5 A in about 10^{-7} sec if the viscosity $\eta = 0.01$ c.p. "Stable" lamellae of very small thickness (in the order of some tens of A) are, consequently, nonexistent unless the rheological "resistance" of the lamella (plasticity, viscosity or elasticity) is strong enough to annihilate any influence of spontaneous temperature fluctuations.

5.7. ACTION OF ANTIFOAMING AGENTS

The mechanism of local thinning of a lamella, as described in Section 5.2, will operate in all cases where a local decrease of surface tension is induced. A well known example is the effect of so-called antifoaming agents on the foam stability. If such an agent is added to a foam, it may either mix with the liquid phase or be adsorbed at the interface (depending on its chemical nature) and cause, in this way, an instantaneous decrease of the surface tension. In the first stage of the process the added component will certainly be unevenly distributed in the foam lamellae and hence local variations of the surface tension will result from the addition (this may even be the case when the surface tension of the pure antifoaming agent or of its solution is higher than that of the foamed liquid). It is not surprising, therefore, that a very large range of chemical compounds appear to exert a destabilizing effect on foams[51], whereas at the same time the solutions of these compounds may be able to form a foam.

This general explanation of the mechanism of film rupture caused by antifoaming agents does not exclude the possibility of specific effects as for instance: diminution of the coherence of the adsorbed monolayer at the interface and a corresponding decrease of the surface viscosity, or surface elasticity, brought forth by the adsorption of the antifoaming agent[52]. It appears nevertheless probable that in many cases film rupture is a direct result of the inhomogeneity of the liquid phase causing local depressions of the surface tension in volume elements of the lamellae that are large enough in order to comply with condition (5.5).

5.8. OTHER CAUSES OF FILM RUPTURE

Another cause of film rupture, proposed by many authors, is the uneven distribution of the normal pressure along the surface of a lamella, which should equally result in a local thinning of the film. Such a disturbance of the mechanical equilibrium might be due to vibrations emanating from any external source or brought about by statistical fluctuations in the gas phase adjacent to the lamella. The last mentioned possibility may be excluded as follows from a calculation similar to that given in Section 5.6 for the temperature fluctuations in the liquid. The result of this calculation shows that the pressure fluctuations to be expected are largely insufficient to cause an appreciable local thinning of the lamella. In order to decide if any mechanical or acoustic vibration may induce rupture of the lamella, two parameters have to be known, viz. the amplitude and the frequency of the vibration. Liquid lamellae are very elastic and largely deformable when the deformation is applied slowly as is shown by the ease with which a lamella of a soap solution may be transformed into a soap bubble. A moderate local increase of the pressure will only lead to rupture of

the film, therefore, if it is applied within a very short interval of time, which is smaller than the "relaxation time" of the film.

As to the amplitude it will be obvious that the local deformation of a lamella must have a value of the order of its thickness for inducing an immediate rupture. If only surface forces are taken into account, the normal force necessary to deform one surface with an ampltidue h (see Figure 5.2) is equal to $(d/dh)(\pi h^2\gamma) = 2\pi h\gamma$, since the increase of total surface area upon deformation will be equal to: $\pi(h^2 + a^2) - \pi a^2$.

For a "black" film ($t \sim 10^{-6}$ cm) of an aqueous soap solution the force must have a value of about $2 \cdot 10^{-4}$ dyne if the film is to be completely pierced. When any force acting on a part of the lamella is insufficiently large to induce its immediate rupture, the motion of the surface will be propagated through the liquid of the film. The properties of the surface waves formed as a function of the characteristics of the liquid, like density and surface tension, may, in principle, be calculated[53] though the solution of the relevant equations in this particular case will present serious difficulties, the more so when the thickness of the lamella is not uniform because of the presence of "black spots". Since, in general, all kinds of pressure disturbances will be present, the surfaces of a lamella will never be at rest but subject to periodic and aperiodic deformations. The probability that a deformation leads to rupture anywhere in the lamella, will be larger the smaller the local thickness, but it might be possible that those parts of the film, where the thickness shows a discontinuity (i.e., at the borders of a "black spot"), are particularly liable to rupture. Neither theoretical nor experimental evidence is, however, available at the moment to lend support to the latter suggestion.

An indication might perhaps be found in the observations reported in Part IV of this series viz. the very rapid growth of the "black" area immediately before rupture. It may be supposed then that the induced surface deformations will facilitate the formation of "black spots" by decreasing the thickness locally over an area large enough to ensure the stability of such a spot (this will most readily occur in the thinnest parts of the film as follows from the considerations in Part IV). Accelerated growth of the spot will follow (if the thickness of the film around the spot is not too large) under influence of the London-van der Waals attraction forces which will tend to increase the area of the spot. In all cases of spontaneous film collapse the sequence of the described accelerated growth and sudden rupture has been noted. The rapidly advancing frontline of the "black spot" will be the seat of high stress concentrations and turbulent flow. It is, therefore, plausible to assume that the rupture will be produced somewhere along this borderline. If this picture is correct, vibrations of any kind have not necessarily to be of very large amplitude in order to decrease the stability of a lamella or a foam. The amplitude (or the sum of the amplitudes in the case of more than one vibration) must, however, be large enough to provoke an appreciable surface deformation of the lamella. Experimental investigations of the influence of forced vibrations on the stability of isolated lamellae should be helpful in a further elucidation of the mechanism of film rupture and foam destabilization, induced by disturbances of the mechanical equilibrium.

VI. SUMMARY *

A foam is a colloidal system in which the dispersed phase is a gas. Foams, as well as other irreversible colloids, are unstable from a thermodynamic

* Translated for RUBBER CHEMISTRY AND TECHNOLOGY by M. A. Golub from the French summary appearing in the original text.

standpoint owing to the presence of an extensive interface. Nevertheless, a large number of foams having a continuous liquid phase display remarkable persistence because the irreversible processes leading to thermodynamic equilibrium often occur at a rather slow rate. The main purpose of this work was to study the mechanism and kinetics of these processes.

The first part (I) considers the various factors, not all of equal importance, governing the stability of foams which had already been described in the scientific literature. That factor whose influence has been the most discussed and even the most contested is the surface tension of the liquid. In fact, a foam can possess a certain stability only when the liquid phase contains one or more surface-active materials. However, there is no general relationship between the lowering of the surface tension and the increase in foam stability.

The gas pressure in the bubbles of a foam is higher than the pressure in the surrounding liquid to an extent which is greater the higher the surface tension and the smaller the radius of curvature (Laplace and Young relationship). The difference in the pressures in the bubbles of various sizes causes the gas to diffuse from the smaller bubbles to the neighboring larger bubbles. As a result the smallest bubbles become progressively still smaller until they completely disappear. The total surface of a foam, polydisperse with respect to the size of the bubbles, therefore decreases spontaneously, and the greater the surface tension the more rapid is this decrease.

A spontaneous reduction in the total interface can likewise be induced by the rupture of the liquid lamellae comprising the walls of the bubbles. Such a rupture causes a coalescence of the bubbles originally separated by the lamella. The rupture follows a deformation of the lamella which is accompanied by a transient increase in area and consequently by an increase in the surface free energy. In fact, this energy is a function of both the surface area and the surface density of the adsorbed substance. Since this density decreases with increase in area, these two effects contribute in the same way towards the total increase of the surface free energy. Gibbs was the first to call attention to the influence of a variation of the surface density on the forces acting at the surface of a lamella, and he has given the name of *surface elasticity* to the phenomena occurring there.

Elementary reasoning shows that, in all practical cases, the contribution of the surface elasticity has an importance comparable to that of the increase in area at constant tension. Consequently the deformation of the walls of the bubbles in a foam and the rupture which can thereby result are not only opposed by the presence of a surface tension but also by the surface elasticity of the liquid walls.

It is shown here that the instantaneous surface elasticity depends upon the compressibility of the adsorption layers.

Drainage or thinning of the lamellae under the influence of gravity leads to a partial separation of the phases without the total interface being reduced. The lamellae become progressively thinner and finally the macroscopic structure of the foam undergoes a remarkable transformation. The bubbles which, from the start, were spherical assume the form of more or less regular polyhedra whose sides meet at angles of 120°. It is especially those foams of very small densities whose lamellae are susceptible of spontaneous rupture.

We studied the gas diffusion across the walls of bubbles in various foams (Hevea rubber latex, aqueous solutions of Tee-pol, oil-in-water emulsions). The bubbles in these foams are all approximately spherical. The rate at which

the diameter of the small bubbles decreases was calculated as a function of the surface tension, the average thickness of the lamellae and the gas permeability of these lamellae (Part II). The experimental results were seen to be in agreement with theory.

We determined the decrease in the total number of bubbles by counting the number of bubbles per unit surface in the plane of contact between the foam and the glass wall of a container (observed with a microscope) as a function of the age of the foam. The required mathematical relations were developed in the second chapter.

If the initial distribution of bubble sizes is known, the reduction in the total number can be deduced from the rate of decrease in size of the small bubbles. We can thus establish a relation between the kinetic results and the different parameters of the foam—surface tension and permeability of the liquid, initial distribution of bubble sizes and the average thickness of the lamellae. The results of our experiments (Part III) fully confirm the theoretical predictions, and lead to the conclusion that the permeability of the lamellae is principally determined by the solubility and diffusion coefficient of the gas. The experimental method described can be used for a rapid evaluation of the foam stability as a function of the gas diffusion across the bubble walls.

In order to have a better understanding of the resistance of the bubble walls to rupture we examined the behavior of isolated lamellae formed from an aqueous solution of Tee-pol and spread on glass or metallic frames. Such lamellae, maintained vertically, spontaneously become thinner as a result of liquid drainage. Optical interference fringes are formed in the upper part of the lamella followed by the appearance of several "black spots". The total area of the "black spots" whose thickness, according to the measurements of various workers, must range between 120 and 500 A, increases sharply to the point of rupture.

High-speed cinematography showed that the rupture is produced in the "black" part of the lamella. The linear dimensions of the perforation formed increase in proportion to the time elapsed; in the lamellae examined the rate of growth was 680 cm/sec. In the thicker lamellae (containing no "black spot") the formation of a perforation can be induced by means of an electrostatic discharge (Part IV). The diameter of the perfectly circular perforation is a linear function of the time. From rate measurements it can be deduced that the surface energy released as a result of the growth of the perforation is nearly completely transformed into kinetic energy of the liquid, as had already been suggested by A. Dupré. Cinematographic pictures of the spontaneous rupture of the lamellae of a foam showed that the rate of rupture in a foam is at least as great as in isolated lamellae.

By means of a geometric model it is shown that the total interface of a lamella increases during the formation and the first stage of growth of a perforation. The increase in the surface free energy must be considered as equal to the minimum value of the activation energy of rupture. This energy is proportional to the square of the lamella thickness, and for a "black" lamella of an aqueous solution of a soap amounts to more than 1000 kT units. For the same reasons the formation of a visible "black spot" in a lamella of much greater thickness requires considerable work.

The electric double-layer repulsion which occurs when the adsorption layer is ionized is of secondary importance when a properly termed rupture is involved, i.e., in the formation of a perforation, because the area of the two sur-

faces which meet is very limited in this case. On the other hand, in the case of the formation of a "black spot" the contribution of the interaction of the double layers to the repulsion energy is far from being negligible. According to the theory of the stability of colloids (see the well-known work of Verwey and Overbeek), the potential energy when plotted as a function of the distance between the charged interfaces must show a "secondary" minimum for a thickness of the spot which, according to the liquid composition, ranges between 100 and 150 A. At this thickness an equilibrium exists between the electric repulsion and the surface forces on the one hand and the mutual attractive forces of the molecules of the liquid (London-van der Waals forces) on the other.

The formation of more or less stable "black spots" is not possible in the lamellae where the electric repulsion is entirely or nearly entirely absent (for example, the lamella of a pure liquid) because the intermolecular attractive forces rapidly give rise to a thinning and then rupture of the lamella. In all other cases, a certain amount of activation energy must be supplied to induce rupture.

The rupture of a "stable" lamella can arise through a local depression of the surface tension as a result of a sharp rise in temperature or a variation in the chemical composition of the liquid (chemical reactions, addition of an antifoaming agent). The minimum dimensions of the small volume element of the lamella in which the lowering of the tension (inducing instantaneous rupture) is produced were calculated as a function of the lamella thickness and the relative decrease in the surface tension (Part V). The influence of a local rise in temperature on the lifetime of the lamellae is explained in terms of the proposed theory.

The magnitude, frequency and average lifetime of the spontaneous temperature fluctuations in the volume element of a lamella were also calculated. It can be deduced that such fluctuations do not generally diminish the stability of a lamella unless its thickness is very small (of the order of some tens of A).

In all cases where the disturbance of the local equilibrium is of a transitory nature the surface viscosity of the liquid can play an important role by virtue of its retarding effect on the rate of deformation of the lamella. Moreover, the surface elasticity is likewise opposed to the deformation of a lamella, as was mentioned above.

The influence of mechanical disturbances on the stability of foams can be explained by supposing that the surface vibrations due to such disturbances facilitate the formation of "black spots". The general observation that rupture is always preceded by a very rapid growth of "black spots" could be interpreted as an indication of the fact that the final rupture is caused by the high concentration of forces at the borders of the growing "black spots". The verification of this hypothesis represents a very complex problem in hydrodynamics.

VII. REFERENCES

[1] Savitskaya, E. M., *Kolloid. Zhur.* 13, 309 (1951).
[2] Laplace, P. S., "Mécanique Céleste", 1806.
[3] Young, T., *Phil. Trans.* (1805).
[4] Dewar, J., *Proc. Roy. Inst. Gt. Brit.* 22, 179, 359 (1918).
[5] Clark, N. O., and Blackman, M., *Trans. Faraday Soc.* 44, 1 (1948).
[6] Gibbs, J. W., "Collected Works", New Haven, 1948, Vol. I, p. 300.
[7] Brady, A. P., *J. Phys. Chem.* 53, 56 (1949); Pethica, B. A., *Trans. Faraday Soc.* 50, 413 (1954).
[8] Meader, Jr., A. L., and Criddle, D. W., *J. Colloid Sci.* 8, 170 (1953).
[9] Dupré, A., "Sur la Théorie Mécanique de la Chaleur", Paris, 1869.
[10] Plateau, J., "Statique Expérimentale et Théorique des Liquides Soumis aux Seules Forces Moléculaires", Paris, 1875.
[11] Brady, A. P., and Ross, S., *J. Am. Chem. Soc.* 66, 1348 (1948).
[12] Gillespie, T., and Rideal, E. K., *Trans. Faraday Soc.* 52, 173 (1956).

[13] Deryagin, B. V., Titievskaya, A. S., Abrikosova, I. I., and Malkina, A. D., *Discussions Faraday Soc.* **18**, 24 (1954).
[14] Joly, M., *Proc. 2nd Intern. Congr. Rheol.*, Oxford, **1954**, p. 365.
[15] Brown, A. G., Thuman, W. C., and McBain, J. W., *J. Colloid Sci.* **8**, 491 (1953).
[16] Adam, N. K., "The Physics and Chemistry of Surfaces", Oxford, **1938**, p. 8.
[17] Amerongen, G. J. van, Thesis, Delft, **1943**.
[18] Korvezee, A. E., and Mol, E. A. J., *J. Polymer Sci.* **2**, 371 (1947).
[19] Amerongen, G. J. van, *J. Applied Phys.* **17**, 972 (1946).
[20] Clark, N. O., and Blackman, M., *Trans. Faraday Soc.* **44**, 1 (1948).
[21] Brown, A. G., Thuman, W. C., and McBain, J. W., *J. Colloid Sci.* **8**, 508 (1953).
[22] Savitskaya, E. M., *Kolloid. Zhur.* **13**, 309 (1951); Chang, R. C., Schoen, H. M., and Grove, Jr., C. S., *Ind. Eng. Chem.* **48**, 2035 (1956).
[23] Kendall, M. G., "The Advanced Theory of Statistics", London, **1952**, Vol. I, p. 137.
[24] Herdan, G., "Small Particle Statistics", Amsterdam, **1953**, p. 167.
[25] Van den Tempel, M., *Rec. trav. chim.* **72**, 433 (1953).
[26] Bikerman, J. J., "Foams, Theory and Industrial Applications", New York, **1953**, Chapter 8.
[27] Reference 9, p. 350.
[28] Reference 26, Chapter 9.
[29] Reinold, A. W. and Rücker, A. W., *Phil. Mag.* [5], **19**, 94 (1885); Johonnot, E. S., *Phil. Mag.* [5], **47**, 501 (1899); Hagenbach, A., *Arch. sci. phys. et nat.* **35**, 329 (1913); Reference 13.
[30] Reference 26, p. 154.
[31] Reinold, A. W., and Rücker, A. W., *Trans. Roy. Soc.* (London) **184**, 505 (1893).
[32] Verwey, E. J. W., and Overbeek, J. Th. G., "Theory of the Stability of Lyophobic Colloids", Amsterdam, 1948.
[33] Overbeek, J. Th. G. and Sparnaay, M. J., *Discussions Faraday Soc.* **18**, 12 (1954); Reference 13; Deryagin, B. V., Abricossova, I. I., and Lifshitz, E. M., *Quart. Rev.* (*London*) **10**, 295 (1956).
[34] Hamaker, H. C., *Physica* **4**, 1058 (1937).
[35] Reference 32, Figure 31, p. 120.
[36] Brady, A. P., and Ross, S., *J. Am. Chem. Soc.* **66**, 1348 (1944).
[37] Brown, A. G., Thuman, W. C., and McBain, J. W., *J. Colloid Sci.* **8**, 491 (1953).
[38] Ward, A. F. H., and Tordai, J., *J. Chem. Phys.* **14**, 453 (1946); Ross, S., *J. Am. Chem. Soc.* **67**, 990 (1945); Posner, A. M., and Alexander, A. E., *J. Colloid Soc.* **8**, 585 (1953).
[39] Harkins, W. D., "The Physical Chemistry of Surface Films", New York, **1952**, p. 79.
[40] Lottermoser, A., and Baumgurtel, B., *Kolloid-Beih.* **41**, 73 (1934).
[41] Rosano, H. L., "Contribution à l'Étude du Pouvoir Mouillant", Paris, **1953**, p. 36.
[42] Reference 39, p. 5.
[43] Carslaw, H. S., and Jaeger, J. C., "Conduction of Heat in Solids", Oxford, **1947**, p. 280.
[44] Gillespie, T., and Rideal, E. K., *Trans. Faraday Soc.* **52**, 173 (1956).
[45] Reference 26, p. 91.
[46] Kraay, G. M., and van den Tempel, M., *Trans. Inst. Rubber Ind.* **28**, 144 (1952); Newnham, L. M., *Trans. Inst. Rubber Ind.* **29**, 160 (1953).
[47] Reference 6, Vol. II, Chapter 7.
[48] Slater, J. C., "Introduction to Chemical Physics", New York, **1939**, Chapter 7.
[49] Reference 43, p. 217.
[50] Stephan, J., *Sits. ber. Akad. Wiss. Wien* (*Math. naturws. Kl. Abt. IIb*) **69**, 713 (1874).
[51] See, e.g., Currie, C. C., in Reference 26, Chapter 15.
[52] Dervichian, D. G., *Bull. soc. chim. France* **1956**, 15; Ross, S., and Butler, J. N., *J. Phys. Chem.* **60**, 1255 (1956).
[53] Lamb, H., "Hydrodynamics", Cambridge, **1924**, Chapter 9.

INDEX

RUBBER CHEMISTRY AND TECHNOLOGY VOLUME XXXI, 1958

AUTHOR INDEX

Page

ADAMS, H. E., STEARNS, R. S., SMITH, W. A., AND BINDER, J. L. cis-1,4 polyisoprene prepared with alkyl aluminum and titanium tetrachloride 838
ALLCROFT, J. B., see Stafford
AMERONGEN, G. J. VAN, BENDERS, J. F., AND DE DECKER, H. C. J. Tire abrasion at different temperatures 650
ANGIER, D. J., CHAMBERS, W. T. AND WATSON, W. F. Mastication of rubber. VI. Viscosity and molecular weight relationships after cold mastication 73
———, AND WATSON, W. F. Mastication. V. Separation and structural investigation of natural rubber-polymethyl methacrylate interpolymers formed by mastication 58
ANGIOLETTI, A., AND FELICE, U. Flight of sounding balloons 211
ANIKANOVA, K. F., BETTS, G. E., ZHAKOVA, V. G., KOMSKAYA, N. F., KARMIN, B. K., PRISS, L. S., RESNIKOVSKII, M. M., CHERNIKINO, L. A., AND SHETEYN, E. B. SKI rubber, polyisoprene 30
ARNIM, E. VON, see Charlesby
AUER, E. E., DOAK, K. W., AND SCHAFFNER, I. J. Laboratory cut growth resistance of cold SBR 185

BARNARD, D. Ozonolytic degradation of interpolymers of natural rubber with methyl methacrylate and styrene 82
BARTENEV, G. Two states in the process of network formation in polymers 592
BATEMAN, L., GLAZEBROOK, R. W., MOORE, C. G., PORTER, M., ROSS, G. W., AND SAVILLE, R. W. VIII. Reaction of sulfur with mono-olefins 1055
———, GLAZEBROOK, R. W., AND MOORE, C. G. IX. Reaction of sulfur with 2,6-dimethylocta-2,5-diene 1065
———, MOORE, C. G., AND PORTER, M. XI. Mechanism of interaction of sulfur with mono-olefins and 1,5-dienes 1090
BELT, R. F., see Semon
BENDERS, J. F., see Amerongen, van
BENISKA, I., see Dogadkin
BENNETT, B., see Kell
BETTS, G. E., see Anikanova
BEVILACQUA, E. M. Efficiency of TMTD vulcanization 559
———. End groups of oxidized rubber 86
BIGGS, B. S. Atmospheric ozone cracking ... 1015
BINDER, J. L., see Adams
BIRGHAN, K., see Scheele
BLOKH, G. A. Radioactive sulfur in vulcanization 1035
———, KORNILTSEVA, Z. P., OLSHANSKAYA, L. A., AND KOLOBENIN, V. A. Diffusion of sulfur in cable rubbers by radioactive sulfur 356
BOUCHER, M., see Le Bras
BRAENDLE, H. A. Carbon-rubber bond 147
BRESLER, S. E., DOLGOPLOSK, B. A., KROL, V. A., AND FRENKEL, S. YA. Degradation of dissolved elastomers by free radicals 278
BUECHE, A. M. Ultimate properties of simple elastomers 19
BUECHE, F. Mechanical properties of rubbers 1

CHAMBERS, W. T., WATSON, W. F., AND ANGIER, D. J. Mastication of rubber. VI. Viscosity and molecular weight relationships after cold mastication 73
CHARLESBY, A., AND VON ARNIM, E. Cross-linking of oriented rubber 98
CHASSET, R., see Desanges
CHERNIKINA, L. A., see Anikanova
CHERUBIM, M., see Scheele
CONANT, F. S., SVETLIK, J. F., AND JUVE, A. E. Equivalent cures in specimens of various shapes 562
CRAIG, DAVID, see Semon

DANJARD, J.-C., see Le Bras
DEAN, W. R., PERERA, V., AND GLAZER, J. Monolayers of some hydroxylated polyolefin rubbers 446
DECKER, H. C. J. DE, see Amerongen, van
DESANGES, H., CHASSET, R., AND THIRION, P. Changes in electrical properties of natural rubber-carbon black stocks during vulcanization 631
DE VRIES, A. J. Foam stability of latex 1142
DOAK, K. W., see Auer
DOBROMYSLOVA, A. V., see Dogadkin
DOGADKIN, B. A., AND BENISKA, I. The action of vulcanization accelerators 329
———, see Feldshtein
———, DOBROMYSLOVA, A. V., TOLSTUKHINA, F. S., AND SAMSONOVA, N. G. The influence of structure on the chemical activity and vulcanizability of butadiene polymers 569
———, B. A., FEDYUKIN, AND GUL, V. E. Effect of swelling on the strength of vulcanizates 756
———, SUSLYAKOV, A. V., ZAKHARCHENKO, P. I., SENATORSKAYA, L. G., AND GUSEVA, V. I. Filler-rubber interaction in latex 655
———, B. LUKIN, TARASOVA, Z., SKORODUMOVA, Z., AND TUTORSKII, I. Theory of reinforcement of rubber: reaction of carbon black with sulfur and rubber 361
———, AND TUTORSKII, I. Mechanism of the action of vulcanization accelerators .. 343
———, TUTORSKII, I. A., AND PEVZNER, D. M. Mechanism of vulcanization in the presence of 2-mercaptobenzothiazole . 751
———, TUTORSKII, I. A., AND PEVZNER, D. M. Mechanism of mill breakdown and vulcanization in the presence of 2-mercaptobenzothiazole 348
DOLGOPLOSK, B. A., see Bresler, see Tinyakova
DOROKHINA, T. V., ZUBOV, P. I., AND NOVIKOV, A. S. Molecular shape on tensile strength of vulcanizates 27
DRUSHEL, H. V., see Hallum

Page

EAGLES, A. E., AND PAYNE, A. R. Simple extensometer for tensile testing of polymers ... 673
ECHTE, ELISABETH, see Lorenz
EDELMANN, KURT, AND HORN, EDITH. Rheological measurements for the characterization of high polymers ... 681
EHRENBURG, E. G., see Poddubnyĭ

FELICE, U., see Angioletti
FOWLER, R. B., see Semon
FEDYUKIN, see Dogadkin
FELDSHTEIN, M., ORLOVSKIĬ, P., AND DOGADKIN, B. Metallic oxides as vulcanization activators ... 526
FLETCHER, W. P., AND FOGG, S. G. The heat aging of natural rubber vulcanized with tetramethylthiuram disulfide ... 327
FLORY, P. J., see Oth
FOGG, S. G., see Fletcher
FRENKEL, S. Y., see Bresler
FUKUDA, HARUKO, see Tsurugi

GEESINK, H. A. O. W., AND PRAT, CL. P. Wear of passenger car tires ... 166
GENT, A. N. Crystallization in natural rubber. V. Chemically modified rubber ... 519
———. Load-deflection relations and surface strain relations for flat rubber pads ... 395
———. On the relation between indentation hardness and Young's modulus ... 896
———, AND LINDLEY, P. B. Tension flaws in bonded soft rubber ... 393
GIBBS, W. E., see Pierson
GLAZEBROOK, R. W., see Bateman
GLAZER, J., see Dean
GRASEMAN, H., see Scheele
GROMOVA, G. N., see Yakubchik
GUL, V. E., see Dogadkin
GUSEVA, V. I., see Dogadkin

HALLUM, J. V., AND DRUSHEL, H. V. The organic nature of carbon black surfaces ... 941
HEIDEMANN, W., see Peter
HERTE, P. Oxidative breakdown of synthetic rubber latex ... 262
HORN, EDITH, see Edelmann

JUVE, A. E., see Conant

KARMIN, B. K., see Anikanova
KELL, R. M., BENNETT, B., AND STICKNEY, P. B. Melting and glass transitions in polyisobutylene ... 499
KHRENNIKOVA, E. K., see Tinyakova
KOLOBENIN, V. A., see Blokh
KOMSKAYA, N. F., see Anikanova
———, AND SLONIMSKIĬ, G. L. Solubility of polymers in each other. 1. Physicomechanical properties of stocks prepared from a mixture of polymers ... 49
———, see Slonimskiĭ, see Anikanova
KORNILTSEVA, Z. P., see Bolkh
KROL, B. A., see Bresler
KUSOV, A. B., TROFIMOVA, V. I., AND NILOVA, Yu. I. Volume changes in stretching of rubber ... 513
KUZMINSKIĬ, A. S., see Postovskaya

LE BRAS, J., DANJARD, J.-C., AND BOUCHER, M. The mechanism of protection of by deactivation effect ... 849
———, PINAZZI, C., AND MILBERT, G. Modification of rubber by reaction with maleic anhydride ... 664
LEE, LIENG-HUENG, see Shelton
LINDLEY, P. B., see Gent
LINNIG, F. J., AND STEWART, J. E. Infrared study of some structural changes in natural rubber during vulcanization ... 719
LORENZ, OTTO, AND ECHTE, ELISABETH. Vulcanization of elastomers. 13. Vulcanization of natural rubber with sulfur and mercaptobenzothiazole. II ... 117

Page

———, AND ECHTE, ELISABETH. Vulcanization of elastomers. 18. The vulcanization of natural rubber with sulfur and mercaptobenzothiazole. III ... 548
LUKIN, B., see Dogadkin
LUTTROPP, H. Thermal vulcanization of Buna ... 132

MCSWEENEY, E. E., see Stickney, see Palinchak
MAU, G., see Scheele
MANDELKERN, L., see Roberts
MERBETT, F. M. Graft polymers with preset molecular configurations ... 829
———. The separation and characterization of graft copolymers from natural rubber. 819
MEYER, G. E., see Pierson
MILBERT, G., see Le Bras
MINOURA, YUJI. Organic sulfides and polysulfides. I. Desulfurization reactions ... 608
II. Reactions with hydrazine, ethylenediamine and ammonia ... 612
III. Reactions with amines ... 615
IV. Reactions with doctor solution, silver nitrate, cupric acetate and lead acetate ... 618
V. Reactions with methyl iodide ... 621
VI. Reactions of metallic oxides with polysulfide rubbers ... 624
———. The structure and molecular refraction of organic polysulfides ... 815
———. Structure and ultraviolet absorption spectra of polysulfides ... 808
MOORE, C. G., AND WATSON, W. F. ... 958
———, see Bateman
MUELLER, W. J., see Stickney, see Palinchak
MULLINS, L., AND TOBIN, N. R. Carbon-black loaded rubber vulcanizates. Volume changes in stretching ... 505

NAKABAYASHI, TAKESHIGE, see Tsurugi
NAPLES, F. J., see Pierson
NILOVA, YU. I., see Kusov
NOVIKOV, A. S., DOROKHINA, T. V., AND ZUBOV, P. I. Molecular shape on tensile strength of vulcanizates ... 27

OLSHANSKAYA, L. A., see Blokh
ORLOVSKIĬ, P., see Feldshtein
OTH, J. F. M., AND FLORY, P. J. Thermodynamics of shrinkage of racked rubber ... 485

PALINCHAK, S. T., see Stickney
———, MCSWEENEY, E. E., MUELLER, W. J., AND STICKNEY, P. B. Bound rubber and mechanical properties of diene polymer stocks ... 374
PANICH, R. M., see Voyutskiĭ
PARKER, C. A. Analysis of accelerators and antioxidants ... 953
PAYNE, A. R., see Eagles
PERERA V., see Dean
PETER, J., AND HEIDEMANN, W. Determination of vulcanization characteristics of rubber ... 105
PEVZNER, D. M., see Dogadkin
PIERSON, R. M., GIBBS, W. E., MEYER, G. E., NAPLES, F. J., SALTMAN, W. M., SCHROCK, R. M., TEWKSBURY, L. B., AND TRICK, G. S. Adduct rubbers: A versatile family of elastomers ... 213
PINAZZI, C., see Le Bras
PISARENKO, A. I., see Voyutskiĭ
PODDUBNYĬ, I. YA., AND EHRENBURG, E. G. Branching in macromolecules of different synthetic rubbers ... 699
PORTER, M., see Bateman
POSTOVSKAYA, A. F., SALIMOV, M. A., AND KUZMINSKIĬ, A. S. Changes caused by light in the number of sulfur atoms in the sulfur structure of vulcanized products ... 747
PRAT, C. Correlation between laboratory abrasion and road testing ... 387
PRAT, CL. P., see Geesink

Page

PRINKLONSKAYA, N. V. Speed of mixing rubber as a factor in processing 907
PRISS, L. S., see Anikanova
PUL, B. I. C. F. VAN. Ozone resistance of natural rubber. I. Apparatus for exposure 866
II. Influence of fillers and waxes 874
III. Influence of accelerators and antioxidants 882

REGENASS, F. A., see Semon
REZNIKOVSKIĬ, M. M., see Anikanova
ROBERTS, D. E., AND MANDELKERN, L. Properties of polymer networks formed from oriented chains of natural rubber ... 469
ROSS, G. W. X. Kinetics of the reaction of sulfur with cyclohexene and other olefins 1077
———, see Bateman

SAKHARCHENKO, P. I., see Dogadkin
SALIMOV, M. A., see Postovskaya
SALTMAN, W. M., see Pierson
SAMOLETOVA, V. V., see Subbotin
SAMSONOVA, N. G., see Dogadkin
SARGENT, D. T., see Stafford
SAVILLE, R. W., see Bateman
SCHAFFNER, I. J., see Auer
SCHALLAMACH, A. Friction and abrasion of rubber 982
SCHEELE, W., AND BIRGHAN, K. The vulcanization of elastomers. 16. The vulcanization of natural rubber with sulfur in the presence of dithiocarbamates (I) . 301
———, AND CHERUBIM, M. The vulcanization of elastomers. 15. The vulcanization of natural rubber and synthetic rubber by sulfur in the presence of organic bases 286
———, GRASEMAN, H., AND MAU, G. Vulcanization of elastomers. 17. Role of oxides in vulcanization with TETD ... 315
———, TOUSSAINT, H.-E, AND STANGE, P. Vulcanization of elastomers. 14. The role of the oxide in vulcanization with compounds of the thiuram series. (I) 539
SCHROCK, R. M., see Pierson
SCHUUR, G. Nature of particle surface in hevea latex and pastes of rubber hydrochloride and polyvinyl chloride 436
SEKHAR, B. C. Aeration of natural rubber latex. I. Effect of polyamines on the hardness and aging characteristics of aerated latex rubber 425
II. Graft polymerization of vinyl monomers with aerated latex rubber 430
SEMON, W. L., CRAIG, DAVID, FOWLER, R. B., REGENASS, F. A., TUCKER, HAROLD, YANKO, JOHN A., SHIPMAN, J. J., AND BELT, R. F. Perdeuterio SN rubber 847
SENATORSKAYA, L. G., see Dogadkin
SHAKOVA, V. G., see Ankianova
SHAPOVALOVA, A. I., VOYUTSKIĬ, S. S., AND PISARENKO, A. P. Adhesion of high polymers. 2. Method for determination of mutual adhesion of high polymers 89
———, see Voyutskiĭ
SHELTON, J. REID, AND LEE, LIENG-HUENG. The structure of cyclized polybutadiene .. 415
SHETEYN, E. B., see Anikanova
SHIMOZATO, J., AND URA, K. Vulcanization accelerators 211
SHIPMAN, J. J., see Semon
SHVARTS, A. G. Evaluation of rubber-solvent interation 691
SKORODUMOVA, Z., see Dogadkin
SLONIMSKIĬ, G. L., AND STRUMINSKIĬ, G. V. The mutual solubility of polymers. IV. Effects of packing density 257
SLONIMSKIĬ, G. L., AND KOMSKAYA, N. F. Mutual solubility of polymers. I. Physicomechanical properties of stocks prepared from a mixture of polymers 49
II. Viscosity of rubber mixtures and behavior of their solutions 244

Page

SMITH, W. A., see Adams
SPASSKOVA, A. I., see Yakubchik
STAFFORD, W. E., ALLCROFT, J. B., AND SARGENT, D. T. Mechanism of devulcanization 202
———, AND WRIGHT, R. A. Modern theories of rubber reclaiming 599
STANGE, P., see Scheele
STEARNS, R. S., see Adams
STEWART, J. E., see Linnig
STICKNEY, P. B., MCSWEENEY, E. E., MUELLER, W. J., AND PALINCHAK, S. T. Bound rubber formation in diene polymer stocks 369
———, see Kell, see Palinchak
STRUMINSKIĬ, G. V., AND SLONIMSKIĬ, G. L. The mutual solubility of polymers. III. Heat of mixing 250
SUBBOTIN, S. A., SAMOLETOVA, V. V., AND ZNAMENSKAYA, A. K. SKI rubber, polyisoprene 44
SUALYAKOV, A. V., see Dogadkin
SVETLIK, J. F., see Conant

TARASOVA, Z., see Dogadkin
TEWKSBURY, L. B., see Pierson
THIRION, P., see Desanges
TINYAKOVA, E. I., KHRENNIKOVA, E. K., AND DOLGOPLOSK, B. A. The role of hydrogen disulfide in vulcanization 353
TOBIN, N. R., see Mullins
TOLSTUKHINA, F. S., see Dogadkin
TOUSSAINT, HORST-ECKART, see Scheele
TRICK, G. S., see Pierson
TROFIMOVA, V. I., see Kusov
TSURUGI, JITSUO AND FUKUDA, HARUKO. Vulcanization. The reaction of diphenylmethane with benzothiazolyl disulfide 800
———. The chemistry of vulcanization. I ... 762
II. Kinetics of hydrogen sulfide evolution during the reaction of diphenylmethane with sulfur 769
III. The action of amines on the reaction of diphenylamine with sulfur 773
———, AND NAKABAYASHI, TAKESHIGE. Vulcanization. IV. Action of mercaptobenzothiazole on the reaction of diphenylmethane with sulfur 779
———, AND FUKUDA, HARUKO. Vulcanization. V. Action of 2,2'-benzothiazolyl disulfide on the reaction of diphenylmethane with sulfur 788
TURNER, D. T. Radiation crosslinking of rubber. Effect of additives 737
TUCKER, HAROLD, see Semon
TUTORSKIĬ, I. A., see Dogadkin

URA, K., see Shimozato

VIEHMANN, W. Surface heating by friction and wear by thermal decomposition 925
VOYUTSKIĬ, S. S., see Shapovalova
———, SHAPOVALOVA, A. I., AND PISARENKO, A. I. Adhesion of high polymers. 3. The effect of size, shape and polarity on adhesion to cellophane 712
———, AND PANICH, R. M. Stability of high polymer latexes and their electrokinetic potentials 1105

WATSON, W. F., AND ANGIER, D. G. Mastication. V. Separation and structural investigation of natural rubber—polymethyl methacrylate interpolymers formed by mastication 58
———, ANGIER, D. J., AND CHAMBERS, W. T. Mastication of rubber. VI. Viscosity and molecular weight relationships after cold mastication 73
———, AND WILSON, D. A uni-rotor mixer for plastics 667
WILSON, D., see Watson
WRIGHT, R. A., see Stafford

Page

Wood, L. A. Glass transition temperatures of copolymers ... 459
———. Rubberlike elasticity ... 959

Yakubchik, A. I., and Gromova, G. N. Hydrogenation of butadiene rubber ... 156
———, and ———. Hydrogenation of butadiene rubber solutions. II. Influence of the solvent with palladium-on-calcium carbonate catalyst ... 588

———, and Spasskova, A. I. The chemical structure of the "popcorn" polymer of butadiene ... 581
Yanko, John A., see Semon

Zakharchenko, P. K., see Dogadkin
Zhakova, V. G., see Anikanova
Znamenskaya, A. K., see Subbotin
Zubov, P. I., see Novikov

SUBJECT INDEX

Abrasion, laboratory and road testing ... 387
Abrasion of tires at different temperatures ... 650
Abrasion resistance, ISO method for measuring ... No. 1, xiv
See friction
Accelerators ... 211, 329, 343, 348, 356, 779, 788, 800, 953
Accelerators, analysis of ... 953
Accelerators, MBTS, Hexa, etc. ... 211
See vulcanization, ozone resistance
Activators, metal oxides as ... 315, 624
See metal oxides, vulcanization
Adduct rubbers, a new family of elastomers ... 213
Adhesion, ISO method for measuring, to textiles ... No. 1, xxi
of high polymers ... 89, 712
Aeration of natural rubber latex. I. ... 425
II. Graft polymerization of vinyl monomers with aerated latex rubber ... 430
Aging, amines on ... 425
Amines
See hardness, vulcanization, aging
Annual report of the progress of rubber technology, Vol. XXI, book, ... No. 2, ix
Antioxidants
Analysis of ... 953
See deactivating effect, ozone resistance

Balloons, sounding ... 211
Bases
See vulcanization
Benzothiazolyl disulfide ... 788, 800
See accelerators
Bound rubber ... 369, 374
Branching ... 699
Butyl ... No. 2 X

Cable rubbers, vulcanization ... 356
Carbon black-rubber bond ... 147, 505
See reinforcement
Carbon black loaded rubber vulcanizates, volume changes in stretching ... 505, 513
Carbon black surfaces ... 941
Reaction with sulfur ... 361
Cellophane, adhesion of rubbers to ... 712
Chemically modified rubber ... 664
Chemistry of natural and synthetic rubber book ... No. 1, xiii
Compounding ingredients for rubber, book ... No. 2, xi
Compression and tension
See stress-strain
Copolymers, glass transition temperatures ... 459
See graft, interpolymers
Crosslinking ... 98
See also radiation
Crystallization in natural rubber ... 469, 485, 505, 513, 519
See also glass transition
Cut growth of cold SBR ... 185

Deactivating effect ... 849
Degradation
See abrasion, ozone resistance, end groups, cut growth, oxidized rubber, oxidative, free radical, heat aging, mill breakdown
Deuterio rubber ... 847
Devulcanization ... 202
See reclaiming

Diffusion of sulfur ... 356
Diphenylmethane reaction with sulfur
See vulcanization

Electrical properties of natural rubber-carbon black stocks, changes during vulcanization ... 631
Electrokinetic potentials of latex ... 1105
End groups of oxidized NR ... 86
Equivalent cures in specimens of various shapes ... 562
Expanded rubber, book ... No. 2, x
Extensometer ... 673

Fillers
See ozone resistance, reinforcement
Filler-rubber interaction in latex ... 655
See reinforcement
Flat pads, stress-strain in ... 395
Flaws
See tensile
Foam stability ... 1142
Free radical degradation ... 278
Free radicals in solution, book, ... No. 2, xi
Friction and abrasion ... 925, 982
Friction and lubrication, book ... No. 2, xiii

Glass transition temperatures ... 459, 499
Glass transitions in polyisobutylene ... 499
Graft polymers ... 58, 82
Fractionation and characterization ... 219
Preset molecular configurations, and ... 829
Prepared in latex ... 430

Hardness, effect of amines on ... 425
Hardness, ISO method for measuring ... No. 1, xxv
Young's modulus and indentation hardness ... 806
Hard rubber, book ... No. 1, x
Heat aging TETD vulcanizates ... 327
Heat of mixing of polymers ... 250
Hydrogen disulfide in vulcanization ... 353
Hydrogen sulfide ... 353, 769
Hydrogen sulfide from diphenylmethane with sulfur ... 769
Hydrogenation of polybutadiene ... 156

Infrared, studies in vulcanization ... 719
Interaction
See rubber solvent interaction, solubility, bound rubber, molecular
Interpolymers formed by mastication ... 58, 82
See grafting and graft polymers
ISO Recommendations ... No. 1, xiv–xxix

Latex and electrokinetic potentials ... 1105
Latex, filler rubber interaction in ... 655
Latex, oxidative degradation of ... 262
Latex, particle surface of ... 436
Latex stability ISO method for measuring ... No. 1, xx
Latex, synthetic, degradation ... 262
Light, effect on vulcanization ... 747
Load-deflection ... 395, 673
See stress-strain

Maleic anhydride, reaction with rubber ... 664
Mastication ... 73, 58
See mixing, mixer, mill breakdown, degradation

Page

Mechanical properties of elastomers....1, 19
Mechanical properties of mixed polymers.. 49
Mechanism of reclaiming.... 202
Mercaptobenzothiazole, as accelerator.... 329, 343, 348, 526, 548, 751, 779
See vulcanization
Metal oxides in vulcanization...315, 526, 539, 624
Mercaptans
See adduct rubbers.... 213
Methyl iodide.... 621
Methyl methacrylate interpolymers from 58, 82, 430
Mill breakdown.... 348
Mixer, uni-rotor.... 667
Mixing, speed of.... 907
Model compounds in vulcanization....211, 608
See diphenylmethane
Molecular packing in polymer mixtures.... 257
Molecular shape, effect on tensile strength.... 27
Molecular weight relationships....73, 681
Monolayers of some hydroxylated polyolefin rubbers.... 446

Natural rubber, mastication of. V....58, 82
Crosslinking of.... 98
Network formation, two stages in.... 592

Oriented rubber, crosslinking of.... 98
Oxidative degradation.... 262
Oxidized rubber.... 86
Ozone cracking.... 1015
Ozone resistance....866, 874, 882
Ozonolytic degradation of NR interpolymers.. 82

Passenger car tires, severity of wear.... 166
See abrasion
Plastics, books....No. 2, xii
Physicomechanical
See mechanical
Polyamines
See amines, aeration of latex
Polybutadiene, cyclized, structure of.... 415
Polybutadiene, "popcorn" polymer.... 581
Polybutadiene, structure and activity of..569, 581
Polybutadiene rubber hydrogenation of...156, 588
Polybutadiene rubber solutions, hydrogenation of.... 588
Polyisobutylene, melting and glass transition.. 499
cis-Polyisoprene.... 838
See SKI rubber
Polyisoprene, SKI....30, 44
Polyolefin rubbers, monolayers of.... 446
Polymer handbook....No. 2, x
Polysulfides
See sulfides
Polysulfide rubbers.... 624
Polysulfide chain length in vulcanization.... 747
Polyvinyl chloride, pastes of.... 436
"Popcorn" polymer of butadiene
See polybutadiene

Racked rubber, shrinkage.... 485
Radiation crosslinking, effect of additives.... 737
Radiosulfur.... 356
Radiosulfur vulcanization....356, 1035
Reclaiming and modern theories of....202, 599
Refraction of polysulfides.... 815
Reinforcement....147, 361, 369, 374, 387, 505
See fillers
Reinforcement, in latex.... 655
Rheological measurements.... 681
Road testing.... 387
Rubberlike elasticity.... 959

Page

Rubber-solvent interaction.... 691
Rubber hydrochloride, pastes of.... 436
SBR, cold, cut growth resistance of.... 185
Shrinkage of racked rubber....469, 485
SKI rubber....30, 44
Solubility, mutual, of polymers...49, 244, 250, 257
Sounding balloons, flight of.... 211
Stress-strain....No. 1, xxiii, 1, 19, 27, 395, 673
Sulfides and polysulfides.... 608, 612, 615, 618, 621, 624, 808, 815
Sulfur, radio-, vulcanization....356, 1035
Sulfur and sulfur compounds with olefins.... 1055
Sulfur vulcanization.... 117, 301, 356, 608, 612, 615, 618, 621, 624, 762, 769, 773, 779, 788, 800, 808, 815, 1035, 1055
Swelling, effect on strength of vulcanizates... 756
Synthetic natural rubber.... 847

Tack.... 89
Tear strength, ISO method for measuring ....No. 1, xviii
Tensile strength, ISO method for measuring tensile stress-strain....No. 1, xxiii
Effect of molecular shape on.... 27
Tensile testing....393, 673
Tetrnethylthiuram disulfide vulcanization.... 315
Thermal vulcanization.... 132
Thiols
See adduct rubbers.... 213
Thiuram vulcanization.... 301
Thiuram vulcanization, efficiency....327, 559
Thiuram vulcanization, oxides in.... 539
Trade directory of Great Britain....No. 1, xiii

Ultraviolet absorption spectra of polysulfides.. 808
Ultimate properties.... 1, 19

Viscosity of polymer mixtures.... 244
Viscosity and molecular weight relationships 73, 681
Effect of mastication on.... 73
Volume changes....469, 485, 499, 505, 513, 519
Vulcanizability of butadiene polymers.... 569
Vulcanization
See thermal, crosslinking, accelerators, metal oxides, model compounds
Vulcanization, chemistry of.... 117, 286, 301, 315, 327, 329, 353, 762, 769, 773, 779, 788, 800
Vulcanization, bases and.... 286
Vulcanization, dithiocarbamates and.... 301
Vulcanization, diphenylmethane as a model for studying....762, 769, 773, 779, 788, 800
Vulcanization, light effects on sulfur chain length.... 747
Vulcanization, effects of MBT.... 329, 343, 348, 548, 751, 779
Effect of MBTS....788, 800
Vulcanization, changes in electrical properties during.... 631
Vulcanization, infrafed study of.... 719
Vulcanization characteristics, new method for measuring.... 105
Vulcanization, effect of specimen shape.... 562
Vulcanization with TMTD, efficiency.... 559
Vulcanization, two stages in.... 592

Waxes
See ozone resistance
Wear of passenger car tires.... 166
Whiting, Research Memorandum....No. 1, xii

Zinc oxide, book....No. 1, x

THE VANDERBILT LABORATORY

...Located in East Norwalk, Connecticut. Maintained as a development and technical service center in the interest of our customers and their efficient use of Vanderbilt materials for Dry Rubber, Latex, and Plastics Compounding.

Consider these Vanderbilt materials when you order SBR

AGERITE* SUPERLITE . . . a good stabilizer in nonstaining, nondiscoloring grades

AGERITE* SUPERFLEX . . . contributes quality to cold rubbers for tires and mechanicals

THERMAX*. . . available now in cold SBR black masterbatch (150 THERMAX : 100 SBR)

Check your SBR supplier for details

* T.M. Reg., U. S. Patent Office

R. T. VANDERBILT CO., INC.

230 Park Avenue, New York 17, N. Y.

ADVERTISE *in*

RUBBER CHEMISTRY AND TECHNOLOGY

KEEP YOUR NAME AND YOUR PRODUCTS CONSTANTLY BEFORE THE RUBBER TECHNOLOGIST

Advertising rates and information about available locations may be obtained from George Hackim, Advertising Manager, Rubber Chemistry and Technology, care of The General Tire & Rubber Company, Chemical Division, Akron 9, Ohio

Famous escape artist meets his match

You've seen what often happens to bales of uncured synthetic rubber during shipment and storage. Subject to a condition called "cold flow," the uncured product was once an incorrigible "escape artist." It flowed, settled and burst from ordinary packages. Escaped rubber stuck to bits of cardboard, paper and dirt. Once contaminated, it was difficult to process the rubber into quality products.

Shell Chemical has solved this "sticky" problem—by caging 42 film-wrapped bales of synthetic rubber in a strong, lightweight, steel-strapped wooden container of unique design called the Flotainer*.

Completely new in principle, the Flotainer keeps rubber in check, prevents contamination, reduces waste, speeds handling, and lets you store 20 tons of rubber on less than 100 sq. ft. of floor space.

Leadership in packaging and delivery, plus versatility of product are qualities that customers have learned to expect from Shell Chemical. In addition—a specialized research and development organization devoted to general-purpose synthetic rubber assures prompt, dependable technical assistance.

**Flotainer* is a Shell Chemical Trademark.

SHELL CHEMICAL CORPORATION

Synthetic Rubber Sales Division
P. O. Box 216, Torrance, California

Fill out and mail this coupon for a complete description of the Flotainer—plus a catalog of Shell synthetic rubbers and latices.

SHELL

Name_____ Title_____

Company_____

Address_____

THE STAMFORD RUBBER SUPPLY CO.
Factice
THE STAMFORD RUBBER SUPPLY CO
Vulcanized Oil
Factice®
A COMPLETE LINE OF
WHITE
BROWN
and AMBER
GRADES
OLDEST AND LARGEST MANUFACTURERS
OF Factice VULCANIZED OIL
SINCE 1900
LEADERS IN THE FIELD
For
RESEARCH and
MANUFACTURING
DEPENDABILITY
THE STAMFORD RUBBER SUPPLY COMPANY, STAMFORD, CONN.

Ameripol 4700 reduces your raw rubber costs almost 10%

New Ameripol 4700 cuts almost two cents per pound off raw material costs when used as a replacement for 37½-part oil-extended rubber. Ameripol 4700 is a 50-part oil-extended rubber. It costs only 17.5 cents per pound and still maintains end product properties for most applications.

Tensile strength of Ameripol 4700 is actually higher than many 37½-part oil-extended polymers. Its modulus is also higher, and hardness is maintained.

Ameripol 4700 is light colored, making it ideal for many color applications. Get samples and data. Fill out the coupon below and drop it in the mail.

Ameripol

Goodrich-Gulf, 3121 Euclid Avenue
Cleveland 15, Ohio

Send ☐ samples ☐ data on Ameripol 4700.

Name_____

Company_____

Address_____

City_____ State_____

Goodrich-Gulf Chemicals, Inc.

To the
Rubber Industry! ~ ~ ~

This Journal is supported by advertising from leading suppliers to the industry. More advertising will permit the publication of a greater number of important technical papers on rubber which will make RUBBER CHEMISTRY AND TECHNOLOGY even more valuable as a convenient reference of "Rubberana."

Specify materials from suppliers listed on page 34. Urge other suppliers to advertise in

RUBBER CHEMISTRY AND TECHNOLOGY

●

Advertising rates and information about available locations may be obtained from George Hackim, Advertising Manager, Rubber Chemistry and Technology, c/o The General Tire & Rubber Company, Chemical Division, Akron 9, Ohio.

Another new development using

B.F.Goodrich Chemical *raw materials*

HERE ARE THE FACTS:

- ***This new series is a major improvement of nitrile rubber to materially aid fabrication, give superior end product properties.***
- **combines a range of oil and water resistance superior to other nitrile rubbers.**
- **improved tensile with higher elongation and lower moduli.**
- **excellent solubility both milled and unmilled to give lower cement viscosities.**
- **excellent aging and abrasion properties.**
- **blends easily with GR-S and other rubbers.**
- **blends easily to modify many resins.**

Get samples or further information on these two new Hycar rubbers by writing Dept. HP-6, B.F.Goodrich Chemical Company, 3135 Euclid Avenue, Cleveland 15, Ohio. Cable address: Goodchemco. In Canada: Kitchener, Ontario.

Hycar
Rubber and Latex

B.F.Goodrich Chemical Company
a division of The B.F.Goodrich Company

B.F.Goodrich

GEON polyvinyl materials • HYCAR rubber and latex
GOOD-RITE chemicals and plasticizers • HARMON colors

DON'T BE AN Old Fashioned COMPOUNDER

...Get Hep to

STABILITE*

ANTIOXIDANT

*Manufactured by Chemico, Inc.
Distributed by The C. P. Hall Co.

AKRON, OHIO
LOS ANGELES, CALIF.
CHICAGO, ILLINOIS
NEWARK, N. J.

The C. P. Hall Co.
CHEMICAL MANUFACTURERS

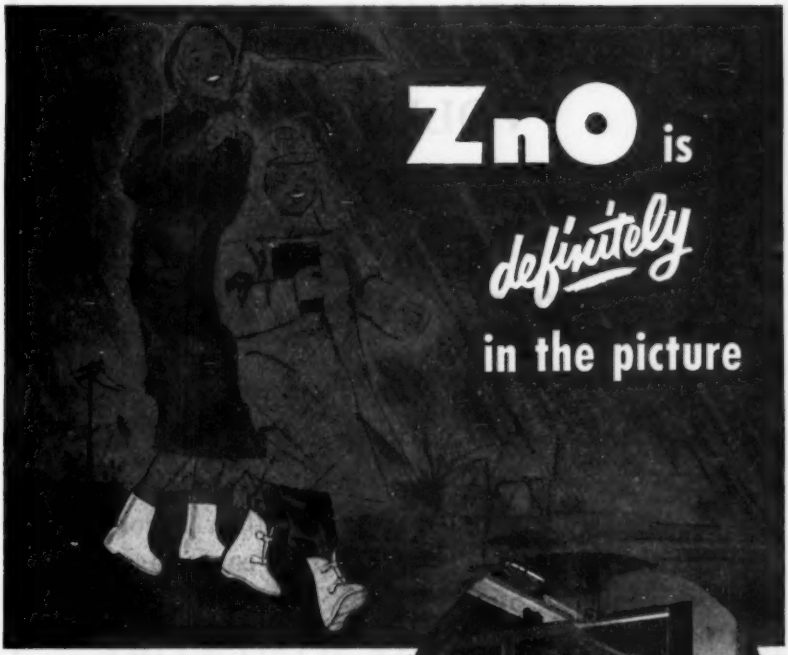

ST. JOE lead-free ZINC OXIDES were first produced by our unique electrothermic smelting process in 1931. Since then these pigments have found steadily increasing acceptance by the rubber industry as primary ingredients in their products.

The various reasons for this acceptance may be summed up thus: By virtue of years of experience with St. Joe pigments, consumers have come to know St. Joe's high and undeviating standards of quality and uniformity. *They rely* on these factors to maintain or increase the *quality* of their own products.

The earned preferential status enjoyed by our pigments in the rubber industry parallels the standing of other well-known products of this company — the largest producer of pig lead and one of the leading producers of slab zinc and lead-free zinc oxides in the United States.

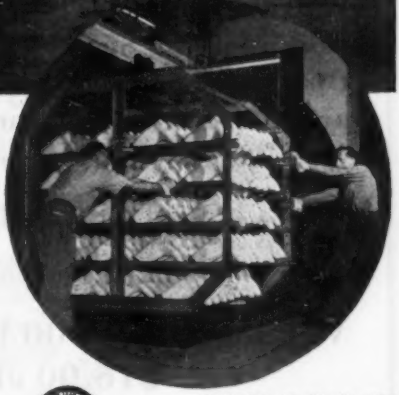

Car loaded with white Grenadier Gaytees is pushed into a gigantic vulcanizer for curing.

Courtesy: U. S. Rubber Co.

SEND FOR YOUR FREE COPY

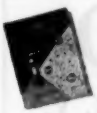

Our recently published 55-page Technical Data Book describes in detail each ST. JOE RUBBER GRADE ZINC OXIDE, and is available — with our compliments — to Purchasing Agents and Technologists.

ST. JOSEPH LEAD CO.

250 Park Avenue, New York 17

Plant & Laboratory:
Monaca (Josephtown), Pa.

ZNO-308A

NOW AVAILABLE

VOLUME II
MACHINERY and EQUIPMENT
for
RUBBER and PLASTICS
Covering
SECONDARY MACHINERY AND EQUIPMENT

Volume 2 has over 700 pages of editorial content with authoritative descriptions for each classification: Types, Specifications, Design Features, Operation, and Applications, as well as names and addresses of the manufacturers or suppliers. More than 300 illustrations. Cloth-bound.

Send for complete prospectus

Over 4,000 Copies of Volume 1 have been sold

Volume 2—$15.00 Postpaid in U.S.A.—$16.00 elsewhere

RUBBER WORLD

630 Third Avenue **New York 17, N. Y.**

SUPERIOR ZINC CORPORATION

121 North Broad Street Philadelphia 7, Penna.

Works at Bristol, Pa.

VULCANIZED VEGETABLE OILS

• RUBBER SUBSTITUTES •

THE CARTER BELL MFG. CO. SINCE CARTER BELL PRODUCTS 1903 SPRINGFIELD, NEW JERSEY

REPRESENTED BY

HARWICK STANDARD CHEMICAL CO.

Akron — Boston — Trenton — Chicago — Denver — Los Angeles — Albertville (Ala.) — Greenville (S. C.)

SCOTT TESTERS - World Standard for conformance with methods of

ASTM, ISO, GOVT., INDUSTRY

NEW "MODEL CRE"

Constant-Rate-of-Extension Tensile Elongation Tester. Inertialess electric weighing up to 1,000 lbs. Designed for speed and simplicity of operation, and eliminating operator fatigue, Model CRE is ideal for production testing.

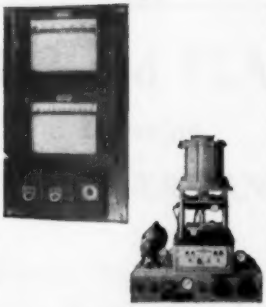

AUTOMATED MOONEY VISCOMETER

Recorders with wired panels now control complete Mooney test cycle. Insert the specimen and push the button. The controls take over, provide a 1-minute warm-up, start the test and record the data, and shut off both Mooney and recorders at the end of the test.

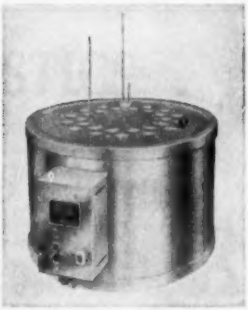

HIGH-TEMPERATURE AGEING

These testers provide contamination-free ageing in individual compartments. For atmospheric pressure, Model LG provides temperatures up to 600°F, and Model LGH to 1,000°F. Model LGP provides high pressures, in air, oxygen or other gas, up to 600°F.

Scott provides a complete line of Testers to evaluate elastomeric compounds and products for tensile, elongation and tear, from −70°F to 600°F, also for state-of-cure and complete curing characteristics, brittle-point, adhesion, rebound, flexing, abrasion, etc.

REQUEST LITERATURE

SCOTT TESTERS, INC.

33 BLACKSTONE ST., PROVIDENCE, R. I.

New Symbol of World Standard Testing

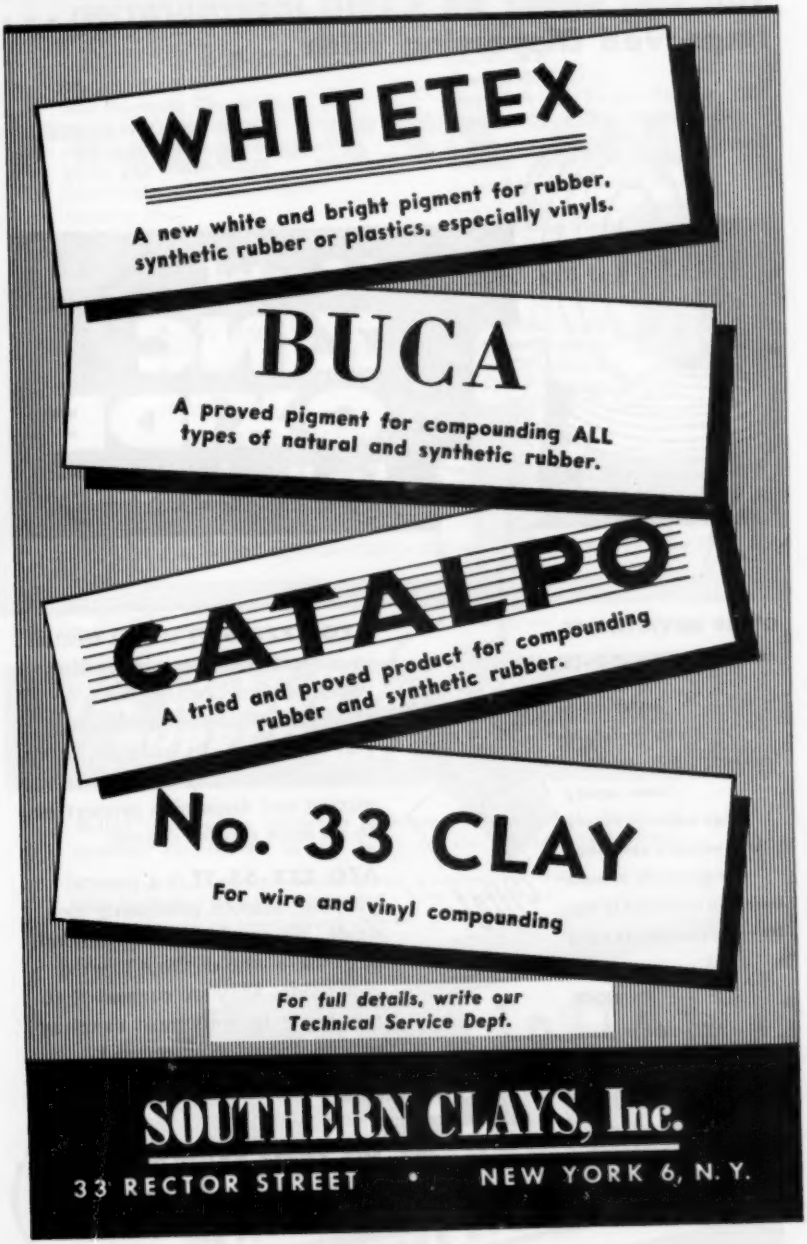
WHITETEX
A new white and bright pigment for rubber, synthetic rubber or plastics, especially vinyls.
BUCA
A proved pigment for compounding ALL types of natural and synthetic rubber.
CATALPO
A tried and proved product for compounding rubber and synthetic rubber.
No. 33 CLAY
For wire and vinyl compounding
For full details, write our Technical Service Dept.
SOUTHERN CLAYS, Inc.
33 RECTOR STREET • NEW YORK 6, N. Y.

You Can Count on Rapid Incorporation . . . Improved Dispersion With . . .

AZO ZZZ-55-TT

A Treated ZINC OXIDE For Use in Rubber

OTHER ADVANTAGES OF AZO ZZZ-55-TT

Faster curing
Safe processing
Improved scorch resistance
Lower acidity
High apparent density
Low moisture absorption
High tensile strength
Increased resistance to tear
Increased resistance to aging

NOTE:

AZO rubber grade zinc oxides are also available as AZODOX (de-aerated). AZODOX has twice the apparent density, half the dry bulk.

AZO ZZZ-55-TT is heat treated in a controlled atmosphere that removes objectionable trace elements and enhances mixing and dispersion. In addition, it is treated chemically to improve mixing and dispersion properties to an even greater degree.

AZO ZZZ-55-TT is a general purpose, smooth processing zinc oxide. We can highly recommend it to users who desire a treated zinc oxide. May we suggest that you try it in your most exacting recipes. Samples on request.

American Zinc sales company

Distributors for AMERICAN ZINC, LEAD & SMELTING COMPANY
COLUMBUS, OHIO • CHICAGO • ST. LOUIS • NEW YORK

HUBER CARBON BLACKS

Wyex EPC
Easy Processing Channel Black

Arrow MPC
Medium Processing Channel Black

Essex SRF
Semi-Reinforcing Furnace Black

Modulex HMF
High Modulus Furnace Black

Arogen GPF
General Purpose Furnace Black

Aromex CF
Conductive Furnace Black

Aromex ISAF Intermediate
Super Abrasion Furnace Black

Arovel FEF
Fast Extruding Furnace Black

Aromex HAF
High Abrasion Furnace Black

HUBER CLAYS

Suprex Clay . . . . . High Reinforcement
LGB . . . . Very Low Grit, High Reinforcement
Paragon Clay . . . . . Easy Processing
LGP . . . . . Very Low Grit, Easy Processing
Hi-White R . . . . . White Color

HUBER RUBBER CHEMICALS

Turgum S, Natac, Butac . . . . . Resin-Acid Softeners
Aktone . . . . . Accelerator Activator
Zeolex 23 . . . . . Reinforcing White Pigment

HUBER **J. M. HUBER CORPORATION** · 100 Park Ave., New York 17, New York

---

The World's only Weekly for
RUBBER AND PLASTICS

World wide news coverage provides international items of interest to readers in all parts of the world every week.

A year's subscription to Rubber Journal & International Plastics costs £2.15s.0d or $7.70 including postage. Write for details to:

Rubber Journal & International Plastics
Subscription Department, Maclaren House
131 Great Suffolk Street
London S E 1
England

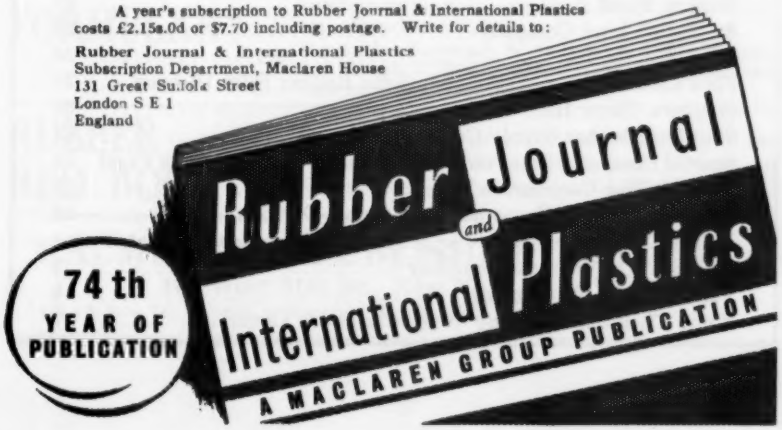

RUBBER CHEMISTRY AND TECHNOLOGY IS SUPPORTED BY ADVERTISING FROM THESE LEADING SUPPLIERS

INDEX TO ADVERTISERS

	Page
American Cyanamid Company, Organic Chemicals Division	7
American Zinc Sales Company	32
Cabot, Godfrey L., Inc.	12
Carter Bell Manufacturing Company, The	29
Columbia-Southern Chemical Corporation	9
Columbian Carbon Company (Opposite Table of Contents)	18
Du Pont, Elastomer Chemicals Department (Chemicals)	4
Du Pont, Elastomer Chemicals Department (HYPALON)	36
Enjay Company, Inc.	6
Goodrich, B. F., Chemical Company (Hycar)	25
Goodrich Gulf Chemicals	23
Goodyear, Chemical Division	5
Hall, C. P. Company, The	26
Harwick Standard Chemical Company	(Inside Back Cover)
Huber, J. M., Corporation	33
Monsanto Chemical Company	10
Naugatuck Chemical Division (U.S. Rubber Company) Chemicals	14
Naugatuck Chemical Division (U.S. Rubber Company) Naugapols	15
New Jersey Zinc Company, The	(Outside Back Cover)
Phillips Chemical Company (Philblack)	2
Phillips Chemical Company (Philprene)	11
Richardson, Sid, Carbon Company	8
Rubber Age	35
Rubber Journal and International Plastics	33
Rubber World	28
St. Joseph Lead Company	27
Scott Testers, Inc.	30
Shell Chemical Corporation, Synthetic Rubber Sales Division	21
Southern Clays, Inc.	31
Stamford Rubber Supply Company	22
Sun Oil Company, Sun Petroleum Products (Opposite Title Page)	16
Superior Zinc Corporation	29
Thiokol Chemical Corporation, Chemical Division	13
United Carbon Company	(Inside Front Cover)
Universal Oil Products Company	3
Vanderbilt, R. T., Company	19
Witco Chemical Company (Opposite Inside Cover)	1

On-the-job literature for Rubber Men

ADHESIVES AGE

A new magazine by the publishers of RUBBER AGE.

As you are well aware, adhesives have become an increasingly important part of today's rubber technology—speeding production, cutting costs, making new and improved products possible throughout the whole of industry.

ADHESIVES AGE is the first magazine to provide urgently-needed information about the chemistry, manufacture, use and application of adhesives. News of new products, new techniques, new methods and new materials—that offer opportunities for growth, expansion, sales and profits.

Now—in as much time as you want to spend with each issue, you can keep yourself expertly informed on the developments *you* are most interested in. For ADHESIVES AGE is factual, authoritative, thorough. You will find it easy to read, easy to use, interesting, practical . . . and filled with useful ideas you can put to work.

You get a full year's subscription (12 issues) of ADHESIVES AGE for only $5.00.

RUBBER AGE

The industry's outstanding technical journal covering the manufacture of rubber and rubberlike plastics products.

SUBSCRIPTION RATES

	U.S.	Canada	Other
1 year	$ 5.00	$ 5.50	$ 6.00
2 years	7.50	8.50	9.50
3 years	10.00	11.50	13.00

Single copies (up to 3 months) 50¢
Single copies (over 3 months) 75¢

THE RUBBER FORMULARY

The "pharmacopeia" for rubber—providing all the rubber compounds published in technical journals and suppliers' releases. Each compound on a separate card with marginal indexes for various physical properties, type of hydrocarbon, etc. A simple mechanical system permits you to select compounds keyed to any property. Issued monthly.

The Rubber Formulary is available on annual subscription through RUBBER AGE at a cost of $95 per year. Back issues available.

RUBBER RED BOOK

Contains complete lists of rubber manufacturers and suppliers of materials and equipment, services, etc. Eleventh issue—1957–58 edition, $12.50* Postpaid.

PALMERTON PUBLISHING CO., INC.

101 West 31st St., New York 1, N. Y.

* Add 3% Sales Tax for copies to New York City addresses.

FOR EXTRA HIGH RESISTANCE

TO DETERIORATION,

MAKE YOUR PRODUCTS WITH

HYPALON® 20

(DU PONT SYNTHETIC RUBBER)

HEAT-RESISTANT—HYPALON shows unusual resistance to hardening at elevated temperatures (250°-350°F.). Ask for Reports 56-4 and BL-306.

OZONE-RESISTANT—Exposure to ozone concentrations up to 150 ppm—a million times atmospheric concentrations—have shown that compounds of HYPALON are unaffected by ozone. Ask for Report 56-4.

WEATHER-RESISTANT—Compounds of HYPALON, brightly colored, white or black, do not lose their physical properties or appearance during long outdoor exposure. Ask for Reports 56-4 and BL-328.

CHEMICAL-RESISTANT — Concentrated sulfuric acid and hypochlorite solutions have little or no effect on compounds of HYPALON. Their superior resistance to oxidizing agents is a distinct advantage over other rubber compositions. Ask for Report 57-10.

HYPALON also offers superior scuff and abrasion resistance—plus oil and grease resistance. Properly compounded vulcanizates of HYPALON will resist flex cracking and crack growth, will not support combustion.

Report 56-4 discusses compounding and processing of HYPALON 20

Ask our District Offices for the reference reports if you don't have them.

E. I. du Pont de Nemours & Co. (Inc.), Elastomer Chemicals Department, Wilmington 98, Delaware

DU PONT
REG. U.S. PAT. OFF.

Better Things for Better Living . . . through Chemistry

DISTRICT OFFICES

Akron 8, Ohio, 40 E. Buchtel Ave. at High St.	POrtage 2-8461
Atlanta, Ga., 1261 Spring St., N. W.	TRinity 5-5391
Boston 10, Mass., 140 Federal St.	HAncock 6-1711
Charlotte 1, N. C., 427 W. 4th St.	FRanklin 5-5561
Chicago 3, Ill., 7 South Dearborn St.	ANdover 3-7000
Detroit 35, Mich., 13000 W. 7 Mile Rd.	UNiversity 4-1963
Houston 6, Texas, 2601A West Grove Lane	MOhawk 7-7429
Los Angeles 58, Calif., 2930 E. 44th St.	LUdlow 2-6464
Palo Alto, Calif., 701 Welch Rd.	DAvenport 6-7550
Trenton 8, N. J., 1750 N. Olden Ave. In New York call WAlker 5-3290	EXport 3-7141

In Canada contact: Du Pont Company of Canada (1956) Ltd., Box 660, Montreal

terial for ALL
BBER and PLASTIC
MPOUNDING

Uniformity

upon the precision char-
ick Standard Chemicals re-
quantity requirement . . .
dible assurance of uniformity
compounding material for
plastics to give *certainty* in
ment and production runs.

are geared to ex-
search toward the
any compounding
our line to your
problems.
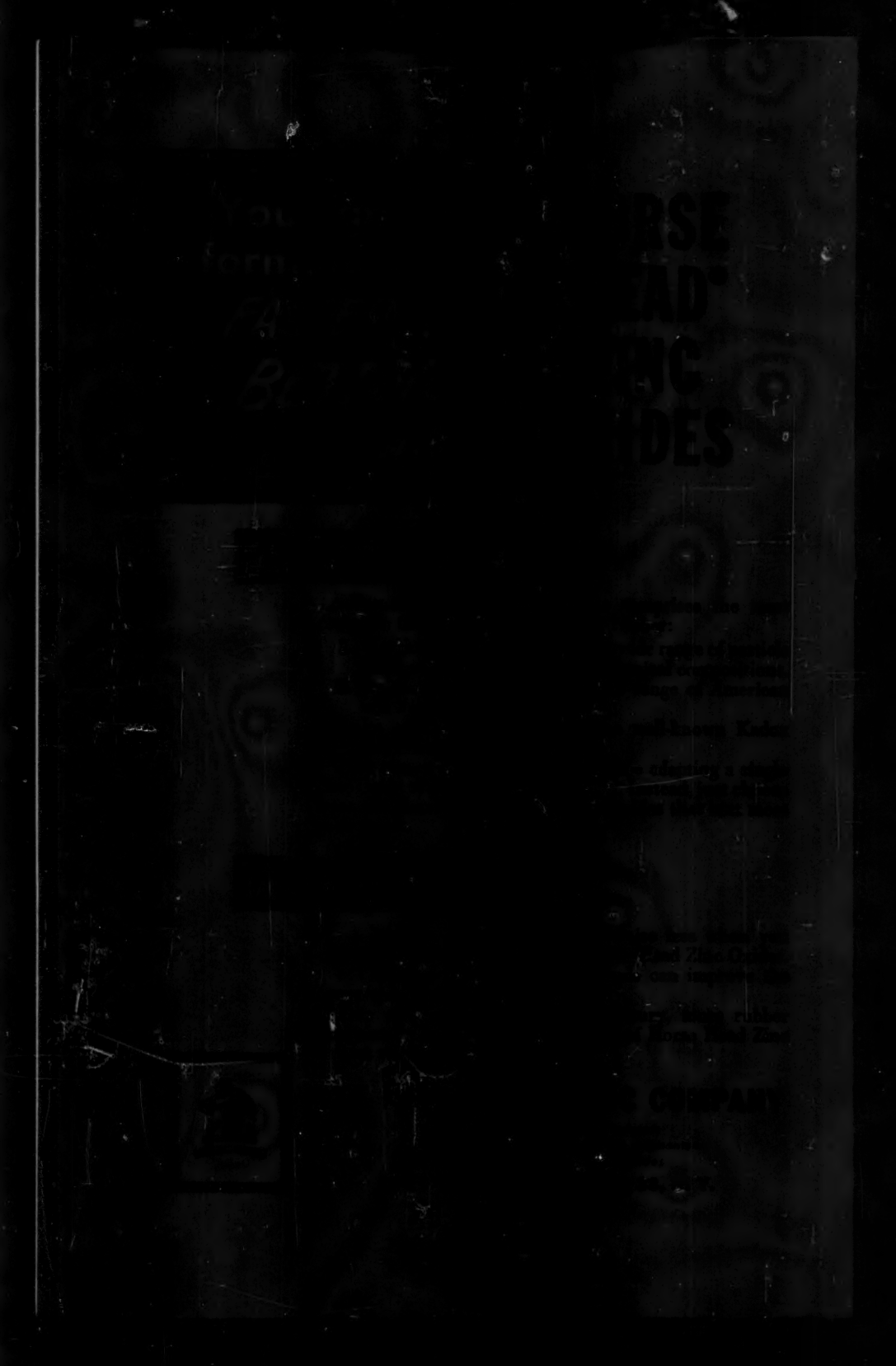
WICK STANDARD CHEMICAL CO.
AKRON 5, OHIO